

**The C-A layers of Sibudu Cave (KwaZulu-Natal,  
South Africa) in the light of the MSA lithic  
technologies in MIS 5**

**Dissertation**

der Mathematisch-Naturwissenschaftlichen Fakultät  
der Eberhard Karls Universität Tübingen  
zur Erlangung des Grades eines  
Doktors der Naturwissenschaften  
(Dr. rer. nat.)

vorgelegt von  
Viola Schmid  
aus Baden bei Wien/Österreich

Tübingen  
2019

Gedruckt mit Genehmigung der Mathematisch-Naturwissenschaftlichen Fakultät der  
Eberhard Karls Universität Tübingen.

Tag der mündlichen Qualifikation:

17.06.2019

Dekan:

Prof. Dr. Wolfgang Rosenstiel

1. Berichterstatter:

Prof. Nicholas J. Conard PhD

2. Berichterstatter:

Prof. Dr. Eric Boëda

## **Les couches C-A de la grotte de Sibudu (KwaZulu-Natal, Afrique du Sud) à la lumière des technologies lithiques du MSA dans MIS 5**

### *Résumé de la thèse*

Au cours des dernières décennies, le *Middle Stone Age* (MSA) a été proclamé comme une période clé de l'évolution de l'homme moderne. Pourtant, la nature des premières innovations nécessite encore d'être clarifiée. L'exploration des séquences régionales et la poursuite des recherches sur les phases supposées anciennes – le Still Bay et l'Howiesons Poort –, ainsi que sur l'ensemble du MSA, est essentielle afin d'élargir nos connaissances.

La grotte de Sibudu en Afrique du Sud contient une longue séquence datée du MSA. Les fouilles en cours, menées par l'Université de Tübingen, ont mis au jour des assemblages du MIS 5 qui contribuent à la discussion sur l'apparition de nouveautés technologiques, leurs mécanismes sous-jacents, ainsi que la variabilité culturelle du MSA à cette époque.

Grâce à la méthode de la chaîne opératoire, j'ai réalisé une analyse technologique des artefacts des couches C-A à Sibudu. Le corpus d'outils se démarque par sa technologie bifaciale. Sa plus grande partie se compose néanmoins d'une variété de formes pointues unifaciales. Les tailleurs ont développé une chaîne opératoire spécifique à l'obtention de produits laminaires, notamment à partir de nucléus à crête latérale opposée à un méplat formant un volume asymétrique triangulaire à exploiter.

Les couches C-A se distinguent en particulier par la présence de pièces crénelées et par le système de production laminaire. Des comparaisons avec d'autres sites du MIS 5 mettent en avant des différences dans les types d'outils et dans la mise en place de la chaîne opératoire. Cependant, les populations de différentes régions visaient un objectif technologique similaire : les lames. Ces données reflètent une organisation de ces populations sur de longues distances, avec des systèmes complexes de réseaux. En conclusion, les strates C-A appartiennent à une adaptation régionale propre au KwaZulu-Natal, attestant la hausse des inventions technologiques et des développements culturels au sein du MSA dans le MIS 5.

### *Mots-clés*

Afrique du Sud, Middle Stone Age, MIS 5, technologie lithique, innovations technologiques, pièces crénelées

# The C-A layers of Sibudu Cave (KwaZulu-Natal, South Africa) in the light of the MSA lithic technologies in MIS 5

## *Abstract of the thesis*

Over the last decades, the Middle Stone Age (MSA) has been heralded as a key period of the evolution of modern humans. Yet the nature of early innovations requires further clarification. The exploration of regional sequences and the extension of the research focus from purportedly precocious phases, Still Bay and Howiesons Poort, to the whole of the MSA are essential to expand our knowledge.

The site of Sibudu Cave, South Africa, comprises a long and well-dated MSA sequence. Ongoing excavations by the University of Tübingen have yielded MIS 5 assemblages that contribute to the discussion about the driving mechanisms as well as appearance of technological novelties and the cultural variability in the MSA during this period.

Following the *chaîne opératoire* approach, I carried out a technological analysis of the artefacts from layers C-A at Sibudu. The tool corpus stands out because of bifacial technology, but the largest part consists of a variety of unifacially pointed forms. The artisans developed a particular reduction strategy to obtain laminar products, involving cores with a lateral crest opposite the so-called lateral plane forming a triangular asymmetric volume for exploitation.

Diagnostic features, including serrated pieces and the laminar reduction system, distinguish the C-A layers. Comparisons with other MIS 5 sites illustrate differences in tool types and organisation of the reduction sequence. However, past populations across different regions aimed at a similar technological goal: blades, thus organising themselves over distances with complex systems of connectedness. In conclusion, the C-A strata belong to a regional adaptation in KwaZulu-Natal attesting the rise of technological inventions and cultural developments within the MSA in MIS 5.

## *Keywords*

South Africa, Middle Stone Age, MIS 5, lithic technology, technological innovations, serrated pieces

# Die C-A-Schichten der Sibudu-Höhle (KwaZulu-Natal, Südafrika) im Hinblick auf die Steintechnologien des MSA im MIS 5

## *Kurzzusammenfassung der Doktorarbeit*

In den letzten Jahrzehnten hat die Forschung mehr und mehr gezeigt, dass das *Middle Stone Age* (MSA) eine Schlüsselperiode der Entwicklung des modernen Menschen darstellt. Die Art der frühen Innovationen bedarf jedoch noch weiterer Klärung. Die Erforschung regionaler stratigraphischer Abfolgen und die Ausweitung des Forschungsschwerpunktes von als früh entwickelt angesehenen Phasen, dem Still Bay und dem Howiesons Poort, auf das gesamte MSA sind für die Vertiefung unseres Wissens unerlässlich.

Die Fundstelle Sibudu-Höhle, Südafrika, umfasst eine lange und gut datierte Sequenz des MSA. Aktuelle Ausgrabungen der Universität Tübingen lieferten Steinartefaktinventare aus MIS 5, die zur Diskussion über die Auslösemechanismen sowie das Auftreten technologischer Neuerungen und die kulturelle Variabilität im MSA während MIS 5 beitragen.

Basierend auf dem *Chaîne opératoire*-Ansatz führte ich eine technologische Analyse der Artefakte aus den Schichten C-A von Sibudu durch. Der Werkzeugbestand zeichnet sich durch bifaziale Technologie aus, aber bei dem größten Teil handelt es sich um unifaziale Spitzenformen. Die Bewohner von Sibudu entwickelten zu dieser Zeit eine spezielle Abbaustrategie, um laminare Grundformen zu erhalten, bei welcher Kerne mit einer lateral angelegten Kernkante gegenüber der breiteren, planaren lateralen Fläche, die zusammen ein dreieckiges asymmetrisches Volumen für den Abbau lieferten, involviert waren.

Diagnostische Merkmale, welche sogenannte ‚serrated pieces‘ und das laminare Abbausystem einschließen, charakterisieren die C-A-Schichten. Vergleiche mit anderen Fundstellen aus MIS 5 zeigen Unterschiede in Bezug auf die Werkzeugtypen und die Organisation der Abbausequenz. Die regional abgegrenzten Populationen zielen jedoch auf ein ähnliches technologisches Ziel, nämlich Klängen, ab, womit ein starker Hinweis dafür vorliegt, dass sich die Menschen über Entfernungen mit komplexen Vernetzungssystemen organisierten. Zusammenfassend lässt sich sagen, dass die C-A-Schichten zu einer regionalen Anpassung in KwaZulu-Natal gehören, die das Aufkommen technologischer Neuerungen und die kulturelle Evolution innerhalb des MSA in MIS 5 belegt.

## *Schlagworte*

Südafrika, Middle Stone Age, MIS 5, lithische Technologie, technologische Innovation, ‚serrated pieces‘



*„I dedicate this work to my sadly deceased grandfathers Manfred Friedrich Schmid and Paul Friedrich Schüller, who always supported me in their very own and different ways, and to my brother Philipp Ludwig Schmid, who stood by my side in my darkest hour.“*

# TABLE OF CONTENTS

<b>LIST OF FIGURES</b>	<b>VII</b>
<b>LIST OF TABLES</b>	<b>XIII</b>
<b>ACKNOWLEDGEMENTS</b>	<b>XX</b>
<b>1. INTRODUCTION AND FOUNDATIONS OF THE STUDY</b>	<b>1</b>
1.1. <i>THE MSA IN AFRICA</i>	1
1.1.1. RESEARCH HISTORY	1
1.1.2. HUMAN REMAINS AND GENETIC DATA	3
1.1.3. NOVELTIES IN LITHIC TECHNOLOGY	5
1.1.4. NON-LITHIC EVIDENCE FOR COGNITIVE COMPLEXITY	8
1.2. <i>THE SOUTHERN AFRICAN MSA SEQUENCE AND MIS 5 EVOLUTIONARY DYNAMICS</i>	11
1.2.1. THE HOWIESONS POORT AND STILL BAY RESEARCH IMBALANCE	11
1.2.2. STATUS QUO OF CHRONO-CULTURAL DEVELOPMENTS IN THE MSA DURING MIS 5	15
1.2.3. RESEARCH OBJECTIVES	19
<b>2. BACKGROUND TO THE SITE</b>	<b>20</b>
2.1. <i>GEOLOGICAL SETTING</i>	20
2.2. <i>RESEARCH HISTORY</i>	21
2.3. <i>STRATIGRAPHY AND CHRONOLOGY</i>	24
2.4. <i>ENVIRONMENTAL BACKGROUND</i>	30
<b>3. METHODS</b>	<b>40</b>
3.1. <i>METHODS OF EXCAVATION</i>	40
3.2. <i>METHODS OF STUDY</i>	44
3.2.1. PROTOCOL OF THE TECHNOLOGICAL STUDY	48
3.2.2. GENERAL ATTRIBUTES	50
3.2.2.1. CORTEX	50
3.2.2.2. FRAGMENTATION	50
3.2.3. MODALITIES OF MEASUREMENTS	50
3.2.4. DEBITAGE SPECIFIC ATTRIBUTES	53
3.2.4.1. TECHNOLOGICAL CLASSIFICATION	53
3.2.4.2. MORPHOLOGICAL ATTRIBUTES	53
3.2.4.3. DORSAL SCAR PATTERN	53
3.2.4.4. DISTAL TERMINATION	53
3.2.5. CORE CLASSIFICATION	54
3.2.6. DIACRITIC DIAGRAM OF CORES	54
3.2.7. ASSESSMENT OF KNAPPING TECHNIQUE	54
3.2.8. TYPOLOGICAL CLASSIFICATION	56
3.2.9. TECHNO-FUNCTIONAL CLASSIFICATION	56
3.2.10. MANUFACTURE PHASES OF BIFACIALS	56
3.2.11. TAPHONOMIC ATTRIBUTES	57
3.2.12. QUANTIFYING SMALL DEBITAGE	57
3.2.13. STATISTICAL TESTS	57
<b>4. ARCHAEOLOGICAL SAMPLE</b>	<b>58</b>
4.1. <i>LAYER ADAM</i>	58
4.2. <i>LAYER ANNIE</i>	60
4.3. <i>LAYER BART</i>	60

4.4.	<i>LAYER BEA</i>	61
4.5.	<i>LAYER CASPER</i>	61
4.6.	<i>LAYER CHANTAL</i>	62
<b>5.</b>	<b>RESULTS</b>	<b>63</b>
5.1.	<i>RAW MATERIALS</i>	63
5.1.1.	RAW MATERIAL AVAILABILITIES	63
5.1.2.	RAW MATERIAL PROCUREMENT	67
5.2.	<i>DEBITAGE</i>	75
5.3.	<i>CORES</i>	98
5.4.	<i>KNAPPING TECHNIQUE</i>	108
5.5.	<i>THE LAMINAR REDUCTION STRATEGY</i>	115
5.5.1.	CORE CONFIGURATION	115
5.5.2.	EARLY PHASE OF REDUCTION	122
5.5.3.	MIDDLE AND LATE PHASE OF REDUCTION	122
5.5.4.	FINAL PHASE OF REDUCTION	124
5.6.	<i>FORMAL TOOLS</i>	125
5.6.1.	UNIFACIAL POINTED FORMS	126
5.6.1.1.	TSPTS	133
5.6.1.2.	ACTS	143
5.6.2.	BIFACIAL PIECES	146
5.6.2.1.	BIFACIAL POINTS	149
5.6.2.1.1.	<i>BIFACIAL POINTS MADE ON DOLERITE, QUARTZITE AND HORNFELS</i>	161
5.6.2.1.2.	<i>BIFACIAL POINTS MADE ON QUARTZ</i>	164
5.6.2.2.	SERRATED PIECES	164
5.6.2.3.	BIFACIALLY BACKED KNIVES	171
5.6.3.	SCRAPER-LIKE FORMS	172
5.6.3.1.	LATERAL SCRAPERS	173
5.6.3.2.	NBTS	174
5.6.4.	DENTICULATES/NOTCH	176
5.7.	<i>TAPHONOMY</i>	177
<b>6.</b>	<b>DISCUSSION</b>	<b>181</b>
6.1.	<i>INSIGHTS INTO THE WAY OF LIFE</i>	181
6.1.1.	TECHNICAL SYSTEM OF THE C-A LAYERS	185
6.1.2.	TECHNO-ECONOMIC SYSTEM OF THE C-A LAYERS (FIGURE 84)	191
6.2.	<i>THE CHRONO-CULTURAL CLASSIFICATION OF THE C-A LAYERS</i>	201
6.2.1.	THE MSA BIFACIAL PHENOMENON	201
6.2.1.1.	THE C-A LAYERS WITHIN THE MIS 5 OCCUPATIONS AT SIBUDU	202
6.2.1.2.	THE C-A LAYERS AND THE STILL BAY	203
6.2.1.3.	THE C-A LAYERS WITHIN THE MIS 5 BIFACIAL EXPRESSIONS	213
6.2.2.	CULTURAL DEVELOPMENTS IN THE MSA CONTEXT OF MIS 5	218
6.2.3.	THE C-A LAYERS OF SIBUDU MATTER – SO WHAT LABEL?	220
<b>7.</b>	<b>SUMMARY</b>	<b>224</b>
<b>8.</b>	<b>RÉSUMÉ</b>	<b>244</b>
<b>9.</b>	<b>ZUSAMMENFASSUNG</b>	<b>267</b>
<b>10.</b>	<b>BIBLIOGRAPHY</b>	<b>291</b>
<b>11.</b>	<b>SUPPLEMENTARY INFORMATION</b>	<b>326</b>



## List of Figures

- Figure 1.** Map of Africa with sites mentioned in the Text: 1 - Apollo 11 Rock Shelter; 2 - Benzú Rock Shelter; 3 - Bestwood 1; 4 - Biesiesput 1; 5 - Blombos Cave; 6 - Border Cave; 7 - Canteen Kopje; 8 - Cap Chatelier; 9 - Cave of Hearths; 10 - Dar es-Soltan 1 Cave; 11 - Diepkloof Rock Shelter; 12 - El Mnasra Cave; 13 - Factory Site; 14 – Florisbad; 15 – Gademotta; 16 - Grotte des Pigeons; 17 – Hackthorne; 18 – Herto; 19 - Jebel Irhoud; 20 - Kalambo Falls; 21 - Katanda; 22 - Kathu Pan; 23 - Keratic Koppie; 24 - Klasies River main site; 25 - Klein Kliphuis Rock Shelter; 26 - Klipdrift Shelter; 27 - Koimilot; 28 - Kudu Koppie; 29 – Kulkuletti; 30 - Leakey Handaxe Area; 31 - Littorines Cave; 32 - Ngaloba; 33 - Nooitegedacht 2; 34 - Ologesailie; 35 - Omo Kibish; 36 - Ounjougou; 37 - Pinnacle Point Cave 13B; 38 - Pniel 1 & 6; 39 - Porc Epic Cave; 40 - Roodam 1 & 2; 41 - Rose Cottage Cave; 42 - Roseberry Plain 1; 43 - Sai Island 8-B-11; 44 - Sibilo School Road Site; 45 - Sibudu Cave; 46 - Strathalan Cave B; 47 - Twin Rivers; 48 - Umhlatuzana Rock Shelter; 49 - Wonderwerk Cave.....2
- Figure 2.** Still Bay points: a) Still Bay point from Pringle Bay (modified after Goodwin and van Riet Lowe, 1929: 128, Text-Figure 2); b-d) Still Bay points from Varsche Rivier 003 (Steele, et al., 2016: Figure 14); e-f) Still Bay points from Mertenhof Rock Shelter (modified after Will, et al., 2015: S2 Figure); g-j) Still Bay points from Hollow Rock Shelter (g-h) Evans, 1993: Appendix 1, i-j) Högberg and Larsson, 2011: Figure 7); k-n) Still Bay points from Diepkloof Rock Shelter (Porráz, et al., 2013: Figure 6); o-q) Still Bay points from Peers Cave (modified after Andreasson, 2010: Figure 25 – 27); r-v) Still Bay points from Dale Rose Parlour (copyright by Pierre-Jean Texier; drawings by Michel Grenet); w-ab) Still Bay points from Blombos Cave (w-y) Villa, et al., 2009: Figure 1, z-ab) Henshilwood, et al., 2001: Figure 7); ac-ae) Still Bay points from Umhlatuzana Rock Shelter (ac-ad) Kaplan, 1990: Figure 11-12, ae) Högberg and Lombard, 2016: Figure 3); af-ai) Still Bay points from Sibudu Cave (Soriano, et al., 2015: S1 Figure A).....14
- Figure 3.** Location of Still Bay sites in southern Africa (Site Abbreviations: BBC - Blombos Cave, DRS - Diepkloof Rock Shelter, DRP - Dale Rose Parlour, HRS - Hollow Rock Shelter, MRS - Mertenhof Rock Shelter, PC - Peers Cave, UMH - Umhlatuzana Rock Shelter, VR3 - Varsche Rivier 003). .....15
- Figure 4.** Location of MSA sites during MIS 5 (Site Abbreviations: AP11 - Apollo 11 Rock Shelter, BBC - Blombos Cave, BC - Border Cave, BRS - Bushman Rock Shelter, CH - Cave of Hearths, CSB - Cape St. Blaize, DRS – Diepkloof Rock Shelter, DRP - Dale Rose Parlour, FL - Florisbad, HBC - Herolds Bay Cave, HDP1 - Hoedjiespunt 1, HRS - Hollow Rock Shelter, KB - Kalkbank, KFR - Klipfonteinrand, KRM - Klasies River main site, MC - Mwulu’s Cave, MLK – Melikane Rock Shelter, MRS - Mertenhof Rock Shelter, NBC - Nelsons Bay Cave, OBP - Olieboompoort, PC - Peers Cave, PL - Plovers Lake, PL8 - Putslaagte 8, PP13B - Pinnacle Point 13B, RCC - Rose Cottage Cave, SH - Sea Harvest, SKC - Swartkrans, UMH - Umhlatuzana Rock Shelter, VR3 - Varsche Rivier 003, WTK - Witkrans, YFT - Ysterfontein 1).....16
- Figure 5.** Sibudu: a) Location of Sibudu in KwaZulu-Natal (left; after: Wadley, 2001a: Figure 1); b) overview of the site in 2016 (photo by Nicholas J. Conard); c) view on the excavation areas in 2017 (photo by Ria Litzenberg).....20
- Figure 6.** Geological context of South Africa (modified after Council for Geoscience).....22
- Figure 7.** Sibudu: Nicholas J. Conard and Lyn Wadley at Sibudu Cave 2011 (Photo by Sarah Rudolf).....22

<b>Figure 8.</b> Sibudu: Plan of the site with elevations in meters amsl, the excavation grid, the two excavation areas, and the location of east profile (modified after Soriano, et al., 2015: Figure 2).....	23
<b>Figure 9.</b> Sibudu: Eastern profile of the Deep Sounding of Sibudu including ages of the archaeological phases and indication of the presence of bifacial or serrated pieces (left) (modified after Rots, et al., 2017). (*Final MSA Mohapi, 2012; **lower Sibudan Will and Conard, 2018; ***Howiesons Poort de la Peña, et al., 2013; ****Still Bay Soriano, et al., 2015); Orthophotography of the east profile (copyright by M.M. Haaland) (right).....	24
<b>Figure 10.</b> Biomes of southern Africa (modified after Meadows and Quick, 2016).....	31
<b>Figure 11.</b> Climate diagram of KwaZulu-Natal Coastal Belt units. MAP: Mean Annual Precipitation; APCV: Annual Precipitation Coefficient of Variation; MAT: Mean Annual Temperature; MFD: Mean Frost Days (days when screen temperature was below 0°C); MAPE: Mean Annual Potential Evaporation; MASMS: Mean Annual Soil Moisture Stress (% of days when evaporative demand was more than double the soil moisture supply) (after Mucina, et al., 2006).....	31
<b>Figure 12.</b> a) Map of southern Africa indicating the location of important MSA sites (EB, Elands Bay Cave; Di, Diepkloof; DK, Die Kelders; Bl, Blombos; Bo, Boomplaas; KR, Klasies River; RC, Rose Cottage; Si, Sibudu; BC, Border Cave; WC, Wolkberg Cave); dominant atmospheric circulation patterns indicated by thin black arrows, major ocean currents indicated by thick grey arrows (labelled as follows: BC, Benguela Current; STC, Subtropical Convergence; AC, Agulhas Current) and Lake Sibayi, Mfabeni peatland as well as marine core MD79254 indicated by filled circles (left; modified after Chase, 2010: Figure 1); b) Indian Ocean faunal SST estimates of marine core MD79254 for past 135 ka (after :van Campo, et al., 1990)....	33
<b>Figure 13.</b> Sea-level fluctuations (bracketed by uncertainty) since 520 ka BP (after Waelbroeck, et al., 2002 in blue, after Rohling, et al., 2009 in red and after Bintanja, et al., 2005 in brown) compared with the sea-level curves for southern Africa above from Ramsay and Cooper, 2002 (filled boxes) and Carr, et al., 2010 (empty boxes) back to 145 ka BP, and from Compton and Wiltshire, 2009 based on a sediment proxy for the timing but not the amplitude of sea-level fluctuations on the western margin back to 440 ka BP (modified after Compton, 2011).....	34
<b>Figure 14.</b> Sibudu: M. Zeidi in the DS in March 14 <sup>th</sup> , 2012 (Photo by Sarah Rudolf).....	40
<b>Figure 15.</b> Sibudu: a) Drawing of Abtrag 3 in layer Bart (GSS) with indication of serrated piece B4-1170 by M. Zeidi (lithics in red; faunal remains in blue, ochre in orange); b) diary of square B4 with diary entries of March 24 <sup>th</sup> and 25 <sup>th</sup> 2013 with drawing of serrated piece B4-1170 from layer Bart (GSS) by M. Zeidi; c) layer form of layer Bart (GSS) filled out by M. Zeidi.....	41
<b>Figure 16.</b> Permanent storage of all lithic specimen from layers Adam to Chantal at the KwaZulu-Natal Museum in Pietermaritzburg (Photo by Viola C. Schmid).....	44
<b>Figure 17.</b> Theoretical framework of the technological approach, including the relationship between project, conceptual scheme, and operational scheme (modified after Soressi and Geneste, 2011: Figure 3; Porraz, et al., 2016: Figure 5); drawing by Heike Würschem).....	45
<b>Figure 18.</b> The three types of contact of a tool (modified after Nicoud, 2011: Figure 9; Lepot, 1993); drawing by Heike Würschem).....	47
<b>Figure 19.</b> Lithic assemblage of Adam laid out on the table to make a first general observation (Photo by Viola C. Schmid).....	48
<b>Figure 20.</b> a) Length, width, thickness, platform width, platform depth and EPA measuring sections on blanks (Drawing by Heike Würschem and Achim Frey); b) Length, width,	

thickness, length of last removal (last removal grey shaded) and EPA measuring sections on cores (Drawing by Heike Würschem); c) Length, width, and thickness of retouched point as well as width and thickness of the base measuring sections on unifacial, bifacial and serrated points (Drawing Guillaume Porraz); d) Width and depth measuring sections on notches of serrated pieces and denticulates (Photo by Viola C. Schmid).....	52
<b>Figure 21.</b> Diacritic diagram of core A5-52 from layer Adam (BMO) (Drawing by Viola C. Schmid).....	55
<b>Figure 22.</b> Sibudu: Overview of the excavation grid (left) and horizontal find distribution of all layers (right).....	59
<b>Figure 23.</b> Sibudu: Orthophotography of the east profile (copyright by M.M. Haaland) (left) and vertical find distribution of all layers, including all objects ≤ 20cm east of the east profile (right).....	60
<b>Figure 24.</b> Map of geological context and raw material source localities in the area of Sibudu. indicating also Sibudu Cave and Umhlatuzana Shelter (modified after Bader, et al., 2015: Figure 1. Top).....	63
<b>Figure 25.</b> a) Dolerite dyke within 200m of the site (Photo by Mohsen Zeidi); b) road cut close to the shelter exposing cobbles of quartzite (size range is shown in the close-up in the upper right corner) (Photo by Mohsen Zeidi); c) Occurrence of dolerite cobbles in Black Mhlasini River close to Colt Shooting Range and next to Oakford Road (Photo by Jonathan A. Baines; d) Verulam sill (close-up of the deposit in the upper right corner) (Photo by Mohsen Zeidi)..	65
<b>Figure 26.</b> Sibudu. C-A layers from the Deep Sounding: Frequency distribution of length and width of completely preserved blades made on dolerite (left) and of width of all in the width completely preserved blades made on dolerite in mm (right).....	69
<b>Figure 27.</b> Sibudu. C-A layers from the Deep Sounding: Ratio of blank to core (the number of complete and proximal flakes and tools divided by the number of cores defined by Dibble and McPherron 2006) and tool to blank (the number of complete and proximal tools divided by the number of complete and proximal flakes defined by Dibble and McPherron 2006)....	71
<b>Figure 28.</b> Sibudu. C-A layers from the Deep Sounding: Initial core made on sandstone (Photo by Viola C. Schmid).....	72
<b>Figure 29.</b> Sibudu. C-A layers from the Deep Sounding: Basal fragment of bifacial made on sandstone (Photos by Guillaume Porraz).....	72
<b>Figure 30.</b> Sibudu. C-A layers from the Deep Sounding: Serrated piece made on light purple fine-grained quartzite variety (Photo by Viola C. Schmid).....	73
<b>Figure 31.</b> Sibudu. C-A layers from the Deep Sounding: Scatter plot of width and length of all complete cores.....	74
<b>Figure 32.</b> Sibudu. C-A layers from the Deep Sounding: Tall, laterally centralized blades with a triangular cross-section. Blades made on dolerite (a-e, g-o) and made on sandstone (f) (Drawing by Mojdeh Lajmiri and Heike Würschem; photos by Viola C. Schmid).....	82
<b>Figure 33.</b> Sibudu. C-A layers from the Deep Sounding: Tall, laterally centralized blades with a triangular cross-section. Blades made on dolerite (a-d, f-q) and made on quartzite (e) (Photos by Viola C. Schmid).....	83
<b>Figure 34.</b> Sibudu. C-A layers from the Deep Sounding: Tall, laterally centralized blades with a triangular cross-section. Blades made on quartzite (a, b) and made on dolerite (c-m) (Photos by Viola C. Schmid).....	84
<b>Figure 35.</b> Sibudu. C-A layers from the Deep Sounding: Flat, laterally diffuse blades with a trapezoidal cross-section. Blades made on dolerite (a-e, g, h, j-o), made on sandstone (f) and	

made on quartzite (i) (Drawing (d) by Mojdeh Lajmiri and Heike Würschem; drawing (j) by Achim Frey and Heike Würschem; photos by Viola C. Schmid).....	85
<b>Figure 36.</b> Sibudu. C-A layers from the Deep Sounding: Technologically diagnostic flakes. Flakes made on dolerite (a-k, m-o, q, r, t-v), made on quartzite (l, s) and made on hornfels (p) (Photos by Viola C. Schmid).....	93
<b>Figure 37.</b> Sibudu. C-A layers from the Deep Sounding: Technologically diagnostic flakes. Flakes made on dolerite (a-j, l-n, p-s, u), made on hornfels (k), made on quartzite (o) and made on quartz (t) (Drawings by Heike Würschem; photos by Viola C. Schmid).....	94
<b>Figure 38.</b> Sibudu. C-A layers from the Deep Sounding: Technologically diagnostic flakes. Flakes made on dolerite (a-f, h, i, k-r) and made on quartzite (g, j) (Photos by Viola C. Schmid).....	95
<b>Figure 39.</b> Sibudu. C-A layers from the Deep Sounding: a) Unidirectional laminar platform core made on quartz; b) Unidirectional laminar platform core made on quartz terminated as bipolar core; c) bipolar core made on quartz (Photos by Viola C. Schmid).....	100
<b>Figure 40.</b> Sibudu. C-A layers from the Deep Sounding: a) Bidirectional laminar platform core made on dolerite (Photo by Viola C. Schmid).....	102
<b>Figure 41.</b> Sibudu. C-A layers from the Deep Sounding: Scatter plot of length and width of completely preserved blades and of blade scars presenting last operation on laminar platform cores.....	105
<b>Figure 42.</b> Sibudu. C-A layers from the Deep Sounding: Quartzite bladelet core (Photo by Viola C. Schmid).....	107
<b>Figure 43.</b> Sibudu. C-A layers from the Deep Sounding: Scatter plot of width and thickness of all in width and thickness completely preserved core types.....	108
<b>Figure 44.</b> Sibudu. C-A layers from the Deep Sounding: Frequency distribution of EPA of blades.....	109
<b>Figure 45.</b> Sibudu. C-A layers from the Deep Sounding: Frequency distribution of platform depth of blades.....	109
<b>Figure 46.</b> Sibudu. C-A layers from the Deep Sounding: Hammerstones. Hammerstones made on sandstone (a, b), and hammerstone made on quartzite (c) (Photo (a) by Julia Becher; photos (b, c) by Viola C. Schmid).....	114
<b>Figure 47.</b> Sibudu. C-A layers from the Deep Sounding: Box plots of dimensions of blade platform cores.....	115
<b>Figure 48.</b> Sibudu. C-A layers from the Deep Sounding: Core configuration of laminar reduction strategy (Drawing after Rots, et al., 2017; photo by Viola C. Schmid).....	117
<b>Figure 49.</b> Sibudu. C-A layers from the Deep Sounding: Laminar cores (a-c) (Drawings by Heike Würschem; photos by Viola C. Schmid).....	118
<b>Figure 50.</b> Sibudu. Layer Bea of the Deep Sounding: Exhausted laminar core, where the lateral crest was completely removed by removals from the exploitation (Drawing by Heike Würschem; photo by Viola C. Schmid).....	120
<b>Figure 51.</b> Sibudu. Layer Bart of the Deep Sounding: Core configuration of laminar reduction strategy with extraction of triangular element in last operational phase (Drawing by Heike Würschem; photo by Viola C. Schmid).....	121
<b>Figure 52.</b> Sibudu. Layer Bart of the Deep Sounding: Distribution of dorsal scar patterns by cortex coverage proportions on the dorsal surface of all lateral crest preparation flakes (n=1,247).....	123

<b>Figure 53.</b> Sibudu. C-A layers from the Deep Sounding: Partial rejuvenation core tablets. Partial rejuvenation core tablets made on dolerite (a, b) and made on sandstone (c) (Photos by Viola C. Schmid).....	124
<b>Figure 54.</b> Sibudu. C-A layers from the Deep Sounding: TSPs. TSPs made on dolerite (a, c-e, g-i, k-o, q, s, t, y, z, ab), made on quartzite (b, j, p, r, u-x, aa), and made on quartz (f) (Drawings by Mojdeh Lajmiri; photos by Viola C. Schmid).....	131
<b>Figure 55.</b> Sibudu. C-A layers from the Deep Sounding: ACTs (a-p) and Tongatis (q, r). ACTs made on hornfels (a), made on dolerite (b-f, i, j, l, m, o), made on quartzite (g, h, k, p), and made on chert (n); Tongati made on quartzite (q) and Tongati made on hornfels (r) (Drawings by Mojdeh Lajmiri; photos by Viola C. Schmid).....	132
<b>Figure 56.</b> Sibudu. C-A layers from the Deep Sounding: Boxplot showing morphometric characteristics of the TSPs.....	134
<b>Figure 57.</b> Sibudu. C-A layers from the Deep Sounding: TSP morphotype.....	138
<b>Figure 58.</b> Sibudu. C-A layers from the Deep Sounding: Morphological and morphometric features of the active part of TSPs.....	139
<b>Figure 59.</b> Sibudu. C-A layers from the Deep Sounding: Techno-functional and functional characterisation of the TSPs (modified after Tringham, et al., 1974: Figure 20). .....	140
<b>Figure 60.</b> Sibudu. C-A layers from the Deep Sounding: Boxplot showing edge angles of both edges of the TSPs and ACTs.....	141
<b>Figure 61.</b> Sibudu. C-A layers from the Deep Sounding: Schematic model of reduction for the TSP cycle in comparison with reduction cycles of other unifacial pointed forms (modified after Conard, et al., 2012: Figure 8).....	142
<b>Figure 62.</b> Sibudu. C-A layers from the Deep Sounding: Boxplot showing length to length of retouched point ratio of TSPs < 40 mm and > 40 mm.....	143
<b>Figure 63.</b> Sibudu. C-A layers from the Deep Sounding: a) ACT morphotype; b) boxplot showing morphometric characteristics of the ACTs; c) techno-functional and functional characterisation of the ACTs.....	144
<b>Figure 64.</b> Sibudu. C-A layers from the Deep Sounding: Profile projection of the bifacial pieces from the Deep Sounding. The numbers in parentheses reflect the number of bifacial pieces; volume refers to the total volume of excavated sediment per layer.....	147
<b>Figure 65.</b> Sibudu. C-A layers from the Deep Sounding: Bifacial points made on dolerite (a-m, p) and hornfels (n, o) according to phase of manufacture (Drawings by Guillaume Porraz; photos (b, c, f, h, k, l) by Julia Becher; photos (i, j, o) by Lucía Cobo-Sánchez; photos (a, d, e, g, m, n, p) by Viola C. Schmid).....	150
<b>Figure 66.</b> Sibudu. C-A layers from the Deep Sounding: Bifacial points made on quartzite (Photos (c, h) by Julia Becher; photos (a, b, d-g, i-k) by Viola C. Schmid).....	151
<b>Figure 67.</b> Sibudu. C-A layers from the Deep Sounding: Bifacial points made on quartz (Drawing by Guillaume Porraz; photos (e-g) by Julia Becher; photo (d) by Lucía Cobo-Sánchez; photos (a-c, h-o) by Viola C. Schmid).....	152
<b>Figure 68.</b> Sibudu. C-A layers from the Deep Sounding: Boxplot showing morphometric characteristics of the bifacial points.....	153
<b>Figure 69.</b> Sibudu. C-A layers from the Deep Sounding: Bifacial point morphotype.....	155
<b>Figure 70.</b> Sibudu. C-A layers from the Deep Sounding: Morphological features, including TPA (a), tip profile (b) and base profile (c).....	156

<b>Figure 71.</b> Sibudu. C-A layers from the Deep Sounding: Shaping flakes made on dolerite. Shaping flakes from initial shaping phase (a-c), shaping flakes from advanced shaping phase (d-f) and shaping flakes from final shaping phase (g-i) (Drawings by by Mojdeh Lajmiri).....	157
<b>Figure 72.</b> Sibudu. C-A layers from the Deep Sounding: Frequency distribution of manufacturing phase attributes.....	159
<b>Figure 73.</b> Sibudu. C-A layers from the Deep Sounding: Boxplot showing thickness of the phases of manufacture of the bifacial points.....	160
<b>Figure 74.</b> Sibudu. C-A layers from the Deep Sounding: a) Removal organisation during manufacture of bifacial points; b) Schematic model showing re-sharpening of bifacial points with two hierarchised surfaces and change of tip outline.....	163
<b>Figure 75.</b> Sibudu. C-A layers from the Deep Sounding: Serrated Pieces. Serrated pieces made on dolerite (f, h, i, k, m, p-x), made on quartz (a-e, n, o), made on hornfels (g, l), and made on quartzite (j) (modified after Rots, et al., 2017).....	166
<b>Figure 76.</b> Sibudu. C-A layers from the Deep Sounding: Pressure flaking experiments. a) Christian Lepers conducting the pressure flaking; b) pressure flaking of crystal quartz (Exp. 84/12 piece fractured in the production sequence); c) pressure flaking of dolerite (Exp. 82/22 piece finished used as projectile (see Rots, et al., 2017: Figure 7).....	168
<b>Figure 77.</b> Sibudu. C-A layers from the Deep Sounding: Bifacial tools. a & b) made on dolerite (Photos by Viola C. Schmid); c) Schematic model showing re-sharpening of bifacial tools and removal organisation.....	172
<b>Figure 78.</b> Sibudu. C-A layers from the Deep Sounding: Lateral scrapers (a-e), NBTs (f-j) and denticulates (k-m). All lateral scrapers made on dolerite; NBTs made on dolerite (f, i, j), made on hornfels (g), and made on quartzite (h); denticulate made on dolerite (k), denticulate made on quartzite (l), and denticulate made on quartz (m) (Drawings by Heike Würschem and Mojdeh Lajmiri; photos by Viola C. Schmid).....	175
<b>Figure 79.</b> Sibudu. C-A layers from the Deep Sounding: Frequency distribution of tool types and shaping flakes.....	182
<b>Figure 80.</b> Sibudu. Deep Sounding: Bifacial tools from BS member. Bifacial tools made on hornfels (a, c, d, e), made on quartzite (b), and made on dolerite (f) (Drawings by Guillaume Porraz; photos by Lucía Cobo-Sánchez).....	183
<b>Figure 81.</b> Sibudu. Deep Sounding: Lamina cores from layers Danny and Darya (a-c) (Drawings by Heike Würschem; photos by Viola C. Schmid).....	184
<b>Figure 82.</b> Sibudu. C-A layers from the Deep Sounding: Box Scheme of laminar reduction system showing early, middle/late and final phase of reduction sequence with diagnostic products.....	186
<b>Figure 83.</b> Sibudu. C-A layers from the Deep Sounding: Summarized comparison of TSPs and ACTs.....	188
<b>Figure 84.</b> Sibudu. C-A layers from the Deep Sounding: Dynamic model of the techno-economic procedures concerning the different raw materials in the assemblage (modified after Porraz, 2005: Figure 60).....	192
<b>Figure 85.</b> Sibudu. C-A layers from the Deep Sounding: Scatter plot of width and length of all complete bifacial points.....	195
<b>Figure 86.</b> Sibudu. C-A layers from the Deep Sounding: Scatter plot of lengths and widths of all complete serrated pieces.....	197

## List of Tables

<b>Table 1.</b> Suggested nomenclature for MSA sub-stages (modified after Wurz, 2002, Wurz, 2016).....	11
<b>Table 2.</b> Summary of Age (ka) $\pm 1\sigma$ .....	25
<b>Table 3.</b> Summary of proxy environmental evidence (modified after Hall, et al., 2014) – Occupation (Wadley and Jacobs, 2006), botanical data (Wadley, 2004; Allott, 2006; Renaut and Bamford, 2006; Sievers, 2006; Murungi, 2017), isotopic data (Hall, et al., 2008; Robinson and Wadley, 2018), and faunal data (Plug, 2004, 2006; Cain, 2006; Glenn, 2006; Wells, 2006; Clark and Plug, 2008; Clark 2011, 2017; Val, 2016), geology and mineralogy (Schiegl, et al., 2004; Pickering, 2006; Schiegl and Conard, 2006) and magnetic susceptibility (Herries 2006).....	35
<b>Table 4.</b> Sibudu. C-A layers from the Deep Sounding: Frequency of lithic single finds and small debitage products, sediment volumes and find density.....	58
<b>Table 5.</b> Sibudu. C-A layers from the Deep Sounding: Frequency of cortex types of blanks with cortex coverage per raw material.....	67
<b>Table 6.</b> Sibudu. C-A layers from the Deep Sounding: Frequency of raw materials.....	67
<b>Table 7.</b> Sibudu. C-A layers from the Deep Sounding: Frequency of dolerite varieties.....	68
<b>Table 8.</b> Sibudu. C-A layers from the Deep Sounding: Frequency of dolerite varieties of tools.....	68
<b>Table 9.</b> Sibudu. C-A layers from the Deep Sounding: Frequency of cortex coverage proportions on the dorsal surface of blanks per raw material.....	69
<b>Table 10.</b> Sibudu. C-A layers from the Deep Sounding: Frequency of raw materials per lithic artefacts >30mm and small debitage (<30mm) in square C4.....	70
<b>Table 11.</b> Sibudu. C-A layers from the Deep Sounding: Frequency of raw material per technological classification.....	70
<b>Table 12.</b> Sibudu. C-A layers from the Deep Sounding: Frequency of quartz types.....	73
<b>Table 13.</b> Sibudu. C-A layers from the Deep Sounding: Frequency of quartz types per technological classification.....	73
<b>Table 14.</b> Sibudu. C-A layers from the Deep Sounding: Descriptive statistics of EL to blank mass-ratio of all completely preserved blanks per raw material.....	74
<b>Table 15.</b> Sibudu. C-A layers from the Deep Sounding: General technological classification....	75
<b>Table 16.</b> Sibudu. C-A layers from the Deep Sounding: Frequency of blank categories.....	75
<b>Table 17.</b> Sibudu. C-A layers from the Deep Sounding: Descriptive statistics of the debitage laminarity of all completely preserved blanks per raw materials.....	76
<b>Table 18.</b> Sibudu. C-A layers from the Deep Sounding: Frequency of fragmentation per blank category.....	76
<b>Table 19.</b> Sibudu. C-A layers from the Deep Sounding: Frequency of raw materials per blank category.....	77

<b>Table 20.</b> Sibudu. C-A layers from the Deep Sounding: Frequency of fragmentation of blades per raw material.....	77
<b>Table 21.</b> Sibudu. C-A layers from the Deep Sounding: Frequency of cortex coverage per blank category.....	78
<b>Table 22.</b> Sibudu. C-A layers from the Deep Sounding: Frequency of cortex position per blank category.....	78
<b>Table 23.</b> Sibudu. C-A layers from the Deep Sounding: Frequency of platform type of completely and proximal preserved blanks.....	78
<b>Table 24.</b> Sibudu. C-A layers from the Deep Sounding: Frequency of dorsal scar pattern per blank category.....	78
<b>Table 25.</b> Sibudu. C-A layers from the Deep Sounding: Frequency of morphology per blank category.....	79
<b>Table 26.</b> Sibudu. C-A layers from the Deep Sounding: Frequency of profile per blank category.....	79
<b>Table 27.</b> Sibudu. C-A layers from the Deep Sounding: Descriptive statistics of the length of all completely preserved blanks per blank category.....	79
<b>Table 28.</b> Sibudu. C-A layers from the Deep Sounding: Descriptive statistics of the width of all in the width completely preserved blanks per blank category.....	80
<b>Table 29.</b> Sibudu. C-A layers from the Deep Sounding: Descriptive statistics of the thickness of all in the thickness completely preserved blanks per blank category.....	80
<b>Table 30.</b> Sibudu. C-A layers from the Deep Sounding: Descriptive statistics of EL to blank mass-ratio of all completely preserved blanks per blank category.....	80
<b>Table 31.</b> Sibudu. C-A layers from the Deep Sounding: Frequency of distal termination of all completely and distal preserved blanks per blank category.....	81
<b>Table 32.</b> Sibudu. C-A layers from the Deep Sounding: Frequency of cross-section per blank category.....	81
<b>Table 33.</b> Sibudu. C-A layers from the Deep Sounding: Comparison of dorsal convexity between blades with a triangular cross-section and blades with a trapezoidal cross-section ( <i>t</i> -test).....	81
<b>Table 34.</b> Sibudu. C-A layers from the Deep Sounding: Frequency of cortex coverage per blade subgroup.....	86
<b>Table 35.</b> Sibudu. C-A layers from the Deep Sounding: Frequency of platform type per blade subgroup.....	86
<b>Table 36.</b> Sibudu. C-A layers from the Deep Sounding: Frequency of cross-sections of in the width completely preserved blades.....	86
<b>Table 37.</b> Sibudu. C-A layers from the Deep Sounding: Descriptive statistics of the width of all in the width completely preserved blades.....	86
<b>Table 38.</b> Sibudu. C-A layers from the Deep Sounding: Descriptive statistics of the thickness of all in the thickness completely preserved blades.....	87



<b>Table 39.</b> Sibudu. C-A layers from the Deep Sounding: Comparison of elements with and without cortex coverage between blades and elongated flakes (chi-squared test).....	88
<b>Table 40.</b> Sibudu. C-A layers from the Deep Sounding: Comparison of elements with plain & cortical platforms and with dihedral & faceted platforms between blades and elongated flakes (chi-squared test).....	88
<b>Table 41.</b> Sibudu. C-A layers from the Deep Sounding: Comparison of width of all in the width completely preserved blanks between blades and elongated flakes ( <i>t</i> -test).....	89
<b>Table 42.</b> Sibudu. C-A layers from the Deep Sounding: Comparison of thickness of all in the thickness completely preserved blanks between blades and elongated flakes ( <i>t</i> -test).....	89
<b>Table 43.</b> Sibudu. C-A layers from the Deep Sounding: Comparison of completely preserved and fragmented elements between blades and elongated flakes (chi-squared test).....	89
<b>Table 44.</b> Sibudu. C-A layers from the Deep Sounding: Comparison of dorsal convexity between elongated flakes with a triangular cross-section and elongated flakes with a trapezoidal cross-section ( <i>t</i> -test).....	90
<b>Table 45.</b> Sibudu. C-A layers from the Deep Sounding: Frequency of cortex coverage per elongated flake subgroup.....	90
<b>Table 46.</b> Sibudu. C-A layers from the Deep Sounding: Frequency of platform type per elongated flake subgroup.....	90
<b>Table 47.</b> Sibudu. C-A layers from the Deep Sounding: Frequency of cross-sections of in the width completely preserved elongated flakes.....	90
<b>Table 48.</b> Sibudu. C-A layers from the Deep Sounding: Descriptive statistics of the length of all completely preserved elongated flakes.....	91
<b>Table 49.</b> Sibudu. C-A layers from the Deep Sounding: Descriptive statistics of the width of all in the width completely preserved elongated flakes.....	91
<b>Table 50.</b> Sibudu. C-A layers from the Deep Sounding: Descriptive statistics of the thickness of all in the thickness completely preserved elongated flakes.....	91
<b>Table 51.</b> Sibudu. C-A layers from the Deep Sounding: Frequency of cortex coverage per flakes with unidirectional dorsal scars compared to such with an orthogonal scar pattern.....	95
<b>Table 52.</b> Sibudu. C-A layers from the Deep Sounding: Frequency of cross-sections of in the width completely preserved flakes.....	96
<b>Table 53.</b> Sibudu. C-A layers from the Deep Sounding: Frequency of dorsal scar patterns of in the width completely preserved flakes.....	96
<b>Table 54.</b> Sibudu. C-A layers from the Deep Sounding: Descriptive statistics of the length of all completely preserved flakes.....	96
<b>Table 55.</b> Sibudu. C-A layers from the Deep Sounding: Descriptive statistics of the width of all in the width completely preserved flakes.....	97
<b>Table 56.</b> Sibudu. C-A layers from the Deep Sounding: Descriptive statistics of the thickness of all in the thickness completely preserved flakes.....	97

<b>Table 57.</b> Sibudu. C-A layers from the Deep Sounding: Comparison of length of all completely preserved blanks between elongated flakes and triangular flakes ( <i>t</i> -test).....	98
<b>Table 58.</b> Sibudu. C-A layers from the Deep Sounding: Comparison of width of all in the width completely preserved blanks between elongated flakes and triangular flakes ( <i>t</i> -test).....	98
<b>Table 59.</b> Sibudu. C-A layers from the Deep Sounding: Frequency of core type per raw material.....	99
<b>Table 60.</b> Sibudu. C-A layers from the Deep Sounding: Frequency of core types.....	99
<b>Table 61.</b> Sibudu. C-A layers from the Deep Sounding: Frequency of original core blanks per core type.....	101
<b>Table 62.</b> Sibudu. C-A layers from the Deep Sounding: Frequency of cortex coverage per core type.....	101
<b>Table 63.</b> Sibudu. C-A layers from the Deep Sounding: Frequency of cortex positions per core type.....	101
<b>Table 64.</b> Sibudu. C-A layers from the Deep Sounding: Frequency of striking platform types per core type.....	102
<b>Table 65.</b> Sibudu. C-A layers from the Deep Sounding: Frequency of exploitation surface shapes per core type.....	102
<b>Table 66.</b> Sibudu. C-A layers from the Deep Sounding: Frequency of back types per core type.....	103
<b>Table 67.</b> Sibudu. C-A layers from the Deep Sounding: Frequency of base types per core type.....	103
<b>Table 68.</b> Sibudu. C-A layers from the Deep Sounding: Descriptive statistics of the length of all completely preserved cores.....	103
<b>Table 69.</b> Sibudu. C-A layers from the Deep Sounding: Descriptive statistics of the width of all in the width completely preserved cores.....	104
<b>Table 70.</b> Sibudu. C-A layers from the Deep Sounding: Descriptive statistics of the thickness of all in the thickness completely preserved cores.....	104
<b>Table 71.</b> Sibudu. C-A layers from the Deep Sounding: Frequency of last operations per core type.....	105
<b>Table 72.</b> Sibudu. C-A layers from the Deep Sounding: Descriptive statistics of the length to width ratio of all completely preserved cores.....	106
<b>Table 73.</b> Sibudu. C-A layers from the Deep Sounding: Comparison of EPA between blades with a triangular cross-section and blades with a trapezoidal cross-section ( <i>t</i> -test).....	110
<b>Table 74.</b> Sibudu. C-A layers from the Deep Sounding: Comparison of platform depth between blades with a triangular cross-section and blades with a trapezoidal cross-section ( <i>t</i> -test).110	110
<b>Table 75.</b> Sibudu. C-A layers from the Deep Sounding: Frequency of dorsal reduction type of completely and proximal preserved blanks.....	110
<b>Table 76.</b> Sibudu. C-A layers from the Deep Sounding: Frequency of platform morphology of completely and proximal preserved blanks.....	111

<b>Table 77.</b> Sibudu. C-A layers from the Deep Sounding: Frequency of blanks with and without lip among completely and proximal preserved blanks.....	111
<b>Table 78.</b> Sibudu. C-A layers from the Deep Sounding: Frequency of bulb type of completely and proximal preserved blanks.....	111
<b>Table 79.</b> Sibudu. C-A layers from the Deep Sounding: Descriptive statistics of EPA of all completely and proximal preserved blanks per blank category.....	113
<b>Table 80.</b> Sibudu. C-A layers from the Deep Sounding: Descriptive statistics of platform depth of all completely and proximal preserved blanks per blank category.....	113
<b>Table 81.</b> Sibudu. C-A layers from the Deep Sounding: Frequencies of striking platform, base, back and last operation of laminar cores.....	119
<b>Table 82.</b> Sibudu. C-A layers from the Deep Sounding: Typological classification. (* Including TSPs, ACTs, and Tongatis; ** including bifacial points, serrated pieces, and bifacially backed knives; *** including lateral scrapers, end-scrapers, and NBTs).....	125
<b>Table 83.</b> Sibudu. C-A layers from the Deep Sounding: Frequency of tool classes.....	125
<b>Table 84.</b> Sibudu. C-A layers from the Deep Sounding: Frequency of raw material per tool types.....	126
<b>Table 85.</b> Sibudu. C-A layers from the Deep Sounding: Descriptive statistics of length of all completely preserved tools.....	127
<b>Table 86.</b> Sibudu. C-A layers from the Deep Sounding: Descriptive statistics of width of all in the width completely preserved tools.....	127
<b>Table 87.</b> Sibudu. C-A layers from the Deep Sounding: Descriptive statistics of thickness of all in the thickness completely preserved tools.....	127
<b>Table 88.</b> Sibudu. C-A layers from the Deep Sounding: Descriptive statistics of EPA of all completely and proximal preserved tools.....	128
<b>Table 89.</b> Sibudu. C-A layers from the Deep Sounding: Descriptive statistics of platform depth of all completely and proximal preserved tools.....	128
<b>Table 90.</b> Sibudu. C-A layers from the Deep Sounding: Frequency of blank type per tool types.....	128
<b>Table 91.</b> Sibudu. C-A layers from the Deep Sounding: Frequency of cortex percentage per tool types.....	129
<b>Table 92.</b> Sibudu. C-A layers from the Deep Sounding: Frequency of platform type of all completely and proximal preserved tools.....	129
<b>Table 93.</b> Sibudu. C-A layers from the Deep Sounding: Frequency of profile per tool types....	129
<b>Table 94.</b> Sibudu. C-A layers from the Deep Sounding: Frequency of cross-section per tool types.....	130
<b>Table 95.</b> Sibudu. C-A layers from the Deep Sounding: Frequency of fragmentation per tool types.....	130
<b>Table 96.</b> Sibudu. C-A layers from the Deep Sounding: Frequency of raw material per tool classes.....	133

<b>Table 97.</b> Sibudu. C-A layers from the Deep Sounding: Frequency of blank type per tool classes.....	135
<b>Table 98.</b> Sibudu. C-A layers from the Deep Sounding: Descriptive statistics of EPA of all completely and proximal preserved unifacial pointed forms by tool class.....	135
<b>Table 99.</b> Sibudu. C-A layers from the Deep Sounding: Descriptive statistics of platform depth of all completely and proximal preserved unifacial pointed forms by tool class.....	136
<b>Table 100.</b> Sibudu. C-A layers from the Deep Sounding: Frequency of platform type per tool classes.....	136
<b>Table 101.</b> Sibudu. C-A layers from the Deep Sounding: Frequency of fragmentation per tool classes.....	137
<b>Table 102.</b> Sibudu. C-A layers from the Deep Sounding: Descriptive statistics of edge angle of ACTs with unretouched and re-sharpened working edge.....	145
<b>Table 103.</b> Sibudu. C-A layers from the Deep Sounding: Frequency of shaping and retouch flakes by raw material in square C4.....	148
<b>Table 104.</b> Sibudu. C-A layers from the Deep Sounding: Frequency of raw material in shaping flakes and in bifacial pieces in square C4.....	148
<b>Table 105.</b> Sibudu. C-A layers from the Deep Sounding: Frequency of cross-section per bifacial tool class (drawings from Boëda and Richter, 1995: 77).....	154
<b>Table 106.</b> Sibudu. C-A layers from the Deep Sounding: Frequency of raw material per phase of manufacture of bifacial points (following Villa, et al., 2009).....	158
<b>Table 107.</b> Sibudu. C-A layers from the Deep Sounding: Descriptive statistics of TCSA in mm <sup>2</sup> .....	163
<b>Table 108.</b> Sibudu. C-A layers from the Deep Sounding: Descriptive statistics of length, width and thickness of the serrated pieces.....	165
<b>Table 109.</b> Sibudu. C-A layers from the Deep Sounding: Descriptive statistics of TPA of all measurable serrated pieces measured with the goniometer and calculated with the formula: $\arctan(\text{width}/10 \text{ mm (known distance from tip)})/\text{Pi} \cdot 180$ .....	167
<b>Table 110.</b> Sibudu. C-A layers from the Deep Sounding: Descriptive statistics of length, width and thickness of the lateral scrapers.....	173
<b>Table 111.</b> Sibudu. C-A layers from the Deep Sounding: Descriptive statistics of length, width and thickness of the NBTs.....	176
<b>Table 112.</b> Sibudu. C-A layers from the Deep Sounding: Frequency of edge damage on all blanks by raw material.....	178
<b>Table 113.</b> Sibudu. C-A layers from the Deep Sounding: Frequency of thermal alteration by raw material.....	179
<b>Table 114.</b> Sibudu. C-A layers from the Deep Sounding: Frequency of heavy sintering by raw material.....	180

**Table 115.** Sibudu. C-A layers from the Deep Sounding: Comparison of finished bifacial points & points from other phases of manufacture between quartz and dolerite (chi-squared test).....196

**Table 116.** Sibudu. C-A layers from the Deep Sounding: Descriptive statistics of width of all in the width completely preserved serrated pieces made on quartz compared to the other raw materials.....198

**Table 117.** Sibudu. C-A layers from the Deep Sounding: Descriptive statistics of thickness of all in the thickness completely preserved serrated pieces made on quartz compared to the other raw materials.....198

**Table 118.** Sibudu. C-A layers from the Deep Sounding: Descriptive statistics of thickness of all in the thickness completely preserved bifacial points of phase 3 and finished serrated pieces made on quartz.....199

**Table 119.** Comparison of the laminar reduction strategy of the C-A layers to other laminar reduction systems in southern Africa (+ = <10%; ++ = >10% and <50%; +++ = >50%) (scheme of pyramidal or flat core modified after Wurz, 2002; scheme of unidirectional recurrent Levallois core modified after Boëda, 1994) (modified after Schmid, et al., 2019).....221

## Acknowledgements

My PhD was a wonderful journey, as I experienced and learned so much. Moreover, I got to visit some of the most beautiful sites there are. On top of it all and most importantly, I collected so many incredible memories with amazing people. I could not imagine a better place to write about and acknowledge all these great personalities, without whom this dissertation could have never been completed, than being back to South Africa for excavations right now.

First, I want to thank my supervisors Nicholas J. Conard and Eric Boëda. Nicholas gave me the unique opportunity to work on material from one of the key sites in southern Africa, Sibudu, and trusted in my scientific capabilities and developments. Eric let me be part of his *équipe* in Paris and provided me with valuable insights about lithic technology in theoretical as well as practical aspects.

Thanks to Michael Bolus and Sylvain Soriano for fruitful discussions and help in bureaucratic matters. I will never forget the proud moment, when I had a meeting with Sylvain and I showed him my diacritic schemes and explained (in my bumpy French) to him the technological details of the laminar reduction strategy of Sibudu, and he commented: “You understood technology now!”.

I express my gratitude to Pierre-Jean Texier, who kindly provided me with information about the site of Dale Rose Parlour and to Michel Grenet, who gave me permission to use his drawings of the bifacial points from Dale Rose Parlour.

I thank the colleagues from the KwaZulu-Natal Museum in Pietermaritzburg, Carolyn Thorp, who kindly provided me with lab space, Gavin Whitelaw, from whom I learned a lot about South African history, Ghilraen Laue, who after the ASAPA conference in Pretoria 2017 told me that she never thought that she could enjoy a talk about lithics, Mudzunga Munzhedzi and Dimakatso Tlhoale, who always helped concerning logistics.

I would also like to express my deepest gratitude to the members of the Sibudu research team. From 2013 until 2017, this excavation meant so much to me from a scientific, but also a personal point of view. I have to thank some people in particular: First and foremost Mohsen Zeidi, who excavated my entire sample and with whom I really enjoyed working in the field together. Furthermore, I thank Gregor D. Bader, with whom I spent probably the most time in South Africa together and, though our personalities are an explosive combination, I really had some amazing and memorable moments, especially celebrations that I would not want to miss for the world. I am so grateful to Heike Würschem, who helped so much with the illustrations and never complained about my sometimes annoying requests! Heike belongs to the by me named *Heinzelmännchen*, including also Svenja Arlt, Ria Litzenberg and Annika Rebentisch. I can honestly say that the name should express my deep appreciation for these great women, who, and of that I am sure of, will make great archaeologists! Furthermore, I want to thank Manuel Will for also being a good teaching team, Chantal Tribolo for providing me with preliminary information about the luminescence dates, Britt M. ‘Bananas’ Starkovich, Feng Li,

Christopher E. Miller (still sorry for the credit card) and Susan M. Mentzer (we will always share our Lady Gaga-moment), Jonathan Baines, Elena Robakiewicz (my buddy), Lennard Schnoor and Sabrina Stempfle. I would like to thank Janet, the good soul of our excavation house in Ballito, who tried so hard to teach me some Zulu. I thank the caretaker of Sibudu, Miriam Dasa, and her husband John as well as her family for taking such good care of the site. Finally, I thank the knappers of the iLembian for producing such amazing technological innovations that I could study.

I am also grateful to the former excavator of Sibudu, Lyn Wadley. Unfortunately, I did not have the chance to spend a lot of time with her, but in the few occasions, this fascinating South African researcher was always very interested and supportive.

As if this was not enough, I am so privileged to be also part of the excavation team of Bushman Rock Shelter and Heuningneskrans. My thanks go firstly to Aurore Val, one of the directors, who now also happens to be my dearest flat mate in Tübingen and without whom I could not imagine a life, especially a party life, in the city, where everything is possible, anymore. I thank Katja Douze (*la meilleure Douze du monde*), with whom I had the most awesome visit to the Victoria Falls. Furthermore, I would like to thank Paloma de la Peña (*meiner kleinen Zuckerschnecke*), May L. Murungi, Léa Feyfant (la Chefe) and Sofia Solana, who let me be part of the greatest day in their lives together, Chrissie Sievers, Christine Verna, Elysandre Puech, Magnus M. Haaland, Liliane Meignen (Sensei), next to whom I had the honour to excavate and who always had an advice for every life situation, the Zimbabwean corner, who includes first and foremost Joseph Matembo, Precious Chiwara and Miniyenkosi 'Minnie' Majoli, and Camille Bourdier for being there with a cup of coffee in the really last moments of the writing. I want to thank the sorting ladies, Emily, Lebo, Immaculate and Bridget, as they accepted me as their *Mkhozi* and provided me with an original African dress that I finally got to wear at my defence.

I am grateful to Veerle Rots and the TraceoLab team, including my dearest best friend from Finland Noora Taipale, furthermore Carol Lentfer, Christian Lepers, Dries Cnuts, Sonja Tommasso, Justin Coppe and Antonin Tomasso.

I want to highlight, how thankful I am to my colleagues and friends from the lab in Paris Nanterre. I do not know what I would have done without the help and effort of Amélie da Costa, *ma héroïne*. Same is true for *mon poulet* Iris Guillmard, with whom my stays in Paris were always awesome. Furthermore, I want to thank Mana Jami Alahmadi, Giulia Ricci (*Capretta*), Roxane Rocca, Daniele Aureli, Marine Massoulié, Lucie Germond, Amir Beshkani and Louis De Weyer (King of the world).

I would like to thank my department in Tübingen, as my colleagues are really great fun – just thinking of our last Karneval – and never let me down, when I needed a coffee or Schnaps. Thus, thanks to Claudio Tennie (chain operator), Yvonne 'Yvi' Tafelmaier, Recha S. 'Rechali' Seitz, Berrin Çep, Elizabeth 'Bethany' Velliky, Ewa Dutkiewicz, Patrick Schmidt (*le docteur*),

Sibylle as well as Sebbi Wolf, Andreas Taller, Guido Bataille, Keiko Kitagawa, Jens Frick, Armando Falcucci, Alexander 'AJ' Janas und Mima F. Batalovic.

I am so glad to have such great friends that enrich my life and made to whole journey worth it. First and foremost, my deepest appreciation for their support and knightliness, especially in the last, most difficult phase of my PhD, goes to my very dear friends, the king of all parties Domenico Giusti and Elisa Bandini. Thank you so much ragazzi! You made it all count in the end! I am so grateful to have Regine E. Stolarczyk (*meine Konstante*), in my life, who with her great personality always found the right words to push me! Stefanie B. Stelzer and I have been through so much together and we always were sure: "*Am Ende wird alles gut!*". Here we are. Thanks so much for never giving up on me! I would like to thank Mareike C. Stahlschmidt, my first flat mate and my dear conference buddy, for believing in me! I hope that we will make our dream come true and one day work side by side on our very own research project and site. Thank you, Dominik Koscielny und Birgit Brandeysky, who made me the proud godmother of their two wonderful daughters Sophie and Marlena, for their warm and loving support! Moreover, I want to thank Anna S. Sonnberger, Andrea 'Platzhirsch' Stadlmayr, Philip R. Nigst, Marjolein D. Bosch, Katja Seidl, Andrea Orendi, my dear lady Sara Rhodes, Tommaso Mori, Lumila 'Lumi' Menéndez, Judith Beier, Hannes Rathmann, Sarah Goll, Madita Kairies, Matthias B. Göden (Herr Göden), Darya 'Dashenka' Anatolyevna Presnyakova and Will Archer, André 'Andrito' Strauß, Gerlinde D. Bigga and Ilona Gold for their friendship and the good memories we are sharing.

I am very grateful to David Witelson and, in particular, Emily Hallinan, for the English editing and constructive feedback. My further thanks go to Nicole LoBianco, who knows me since high school and takes me as I am with all my flaws, for managing the layout.

Concerning the financial support, I luckily earned a Doctoral Dissertation Grant in the research project "The Evolution of Cultural Modernity" under the state of Baden-Württemberg law for the promotion of graduates (LGFG). My research in South Africa was made possible by the Heidelberger Akademie der Wissenschaften (ROCEEH) and the Deutsche Forschungsgemeinschaft (DFG), who funded most of the excavations and analytical studies in South Africa. Travel grants from Universitätsbund Tübingen e. V. and Deutscher Akademischer Austausch Dienst (DAAD) helped me to present the results of my research to the scientific community at international congresses.

I am so grateful to my family, as all of them, in their own, very different and very particular styles, always had my back and supported me. I especially would like to thank my parents for giving me the opportunity and, above all, the freedom to take this path without any ifs or buts. I furthermore want to thank you for being there for me despite all my peculiarities with your kindness as well as your calming nature and for pushing me to finally accomplish this mission so that we can start a new chapter of our lives together.

Last, but not least, actually the opposite, I want to thank Guillaume Porraz (meinem lieben Dr. Porraz), whom I met in 2009 and who since then, if from close or far, was always there for me,



for his eternal trust, for his everlasting encouragement and for always making me keep the force! I probably would not be the person I am today, if it was not for him! *Au bonheur de la chance!*

# 1. Introduction and foundations of the study

„Giving substance to shadows.“

— Sixto Díaz Rodríguez

Song 'Crucify Your Mind'  
Album 'Cold Fact'  
1970

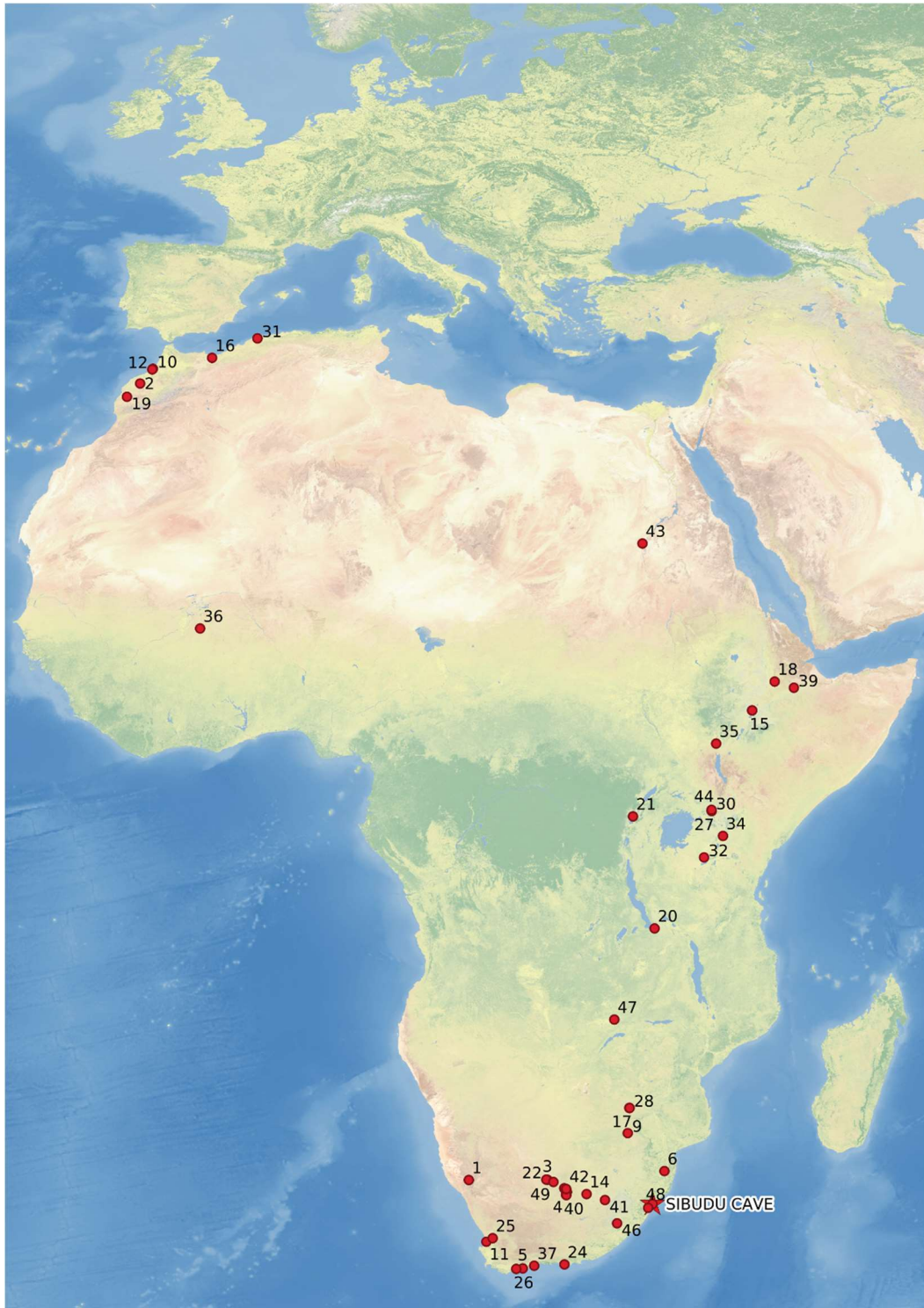
## 1.1. The MSA in Africa

*In this chapter, I will provide an overview of the African Middle Stone Age (MSA). I start with a summary on the research history and definition of the term. I then discuss the fossil record and the genetic evidence in the MSA highlighting the complex scenario of the emergence of Homo sapiens. Finally, I focus on the material culture; I introduce the innovations in lithic technology first and then elaborate on other cultural material objects indicating the appearance of new behaviours linked to the MSA. Figure 1 shows all of the sites mentioned in the text.*

### 1.1.1. Research history

The MSA represents a key period in the biological and cultural evolution of modern humans in Africa. While a clear-cut chronological or technological break that announces the advent of the MSA is difficult to identify, many researchers have reached **the consensus that the MSA began roughly 300 ka ago** (Deacon and Deacon, 1999; McBrearty and Brooks, 2000; Klein, 2009; Herries, 2011; Conard, 2012; Wadley, 2015; Wurz, 2016; Scerri, 2017). In East Africa long sequences (e.g. Wendorf and Schild, 1974; McBrearty, 2005; Brooks, et al., 2018) point to a transition from the Earlier Stone Age (ESA) to the MSA between 300 ka and 250 ka (McBrearty and Brooks, 2000; McBrearty and Tryon, 2005; Tryon, et al., 2005; Herries, 2011), but little data on the onset of the MSA is available from southern Africa (Herries, 2011; Lombard, et al., 2012; Wurz, 2014; Wadley, 2015). The emergence of and/or, depending on the region, the shift to predominantly microlithic technology signals the end of the MSA between approximately 40 and 20 ka (Deacon and Deacon, 1999; Lombard, et al., 2012; Mackay, et al., 2014; Wadley, 2015). At some sites, such as Strathalan Cave B, Eastern Cape, diagnostic MSA artefacts persist until around 24 ka (Opperman, 1996), whereas Border Cave (BC), KwaZulu-Natal, has yielded assemblages dated to approximately 40 ka bearing Later Stone Age (LSA) technologies (Beaumont, 1978; d'Errico, et al., 2012a; Villa, et al., 2012). As with the ESA to MSA transition, a neat delimitation of the subsequent LSA is hampered by the lack of high resolution regional data and a valid definition of the LSA (Mitchell, 2008; Ossendorf, 2013).

**The term MSA was originally defined in the pioneering monograph 'The Stone Age cultures of South Africa'** by Astley John Hillary Goodwin and Clarence ('Peter') van Riet Lowe (1929) based on their research in South Africa. Goodwin, born in 1900 in Pietermaritzburg, was the first South African trained in archaeology graduating with an honours degree at Cambridge University in 1922. After his return to South Africa in 1923, he was based at the University of Cape Town and



**Figure 1.** Map of Africa with sites mentioned in the Text: 1 - Apollo 11 Rock Shelter; 2 - Benzú Rock Shelter; 3 - Bestwood 1; 4 - Biesiesput 1; 5 - Blombos Cave; 6 - Border Cave; 7 - Canteen Kopje; 8 - Cap Chatelier; 9 - Cave of Hearths; 10 - Dar es-Soltan 1 Cave; 11 - Diepkloof Rock Shelter; 12 - El Mnasra Cave; 13 - Factory Site; 14 - Florisbad; 15 - Gademotta; 16 - Grotte des Pigeons; 17 - Hackthorne; 18 - Herto; 19 - Jebel Irhoud; 20 - Kalambo Falls; 21 - Katanda; 22 - Kathu Pan; 23 - Keratic Koppie; 24 - Klasies River main site; 25 - Klein Kliphuis Rock Shelter; 26 - Klipdrift Shelter; 27 - Koimilot; 28 - Kudu Koppie; 29 - Kulkuletti; 30 - Leakey Handaxe Area; 31 - Littorines Cave; 32 - Ngaloba; 33 - Nooitgedacht 2; 34 - Olorgesailie; 35 - Omo Kibish; 36 - Ounjougou; 37 - Pinnacle Point Cave 13B; 38 - Pniel 1 & 6; 39 - Porc Epic Cave; 40 - Rooidam 1 & 2; 41 - Rose Cottage Cave; 42 - Roseberry Plain 1; 43 - Sai Island 8-B-11; 44 - Sibilo School Road Site; 45 - Sibudu Cave; 46 - Strathalan Cave B; 47 - Twin Rivers; 48 - Umhlatuzana Rock Shelter; 49 - Wonderwerk Cave.

the South African Museum in Cape Town (Deacon, 1990; Schlanger, 2003; Underhill, 2011a; Conard, 2012). Van Riet Lowe, born in 1894 in Aliwal North, found several archaeological sites in the Free State province by training as a civil engineer based in Bloemfontein. He was appointed as Director of the Bureau of Archaeology in 1934 (Conard, 2012; Schlanger, 2003; Deacon, 1990; Malan, 1962). The two authors aimed to create a new indigenous taxonomic system for African prehistory that was clearly independent of European terminology (Goodwin, 1958; Deacon, 1990; Schlanger, 2003; Underhill, 2011a; Conard, 2012). Goodwin (Goodwin, 1928, 1958) had in fact already introduced the MSA with a first basic description in 1928, but the publication of Goodwin and van Riet Lowe (1929) fully clarified the tripartite division of the African Stone Age into ESA, MSA and LSA (Deacon, 1990; Schlanger, 2003; Underhill, 2011a; Conard, 2012). Despite subsequent re-assessments and modifications, the classificatory scheme describing the major technological Stone Age periods in sub-Saharan Africa and their geographical distribution has maintained its overall validity (e.g. Clark, 1959; Clark, et al., 1966; Sampson, 1974; Singer and Wymer, 1982; Deacon, 1990; Underhill, 2011a; Lombard, et al., 2012). In 1965, the Burg-Wartenstein Symposium, an inter-congress meeting between the 5<sup>th</sup> and the 6<sup>th</sup> Pan-African Congress, was held in Austria. The outcome of this meeting recommended the abandonment of the chronological scheme in Africa mainly due to an absence of supporting field evidence (Clark, et al., 1966; Bishop and Clark, 1967); however, this was not completely implemented and only the 'First and Second Intermediate' periods identified between the ESA/MSA and MSA/LSA were abandoned (McBrearty, 1988). Today, prehistorians are still confronted with problems related to the chrono-cultural sequence owing to a scarcity of well-dated and well-documented type assemblages during certain time periods (Underhill, 2011a). Until recently, the terms ESA, LSA and, in particular, the MSA have been almost exclusively used in sub-Saharan Africa and the Eurasian terminology, namely Lower, Middle and Upper Palaeolithic, was applied in North and West Africa due to historical reasons (McBrearty and Brooks, 2000; Conard, 2012; Dibble, et al., 2013). However, lately researchers are increasingly using the terminological system of ESA, MSA and LSA across the whole of Africa (see e.g. Conard, 2012; Dibble, et al., 2013; Tribolo, et al., 2015). Stimuli for having a uniform terminology for the major classification of the African Stone Age are the similarities between assemblages across Africa and the developments and events in the pan-African archaeological and fossil record distinctive from that in Eurasia from MIS 5 onwards.

#### 1.1.2. Human remains and genetic data

The fossil record for the beginnings of *Homo sapiens* reveals variations that, as for the archaeological record, present a complex emergence. The fossil evidence indicates an African origin of *Homo sapiens* that has recently been shown to coincide with the MSA (Wurz, 2014; Wadley, 2015; Stringer, 2016; Hublin, et al., 2017; Scerri, et al., 2018). While the accumulating fossil record endorses Africa as the cradle of anatomically modern humans (AMH), the extreme 'Out-of-Africa' model which posits a complete replacement of archaic hominin populations by AMH (for definition see Bräuer, 1984, 1992; Stringer and Andrews, 1988; Stringer, 1992) is not supported. **The diversity of the morphological features by early representatives of our species, together with the genetic data,** rejects a human ancestry deriving from a single African

region and rather **suggest a 'African multi-regionalism' scenario with subdivided populations connected by sporadic gene flow**, maybe also interbreeding with other contemporaneous hominin species (Lahr and Foley, 1998; Gunz, et al., 2009; Stringer, 2016; Scerri, et al., 2018). The oldest currently identified members of the *Homo sapiens* clade come from Jebel Irhoud, Morocco, dated by thermoluminescence to  $315 \pm 34$  ka (Richter, et al., 2017). These biologically modern humans are associated with one of the oldest MSA assemblages (Hublin, et al., 2017). The facial morphology and endocranial volumes fall within the range of extant modern humans, while the braincase shapes are elongated rather than globular suggesting that this diagnostic feature evolved over time within the *Homo sapiens* lineage (Gunz, et al., 2009; Hublin, et al., 2017). The rich East African fossil record has provided important data for the origins of *Homo sapiens* as well. The human material from Omo Kibish, Ethiopia, includes *inter alia* the partial skeleton Omo 1 and the calvaria Omo 2 (Day, 1969; Stringer, 2016). These two individuals have an age of ca. 195 ka (McDougall, et al., 2005; Aubert, et al., 2012; Brown, et al., 2012). While the preserved elements of Omo 1 can be attributed to early *Homo sapiens*, Omo 2 can only tentatively be ascribed to this clade (Stringer, 2016). Several cranial and dental human fossils, including an almost complete adult skull, an immature calvaria and parts of another probably adult cranial vault, were recovered from the site of Herto, Ethiopia, and date to between 167 and 154 ka (Clark, et al., 2003; White, et al., 2003). The Herto specimens show features that fall outside the variation of recent modern humans, which has led some researchers to classify them as the subspecies *Homo sapiens idaltu* (White, et al., 2003). However, cranial metrical studies and the relatively globular shape of the braincase support their assignment to early *Homo sapiens* (Lubsen and Corruccini, 2011; McCarthy and Lucas, 2014; Stringer, 2016; Scerri, et al., 2018). The Ngaloba Laetoli Hominid 18, Tanzania, represents a partial cranium dating to the late Middle or early Late Pleistocene and was discovered alongside MSA lithic artefacts (Day, et al., 1980; Magori and Day, 1983; Grove, et al., 2015). The specimen belongs to the *Homo sapiens* clade, but shows both archaic traits (the retention of particular traits typically associated with archaic hominins (for definition see Scerri, et al., 2018), and modern features (Stringer, 2016). South Africa has also yielded early *Homo sapiens* fossils. A partial cranium was found at Florisbad, Free State, dated by ESR to  $259 \pm 35$  ka and associated with MSA artefacts (Dreyer, 1935; Grün, et al., 1996; Kuman, et al., 1999; Dusseldorp, et al., 2013; Lombard, et al., 2013). Due to the combination of modern and archaic morphological characteristics, some researchers have proposed ascribing this specimen to a more primitive species, *Homo helmei* (Stringer, 1996). Bed 3 of Cave of Hearths (CH), Limpopo, yielded a mandible and a radius of early *Homo sapiens*, formerly described as *Homo rhodesiensis* with an age estimate of around 500–200 ka (Tobias, 1971; Dusseldorp, et al., 2013; Lombard, et al., 2013; Wadley, 2015). The fossil material from Klasies River main site (KRM), Eastern Cape, comprises more than 50 human remains, including cranial and post-cranial elements (Singer and Wymer, 1982; Rightmire and Deacon, 1991; Grine, et al., 1998, 2017; Deacon, 2008; Grine, 2012). Some of the fossils originate from the 'MSA I' (or 'Klasies River') layers dating to approximately 110 ka, and a large number comes from the 'MSA II' (or 'Mossel Bay') layers with age estimates between 100 and 80 ka (for a summary of the dates see Grine, et al., 2017). The human remains display primarily

AMH morphological traits, but some specimens retain archaic characteristics (Dusseldorp, et al., 2013; Wurz, 2016; Grine, et al., 2017).

Since the 1980s, several independent genetic studies examining patterns of genetic variation from living people and using ancient DNA (aDNA) preserved in human fossils have shown that **Africa is the original homeland of *Homo sapiens*** (e.g. Cann, et al., 1987; Vigilant, et al., 1991; Templeton, et al., 1992; Ingman, et al., 2000). With regard to the temporal depth of present-day diversity between and within African populations, most studies have used demographic models and model assumptions simplifying population structure and favouring a single origin model of modern humans (Scerri, et al., 2018). The results of these analyses demonstrate a variety of split-time estimates at 300 to 150 ka and identify the deepest genetic divergence to be associated with Khoe-San groups, (i.e. 'non-Bantu' indigenous people) from southern Africa (Tishkoff, et al., 2009; Veeramah, et al., 2011; Lachance, et al., 2012; Scally and Durbin, 2012; Schlebusch, et al., 2012, 2013; Mallick, et al., 2016). Schlebusch et al. (2017) recently published a new genetic study from southern Africa using both traditional and novel approaches. This study points towards a divergence time of the first modern humans between 350 and 260 ka ago, located in various regions including southern Africa, concurring closely with the anatomical developments of early *Homo sapiens* and the onset of the MSA. However, other models incorporating more complex population structures (e.g. Skoglund, et al., 2017) are needed to allow a more generalised and flexible view of past demographic trends. The increased availability of genomic data from contemporary and ancient humans and the constant progress of analytical methodologies pave the way to more complex and realistic models (Chimusa, et al., 2018; Scerri, et al., 2018).

### 1.1.3. Novelties in lithic technology

**The material culture of the African MSA heralds a period of unique technological and behavioural innovations and accomplishments happening at diverse *tempi* in different regions. The major technological changes in the MSA are characterised by the disappearance of large cutting tools (LCTs), i.e. blanks shaped into large tools for cutting functions such as handaxes and cleavers, the development of prepared core technologies that guarantee the production of pre-determined blanks such as flakes, blades and triangular flakes (points), and the manufacture of new tool types more suitable for hafting** (Goodwin and van Riet Lowe, 1929; Clark, 1988; McBrearty and Brooks, 2000; Wurz, 2014; Wadley, 2015; Scerri, et al., 2018). The appearance of the MSA can thus be considered as a shift in the ways that people were producing and using their tools, and consequently in the ways that they were organising their subsistence (Schmid, et al., 2016). Several researchers associate the dawn of the MSA with a diversification in lithic technology that is related to cultural regionalisation of past populations resulting in different spatial trajectories of change (Goodwin and van Riet Lowe, 1929; Clark, 1988; McBrearty and Brooks, 2000; Tryon, et al., 2005; McBrearty and Tryon, 2006; Wurz, 2012; Douze and Delagnes, 2016).

The East and southern African archaeological records indicate that the transition from the ESA to the MSA was an asynchronous adaptive process rather than an abrupt event (Tryon, et al., 2005; McBrearty and Tryon, 2006; Tryon and Faith, 2013; Wadley, 2015). East African Late

Acheulean sites, such as the Leakey Handaxe Area and the Factory Site (Kaphthurin Formation, Kenya), both dated to between approximately 509 and 284 ka, demonstrate that the Levallois concept – the most distinctive prepared core technology – has an Acheulean origin and occurs alongside handaxe and cleaver production (Tryon, et al., 2005; McBrearty and Tryon, 2006; Tryon and Faith, 2013). The oldest MSA occupations that lack LCTs, include prepared core technologies and production of triangular flakes, and show long-distance raw material transport ( $\geq 25$  km – 50 km) are documented at Localities B and G from Olorgesailie, Kenya, dated to ca. 320 to  $\geq 295$  ka (Brooks, et al., 2018; Deino, et al., 2018). Loci 1 and 2 from Koimilot (Kaphthurin Formation, Kenya), dating to 250-200 ka, also demonstrate an absence of LCTs and the early employment of prepared core technologies to produce pre-determined blanks (McBrearty and Tryon, 2006; Tryon, 2006). Sibilo School Road Site (GnJh-79), Kenya, with a minimum age of 200 ka, includes Levallois points and reduction methods as well as early evidence of long-distance obsidian import from up to 166 km away (Blegen, 2017). Further early MSA sites from the East African record are ETH-72-8B (Gademotta area, Ethiopia), dated to between 281 ka and 269 ka (Morgan and Renne, 2008; Sahle, et al., 2014), and ETH-72-1 (Kulkuletti area, Ethiopia), dated to between  $280 \pm 8$  ka and  $183 \pm 10$  ka (Morgan and Renne, 2008). These sites demonstrate a strong focus on the manufacture of convergent tools (Wendorf and Schild, 1974; Wendorf, et al., 1994; Douze, 2012; Douze and Delagnes, 2016). In the Acheulean at Canteen Kopje, South Africa, early ‘Victoria West’ prepared core technology appears between 1.1 Ma and 800 ka (McNabb and Beaumont, 2012; Li, et al., 2017). The Victoria West cores produce large pre-determined flakes which are subsequently shaped into LCTs. At the site of Kudu Koppie, South Africa, both late ESA and MSA occupations show the application of Levallois methods (Wilkins, et al., 2010). The earliest MSA assemblages of southern Africa (for summary see Schmid, et al., 2016) come from Stratum 3 at Kathu Pan 1, South Africa, dated to  $291 \pm 45$  ka (Porat, et al., 2010; Wilkins, 2013) and the basal deposits P, O and N of Florisbad, associated with the hominid cranium mentioned above (Kuman, et al., 1989, 1999).

The emergence of MSA traditions in North Africa has broadly similar timing to East and sub-Saharan African MSA lithic assemblages, all containing retouched points and using the Levallois concept (Scerri, 2017). A long sequence from Casablanca in Morocco comprises late Acheulean occupations, such as Littorines Cave and Cap Chatelier at Sidi Abderrahmane, dating to the late Middle Pleistocene. These sites provide assemblages with Levallois reduction methods alongside handaxes and cleavers, again pointing to the development of prepared core technologies in the late Acheulean (Biberson, 1956; Debenath, et al., 1984; Raynal, et al., 2001, 2009). The earliest MSA assemblages in North Africa are known from Jebel Irhoud at  $315 \pm 34$  ka BP (Richter, et al., 2017) and Benzú Rock Shelter at ca. 250 ka (Ramos, et al., 2008). The West African MSA has yielded younger dates for the onset of the MSA; however, it must be acknowledged that research in this region is hindered by political conditions and the lack of well-dated long chronostratigraphic sequences (Chevrier, et al., 2018). The site of Ounjougou, Mali, yielded MSA layers tentatively dated to 160-150 ka representing the oldest known evidence of Levallois technology in this region (Rasse, et al., 2004; Soriano, et al., 2010; Chevrier, et al., 2018).

The study of the transition from the ESA to the MSA has a long history and is historically associated with three entities: the Fauresmith, Sangoan and Lupemban (e.g. Goodwin and van Riet Lowe, 1929; Clark, 1959, 1970; Sampson, 1974; Barham and Mitchell, 2008; Underhill, 2011b). All three phases are in need of more well-dated undisturbed sites with clear and detailed descriptions.

The Fauresmith occurs in the interior of southern Africa (Goodwin and van Riet Lowe, 1929; Underhill, 2011b; Lombard, et al., 2012; Chazan, 2015) and available chronometric dates strongly suggest a Middle Pleistocene age between approximately 550 and 300 ka BP (Porat, et al., 2010; Wilkins and Chazan, 2012; Chazan, 2015; but see Herries, 2011). Several sites exist in the Northern Cape of South Africa, such as Kathu Pan 1 (KP1) (Wilkins and Chazan, 2012; Wilkins, 2013), Excavation 6 at Wonderwerk Cave (Chazan and Horwitz, 2009, 2015; Chazan, 2015), Bestwood 1 (Chazan, et al., 2012; Chazan, 2015), Canteen Kopje (Beaumont and McNabb, 2000; McNabb and Beaumont, 2011; Shadrach, 2018), Pniel 1 and 6 (Beaumont, 1990a, 1990b; Ecker and Morris, 2017), Rooidam 1 and 2 (Beaumont, 1990c), Biesiesput 1 (Beaumont, 1990c), Nooitegedacht 2 (Beaumont, 1990d) and Roseberry Plain 1 (Beaumont, 1990d). Chazan (2015) proposed that diagnostic features of the Fauresmith are the production of blades from prepared cores and typical tools are small ovate bifacial tools and bifaces.

The Sangoan entity is named after surface collections discovered in the surroundings of Sango Bay, Uganda (Wayland and Smith, 1923). The Sangoan is mainly a central African phenomenon (McBrearty, 1988; Clark, 1970, 1982), but its geographic distribution extends to southern Africa, including sites from the Mapungubwe National Park (Keratic Koppie, Hackthorne, and Kudu Koppie), South Africa (Kuman, et al., 2005), as well as to northern Africa at site 8-B-11, Sai Island, Sudan (Van Peer, et al., 2003, 2004; Rots and Van Peer, 2006). The maximum age estimates for this technocomplex come from the Sangoan deposits at site 8-B-11, Sai Island, which have an OSL age range between 242-204 ka (Van Peer, et al., 2003). The typical features of Sangoan lithic assemblages are heavy-duty tools, such as bifacially shaped picks and core-axes, denticulates, and denticulated scrapers, together with Levallois blanks and cores (Clark, 1982; McBrearty, 1988).

The Lupemban was named after lithic assemblages exposed by mining activities along the Lupemba stream, Democratic Republic of the Congo, by (Breuil, 1944). The majority of sites assigned to the Lupemban is located in Central Africa, clustering in the Congo Basin and neighbouring areas (Clark, 1982, 1988; Barham, 2000; Taylor, 2016), but the technocomplex is documented as far south as Peperkorrel in Namibia (MacCalman and Viereck, 1967) and as far north as 8-B-11, Sai Island (Van Peer, et al., 2003, 2004). Lupemban assemblages are characterised by distinctive elongated bifacial (lanceolate) points, as well as core-axes and picks, prepared core technology, blades and backed blades (Clark, 2001; Clark and Brown, 2001; Barham, 2002; Taylor, 2016). At stratified sites where both Lupemban and Sangoan entities are present, the Lupemban layers always occur above the Sangoan, as at Sai Island, Twin Rivers and Kalambo Falls (Zambia) (Barham, 2000, 2012; Clark, 2001; Clark and Brown, 2001; Van Peer, et al., 2003, 2004; Barham, et al., 2015; Duller, et al., 2015). These three sites have also yielded



dates for the Lupemban. U-series dates from the collapsed cave site Twin Rivers and luminescence dates from Kalambo Falls indicate a solid pre-200 ka age (Barham, 2000, 2012; Barham, et al., 2015; Duller, et al., 2015; Taylor, 2016), while the OSL dates from Sai Island range between  $182 \pm 20$  ka and  $152 \pm 10$  ka (Van Peer, et al., 2004).

#### 1.1.4. Non-lithic evidence for cognitive complexity

**In addition to advances in lithic technology, a variety of other material cultural items make an appearance as novelties in the MSA, signalling the emergence of more complex social behaviours, such as technological diversification, new hunting practices, personal adornment, symbolism, hafting and manufacture of composite tools** (McBrearty and Brooks, 2000; Conard, 2004; Henshilwood and Lombard, 2014; Wurz, 2014; Wadley, 2015).

An array of MSA **bone tools** attests to a diversity of organic technologies, challenging the notion that bone working, such as grinding, polishing, knapping, and retouching of bones, is a hallmark of the European Upper Palaeolithic and African LSA (McBrearty and Brooks, 2000; Conard, 2004; Henshilwood and Lombard, 2014). Bone tools, including knives and a spear point, come from deposits at El Mnasra Cave, Morocco, dated by OSL to ca. 111 ka and 106 ka and by ESR-U/Th to approximately 89-67 ka (El Hajraoui, 1994; El Hajraoui and Debenath, 2012; Jacobs, et al., 2012; Backwell and d'Errico, 2016; Campmas, et al., 2016). Another bone knife was found at Dar es-Soltan 1 Cave, Morocco, from a layer with an age of ca. 90 ka (Bouzouggar, et al., 2018). Three MSA occurrences, Kt-2, Kt-9 and Kt-16 at Katanda, Democratic Republic of the Congo, have yielded finely manufactured barbed and unbarbed bone harpoons discovered within secure stratigraphic context dated to ca. 90 ka (Brooks, et al., 1995; Yellen, et al., 1995; Yellen, 1998; McBrearty and Brooks, 2000). The M1 and M2 Upper layers at Blombos Cave (BBC), Western Cape Province, South Africa, dated to ca. 77-72 ka, include bone points, awls and engraved bone (Henshilwood, et al., 2001a, 2001b; d'Errico and Henshilwood, 2007; Henshilwood and Lombard, 2014). The awls were produced on long bone diaphysis fragments by scraping and were used to pierce materials, while the points were finished by polishing and probably represent hafted spear points (Henshilwood, et al., 2001a; d'Errico and Henshilwood, 2007). Sibudu Cave also contains a bone assemblage including bone points, wedges, awls, pins, scaled pieces (*pièces esquillées*), smoothers, compressors and percussors, and notched pieces (d'Errico, et al., 2012b; Rots, et al., 2017). Several of the bone points are associated with layers dating to approximately 62-56 ka (d'Errico, et al., 2012b; Jacobs and Roberts, 2017). One of these points from layer GR at Sibudu shows features suggestive of use as arrowhead. This finding suggests that organic projectile weaponry, including bow-and-arrow technology, was a part of the hunting toolkit of MSA people (Wadley, 2006; Backwell, et al., 2008, 2018a). Three undoubted bone objects are known from KRM (Singer and Wymer, 1982; Wurz, 2000; d'Errico and Henshilwood, 2007). Two of these are notched bone elements dated to ca. 100-80 ka. They were most likely used on soft materials. The third piece, originating from the Howiesons Poort (HP) deposits, shows engravings (d'Errico and Henshilwood, 2007). Apollo 11 Rock Shelter (AP11) (Karas region, Namibia) contains two notched rib fragments from a context dated to around 70 ka (Vogelsang, 1998; Vogelsang, et al., 2010). The presence of markings on bone

implements from BBC, KRM, AP11, and Sibudu potentially represent symbolic cultural items (d'Errico and Henshilwood, 2007).

Personal ornaments are considered explicit expressions of symbolism and their emergence in the MSA highlights that past social groups must have had a system of symbolic communication to mediate information and had a well-developed aesthetic sensitivity (Wadley, 2001b; Henshilwood and Marean, 2003; Conard, 2004; Henshilwood and Lombard, 2014). Early **marine shell beads** occur at several North African sites (Vanhaeren, et al., 2006; Bouzouggar, et al., 2007; d'Errico, et al., 2009). The site of Grotte des Pigeons, Taforalt, Morocco, yielded perforated *Nassarius gibbosulus* shell beads from layers dating back to around 82 ka ago (Bouzouggar, et al., 2007). Wear patterns on some of the specimens indicate stringing of the beads and residues of pigment show that they were covered with red ochre. The East African site of Porc-Epic Cave, Ethiopia, contains a large number of opercula of the terrestrial gastropod *Revoilia guillainopsis* with central perforations that might have been used as beads, occurring in MSA layers dated by AMS to between 43 ka and 33 ka (Assefa, et al., 2008). From the South African record, *Nassarius kraussianus* shell beads were recovered from deposits of an age around 72 ka at BBC, also with use-wear traces and some covered in red pigment (Henshilwood, et al., 2004; d'Errico, et al., 2005). Further possible examples are six *Afrolittorina africana* shells coming from layers dated to 70 ka at Sibudu Cave (d'Errico, et al., 2008). At BC, an infant individual was discovered with a perforated *Conus* shell in a pit excavated in a layer dated to  $74 \pm 4$  ka BP (d'Errico and Backwell, 2016). This discovery represents the oldest modern human burial from Africa and the earliest evidence of a decedent equipped with a personal ornament. Other objects related to symbolically mediated behaviour occur in the sub-Saharan MSA contexts, such as **engraved ochre pieces and ostrich eggshell**. Several ochre pieces exhibiting engravings of geometric patterns come from strata dating to between ca. 100 ka and 72 ka at BBC (Henshilwood, et al., 2002, 2009). Additionally, an abstract drawing on a silcrete flake made by an ochre crayon was recovered from layers with an age of approximately 73 ka at BBC (Henshilwood, et al., 2018). The site of Pinnacle Point Cave 13B (PP13B), Western Cape Province, South Africa, yielded engraved ochre nodules dated to ca. 100 ka (Watts, 2010). A fragmented ochre pebble with incised markings was discovered in deposits dating between 100 ka and 85 ka at KRM (d'Errico, et al., 2012b). Klein Kliphuis Rock Shelter, South Africa, also provided an engraved ochre piece from a layer with an age most probably between 80 ka and 50 ka (Mackay and Welz, 2008; Mackay, 2010). The site of Diepkloof Rock Shelter (DRS), South Africa, contains a large assemblage of fragmented ostrich eggshell engraved with parallel lines and cross-hatched patterns dated to ca. 65-55 ka (Rigaud, et al., 2006; Texier, et al., 2010). The motifs were placed on functional items, i.e. eggshell containers, which played a role in the daily life of hunter-gatherers. The standardisation and repetition of the markings suggest a system of symbolic practice imparting group identity and individual expressions (Texier, et al., 2010). An assemblage of engraved ostrich eggshells was also discovered in layers with an age of approximately  $65.5 \pm 4.8$  ka to  $59.4 \pm 4.6$  ka at Klipdrift Shelter, South Africa (Henshilwood, et al., 2014).

The manufacture of **compound paint** is attested to as early as the MSA (Wadley, 2015). At BBC, a toolkit dedicated to producing pigmented compounds was discovered in layers dating to 100 ka, consisting of two shell containers with a mixture of ochre, charcoal and bone, together with utilised ochre pieces, stone grinders, fragmented bones and bone tools (Henshilwood, et al., 2011; Henshilwood and Lombard, 2014). Though the exact purpose of the red paint is unclear – possibly used as decoration or skin protection – it highlights the behavioural complexity that MSA toolmakers possessed in terms of combining different raw materials and the forward planning of several steps of the procedure (Henshilwood and Lombard, 2014).

The production of **adhesives for hafting tools** is a complex technology associated with modern cognitive abilities, including long-term planning, multitasking and the use of abstraction as well as recursion (Wadley, 2010a). The emergence of hafting technologies with compound adhesives is interrelated with the use of composite tools, enabling new complex hunting systems (Clark, 1988; McBrearty and Brooks, 2000; Wadley, 2010a; Henshilwood and Lombard, 2014). For layers at Sibudu Cave dating to ca. 60 ka, there is strong evidence that MSA artisans used compound adhesives (Lombard, 2007). They made the glue from red ochre mixed with plant gum, with ochre transforming the physical properties of the glue (Wadley, et al., 2009). Additionally, other South African sites from the time period between 65-58 ka, such as Rose Cottage Cave and Umhlatuzana Rock Shelter (UMH), have yielded evidence for hafting of backed pieces with compound adhesives (Gibson, et al., 2004 Lombard, 2007). However, Sibudu Cave involves even earlier direct evidence for ochre-enriched adhesives from layers dated to ca. 70 ka (Lombard, 2006a) and older than 77 ka (Rots, et al., 2017).

**All of these technological enhancements nascent in the MSA are behavioural proxies for the emergence of complex cognition** formerly termed ‘modern human behaviour’ or ‘cultural modernity’ (McBrearty and Brooks, 2000; Wadley, 2015). **Cognitive complexity is defined as a set of capabilities, including abstract thought, analogical reasoning, cognitive fluidity, flexibility in problem-solving, multitasking and long-term planning, comparable with the mental competency of living people and falling within the variability of modern populations** (Conard, 2004, 2010; Wadley, 2013a, 2015). The above-mentioned outcomes of several decades of research in the African MSA have led to the rejection of the Eurocentric model which has long been the dominant paradigm claiming that cognitive complexity arose suddenly in a dramatic shift known as the ‘human revolution’ throughout Europe at ca. 40 ka (Mellars, 1989; Mellars and Stringer, 1989; Mithen, 1996; Bar-Yosef, 1998). Currently, different models for the origin and expansion of complex cognition exist and they are all attempting to provide interpretations in accordance with the increasing bulk of archaeological data (Henshilwood and Marean, 2003; Conard, 2007, 2008). These models are: a gradual emergence of African origin (McBrearty and Brooks, 2000), an African origin in the early Late Pleistocene based on the intensified use of coastal resources (Parkington, 2001, 2010; Kyriacou, et al., 2014), a punctuated late African origin in connection with a genetic mutation triggering major advances in linguistic capacities (Klein and Edgar, 2002; Klein, 2009), gradual origins across multiple human taxa and multiple continents (d’Errico, 2003; d’Errico, et al., 2003), relatively late origins

among multiple human taxa (Zilhão, 2001, 2011; Hoffmann, et al., 2018), and the mosaic, polycentric, non-exclusively African origin of modernity (Conard, 2005, 2008).

This overview illustrates the significance of the palaeoanthropological, genetic and archaeological record of the MSA concerning the history of mankind. The MSA is especially important regarding the development of cognitive complexity and the first appearance of AMH. However, more and especially high-resolution data is necessary to understand the evolutionary processes happening during this phase.

### 1.2. The southern African MSA sequence and MIS 5 evolutionary dynamics

*After discussing the African MSA in general, I will elaborate here on cultural developments and the subdivision of the southern African MSA with a particular focus on Marine Isotope Stage (MIS) 5, ranging from 130 ka to 71 ka (see for a definition of MIS 5 Lisiecki and Raymo, 2005) (Table 1). The previous section has already introduced the wealth of data originating from the MSA from sub-Saharan Africa. The sub-Saharan MSA is linked to a long research tradition, benefitting from current research conditions that, unlike other parts of Africa, are not hampered by political unrest, problematic infrastructures, dense vegetation, soil erosion, and drastic disruption of stratigraphies (see for example Taylor, 2016).*

**Table 1.** Suggested nomenclature for MSA sub-stages (modified after Wurz, 2002, 2016).

Volman 1981	Singer and Wymer 1982	Lombard et al. 2012	Marine Isotope Stage (MIS) association	Approximate time period (ka BP)
Post Howiesons Poort	MSA III & IV	Sibudu technocomplex	3 - 2	60 - 45
Howiesons Poort	Howiesons Poort	Howiesons Poort	4 - 3	70 - 58
		Still Bay	5 - 4	77 - 70
		pre-Still Bay	5	96 - 72
MSA 2b	MSA II	Mossel Bay	5	105 - 77
MSA 2a	MSA I	Klasies River	5	130 - 105
MSA 1		early MSA	8 - 6	300 - 130

#### 1.2.1. The Howiesons Poort and Still Bay research imbalance

Over the last two decades, **researchers have concentrated on investigation of two distinct Late Pleistocene technocomplexes, the Howiesons Poort (HP) and the preceding Still Bay (SB)**, because these two MSA phases were considered particularly innovative compared to the ones before and after (Henshilwood, 2012; Wurz, 2013, 2016; Wadley, 2015). It was suggested that these two sub-stages were short-lived and represent clear cultural markers (Jacobs, et al., 2008a). The HP is characterised by blade production on high quality raw materials of good knapping suitability to be transformed into backed tools (Henshilwood, 2012; Wadley, 2015) as well as the manufacture of bone tools (d'Errico, et al., 2012b), engraved ostrich eggshell (Texier, et al., 2010; Henshilwood, et al., 2014), and varied usage of ochre (Lombard, 2006b, 2007; Wadley, et al., 2009; Dayet, et al., 2013). The SB features objects of symbolic expression, such

as engraved ochre (Henshilwood, et al., 2002, 2009), abstract drawings (Henshilwood, et al., 2018), and shell beads (Henshilwood, et al., 2004; d'Errico, et al., 2005, 2008; Wadley, 2012a), the creation of compound adhesives for hafting (Lombard, 2006a), and the production of bone implements (Henshilwood, et al., 2001a; d'Errico and Henshilwood, 2007; d'Errico, et al., 2012b). However, the most diagnostic, even iconic characteristic of the SB is its bifacial lithic technology (Henshilwood, 2012), partially produced by pressure-flaking (Mourre, et al., 2010) and silcrete heat-treatment that was used to improve the knapping properties (Brown, et al., 2009; Mourre, et al., 2010; Schmidt, et al., 2013; Schmidt and Högberg, 2018). All of these characteristic features of the HP and SB are interpreted as proxies for drastic change in technology, economy and social organisation.

In recent years, several studies of HP assemblages have confirmed the definition of the HP as a cultural unit with a wide geographic range, but with a relatively long-lasting temporal duration ranging from MIS 5 to MIS 3, encompassing diachronic technological change and regional variability (Soriano, et al., 2007, 2015; Villa, et al., 2010; Porraz, et al., 2013; Tribolo, et al., 2013; Mackay, et al., 2014; de la Peña, 2015; Douze, et al., 2018). The broad defining consistencies and similar patterns of change over time of this dynamic cultural entity indicate inter-regional social interactions and connectivity between HP populations. In lithic assemblages, this is seen in the production of elongated blanks involving similar methods and techniques, the repertoire of retouched elements and the ways of modifying them, assemblage sizes and the on-site manufacture of blanks and tools (Porraz, et al., 2013; Mackay, et al., 2014; de la Peña, 2015; Soriano, et al., 2015).

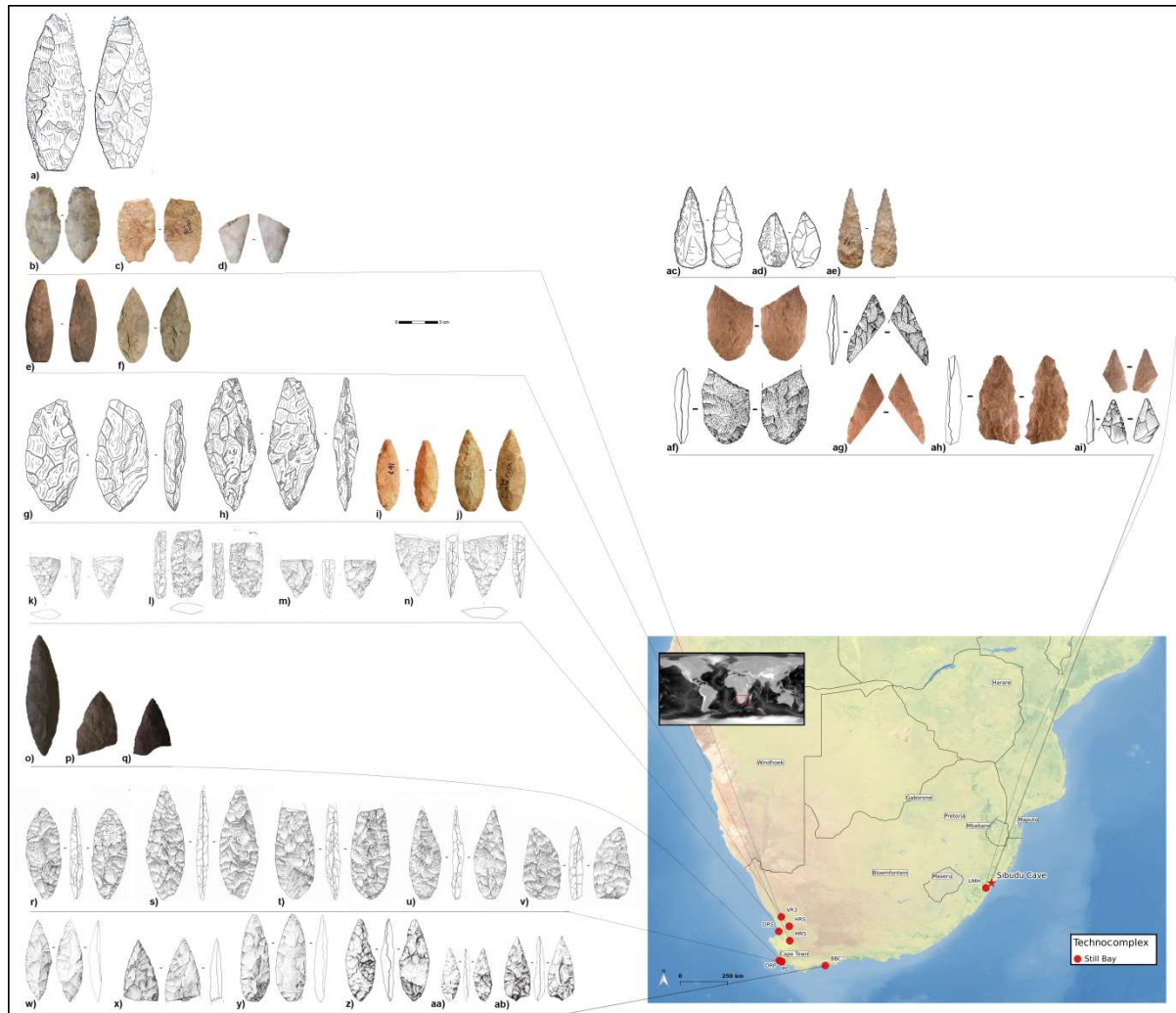
In contrast, **the older SB period dating to MIS 5 and 4 is less well-defined and has a more complex research history.** A.J.H. Goodwin and C. van Riet Lowe (1929) provided a detailed definition of the SB based on several unstratified, undated MSA open-air sites in the Western Cape Province in their pioneering monograph about the subdivision of the southern African Stone Age. The term SB was introduced in memory of C.H.T.D. Heese, a retired headmaster from Riversdale, who collected leaf-shaped lithic points in the dunefield close to the village of Still Bay in 1906 (Goodwin, 1958). Goodwin and van Riet Lowe considered the SB industry as a probable 'Neo-anthropoc' (modern) invasion, "[...] *in which a technique and a beauty of form very comparable to the Lower Solutrean of Europe make their appearance*" (Goodwin and van Riet Lowe, 1929: 100). The *fossile directeur* of the SB was the bifacial lance-head, which was a bifacially worked foliate or lanceolate point (Figure 2) (Goodwin and van Riet Lowe, 1929; Wadley, 2007). The most common shape is described as a laurel leaf tip with a semi-circular or a wide-angled pointed base. In addition to the typical bifacial foliates, two other types of points occurred, namely the convergent flake and the oakleaf, i.e. denticulated, point. Side-scrapers and backed pieces were also present in low proportions. Goodwin and van Riet Lowe stated that from their present knowledge, the distribution of the SB was confined to the southernmost coast of Africa (Goodwin and van Riet Lowe, 1929). After this initial description, confusion arose about the chronological position of this technocomplex relative to the HP. During excavations at Peers Cave (PC) in 1947 and 1948, also known as Skildergat Cave, South Africa, K. Jolly could

not clarify whether the SB was stratigraphically above or below the HP (Jolly, 1948). Bifacially worked points were also regarded as elements associated with the HP, for example at Tunnel Cave and Skildergat Kop also located on the Cape Peninsula (Malan, 1955). Moreover, the taxonomic unit SB was applied to many African MSA assemblages, some of which lacked the *fossile directeur* of this industry, while others had problematic stratigraphic contexts. The result was that in Sampson's summary (Sampson, 1974) of the chrono-cultural framework of southern Africa, he called the validity of the term 'Still Bay' into question. Following this, the SB industry lost its credibility (Wadley, 2007) and was not listed in Volman's revised classification scheme of the MSA phases (see Table 1) (Volman, 1981, 1984). Volman's publication, based on his own study of the Southern African archaeological record as well as Singer and Wymer's work at KRM (1982), represented the first formal subdivisions of the MSA after the early model established by Goodwin and van Riet Lowe (1929).

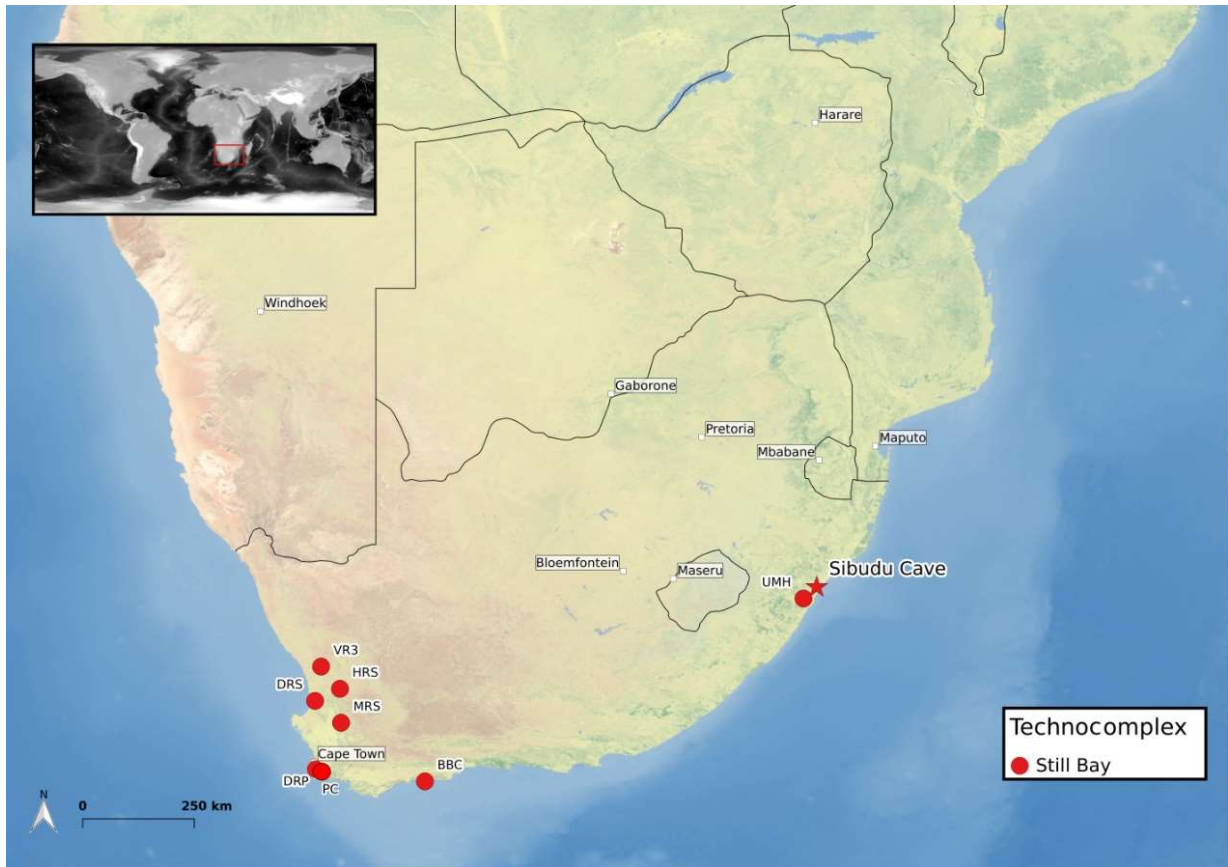
The term SB was not revived until the 1990s when excavations at Hollow Rock Shelter (HRS), Western Cape Province, South Africa (Evans, 1993, 1994), and at BBC (Henshilwood, et al., 2001b), yielded stratified assemblages fitting original definition of the SB. The excavation at BBC prompted the proposal to reinstate the SB as a MSA sub-stage (Henshilwood, et al., 2001b). The latest revision of the South African and Lesotho Stone Age sequence reaffirmed the SB as a technocomplex within the MSA (Lombard, et al., 2012). The synthesised chronological model of Jacobs et al. (2008a) led to the proposal that the SB sub-stage of the MSA is short-lived, lasting only from ca. 75 ka to 71 ka BP. However, Tribolo et al. (2013) demonstrated that the SB layers of DRS are significantly older, extending up to  $109 \pm 10$  ka BP, directly followed by the Early HP, and thus the SB potentially has a longer duration. New dates and different mathematical models concerning the chronology have further challenged the short-lived nature of the SB from only ca. 75 ka to 71 ka BP (Guérin, et al., 2013; Jacobs, et al., 2013; Feathers, 2015; Galbraith, 2015; Jacobs and Roberts, 2015, 2017).

Sites containing assemblages assigned to the SB technocomplex include Varsche Rivier 003 (VR3) (Steele, et al., 2016), Mertenhof Rock Shelter (MRS) (Will, et al., 2015), HRS (Evans, 1994; Högberg and Larsson, 2011; Högberg and Lombard, 2016a; Schmidt and Högberg, 2018), DRS (Porraz, et al., 2013; Porraz, et al., 2014), PC (formerly known as Skildergat (Andreasson, 2010; Minichillo, 2005)), Dale Rose Parlour (DRP) (also known as Eales Cave (Schirmer, 1975; Minichillo, 2005)), BBC (Henshilwood, et al., 2001b; Villa, et al., 2009; Mourre, et al., 2010; Archer, et al., 2015; Soriano, et al., 2015), UMH (Kaplan, 1990; Lombard, et al., 2010; Mohapi, 2013; Högberg and Lombard, 2016a, 2016b) and Sibudu Cave (Wadley, 2007; Soriano, et al., 2009, 2015) (Figure 3). The technological descriptions of VR3 and MRS are preliminary, PC and DRP have a very problematic research history (Andreasson, 2010; Minichillo, 2005) and UMH lacks stratigraphic integrity leaving a paucity of stratified well-dated and well-studied SB-sites, the majority of which occurs in the Western Cape Province of South Africa. These few SB assemblages have bifacial technology in common; however, they also exhibit variability in the shaping and use of bifacial tools and their importance within the SB technical system. Additionally, differences are seen in raw material procurement, other reduction strategies and

tool types present. In response to this diversity and the chronological inconsistencies, more and more researchers are calling for caution in grouping these assemblages together under one cultural label (Porraz, et al., 2013; Archer, et al., 2015, 2016; Conard and Porraz, 2015; Soriano, et al., 2015; Rots, et al., 2017).



**Figure 2.** Still Bay points: a) Still Bay point from Pringle Bay (modified after Goodwin and van Riet Lowe, 1929: 128, Text-Figure 2); b-d) Still Bay points from Varsche Rivier 003 (Steele, et al., 2016: Figure 14); e-f) Still Bay points from Mertenhof Rock Shelter (modified after Will, et al., 2015: S2 Figure); g-j) Still Bay points from Hollow Rock Shelter (g-h) Evans, 1993: Appendix 1, i-j) Högberg and Larsson, 2011: Figure 7); k-n) Still Bay points from Diepkloof Rock Shelter (Porraz, et al., 2013: Figure 6); o-q) Still Bay points from Peers Cave (modified after Andreasson, 2010: Figure 25 – 27); r-v) Still Bay points from Dale Rose Parlour (copyright by Pierre-Jean Texier; drawings by Michel Grenet); w-ab) Still Bay points from Blombos Cave (w-y) Villa, et al., 2009: Figure 1, z-ab) Henshilwood, et al., 2001: Figure 7); ac-ae) Still Bay points from Umhlatuzana Rock Shelter (ac-ad) Kaplan, 1990: Figure 11-12, ae) Högberg and Lombard, 2016: Figure 3); af-ai) Still Bay points from Sibudu Cave (Soriano, et al., 2015: S1 Figure A).

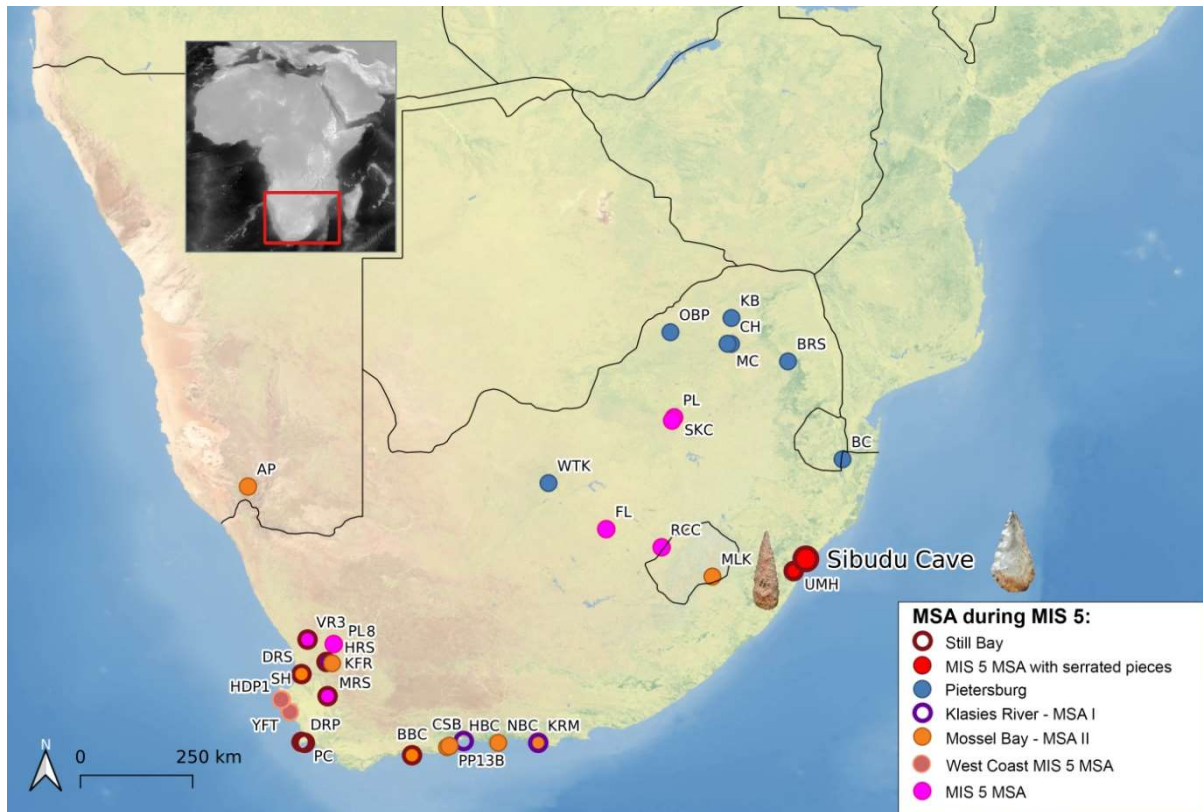


**Figure 3.** Location of Still Bay sites in southern Africa (Site Abbreviations: BBC - Blombos Cave, DRS - Diepkloof Rock Shelter, DRP - Dale Rose Parlour, HRS - Hollow Rock Shelter, MRS - Mertenhof Rock Shelter, PC - Peers Cave, UMH - Umhlatuzana Rock Shelter, VR3 - Varsche Rivier 003).

### 1.2.2. Status quo of chrono-cultural developments in the MSA during MIS 5

The findings of recent years demonstrating **the heterogeneity and temporal expansiveness of the SB and the growing body of technological studies on MIS 5 assemblages present a more complex picture of cultural evolution** than the uniform scenario previously assumed. The Early MSA (EMSA), embracing all late Middle Pleistocene MSA technologies from ca. 300-130 ka (see Lombard, et al., 2012; Schmid, et al., 2016) involves only a few sites and lacks definitive spatial or chronological patterns due to preservation issues, study biases, or lower population densities or sizes (Wurz, 2013; Schmid, et al., 2016). In contrast, MIS 5 marks a time period in the MSA after which technological trends are archaeologically more clearly visible in space and time (Figure 4):





**Figure 4.** Location of MSA sites during MIS 5 (Site Abbreviations: AP11 - Apollo 11 Rock Shelter, BBC - Blombos Cave, BC - Border Cave, BRS - Bushman Rock Shelter, CH - Cave of Hearths, CSB - Cape St. Blaize, DRS – Diepkloof Rock Shelter, DRP - Dale Rose Parlour, FL - Florisbad, HBC - Herolds Bay Cave, HDP1 - Hoedjiespunt 1, HRS - Hollow Rock Shelter, KB - Kalkbank, KFR - Klipfonteinrand, KRM - Klasies River main site, MC - Mwulu’s Cave, MLK – Melikane Rock Shelter, MRS - Mertenhof Rock Shelter, NBC - Nelsons Bay Cave, OBP - Olieboompoort, PC - Peers Cave, PL - Plovers Lake, PL8 - Putslaagte 8, PP13B - Pinnacle Point 13B, RCC - Rose Cottage Cave, SH - Sea Harvest, SKC - Swartkrans, UMH - Umhlatuzana Rock Shelter, VR3 - Varsche Rivier 003, WTK - Witkrans, YFT - Ysterfontein 1).

**In the north-eastern interior part of South Africa, the so-called Pietersburg technocomplex** was said to be one of the earliest distinguishable phases of the MSA (Goodwin and van Riet Lowe, 1929; Tobias, 1949; Mason, 1962; Sampson, 1974; Wadley, 2015). A number of sites mostly located in the Limpopo and Gauteng Provinces were excavated between the 1940’s and the 1960’s, with the long sequence of Pietersburg occupations at CH serving as a reference sequence (Mason, 1957; Mason, et al., 1988; McNabb and Sinclair, 2009). Based on the analysis of the lithic assemblage at CH by Mason (1957), the Pietersburg was subdivided into Lower, Middle and Upper phases. The corresponding layers at BC yielded an age for the Pietersburg MSA sub-stage between 238-75 ka BP (Grün and Beaumont, 2001; Grün, et al., 2003). Some general characteristics include the exploitation of local raw materials, production of blades and elongated products from Levallois cores (Mason, 1962). Different research teams are currently reinvestigating Pietersburg sites such as Bushman Rock Shelter (BRS) (Porráz, et al., 2015, 2018), BC (Backwell, et al., 2018b), Mwulu’s Cave (MC) (de la Peña, et al., 2018), and Olieboompoort (OBP) (Mason, 1957; Val, personal communication) to provide a refined chronology and technological revision of the Pietersburg. At BRS, Porráz et al. (2015, 2018) recognised two

techno-typological phases, namely an upper phase (called 21), characterised by both unifacial and bifacial points, and a lower Phase (called 28), featuring end-scrapers.

**The 'MSA I' or 'Klasies River' and the 'MSA II' or 'Mossel Bay' technocomplexes** were originally defined by Singer and Wymer (1982) based on assemblages at KRM. The subsequent analysis by Wurz (2000, 2002) confirmed this subdivision. The 'MSA I' layers are dated to between ca. 115-110 ka and the 'MSA II' has an age between approximately 108-63 ka (Feathers, 2002).

The assemblage of the Klasies River sub-stage is characterised by the exploitation of local quartzite cobbles, the use of both internal direct hard hammer percussion and marginal direct soft hammer percussion, the manufacture of blades with prepared platforms from unidirectional pyramidal or flat cores, and a small tool corpus including retouched blades (Wurz, 2000, 2002, 2012). HRS has deposits below the SB dated to  $87 \pm 6$  ka (Högberg and Larsson, 2011). The lithic assemblage features the use of local quartzite, the production of flakes and blades, with scrapers and denticulates as the main tool types (Evans, 1994). Evans (1994) suggested a possible designation of the assemblage to MSA 2a as defined by Volman (1981), corresponding to the Klasies River sub-stage. The undated site of Herolds Bay Cave, Western Cape Province, shows similar technological features and has been designated to the Klasies River phase (Volman, 1981, 1984; Hendeby and Volman, 1986; Lombard, et al., 2012).

The Mossel Bay lithic assemblage of KRM features the exploitation of mainly local quartzite, the exclusive employment of hard hammer percussion, a reduction system aiming at the production of triangular flakes and blades by the use of unidirectional convergent and parallel Levallois methods on split cobbles, and notched and denticulated blades as formal tools (Wurz, 2000, 2002, 2012; Wurz, et al., 2018). MSA-Mike from DRS (Porraz, et al., 2013), M3 phase of BBC (Douze, et al., 2015), and PP13B dating to MIS 5 (Thompson, et al., 2010) are reminiscent of the KRM Mossel Bay regarding the dominant use of local raw materials, the prevalence of parallel (Levallois-like) core reduction methods, the strong emphasis on production of triangular flakes and the low proportion of tools. AP11 was originally defined as MSA 2 (Vogelsang, 1998), but due to the presence of four bifacial points an affiliation to the SB technocomplex was proposed (Vogelsang, et al., 2010; Lombard and Högberg, 2018). However, Vogelsang et al. (2010) suggested this with reservations and stated that *"Indeed, the definition of Still Bay bifacial points used by Villa et al. (2009) [...] calls the classification of the Apollo 11 specimens into question"* (Vogelsang, et al., 2010: 197). Porraz et al. (2013, 2018) made similar claims rejecting the idea that a handful bifacial pieces in an assemblage may be indicative of the SB or have some degree of association with the SB. Furthermore, undated MSA layers of Cape St. Blaize (Thompson and Marean, 2008), Nelson Bay Cave (Volman, 1981, 1984), and Klipfonteinrand (Volman, 1981; Mackay, et al., 2014), Western Cape Province, have been tentatively assigned to the MSA II or Mossel Bay sub-stage (Volman, 1981; Lombard, et al., 2012). Melikane Rock Shelter, Qacha's Nek District, Lesotho, yielded an assemblage with an age between 89.4-76.4 ka dominated by regular, large blades resembling those of the Klasies River sub-stage (Stewart, et al., 2012), but due to the dating results, these layers have been designated as Mossel Bay (Lombard, et al., 2012).

**Three coastal sites from the West Coast**, Ysterfontein 1 (YFT) (Halkett, et al., 2003; Avery, et al., 2008; Wurz, 2012), Hoedjiespunt 1 (HDP 1) (Will, 2011; Will, et al., 2013), and Sea Harvest (SH) (Volman, 1978, 1981; Grine and Klein, 1993), share great similarities **suggesting a chronologically and/or regionally distinct variant** (Wurz, 2012, 2013). These three assemblages, probably all dating to the Last Interglacial, strongly conform in technology as well as economy. The majority of artefacts is made on raw materials from within 20 km of the sites. The assemblages comprise a relatively high tool component dominated by denticulates, notched pieces and scrapers. The reduction strategies are oriented towards the manufacture of flakes demonstrating no or minimal preparation (Wurz, 2013; Mackay, et al., 2014; Douze, et al., 2015).

Additionally, DRS contains between MSA-Mike and SB type 'Larry' another phase **Pre-SB type 'Lynn'** (Porraz, et al., 2013, 2014). The assemblage is primarily made on local raw materials. The blank production follows two reduction strategies concerning the exploitation of the cores either with centripetal removals or in a unidirectional manner by the use of direct internal hard hammer percussion. The formal tools comprises a high frequency of lateral scrapers and convergent scrapers, but notched pieces, denticulates, *pieces esquillées* and a few bifacial pieces occur as well. Tools on exotic fine-grained rocks are more often and more intensely re-sharpened. Porraz et al. (2013) argue that Pre-SB type 'Lynn' is a transitional unit showing a gradual change from the preceding MSA-Mike noticeably by a shift in raw material economy and a discontinuity to the subsequent Still Bay type Larry due to the appearance and dominance of bifacial technology.

Further MIS 5 deposits are known from VR3 (Mackay, et al., 2014; Steele, et al., 2012, 2016), Putslaagte 8 (Mackay, et al., 2015), MRS (Will, et al., 2015), Rose Cottage Cave (Harper, 1997; Pienaar, et al., 2008), Florisbad (Kuman, 1989; Grün, et al., 1996; Kuman, et al., 1999), Swartkrans Cave (Sutton, et al., 2009; Sutton, 2013) and Plovers Lake (de Ruiter, et al., 2008). These assemblages either have been described in very preliminary terms or need a re-evaluation in the light of more comprehensive new evidence on the technological trends within MIS 5.

Increasingly, the archaeological record seems to indicate that cultural change and innovativeness are not restricted to the HP and SB technocomplexes and, beyond that, hint at a complex scenario of distinct co-existing techno-typological traditions, adaptations, and innovations in different regions of southern Africa during MIS 5. This process of regionally differentiated populations would have influenced the way in which groups organised themselves territorially and socially, and impacted on the appearance, assimilation, diffusion and implementation of inventions. Clark (1988: 251) proposed this in his publication on the MSA and the beginnings of regional identities. However, in order to corroborate and elaborate on this hypothesis, and to determine cultural, demographic and/or ecological triggers and mechanisms for the development of early complex behaviours, a robust understanding of the regional chrono-cultural framework requires long regional sequences.

An excellent case study is the site of Sibudu Cave, which contains a long continuous sequence from MSA occupations dating to MIS 5 with overlying SB layers, through to final MIS strata in a well-controlled and well-documented stratigraphy (see Wadley and Whitelaw, 2006; Goldberg, et al., 2009; Conard, et al., 2012; Wadley, 2013b; Will and Conard, 2018; Rots, et al., 2017). **This thesis uses lithic assemblages from Sibudu Cave to test dynamics during MIS 5 in KwaZulu-Natal – a very different ecological and geological zone from the Western and Eastern Cape Province** where many other studies are focused (e.g. Wurz, 2002; Porraz, et al., 2013; Miller, 2014; Douze, et al., 2015; Mackay, et al., 2015; Steele, et al., 2016). Thus, the study of Sibudu will provide crucial insights from the eastern part of southern Africa and it will pave the way for syntheses and prospects on cultural evolution on a broader geographical scale.

### 1.2.3. Research objectives

I started the introduction with the quote '*Giving substance to shadows*' from the song '*Crucify your mind*' by Sixto Rodriguez, as in my opinion, these four words describe in essence the central research questions that I want to address in my thesis, as my goal is to give substance to an assemblage of a period and in a region that has remained in the shadows for a long time:

- What are the technological and techno-economic features of the assemblage from the C-A layers of Sibudu?
- How is the relationship to bifacial-bearing industries in MIS 5, particularly to the SB?
- What connections and/or differences exist, in general, to MSA assemblages of MIS 5?
  - What technological novelties do I observe during this period in this region respectively ecological zone?
  - What are possible mechanisms that drive the technological changes, dynamics and variability during MIS 5?
- Do I identify techno-cultural markers and how do the C-A layers of Sibudu fit in the chrono-cultural framework of the MSA?

## 2. Background to the site

Sibudu Cave (ID no. 2931CA; 29°31'21.5" S, 31°05'09.2" E) is situated about 40 km north of Durban and 15 km inland of the Indian Ocean. The site is perched on a steep, forested cliff 20 m above the uThongathi River (alternatively Tongati River) in the local municipality KwaDukuza belonging to the district municipality iLembe (formerly named King Shaka District Municipality) in the northern part of KwaZulu-Natal Province, South Africa (Figure 5).



**Figure 5.** Sibudu: a) Location of Sibudu in KwaZulu-Natal (left; after Wadley, 2001a: Figure 1); b) overview of the site in 2016 (photo by Nicholas J. Conard); c) view on the excavation areas in 2017 (photo by Ria Litzenberg).

The site was historically considered as a cave probably due to its large size: 55 m long and ca. 18 m wide, but in fact, the site is more appropriately described as a rock shelter since it is wider than it is deep, and daylight reaches everywhere (Wadley and Jacobs, 2006).

In this chapter, I will give an overview of the geological setting as well as the research history of Sibudu. Furthermore, I will detail the long stratigraphy and chronology of the site. Finally, I will discuss what data are so far available to reconstruct palaeoenvironments and palaeoclimates.

### 2.1. Geological setting

The rock shelter was formed during a marine regression when the uThongathi River cut its bed into the Cambrian to Ordovician (490 million years ago) Natal Group sandstone cliff. These sandstones comprise a thick sequence of sediments, deposited onto the stable platform created by erosion of the primarily granitic rocks of the Natal Metamorphic Province, a geological formation dated to approximately 1000 million years ago (Figure 6). They consist of purple-red quartz, feldspar-rich medium sand and some silt (Pickering, 2006). Clay occurs as an interstitial binder between the coarser grains (Goldberg, et al., 2009). The sandstone deposits reach a thickness of between 300 and 400 m, are planar and cross-bedded by ca. 0.8 m thick units. Individual sets of cross-beds demonstrate pronounced changes in dip and are often capped by fine-grained generally eroded siltstone, revealing the stepped morphology of the sandstone cliff in the shelter. The south-western part of the shelter is more exposed and thus, more affected by weathering and erosion than the north-eastern part (Pickering, 2006). The bedrock and sediments of the shelter slope steeply from north to south. The excavation area is located at an altitude of approximately 100 m above mean sea-level (amsl) in the north-eastern part of the shelter where the sediments are thickest and best preserved (Wadley and Jacobs,

2004, 2006). A large rockfall cone formed by large boulders fallen from the cliff is situated at the northern portion of the shelter, adjacent to the excavation (Pickering, 2006).

## *2.2. Research History*

A first trial trench of about one metre in depth was excavated in 1983 by Aron Mazel (Natal Museum). The unpublished field notes, stratigraphic drawings, photographs and excavated finds are stored in the Natal Museum, Pietermaritzburg. Mazel documented that the uppermost part of the sequence contained Late Iron Age pottery mixed with MSA lithic artefacts, followed by deposits with only MSA materials below a depth of 30 cm. From the two reversed radiocarbon dates on charcoal Mazel obtained, one (Pta-3765) from layer MOD2 at a depth of 20-30 cm from the surface provided an age of  $26,000 \pm 420$  uncal BP, while the other with an age of  $24,200 \pm 290$  BP (Pta-3767) was out of context and should be rejected (Wadley, 2001a). Further excavations conducted by Lyn Wadley (University of the Witwatersrand) started in September 1998 and continued until 2011 (Figure 7) (Wadley, 2013b). Following standard excavation procedures, an excavation grid was set up in one-metre squares labelled by alphabetic letters from north to south and Arabic numerals from the rear to the front of the shelter. Each square is subdivided into four 50 by 50 cm quadrants, which are identified by lower case letters: quadrant *a* is in the northeast, *b* is in the southeast, *c* is in the northwest and *d* is in the southwest (Sievers, 2013). The grid of 21 square metres comprised squares A6-4, B6-4, C6-2, D6-2 and E6-2 (Figure 8). The excavation followed the natural stratigraphy and material is collected according to quadrant and layer. The colour and texture of each layer is pivotal and thus, generally reflected in the name of the layer; for example, the appended Sp in layers RSp, BSp and YSp refers to the speckled nature conferred by gypsum spots that are predominantly red, brown and yellow. In case a natural layer is deeper than ca. 10 cm, it is arbitrarily split, e.g. LBG, LBG2, LBG3 and LBG4 (Wadley and Jacobs, 2006). Munsell colour readings were taken for each stratigraphic unit. Features were removed separately and in the case of hearths, the top, middle and base were excavated individually to record the preservation of carbonised organic material in different parts of the hearths. Soil samples were taken for each layer and feature. Volumes of excavated deposit are recorded according to measurement markings on the sides of buckets, which hold a maximum of 10 litres. All excavated sediments were dry-sieved through stacked 2 mm and 1 mm sieves, although 1 mm sieves were not used prior to 2003 (Sievers, 2013). Dry-sieving was preferred over flotation, as the moisture can cause disintegration of the fragile material. The volumes in each sieve were additionally recorded. A permanent datum line was painted 1.3 m above the ground surface on the cave wall and the depth of each layer is measured from this datum using a theodolite (Wadley, 2001a). Wadley's excavation began in 1998 with a two square metre trial trench comprising squares B6 and B5. During Wadley's excavation campaigns until 2011, strata dating to around 58 ka BP were reached in all 21 squares of the excavation area. Older occupations, including pre-SB, SB and HP layers, were exposed in a total of six square metres (B6-4 and C6-4) to a depth more than three metres below the surface (Wadley, 2013b). Since 2011, a team led by Nicholas J. Conard (University of Tübingen) continues the fieldwork (for further details see Chapter 3.1.).

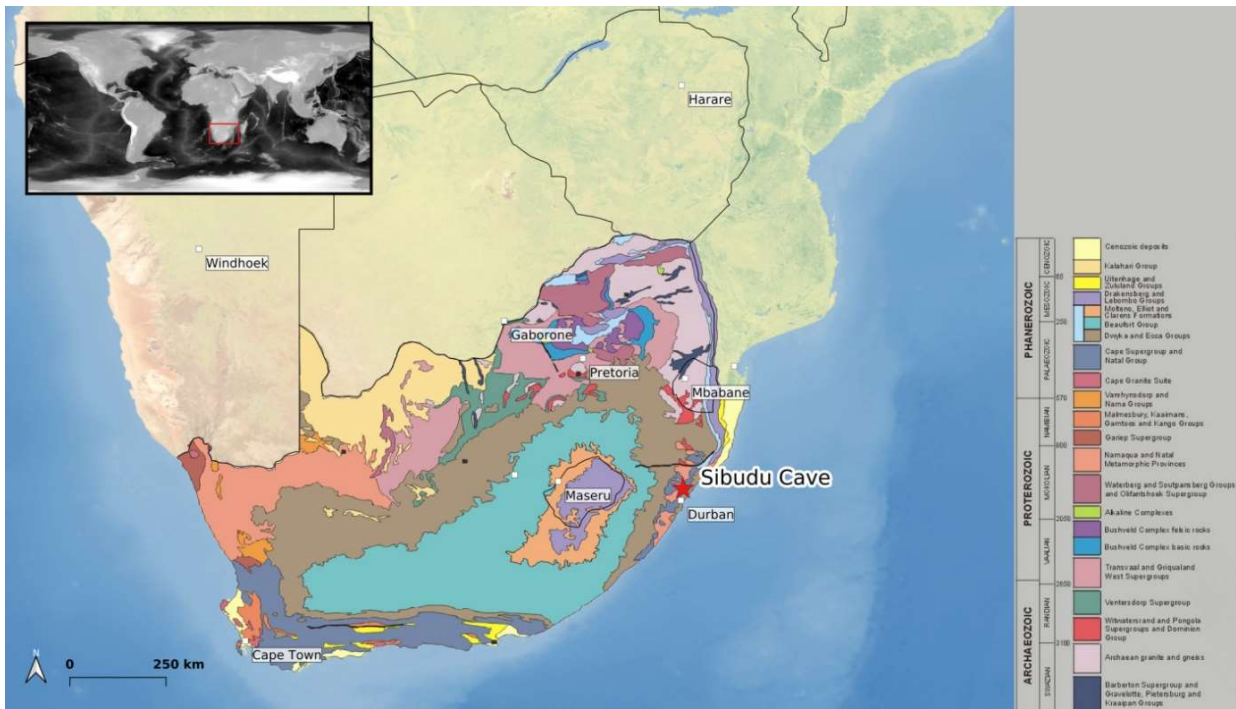
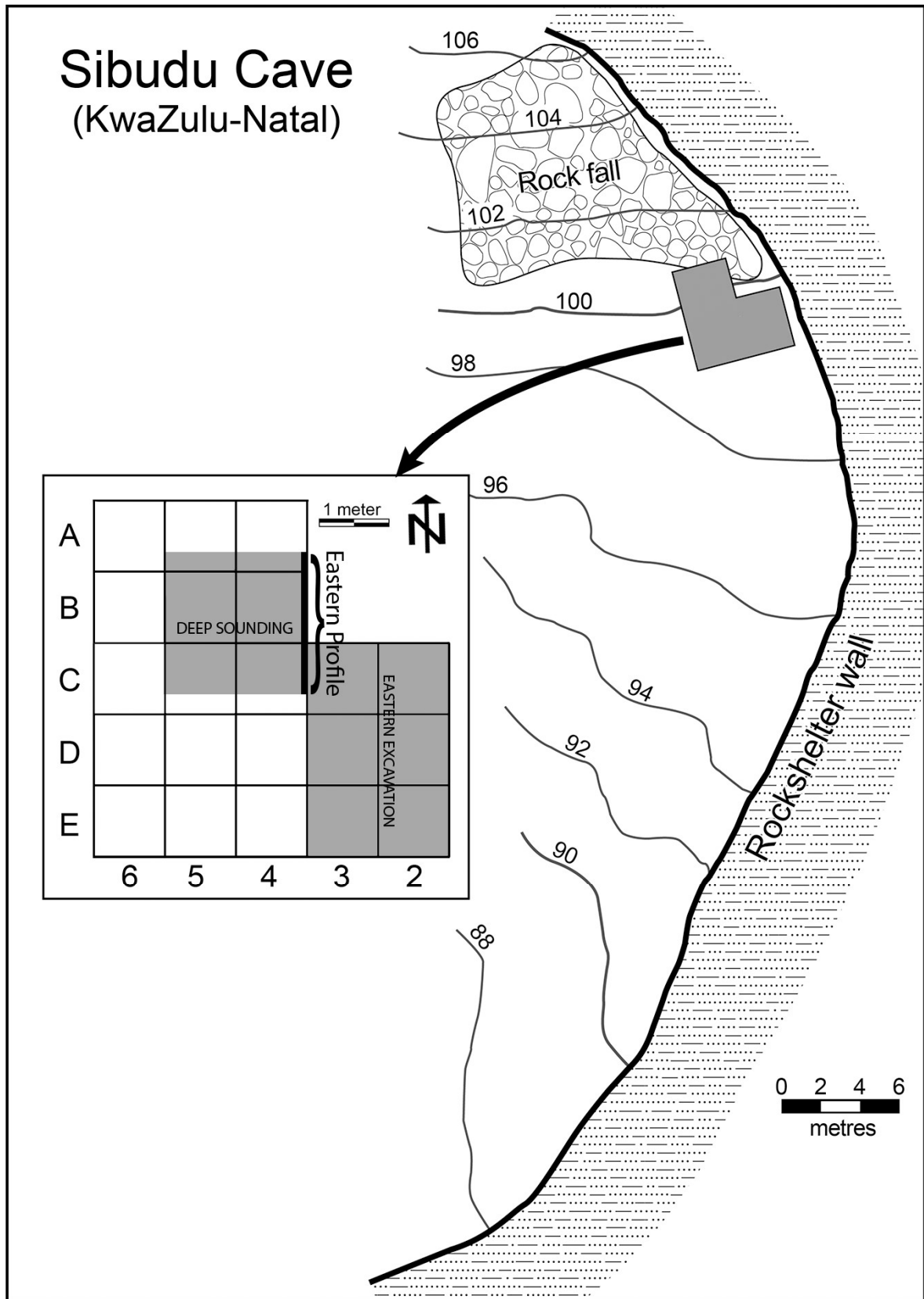


Figure 6. Geological context of South Africa (modified after Council for Geoscience).



Figure 7. Sibudu: Nicholas J. Conard and Lyn Wadley at Sibudu Cave 2011 (photo by Sarah Rudolf).



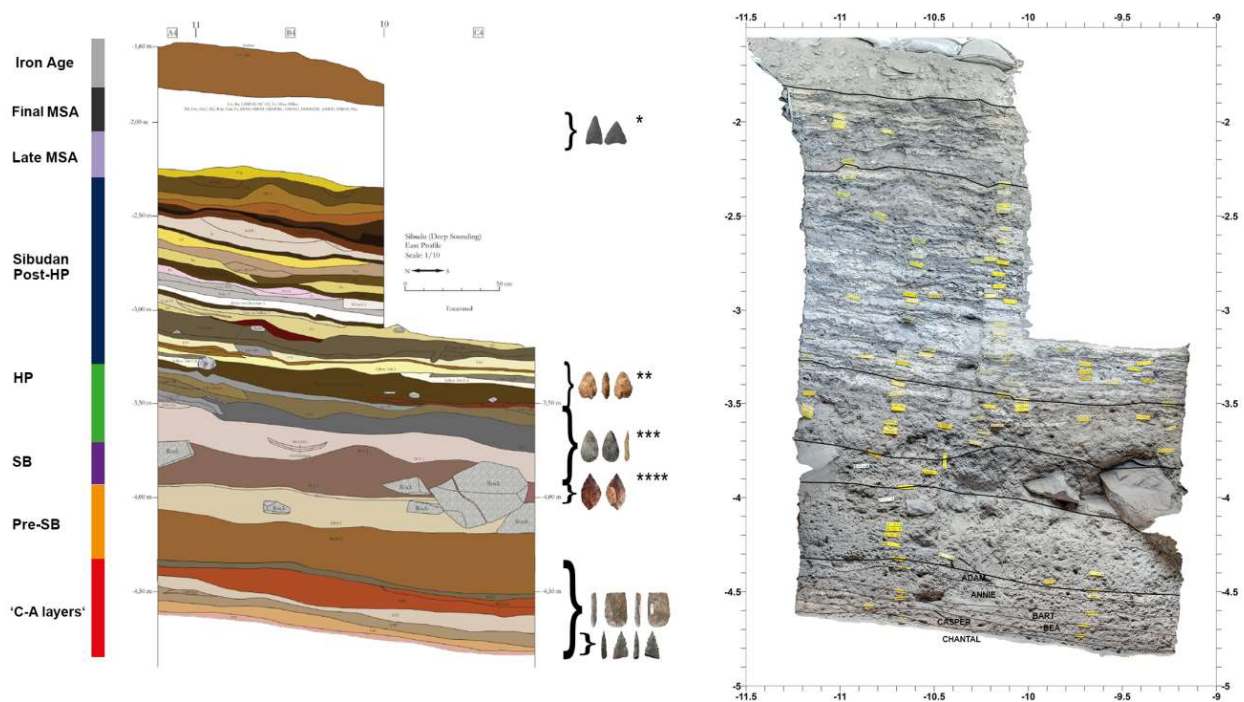
**Figure 8.** Sibudu: Plan of the site with elevations in meters amsl, the excavation grid, the two excavation areas, and the location of east profile (modified after Soriano, et al., 2015: Figure 2).



### 2.3. Stratigraphy and Chronology

Sibudu preserves a thick, stratified and high-resolution sequence over 3.5 m deep, mainly consisting of MSA layers that span a time range of more than 74 to 33 ka BP followed by much later Iron Age occupations (Figure 9).

The stratigraphy is predominantly composed of anthropogenic deposits, including numerous ashy and charcoal-rich lenses that are related to combustion events, with relatively lower amounts of geogenic input, such as inclusions of *éboulis* derived from rock fall (Pickering, 2006; Goldberg, et al., 2009). Analyses of the sediments show that little-to-no water-borne transportation or remobilisation occurred (Pickering, 2002). The organic preservation is generally good. Several OSL and radiocarbon dates have been obtained from the MSA deposits (Wadley and Jacobs, 2004, 2006; Jacobs, et al., 2008a, 2008b, 2008c; Jacobs and Roberts, 2008, 2017) and new luminescence dates are in progress by Chantal Tribolo (Université de Bordeaux-III, IRAMAT) (Table 2).



**Figure 9.** Sibudu: Eastern profile of the Deep Sounding of Sibudu including ages of the archaeological phases and indication of the presence of bifacial or serrated pieces (left) (modified after Rots, et al., 2017). (\*Final MSA Mohapi, 2012; \*\*lower Sibudan Will and Conard, 2018; \*\*\*Howiesons Poort de la Peña, et al., 2013; \*\*\*\*Still Bay Soriano, et al., 2015); Orthophotography of the east profile (copyright by M.M. Haaland) (right).

**Table 2.** Summary of Age (ka)  $\pm 1\sigma$ .

Occupation	Munsell colour	<sup>14</sup> C ages	Wadley and Jacobs, 2006	Jacobs, et al., 2008a	Jacobs, et al., 2008b	Guérin, et al., 2013*	Jacobs and Roberts, 2017	Tribolo, personal communication
<i>serrates layers</i>								
Chantal								91 - 75
Casper								
Bea								77 - 63
Bart								86 - 72
Annie								
Adam								92 - 76
<i>pre-SB</i>								
BS 1-16	7.5 yr 4/3 brown			77.3 $\pm$ 2.7			72.4 $\pm$ 1.9	
LBG 4	light brownish-grey							
LBG 2, LBG 3	light brownish-grey			73.2 $\pm$ 2.7			70.8 $\pm$ 3.2	
LBG	10 YR 6/2			72.5 $\pm$ 2.5			70.9 $\pm$ 2.2	
<i>SB</i>								
RGS 2	5 YR 5/2 reddish-grey							
RGS	5 YR 5/2 reddish-grey			70.5 $\pm$ 2.4			69.5 $\pm$ 2.1	
<i>HP</i>								
PGS	5 YR 6/2 pinkish-grey			64.7 $\pm$ 2.3			60.5 $\pm$ 1.8	
GS 2	5 YR 5/1 grey			63.8 $\pm$ 2.8			60.5 $\pm$ 2	
GS	5 YR 5/1 grey							
GR 2	5 YR 6/1 light brownish-grey			61.7 $\pm$ 2			58 $\pm$ 1.7	
GR	5 YR 6/1 light brownish-grey							
DRG	10 R 3/1 dark reddish-grey							
<i>post-HP</i>								
RB								
LBYA								
BYA2i								
YA2i								
Br under YA 2	5 YR 3/2 greyish-brown							
YA 2	10 YR 8/2 very pale orange							
YA 1	10 YR 8/2 very pale orange							
Bor, Ymix	5 YR 2.5/2 dark reddish-brown							
BL 2, BL 3	10 R 2.5/1 reddish-black							
B/Gmix, B/Gmix 2	5 YR 3/2 greyish-brown		59.4 $\pm$ 2.3		58.2 $\pm$ 2.4	56 $\pm$ 3		
Y 1	10 YR 8/6 pale yellowish-orange		59.4 $\pm$ 2.4		58.6 $\pm$ 2.1	61 $\pm$ 3		
Ch 2	10 R 3/1 dark reddish-grey		61.6 $\pm$ 1.9		58.3 $\pm$ 2	57 $\pm$ 3		
G 1	10 YR 6/1 grey							
WOG 1								
P 1								
Ch	7.5 YR 2.5/2 very dark brown							
Sp								
Su, Su 2	5 Y 6/6 olive-yellow							
BP	10 YR 5/3 brown							
OP	7.5 YR 4/6 strong brown							
POX	10 YR 5/6 yellowish-brown		64.1 $\pm$ 2.9		59 $\pm$ 2.2	51 $\pm$ 2	50.2 $\pm$ 2	
BM	5 Y 2.5/1 black							
BO	7.5 YR 4/4 brown							
Iv	10 YR 7/3 very pale brown							
Ma, MY	2.5 YR 2.5/3 dark reddish-brown							
Che, Eb	5 YR 4/4 moderate brown, 10 YR 2/2 very dark brown							
SS	5 YR 7/3 pink		56.2 $\pm$ 1.9		59.6 $\pm$ 2.3	56 $\pm$ 3		
Mi	5 Y 2.5/1 black							
BL, Or	5 Y 2.5/1 black, 5 YR 5/6 light brown		61.5 $\pm$ 2.2					
SPCA	10 YR 5/4 yellowish-brown							
BSp 2	10 YR 5/3 brown	28.88 $\pm$ 0.17						
BSp	10 YR 5/3 brown		61.3 $\pm$ 2.0		57.6 $\pm$ 2.1	55 $\pm$ 2		
<i>late MSA</i>								
Ysp	10 YR 5/4 yellowish-brown							
RSp	7.5 YR 6/2 pinkish-grey	>41.4	48.4 $\pm$ 1.7		46 $\pm$ 1.9	49 $\pm$ 3		
GMOD, BMOD	10 YR 6/1 grey, 5 YR 2/2 dusky brown							
OMOD 2 BL	10 YR 2/2 very dark brown	>45						
OMOD 2	5 YR 5/6 light brown	34.3 $\pm$ 2						
OMODBL	10 YR 2/2 very dark brown		50.2 $\pm$ 1.7		47.6 $\pm$ 1.9	46 $\pm$ 3		
OMOD	5 YR 5/6 light brown late MSA		50.3 $\pm$ 2.1		46.6 $\pm$ 2.3	47 $\pm$ 3		
MOD	5 YR 3/4 moderate brown		49.7 $\pm$ 1.8		49.1 $\pm$ 2.1	46 $\pm$ 3		
Cad, Pu	10 YR 2/2 dark brown, 5 YR 3/4 moderate brown							
RD	7.5 YR 6/2 pinkish-grey		49.0 $\pm$ 2.0		49.4 $\pm$ 2.3	49 $\pm$ 2		
Ore, Ore 2	5 YR 2/2 dusky brown							
PB	7.5 YR 6/2 pinkish-grey							
<i>final MSA</i>								
Mou, Dmou	10 YR 4/2 dark yellowish-brown							
Es	10 YR 6/2 pale yellowish-brown							
MC (hearth)								
LBMOD	10 YR 4/2 dark yellowish-brown		50.4 $\pm$ 1.8		49.9 $\pm$ 2.5	48 $\pm$ 2		
Bu	10 YR 6/2 pale yellowish-brown	42.3 $\pm$ 1.3	36.7 $\pm$ 1.7		39.1 $\pm$ 2.5	37 $\pm$ 2		
Co	5YR 5/2 pale brown		37.1 $\pm$ 1.5		38 $\pm$ 2.6	35 $\pm$ 2		
<i>Iron Age</i>								
BSS		0.96 $\pm$ 25						
BSV								

The stratigraphic sequence shows large differences in the deposits above and below layer YA2, which represents the base of the post-HP occupations and is roughly the contact between the post-HP and the preceding HP. The results of the micromorphological and microfacies analysis (Goldberg, et al., 2009; Miller, 2014) show that the lower part of the sequence (the HP, SB, pre-SB and underlying recently named 'serrates layers' (Rots, et al., 2017) consists of greyish, fairly compacted, homogeneous, non-bioturbated ashy deposits with input of rock fall. These basal strata are interpreted as remains of hearths which were homogenised and redistributed through trampling (Goldberg, et al., 2009; Miller, 2014). Numerous lenses of white-coloured sediment with dark-coloured bases that were interpreted as intact hearth features also occur within the deposits (Miller, 2014). In contrast, the stratigraphic units of the upper part of the sequence are laminated and much less homogenous. These deposits are mainly dominated by microfacies of a loose mixture of calcareous or phosphatised ashes, phytoliths, and fragments of burnt bone and charcoal which do not display any clear structuring. The heat-altered components were most probably burnt elsewhere and afterwards redeposited by human actions, such as hearth rake-out or dumping (Miller, 2014). Combustion features exhibiting characteristics typical of burnt bedding material are very common in the upper deposits but almost absent in the lower ones (Wadley, et al., 2011). Few intact hearths are documented in the upper part as well.

The variation between the lower and upper parts of the sequence highlight a change in the mode of occupation, involving the daily activities carried out at the site (Goldberg, et al., 2009; Miller, 2014). During the earlier occupations, inhabitants constructed hearths and afterwards abandoned them without cleaning them out for reuse. In the lower strata, past people lived directly on the bare ground surface of the shelter and only sporadically constructed bedding areas which are thinner and not as laterally extensive as the ones from the upper part. Inhabitants of the later phase seem to have placed great value on the structuring and maintenance of their domestic space. They constructed, used, maintained and cleaned out hearths indicating their reuse. Furthermore, the upper stratigraphic units show the repeated construction and burning of bedding. Some of the burnt bedding additionally shows evidence for refurbishment. Trampling has played an important role in the modification of the deposits throughout the whole stratigraphic sequence. In the lower part, trampling has had the effect of homogenising the deposits, whereas due to the prepared coverage of the floor with soft plant bedding material in the upper part, trampling caused compaction but no horizontal dispersion of the original combustion deposits. The shift of behavioural patterns suggests more intense occupation during the upper stratigraphic units. This intensification could be related to longer visits, more frequent visits, or occupation by larger groups than before (Wadley, et al., 2011).

The chrono-cultural sequence (Figure 9) that provides the core of my thesis encompasses at the lowest six layers identified since the beginning of the new excavations in 2011 by our team from the University of Tübingen. These strata include (from the youngest to the oldest): Burnt Mouse (BMo), Red-Brown Silt (RBS), Grey Sandy Silt (GSS), Gray-Brown Patchy (GBP), Light Brown Compact (LBC) and Pink Sandy Silt (PSS). In addition to these descriptive field designations, we gave layers the names of people, modified from the system used by Parkington and colleagues

in the Western Cape (Rots, et al., 2017). According to our system, we assign first a male and then a female name to every new layer in alphabetical order, starting with the letter A highest in the sequence. Most of these names relate to people involved in the Sibudu project, e.g. excavation team members Jonathan Adam Baines and Beatrix 'Bea' Welte, deputy director of AMAFA Annie van de Venter Radford and dating specialist Chantal Tribolo. The preliminary results of luminescence dating suggest that these layers date to between 92 and 72 ka BP, excluding an outlier from layer Bea that represents an underestimation (Tribolo, personal communication). Finds from these layers include non-lithic artefacts such as bone tools, comprising points, a wedge (Conard, 2015; Becher, 2016), bone compressors and percussors (Rots, et al., 2017), and modified ochre (Conard, 2015). Furthermore, a human tooth fragment was discovered in layer Casper (Will, et al., 2019).

The lowermost layers excavated by Wadley, namely Brown Sand (BS) and Light Brownish Grey (LBG), informally named 'pre-SB', are stratigraphically located above the layers discussed here. Jacobs and colleagues (2008a) published a first series of OSL dates from the 'pre-SB' to the HP of Sibudu but ages were subsequently argued to be overestimates due to significantly underestimated uncertainties on measured beta dose rates in their model (Guérin, et al., 2013). In a new study, the beta dose rate errors were re-examined and the OSL dates with revised estimates of dose rate errors were presented (Jacobs and Roberts, 2017). Consequently, the single age obtained for the older 'pre-SB' stratum (BS) is  $72.4 \pm 1.9$  ka BP. The lithic artefacts in BS show that toolmakers manufactured flakes and large blades on mainly dolerite and hornfels, as well as quartz, quartzite and other raw materials. A change in the typological corpus stands out within the BS sequence. The tools characterising the deepest layers, BS 11 to BS 16, comprise a few thin bifacial points, while the formal tools of BS to BS 10 only include rare unifacial points and denticulates (Wadley, 2012a, 2013). The younger 'pre-SB' stratum (LBG) yielded two OSL ages of  $70.8 \pm 3.2$  and  $70.9 \pm 2.2$  ka BP (Jacobs and Roberts, 2017). This assemblage is characterised by flakes and blades made on hornfels and dolerite. The rare retouched pieces include unifacial points and denticulates (Wadley, 2012a, 2013). Notched bone fragments and a bone wedge were found in the 'pre-SB' layers (d'Errico, et al., 2012b). One deciduous human tooth, a lower left first molar, comes from the base of layer BS 5 (Riga, et al., 2018).

The deposits belonging to the SB, with an age of  $69.5 \pm 2.1$  ka BP, lie directly above the 'pre-SB' and show technological discontinuity. The most significant and dominant characteristic is bifacial lithic technology, in particular, bifacial points (Wadley, 2007; Soriano, et al., 2009, 2015). Additionally, only the SB layers have yielded specimens of the marine gastropod *Afrolittorina africana*. Some of these small shells exhibit perforations and were putatively used as personal ornaments by the SB occupants (d'Errico, et al., 2008).

Strata assigned to the HP overlie the SB without any sterile layers in between. They have ages between  $60.5 \pm 1.8$  and  $58 \pm 1.7$  ka BP suggesting a chronological gap (Jacobs and Roberts, 2017), but see (Guérin, et al., 2013). The HP toolmakers of Sibudu predominantly employed different lithic reduction strategies, including HP cores, prismatic cores and cores on flakes, to produce blades using marginal percussion (Wadley, 2008; de la Peña and Wadley, 2014a, 2014b; de la Peña, 2015; Soriano, et al., 2015). The lithics of this period are also characterised

by the frequent transformation of large and small blades made on hornfels, dolerite and quartz (both translucent and milky) into a variety of backed tools (Delagnes, et al., 2006; Mohapi, 2008; Wadley, 2008; Wadley and Mohapi, 2008; de la Peña, 2015; Soriano, et al., 2015). Ochre and plant adhesive traces associated with hafting often occur on the backed edge of these backed pieces (Lombard, 2006, 2007, 2008; Wadley, et al., 2009). Both hafting lines and impact fractures support the hypothesis that the backed elements made on dolerite and hornfels were hafted diagonally and longitudinally as part of composite tools. Backed tools seem to have served as tips or barbs for hunting weapons, but also as cutting edges for domestic tools, with differences linked to raw material (Soriano, et al., 2015). The backed pieces made on dolerite and hornfels seem to represent an innovative way of hafting spear tips rather than armatures involved in bow and arrow technology (Wadley and Mohapi, 2008; Villa and Soriano, 2010). However, several lines of evidence suggest that the quartz backed tools may have been hafted as transverse arrowheads (Wadley and Mohapi, 2008; Lombard and Phillipson, 2010). A new study shows that unretouched quartz blanks were also mounted as barbs in hunting weapons (de la Peña, et al., 2018). Furthermore, the manufacture of small quartz bifacial points took place at the site, currently idiosyncratic to the Sibudu HP (de la Peña, et al., 2013). The HP layers also feature distinctive forms of bone technology including points, awls, smoothers, *pieces esquillées* and tools used for pressure flaking (Backwell, et al., 2008, 2018; d'Errico, et al., 2012b). Finally, more deciduous human teeth, a lower right central incisor and a lower right molar, originate from layer PGS and, like the teeth from strata BS 5 and Casper, are identified as Late Pleistocene MSA (Riga, et al., 2018; Will, et al., 2019).

The following extended part of the sequence has an age of roughly 58 ka BP and corresponds to the post-HP. Despite the short time period involved, repeated occupations seem to have taken place leaving 0.9 m of deposit (Wadley, 2013b). Several anthropogenic burning events were identified, some associated with the burning of reed/grass bedding material and others with discrete hearths as well as larger combustion features (Goldberg, et al., 2009; Wadley, et al., 2011; Wadley, 2012b). de la Peña and Wadley (2017) performed a cladistic analysis with the technological traits of the youngest HP layer (GR) and the oldest post-HP layers (RB-YA) to explore technological variability, identifying numerous technological changes over time. Some reduction strategies that were not part of the technical system in the HP become common in the post-HP, while others that are deeply-rooted in the HP are of minor importance in the post-HP. The outstanding new features in layers RB-YA are the Discoid reduction method, the low frequency of unstandardized retouched elements, and the high frequency of grindstones. The explanation proposed for the transformation of more formal HP technology to the more expedient post-HP relates to a trend towards reduced residential mobility (de la Peña and Wadley, 2017).

In response to problems surrounding the informal name of 'post-HP', it has been suggested that Sibudu should be considered as type-site for this phase (Conard, et al., 2012; Lombard, et al., 2012). Lombard and colleagues (2012) proposed the term 'Sibudu technocomplex', characterised by an emphasis on point production using the Levallois concept and typical Sibudu unifacial points with faceted platforms and elongated shapes. The type assemblage of

Sibudu itself shows subtle changes through time and is characterised by, on the one hand, two kinds of cores – unidirectional or bidirectional Levallois-like cores and bladelet cores – and on the other hand, a toolkit dominated by unifacial points and scrapers (Cochrane, 2006, 2008; Lombard, et al., 2012; Mohapi, 2012). Conard et al. (2012) coined the term ‘Sibudan’ and, based on their techno-functional analysis, identify the tool classes Tongatis, Ndwedwes, *biseaux* and naturally backed tools as the distinctive signatures of this technocomplex. Further technotypological studies of this high-resolution sequence dating to around 58 ka BP revealed short-term changes and strong diachronic signals so that the ‘Sibudan’ can be further subdivided into four facies that building on each other in a gradual and incremental manner (Will, et al., 2014; Conard and Will, 2015; Will and Conard, 2018; Bader and Will, 2017). The following informal descriptions denote the ‘Sibudan’ sequence (Will and Conard, 2018): ‘Lower Sibudan’ for the oldest layers RB-G 1, ‘Lower middle Sibudan’ for layers WOG 1 and Sp, ‘Upper middle Sibudan’ for layers Su-POX and ‘Upper/classic Sibudan’ for BM-BSp. The uppermost/classic phase constitutes the basis for the original definition of the ‘Sibudan’ and is distinguished by a rich tool corpus featuring primarily Tongati and Ndwedwe tools, asymmetric convergent tools and naturally backed tools, an increased use of hornfels, different methods of the Levallois concept to produce flakes including triangular flakes, and the frequent production of blades from platform cores. The preceding layers, Su-POX, show an almost exclusive use of dolerite, a predominance of the Discoid method and the earliest appearance of the four main techno-functional tool classes. The ‘Lower middle Sibudan’ exhibits the primary use of dolerite and sandstone, a prevalence of the Levallois concept, lesser emphasis on retouched elements which include notched pieces and denticulates, lower overall artefact density and a near-absence of the techno-functional tool classes. The ‘Lower Sibudan’ is characterised by the use of dolerite, sandstone, quartz and quartzite, the frequent employment of bipolar cores along with the lesser use of the Levallois concept, a low frequency of retouch, a complete absence of Tongati and Ndwedwe tools, and the occurrence of invasively shaped bifacial points made preferentially on quartz. Rare worked bone is present (d’Errico, et al., 2012b) and extensive use of ochre is observed in these layers (Wadley, 2010b; Hodgskiss, 2013).

The strata overlying the post-HP or Sibudan are referred to as late MSA (but the name is only used at Sibudu) and are dated to ca. 48 ka BP (Wadley, 2013b). The late MSA layers are characterised by a high frequency of retouched pieces, mainly unifacial points (Villa, et al., 2005).

The layers at the top of the MSA sequence are described as final MSA, with an age of around 38 ka BP. The toolkit encompasses bifacial and unifacial points, scrapers, wide segments, *pieces esquillées* and notched pieces. The most characteristic feature is the appearance of rare hollow-based points – bifacial, triangular points with bases thinned and shaped to a concave form (Wadley, 2005). An incised flake (Wadley, 2005) and a few worked bone tools also occur (Cain, 2004).

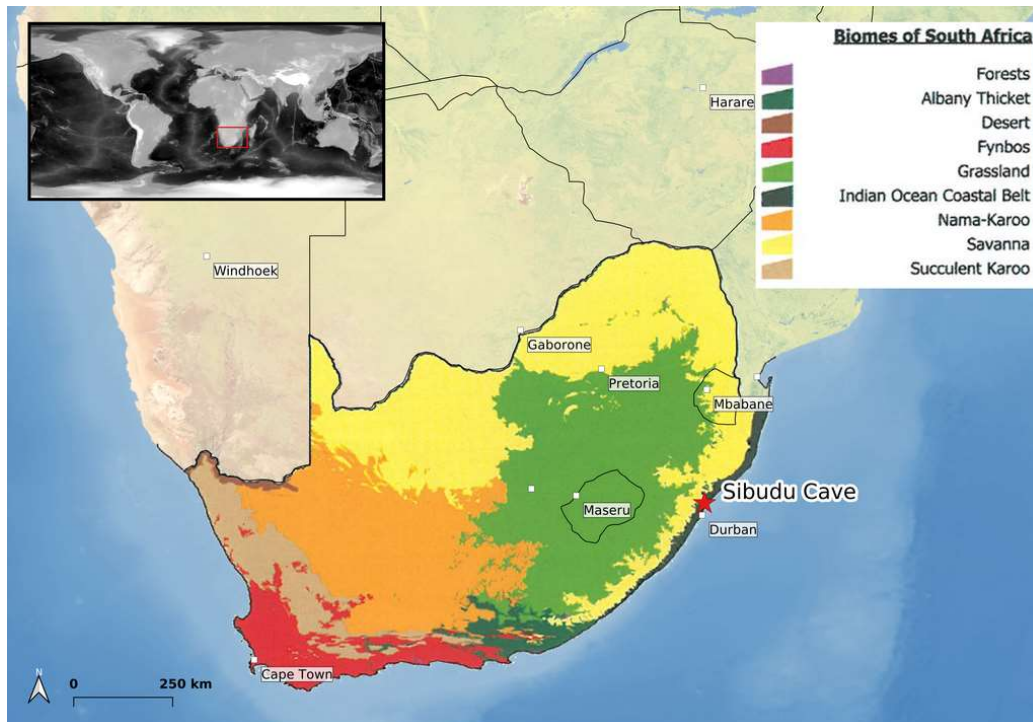
Below the modern surface, there are layers BSV (Brown Silt with Vegetation) and BSS (Brown Silt with Stones) containing Iron Age (IA) material culture. Charcoal from a pit of BSS provided an age of  $960 \pm 25$  BP (Pta-8015). Numerous pits were dug into the MSA deposits, causing a mixture of MSA and IA artefacts (Wadley and Jacobs, 2004).

#### *2.4. Environmental background*

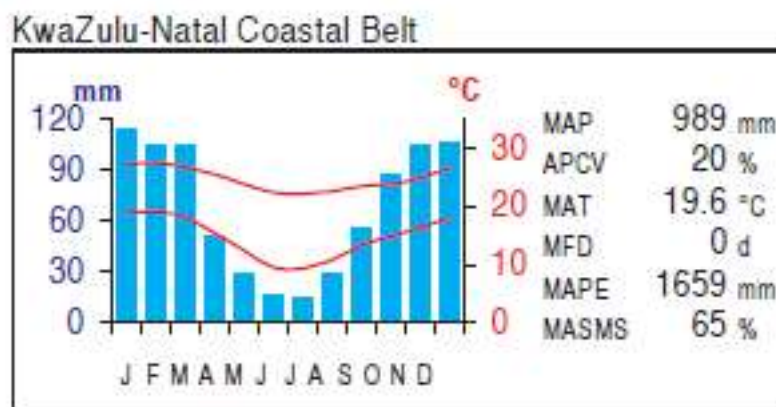
The environmental context of Sibudu Cave today is in the 800 km-long Indian Ocean Coastal Belt (IOCB) Biome (Figure 10). This stretches the coastline from Port Elizabeth in the south to the Limpopo River in Mozambique in the north, encompassing altitudes of 0 to 450 m (Wadley and Jacobs, 2004; Mucina, et al., 2006). Following the work of Bews (1920), Moll and White (1978), and Mucina et al. (2006), this coastal belt is dominated by forest cover featuring varying proportions of deciduous and semi-deciduous species, interrupted by patches of grassland. The biome is characterised by pronounced hot and moist tropical climatic conditions in the summer and mild, slightly drier subtropical conditions in winter, controlled by several global and macro-regional factors. Two atmospheric circulation systems are of great importance, namely the Intertropical Convergence Zone (ITCZ) and the warm Agulhas Current. These factors enable the globally southernmost occurrences of typical on shore (mangroves) and off-shore (corals) tropical flora and fauna (Mucina, et al., 2006).

The site lies in the section of IOCB referred to as the KwaZulu-Natal Coastal Belt, spanning from Mtunzini in the north to Port Edward in the south, which used to be mainly covered by various types of subtropical coastal forest (Figure 10) (Mucina, et al., 2006). The region falls within the Summer Rainfall Zone (SRZ), receiving less than 33% of its annual precipitation during the winter months of April to September (Chase and Meadows, 2007), but rain falls throughout the year (Figure 11). The mean total annual rainfall ranges between 819 and 1,272 mm. The mean annual air humidity is high, recorded as 79% in Durban. This humidity is comparable to regions further north on the east coast of Africa within the tropics, e.g. in Dar-es-Salaam (Tanzania) at 73% and in Mombasa (Kenya) at 74%. The mean maximum monthly temperature for Durban is 32.6°C in January (summer) and the mean minimum temperature is 5.8°C in July (winter). Frost does not occur.

Today, the natural vegetation of the coastal belt is poorly preserved due to its extensive eradication by deforestation and cultivation of sugar plantations; around 39% of the area of the IOCB has been already transformed and only 7% is formally protected in statutory reserves (Mucina, et al., 2006). This being said, the indigenous vegetation directly around Sibudu Cave has survived because the rugged cliff has prevented the expansion of sugarcane plantations and agricultural development. The valley and cliff where the rock shelter is situated are south-facing, offering shade until mid-afternoon and thus cooler aspects (Sievers, 2013). Evergreen species grow on the south-western slope adjacent to the shelter, while deciduous savannah woodland and grassland are found on the hot, exposed plateau above the shelter and on the nearby north-facing hill-slope (Wadley, 2013b). The riverine habitat of the uThongathi River includes grasses, sedges, small shrubs and trees (Sievers, 2013). Unfortunately, even these remains of the forest are threatened by invasive alien plants and are still exploited by local people for firewood, grazing, crafts, food, medicines as well as ritual purposes. For further



**Figure 10.** Biomes of southern Africa (modified after Meadows and Quick, 2016).



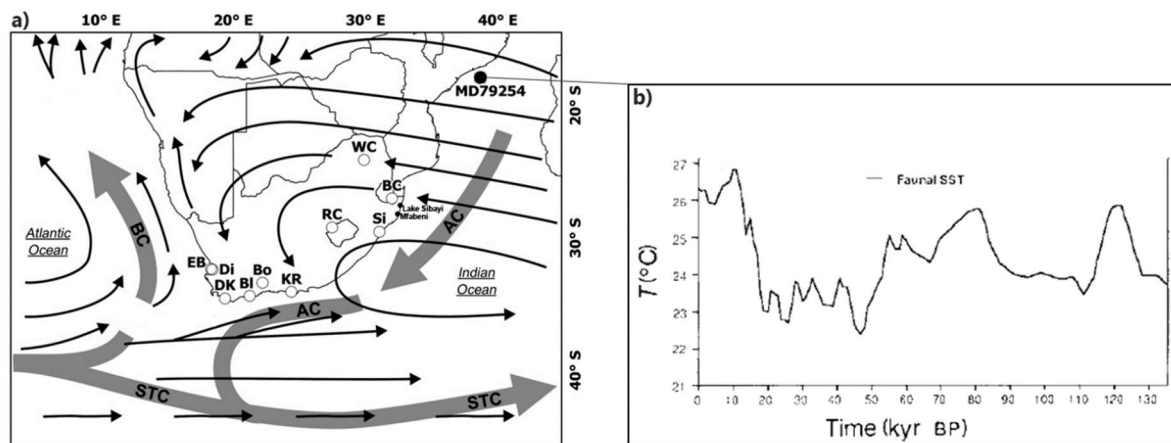
**Figure 11.** Climate diagram of KwaZulu-Natal Coastal Belt units. MAP: Mean Annual Precipitation; APCV: Annual Precipitation Coefficient of Variation; MAT: Mean Annual Temperature; MFD: Mean Frost Days (days when screen temperature was below 0°C); MAPE: Mean Annual Potential Evaporation; MASMS: Mean Annual Soil Moisture Stress (% of days when evaporative demand was more than double the soil moisture supply) (after Mucina, et al., 2006).

information, (Sievers, 2013) provides an extensive list of the remaining indigenous plant species in the modern Sibudu area.

The reconstruction of late Pleistocene palaeoenvironmental fluctuations for KwaZulu-Natal is difficult because of, firstly, the uncertainty surrounding climatic changes that triggered environmental variation and, secondly, the lack of sites providing high-resolution regional proxy data and reliable chronologies (Wadley and Jacobs, 2006; Chase, 2010; Meadows and Quick, 2016). In the past, this situation has led researchers – though aware of the limitations and caveats – to the application of coarse conceptual models. The interpretations of southern

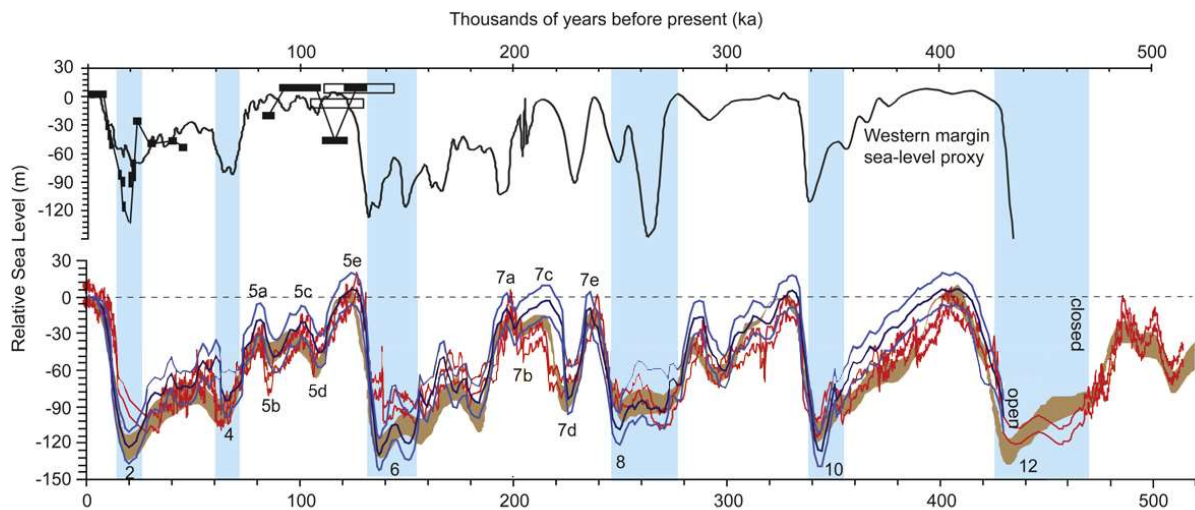


African archaeological sequences in general have been especially influenced by a model of environmental change inclined towards northern hemispheric or global patterns in which glacial and interglacial conditions correspond to 'cold and dry' and 'warm and wet' respectively (Chase, 2010). However, this approach poses several problems and should not readily be applied uncritically. The variety of mechanisms controlling southern African climate rules out a uniform or globally representative response to periods of global warming and cooling (Chase and Meadows, 2007). Moreover, the great heterogeneity of palaeoenvironments on a local and regional level prevent a simplistic broad classification into glacial and interglacial. Finally, the available southern African climate record indicates that using marine isotope stages as indicator of global conditions is inadequate for precisely reconstructing southern African palaeoenvironments (Chase, 2010). Returning to the first difficulty identified: although the tropical and temperate circulation systems that determine southern African climate and drive climatic change are still not understood in detail, the existing data allow of establishing hypotheses how they interacted (Chase, 2010). KwaZulu Natal falls within the SRZ so its climate is primarily driven by southwest (SW) Indian Ocean sea-surface temperatures (SSTs) and their impact on the moisture-bearing capacity of the easterly flows associated with the ITCZ and the temperature and competence of the Agulhas Current (Tyson, 1986; Chase and Meadows, 2007; Chase, 2010). The marine core MD79254 represents an important dataset documenting the SW Indian Ocean SSTs variations from MIS 5 until today (Figure 12) (van Campo, et al., 1990). Warmer SSTs result in more precipitation on the sub-continent, indicating that the warmest SSTs occurred during ~120 ka, ~80 ka, and ~10 ka and the coldest SSTs during ~50–18 ka. In agreement with this, (Finch and Hill, 2008) identified greater aridity around 24 cal ka BP along the KwaZulu-Natal coast causing the Mfabeni peatland and coastal forests to retreat. With regard to the second major difficulty in reconstructing palaeoenvironments, most regional data come from studies of stratigraphic sequences exposed in gully (donga) sidewalls across KwaZulu-Natal, where palaeosols are interposed with colluvial deposits demonstrating cyclical accretion and erosion (Wadley and Jacobs, 2006; Botha, et al., 2016). Pleistocene colluvium is considered to have been accumulated either during aridity or during transitions from dry to wet conditions when precipitation has increased but vegetation is still reduced (Botha and Partridge, 2000; Botha, et al., 2016). Conversely, pedogenesis may have occurred under periods of relative hill-slope stability influenced by greater humidity and thicker vegetation cover. A comprehensive chronological framework spanning over 135 ka was based on a combination of radiocarbon and luminescence dating methods to determine arid and wet periods in Kwa-Zulu-Natal (Botha, et al., 1992; Wintle, et al., 1995; Botha, 1996; Clarke, et al., 2003). Discrete phases of colluviation took place at ~110–96 ka, 56–52 ka, 47–41 ka and ~11 ka (Botha and Partridge, 2000). Additionally, an undated colluvial wedge from the Voordrag palaeosol succession bracketed by two radiocarbon dated palaeosols indicates that the period between ~42 and 37 ka was also arid (Botha, et al., 1992; Clarke, et al., 2003). At the western shores of Lake Sibayi, freshwater diatomite beds and calcareous clays developed between about 45 and 24.8 ka ago, suggesting drying out of the lake and thus providing further evidence for an arid period (Maud and Botha, 2000).



**Figure 12.** a) Map of southern Africa indicating the location of important MSA sites (EB, Elands Bay Cave; Di, Diepkloof; DK, Die Kelders; Bl, Blombos; Bo, Boomplaas; KR, Klasies River; RC, Rose Cottage; Si, Sibudu; BC, Border Cave; WC, Wolkberg Cave); dominant atmospheric circulation patterns indicated by thin black arrows, major ocean currents indicated by thick grey arrows (labelled as follows: BC, Benguela Current; STC, Subtropical Convergence; AC, Agulhas Current) and Lake Sibayi, Mfabeni peatland as well as marine core MD79254 indicated by filled circles (left; modified after Chase, 2010: Figure 1); b) Indian Ocean faunal SST estimates of marine core MD79254 for past 135 ka (after van Campo, et al., 1990).

During the last glaciation (ca. 115–11.7 ka ago), sea-level lowering affected the shoreline of KwaZulu-Natal. A sea-level curve from the Last interglacial until the present day has been reconstructed from a range of sea-level indicators at various locations along the South African margin, including beach rock formation, barnacles and attached oysters, locations of coastal wetlands and incised valley fills (Ramsay and Cooper, 2002; Carr, et al., 2010). The timing of sea-level fluctuations has also been extended to 440 ka (Compton and Wiltshire, 2009) (Figure 13). The South African sea-level curve is in general agreement with global sea-level records from the marine  $\delta^{18}\text{O}$  record of benthic foraminifera (Waelbroeck, et al., 2002; Bintanja, et al., 2005) and the  $\delta^{18}\text{O}$  record of foraminifera from the Red Sea (Rohling, et al., 2009) (Figure 13). During both MIS 5e and 5c, the South African shoreline is approximately +4 m amsl (Ramsay and Cooper, 2002). Until the end of MIS 3, sea-levels fluctuated between -40 and -70 m amsl. Due to the steepness of the continental shelf around the coastal margin of KwaZulu-Natal, this drop in sea-level did not lead to the exposure of much more land than is the case today. However, during MIS 2, the sea-level dropped to maximum low of -130 m amsl (Wadley and Jacobs, 2006). At the last glacial maximum, the shoreline in the Durban region was 30 to 40 km offshore of its present-day position and similar distances could be expected for the coastline off the Tongati River mouth (Wadley and Jacobs, 2004).



**Figure 13.** Sea-level fluctuations (bracketed by uncertainty) since 520 ka BP Waelbroeck, et al., 2002 in blue, Rohling, et al., 2009 in red and Bintanja, et al., 2005 in brown) compared with the sea-level curves for southern Africa above from Ramsay and Cooper (2002; filled boxes) and Carr et al. (2010; empty boxes) back to 145 ka BP, and from Compton and Wiltshire, 2009 based on a sediment proxy for the timing but not the amplitude of sea-level fluctuations on the western margin back to 440 ka BP (modified after Compton, 2011).

Sibudu itself provides a wide range of high-resolution proxy environmental data offering several lines of evidence. Analyses include geomagnetic susceptibility (Herries, 2006), mineralogy (Schiegl, et al., 2004; Schiegl and Conard, 2006), geology (Pickering, 2006), taxa identification from charcoals (Allott, 2006), charcoal carbon isotopes (Hall, et al., 2008, 2014), stable carbon and oxygen isotopes from faunal tooth enamel (Robinson and Wadley, 2018), macrobotanical remains (Wadley, 2004; Sievers, 2006, 2013), pollen (Renaut and Bamford, 2006), phytoliths (Murungi, 2017) and macro- as well as micro-faunal remains (Plug, 2004, 2006; Cain, 2006; Glenny, 2006; Wells, 2006; Plug and Clark, 2008; Wadley, et al., 2008; Clark, 2009, 2013; Val, 2016). This multi-disciplinary evidence from Sibudu combined with the albeit limited palaeoclimatic record of KwaZulu-Natal allows for fairly good reconstruction of the fluctuating palaeoclimates and environments around the site and their impact on the occupational history of past people (Table 3) (Hall, et al., 2014). A mosaic of habitats seems to have persisted during all occupation layers of Sibudu due to the aspect of the site and the proximity to the uThongathi River (Wadley, 2006, 2013; Robinson and Wadley, 2018). The river possibly paved the way to the localised occurrence of certain species that would not have survived in drier conditions. The greater exposure of the north-eastern slopes and the plateau to sunlight, compared to the southern slopes, support the growth of deciduous woodland, savannah and grassland plant communities. The cooler, sheltered south-western cliffs provide optimal conditions for evergreen forest taxa and also would serve as refugia for forest species during drier periods (Hall, et al., 2014). The charcoal (Allott, 2006) and seed analyses (Sievers, 2006) demonstrate that a lot of the taxa growing in and around Sibudu today were also present during the MSA, indicating at least some similar conditions to today. However, some plant species occur that are absent today, implying that more northerly vegetation elements

**Table 3.** Summary of proxy environmental evidence (modified after Hall, et al., 2014) – Occupation (Wadley and Jacobs, 2006), botanical data (Wadley, 2004; Allott, 2006; Renaut and Bamford, 2006; Sievers, 2006; Murungi, 2017), isotopic data (Hall, et al., 2008; Robinson and Wadley, 2018), and faunal data (Plug, 2004, 2006; Cain, 2006; Glenny, 2006; Wells, 2006; Clark and Plug, 2008; Clark 2009, 2011, 2017; Val, 2016), geology and mineralogy (Schiegl, et al., 2004; Pickering, 2006; Schiegl and Conard, 2006) and magnetic susceptibility (Herries 2006).

Occupation	General vegetation	General Climate	Seeds	Charcoal	Charcoal Carbon isotopes	Enamel Carbon and Oxygen isotopes	Phytolith & Pollen	Macrofauna	Microfauna	Avifauna	Mineralogy	Magnetic susceptibility
Chardal												
Casper												
Bra	Forest communities							Blue duiker, bush pig				
Balf												
Aminie												
Adam												
BS 1-16	Evergreen and deciduous forest communities, more closed	Warm and moist				pre-SB low $\delta^{13}C$ and $\delta^{18}O$ values	grass, sedge, woody plants			forest-dwelling species		
LBS, LBS 2-4						SB	grass, sedge, dicotyledonous plants					
RGS RGS 2	Evergreen and deciduous forest communities	Moist				similar $\delta^{13}C$ and $\delta^{18}O$ values to pre-SB				forest-dwelling species		
FGS						HP						
GS, GS 2	Predominance of evergreen forest	Cold, humid and moist	Sedge species	Poaceae dominates, other forest species are present	Cella & Potoocarpus $\delta^{13}C$ values more negative, Potoocarpus values have high variability	similar $\delta^{13}C$ and $\delta^{18}O$ values to pre-SB	Dominance of warm and wet climate grasses	Small forest species and many aquatic species. Blue duiker dominant small bodied	Crocomys gambianus, Rhinoceros chirox	forest-dwelling species	Layers dominated by calcite and the presence of some gypsum	
GR, GR 2												
DRG												
RB												
LBYA												
BYA2												
YA2												
BT under YA 2												
YA 1, YA 2	More open savanna and grassland environments	Coldest period in the MSA	Sedge species			similar $\delta^{13}C$ and $\delta^{18}O$ values to pre-SB	Grass, sedge, Acacia	Large bovids			High gypsum, increasing amounts in lower layers and also the presence of calcite	Indications of cold conditions
Box, Ymk												
BL 2, BL 3												
BGMix, BGMix 2												
Y 1												
Ch 2												
G 1												
MOG 1												
P 1												
Sp												
Su, Su 2	More open savanna and grassland environments	Warming period, cooler and drier than present	Asparagus sp. Poaceae occur in the majority of these layers			similar $\delta^{13}C$ and $\delta^{18}O$ values to pre-SB	Acacia, grass, fern, sedge species	Large bovids including species such as buffalo and equids			Gypsum in all the layers, increasing amounts in lower layers	A warming trend is indicated
Ch												
BM												
IV												
BP												
OP	Very reduced forested areas	Cold phase and very dry	Asparagus sp.	Acacia, Erica, Ziziphus		similar $\delta^{13}C$ and $\delta^{18}O$ values to pre-SB		Large bovids			Gypsum	Warm
POX												
BO												
Ma, MY		Warm and dry		Dry-adapted species		similar $\delta^{13}C$ and $\delta^{18}O$ values to pre-SB		Large bovids	Mastomys natalensis		Gypsum	Cool
Cha, Ea												
SS	More grassland	Cooler phase	Evergreen species dominates			similar $\delta^{13}C$ and $\delta^{18}O$ values to pre-SB	Grass	Large bovids			High gypsum	
BL, Or	Increased woodlands	Warmer conditions	Asparagus sp., Sedge	Erica, Potoocarpus, Leucosidea	Cella & Potoocarpus $\delta^{13}C$ values less negative	similar $\delta^{13}C$ and $\delta^{18}O$ values to pre-SB	Sedge, Acacia	Large and medium sized bovids present			High calcite, high gypsum	
SPCA	Increased grasslands	Cooler and drier phase	Asparagus sp., sedge	Erica, Acacia, Ficus		similar $\delta^{13}C$ and $\delta^{18}O$ values to pre-SB		Large and medium sized bovids present			High calcite, gypsum	
BSP												
BSP 2												
Ysp	Highly mosaic environment	Warming period, dry	Phoenix, ricinida, Pavetta sp., sedge	Acacia, Erica, Potoocarpus	Potoocarpus $\delta^{13}C$ values more negative	final MSA high $\delta^{13}C$ and $\delta^{18}O$ values	Grass	Large and medium sized bovids present	Mastomys natalensis		Calcite, high gypsum	Warmer
RSP												
GMOD, BMOD												
OMOD 2BL												
OMOD 2	More deciduous taxa	Cooler, dry	Pavetta sp. and sedge species present in most layers	Acacia, Erica present in upper layers	Cella $\delta^{13}C$ values less negative	high $\delta^{13}C$ and $\delta^{18}O$ values		Large and medium sized bovids present			High amounts of calcite and gypsum	Warmer conditions indicated NOTE: contradiction between Magnetic susceptibility and other proxies
OMODBL												
OMOD												
MOD												
Mod, Pu												
RD	open	Dry	Overall increase in deciduous species			high $\delta^{13}C$ and $\delta^{18}O$ values					High amounts of calcite and gypsum	
Ore, Ore 2												
PB												
Mou, Omou												
E5	Deciduous and evergreen forest	Warm similar to today but drier	Brachylaena spp., Acacia spp., Miconia spp., Chepochia spp., Phoenix ricinida, Kivua sp.			final MSA high $\delta^{13}C$ and $\delta^{18}O$ values						
ILC (Health)												
LEIOD												
Bu												
Co												

once grew in the region and that the dry woodland component of the vegetation may have been more extensive (Wadley and Jacobs, 2006).

A new quantitative method, the GIS-based Coexistence Approach (Bruch, et al., 2012), was applied to the fossil plant material from Sibudu which allowed researchers to quantify palaeoclimate and vegetation parameters despite the anthropogenically introduced bias of an archaeological site. This study demonstrates that during the HP, winters were slightly colder and drier than present, whereas summer temperatures and precipitation were similar. During the post-HP, winters were prominently drier and colder than present, possibly colder than during the HP. Summer temperatures remained the same, but summer precipitation decreased from the preceding HP to the post-HP. The late MSA is associated with a pronounced warmer phase than before, especially during winter. At the same time, summer precipitation slightly increased (Bruch, et al., 2012).

With regard to layers Chantal to Adam relevant for this study here, I can only make a very first statement. A preliminary faunal identification of layer Casper (Conard, 2013) revealed the presence of blue duiker (*Philantomba monticola*), and *Potamochoerus porcus* (bush pig), which are commonly found in forest habitats.

Palaeoenvironmental information available for the pre-SB and SB is limited. However, the avifaunal analysis of the pre-SB and SB layers (Val, 2016) revealed the presence of forest-dwelling species, such as the African olive pigeon (*Columba arquatrix*), trumpeter hornbill (*Bycanistes bucinator*), buff-spotted flufftail (*Sarothrura elegans*) and turacos (*Musophagidae* sp.). These taxa highlight the importance of an evergreen forest component in the vicinity of the rock shelter during the pre-SB and SB. The Cape parrot (*Poicephalus robustus*) was identified in the late pre-SB layers, BS, LBG3 and LBG2 (Val, 2016). This species exists today only in KwaZulu-Natal and is almost extinct in the rest of South Africa (Sinclair, et al., 2011). The Cape parrots need tall trees for nesting and they live in temperate forests, preferably *Podocarpus* (yellowwood) spp. forests (Wirminghaus, et al., 2012). The bird assemblage of the pre-SB encompasses only a few species indicating open conditions (Val, 2016) contradicting the assumption of a mosaic of habitats at the end of an interglacial stage (>77 ka BP) (Plug and Clark, 2008). This being said, one possible bias can be that certain taxa associated with savannah or grasslands neither inhabited rock shelters nor were preyed upon by rock-dwelling birds of prey. Therefore, if they are not introduced into the site by humans, they do not appear in the archaeological assemblage (Val, 2016). The phytolith record (Murungi, 2017) confirms warm and moist conditions coinciding with the end of an interglacial period and attests to a mixed vegetation of grasses, sedges and woody plants in the vicinity of Sibudu during the pre-SB. The low stable carbon and oxygen isotopes collected from faunal tooth enamels imply a more closed, likely forested, and wet habitat compared to the rest of the sequence (Robinson and Wadley, 2018). The phytoliths of the SB suggest continuing moist conditions and a mixed environment of grasses, sedges, and dicotyledonous plants (Murungi, 2017).

The micro-faunal analysis (Glenny, 2006) shows that the Gambian giant rat (*Cricetomys gambianus*) occurred in the HP layer GS. This animal is not present in KwaZulu-Natal today, preferring evergreen forests and woodland that receive more than 800 mm rainfall per annum, thus indicating at least partially more humid or moister conditions than today (Wadley, 2013b). Additionally the Geoffroy's horseshoe bat (*Rhinolophus clivosus*), which occurs in the HP layers GS and GR (Glenny, 2006), prefers sandstone caves with humid conditions. The sediments belonging to the HP contain more calcite than gypsum (Schiegl and Conard, 2006). Both calcite and gypsum require moisture for their formation and are water-soluble, but calcite dissolves less readily after its formation. The high frequency of calcite, yet absence of gypsum, in the HP implies a period of greater humidity than after ~58 ka in the post-HP when large quantities of gypsum suggest arid conditions (Wadley, 2013b). Furthermore in the HP, charcoal is dominated by *Podocarpus* spp. (Allott, 2006), indicating evergreen forest around Sibudu in the final stage of MIS 4. The identification of Cape parrots in the HP layers additionally emphasises the evergreen forest component (Val, 2016). This is supported by the presence of other fauna that prefer forest habitats including *Cephalophus natalensis* (red duiker), blue duiker, bush pig, *Tragelaphus scriptus* (bushbuck), and *Chlorocebus aethiops* (vervet monkey) (Clark and Plug, 2008; Clark, 2011, 2017; Wadley, 2013b). The lowermost layer of the HP contains the highest frequency of blue duiker, small ungulates and closed-dwelling taxa. The significant decline of these species over the course of the HP relates primarily to changes in the local environment, but also reflects changes in subsistence strategies, hunting weaponry and/or site use (Clark, 2017). The HP seems to represent cooler conditions than today that possibly allowed for more effective moisture retention supporting a substantial evergreen forest with patches of open woodland/savannah (Hall, et al., 2014).

Archaeomagnetic based studies (Herries, 2006) for the early post-HP layers YA2 to G1 imply that this is the coldest phase within the whole sequence. However, since the deposits were accumulating mostly from anthropogenic activities and were not climatically driven (Goldberg, et al., 2009), the magnetic susceptibility data must be treated with caution. The near-disappearance of forest birds during the post-HP corresponds to a decrease of forest cover and a shift towards drier and more open conditions (Val, 2016). In layer Eb, towards the top of these layers with an age of ~58 ka BP, charcoals of *Erica* sp., *Acacia* spp., *Morella* sp., *Ziziphus* sp. and *Leucosidea sericea* (Allott, 2006) are identified, which are not part of the vegetation community today. *Leucosidea sericea* can represent a pioneer species and is most often found in higher altitudes and in areas with cold winters. The appearance of this taxon implies that rapid environmental change may have been taking place at the time (Wadley, 2013b). Correspondence analysis of seed and faunal data (Reynolds, 2006) from this period confirms fluctuations in response to a changing environment. The seed assemblage contains a mixture of sedges and woody trees as well as shrub species. The presence of Cyperaceae nutlets in the lower post-HP layers implies open or semi-permanent water. Most of the other identified seeds come from evergreen forest species, but deciduous taxa increase in the younger post-HP strata coinciding with the warming trend (Sievers, 2006). Woody species from charcoal analysis suggest the continuous presence of an evergreen riverine forest component (Allott, 2006).

*Podocarpus* spp. does not occur in the earlier post-HP deposits and only reappears in layer SPCA (Wadley and Jacobs, 2006). The pioneer species Natal multimammate mouse (*Mastomys natalensis*) was identified in the upper post-HP deposit MY (Glenny, 2006). This taxon is not forest-dwelling and can inhabit dry areas due to its degree of water independence (Skinner and Chimimba, 2005). The earlier and younger post-HP layers show great differences in their faunal composition. Small bovids decrease and are almost absent in the uppermost part which is instead dominated by large species such as equids and large to very large bovids (Plug, 2004). Grazers occur throughout the post-HP sequence but in higher frequencies in the younger layers (Plug, 2004; Clark and Plug, 2008), suggesting a shift from subsistence based on fauna from closed forest environments to exploitation of animals in drier, more open savannah/grassland communities. The initial phase of the HP was most likely a cold phase, followed by a warming trend. However, in contrast to the afforestation occurring in the HP, open woodland and grassland vegetation was more common during the post-HP (Hall, et al., 2014). The data resulting from the enamel stable isotopes are suggestive of stable conditions during the SB, HP and post-HP characterised by a closed forested vegetation, but with a slightly drier climate than in the pre-SB (Robinson and Wadley, 2018).

Magnetic susceptibility data (Herries, 2006) imply a warming trend in the late MSA. Proportions of gypsum are high suggesting arid conditions in the shelter (Schiegl and Conard, 2006). The presence of Cyperaceae nutlets (Sievers, 2006) and the occurrence of hippopotamus (*Hippopotamus amphibious*) (Plug, 2006) point to the presence of a permanent water source. Seeds of evergreen species persist, but the proportion of deciduous species increases during the late MSA. Charcoal analysis attests to a typical plant community for deciduous savannah woodland, including *Acacia* spp., *Albizia* spp., and *Celtis* spp. (Allott, 2006). Layer RSp is the youngest to contain *Podocarpus*. The faunal remains indicate mixed environment with savannah, grassland, and woodland habitats (Plug, 2004; Wells, 2006). The Gambian giant rat is present in layer RSp suggesting the presence of forested areas (Glenny, 2006). The re-occurrence of the Natal multimammate mouse implies an environmental change and the onset of a cooler period prior to or during the deposition of RSp (Glenny, 2006). The late MSA seems to represent a warmer and more humid phase than the post-HP, with more open vegetation (Hall, et al., 2014).

The final MSA may represent a relatively warm phase within MIS 3, possibly drier than today (Wadley, 2013b). *Brachylaena* spp., *Acacia* spp., *Mystroxydon aethiopicum*, *Erica* sp., *Clerodendrum glabrum*, cf. *Phoenix reclinata* and *Kirkia* sp. occur and are reminiscent of bushveld vegetation that is nowadays restricted to northern South Africa (Allott, 2006). The faunal stable isotope analysis demonstrate higher  $\delta^{13}\text{C}$  and  $\delta^{18}\text{O}$  values in the late MSA and final MSA indicating more open and drier environmental conditions than before (Robinson and Wadley, 2018).

Interestingly, two hiatuses occur between the post-HP and the late MSA and between the late MSA and the final MSA, which correspond to periods of colluviation. It seems that MSA people

rather inhabited Sibudu during phases of pedogenesis reflecting more humid conditions than during colluviation. Thus, climate and environmental forces may have partially contributed to determining occupation or abandonment of Sibudu Cave in MIS 3 and other periods (Wadley and Jacobs, 2006). However, the scenario is clearly more complex because the long occupational hiatus between the final MSA at ca. 38 ka BP and the Iron Age and the accompanying lack of LSA occupations cannot be explained by climatic and environmental causes alone.



### 3. Methods

In this chapter, firstly I expand on the method of excavation to illustrate the high-value and high-resolution documentation of the lithic material within the archaeological context. I then describe the strict protocol we follow to process all the finds in such a way that subsequent analyses and later final archiving in the museum are well ensured. Secondly, I elaborate on the technological, techno-economic, techno-typological, and techno-functional methodological procedures that I applied to study the lithic artefacts of the basal deposits from Sibudu. I provide the theoretical background to these approaches and highlight that due to the comprehensive framework, I was able to gain a wide range of data to address my research questions concerning the characterisation of the assemblage, human behaviours and technological variability in time and space. Finally, I explain how the analysis proceeded in practice, what analytical tools I used and what attributes I recorded.

#### *3.1. Methods of excavation*

The new excavation of the University of Tübingen is carried out in two excavation areas, the Deep Sounding (DS), including squares A5-4, B5-4 and C5-4, and the Eastern Excavation (EE), involving squares C3-2, D3-2 and E3-2 (Figure 8) (Conard 2013). The research team adopted the excavation grid and layer definition and designation introduced by Wadley and established reliable chrono-facies that link stratigraphic units of the previous excavations with the new areas (Conard, et al., 2012). The excavation method used by our team complies with modern standards and follows a strict protocol, allowing the optimal documentation of the context of the finds.

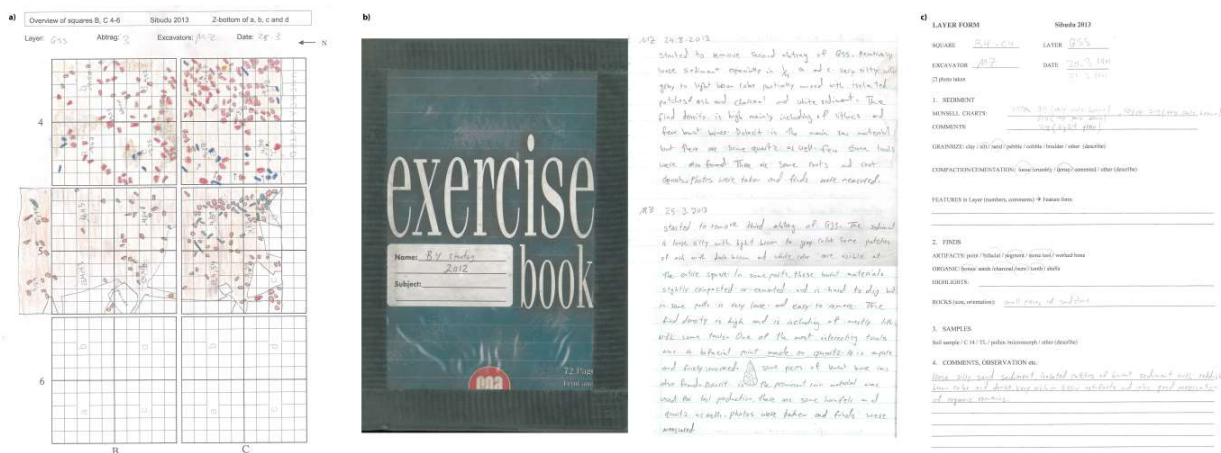
With regard to my data, it is important to mention that one single archaeologist excavated all of the assemblage. Since 2012, Mohsen Zeidi (University of Tübingen) has had the delicate task of exposing the new layers in the DS (Figure 14). His expertise and excavating accuracy ensure a unified high-quality documentation of the archaeological record. The protocol used for the fieldwork at Sibudu adheres to a slightly adjusted version of the Tübingen excavation conventions originally established by (Hahn, 1988).



**Figure 14.** Sibudu: M. Zeidi in the DS in March 14<sup>th</sup>, 2012 (Photo by Sarah Rudolf).

Following standard excavation procedures adopted by Wadley's team as well, every square metre is subdivided into four 50x50 cm quadrants. These are identified by lower case letters whereby quadrant *a* is located in the northwest, *b* in northeast, *c* in the southwest and *d* in the southeast. In each quadrant, excavation proceeds in ca. 10-30 mm thick *Abträge* that follow the natural slope of the sediments and never crosscut geological strata. These *Abträge* represent the smallest time-unit discerned at Sibudu and sometimes equate to defined archaeological layers. The *Abträge* are numbered and documented by layers and features. Features are defined as sedimentary events that do not spread over an area larger than a quarter square metre, are excavated separately from layers and are numbered within the associated layer. Zeidi always starts digging a new *Abtrag* in the northwest corner, i.e. in quadrant *a* of square A5, following the natural southeast slope of the deposits. As logistical limitations make it impossible to expose one *Abtrag* on the whole excavation surface of the DS at once, Zeidi excavates every *Abtrag* square by square using a stuccoer's iron. He takes soil samples of each *Abtrag* in each square in quadrant *c*. Micromorphological samples are taken as well, whenever found necessary.

After the completion of an *Abtrag* in one whole square metre, Zeidi starts the documentation procedure. This includes a drawing of the situation of any finds present (Figure 15a), writing an entry in the square diary to provide information of sediment changes, particular features and/or finds (FIGURE 15b) and taking photos. Photos with target points for photogrammetry were taken following the workflow suggested and implemented by Magnus H. Haaland so that later image-based 3D models can be generated. Furthermore, for every new layer, Zeidi fills out a new layer form, which includes information on colour, grain size, compaction of the sediment, find density and presence of artefacts, features and rocks (FIGURE 15c). Where a new feature is identified, he also fills out a new feature form, including information on sediment and finds.



**Figure 15.** Sibudu: a) Drawing of *Abtrag* 3 in layer Bart (GSS) with indication of serrated piece B4-1170 by M. Zeidi (lithics in red; faunal remains in blue, ochre in orange); b) diary of square B4 with diary entries of March 24<sup>th</sup> and 25<sup>th</sup> 2013 with drawing of serrated piece B4-1170 from layer Bart (GSS) by M. Zeidi; c) layer form of layer Bart (GSS) filled out by M. Zeidi.

Our team then piece-plots all lithic single finds over 30 mm in maximum dimension and all faunal remains larger than 40 mm – making exceptions for smaller identifiable items like worked boned, retouched objects or cores – with a Leica total station and the EDM program (Dibble and McPherron, 1996). Due to the depth of the DS, we measure most of the finds with a prism. In the western part of the excavation area, logistical difficulties, namely the poles to stabilise the profiles, force us to use offsets. All individual finds with no significant long axis are measured at the middle point on the topside of the object. Single finds with a significant long axis (long axis ratio over 1.8) are measured at three points on the exposed surface of the object: at the middle, the highest point, and the lowest point. For the recorded pieces with a significant long axis, the inclination and orientation are also noted in order to retrieve information about the embedding conditions, e.g. if sorting by solifluction occurred. The artefact inclination or ‘dip’ is indicated by numbers 1 to 5, whereby 1 stands for completely horizontal and 5 for completely vertical. The orientation description is organised into a military clock system with 12:00 representing north. The lowest point of the artefact is the measured origin on the clock, for example a base point of 6:00 would indicate the artefact is sloping downwards to the south. For horizontal finds with a dip measurement of 1, their orientation is recorded as afternoon times, so a north-south oriented artefact would be recorded as 18:00.

After finds have been recorded *in situ* with the total station, each is then put into a small plastic bag with an individual find tag giving details of the square, find number successive per square, layer, feature where relevant, archaeological designation (e.g. blank, tool, core), date, excavator and z-value. Since 2014, Zeidi has collected sediment samples close to specific lithic artefacts which is added to the find bag. He then also marks the bag with a cross, meaning that it should not be washed as it is designated for residue analysis. Rocks larger than 10 cm are measured after being fully exposed with as many points as necessary to record three different aspects: the long axis of the rock, the outline and the highest and the lowest point of the long axis. With regard to features, when their full extent is uncovered, we measure the outline and highest and lowest points. To record the top surface of a newly exposed layer, we take a sufficient amount of measuring points on the surface. To finish a measuring session, we record one central point in each quadrant which refers to the bucket with the collected excavated sediment. We give every bucket a plastic bag with a find tag that includes all the information provided for the single finds, together with its own information. The archaeological designation is always EI, referring to the German word for bucket ‘Eimer’, with the quadrant as a suffix in lower case and the volume of the excavated deposit, taken from measurement markings on the sides of buckets which hold a maximum of 10 litres. After the measuring session, we dry sieve every bucket of sediment with superimposed screens of 5 mm and 1 mm mesh to retrieve all the smaller pieces as well as any larger objects that were not detected during excavation. The volume of residue left in each sieve is additionally recorded on the back of the find tag, meaning that the provenience of small screen residues can be allocated to within a quadrant and a maximum thickness of 30 mm.

To keep track of layer boundaries, Zeidi marks the bottom surface of every layer with pins in the same colour and attaches a plastic label to the profile wall. At the end of every excavation season, before the refilling of the DS to secure the site, we document all of the profiles.

All of archaeological material recovered is further processed in our excavation house in Ballito according to our comprehensive manual.

Firstly, all single finds are hand-washed in water with latex free gloves. The residue analyses have shown that although the washing process is not optimal, residues are still preserved on the artefacts after washing. Faunal remains and lithics are all labelled with the exception of bifacial pieces. Bifacial pieces follow a different protocol to avoid that the labelling conceals shaping removals.

Secondly, the coarse fraction of the sediment (from the 5 mm screen), so-called 'bucket finds', are sorted. During the process of sorting, if an artefact is found that complies with the single find category (lithic blank >30 mm, worked bone, worked ochre, etc.) then it is 'upgraded', washed, labelled and catalogued with the single finds. Each upgraded find is allocated a sub-number that is added to the final find number for that bucket. For example, if the final find number of the bucket is 832, the number of the first upgraded find will be 832.1, the second upgraded find will be 832.2 and so on.

All remaining finds that are not upgraded are sorted according to their category. We put each category in one bag that is labelled with the respective abbreviation and the number (n) or weight (g). All lithic small debitage is sorted and counted according to three size categories: KD 30 = all small debitage >20 mm and <30 mm, KD = all small debitage >10 mm and <20 mm, and MD = all micro debitage >5mm and <10mm. When the sorting and packing is finished, the categories are put together in a large find-bag labelled with the site name, excavation year, square, quadrant, find number, layer and z-value.

Thirdly, we also sort the fine fraction (from the 1 mm screen). Because of the large quantity recovered, fine sediment is only sorted in selected DS quadrants since 2012: quadrants *b* of B4, B5, C4 and C5. From this fine fraction material, micro-debitage, microfauna, fish remains, molluscs and botanical remains are separated. The fine sediments are analysed under the microscope to detect any botanical remains that are too small to catch with the naked eye. Each find category from the fine fraction is put into a bag and then packed together in the large find-bag with the remains from the coarse fraction.

Fourthly, after all bucket sediments are sorted, we enter their information into the superordinate main Microsoft Access database for Sibudu in the form 'Eimer'.

For all upgraded lithic finds and lithic single finds, I enter the attributes, including raw material unit (dolerite, hornfels, quartz, quartzite, sandstone, chert, indetermined), technological classification (blank, angular debris, tool, core, hammerstone) and blank description (blade, bladelet, flake, triangular flake), in the form 'lithic analysis' of the Sibudu main database during the field season.

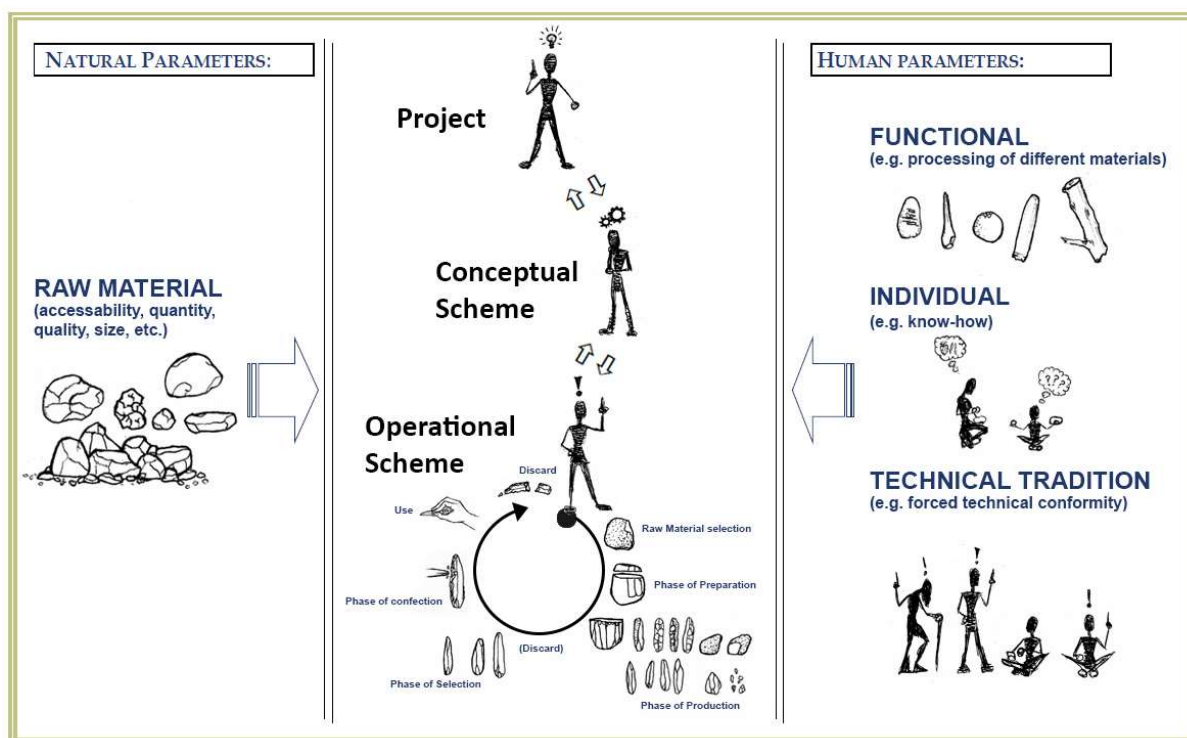
Finally, after data have been entered into the database, all find categories (e.g. lithic artefacts, bones, ochre pieces, etc.) are separated and sorted into larger bags by layers. They are then stored in respective boxes in such a way that they can be readily access for subsequent analyses. All recovered archaeological specimens are permanently stored at the KwaZulu-Natal Museum in Pietermaritzburg (South Africa, 237 Jabu Ndlovu Street) (Figure 16).



**Figure 16.** Permanent storage of all lithic specimen from layers Adam to Chantal at the KwaZulu-Natal Museum in Pietermaritzburg (Photo by Viola C. Schmid).

### 3.2. Methods of Study

I apply a technological approach to study the lithic assemblage. Lithic technology is defined here as concerning all activities of prehistoric humans related to the creation, transformation and use of lithic objects (Haudricourt, 1964; Inizan, et al., 1999). I implement the technological approach of the *chaîne opératoire* which uses each artefact in the assemblage to reconstruct the temporal operational sequence of the different technical stages, from raw material acquisition, blank production, tool manufacture and use to discard (Leroi-Gourhan, 1943, 1964; Lemonnier, 1976; Tixier, 1980; Cresswell, 1983; Pelegrin, et al., 1988; Boëda, et al., 1990; Geneste, 1991; Karlin, et al., 1991; Inizan, et al., 1999; Wurz, 2000; Soressi and Geneste, 2011). The nature of the analysis itself is descriptive based on rigorous, in-depth observations and, because stone tools represent the work of craftsmanship, strives to expose the intentions and knowledge of the craftspeople (Tixier, 2012; Porraz, et al., 2016). The interpretations, in terms of variability and diversity in intentions/technical choices, are founded on a theoretical framework aligned with the analyst and the research questions (Porraz, et al., 2016). In my theoretical background here, I propose that the lithic production first emerged as a cognitive project which was then converted, on an intellectual level, into a conceptual scheme that finally underwent concretisation through a series of operations representing the operational scheme (Figure 17) (Pigeot, 1991; Inizan, et al., 1999; Soressi and Geneste, 2011).



**Figure 17.** Theoretical framework of the technological approach, including the relationship between project, conceptual scheme, and operational scheme (modified after Soressi and Geneste, 2011: Figure 3; Porraz, et al., 2016: Figure 5; drawing by Heike Würschem).

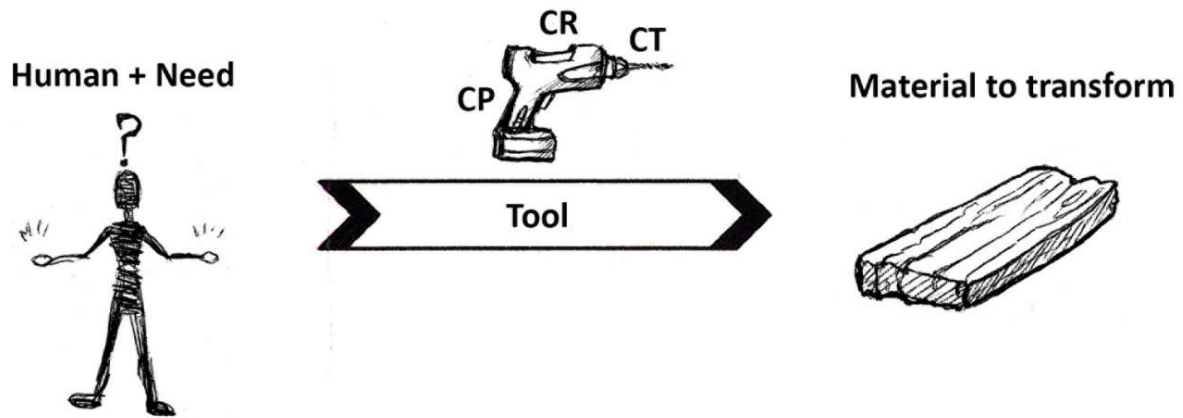
Each of these steps is dependent upon and influenced by several, partly interacting, natural (raw material accessibility, quantity, quality, size, etc.) and human parameters (functional needs, individual know-how, technical traditions, subsistence, belief systems, etc.) (Jelinek, 1976; Boëda, et al., 1990; Pigeot, 1991; Inizan, et al., 1999; Soressi and Geneste, 2011; Porraz, et al., 2016). Thus, the constancy or recurrence of pattern(s) in a lithic assemblage allow for this to be interpreted as intentional (Soressi and Geneste, 2011).

The basic analytical principle of a lithic technological analysis is that the production of stone tools is a reductive technology that depends on the property of conchoidal fracture. The process of conchoidal fracturing is governed by three main physical constraints (Collins, 1975: 16; Porraz, et al., 2016: 208), namely the mechanical properties of the rock, the geometric shape of volume, and the application and control of force (Goodman, 1944; Kerkhof and Müller-Beck, 1969; Crabtree, 1972; Speth, 1972; Tsirk, 1974; Dies, 1975; Callahan, 1979; Cotterell and Kamminga, 1979; Johnson, 1979; Roche and Tixier, 1982; Cotterell, et al., 1985; Cotterell and Kamminga, 1987, 1990; Bertouille, 1989; Dibble and Whittaker, 1981; Hahn, 1991; Weißmüller, 1991; Pelcin, 1996, 1998; Dibble and Pelcin, 1995; Pelegrin, 2000; Dibble and Rezek, 2009; Rezek, et al., 2011; Magnani, et al., 2014). Once the toolmaker has empirically incorporated these constraints, they become rules. By following these established rules, it is possible to control and predict the fracture (Porraz, et al., 2016). Consequently, technological analysis allows one to assess deterministic constraints before making assumptions about cultural choices (Inizan, et al., 1999: 13).

The intention of knappers is ultimately to produce a tool designed in a way to serve a distinct function (Porraz, et al., 2016). The tool obtains its specific technological characteristics as a pre-determined blank resulting from *débitage* (knapping, for definition see Boëda, 1991: 41; Chevrier, 2012: 141); Boëda, 2013: 52f.) and/or by a stage of *confection* (for definition see Boëda, 2013: 52). If a *confection* is applied to the pre-determined blank, I refer to the tool as retouched tool (*outil retouché*). If the pre-determined blank is used as tool without *confection*, I refer to the tool as utilised tool (*outil brut*) (Bonilauri, 2010: 27ff.). To understand a tool itself, we, as analysts, should take into account all technical steps behind its manufacture which will vary according to foreseen intended actions/tasks, the availability of geological resources, the skill of the knappers, the technical subsystem (e.g. the hafting mode, the mode of propulsion of the tool), the subsistence strategy and the traditions of the tool-manufacturing population (Porraz, et al., 2016). I hypothesise that these traditions are products of cumulative culture (Tomasello, 1999) or constituted culture-dependant traits (Reindl, et al., 2017); that is, they required cultural contact or transmission, including active teaching plus a high selective social pressure towards standardisation (compare Whiten, et al., 2003). The tool is considered as the integral part of a deliberate, non-random system of fabrication, maintenance and abandonment. Hence, strong connections are expected between raw material selection, core reduction strategies, outcome of (pre-determined) blanks and the production, use and discard of tools (Conard, et al., 2012).

I propose that the inhabitants of Sibudu aimed to produce specific tool forms at specific times and these tools underwent life-histories reflecting their manufacture, use, curation, recycling and discard (Conard and Adler, 1997). Accordingly, the tool types are governed by dynamics of re-sharpening, continued utilisation, and recycling in their life-cycles, partly explaining the variability in intensity of modification seen in a lithic assemblage (Krukowski, 1939; Frison, 1968; Dibble, 1987; Kuhn, 1990; Clarkson, 2002a; Andrefsky, 2006; see Hiscock and Tabrett, 2010 for review). Moreover, the investigation of the life-history of tools allows us to make statements about raw material economy (Dibble, 1991; Andrefsky, 1994; Clarkson, 2002b), occupation duration and intensity (Rolland and Dibble, 1990; Kuhn 1991; Surovell, 2012) , and mobility strategies (Kuhn, 1992; Odell, 1996; Holdaway and Douglass, 2015). Therefore, in addition to adopting a traditional typological approach, I follow the concept of the Pradnik Cycle (Krukowski, 1939). I assume that well-defined regulated phases of tool production, usage and discard left its recurrent marks on the lithic assemblage as tools from different stages occur, enabling the reconstruction of clear patterns and ultimately determining the life-cycle of the tool (Conard, et al., 2012).

I also adopt a techno-functional approach to provide functional characterisations of the tools based on technical features (Lepot, 1993; Boëda, 1997, 2001, 2013; Bourguignon, 1997; Soriano, 2000, 2001; Bonilauri, 2010; Lourdeau, 2010; Nicoud, 2011; Chevrier, 2012; Conard, et al., 2012). A tool consists essentially of three techno-functional units (*Unité Techno-Fonctionnelle* (UTF)): a transformative part (*Contact Transformatif* (CT)) intended to be in contact with the worked material, a passive part (*Contact Préhensif* (CP)) intended to be handled, and an intermediate part (*Contact Réceptif* (CR)) that connects the working edge and the prehensile end, passing on the transmitted energy during an action (Figure 18).



**Figure 18.** The three types of contact of a tool (modified after Nicoud, 2011: Figure 9; Lepot, 1993; drawing by Heike Würschem).

UTFs are defined as an ensemble of technical elements and/or characteristics that coexist in a synergy of effects (Boeda, 1997: 34). The three units, depending on the tool, can be very pronounced or rather subtle, but the basic principles are universal. One of the central aspects of the techno-functional approach is the study of the patterns of retouch. They depend on a couple of variables, including the physical attributes of the hammer substrate, and the motion and force of percussion applied by the toolmakers determining the edge characteristics with respect to the intended task(s) (Conard, et al., 2012).

These technological and techno-functional approaches, combined with use-wear and residue analyses, and supplemented further with experimental data, provide multiple lines of evidence to underpin and strengthen certain hypotheses about the dynamics of production, use and discard of stone tools within an assemblage (Conard, et al., 2012; Rots, et al., 2017). In collaboration with the use-wear specialist Veerle Rots (TraceoLab/University of Liège, University of Tübingen), the residue analyst Carol Lentfer (TraceoLab/University of Liège) and the experimental archaeologist Christian Lepers (TraceoLab/University of Liège), we had the opportunity to integrate of all these fields to yield a combined, robust set of results on the manufacture and function of the tool class of serrated pieces (for further details see Chapter 5.6.2.2.) (Rots, et al., 2017).

By applying such a comprehensive framework and incorporating different technological methodological procedures, my goal is to maximise the information that can be obtained from limited archaeological data (Collins, 1975: 15) to describe the different technical events underlying the lithic assemblage, to decipher their associations and characteristics (Porraz, et al., 2016) and to make inferences about human behaviours in layers Adam to Chantal from Sibudu. To achieve a more holistic picture of past behavioural patterns, one has to explore the relationship of the lithic technical sub-system to other interrelated technical sub-systems, such as food collection/hunting or food processing (Soressi and Geneste, 2011). As research into the



faunal remains is still in progress, this must be part of future work. Moreover, as stated above, groups of hunter-gatherers made different technical choices and passed them on from one generation to the next. Consequently, they established different traditions, creating variability. Detailed technological analyses allow comparison with other assemblages to examine similarities and differences in technical choices to achieve a better understanding of temporal and spatial variability of lithic technology in broader cultural context (see Jelinek, 1976; Lechtman, 1977; Sackett, 1982; Wiessner, 1983).

### 3.2.1. Protocol of the technological Study

To highlight the technical choices made during each step of the knapping process, I followed a specific study protocol inspired by (Soressi, 2002; Soressi and Geneste, 2011):

As mentioned above, I undertook an initial classification of the lithic finds during the excavation and accordingly, the lithic artefacts are separated into blanks, angular debris, tools and cores. I then continued with the study protocol at my provided working space in the KwaZulu-Natal Museum in Pietermaritzburg.

First, I laid out the whole lithic assemblage of each layer on a table to make a first general observation, keeping artefacts separated according to technological classification (see for example Figure 19).

Based on this superficial, visual examination, I defined *a posteriori* (vs. *a priori*, see Soressi and Geneste, 2011) the attributes to be recorded, allowing for quantification on each individual



**Figure 19.** Lithic assemblage of Adam laid out on the table to make a first general observation (Photo by Viola C. Schmid).

piece, or, if specifically for a particular technological category (e.g. cores), on each individual piece of this category. In this way, I had the opportunity to use attributes that are specific to the actual operational scheme. As an interpretation is only possible for what we, as the analysts, understand from the assemblage, this *a posteriori* definition of attributes is no less objective than an *a priori* attribute definition (Soressi and Geneste, 2011: 342). As one major outcome of my analysis concerns the global description of the lithic assemblages, I tried to be exhaustive in my definition of attributes. I added some attributes later, especially for cores and tools, as I gained more experience of the assemblage and specific features I observed on blanks, cores and tools raised new questions that I wanted to elaborate on.

In the next step, each artefact of each technological category was grouped by raw material, based on macroscopic observations. Because the petrographic properties of rocks have an influence on the knapping process, this allowed me to establish a first impression of techno-economic patterns.

Next, I aimed to gain a thorough understanding of the knapping techniques and methods of reduction used by the knappers producing the assemblage. These terms are introduced and distinguished by (Tixier, 1967). Knapping technique refers to the physical means of the transferred energy associated with the removal of the blanks ( Pelegrin, 1995; Soressi and Geneste, 2011). Method of reduction refers to the intellectual steps intentionally followed throughout the knapping process, expressed by the volumetric and sequential organization of the removals in space and time (Pelegrin, 2000, 2005, 2006; Soressi and Geneste, 2011). An accurate determination of the techniques involved for each piece is very difficult, so I tried to gauge more general tendencies. The examination of the methods of reduction is paramount and I proceeded by considering the organisation of removals on each artefact in order to retrace short sequences of the reduction. By placing these sequences in sequential order, I could then reconstruct the global method(s) underlying the assemblage. Some of the products are obviously more informative than others, e.g. primary crested blade, as their short sequence of removals are more characteristic of a specific stage within the knapping process. Additionally, some stages are so essential to the operational sequence that their presence or absence is always significant, e.g. first flakes.

After organising all lithic objects, I aimed to highlight morphological and technological characteristics of the products within the operational sequence in order to provide a detail-rich reconstruction of the operational scheme. Mental refitting guided my observations, but the proposed model can be tested by physical refitting and experimentation (Tixier, 1980; Pelegrin, 1986, 1995, 2006; Geneste, 1991).

The last step concerned identifying whether every phase of the operational sequence was carried out for each raw material at the site or whether certain phases are not observed in the assemblage and therefore might have been conducted away from the excavated site.

Observations, attributes and attribute combinations judged as relevant during the classification stages were then recorded in a database and quantified to enable the application of descriptive and comparative statistical tests. The attribute list compiled for the assemblage of the lower deposits from Sibudu contains attributes similar to those already existing in the literature (Hahn, 1977, 1982; Auffermann, et al., 1990; Kieselbach 1993; Ott 1996; Tostevin, 2000, 2003,

2012; Adler, 2002; Nigst, 2012) as well as some specially selected attributes to address particular technological, techno-typological or techno-economic research questions. I created an input mask of the attribute list to enter all the data into a Microsoft Access database. The input mask and the data acquisition were realised by the software E4 (<http://www.oldstoneage.com/software/e4.shtml>). The whole attribute list can be found in Supplementary Information.

### 3.2.2. General Attributes

#### **3.2.2.1. Cortex**

The proportion and position of cortex coverage provide information about the organisation and intensity of the reduction sequence, import and export of raw material, site use and mobility patterns (e.g. Newcomer, 1971; Geneste, 1985; Hahn, 1991; Kuhn, 1991, 2004; Reher, 1991; Roth and Dibble, 1998; Andrefsky, 2005; Dibble, et al., 2005, Marwick, 2008). I recorded the cortex coverage for all technological categories. For blanks, this attribute concerns only the dorsal surface, while for the cores and angular debris it relates to the overall surface (Nigst, 2012). I determined the percentage of cortex coverage and divided the artefacts into groups based on the coverage percentage. These groups are as follows: 0%, <20%, >20%, >50% and 100%. I additionally specified the location of the cortex.

#### **3.2.2.2. Fragmentation**

Fragmentation was recorded for all artefacts but information on which part is preserved was only recorded for blanks. The data concerning artefact dimensions are strongly affected by the degree of fragmentation in the assemblage.

### 3.2.3. Modalities of Measurements

Measurements were only taken if the lithic object was completely preserved in this dimension and the measurement was easy to take as well as reproducible. I took measurements of length, width, thickness and maximum dimension in millimetres with a calliper. All objects were weighed in grams using a digital scale (Nigst, 2012). All values are recorded accurate to one decimal place.

The measurements of length, width and thickness on blanks follow the definitions of (Auffermann, et al., 1990; Soressi, 2002; Nigst, 2012) (Figure 20a). The length is obtained by taking the longest measuring distance from the platform to the most distal point of the artefact parallel to the axis of flaking. The axis of flaking of a piece is defined as the imaginary line following the direction of percussion (De Loecker and Schlanger, 2004: 304). I measured the width as the maximum distance between the two edges of the object perpendicular to the length axis. I took the value for the thickness at the thickest part of the blank perpendicular to

the ventral face including the bulb of percussion. I additionally recorded the maximum dimension defined as the longest measurement distance across a blank (Mackay, 2008). The depth and width of the platform were also recorded (Figure 20a). The platform depth is defined as the distance from the exterior edge of the platform to the impact point of percussion (Dibble and Whittaker, 1981; Dibble and Pelcin, 1995; Dibble and Rezek, 2009). The platform width was measured perpendicularly to the platform depth (Auffermann, et al., 1990; Nigst, 2012).

By using combinations of different measurements, I could calculate different informative ratios and formulae; for example, debitage laminarity and dorsal convexity. The debitage laminarity is calculated from the average ratio of the blank length to the blank width of all blanks (Adler 2002: 196; Tostevin 2003: 85). An assemblage showing a high debitage laminarity of or above 2.0 indicates that the knappers aimed primarily for elongated objects. The dorsal or vertical convexity is determined by the average ratio of the blank width to the blank thickness. This value serves to identify whether a tall, laterally centralised convexity or a flat, laterally diffuse convexity dominates the assemblage (Tostevin 2003: 86). Furthermore, I used the formula following (Mackay, 2008) to generate an estimate of the edge length (EL):  $EL = \text{length} + \text{width} + \text{maximum dimension}$ . The EL-weight-ratio allows one to make statements on the efficiency with which knappers converted core mass into cutting edge by applying their preferred reduction strategies (Mackay, 2008).

I used a goniometer to determine the exterior platform angle (EPA), defined as the angle between the platform and dorsal surface of completely and proximally preserved blanks (Figure 20a) as well as between the platform and removal surface of cores (Figure 20b) (Dibble and Whittaker, 1981; Dibble and Rezek, 2009; Nigst, 2012). In addition, on cores I measured the angles between the lateral surfaces and the final main removal surface.

The measurements taken on cores followed (Hahn, 1982; Nigst, 2012) (Figure 20b). The length of the core was measured from the platform to the most distant point at the base, parallel to final main reduction axis. The width was recorded as the maximum distance between the two edges of the core, perpendicular to the length. I measured thickness from the thickest part of the core between the final main removal surface and the core back, perpendicular to the length. I recorded the length of the last removal on the final main removal surface as the measurement distance from the platform of the core to the most distal point of the removal.

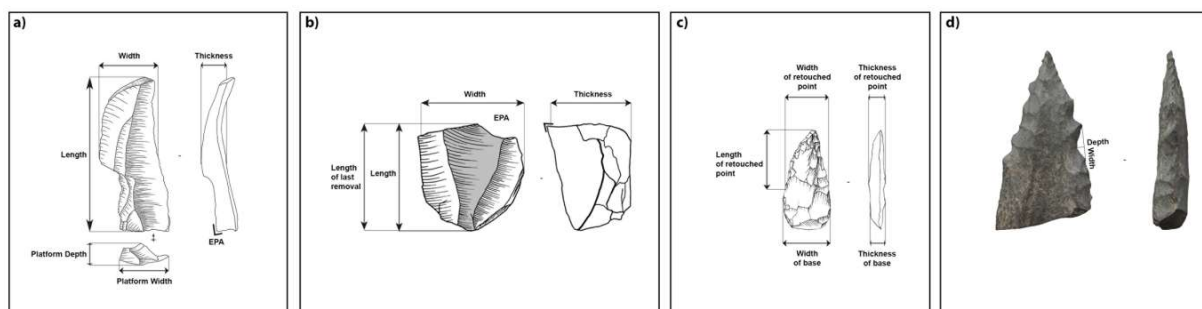
For retouched elements such as unifacial pointed forms, bifacial points and serrated pieces, I recorded the length of the retouched point, the maximum width and thickness of the point, and the length, maximum width and thickness of the base (Figure 20c) (compare Conard, et al., 2012: Figure 9).

Due to time constraints, I took measurements with a goniometer in degrees to determine the edge-angles of the edges of unifacial pointed forms. The artefact was placed in the device so that one surface was flat against one of the arms (Dibble and Bernard, 1980). To calculate the edge-angles of bifacial and serrated pieces, I took thickness measurements with a calliper at a known medial distance of 2 mm from the edge of the artefact and then used the formula for

calculating the edge-angle according to (Soressi, 2002; Dibble and Bernard, 1980): edge angle = tangent arc [thickness/ 2 mm (known edge depth) / Pi \* 180]. This measuring method has been demonstrated to be most reliable (Dibble and Bernard, 1980; McPherron, et al., 2014).

As demonstrated by several ethnographic studies (see for example Leroi-Gourhan, 1943), the edge-angle constrains whether a tool can perform a vertical incision, a horizontal incision or both. An edge-angle of 35° or less corresponds to a cutting referred to as *coupe rentrante*, including piercing, slicing, and stabbing; edge-angles exceeding 65° are so-called *coupe sortante*, suitable for scraping, whittling, and smoothing. An intermediary angle between 35° and 65° allows for both directions of cutting (Soressi, 2002, 2004). The *coupe rentrante* is defined as a cutting edge where the active part of the piece is moved in the same plane as its length, parallel to the direction of use. In contrast, for the *coupe sortante*, the transformative part is moved perpendicular to the direction of motion (Soressi, 2002). The results of several analyses attest to the limits of angles suited to different directions of cutting (Wilmsen, 1968; Gould, et al., 1971; Hayden, 1979; Siegel, 1985).

I determined the tip-penetrating-angle (TPA) and the tip cross-sectional area (TCSA) of the bifacial points and serrated pieces as two proxies to make a suggestive discrimination of armatures of different weapon systems (thrusting or throwing spears, spear thrower darts or arrows) (Shea, 2003, 2006, 2009; Villa and Lenoir, 2006). This was complemented by residue and use-wear analysis that demonstrated the use of the serrated pieces as projectiles through multiple lines of evidence (Rots, et al., 2017). The TPA is defined as the angle (seen in plan view) at which the lateral edges converge at the tip of the retouched point (Peterkin, 1993). I measured the TPA with a goniometer in degrees. For serrated pieces, I also measured the TPA using the same formula as for the edge-angle, but instead of measuring the thickness, I measured the width at a known distance of 10 mm from the tip with a calliper following (Villa and Lenoir, 2006). To calculate the TCSA, I used the formula established by (Hughes, 1998):  $TCSA = (0.5 * \text{maximum width}) * \text{maximum thickness of the point}$ .



**Figure 20.** a) Length, width, thickness, platform width, platform depth and EPA measuring sections on blanks (Drawing by Heike Würschem and Achim Frey); b) Length, width, thickness, length of last removal (last removal grey shaded) and EPA measuring sections on cores (Drawing by Heike Würschem); c) Length, width, and thickness of retouched point as well as width and thickness of the base measuring sections on uniface, bifacial and serrated points (Drawing Guillaume Porraz); d) Width and depth measuring sections on notches of serrated pieces and denticulates (Photo by Viola C. Schmid).

For serrated pieces and denticulates, I took measurements of the width and depth of all notches of each tool on high-resolution photos using the software Adobe Photoshop (Figure 20d) (Rots, et al., 2017).

#### 3.2.4. Debitage Specific Attributes

##### **3.2.4.1. Technological Classification**

I classified all blanks that were twice as long as wide and featuring regular, parallel edges and a width  $\geq 10$  mm as blades, following the definition of (Sonneville-Bordes, 1960; Crabtree, 1972; Hahn, 1977; Inizan, et al., 1999). Bladelets conform to these criteria as well but have a width  $< 10$  mm (Hahn, 1977). Moreover, I distinguished elongated flakes (*éclats laminaires*) which exhibit parallel dorsal ridges, regular morphologies. In contrast to blades, they do not fulfil the size ratio of length  $\geq 2 \times$  width, but have a lower limit of length-to-width ratio of 1.5 (Sonneville-Bordes, 1960; Moreau, 2009). I referred to blanks with converging edges as triangular flakes (Porraz, et al., 2013).

##### **3.2.4.2. Morphological Attributes**

I recorded blank morphology to establish whether a specific shape dominated among the blanks. I also determined thedebitage profile to get an understanding of the management of the longitudinal convexities of the removal surfaces of cores (Tostevin, 2000: 99, Tostevin, 2003: 86). I also assessed the cross-section at the midpoint of the blank length to identify how knappers organised the ridge patterns on the removal surfaces of cores to achieve the propagation of the products (Tostevin, 2000: 99, Tostevin, 2003: 86).

##### **3.2.4.3. Dorsal Scar Pattern**

I recorded the number and orientation of dorsal scars for each blank. The number and direction of the dorsal scars yield information about the organisation and intensity of the reduction strategy used during the previous flaking of the core (De Loecker and Schlanger, 2004: 318).

##### **3.2.4.4. Distal Termination**

The nature of the distal end allows one to make statements about successful exploitation, maintenance, correction and knapping accidents. In most cases, knappers aimed at feather terminations as these produce a sharp cutting edge on the blank and leave the core with a removal surface morphology suitable for the detachment of further products. Blanks exhibiting a hinge or step termination usually represent knapping accidents related to suboptimal management of angles and convexities of the core. These accidents cause irregularities on the removal surface which complicate the further reduction of usable end-products (Dibble and Whittaker, 1981: 287ff.). By contrast, plunging blanks, which remove part of the opposing end of a core, are influenced by the shape of the core base and thus may be desired to correct or maintain the distal convexity of the core (Cotterell and Kamminga, 1987: 701).

### 3.2.5. Core Classification

To provide a first general classification of the patterns of reduction of each core, I followed the framework of the 'Unified Taxonomy' defined by (Conard, et al., 2004).

### 3.2.6. Diacritic Diagram of Cores

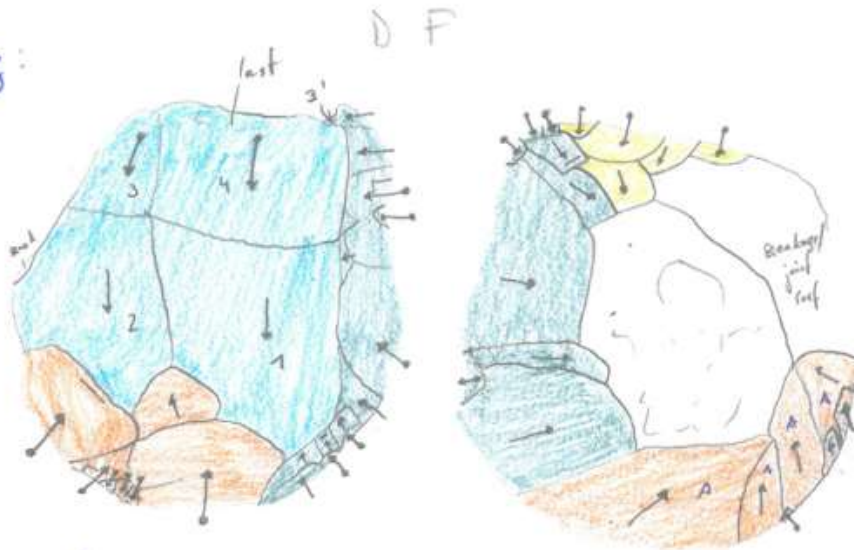
I systematically constructed diacritic diagrams of all cores and core fragments which represent schematic drawings to highlight the final sequence of actions preserved on these artefacts (Figure 21).

To determine the organisation concerning direction and chronology of the removals on each object, I took into account criteria, such as ripples or undulations, hackle fractures or 'lances', and the morphology of the ridges (Dauvois, 1976; Inizan, et al., 1999; Soressi, 2002; Soressi and Hays, 2003). Based on these diacritic diagrams portraying each stage of the reduction sequence, I established a schematic representation of the reduction sequence to illustrate the entire sequence of technical actions involved (Inizan, et al., 1999). I used Adobe Photoshop to realise the schematic illustration. Additionally, I took photos of each core with a Canon EOS 1100D and processed them with the software Helicon to gain high-resolution images. Furthermore, 3D artefact models were rendered from photos of selected cores using the same camera to systematically rotate all around them and the images were processed with the software Agisoft PhotoScan.

### 3.2.7. Assessment of Knapping Technique

The knapping technique depends on three parameters defined by (Tixier, 1967): the mode of application of force, the motion involved in the knapping, and the nature and morphology of the knapping tool. Several recurrent criteria associated with platform preparation and regularity of the products enable the identification of these parameters and subsequently the knapping technique(s) (Pelegrin, 1995, 2000; Valentin, 2000; Soriano, et al., 2007). The characteristics include lip, bulb, bulbar scar, cone, and impact point as well as platform type and shape, platform depth, dorsal reduction/thinning, and EPA (Nigst, 2012: 55). I recorded technological accidents, such as Siret breaks, which can yield additional information about the percussion technique (Crabtree, 1972; Roche and Tixier, 1982; Inizan, et al., 1999; Pelegrin, 2000). Some setbacks in assessing knapping technique must be acknowledged, such as the difficulty of differentiating soft and hard hammerstones or of anticipating a change of motion during the reduction sequence. I followed, on a general level, the distinction of knapping techniques described by Pelegrin (2000) and, on a more specific level, the list of criteria developed to diagnose the percussion technique used in the blade reduction system of the HP and post-HP at Rose Cottage Cave (Soriano, et al., 2007). However, I note that all diagnostic criteria should be based on and controlled by specific experimental data using similar raw materials and reduction strategies, which will be the focus of future work.

Drawing:



Chron:

2 3 4 3'  
1

5 main removals: 2 blades, 2 accidental flakes, 1 indet

Descriptions: crest alternating, distal trimming <sup>on back</sup> on Face B,  
Face B not clear, but probably breakage/joint surface  
rem surface too flat hinges last removals  
dist → / plat → crest → prod → dist → prod acc

Matrix:

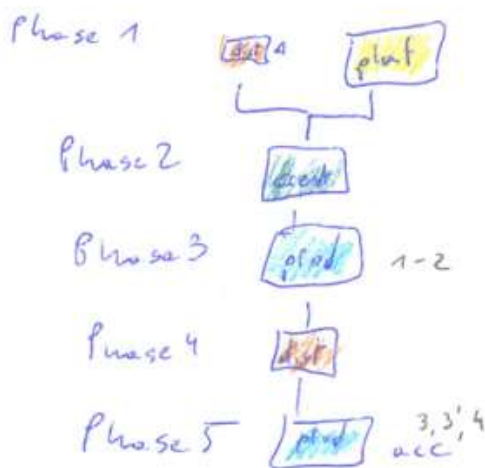


Figure 21. Diacritic diagram of core A5-52 from layer Adam (BMO) (Drawing by Viola C. Schmid).



### 3.2.8. Typological Classification

The typological classification complied with the commonly used terminology for the southern African MSA (Wurz, 2000; Porraz, et al., 2013; Volman, 1981; Singer and Wymer, 1982) and I classified specific tools according to the recently defined terms based mainly on techno-functional analysis, including Tongatis, naturally backed tools (NBTs) and asymmetric convergent tools (ACTs) (see for definitions: Conard, et al., 2012; Will, et al., 2014; Conard and Will, 2015). Moreover, within the bifacial pieces, I identified pieces with serrated edges and assigned them to an autonomous tool class. The serrated pieces are clearly differentiated from denticulates by bifacial working preceding the serration and the regularity as well as dimensions of the notches.

### 3.2.9. Techno-Functional Classification

The distinct UTFs of a tool, namely CT, CR, and CP, were treated differently during manufacture and re-sharpening (Lepot, 1993; Boeda, 1997; Soriano, 2000, 2001; Nicoud, 2011; Chevrier, 2012; Kot, 2013). To identify one or more of these UTFs on a tool, each of which is designed in a specific way by the toolmakers to equip this section of the object with the intended set of techno-functional features, I examined features from the tool manufacturing to the final phase of transformation which give the functional characteristics to the tool. In addition to identifying the chronological order of the removals of retouch, I also took into consideration the orientation, size, presence or absence of counter-bulbs, and the profile of the retouch removals (Soriano, 2001: 78).

Alongside the retouch removals, I documented the location and distribution of the various macro-removals, , which are visible with the naked eye, and micro-removals, which were identified under the microscope, on the different parts of the tools at a low magnification (x10-x40) with an Euromex stereomicroscope EduBlue to characterise the intentional (i.e. technological) and unintentional (i.e. functional) traces the tools bear (Porraz, et al., 2018).

### 3.2.10. Manufacture Phases of Bifacials

To study the bifacial pieces of the lower layers from Sibudu, I followed the classification of manufacture phases proposed by (Villa, et al., 2009) based on the SB point assemblage from BBC, and expanded on by (Högberg and Larsson, 2011) based on the SB point assemblage from HRS. The manufacturing of SB points is a progressive process which is valid for all bifacial shaping processes (Whittaker, 1994). However, the term 'manufacture phase' was explicitly chosen instead of reduction stage, as it is difficult to achieve a clear distinction of stages for the manufacturing of SB points which seems to be less regular and less standardised than the production of Folsom and other bifacial Paleoindian points (Villa, et al., 2009: 446). Villa and colleagues (2009) divided the manufacturing sequence into four phases (1-4): initial shaping, advanced shaping, finished product and recycling, with a subdivision of phase 2 (advanced shaping) into phase 2a and 2b. Högberg and Larsson (2011) defined an additional phase between phases 2a and 2b, referred to as phase 2ab. To determine the production phase, I

accordingly assessed different attributes, such as portion of unmodified edge, regular outline of tip and base, regular profile of tip and base, bifacial symmetry, and bilateral symmetry.

#### 3.2.11. Taphonomic Attributes

I determined edge damage and thermal alterations on each artefact to evaluate the condition of the lithic material. Additionally, some of the artefacts exhibited a heavy encrustation of sediment, including fossilised grass leaves and stems (Conard, 2016). I recorded these features to document the extent to which assemblages were affected by diagenetic processes and to identify potential spatial differences of post-depositional influences.

#### 3.2.12. Quantifying Small Debitage

The fraction of small lithic objects (<30-5 mm) was quantified according to raw material to draw additional conclusions on techno-economic patterns. Furthermore, I recorded the proportion of retouch and shaping flakes not only to quantify the intensity of on-site tool manufacturing and recycling, but also to identify the different procedures to modify the blanks into tools. I chose square C4 as a representative sample. I used the description of the attributes established by Soriano et al. (2009: 44f., 2015: S2 Table D) to determine shaping flakes involving initial, advanced and final shaping, and the description of Conard et al. (2012: 195) to determine retouch flakes. The main attribute to distinguish between shaping and retouch flakes concerns the platform type. Retouch debitage shows plain striking platforms formed by the original ventral surface of the blank, and shaping debitage demonstrates dihedral or faceted striking platforms formed by former bifacial preparation, especially in the advanced and final stages of shaping. Besides the platform type, if I identified at least two further characteristics on a piece, I classified it accordingly. This approach is conservative and most probably yields an underestimate of the effective amount of retouch and shaping debitage, as also shown by experiments (Porraz, 2005).

#### 3.2.13. Statistical Tests

I used the statistics software Past (Hammer, et al., 2001) to conduct univariate descriptive and comparative tests to underpin my proposed hypotheses, including the Shapiro-Wilk test, Student's *t*-test, and chi-squared test. I used the Shapiro-Wilk test to determine whether a data set is normally distributed. Student's *t*-test tests the equivalence of the averages of two data sets. The chi-squared test is used to determine the independence of two data sets. A probability greater than 0.05 ( $p > 0.05$ ) indicates that the hypothesis tested must be significantly rejected at the 95% confidence level; a probability less than 0.05 ( $p < 0.05$ ) indicates that the hypothesis tested cannot be rejected at the 95% confidence level.

## 4. Archaeological Sample

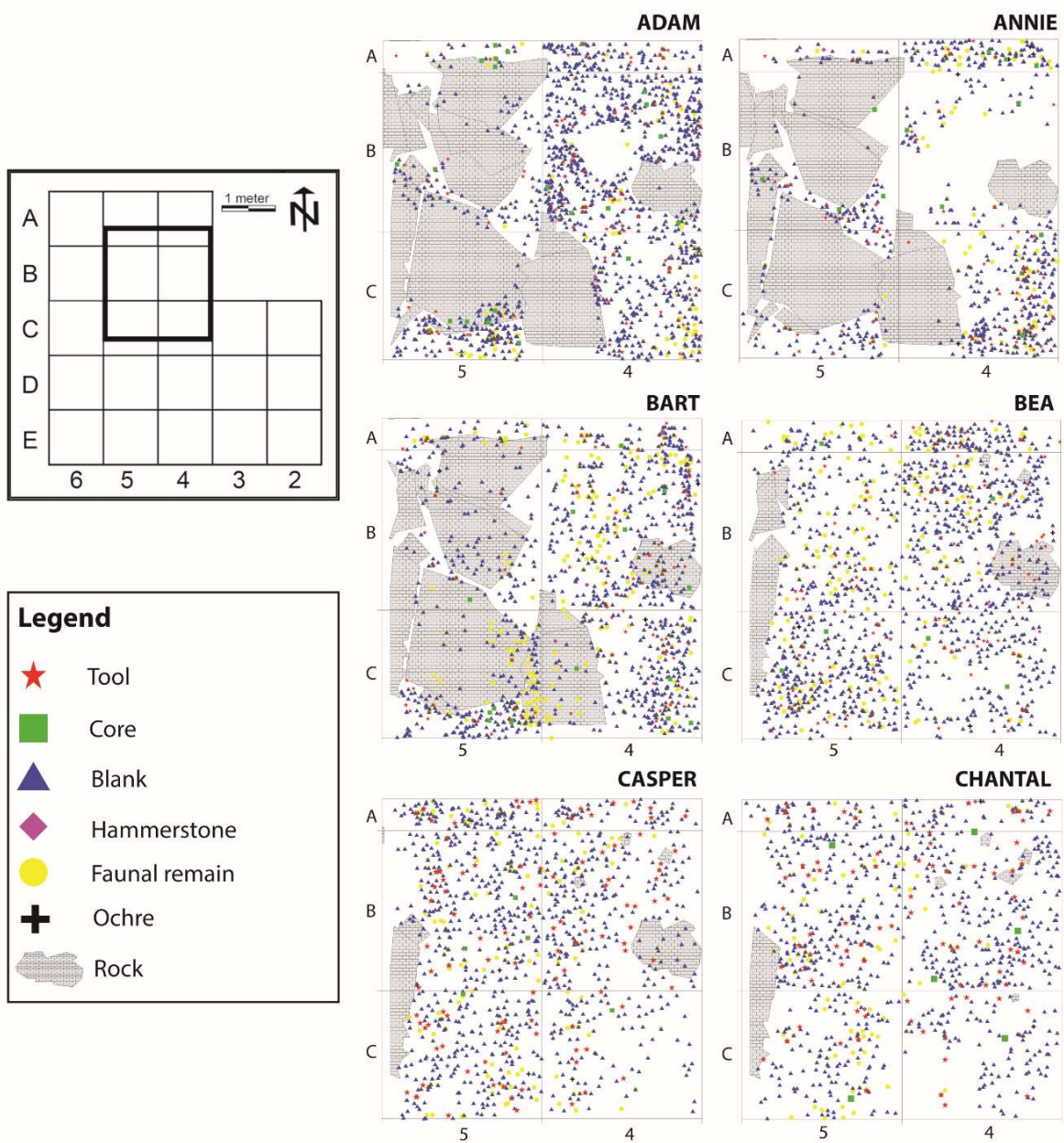
The archaeological sample providing the basis for the lithic analysis performed here includes all of the lithic artefacts  $\geq 30$  mm, plus all cores, core fragments, tools and tool fragments regardless of their size from layers Adam, Annie, Bart, Bea, Casper, and Chantal. The artefacts come from squares A4, B4, C4, A5, B5 and C5, which represent an excavation area of approximately 4 m<sup>2</sup> and a volume of about 1 m<sup>3</sup> (989 litres of sediment) that were excavated in five field seasons from 2012-2016. The six archaeological units analysed comprise a total of 8,164 lithic objects. The small debitage products (<30mm and <5mm) form a total of 76,945 pieces. The total find density of Adam to Chantal is high with a value of 86,081 n/m<sup>3</sup> (Table 4), exceeding the value of 34,790 n/m<sup>3</sup> of the very dense Sibudan layers (Will and Conard, 2018). In this chapter, I provide a description of each layer, including the general composition of the lithic assemblage.

**Table 4.** Sibudu. C-A layers from the Deep Sounding: Frequency of lithic single finds and small debitage products, sediment volumes and find density.

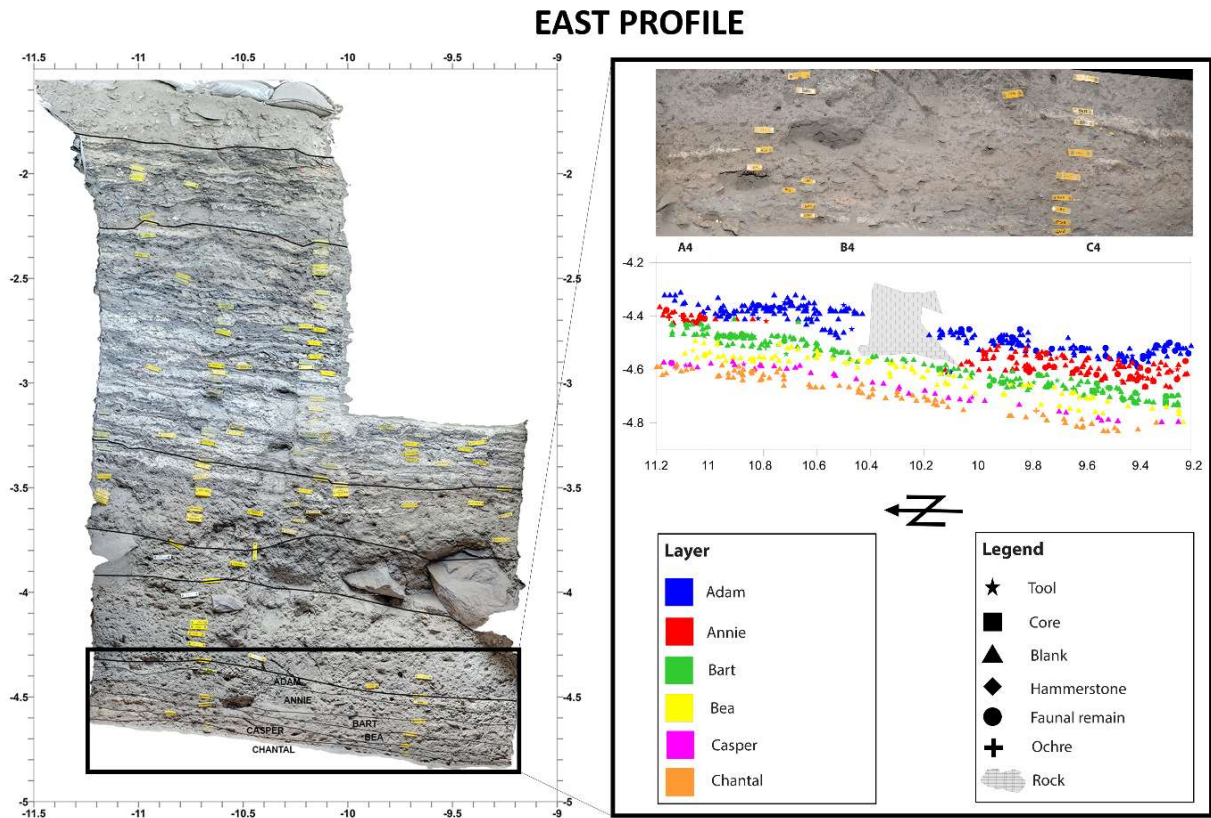
Layer	Lithics (>30 mm)		Density (>30 mm)	Lithics (<30-5 mm)		Density (<30-5 mm)	Total		Density Total	Excavated Volume
	n	%	(n/m <sup>3</sup> )	n	%	(n/m <sup>3</sup> )	n	%	(n/m <sup>3</sup> )	m <sup>3</sup>
ADAM	1,814	10.6%	14,227.5	1,5245	89.4%	119,568.6	17,059	100%	133,796.1	0.128
ANNIE	1,057	10.4%	11,044.9	9,094	89.6%	95,026.1	10,151	100%	106,071.1	0.96
BART	1,183	10.1%	6,411.9	10,563	89.9%	57,252.0	11,746	100%	63,664.0	0.185
BEA	1,595	8.8%	6,980.3	16,588	91.2%	72,595.2	18,183	100%	79,575.5	0.229
CASPER	1,393	7.8%	7,143.6	16,505	92.2%	84,641.0	17,898	100%	91,784.6	0.195
CHANTAL	1,122	11.1%	7,123.8	8,950	88.9%	56,825.4	10,072	100%	63,949.2	0.158
<b>Total</b>	<b>8,164</b>	<b>9.6%</b>	<b>8,257.3</b>	<b>76,945</b>	<b>90.4%</b>	<b>77,824.4</b>	<b>85,109</b>	<b>100%</b>	<b>86,081.7</b>	<b>0.989</b>

### 4.1. Layer Adam

The uppermost layer corresponds to an important marker in the stratigraphic subdivision within the otherwise fairly homogenous deposits of the DS (Conard, 2013). Adam is a distinctive slightly cemented mostly greyish brown (Munsell 10 YR 5/2) silty to sandy layer with patches of white colour, hence the field name Burnt Mouse (BMo). Patches of ash and charcoal are visible. Natural cobbles and boulders occur. The deposit formed after an earlier major rock fall event and partly abuts against the large rocks with dimensions of over 50 cm (Figure 22 & Figure 23). Few bones were recovered and the majority of bone is present as fragments. In a large portion of the excavation area, the archaeological unit comprised only three *Abträge*. However, in sub-square metres c and d of square C5, eight *Abträge* were removed, following the natural slope of the deposits. The lithic assemblage consists of 1,814 artefacts  $\geq 30$  mm and 15,245 small debitage products (Table 4). The lithic find density is extremely high with a value of 133,796 n/m<sup>3</sup>.



**Figure 22.** Sibudu: Overview of the excavation grid (left) and horizontal find distribution of all layers (right).



**Figure 23.** Sibudu: Orthophotography of the east profile (copyright by M.M. Haaland) (left) and vertical find distribution of all layers, including all objects  $\leq 20\text{cm}$  east of the east profile (right).

#### 4.2. Layer Annie

Layer Annie is described as loose, reddish-brown (Munsell 5 YR 4/3, 5/3), silty sediment mixed with dark grey ash, charcoal and whitish cemented sediment containing small natural sandstones. In general, the deposit is less strongly cemented than the layer above but is also affected by the same rock fall event (Figure 22 & Figure 23). Few bones and bone fragments appear in this archaeological unit. In most squares of the excavation area, the excavation of the archaeological unit was finished after removing two *Abträge*. In square C4, nine *Abträge* were completed, following the natural slope of the deposits. The lithic assemblage contains 1,057 finds  $\geq 30\text{ mm}$  and 9,094 small debitage products (Table 4). The lithic find density is high, but lower than in layer Adam with a value of  $106,071\text{ n/m}^3$ .

#### 4.3. Layer Bart

This very pale brown (Munsell 10 YR 8/3, 8/4, 7/3) to light grey (Munsell 10 YR 7/2) deposit is loose to dense, silty to sandy. Small pieces of natural sandstone are present. Isolated reddish-brown patches of burnt sediment showing a high density of lithic artefacts and good preservation of organic remains occur. A major phase of rocks fell on the exposed surface of

this deposit, the largest of which have dimensions of over 50 cm and protrude on the upper layers Adam and Annie (Figure 22 & Figure 23). Noticeable concentrations of lithic artefacts and sometimes well-preserved bones were documented in the areas along the edges and gaps between the large boulders, particularly in square C5 (Figure 22) (Conard, 2014). Excavation of the layer was finished after the removal of four *Abträge* across the whole excavation area. The lithic assemblage encompasses 1,183 pieces  $\geq 30$  mm and 10,563 small debitage elements (Table 4). The lithic find density is the lowest in the whole archaeological sample with a value of 63,664 n/ m<sup>3</sup>.

#### 4.4. Layer Bea

Layer Bea received the field description Gray Brown Patchy (GBP) because the texture varies from loose, crumbly, dense to cemented, and the colour ranges from brown (Munsell 7.5 YR 4/2, 5/2), greyish brown (Munsell 10 YR 5/2) to dark greyish brown (Munsell 10 YR 4/2). Natural small fragments of sandstone appear in the silty to sandy sediment. Yellow-white patches of compaction mixed with ash also occur. The low-to-moderate amount of faunal remains is in a good state of preservation. It is noticeable that in the south-eastern part of squares B4 and C4 no bones are preserved in the area from the edge to approximately 20 cm inside of the square due to diagenetic alteration (Figure 22). This stratum lacks the large rock falls that affected the layers higher up in the sequence (Figure 22 & Figure 23). Excavation of the whole archaeological unit was completed after removing three *Abträge*. The lithic assemblage comprises 1,595 artefacts  $\geq 30$  mm and 16,588 small debitage products (Table 4). The lithic find density has a value of 79,576 n/m<sup>3</sup>, higher than in layer Bart but lower than the uppermost layers, even though the greatest volume was excavated.

#### 4.5. Layer Casper

This layer is brown (Munsell 7.5 YR 5/2, 5/3) to very pale brown (Munsell 10 YR 7/3, 7/4) in colour. Brown compact patches occur in a loose, silty to sandy sediment containing small natural pieces of sandstone. A complete absence of faunal preservation in the south-eastern part of squares B4 and C4, from the square limits to approximately 25 cm into the square area, extends slightly towards the west and the north (Figure 22). Stones from rock falls were not encountered (Figure 22 & Figure 23). In a large portion of the excavation area, excavation of the archaeological unit was finished after the removal of three *Abträge*. In squares A5 and B5, six *Abträge* were excavated due to adjustments concerning the stratigraphic situation. The layer yielded a lithic assemblage of 1,393 artefacts  $\geq 30$  mm and 16,505 small debitage elements (Table 4). The stratum shows the highest proportion of small debitage. The lithic find density has a value of 91,785 n/m<sup>3</sup>, again higher than layer Bea but lower than the uppermost layers.

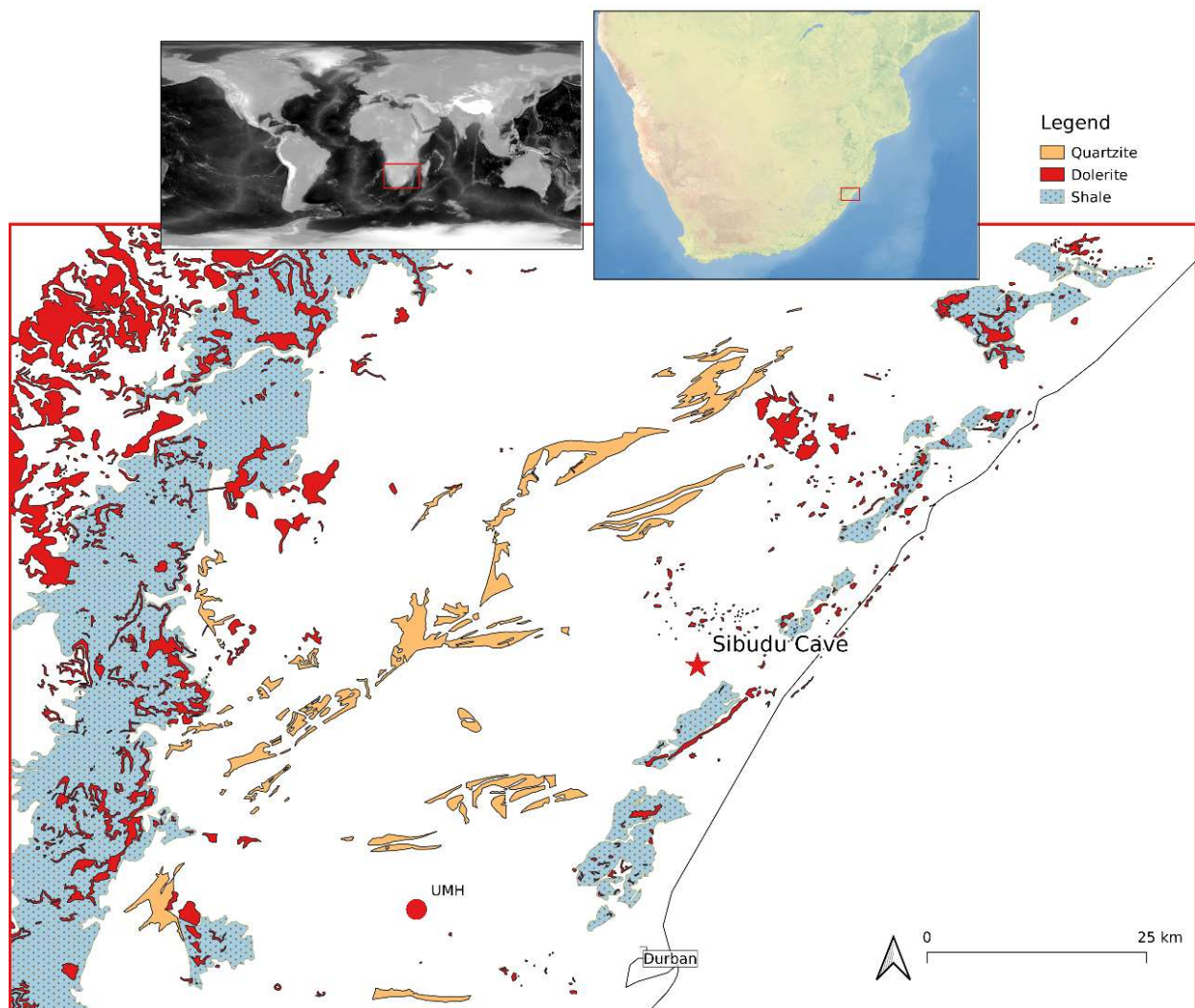
#### 4.6. Layer Chantal

This deposit was referred to in the field as Pinkish Sandy Silt (PSS) due to the silty, sandy texture and the pinkish grey (Munsell 5 YR 6/2, 7/2; 7.5 YR 6/2) to brown (Munsell 7.5 YR 5/2) colour. The sediment is loose, dense to cemented. Small natural pieces of sandstone are present, and some bones and charcoals occur. However, the area with no faunal preservation noted in layer Caspar continues to spread towards the west and the north (Figure 22). Large rocks associated with rock fall are not present (Figure 22 & Figure 23). A mix of compact orange sediment and deposits with white mineral nodules were discovered in this layer and could represent a combustion feature (Conard, 2015). In most squares of the excavation area, the layer excavation was completed after removing two *Abträge*. In squares A5 and B5 four *Abträge* were excavated, again due to adjustments concerning the stratigraphic situation. The lithic assemblage consists of 1,122 finds  $\geq 30$  mm and 8,950 small debitage products (Table 4). The archaeological unit shows the lowest proportion of small debitage. The lithic find density has a value of 63,949 n/m<sup>3</sup>, the second lowest after layer Bart.

## 5. Results

### 5.1. Raw Materials

In this section, I introduce the different rock categories that occur, their properties and availability. I then touch upon the completeness of the reduction sequence, the intensity of on-site knapping, degree of reduction, and investment in curation of the different raw materials. I address these in descending order of their proportion within the assemblage.



**Figure 24.** Map of geological context and raw material source localities in the area of Sibudu. indicating also Sibudu Cave and Umhlatuzana Shelter (modified after Bader, et al., 2015: Figure 1. Top).

#### 5.1.1. Raw Material Availabilities

The characterisation of the geological environment, and therefore raw material availability, yields essential information about the adaptations and requirements of the lithic technical sub-system, land use patterns and mobility strategies of past populations. The selection of the rock types as well as their original morphologies (cobble, slab, block) substantially influences the

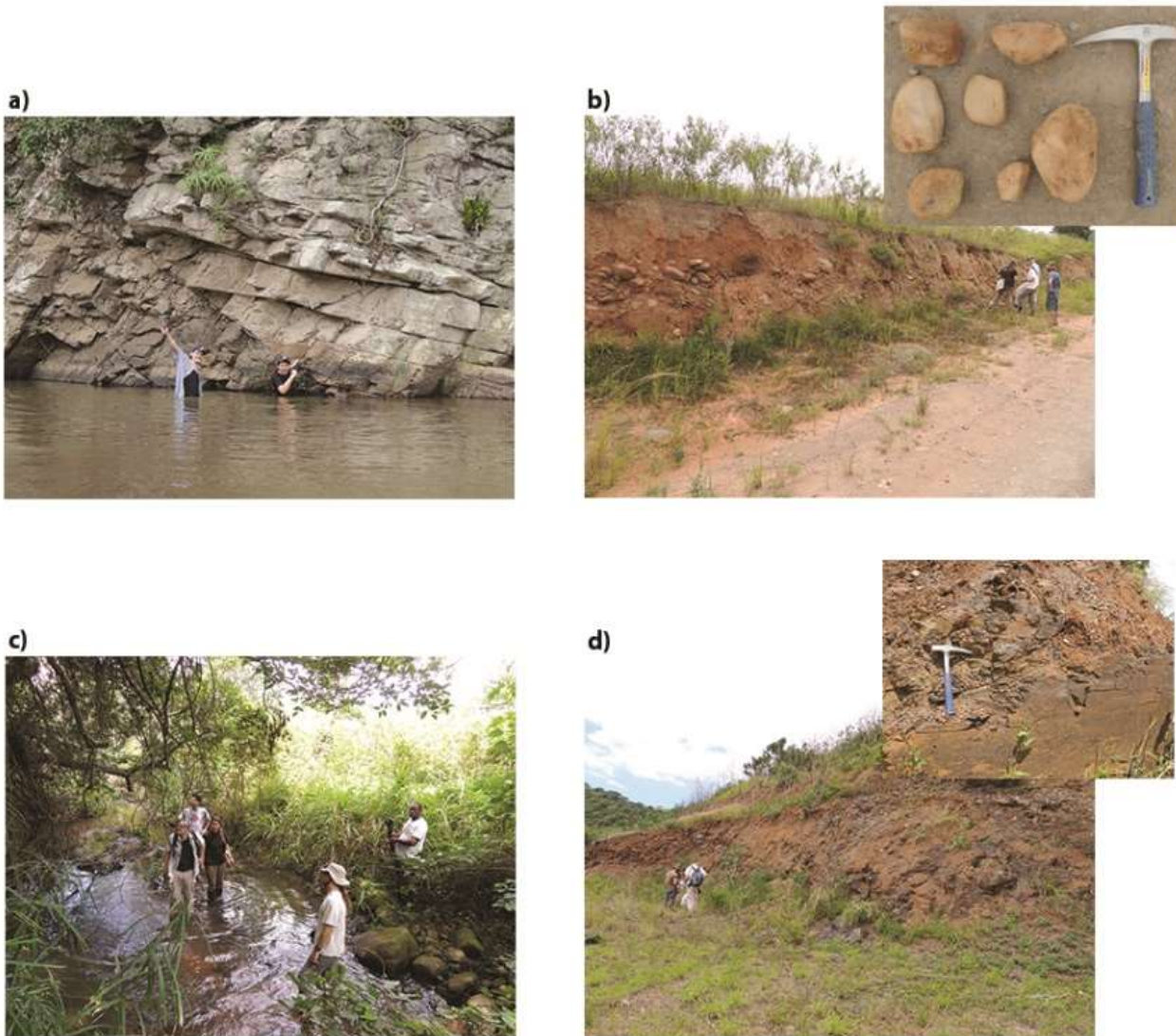


operational sequence and consequently the composition of the assemblage (Nigst, 2012; Vaquero, et al., 2001; Schmid, et al., 2016). Systematic geological fieldwork can help to increase the knowledge of the geology and available raw materials in a region to better inform in-depth statements about the techno-economic organisation. This information comes not only from previous work on the available raw material sources in the area (Figure 24) (de la Peña and Wadley, 2014a, Wadley and Kempson, 2011) but also from new fieldwork carried out by a team from the University of Tübingen (including Mohsen Zeidi, Gregor D. Bader, Jonathan A. Baines, Manuel Will, Lawrence 'Muzy' Msimanga and myself). This team surveyed the site surroundings and neighbouring areas in February 2015 to explore raw material availability (Figure 25). A key observation from our raw material survey is that the rivers in the region of Sibudu Cave served as important raw material suppliers.

The current state of knowledge suggests that the inhabitants of Sibudu Cave had most of their raw material spectrum available locally and thus mostly had short transportation distances (see de la Peña and Wadley, 2014a, Wadley and Mohapi, 2008; Cochrane, 2006; Villa, et al., 2005). In accordance with ethnographic and archaeological observations, I refer to a local economic sector as less than 5 km around the site, while the semi-local zone means more than 5 km but less than 20 km, and the exotic or non-local sector is more than 20 km from the site (Geneste, 1985, 1988; Weißmüller, 1995; Porraz, et al., 2008, 2013).

I divided the archaeological assemblage into six main rock categories, identified as dolerite, hornfels, sandstone, quartzite, quartz and chert. Additionally, I distinguished three cortex types to determine the kind of depositional context the raw materials originated from: 1) weathered cortex, well-polished and shiny, 2) natural surface, often flat, stepped, and occasionally oxidised, and 3) alluvial cobble cortex with a regular surface, generally convex, with numerous shocks (see also Porraz, et al., 2013). In the following section, I provide a short geological description of each of the different rock categories (for further definitions see: Cochrane, 2006; Wadley and Kempson, 2011; Clarke, et al., 2007; Cairncross, 2004):

**Dolerite** represents typically a relatively coarse-grained igneous rock with a hardness of approximately 6 on the Mohs scale. Dolerite is abundant in the surroundings of Sibudu, originating from intrusive Jurassic volcanic features. The majority of dolerite occurs as sills, though a true dolerite dyke is located within 200 m of the site (Figure 25a). Dolerite sills in the area include the prominent, fine-grained Mhlasini sill, which outcrops extensively inland of the Indian Ocean. Both dolerite sills and dykes provide tabular slabs of raw material. Rounded and weathered dolerite cobbles occur in the riverbanks of the uThongathi. As dolerite is chemically similar across large regions, it is not feasible to allocate dolerite artefacts to a specific source in KwaZulu-Natal. Macroscopically, I identified differences in granularity, roughness of the fracture surfaces, and inclusions of crystals most probably affecting the knapping suitability. Thus, in order to connect the classification more closely with my technological study, I followed the approach presented by (Porraz, et al., 2018) and subdivided the dolerite into three categories based on grain-size: fine, medium and coarse.



**Figure 25.** a) Dolerite dyke within 200m of the site (Photo by Mohsen Zeidi); b) road cut close to the shelter exposing cobbles of quartzite (size range is shown in the close-up in the upper right corner) (Photo by Mohsen Zeidi); c) Occurrence of dolerite cobbles in Black Mhlasini River close to Colt Shooting Range and next to Oakford Road (Photo by Jonathan A. Baines; d) Verulam sill (close-up of the deposit in the upper right corner) (Photo by Mohsen Zeidi).

**Hornfels** is a fine-grained black to grey metamorphic rock with a hardness of 2-3 on the Mohs scale, originating from sedimentary rocks, such as shale or mudstone, at the contact with an igneous intrusion of dolerite or granite. Shales and mudstones occur widely in the region and bands of hornfels of varying qualities are sometimes formed along the margins of dolerite intrusions into the shale. Sources of high-quality hornfels are hardly ever observed in the area but outcrops close to the shelter might have existed in the past. Today the closest good-quality hornfels outcrop occurs in the Verulam district on the Black Mhlasini River, approximately 15 km away from Sibudu. This hornfels occurs as thin slabs of only few centimetres in thickness and is often poorly metamorphosed. Upstream, the geology of the uThongathi River suggests that a few hornfels boulders might have existed in the paleo-river. Varying temperatures arise

in the zone of thermal metamorphism where a dolerite intrusion occurs, with the result of different grades of metamorphic hornfels and igneous dolerite which can be difficult to discriminate macroscopically.

**Sandstone** is a primarily coarse-grained clastic sedimentary rock composed mainly of sand-sized mineral particles between 2 and 1.16 mm in tangential contact with a system of empty spaces in between the grains. This rock exhibits variable hardness from soft to hard (6-7 on the Mohs scale) depending on clast and cement composition. The shelter itself is located in a sandstone cliff cut into the Mariannahill formation of the Natal Group and sandstone was occasionally used for blank production and tool manufacture.

**Quartz** represents generally the crystalline form of the mineral silica or silicon dioxide ( $\text{SiO}_2$ ) and is a very hard rock at 7 on the Mohs scale. Two types of quartz occur in the assemblage: milky (also called vein or xenomorphic) quartz and crystal (also called hyaline or automorphic) quartz equalling translucent quartz, which have fairly different knapping and functional characteristics. Milky quartz has a white colour due to the presence of many small fluid inclusions, while crystal quartz is translucent and pure. Due to its internal structure, crystal quartz does not break according to the mechanics of conchoidal fracture causing a degree of unpredictability during the knapping process. However, the cutting edges of this quartz type are considerably smoother and sharper than those of other hard rocks (Mourre, 1996; Delagnes, et al., 2006; Pargeter and Hampson, 2019). Both types of quartz most likely come from the same outcrops because milky portions adjoining crystal ones were observed (Delagnes, et al., 2006). Milky and crystal quartz are found mostly as small pebbles with a length of ca. 60 mm in the uThongathi River and exposed river terrace gravels. The quartz may have originated in the granite outcrops 20 km north-west of Sibudu (Wadley, 2001a). Conglomerates with quartz clasts of up to 80 mm in size occur in the Verulam area.

**Quartzite** results from the diagenesis or metamorphism of sandstones, also known as arenaceous rock. The changes of the sandstone under heat or pressure cause the recrystallisation of particles into an interlocking mosaic texture without trace of cementation. Due to varying degrees of metamorphism, the occurrence of some intergrading between quartzite and sandstone is possible. Other minerals can form in the quartzite owing to impurities in the original rock. The hardness of this rock type is between 6 and 7 on the Mohs scale. Different variations of quartzite occur within the assemblage. Two quartzite variants are most common: a fine-grained, light purple rock and a medium-grained dark purple rock. Quartzite cobbles are also observed in the uThongathi River and exposed river terrace gravels (Figure 25b). Additionally, the conglomerates in the area contain clasts with quartzite dominating the clastic content.

**Chert** is a fine-grained sedimentary rock composed of microcrystalline or cryptocrystalline silica. This rock has a hardness of 6.5 to 7 on the Mohs scale. Chert also appears in the conglomerates of this area.

### 5.1.2. Raw Material Procurement

All rock types exhibit all three cortex types, albeit with a different emphasis (Table 5). The blanks made on dolerite and sandstone primarily have weathered cortex. Quartzite involves a similar percentage of pieces with alluvial and weathered cortex. Blanks made on quartz and hornfels exhibit increased natural surfaces. This variability in cortex shows that the blanks available originate from different sources and thus have variable shapes as well as physical characteristics.

Dolerite dominates the assemblage of the basal layers of Sibudu, accounting for 81.5% of the raw material total (Table 6), followed by sandstone and quartzite. Quartz and hornfels make up only a small proportion of the assemblage. A few pieces of chert are also present.

**Table 5.** Sibudu. C-A layers from the Deep Sounding: Frequency of cortex types of blanks with cortex coverage per raw material.

Raw Material	alluvial		natural surface		weathered		thermal		Total	
	n	%	n	%	n	%	n	%	n	%
Dolerite	507	17.3%	546	18.7%	1,867	63.8%	6	0.2%	<b>2,926</b>	<b>100%</b>
Hornfels	2	4.5%	30	68.2%	12	27.3%	-	0.0%	<b>44</b>	<b>100%</b>
Quartz	13	29.5%	23	52.3%	8	18.2%	-	0.0%	<b>44</b>	<b>100%</b>
Quartzite	69	49.6%	15	10.8%	55	39.6%	-	0.0%	<b>139</b>	<b>100%</b>
Sandstone	50	10.4%	89	18.5%	343	71.2%	-	0.0%	<b>482</b>	<b>100%</b>
Chert	1	8.3%	2	16.7%	9	75.0%	-	0.0%	<b>12</b>	<b>100%</b>
<b>Total</b>	<b>642</b>	<b>17.6%</b>	<b>705</b>	<b>19.3%</b>	<b>2,294</b>	<b>62.9%</b>	<b>6</b>	<b>0.2%</b>	<b>3,647</b>	<b>100%</b>

**Table 6.** Sibudu. C-A layers from the Deep Sounding: Frequency of raw materials. (\*Bias in distinguishing knapped sandstone from natural spalls.)

Layer	Dolerite		Hornfels		Quartz		Quartzite		Sandstone		Chert		Indetermined		Total	
	n	%	n	%	n	%	n	%	n	%	n	%	n	%	n	%
ADAM	1,584	87.3%	32	1.8%	33	1.8%	97	5.3%	61*	3.4%	7	0.4%	-	0.0%	<b>1,814</b>	<b>100%</b>
ANNIE	859	81.3%	21	2.0%	10	0.9%	78	7.4%	87*	8.2%	2	0.2%	-	0.0%	<b>1,057</b>	<b>100%</b>
BART	962	81.3%	16	1.4%	38	3.2%	66	5.6%	94*	7.9%	5	0.4%	2	0.2%	<b>1,183</b>	<b>100%</b>
BEA	1,304	81.8%	18	1.1%	32	2.0%	75	4.7%	157	9.8%	9	0.6%	-	0.0%	<b>1,595</b>	<b>100%</b>
CASPER	1,068	76.7%	23	1.7%	44	3.2%	69	5.0%	181	13.0%	6	0.4%	2	0.1%	<b>1,393</b>	<b>100%</b>
CHANTAL	879	78.3%	9	0.8%	18	1.6%	88	7.8%	126	11.3%	2	0.2%	-	0.0%	<b>1,122</b>	<b>100%</b>
<b>Total</b>	<b>6,656</b>	<b>81.5%</b>	<b>119</b>	<b>1.5%</b>	<b>175</b>	<b>2.1%</b>	<b>473</b>	<b>5.8%</b>	<b>706</b>	<b>8.6%</b>	<b>31</b>	<b>0.4%</b>	<b>4</b>	<b>0.0%</b>	<b>8,164</b>	<b>100%</b>

The majority of all artefacts is made on dolerite (Table 6), varying from 87.4% in the uppermost layer Adam to 76.7% in layer Casper and 78.3% in layer Chantal at the base. These differences between the uppermost and lowermost deposits partly relate to a bias in distinguishing knapped sandstone from natural spalls from the shelter in the earlier excavation campaigns. Accordingly, layer Adam yielded 3.4% of products made on sandstone as opposed to layers Casper and Chantal with 13% and 11.3% respectively. I nevertheless assume that sandstone

played a minor but constant role in blank production in all layers and that, consequently, sandstone has been underestimated in the upper layers.

**Table 7.** Sibudu. C-A layers from the Deep Sounding: Frequency of dolerite varieties.

Layer	Fine		Medium		Coarse		Indetermined		Total	
	n	%	n	%	n	%	n	%	n	%
ADAM	130	8.2%	1,059	66.8%	391	24.7%	4	0.3%	<b>1,584</b>	<b>100%</b>
ANNIE	65	7.6%	577	67.2%	212	24.7%	5	0.6%	<b>859</b>	<b>100%</b>
BART	40	4.2%	525	54.6%	382	39.7%	15	1.6%	<b>962</b>	<b>100%</b>
BEA	57	4.4%	655	50.2%	552	42.3%	40	3.1%	<b>1,304</b>	<b>100%</b>
CASPER	39	3.7%	518	48.5%	478	44.8%	33	3.1%	<b>1,068</b>	<b>100%</b>
CHANTAL	50	5.7%	403	45.8%	397	45.2%	29	3.3%	<b>879</b>	<b>100%</b>
<b>Total</b>	<b>381</b>	<b>5.7%</b>	<b>3,737</b>	<b>56.1%</b>	<b>2,412</b>	<b>36.2%</b>	<b>126</b>	<b>1.9%</b>	<b>6,656</b>	<b>100%</b>

The dominant material dolerite appears in different qualities in the assemblage (Table 7). The medium-grained dolerite consistently makes up the largest part. The coarse-grained variety decreases in the two uppermost layers Adam and Annie which contain the highest proportion of fine-grained dolerite. A similar trend applies to the tools, as tool-makers in the lower layers more frequently used coarse-grained dolerite to produce retouched elements (Table 8). However, the lowermost layer Chantal yielded the highest percentage of tools made on fine-grained dolerite. The proportions of cortex coverage of the dolerite blanks imply that knappers pursued a provisioning strategy where they partially carried out the earliest stages of the reduction at the site (Table 9). A total of 3.4% of the pieces (n=210) made on dolerite represent

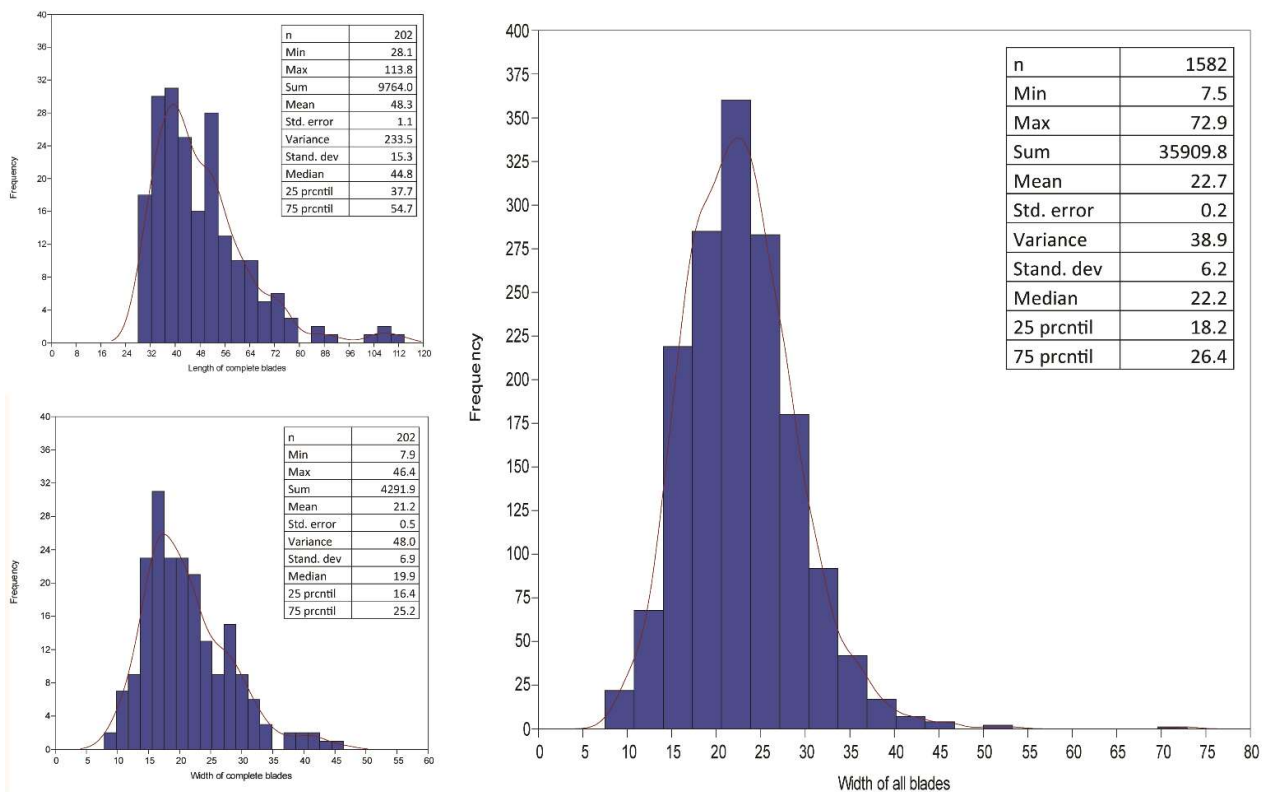
**Table 8.** Sibudu. C-A layers from the Deep Sounding: Frequency of dolerite varieties of tools.

Layer	Fine		Medium		Coarse		Indetermined		Total	
	n	%	n	%	n	%	n	%	n	%
ADAM	15	16.3%	62	67.4%	12	13.0%	3	3.3%	<b>92</b>	<b>100%</b>
ANNIE	11	21.6%	32	62.7%	6	11.8%	2	3.9%	<b>51</b>	<b>100%</b>
BART	4	7.8%	30	58.8%	12	23.5%	5	9.8%	<b>51</b>	<b>100%</b>
BEA	17	17.7%	53	55.2%	23	24.0%	3	3.1%	<b>96</b>	<b>100%</b>
CASPER	6	9.1%	44	66.7%	15	22.7%	1	1.5%	<b>66</b>	<b>100%</b>
CHANTAL	13	23.6%	30	54.5%	10	18.2%	2	3.6%	<b>55</b>	<b>100%</b>
<b>Total</b>	<b>66</b>	<b>16.1%</b>	<b>251</b>	<b>61.1%</b>	<b>78</b>	<b>19.0%</b>	<b>16</b>	<b>3.9%</b>	<b>411</b>	<b>100%</b>

blanks from these early stages, of which 16 are first flakes (*entame*). Two behavioural factors are likely to have been of importance: firstly, long reduction sequences and, secondly, the transport of products prepared beforehand to the shelter indicating an off-site initial stage of decortication (Geneste, 1985, 1988; Weißmüller, 1995; Geneste, 1992; Dibble, et al., 2005). The presence of isolated large blades exceeding the length distribution of the majority of

**Table 9.** Sibudu. C-A layers from the Deep Sounding: Frequency of cortex coverage proportions on the dorsal surface of blanks per raw material.

Raw Material	0%		<20%		>20%		>50%		100%		Indetermined		Total	
	n	%	n	%	n	%	n	%	n	%	n	%	n	%
Dolerite	3,209	52.3%	817	13.3%	1,288	21.0%	611	10.0%	210	3.4%	1	0.0%	6,136	100%
Hornfels	29	39.7%	12	16.4%	22	30.1%	8	11.0%	2	2.7%	-	0.0%	73	100%
Quartz	45	50.6%	6	6.7%	23	25.8%	9	10.1%	6	6.7%	-	0.0%	89	100%
Quartzite	192	58.0%	32	9.7%	65	19.6%	24	7.3%	18	5.4%	-	0.0%	331	100%
Sandstone	208	30.1%	57	8.2%	173	25.0%	113	16.4%	139	20.1%	1	0.1%	691	100%
Chert	8	40.0%	1	5.0%	7	35.0%	3	15.0%	1	5.0%	-	0.0%	20	100%
<b>Total</b>	<b>3,691</b>	<b>50.3%</b>	<b>925</b>	<b>12.6%</b>	<b>1,578</b>	<b>21.5%</b>	<b>768</b>	<b>10.5%</b>	<b>376</b>	<b>5.1%</b>	<b>2</b>	<b>0.0%</b>	<b>7,340</b>	<b>100%</b>



**Figure 26.** Sibudu. C-A layers from the Deep Sounding: Frequency distribution of length and width of completely preserved blades made on dolerite (left) and of width of all in the width completely preserved blades made on dolerite in mm (right).

artefacts strengthens the assumption that end-products were imported (Figure 26). A large portion of the completely preserved blades exhibit a length between 35 mm and 55 mm, however four laminar end-products exceed 100 mm. The high ratio (9:1) of small debitage elements to single lithic finds of all raw materials indicates intense on-site knapping activities with few post-depositional disturbances (Table 10). Dolerite makes up 56.3% of the cores (Table 11). With regards to the blank-to-core ratio (see for a definition Dibble and McPherron, 2006), knappers exploited dolerite intensively at the site (Figure 27) Most retouched elements (65.3%)

**Table 10.** Sibudu. C-A layers from the Deep Sounding: Frequency of raw materials per lithic artefacts >30mm and small debitage (<30mm) in square C4.

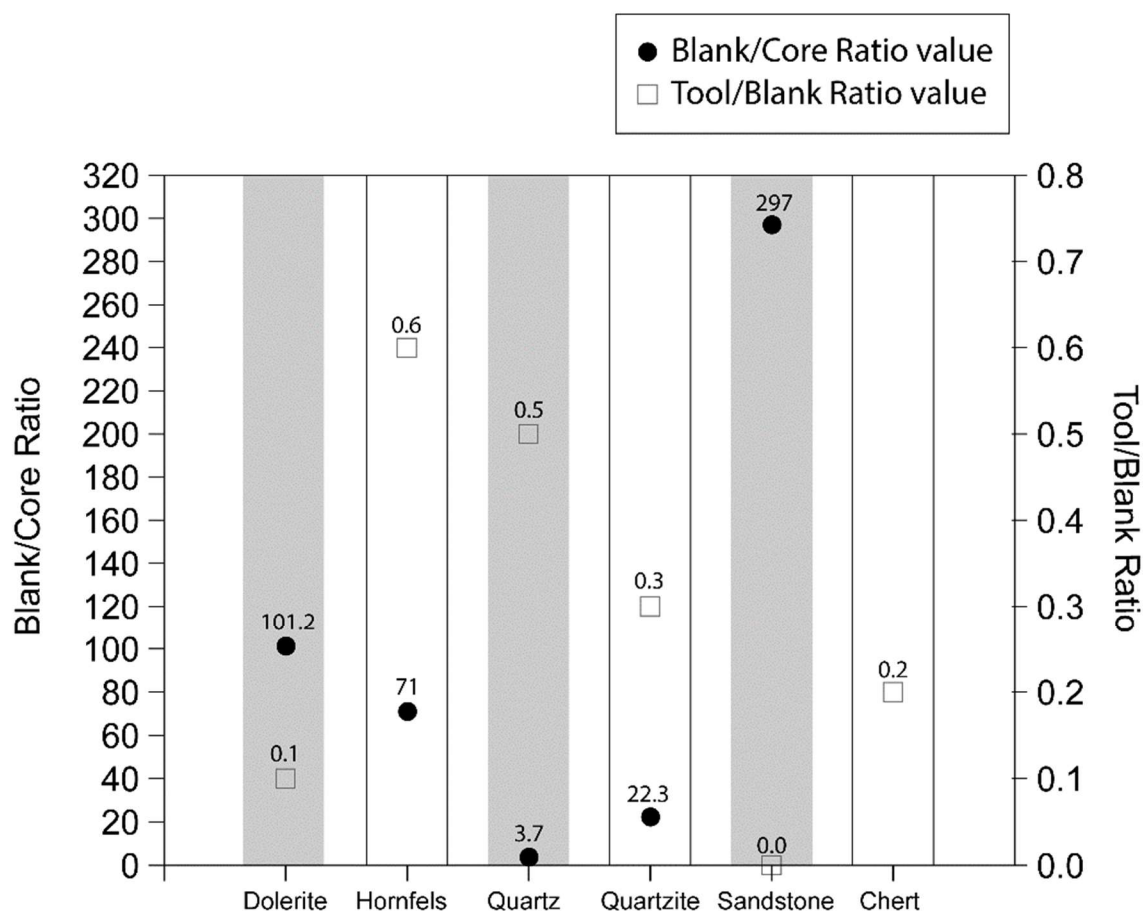
Lithic material	Dolerite		Hornfels		Quartzite		Quartz		Sandstone		Chert		Total	
	n	%	n	%	n	%	n	%	n	%	n	%	n	%
Lithic artefacts (>30 mm)	1,331	9.0%	27	5.2%	87	9.4%	18	2.4%	119	11.5%	4	23.5%	<b>1,586</b>	<b>8.8%</b>
Small debitage (<30 mm)	13,401	91.0%	494	94.8%	842	90.6%	720	97.6%	916	88.5%	13	76.5%	<b>16,386</b>	<b>91.2%</b>

**Table 11.** Sibudu. C-A layers from the Deep Sounding: Frequency of raw material per technological classification.

Technological Classification	Dolerite		Hornfels		Quartz		Quartzite		Sandstone		Chert		Indetermined		Total	
	n	%	n	%	n	%	n	%	n	%	n	%	n	%	n	%
Blades/Flakes	6,136	83.6%	73	1.0%	89	1.2%	331	4.5%	691	9.4%	20	0.3%	-	0.0%	<b>7,340</b>	<b>100%</b>
Tools	411	65.3%	31	4.9%	62	9.9%	117	18.6%	1	0.2%	6	1.0%	1	0.2%	<b>629</b>	<b>100%</b>
Cores	40	56.3%	1	1.4%	18	25.4%	11	15.5%	1	1.4%	-	0.0%	-	0.0%	<b>71</b>	<b>100%</b>
Hammerstones	5	17.2%	-	0.0%	1	3.4%	13	44.8%	8	27.6%	-	0.0%	2	6.9%	<b>29</b>	<b>100%</b>
Angular Debris	64	67.4%	14	14.7%	5	5.3%	2	2.1%	5	5.3%	5	5.3%	-	0.0%	<b>95</b>	<b>100%</b>
<b>Total</b>	<b>6,656</b>	<b>81.5%</b>	<b>119</b>	<b>1.5%</b>	<b>175</b>	<b>2.1%</b>	<b>474</b>	<b>5.8%</b>	<b>706</b>	<b>8.6%</b>	<b>31</b>	<b>0.4%</b>	<b>3</b>	<b>0.0%</b>	<b>8,164</b>	<b>100%</b>

are made on dolerite (Table 11), although in terms of the tool-to-blank ratio (see for a definition Dibble and McPherron, 2006), dolerite shows a low overall degree of modification (0.1) (Figure 27). The second most common raw material is sandstone. The reduction of this rock largely, if not entirely, occurred on-site since only 30.1% of the products exhibit no cortex and 20.1% are flakes with cortex remains (n=139), including 38 first flakes. One sandstone core left in an initial stage is present in the total core assemblage (Figure 28). Sandstone demonstrates the highest blank-to-core ratio at 297, reflecting its intense utilisation in the shelter. Accordingly, this raw material demonstrates the lowest degree of modification (Figure 27), with only one bifacial tool – a basal fragment – made on sandstone (Figure 29).

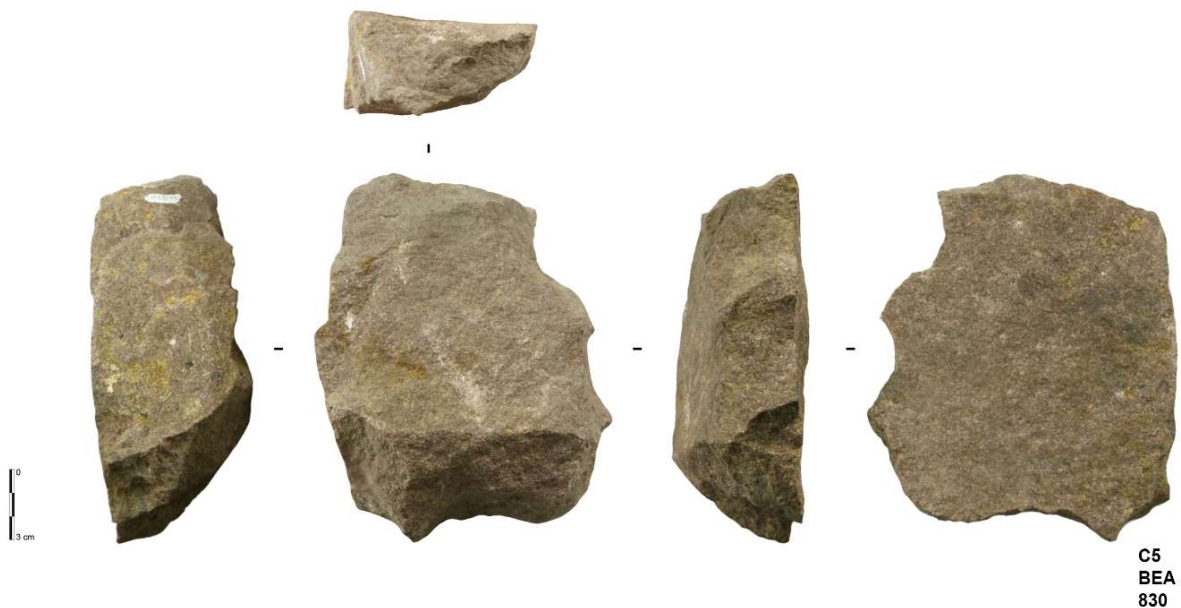
Quartzite accounts for 5.8% of the total assemblage (Table 11). Different varieties of quartzite are present, but the knappers of Sibudu primarily used a light to dark purple fine-grained variant. This variant represents 64.1% of the quartzite artefact total and 81.4% of the quartzite tools, including the only serrated piece made on quartzite (Figure 30). Some rocks were introduced to the site without preceding preparation, with the whole reduction sequence carried out on-site. Quartzite exhibits low frequencies of blanks with cortex coverage (5.4%; n=18) (Table 9), including three first flakes. The raw material demonstrates a low degree of reduction. The predominant transport of already finished blanks to the site could explain the highest proportion of blanks without any cortex coverage at 58% and the paucity of pieces with over 50% cortex. A total of 15.5% of the cores were made on quartzite (Table 11). Fittingly, the blank-to-core ratio indicates the relatively low exploitation of quartzite at the site (Figure 27). The tool corpus consists of 18.8% elements made on quartzite. Considering the tool-to-blank ratio, the increased investment in the curation of quartzite compared to dolerite and sandstone stands out (Figure 27).



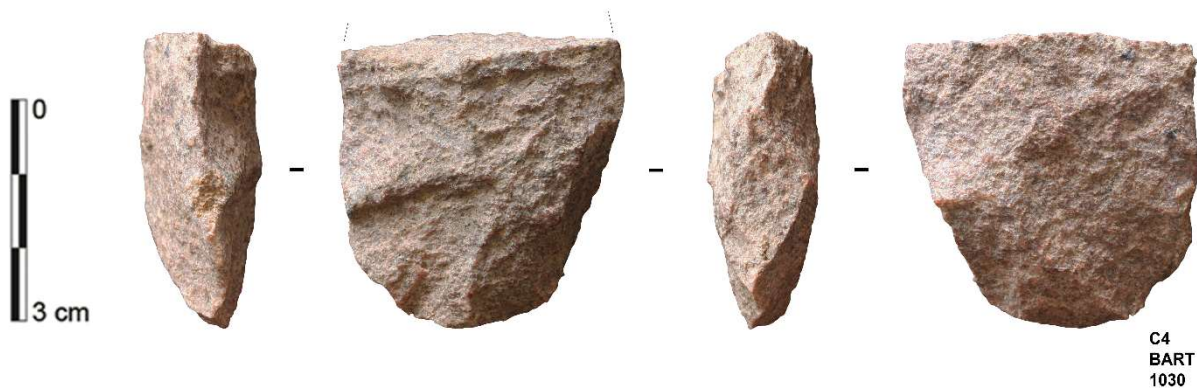
**Figure 27.** Sibudu. C-A layers from the Deep Sounding: Ratio of blank to core (the number of complete and proximal flakes and tools divided by the number of cores defined by Dibble and McPherron 2006) and tool to blank (the number of complete and proximal tools divided by the number of complete and proximal flakes defined by Dibble and McPherron 2006).

Quartz comprises 2.1% of the total lithic assemblage (Table 11). Milky quartz dominates throughout the sequence and is the almost exclusive quartz type in layer Chantal (Table 12). The frequency of crystal quartz is highest in layers Annie, Bart, and Bea. Interestingly, in layer Annie tools and cores are exclusively made on crystal quartz. In general, the proportion of crystal quartz among the blanks is low and no angular debris of this quartz type occur (Table 13). The appearance of six completely cortical quartz blanks (6.7%), including one first flake, also reflects that the initial stage of the reduction sequence partially took place at the site. A total of 25.4% of the cores are made on quartz. This rock has the second largest number of cores in the assemblage. The very low intensity of utilisation evident from the blank-to-core ratio (Figure 27) is, to a certain degree, related to the small-sized original core blanks and the cut-off size of 30 mm applied to this analysis. The cores made of quartz, most of which still exhibit cortical remains, are the smallest in size compared to the others (Figure 31). This rock has the highest ratio of small debitage products to single lithic finds of all raw materials. This not only attests to intense on-site knapping events, but also implies small-sized natural raw



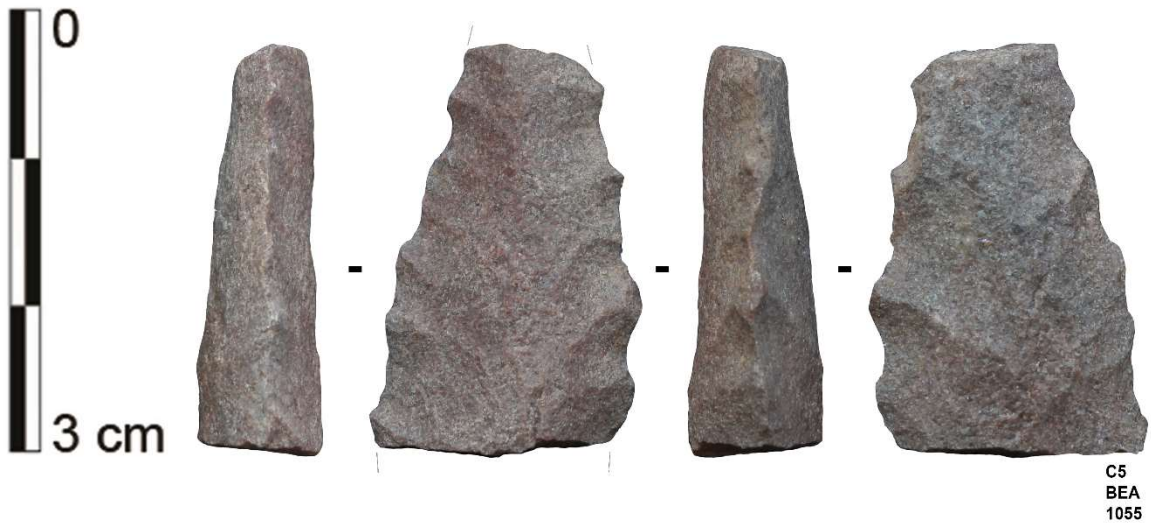


**Figure 28.** Sibudu. C-A layers from the Deep Sounding: Initial core made on sandstone (Photo by Viola C. Schmid).



**Figure 29.** Sibudu. C-A layers from the Deep Sounding: Basal fragment of bifacial made on sandstone (Photos by Guillaume Porraz).

material occurrences (Table 10). The toolmakers frequently chose to transform quartz blanks into tools (Figure 27). The importance of quartz, especially crystal quartz, in the production of tools, particularly bifacial and serrated pieces, can be seen in the proportion of 35% made on quartz, following 40% made on dolerite – a far more commonly used raw material.



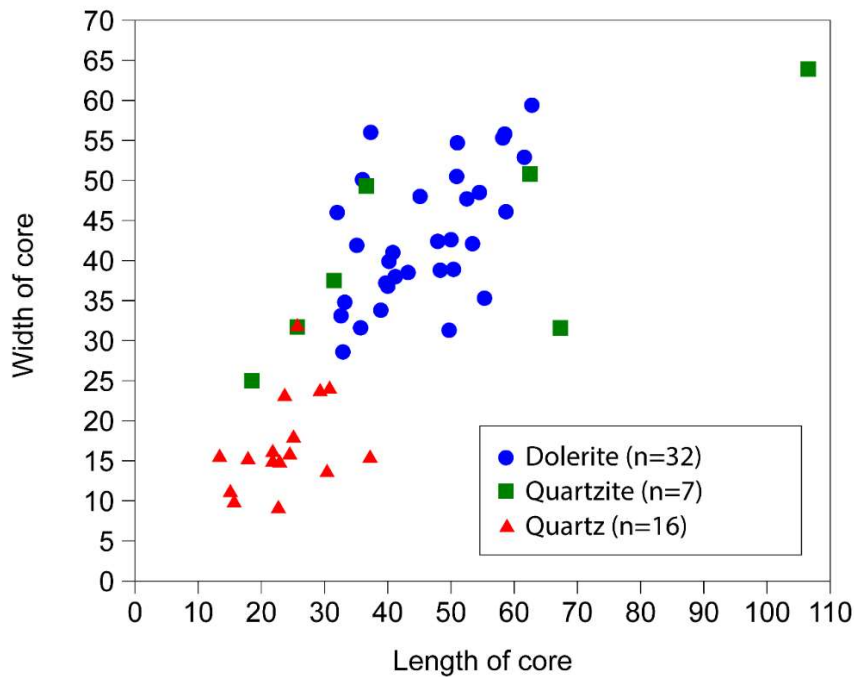
**Figure 30.** Sibudu. C-A layers from the Deep Sounding: Serrated piece made on light purple fine-grained quartzite variety (Photo by Viola C. Schmid).

**Table 12.** Sibudu. C-A layers from the Deep Sounding: Frequency of quartz types.

Layer	crystal		milky		Total	
	n	%	n	%	n	%
ADAM	6	18.2%	27	81.8%	<b>33</b>	<b>100%</b>
ANNIE	4	40.0%	6	60.0%	<b>10</b>	<b>100%</b>
BART	13	34.2%	25	65.8%	<b>38</b>	<b>100%</b>
BEA	11	34.4%	21	65.6%	<b>32</b>	<b>100%</b>
CASPER	7	15.9%	37	84.1%	<b>44</b>	<b>100%</b>
CHANTAL	1	5.6%	17	94.4%	<b>18</b>	<b>100%</b>
<b>Total</b>	<b>42</b>	<b>24.0%</b>	<b>133</b>	<b>76.0%</b>	<b>175</b>	<b>100%</b>

**Table 13.** Sibudu. C-A layers from the Deep Sounding: Frequency of quartz types per technological classification.

Technological classification	crystal		milky		Total	
	n	%	n	%	n	%
Blanks	6	6.7%	83	93.3%	<b>89</b>	<b>100%</b>
Tools	29	46.8%	33	53.2%	<b>62</b>	<b>100%</b>
Cores	7	38.9%	11	61.1%	<b>18</b>	<b>100%</b>
Hammerstones	-	0.0%	1	100.0%	<b>1</b>	<b>100%</b>
Angular Debris	-	0.0%	5	100.0%	<b>5</b>	<b>100%</b>
<b>Total</b>	<b>42</b>	<b>24.0%</b>	<b>133</b>	<b>76.0%</b>	<b>175</b>	<b>100%</b>



**Figure 31.** Sibudu. C-A layers from the Deep Sounding: Scatter plot of width and length of all complete cores.

1.5% of the artefacts are made on hornfels (Table 6). The inhabitants of Sibudu transported hornfels partly without preceding preparation to the site. This raw material exhibits the lowest frequency of cortical blanks at 2.7% and I observed no first flakes (Table 9). Similar to quartzite, hornfels shows a low degree of reduction and the scarcity of pieces with over 50% cortex is most likely related to the increased import of already finished blanks to the shelter. One hornfels core, indeterminate and broken, exists in the total core assemblage. The blank-to-core ratio indicates the moderate exploitation of hornfels at the site (Figure 27). However, the EL-to-blank mass ratio shows that knappers most successfully converted hornfels rock mass into blank edges (Table 14).

**Table 14.** Sibudu. C-A layers from the Deep Sounding: Descriptive statistics of EL-to-blank mass ratio of all completely preserved blanks per raw material.

	Dolerite	Hornfels	Quartz	Quartzite	Sandstone
n	1,786	23	22	78	130
Min	1.3	4.9	2.3	4.7	1.7
Max	71	44.8	25.2	73.9	42.7
Sum	28,014.8	532.7	302	1,409.4	1,788.4
Mean	15.7	23.2	13.7	18.1	13.8
Std. error	0.2	2.2	1.4	1.2	0.7
Variance	75.3	110.2	41.7	116.3	57.4
Stand. dev.	8.7	10.5	6.5	10.8	7.6
Median	14.1	20.1	12.8	15.5	12
25 prcntil	9.7	16.2	8.5	11.1	8.3
75 prcntil	19.8	30.3	18	21.6	17.4

Only 4.9% of the tool corpus is comprised of hornfels (Table 11), yet the toolmakers chose more often to transform hornfels blanks into tools. Hornfels exhibits the highest tool-to-blank ratio reflecting a high investment in the curation of this raw material (Figure 27).

The small number of pieces (n=31) and the lack of cores made on chert (Table 11) indicate that past people rarely exploited this rock, confirmed by the lowest ratio of small debitage products to single lithic finds (8:2) (Table 10). Conversely, the toolmakers selected chert blanks relatively often to manufacture tools (Figure 27).

## 5.2. Debitage

All layers comprise a high frequency of blanks, between 89.6% to 90.3% of the assemblage (Table 15). The assemblage demonstrates a strong emphasis on the production of laminar elements among the blanks (Table 16). The proportion of blades varies from 23.5% to 29.3% per layer and elongated flakes also account for between 11.3% and 16.1%. Even though the total debitage laminarity (for a definition see Tostevin, 2003) of all completely preserved products is relatively low at 1.2 (Table 17), one has to take under consideration that only 27.9%

**Table 15.** Sibudu. C-A layers from the Deep Sounding: General technological classification.

Layer	Blanks		Tools		Cores		Hammerstones		Angular Debris		Total	
	n	%	n	%	n	%	n	%	n	%	n	%
ADAM	1,630	89.9%	124	6.8%	22	1.2%	10	0.6%	28	1.5%	1,814	100%
ANNIE	954	90.3%	74	7.0%	15	1.4%	6	0.6%	8	0.8%	1,057	100%
BART	1,067	90.2%	83	7.0%	16	1.4%	8	0.7%	9	0.8%	1,183	100%
BEA	1,429	89.6%	147	9.2%	6	0.4%		0.0%	13	0.8%	1,595	100%
CASPER	1,248	89.6%	113	8.1%	6	0.4%	1	0.1%	25	1.8%	1,393	100%
CHANTAL	1,012	90.2%	88	7.8%	6	0.5%	4	0.4%	12	1.1%	1,122	100%
<b>Total</b>	<b>7,340</b>	<b>89.9%</b>	<b>629</b>	<b>7.7%</b>	<b>71</b>	<b>0.9%</b>	<b>29</b>	<b>0.4%</b>	<b>95</b>	<b>1.2%</b>	<b>8,164</b>	<b>100%</b>

**Table 16.** Sibudu. C-A layers from the Deep Sounding: Frequency of blank categories.

Layer	Blades		Bladelets		Elongated flakes		Flakes		Triangular flakes		Total	
	n	%	n	%	n	%	n	%	n	%	n	%
ADAM	477	29.3%	5	0.3%	254	15.6%	841	51.6%	53	3.3%	1,630	100%
ANNIE	247	25.9%	1	0.1%	154	16.1%	519	54.4%	25	2.6%	954	100%
BART	255	23.9%	1	0.1%	144	13.5%	641	60.1%	26	2.4%	1,067	100%
BEA	342	23.9%	3	0.2%	162	11.3%	910	63.7%	19	1.3%	1,429	100%
CASPER	293	23.5%	3	0.2%	155	12.4%	809	64.8%	14	1.1%	1,248	100%
CHANTAL	273	27.0%	4	0.4%	129	12.7%	571	56.4%	10	1.0%	1,012	100%
<b>Total</b>	<b>1,887</b>	<b>25.7%</b>	<b>17</b>	<b>0.2%</b>	<b>998</b>	<b>13.6%</b>	<b>4,291</b>	<b>58.5%</b>	<b>147</b>	<b>2.0%</b>	<b>7,340</b>	<b>100%</b>

**Table 17.** Sibudu. C-A layers from the Deep Sounding: Descriptive statistics of the debitage laminarity of all completely preserved blanks per raw materials.

	Dolerite	Hornfels	Quartz	Quartzite	Sandstone	Chert	Total
n	1786	23	22	78	129	6	<b>2044</b>
Min	0.2	0.5	0.5	0.5	0.2	0.8	<b>0.2</b>
Max	4.3	3.6	1.8	2.1	2.9	1.9	<b>4.3</b>
Sum	2234.0	34.2	23.5	83.8	127.0	6.7	<b>2509.2</b>
Mean	1.3	1.5	1.1	1.1	1.0	1.1	<b>1.2</b>
Std. error	0.0	0.2	0.1	0.0	0.0	0.2	<b>0.0</b>
Variance	0.3	0.5	0.2	0.2	0.2	0.2	<b>0.3</b>
Stand. dev.	0.6	0.7	0.4	0.4	0.5	0.4	<b>0.6</b>
Median	1.2	1.3	1.1	1.0	0.9	0.9	<b>1.1</b>
25 prcntil	0.9	0.9	0.7	0.7	0.6	0.9	<b>0.8</b>
75 prcntil	1.5	1.8	1.4	1.4	1.2	1.4	<b>1.5</b>

**Table 18.** Sibudu. C-A layers from the Deep Sounding: Frequency of fragmentation per blank category.

Blank categories	all		proximal		medial		distal		lateral		lateral-proximal		lateral-medial		lateral-distal		indetermined		Total	
	n	%	n	%	n	%	n	%	n	%	n	%	n	%	n	%	n	%	n	%
Blades	217	11.5%	835	44.3%	484	25.6%	254	13.5%	8	0.4%	40	2.1%	37	2.0%	11	0.6%	1	0.1%	<b>1,887</b>	<b>100%</b>
Bladelets	2	11.8%	2	11.8%	9	52.9%	4	23.5%	-	0.0%	-	0.0%	-	0.0%	-	0.0%	-	0.0%	<b>17</b>	<b>100%</b>
Elongated flakes	327	32.8%	285	28.6%	131	13.1%	100	10.0%	36	3.6%	64	6.4%	31	3.1%	24	2.4%	-	0.0%	<b>998</b>	<b>100%</b>
Flakes	1,430	33.3%	789	18.4%	308	7.2%	553	12.9%	285	6.6%	319	7.4%	312	7.3%	294	6.9%	1	0.0%	<b>4,291</b>	<b>100%</b>
Triangular flakes	69	46.9%	29	19.7%	15	10.2%	26	17.7%	3	2.0%	3	2.0%	1	0.7%	1	0.7%	-	0.0%	<b>147</b>	<b>100%</b>
<b>Total</b>	<b>2,045</b>	<b>27.9%</b>	<b>1,940</b>	<b>26.4%</b>	<b>947</b>	<b>12.9%</b>	<b>937</b>	<b>12.8%</b>	<b>332</b>	<b>4.5%</b>	<b>426</b>	<b>5.8%</b>	<b>381</b>	<b>5.2%</b>	<b>330</b>	<b>4.5%</b>	<b>2</b>	<b>0.0%</b>	<b>7,340</b>	<b>100%</b>

of all the blanks are not broken (Table 18). The unimodal distribution of blade/bladelet widths supports a continuum of blade production at an advanced stage and not a separate reduction sequence (Figure 26). There is a small proportion of bladelets in the assemblage (Table 16) but I follow the proposal of (Tixier, 1967) and Inizan et al. (1999) to waive the arbitrary dimensional boundary. In the following, I give an overview of each blank category highlighting the general diagnostic features within this assemblage:

Regarding the overall blank population, hornfels demonstrates the highest proportion of blades at 32.9% (Table 19). Fittingly, this raw material has also the highest debitage laminarity value (Table 17), although the percentage of completely preserved blades is comparable to dolerite (Table 20). Chert stands at 30% though the total sample of 20 pieces is small. Quartzite and dolerite show similar blade frequencies at 27.5% and 26.8%. Sandstone follows at 16.8%, while only 6.7% of the quartz blanks are blades, none of which is completely preserved suggesting a minor importance of these raw materials in blade production. In general, most of the blades are non-cortical (55.5%) (Table 21). Only 1.8% exhibit a complete dorsal cortex coverage. However, lateral and (to a certain degree) backed cortical end-products are common as well (Table 22). Most blades have plain butts indicating limited preparation of the striking platforms (Table 23). Furthermore, most of the blades exhibit unidirectional dorsal scars (74.1%) (Table

24). Some of the laminar end-products show orthogonal negatives (11.8%) and some bidirectional negatives (6.5%), attesting to lateral and distal preparation and/or exploitation. A rectangular shape clearly distinguishes the laminar end-products (Table 25). The knappers strived for straight to slightly curved end-products indicated by the artefact profiles (Table 26). The length of blades averages between 39 mm and 55 mm (Table 27). The mean length stands at 48.5 mm which significantly differentiates blades from flakes and even elongated flakes. The width ranges mainly between 18 mm and 26 mm (Table 28) and the thickness between 6 mm and 9 mm (Table 29). Additionally, the blades are clearly narrower and thinner than the other blanks. Large specimens (n=4), namely larger than 100 mm, occur occasionally (Figure 32c, e and n & Figure 35d and j). As expected, laminar end-products demonstrate a higher EL-to-blank mass ratio compared to the other blank categories (Table 30), indicating a greater efficiency in converting stone mass into edge length. While blade length encompasses a wide range, the other two dimensions show a higher degree of standardisation. Most of the blades terminate in a feather termination and the distal end is either convex or pointed (Table 31). Plunging blades occur, some of which show distal preparation. Knapping accidents, in the form

**Table 19.** Sibudu. C-A layers from the Deep Sounding: Frequency of raw materials per blank category.

Blank categories	Dolerite		Hornfels		Quartz		Quartzite		Sandstone		Chert		Total	
	n	%	n	%	n	%	n	%	n	%	n	%	n	%
Blades	1,644	26.8%	24	32.9%	6	6.7%	91	27.5%	116	16.8%	6	30.0%	<b>1,887</b>	<b>25.7%</b>
Bladelets	11	0.2%	2	2.7%	2	2.2%	2	0.6%	-	0.0%	-	0.0%	<b>17</b>	<b>0.2%</b>
Elongated flakes	865	14.1%	10	13.7%	9	10.1%	48	14.5%	64	9.3%	2	10.0%	<b>998</b>	<b>13.6%</b>
Flakes	3,487	56.8%	36	49.3%	71	79.8%	184	55.6%	501	72.5%	12	60.0%	<b>4,291</b>	<b>58.5%</b>
Triangular flakes	129	2.1%	1	1.4%	1	1.1%	6	1.8%	10	1.4%	-	0.0%	<b>147</b>	<b>2.0%</b>
<b>Total</b>	<b>6,136</b>	<b>100%</b>	<b>73</b>	<b>100%</b>	<b>89</b>	<b>100%</b>	<b>331</b>	<b>100%</b>	<b>691</b>	<b>100%</b>	<b>20</b>	<b>100%</b>	<b>7,340</b>	<b>100%</b>

**Table 20.** Sibudu. C-A layers from the Deep Sounding: Frequency of fragmentation of blades per raw material.

Raw Material	all		proximal		medial		distal		lateral		lateral-proximal		lateral-medial		lateral-distal		indetermined		Total	
	n	%	n	%	n	%	n	%	n	%	n	%	n	%	n	%	n	%	n	%
Dolerite	202	12.2%	751	45.4%	413	25.0%	216	13.1%	7	0.4%	29	1.8%	31	1.9%	5	0.3%	1	0.1%	<b>1,655</b>	<b>100%</b>
Hornfels	3	11.5%	13	50.0%	5	19.2%	2	7.7%	-	0.0%	2	7.7%	1	3.8%	-	0.0%	-	0.0%	<b>26</b>	<b>100%</b>
Quartz	-	0.0%	3	37.5%	4	50.0%	1	12.5%	-	0.0%	-	0.0%	-	0.0%	-	0.0%	-	0.0%	<b>8</b>	<b>100%</b>
Quartzite	6	6.5%	42	45.2%	24	25.8%	13	14.0%	1	1.1%	4	4.3%	2	2.2%	-	0.0%	-	0.0%	<b>93</b>	<b>100%</b>
Sandstone	7	6.0%	26	22.4%	46	39.7%	23	19.8%	-	0.0%	5	4.3%	3	2.6%	6	5.2%	-	0.0%	<b>116</b>	<b>100%</b>
Chert	1	16.7%	2	33.3%	1	16.7%	2	33.3%	-	0.0%	-	0.0%	-	0.0%	-	0.0%	-	0.0%	<b>6</b>	<b>100%</b>
<b>Total</b>	<b>219</b>	<b>11.5%</b>	<b>837</b>	<b>44.0%</b>	<b>493</b>	<b>25.9%</b>	<b>258</b>	<b>13.6%</b>	<b>8</b>	<b>0.4%</b>	<b>40</b>	<b>2.1%</b>	<b>37</b>	<b>1.9%</b>	<b>11</b>	<b>0.6%</b>	<b>1</b>	<b>0.1%</b>	<b>1,904</b>	<b>100%</b>

**Table 21.** Sibudu. C-A layers from the Deep Sounding: Frequency of cortex coverage per blank category.

Blank Categories	0%		<20%		>20%		>50%		100%		indetermined		Total	
	n	%	n	%	n	%	n	%	n	%	n	%	n	%
Blades	1,056	55.5%	205	10.8%	438	23.0%	169	8.9%	35	1.8%	1	0.1%	<b>1,904</b>	<b>100%</b>
Elongated flakes	539	54.0%	138	13.8%	220	22.0%	82	8.2%	19	1.9%	-	0.0%	<b>998</b>	<b>100%</b>
Flakes	2,020	47.1%	571	13.3%	881	20.5%	502	11.7%	316	7.4%	1	0.0%	<b>4,291</b>	<b>100%</b>
Triangular flakes	76	51.7%	11	7.5%	39	26.5%	15	10.2%	6	4.1%	-	0.0%	<b>147</b>	<b>100%</b>
<b>Total</b>	<b>3,691</b>	<b>50.3%</b>	<b>925</b>	<b>12.6%</b>	<b>1,578</b>	<b>21.5%</b>	<b>768</b>	<b>10.5%</b>	<b>376</b>	<b>5.1%</b>	<b>2</b>	<b>0.0%</b>	<b>7,340</b>	<b>100%</b>

**Table 22.** Sibudu. C-A layers from the Deep Sounding: Frequency of cortex position per blank category.

Blank Categories	0%		100% cortex		backed		lateral		distal		proximal		middle/centre		indetermined		Total	
	n	%	n	%	n	%	n	%	n	%	n	%	n	%	n	%	n	%
Blades	1,056	55.5%	35	1.8%	143	7.5%	566	29.7%	71	3.7%	6	0.3%	26	1.4%	1	0.1%	<b>1,904</b>	<b>100%</b>
Elongated flakes	539	54.0%	19	1.9%	57	5.7%	266	26.7%	98	9.8%	4	0.4%	15	1.5%	-	0.0%	<b>998</b>	<b>100%</b>
Flakes	2,020	47.1%	316	7.4%	295	6.9%	1,001	23.3%	552	12.9%	35	0.8%	71	1.7%	1	0.0%	<b>4,291</b>	<b>100%</b>
Triangular flakes	76	51.7%	6	4.1%	4	2.7%	56	38.1%	5	3.4%	-	0.0%	-	0.0%	-	0.0%	<b>147</b>	<b>100%</b>
<b>Total</b>	<b>3,691</b>	<b>50.3%</b>	<b>373</b>	<b>5.1%</b>	<b>499</b>	<b>6.8%</b>	<b>1,892</b>	<b>25.8%</b>	<b>726</b>	<b>9.9%</b>	<b>45</b>	<b>0.6%</b>	<b>112</b>	<b>1.5%</b>	<b>2</b>	<b>0.0%</b>	<b>7,340</b>	<b>100%</b>

**Table 23.** Sibudu. C-A layers from the Deep Sounding: Frequency of platform type of completely and proximal preserved blanks.

Blank Categories	plain		cortical		faceted		dihedral		crushed		indetermined		Total	
	n	%	n	%	n	%	n	%	n	%	n	%	n	%
Blades	825	74.7%	74	6.7%	97	8.8%	101	9.1%	5	0.5%	2	0.2%	<b>1,104</b>	<b>100%</b>
Elongated flakes	550	77.4%	59	8.3%	37	5.2%	62	8.7%	1	0.1%	2	0.3%	<b>711</b>	<b>100%</b>
Flakes	1,996	70.7%	390	13.8%	102	3.6%	287	10.2%	40	1.4%	7	0.2%	<b>2,822</b>	<b>100%</b>
Triangular flakes	69	66.3%	11	10.6%	11	10.6%	13	12.5%	-	0.0%	-	0.0%	<b>104</b>	<b>100%</b>
<b>Total</b>	<b>3,440</b>	<b>72.6%</b>	<b>534</b>	<b>11.3%</b>	<b>247</b>	<b>5.2%</b>	<b>463</b>	<b>9.8%</b>	<b>46</b>	<b>1.0%</b>	<b>11</b>	<b>0.2%</b>	<b>4,741</b>	<b>100%</b>

**Table 24.** Sibudu. C-A layers from the Deep Sounding: Frequency of dorsal scar pattern per blank category.

Blank Categories	unidirectional		unidirectional convergent		bidirectional		opposed		orthogonal		crossed		Kombewa		cortex		indetermined		Total	
	n	%	n	%	n	%	n	%	n	%	n	%	n	%	n	%	n	%	n	%
Blades	1,411	74.1%	85	4.5%	124	6.5%	5	0.3%	224	11.8%	15	0.8%	3	0.2%	36	1.9%	1	0.1%	<b>1,904</b>	<b>100%</b>
Elongated flakes	809	81.1%	59	5.9%	51	5.1%	3	0.3%	54	5.4%	3	0.3%	-	0.0%	19	1.9%	-	0.0%	<b>998</b>	<b>100%</b>
Flakes	2,233	52.0%	108	2.5%	168	3.9%	13	0.3%	1,372	32.0%	67	1.6%	2	0.0%	314	7.3%	14	0.3%	<b>4,291</b>	<b>100%</b>
Triangular flakes	50	34.0%	81	55.1%	6	4.1%	-	0.0%	3	2.0%	1	0.7%	-	0.0%	6	4.1%	-	0.0%	<b>147</b>	<b>100%</b>
<b>Total</b>	<b>4,503</b>	<b>61.3%</b>	<b>333</b>	<b>4.5%</b>	<b>349</b>	<b>4.8%</b>	<b>21</b>	<b>0.3%</b>	<b>1,653</b>	<b>22.5%</b>	<b>86</b>	<b>1.2%</b>	<b>5</b>	<b>0.1%</b>	<b>375</b>	<b>5.1%</b>	<b>15</b>	<b>0.2%</b>	<b>7,340</b>	<b>100%</b>

**Table 25.** Sibudu. C-A layers from the Deep Sounding: Frequency of morphology per blank category.

Blank Categories	rectangular		trapezoidal		triangular		irregular		indetermined		Total	
	n	%	n	%	n	%	n	%	n	%	n	%
Blades	1,736	91.2%	2	0.1%	121	6.4%	1	0.1%	44	2.3%	<b>1,904</b>	<b>100%</b>
Elongated flakes	906	90.8%	11	1.1%	51	5.1%	2	0.2%	28	2.8%	<b>998</b>	<b>100%</b>
Flakes	970	22.6%	2,251	52.5%	125	2.9%	20	0.5%	925	21.6%	<b>4,291</b>	<b>100%</b>
Triangular flakes	-	0.0%	-	0.0%	147	100.0%	-	0.0%	-	0.0%	<b>147</b>	<b>100%</b>
<b>Total</b>	<b>3,612</b>	<b>49.2%</b>	<b>2,264</b>	<b>30.8%</b>	<b>444</b>	<b>6.0%</b>	<b>23</b>	<b>0.3%</b>	<b>997</b>	<b>13.6%</b>	<b>7,340</b>	<b>100%</b>

**Table 26.** Sibudu. C-A layers from the Deep Sounding: Frequency of profile per blank category.

Blank Categories	straight		slightly curved		curved		highly curved		indetermined		Total	
	n	%	n	%	n	%	n	%	n	%	n	%
Blades	1,166	61.2%	603	31.7%	132	6.9%	1	0.1%	2	0.1%	<b>1,904</b>	<b>100%</b>
Elongated flakes	581	58.2%	345	34.6%	72	7.2%	-	0.0%	-	0.0%	<b>998</b>	<b>100%</b>
Flakes	2,239	52.2%	1,453	33.9%	508	11.8%	78	1.8%	13	0.3%	<b>4,291</b>	<b>100%</b>
Triangular flakes	85	57.8%	41	27.9%	21	14.3%	-	0.0%	-	0.0%	<b>147</b>	<b>100%</b>
<b>Total</b>	<b>4,071</b>	<b>55.5%</b>	<b>2,442</b>	<b>33.3%</b>	<b>733</b>	<b>10.0%</b>	<b>79</b>	<b>1.1%</b>	<b>15</b>	<b>0.2%</b>	<b>7,340</b>	<b>100%</b>

**Table 27.** Sibudu. C-A layers from the Deep Sounding: Descriptive statistics of the length of all completely preserved blanks per blank category.

	Blades	Elongated flakes	Flakes	Triangular flakes
n	219	326	1430	69
Min	28.1	23.9	6.3	25.1
Max	113.8	81.7	94	70.4
Sum	10,619.9	13,098.4	45,640.4	2,695.9
Mean	48.5	40.2	31.9	39.1
Std. error	1.0	0.6	0.3	1.3
Variance	226.2	99.0	112.7	114.7
Stand. dev.	15.0	9.9	10.6	10.7
Median	45.2	37.6	30.2	36.3
25 prcntil	38.5	33	25.2	30.6
75 prcntil	55.4	45.7	37	44.4



**Table 28.** Sibudu. C-A layers from the Deep Sounding: Descriptive statistics of the width of all in the width completely preserved blanks per blank category.

	Blades	Elongated flakes	Flakes	Triangular flakes
n	1,807	843	3,077	139
Min	5.8	12.8	9	15.3
Max	72.9	57.2	100.3	48.3
Sum	40,891.7	22,956	101,493	3,874.1
Mean	22.6	27.2	33.0	27.9
Std. error	0.1	0.2	0.2	0.6
Variance	40.1	47.8	73.3	43.3
Stand. dev.	6.3	6.9	8.6	6.6
Median	22.2	26.1	31.5	27
25 prcntil	18.2	22.3	27.5	23.4
75 prcntil	26.2	30.9	37	31.2

**Table 29.** Sibudu. C-A layers from the Deep Sounding: Descriptive statistics of the thickness of all in the thickness completely preserved blanks per blank category.

	Blades	Elongated flakes	Flakes	Triangular flakes
n	1,903	997	4,287	147
Min	2	2.4	2.2	4.6
Max	27.4	27.6	41.5	26.6
Sum	14,893.4	8,213	38,310.4	1337.9
Mean	7.8	8.2	8.9	9.1
Std. error	0.1	0.1	0.1	0.3
Variance	8.8	10.1	14.3	9.2
Stand. dev.	3.0	3.2	3.8	3.0
Median	7.5	7.7	8.1	8.8
25 prcntil	5.7	6	6.4	6.8
75 prcntil	9.3	9.8	10.7	10.9

**Table 30.** Sibudu. C-A layers from the Deep Sounding: Descriptive statistics of EL-to-blank mass ratio of all completely preserved blanks per blank category.

	Blade	Elongated flakes	Flakes	Triangular flakes
n	219	326	1430	69
Min	2.4	2.9	1.3	3.8
Max	71.0	63.3	73.9	42.4
Sum	4,188.6	5,342.7	21,588.5	1,001.0
Mean	19.1	16.4	15.1	14.5
Std. error	0.8	0.5	0.2	0.8
Variance	142.4	78.0	65.6	41.2
Stand. dev.	11.9	8.8	8.1	6.4
Median	16.1	14.7	13.8	12.9
25 prcntil	11.4	10.3	9.3	10.2
75 prcntil	24.3	20.9	19.4	18.1



**Table 31.** Sibudu. C-A layers from the Deep Sounding: Frequency of distal termination of all completely and distal preserved blanks per blank category.

Blank Categories	pointed		convex		concave		straight		irregular		hinged		plunging		step		indetermined		Total	
	n	%	n	%	n	%	n	%	n	%	n	%	n	%	n	%	n	%	n	%
Blades	158	32.4%	166	34.0%	10	2.0%	57	11.7%	-	0.0%	44	9.0%	40	8.2%	2	0.4%	11	2.3%	<b>488</b>	<b>100%</b>
Elongated flakes	51	11.3%	205	45.6%	14	3.1%	79	17.6%	2	0.4%	81	18.0%	13	2.9%	-	0.0%	5	1.1%	<b>450</b>	<b>100%</b>
Flakes	107	4.7%	927	40.8%	119	5.2%	524	23.1%	-	0.0%	332	14.6%	223	9.8%	3	0.1%	36	1.6%	<b>2,271</b>	<b>100%</b>
Triangular flakes	78	81.3%	11	11.5%	-	0.0%	-	0.0%	-	0.0%	6	6.3%	-	0.0%	-	0.0%	1	1.0%	<b>96</b>	<b>100%</b>
<b>Total</b>	<b>394</b>	<b>11.9%</b>	<b>1,309</b>	<b>39.6%</b>	<b>143</b>	<b>4.3%</b>	<b>660</b>	<b>20.0%</b>	<b>2</b>	<b>0.1%</b>	<b>463</b>	<b>14.0%</b>	<b>276</b>	<b>8.4%</b>	<b>5</b>	<b>0.2%</b>	<b>53</b>	<b>1.6%</b>	<b>3,305</b>	<b>100%</b>

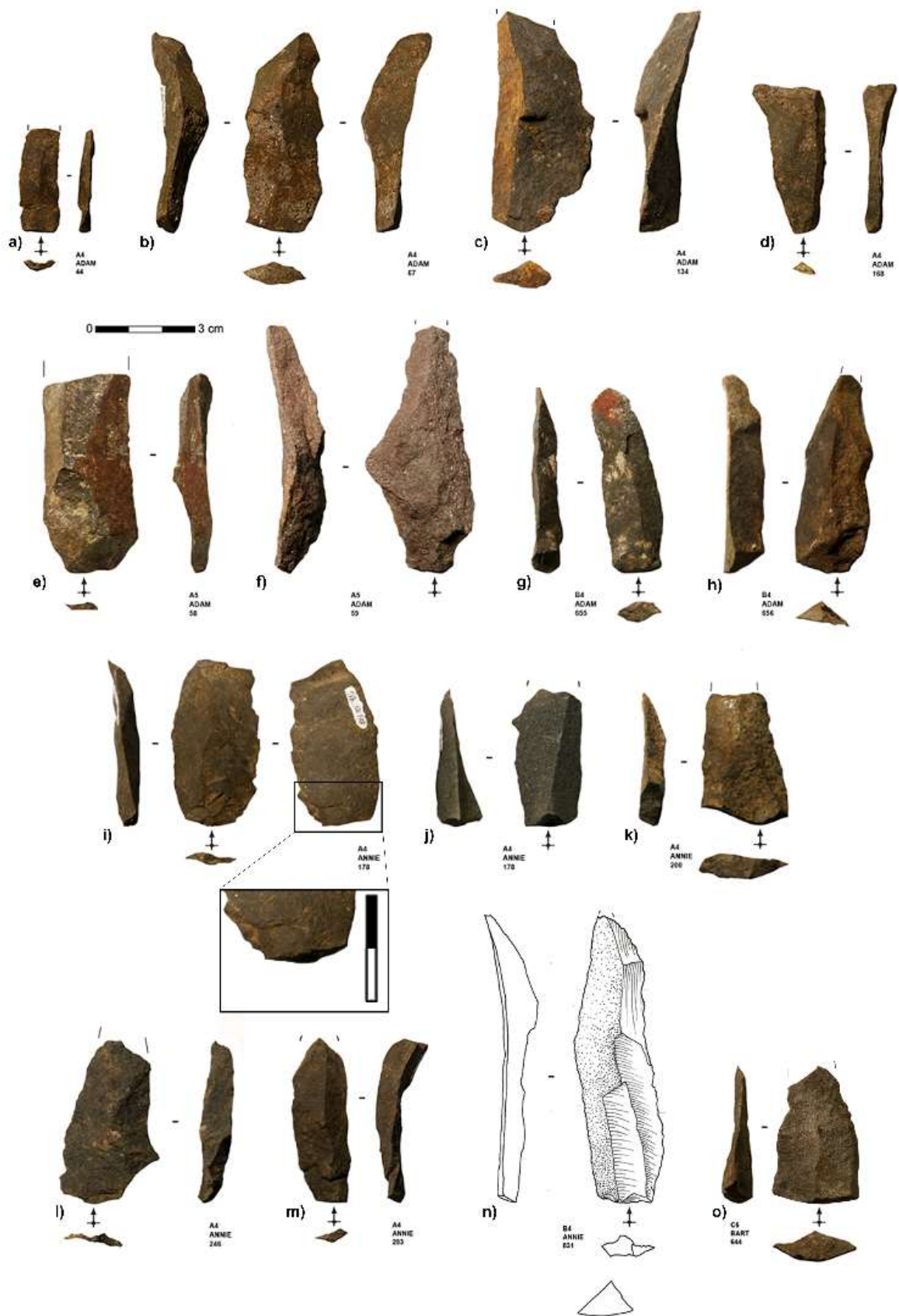
**Table 32.** Sibudu. C-A layers from the Deep Sounding: Frequency of cross-section per blank category.

Blank Categories	triangular		trapezoidal		lenticular		irregular		indetermined		Total	
	n	%	n	%	n	%	n	%	n	%	n	%
Blades	1,151	63.7%	491	27.2%	152	8.4%	3	0.2%	10	0.6%	<b>1,807</b>	<b>100%</b>
Elongated flakes	462	54.8%	298	35.3%	78	9.3%	1	0.1%	4	0.5%	<b>843</b>	<b>100%</b>
Flakes	1,166	37.9%	1,212	39.4%	596	19.4%	82	2.7%	24	0.8%	<b>3,080</b>	<b>100%</b>
Triangular flakes	91	65.5%	40	28.8%	8	5.8%	-	0.0%	-	0.0%	<b>139</b>	<b>100%</b>
<b>Total</b>	<b>2,870</b>	<b>48.9%</b>	<b>2,041</b>	<b>34.8%</b>	<b>834</b>	<b>14.2%</b>	<b>86</b>	<b>1.5%</b>	<b>38</b>	<b>0.6%</b>	<b>5,869</b>	<b>100%</b>

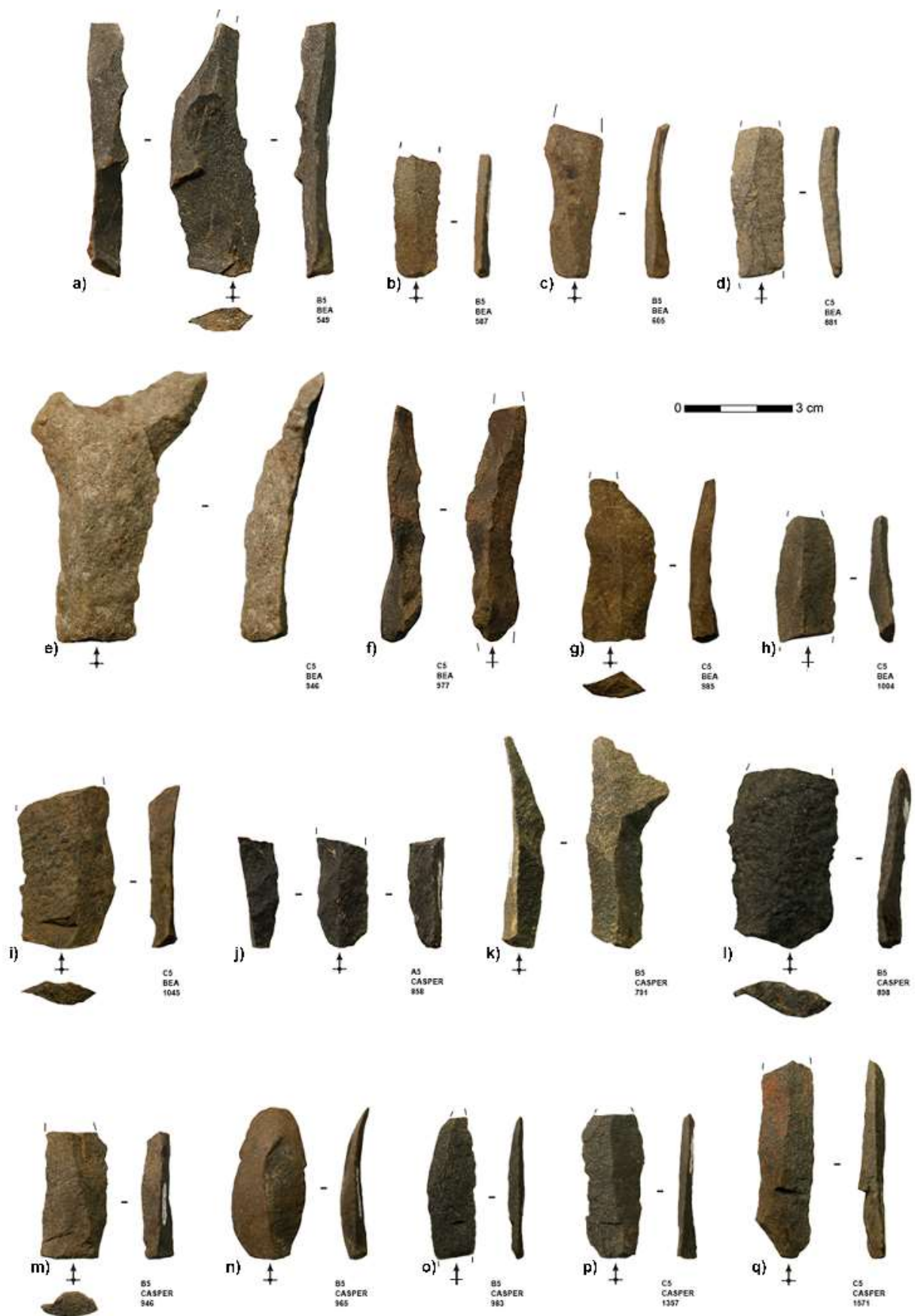
**Table 33.** Sibudu. C-A layers from the Deep Sounding: Comparison of dorsal convexity between blades with a triangular cross-section and blades with a trapezoidal cross-section (t-test).

		
n:	1,151	491
Mean:	2.936	3.3703
Stand. dev.	0.0546	0.0998
Variance:	0.89016	1.2665
<b>F:</b>	<b>1.4228</b>	
<b>t:</b>	<b>-8.0467</b>	
<b>p:</b>	<b>0.0001</b>	

of hinged terminations, account for 9% of the laminar end-products. A large proportion of the blades (only 11.5% completely preserved) is fragmented (Table 18), but 55.3% of the blades have two-thirds (proximal-medial or medial-distal) preserved. The majority of laminar end-products has a triangular cross-section followed by those with a trapezoidal cross-section (Table 32). Within the blade category, I observed the existence of two significantly different groups when using the cross-section and the width-to-thickness ratio as proxies for the lateral and vertical convexity (for a definition see Tostevin, 2003): (1) tall, laterally centralised blades with



**Figure 32.** Sibudu. C-A layers from the Deep Sounding: Tall, laterally centralised blades with a triangular cross-section. Blades made on dolerite (a-e, g-o) and made on sandstone (f) (Drawing by Mojdeh Lajmiri and Heike Würschem; photos by Viola C. Schmid).



**Figure 33.** Sibudu. C-A layers from the Deep Sounding: Tall, laterally centralised blades with a triangular cross-section. Blades made on dolerite (a-d, f-q) and made on quartzite I (Photos by Viola C. Schmid).



**Figure 34.** Sibudu. C-A layers from the Deep Sounding: Tall, laterally centralised blades with a triangular cross-section. Blades made on quartzite (a, b) and made on dolerite (c-m) (Photos by Viola C. Schmid).



**Figure 35.** Sibudu. C-A layers from the Deep Sounding: Flat, laterally diffuse blades with a trapezoidal cross-section. Blades made on dolerite (a-e, g, h, j-o), made on sandstone (f) and made on quartzite (i) (Drawing (d) by Mojdeh Lajmiri and Heike Würschem; drawing (j) by Achim Frey and Heike Würschem; photos by Viola C. Schmid).

**Table 34.** Sibudu. C-A layers from the Deep Sounding: Frequency of cortex coverage per blade subgroup.

Blade Subgroups	0%		<20%		>20%		>50%		100%		Total	
	n	%	n	%	n	%	n	%	n	%	n	%
△	606	54.4%	100	9.0%	266	23.9%	126	11.3%	16	1.4%	<b>1,114</b>	<b>100%</b>
▱	264	55.9%	80	16.9%	119	25.2%	9	1.9%	-	0.0%	<b>472</b>	<b>100%</b>
<b>Total</b>	<b>870</b>	<b>54.9%</b>	<b>180</b>	<b>11.3%</b>	<b>385</b>	<b>24.3%</b>	<b>135</b>	<b>8.5%</b>	<b>16</b>	<b>1.0%</b>	<b>1,586</b>	<b>100%</b>

**Table 35.** Sibudu. C-A layers from the Deep Sounding: Frequency of platform type per blade subgroup.

Blade Subgroups	plain		cortical		faceted		dihedral		crushed		indetermined		Total	
	n	%	n	%	n	%	n	%	n	%	n	%	n	%
△	475	76.1%	45	7.2%	42	6.7%	58	9.3%	3	0.5%	1	0.2%	<b>624</b>	<b>100%</b>
▱	233	72.6%	13	4.0%	39	12.1%	34	10.6%	1	0.3%	1	0.3%	<b>321</b>	<b>100%</b>
<b>Total</b>	<b>708</b>	<b>74.9%</b>	<b>58</b>	<b>6.1%</b>	<b>81</b>	<b>8.6%</b>	<b>92</b>	<b>9.7%</b>	<b>4</b>	<b>0.4%</b>	<b>2</b>	<b>0.2%</b>	<b>945</b>	<b>100%</b>

**Table 36.** Sibudu. C-A layers from the Deep Sounding: Frequency of cross-sections of in the width completely preserved blades.

Layer	triangular		trapezoidal		lenticular		irregular		indetermined		Total	
	n	%	n	%	n	%	n	%	n	%	n	%
ADAM	279	60.9%	114	24.9%	61	13.3%	2	0.4%	2	0.4%	<b>458</b>	<b>100%</b>
ANNIE	160	68.7%	65	27.9%	7	3.0%	-	0.0%	1	0.4%	<b>233</b>	<b>100%</b>
BART	151	61.6%	81	33.1%	12	4.9%	-	0.0%	1	0.4%	<b>245</b>	<b>100%</b>
BEA	220	66.9%	85	25.8%	21	6.4%	-	0.0%	3	0.9%	<b>329</b>	<b>100%</b>
CASPER	178	63.6%	75	26.8%	24	8.6%	-	0.0%	3	1.1%	<b>280</b>	<b>100%</b>
CHANTAL	126	61.5%	52	25.4%	26	12.7%	1	0.5%	-	0.0%	<b>205</b>	<b>100%</b>
<b>Total</b>	<b>1,114</b>	<b>63.7%</b>	<b>472</b>	<b>27.0%</b>	<b>151</b>	<b>8.6%</b>	<b>3</b>	<b>0.2%</b>	<b>10</b>	<b>0.6%</b>	<b>1,750</b>	<b>100%</b>

**Table 37.** Sibudu. C-A layers from the Deep Sounding: Descriptive statistics of the width of all in the width completely preserved blades.

	ADAM	ANNIE	BART	BEA	CASPER	CHANTAL
n	458	233	245	329	280	262
Min	6.9	9.2	9.6	6	8.6	5.8
Max	53.2	48.3	72.9	45.1	43	40
Sum	10,118.4	5,503.3	5,579.3	7,266.2	6,231.9	6,192.6
Mean	22.1	23.6	22.8	22.1	22.3	23.6
Std. error	0.3	0.4	0.4	0.3	0.3	0.4
Variance	45.0	41.7	48.0	34.1	34.1	34.4
Stand. dev.	6.7	6.5	6.9	5.8	5.8	5.9
Median	21.1	22.7	22.1	21.8	22.3	23.5
25 prcntil	17.4	19.1	18.3	17.9	17.8	19.6
75 prcntil	25.9	27.2	25.8	25.6	26.7	27.4

**Table 38.** Sibudu. C-A layers from the Deep Sounding: Descriptive statistics of the thickness of all in the thickness completely preserved blades.

	ADAM	ANNIE	BART	BEA	CASPER	CHANTAL
n	482	248	256	345	296	276
Min	2	3.2	3	2.1	2.9	2.9
Max	22.7	27.4	27	17.1	17.1	22.5
Sum	3,670.1	2,134.2	2,068.9	2,561.8	2,253.6	2,204.8
Mean	7.6	8.6	8.1	7.4	7.6	8
Std. error	0.1	0.2	0.2	0.1	0.1	0.2
Variance	8.6	12.1	9.7	7.1	6.3	9.3
Stand. dev.	2.9	3.5	3.1	2.7	2.5	3
Median	7.2	8.1	7.7	6.9	7.5	7.4
25 prcntil	5.5	6.1	5.9	5.5	5.5	5.9
75 prcntil	9.1	10.1	9.5	9.1	8.9	9.7

a triangular cross-section (Figure 32 – Figure 34), and (2) flat, laterally diffuse blades with a trapezoidal cross-section (Figure 35). The former shows significantly lower vertical convexities (*t*-test,  $t = -8.0467$ ;  $p < 0.0001$ ) (Table 33). In contrast to subgroup (1), no blade of subgroup (2) has complete dorsal cortex coverage and only 1.9% have more than 50% of cortex on their dorsal face (Table 34), implying that subgroup (2) is not involved in the earliest stages of reduction. Additionally, subgroup (2) includes fewer pieces with a cortical platform and more with either a dihedral or faceted platform (Table 35). Subgroup (1) dominates throughout the sequence (Table 36). In general, no distinct diachronic trends in size (Table 37 & Table 38) and morphological traits of the blades are evident. In fact, the blades exhibit similar metric dimensions and shapes throughout the layers, indicative of similar objectives.

In general, elongated flakes display similar tendencies to blades. However, quartzite encompasses the highest proportion of elongated flakes among the blanks at 14.5%, followed by dolerite at 14.1% and hornfels at 13.7% (Table 19). Compared to the blades, more elongated flakes show cortical remains on their dorsal face (Table 21) and more elements with distal cortex coverage occur (Table 22), but the difference in dorsal cortex percentage is not significant (Table 39). The elongated flake population involves significantly more pieces with plain and cortical platforms and fewer with dihedral and faceted platforms (Table 23 & Table 40). Additionally, a higher proportion demonstrates unidirectional dorsal scars (Table 24). Elongated flakes are shorter than blades, averaging between 33 mm and 46 mm in length, and are significantly wider (Table 41) and thicker (Table 42) than blades. Elongated flakes and blades resemble one another in terms of morphology (Table 25) and profile (Table 26), but they differ regarding the distal termination (Table 31). The major part of elongated flakes also terminates in a feather termination, but the distal end is primarily convex. Plunging elements occur, but rarely. Hinged terminations amount to 18%, suggesting that the knappers most likely intended to produce blades but failed. Most of the elongated flakes (32.8%) are not fragmented (Table 18) and a further 38% have two-thirds (proximal-medial or medial-distal) preserved. The elongated flakes show a significantly higher percentage of completely preserved pieces than the blade population (Table 43). Finally, the majority of elongated flakes has a triangular cross-



section at 54.8%, followed by artefacts with a trapezoidal cross-section at 35.3% (Table 32). The trend is again similar to the blades, but the proportion of elongated flakes with a trapezoidal cross-section is higher. The elongated flakes also show a dichotomy of laterally centralised specimens with a triangular cross-section and flat, laterally diffuse ones with a trapezoidal cross-section (*t*-test, *t* = -4.8726; *p* < 0.0001) (Table 44). The laterally centralised elongated flakes with a triangular cross-section include more pieces with over 50% dorsal cortex coverage than the flat, laterally diffuse elongated flakes with a trapezoidal cross-section (Table 45). More

**Table 39.** Sibudu. C-A layers from the Deep Sounding: Comparison of elements with and without cortex coverage between blades and elongated flakes (chi-squared test).

Blank categories	without cortex	with cortex	Total
Blade	1,056	848	1,904
Elongated flakes	539	459	998
<b><i>chi-squared test</i></b>			
<b>F=</b>	<b>1</b>		
<b>χ<sup>2</sup>=</b>	<b>0,55936</b>		
<b>p=</b>	<b>0,45452</b>		
<b>Fisher exact p=</b>	<b>0,45586</b>		

**Table 40.** Sibudu. C-A layers from the Deep Sounding: Comparison of elements with plain & cortical platforms and with dihedral & faceted platforms between blades and elongated flakes (chi-squared test).

Blank categories	with plain and cortical platform	with dihedral and faceted platform	Total
Blade	909	198	1,107
Elongated flakes	609	99	708
<b><i>chi-squared test</i></b>			
<b>F=</b>	<b>1</b>		
<b>χ<sup>2</sup>=</b>	<b>4,8068</b>		
<b>p=</b>	<b>0,028348</b>		
<b>Fisher exact p=</b>	<b>0,031726</b>		

**Table 41.** Sibudu. C-A layers from the Deep Sounding: Comparison of width of all in the width completely preserved blanks between blades and elongated flakes (*t*-test).

	Blades	Elongated flakes
n:	1,807	843
Mean:	22.6	27.2
Stand. dev.	0.293	0.467
Variance:	40.102	47.827
<b>F :</b>	<b>1.1926</b>	
<b>t :</b>	<b>-16.912</b>	
<b>p :</b>	<b>0.0001</b>	


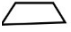
**Table 42.** Sibudu. C-A layers from the Deep Sounding: Comparison of thickness of all in the thickness completely preserved blanks between blades and elongated flakes (*t*-test).

	Blades	Elongated flakes
n:	1,903	997
Mean:	7.8263	8.2377
Stand. dev.	0.1332	0.1974
Variance:	8.7782	10.087
<b>F :</b>	<b>1.1491</b>	
<b>t :</b>	<b>-3.4643</b>	
<b>p :</b>	<b>0.0008</b>	


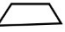
**Table 43.** Sibudu. C-A layers from the Deep Sounding: Comparison of completely preserved and fragmented elements between blades and elongated flakes (chi-squared test).

Blank categories	completely preserved	fragmented	Total
Blade	219	1,685	1,904
Elongated flakes	327	671	998
<b><i>chi-squared test</i></b>			
<b>F=</b>		<b>1</b>	
<b>χ<sup>2</sup>=</b>		<b>193,82</b>	
<b>p=</b>		<b>0,0001</b>	
<b>Fisher exact p=</b>		<b>0,0001</b>	


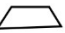
**Table 44.** Sibudu. C-A layers from the Deep Sounding: Comparison of dorsal convexity between elongated flakes with a triangular cross-section and elongated flakes with a trapezoidal cross-section (*t*-test).

		
n:	461	298
Mean:	3.4168	3.8217
Stand. dev.	0.0942	0.1418
Variance:	1.0583	1.5474
<b>F:</b>	<b>1.4623</b>	
<b>t:</b>	<b>-4.8726</b>	
<b>p:</b>	<b>0.0001</b>	

**Table 45.** Sibudu. C-A layers from the Deep Sounding: Frequency of cortex coverage per elongated flake subgroup.

Elongated flake Subgroups	0%		<20%		>20%		>50%		100%		Total	
	n	%	n	%	n	%	n	%	n	%	n	%
	245	53.0%	49	10.6%	116	25.1%	44	9.5%	8	1.7%	<b>462</b>	<b>100%</b>
	161	54.0%	55	18.5%	69	23.2%	12	4.0%	1	0.3%	<b>298</b>	<b>100%</b>
<b>Total</b>	<b>406</b>	<b>53.4%</b>	<b>104</b>	<b>13.7%</b>	<b>185</b>	<b>24.3%</b>	<b>56</b>	<b>7.4%</b>	<b>9</b>	<b>1.2%</b>	<b>760</b>	<b>100%</b>

**Table 46.** Sibudu. C-A layers from the Deep Sounding: Frequency of platform type per elongated flake subgroup.

Elongated flake Subgroups	plain		cortical		faceted		dihedral		crushed		indetermined		Total	
	n	%	n	%	n	%	n	%	n	%	n	%	n	%
	255	59.3%	23	5.3%	17	4.0%	27	6.3%	1	0.2%	107	24.9%	<b>430</b>	<b>100%</b>
	172	59.3%	19	6.6%	12	4.1%	25	8.6%	-	0.0%	62	21.4%	<b>290</b>	<b>100%</b>
<b>Total</b>	<b>427</b>	<b>59.3%</b>	<b>42</b>	<b>5.8%</b>	<b>29</b>	<b>4.0%</b>	<b>52</b>	<b>7.2%</b>	<b>1</b>	<b>0.1%</b>	<b>169</b>	<b>23.5%</b>	<b>720</b>	<b>100%</b>

**Table 47.** Sibudu. C-A layers from the Deep Sounding: Frequency of cross-sections of in the width completely preserved elongated flakes.

Layer	triangular		trapezoidal		lenticular		irregular		indetermined		Total	
	n	%	n	%	n	%	n	%	n	%	n	%
ADAM	115	52.3%	82	37.3%	20	9.1%	1	0.5%	2	0.9%	<b>220</b>	<b>100%</b>
ANNIE	76	61.3%	42	33.9%	5	4.0%	-	0.0%	1	0.8%	<b>124</b>	<b>100%</b>
BART	62	50.4%	59	48.0%	2	1.6%	-	0.0%	-	0.0%	<b>123</b>	<b>100%</b>
BEA	91	66.9%	30	22.1%	14	10.3%	-	0.0%	1	0.7%	<b>136</b>	<b>100%</b>
CASPER	61	47.3%	39	30.2%	29	22.5%	-	0.0%	-	0.0%	<b>129</b>	<b>100%</b>
CHANTAL	57	51.4%	46	41.4%	8	7.2%	-	0.0%	-	0.0%	<b>111</b>	<b>100%</b>
<b>Total</b>	<b>462</b>	<b>54.8%</b>	<b>298</b>	<b>35.3%</b>	<b>78</b>	<b>9.3%</b>	<b>1</b>	<b>0.1%</b>	<b>4</b>	<b>0.5%</b>	<b>843</b>	<b>100%</b>

**Table 48.** Sibudu. C-A layers from the Deep Sounding: Descriptive statistics of the length of all completely preserved elongated flakes.

	ADAM	ANNIE	BART	BEA	CASPER	CHANTAL
n	100	51	51	39	45	40
Min	25	27.2	26.4	27.3	26.8	23.9
Max	81.7	67.7	70.3	59.4	57.5	74.5
Sum	3991.9	2043.7	2059.1	1540.2	1752.8	1710.7
Mean	39.9	40.1	40.4	39.5	39	42.8
Std. error	1.1	1.2	1.6	1.1	1.2	1.6
Variance	129.5	72.2	130.6	51.5	63.9	104.6
Stand. dev.	11.4	8.5	11.4	7.2	8	10.2
Median	36.4	37.9	36.6	37.9	36.6	41.2
25 prcntil	32.1	33.3	31.1	35.2	33.1	34.9
75 prcntil	45.6	44.3	47.7	42.9	45.2	50.2

**Table 49.** Sibudu. C-A layers from the Deep Sounding: Descriptive statistics of the width of all in the width completely preserved elongated flakes.

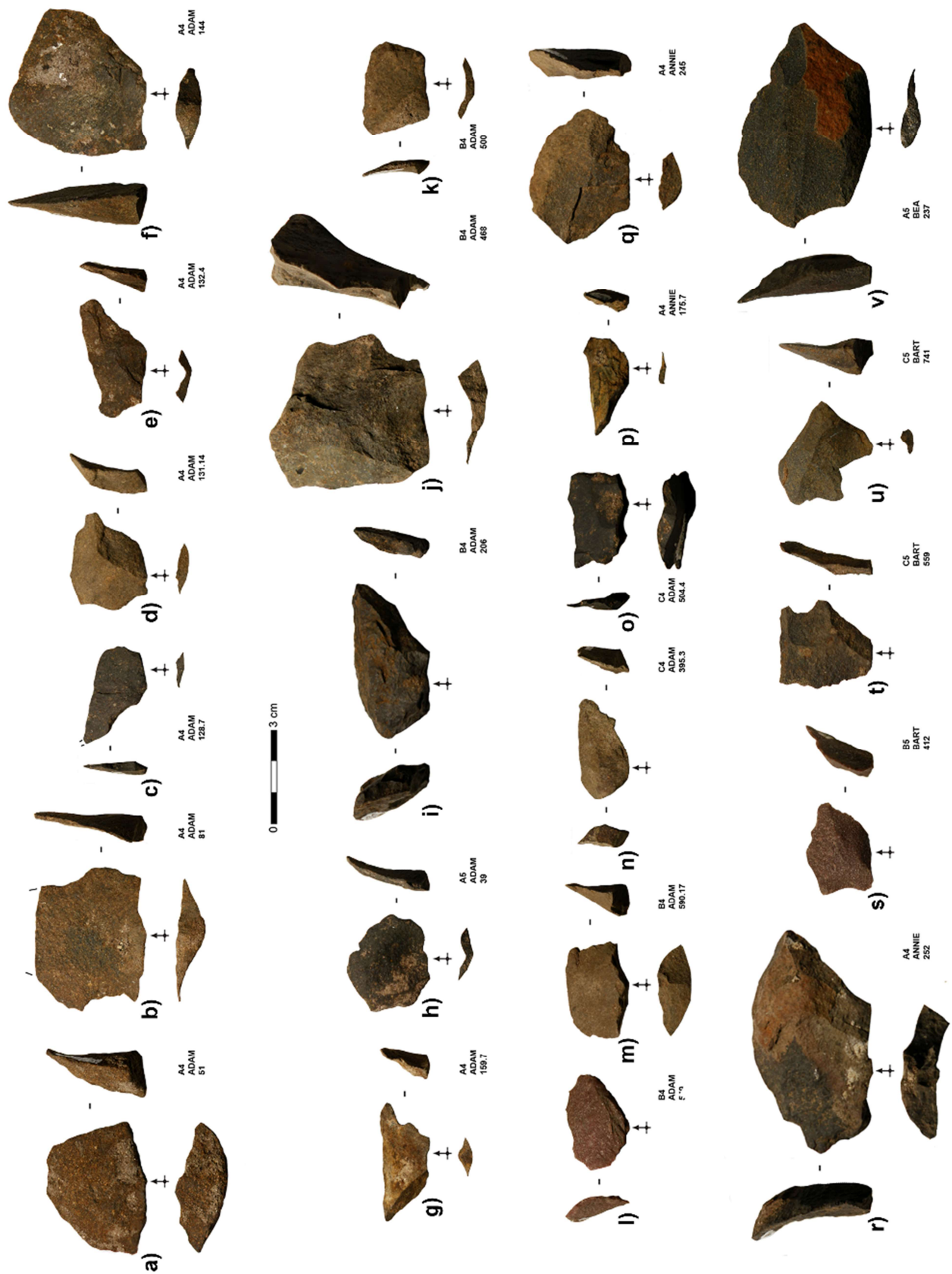
	ADAM	ANNIE	BART	BEA	CASPER	CHANTAL
n	220	124	123	136	129	111
Min	12.8	13	15.4	15.5	15.1	18.7
Max	53.7	52	54	57.2	44.1	50
Sum	5,999	3,291	3,237.3	3,623.3	3,553	3,252.4
Mean	27.3	26.5	26.3	26.6	27.5	29.3
Std. error	0.5	0.6	0.6	0.6	0.5	0.7
Variance	54.2	43.5	44.1	50.9	35.1	51.1
Stand. dev.	7.4	6.6	6.6	7.1	5.9	7.1
Median	25.8	25.7	25.1	24.9	27.3	28.7
25 prcntil	22.1	21.6	22.1	21.6	23.7	23
75 prcntil	31.2	30	29	29.8	31	33.7

**Table 50.** Sibudu. C-A layers from the Deep Sounding: Descriptive statistics of the thickness of all in the thickness completely preserved elongated flakes.

	ADAM	ANNIE	BART	BEA	CASPER	CHANTAL
n	254	154	144	162	155	128
Min	2.8	3.7	3.2	2.4	3	3.2
Max	27.6	21.4	17.7	23.4	17.5	25.6
Sum	2,091.2	1,309	1,165.7	1,348.6	1,237.2	1,061.3
Mean	8.2	8.5	8.1	8.3	8	8.3
Std. error	0.2	0.3	0.2	0.3	0.2	0.3
Variance	10.9	9.7	8.8	10.7	9.2	11
Stand. dev.	3.3	3.1	3	3.3	3	3.3
Median	7.6	8	7.4	7.7	7.3	7.6
25 prcntil	5.9	6.1	6.1	5.9	5.8	5.9
75 prcntil	9.8	9.8	9.7	10.1	9.8	9.9

blanks with faceted or dihedral platforms are present among the flat, laterally diffuse elongated flakes with a trapezoidal cross-section, though there are also more pieces with cortical platforms (Table 46). Generally, elongated flakes with triangular cross-sections dominate throughout the sequence followed by pieces with trapezoidal cross-sections, but the proportions differ (Table 47). As for the blades, I observed similar trends in all layers in terms of elongated flake size (Table 48 – Table 50) and shape.

Regarding raw materials, I documented that quartz and sandstone, in contrast to the other raw materials, contribute a low frequency of laminar products but a high frequency of flakes (Table 19). Hornfels yielded the lowest percentage of flakes at 49.3%. The hornfels flake population comprises 7.4% of products with 100% dorsal cortex coverage and fewer non-cortical elements than the laminar products, at 47.1% (Table 21). Lateral cortical products are numerous but less common than among the blades (Table 22). Flakes with distal cortex coverage occur relatively frequently at 12.9%. Most of their platforms are plain, as for the laminar products (Table 23). However, flakes make up the highest proportion of pieces with cortical platforms at 13.8%, suggesting again a low investment in the preparation of the striking platforms. However, 10.2% of the flakes exhibit a dihedral platform. The predominant dorsal scar pattern is unidirectional at 52%, but a large part demonstrates orthogonal negatives (32%) (Figure 36 – Figure 38 & Table 24). Interestingly, the flakes with an orthogonal scar pattern show a higher frequency of non-cortical elements (63%) than the flakes with unidirectional dorsal scars (42.6%) and additionally involve fewer pieces with over 50% cortical remains on the dorsal face, plus no completely cortical artefacts (Table 51). Thus, the orthogonal flakes presumably come from more advanced stages of the reduction sequence. Most of the flakes (52.5%) are trapezoidal in shape (Table 25) and straight to slightly curved in profile, while 11.8% exhibit a curved profile (Table 26). The flakes show a mean length of 31.9 mm (Table 27) with a corresponding mean width of 33 mm (Table 28) and a mean thickness of 8.9 mm. Compared to their laminar counterparts, flakes are significantly shorter, wider and thicker. The majority of the flakes displays a feather termination and the distal end is predominantly convex or straight (Table 31). Elements with triangular and trapezoidal cross-sections dominate, but in contrast to the laminar population, their frequencies are relatively balanced (Table 32). A total of 33.3% of the flakes are completely preserved (Table 18) and 30.1% have two-thirds (proximal-medial or medial-distal) preserved. Throughout the sequence, flakes with triangular or trapezoidal cross-sections prevail (Table 52). Flakes with a trapezoidal cross-section are more frequent than flakes with a triangular cross-section in the upper layers Adam to Bart, while blanks with a triangular cross-section dominate the lower layers. All layers demonstrate a predominance of flakes with unidirectional dorsal scars, followed by flakes with an orthogonal scar pattern (Table 53). The proportion of unidirectional flakes increases towards the lower strata, while the frequency of orthogonal flakes decreases. In terms of the metric dimensions (Table 54 – Table 56), the diachronic tendencies are similar.



**Figure 36.** Sibudu. C-A layers from the Deep Sounding: Technologically diagnostic flakes. Flakes made on dolerite (a-k, m-o, q, r, t-v), made on quartzite (l, s) and made on hornfels (p) (Photos by Viola C. Schmid).



**Figure 37.** Sibudu. C-A layers from the Deep Sounding: Technologically diagnostic flakes. Flakes made on dolerite (a-j, l-n, p-s, u), made on hornfels (k), made on quartzite (o) and made on quartz (t) (Drawings by Heike Würschem; photos by Viola C. Schmid).



**Figure 38.** Sibudu. C-A layers from the Deep Sounding: Technologically diagnostic flakes. Flakes made on dolerite (a-f, h, l, k-r) and made on quartzite (g, j) (Photos by Viola C. Schmid).

**Table 51.** Sibudu. C-A layers from the Deep Sounding: Frequency of cortex coverage per flakes with unidirectional dorsal scars compared to such with an orthogonal scar pattern.

Dorsal Scar Patterns	0%		<20%		>20%		>50%		100%		Total	
	n	%	n	%	n	%	n	%	n	%	n	%
unidirectional	955	42.8%	314	14.1%	563	25.2%	398	17.8%	3	0.1%	<b>2,233</b>	<b>100%</b>
orthogonal	865	63.0%	199	14.5%	236	17.2%	72	5.2%	-	0.0%	<b>1,372</b>	<b>100%</b>
<b>Total</b>	<b>1,820</b>	<b>50.5%</b>	<b>513</b>	<b>14.2%</b>	<b>799</b>	<b>22.2%</b>	<b>470</b>	<b>13.0%</b>	<b>3</b>	<b>0.1%</b>	<b>3,605</b>	<b>100%</b>



**Table 52.** Sibudu. C-A layers from the Deep Sounding: Frequency of cross-sections of in the width completely preserved flakes.

Layer	triangular		trapezoidal		lenticular		irregular		indetermined		Total	
	n	%	n	%	n	%	n	%	n	%	n	%
ADAM	238	34.2%	314	45.1%	112	16.1%	21	3.0%	11	1.6%	696	100%
ANNIE	140	35.9%	188	48.2%	56	14.4%	5	1.3%	1	0.3%	390	100%
BART	161	34.6%	210	45.2%	82	17.6%	11	2.4%	1	0.2%	465	100%
BEA	233	38.9%	214	35.7%	130	21.7%	17	2.8%	5	0.8%	599	100%
CASPER	224	43.4%	151	29.3%	122	23.6%	17	3.3%	2	0.4%	516	100%
CHANTAL	170	41.1%	135	32.6%	94	22.7%	11	2.7%	4	1.0%	414	100%
<b>Total</b>	<b>1,166</b>	<b>37.9%</b>	<b>1,212</b>	<b>39.4%</b>	<b>596</b>	<b>19.4%</b>	<b>82</b>	<b>2.7%</b>	<b>24</b>	<b>0.8%</b>	<b>3,080</b>	<b>100%</b>

**Table 53.** Sibudu. C-A layers from the Deep Sounding: Frequency of dorsal scar patterns of in the width completely preserved flakes.

Layer	unidirectional		unidirectional convergent		bidirectional		opposed		orthogonal		crossed		Kombewa		cortex		indetermined		Total	
	n	%	n	%	n	%	n	%	n	%	n	%	n	%	n	%	n	%	n	%
ADAM	378	44.9%	37	4.4%	44	5.2%	5	0.6%	307	36.5%	29	3.4%	-	0.0%	39	4.6%	2	0.2%	841	100%
ANNIE	245	46.5%	21	4.0%	19	3.6%	1	0.2%	197	37.4%	7	1.3%	-	0.0%	36	6.8%	1	0.2%	527	100%
BART	307	47.9%	19	3.0%	32	5.0%	2	0.3%	219	34.2%	12	1.9%	2	0.3%	47	7.3%	1	0.2%	641	100%
BEA	506	56.0%	19	2.1%	30	3.3%	1	0.1%	258	28.6%	8	0.9%	-	0.0%	74	8.2%	7	0.8%	903	100%
CASPER	452	57.7%	7	0.9%	25	3.2%	2	0.3%	221	28.2%	6	0.8%	-	0.0%	68	8.7%	2	0.3%	783	100%
CHANTAL	345	57.9%	5	0.8%	18	3.0%	2	0.3%	170	28.5%	5	0.8%	-	0.0%	50	8.4%	1	0.2%	596	100%
<b>Total</b>	<b>2,233</b>	<b>52.0%</b>	<b>108</b>	<b>2.5%</b>	<b>168</b>	<b>3.9%</b>	<b>13</b>	<b>0.3%</b>	<b>1,372</b>	<b>32.0%</b>	<b>67</b>	<b>1.6%</b>	<b>2</b>	<b>0.0%</b>	<b>314</b>	<b>7.3%</b>	<b>14</b>	<b>0.3%</b>	<b>4,291</b>	<b>100%</b>

**Table 54.** Sibudu. C-A layers from the Deep Sounding: Descriptive statistics of the length of all completely preserved flakes.

	ADAM	ANNIE	BART	BEA	CASPER	CHANTAL
n	355	175	211	277	213	199
Min	9.8	9.2	7.6	6.3	8.7	8.3
Max	79	83	82.3	64.6	77.9	94
Sum	11,347.3	5,898	6,745.6	8,337.4	6,799.5	6,512.6
Mean	32	33.7	32	30.1	31.9	32.7
Std. error	0.5	0.9	0.7	0.6	0.7	0.8
Variance	104	135.5	108	103.1	111	123.2
Stand. dev.	10.2	11.6	10.4	10.2	10.5	11.1
Median	30.2	32.3	30.8	29.3	30.3	30.2
25 prcntil	25.8	25.6	25.2	23.6	25	25.6
75 prcntil	36.4	40.9	36.8	35.6	37.85	37.5

**Table 55.** Sibudu. C-A layers from the Deep Sounding: Descriptive statistics of the width of all in the width completely preserved flakes.

	ADAM	ANNIE	BART	BEA	CASPER	CHANTAL
n	696	390	465	598	515	413
Min	14	12.8	9	16.7	15	13.8
Max	86	100.3	73	78	72	91.4
Sum	22,888.3	13,563.9	15,093.7	19,336.5	16,688.5	13,922.1
Mean	32.9	34.8	32.5	32.3	32.4	33.7
Std. error	0.3	0.5	0.4	0.3	0.3	0.4
Variance	74.9	98.3	70	63.5	60.6	76.7
Stand. dev.	8.7	9.9	8.4	8	7.8	8.8
Median	31.2	32.9	31.2	31.1	31.3	31.8
25 prcntil	27.1	29	27.2	27.1	27.6	28.1
75 prcntil	38	39	36.5	35.9	35.9	37.9

**Table 56.** Sibudu. C-A layers from the Deep Sounding: Descriptive statistics of the thickness of all in the thickness completely preserved flakes.

	ADAM	ANNIE	BART	BEA	CASPER	CHANTAL
n	841	527	640	903	783	593
Min	2.2	2.2	3	2.3	2.8	2.2
Max	30.4	38.2	25.5	41.5	27.8	28.4
Sum	7,809.4	5,155.6	5,634.8	7,685	6,728.6	5,297
Mean	9.3	9.8	8.8	8.5	8.6	8.9
Std. error	0.1	0.2	0.1	0.1	0.1	0.2
Variance	14.8	19.7	13.5	12	11.5	15.9
Stand. dev.	3.8	4.4	3.7	3.5	3.4	4
Median	8.5	8.8	7.9	7.9	7.9	8
25 prcntil	6.7	6.8	6.4	6.1	6.2	6.2
75 prcntil	11	11.5	10.3	10.2	10.3	10.7

The assemblage contains a low proportion of triangular flakes at 2% (Table 16). Most of the triangular elements are made on dolerite (Table 19). The majority of these blanks (51.7%) is non-cortical (Table 21); however, triangular flakes show the second highest proportion of products with more than 50% cortex coverage following the flakes. The position of cortical remains is most frequently lateral (Table 22). Triangular elements attest to the highest frequency of pieces with a prepared platform, either faceted or dihedral (Table 23). The products exhibit either unidirectional or unidirectional convergent dorsal negatives (Table 24). Most of the triangular flakes are straight in their profile (57.8%), followed by slightly curved (27.9%) (Table 26). However, this blank category shows the highest percentage of curved pieces at 14.3%. The length of triangular elements averages 39.1 mm (Table 27) and the width has a mean value of 27.9 mm (Table 28). Concerning both of these dimensions, the triangular flakes resemble the elongated flakes in their actual dimensions (Table 57 & Table 58). The triangular elements have an average thickness of 9.1 mm (Table 29) and they are thicker than all other blank categories. The triangular flakes show the lowest EL-to-blank mass ratio (Table 30). Most

of the products have a feather termination and a pointed distal end (Table 31). Triangular flakes encompass the highest proportion of completely preserved elements (Table 18). Pieces with a triangular cross-section dominate, followed by those with a trapezoidal cross-section (Table 32). The number of triangular flakes decreases throughout the sequence (Table 16).

**Table 57.** Sibudu. C-A layers from the Deep Sounding: Comparison of length of all completely preserved blanks between elongated flakes and triangular flakes (*t*-test).

	Elongated flakes	Triangular flakes
n:	326	69
Mean:	40.2	39.1
Stand. dev.	1.6	2.6
Variance:	99	114.7
<b>F :</b>	<b>1.1587</b>	
<b>t :</b>	<b>-0.82919</b>	
<b>p :</b>	<b>0.4083</b>	

**Table 58.** Sibudu. C-A layers from the Deep Sounding: Comparison of width of all in the width completely preserved blanks between elongated flakes and triangular flakes (*t*-test).

	Elongated flakes	Triangular flakes
n:	843	139
Mean:	27.2	27.9
Stand. dev.	0.5	1.1
Variance:	47.8	43.3
<b>F :</b>	<b>1.1034</b>	
<b>t :</b>	<b>-1.0175</b>	
<b>p :</b>	<b>0.3128</b>	

### 5.3. Cores

The majority of the 71 cores from layers Adam to Chantal is made on dolerite, followed by quartz and quartzite (Table 59). According to the unified taxonomy by Conard et al. (2004), the main proportion of the cores corresponds to platform types (n=49) (Table 60). These cores are almost exclusively oriented towards laminar blank production (n=48). In this section, I deal with the different core types appearing in the assemblage and describe their general characteristics: The blade platform cores are primarily made on dolerite and quartzite (Table 59). However, one core made on quartz corresponds to the configuration of these platform cores (Figure 39a). The knappers predominately selected slabs (n=22) as original core blanks compared to cobbles (n=10) and flakes (n=8) (Table 61). A total of 16.7% of the cores have no cortex coverage at all,

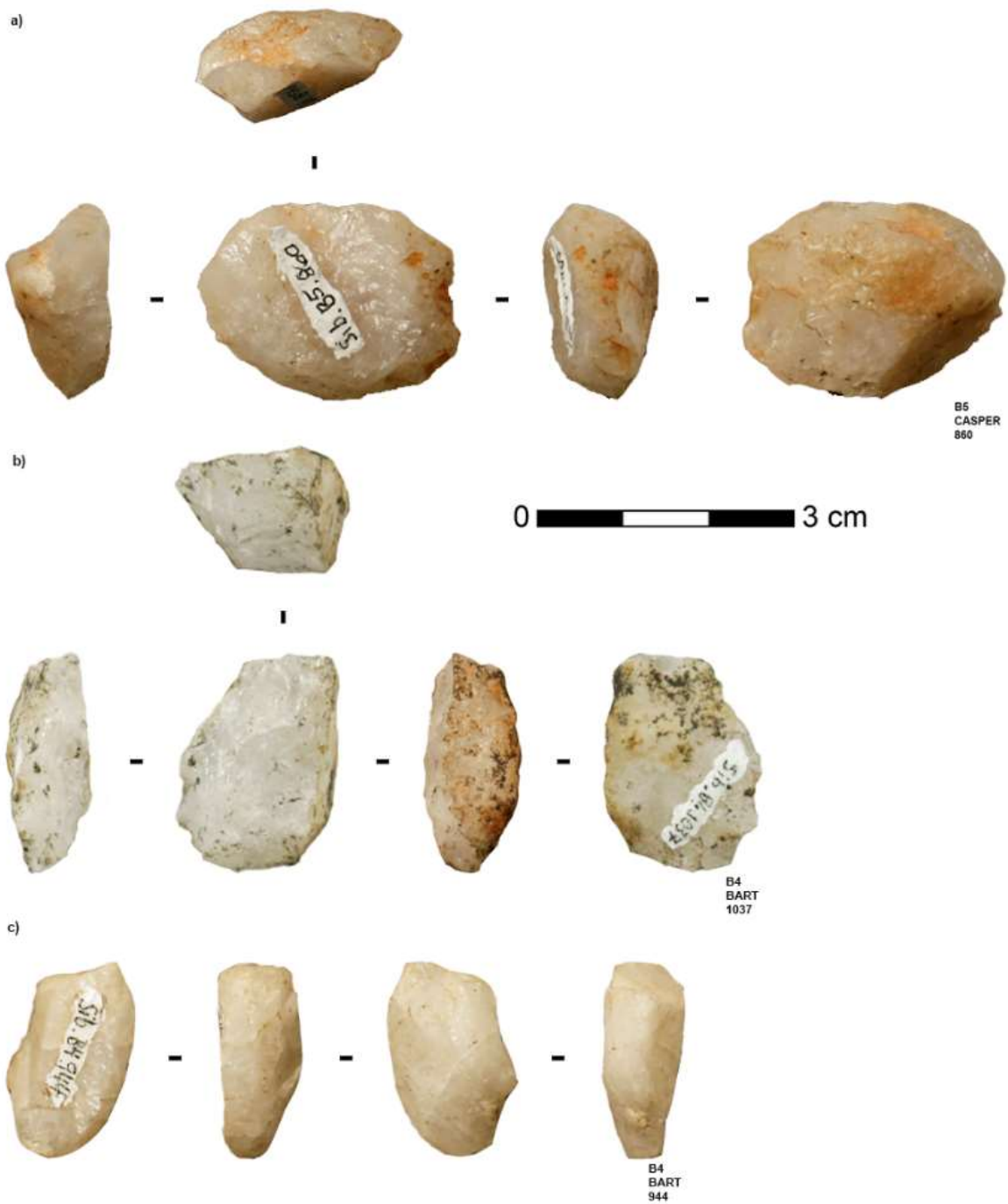
**Table 59.** Sibudu. C-A layers from the Deep Sounding: Frequency of core type per raw material.

Raw Material	platform blade		platform bladelet		platform blade/ bipolar		bipolar		initial core		indetermined		Total	
	n	%	n	%	n	%	n	%	n	%	n	%	n	%
Dolerite	37	92.5%	-	0.0%	-	0.0%	-	0.0%	2	5.0%	1	2.5%	40	100%
Hornfels	-	0.0%	-	0.0%	-	0.0%	-	0.0%	-	0.0%	1	100.0%	1	100%
Quartz	1	5.6%	-	0.0%	1	5.6%	16	88.9%	-	0.0%	-	0.0%	18	100%
Quartzite	10	90.9%	1	9.1%	-	0.0%	-	0.0%	-	0.0%	-	0.0%	11	100%
Sandstone	-	0.0%	-	0.0%	-	0.0%	-	0.0%	1	100.0%	-	0.0%	1	100%
<b>Total</b>	<b>48</b>	<b>67.6%</b>	<b>1</b>	<b>1.4%</b>	<b>1</b>	<b>1.4%</b>	<b>16</b>	<b>22.5%</b>	<b>3</b>	<b>4.2%</b>	<b>2</b>	<b>2.8%</b>	<b>71</b>	<b>100%</b>

**Table 60.** Sibudu. C-A layers from the Deep Sounding: Frequency of core types.

Layer	platform blade		platform bladelet		platform blade/ bipolar		bipolar		initial core		indetermined		Total	
	n	%	n	%	n	%	n	%	n	%	n	%	n	%
ADAM	17	77.3%	-	0.0%	-	0.0%	4	18.2%	1	4.5%	-	0.0%	22	100%
ANNIE	12	80.0%	-	0.0%	-	0.0%	2	13.3%	-	0.0%	1	6.7%	15	100%
BART	9	56.3%	-	0.0%	1	6.3%	5	31.3%	1	6.3%	-	0.0%	16	100%
BEA	4	66.7%	-	0.0%	-	0.0%	1	16.7%	1	16.7%	-	0.0%	6	100%
CASPER	1	16.7%	1	16.7%	-	0.0%	3	50.0%	-	0.0%	1	16.7%	6	100%
CHANTAL	5	83.3%	-	0.0%	-	0.0%	1	16.7%	-	0.0%	-	0.0%	6	100%
<b>Total</b>	<b>48</b>	<b>67.6%</b>	<b>1</b>	<b>1.4%</b>	<b>1</b>	<b>1.4%</b>	<b>16</b>	<b>22.5%</b>	<b>3</b>	<b>4.2%</b>	<b>2</b>	<b>2.8%</b>	<b>71</b>	<b>100%</b>

while 77.1% exhibit cortical remains on less than 50% of their complete surface (Table 62). Only 6.3% have more than 50% cortex, showing that past people highly exhausted most of their cores. Cortex is most often located on the backs and/or one lateral surface of the cores (Table 63). All the specimens are equipped with one striking platform, but one exception has two platforms due to a re-orientation during the reduction sequence. The platforms of the blade platform cores are usually plain with one exception that exhibits a faceted platform (Table 64). The main removal surfaces are mostly quadrangular (60.4%) or oval-shaped (29.2%) (Table 65). The blade platform cores are almost solely exploited by unidirectional removals, apart from one core that shows bidirectional removals indicating bidirectional reduction (Figure 40). The largest proportion of these cores demonstrates preparatory removals and/or cortex coverage on their back (Table 66). Toolmakers most frequently prepared the base of the blade platform cores with distal trimming (Table 67). A total of 79.2% of the blade platform cores are completely preserved. The length averages between 36.5 mm and 54.7 mm (Table 68), the width between 35.9 mm and 49.7 mm (Table 69), and the thickness between 18.9 mm and 30.4 mm (Table 70). The variability within the laminar platform cores reflects different stages of



**Figure 39.** Sibudu. C-A layers from the Deep Sounding: a) Unidirectional laminar platform core made on quartz; b) Unidirectional laminar platform core made on quartz terminated as bipolar core; c) bipolar core made on quartz (Photos by Viola C. Schmid).

**Table 61.** Sibudu. C-A layers from the Deep Sounding: Frequency of original core blanks per core type.

Core type	slab		cobble		flake		crystal facet		indetermined		Total	
	n	%	n	%	n	%	n	%	n	%	n	%
platform blade	22	45.8%	10	20.8%	8	16.7%	-	0.0%	8	16.7%	<b>48</b>	<b>100%</b>
platform bladelet	-	0.0%	-	0.0%	1	100.0%	-	0.0%	-	0.0%	<b>1</b>	<b>100%</b>
platform blade/bipolar	-	0.0%	1	100.0%	-	0.0%	-	0.0%	-	0.0%	<b>1</b>	<b>100%</b>
bipolar	-	0.0%	3	18.8%	2	12.5%	4	25.0%	7	43.8%	<b>16</b>	<b>100%</b>
initial core	3	100.0%	-	0.0%	-	0.0%	-	0.0%	-	0.0%	<b>3</b>	<b>100%</b>
indetermined	1	50.0%	-	0.0%	1	50.0%	-	0.0%	-	0.0%	<b>2</b>	<b>100%</b>
<b>Total</b>	<b>26</b>	<b>36.6%</b>	<b>14</b>	<b>19.7%</b>	<b>12</b>	<b>16.9%</b>	<b>4</b>	<b>5.6%</b>	<b>15</b>	<b>21.1%</b>	<b>71</b>	<b>100%</b>

**Table 62.** Sibudu. C-A layers from the Deep Sounding: Frequency of cortex coverage per core type.

Core type	0%		<20%		>20%		>50%		Total	
	n	%	n	%	n	%	n	%	n	%
platform blade	8	16.7%	22	45.8%	15	31.3%	3	6.3%	<b>48</b>	<b>100%</b>
platform bladelet	-	0.0%	1	100.0%	-	0.0%	-	0.0%	<b>1</b>	<b>100%</b>
platform blade/bipolar	-	0.0%	-	-0.0%	1	100.0%	-	0.0%	<b>1</b>	<b>100%</b>
bipolar	5	31.3%	4	25.0%	6	37.5%	1	6.3%	<b>16</b>	<b>100%</b>
initial core	-	0.0%	-	-0.0%	-	0.0%	3	100.0%	<b>3</b>	<b>100%</b>
indetermined	1	50.0%	-	-0.0%	1	50.0%	-	0.0%	<b>2</b>	<b>100%</b>
<b>Total</b>	<b>14</b>	<b>19.7%</b>	<b>27</b>	<b>38.0%</b>	<b>23</b>	<b>32.4%</b>	<b>7</b>	<b>9.9%</b>	<b>71</b>	<b>100%</b>

**Table 63.** Sibudu. C-A layers from the Deep Sounding: Frequency of cortex positions per core type.

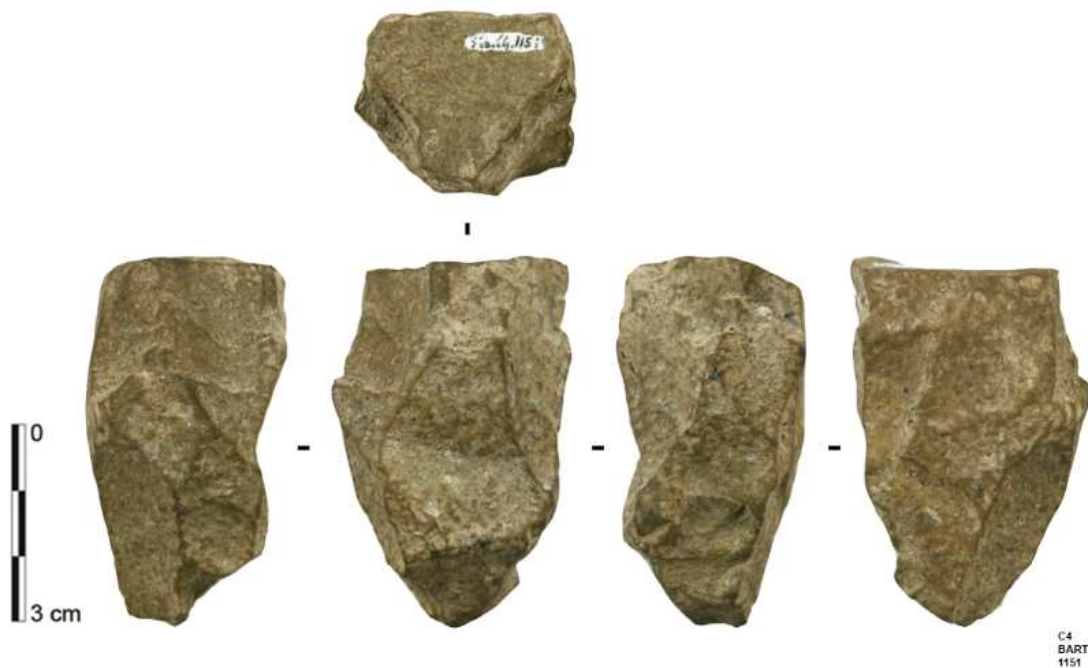
Core type	no cortex		back		back & lateral		lateral		lateral & base		base		central		platform		Total	
	n	%	n	%	n	%	n	%	n	%	n	%	n	%	n	%	n	%
platform blade	8	16.7%	15	31.3%	9	18.8%	11	22.9%	2	4.2%	1	2.1%	2	4.2%	-	0.0%	<b>48</b>	<b>100%</b>
platform bladelet	-	0.0%	-	0.0%	-	0.0%	-	0.0%	-	0.0%	-	0.0%	1	100.0%	-	0.0%	<b>1</b>	<b>100%</b>
platform blade/bipolar	-	0.0%	-	0.0%	1	100.0%	-	0.0%	-	0.0%	-	0.0%	-	0.0%	-	0.0%	<b>1</b>	<b>100%</b>
bipolar	5	31.3%	5	31.3%	-	0.0%	2	12.5%	-	0.0%	2	12.5%	1	6.3%	1	6.3%	<b>16</b>	<b>100%</b>
initial core	-	0.0%	1	33.3%	2	66.7%	-	0.0%	-	0.0%	-	0.0%	-	0.0%	-	0.0%	<b>3</b>	<b>100%</b>
indetermined	1	50.0%	1	50.0%	-	0.0%	-	0.0%	-	0.0%	-	0.0%	-	0.0%	-	0.0%	<b>2</b>	<b>100%</b>
<b>Total</b>	<b>14</b>	<b>19.7%</b>	<b>22</b>	<b>31.0%</b>	<b>12</b>	<b>16.9%</b>	<b>13</b>	<b>18.3%</b>	<b>2</b>	<b>2.8%</b>	<b>3</b>	<b>4.2%</b>	<b>4</b>	<b>5.6%</b>	<b>1</b>	<b>1.4%</b>	<b>71</b>	<b>100%</b>

**Table 64.** Sibudu. C-A layers from the Deep Sounding: Frequency of striking platform types per core type.

Core type	plain		cortical		faceted		splitted out		Total	
	n	%	n	%	n	%	n	%	n	%
platform blade	42	97.7%	-	0.0%	1	2.3%	-	0.0%	<b>43</b>	<b>100%</b>
platform bladelet	1	100.0%	-	0.0%	-	0.0%	-	0.0%	<b>1</b>	<b>100%</b>
platform blade/bipolar	-	0.0%	-	0.0%	-	0.0%	1	100.0%	<b>1</b>	<b>100%</b>
bipolar	-	0.0%	-	0.0%	-	0.0%	14	100.0%	<b>14</b>	<b>100%</b>
initial core	-	0.0%	1	100.0%	-	0.0%	-	0.0%	<b>1</b>	<b>100%</b>
indetermined	1	100.0%	-	0.0%	-	0.0%	-	0.0%	<b>1</b>	<b>100%</b>
<b>Total</b>	<b>44</b>	<b>72.1%</b>	<b>1</b>	<b>1.6%</b>	<b>1</b>	<b>1.6%</b>	<b>15</b>	<b>24.6%</b>	<b>61</b>	<b>100%</b>

**Table 65.** Sibudu. C-A layers from the Deep Sounding: Frequency of exploitation surface shapes per core type.

Core type	quadrangular		oval		triangular		indetermined		Total	
	n	%	n	%	n	%	n	%	n	%
platform blade	29	60.4%	14	29.2%	3	6.3%	2	4.2%	<b>48</b>	<b>100%</b>
platform bladelet	-	0.0%	-	0.0%	1	100.0%	-	0.0%	<b>1</b>	<b>100%</b>
platform blade/bipolar	1	100.0%	-	0.0%	-	0.0%	-	0.0%	<b>1</b>	<b>100%</b>
bipolar	-	0.0%	-	0.0%	-	0.0%	16	100.0%	<b>16</b>	<b>100%</b>
initial core	3	100.0%	-	0.0%	-	0.0%	-	0.0%	<b>3</b>	<b>100%</b>
indetermined	2	100.0%	-	0.0%	-	0.0%	-	0.0%	<b>2</b>	<b>100%</b>
<b>Total</b>	<b>35</b>	<b>49.3%</b>	<b>14</b>	<b>19.7%</b>	<b>4</b>	<b>5.6%</b>	<b>18</b>	<b>25.4%</b>	<b>71</b>	<b>100%</b>



**Figure 40.** Sibudu. C-A layers from the Deep Sounding: a) Bidirectional laminar platform core made on dolerite (Photo by Viola C. Schmid).

**Table 66.** Sibudu. C-A layers from the Deep Sounding: Frequency of back types per core type.

Core type	removals		cortex & removals		cortex		ventral		indetermined		Total	
	n	%	n	%	n	%	n	%	n	%	n	%
platform blade	12	25.0%	10	20.8%	16	33.3%	8	16.7%	2	4.2%	<b>48</b>	<b>100%</b>
platform bladelet	-	0.0%	-	0.0%	-	0.0%	1	100.0%	-	0.0%	<b>1</b>	<b>100%</b>
platform blade/bipolar	-	0.0%	-	0.0%	1	100.0%	-	0.0%	-	0.0%	<b>1</b>	<b>100%</b>
bipolar	11	68.8%	-	0.0%	5	31.3%	-	0.0%	-	0.0%	<b>16</b>	<b>100%</b>
initial core	-	0.0%	-	0.0%	3	100.0%	-	0.0%	-	0.0%	<b>3</b>	<b>100%</b>
indetermined	1	50.0%	-	0.0%	-	0.0%	-	0.0%	1	50.0%	<b>2</b>	<b>100%</b>
<b>Total</b>	<b>24</b>	<b>33.8%</b>	<b>10</b>	<b>14.1%</b>	<b>25</b>	<b>35.2%</b>	<b>9</b>	<b>12.7%</b>	<b>3</b>	<b>4.2%</b>	<b>71</b>	<b>100%</b>

**Table 67.** Sibudu. C-A layers from the Deep Sounding: Frequency of base types per core type.

Core type	distal trimming		cortex		no base		splitted out		Total	
	n	%	n	%	n	%	n	%	n	%
platform blade	32	76.2%	9	21.4%	1	2.4%	-	0.0%	<b>42</b>	<b>100%</b>
platform bladelet	-	0.0%	-	0.0%	1	100.0%	-	0.0%	<b>1</b>	<b>100%</b>
platform blade/bipolar	-	0.0%	-	0.0%	-	0.0%	1	100.0%	<b>1</b>	<b>100%</b>
bipolar	-	0.0%	-	0.0%	-	0.0%	16	100.0%	<b>16</b>	<b>100%</b>
initial core	2	66.7%	1	33.3%	-	0.0%	-	0.0%	<b>3</b>	<b>100%</b>
<b>Total</b>	<b>34</b>	<b>54.0%</b>	<b>10</b>	<b>15.9%</b>	<b>2</b>	<b>3.2%</b>	<b>17</b>	<b>27.0%</b>	<b>63</b>	<b>100%</b>

**Table 68.** Sibudu. C-A layers from the Deep Sounding: Descriptive statistics of the length of all completely preserved cores.

	Platform blade	platform bladelet	platform blade/bipolar	bipolar	initial Core
n	38	1	1	14	1
Min	25.7			13.4	
Max	106.5			37.2	
Sum	1,796.5			322.1	
Mean	47.3	18.5	25.1	23	32
Std. error	2.3			1.7	
Variance	209.6			41.8	
Stand. dev.	14.5			6.5	
Median	46.5			22.8	
25 prcntil	36.5			17.5	
75 prcntil	54.7			26.6	



discard. The last operation is predominantly related to knapping accidents (47.9%), followed by preparational activities (27.1%) (Table 71). The extraction of end-products as a final reduction stage amounts to 25%. The last production operation on most of these platform cores (n=12) clearly highlights the focus on laminar elements, as six cores exhibit an elongated flake scar and three a blade negative as the last end-product. Two further cores demonstrate flake scars and one core has a triangular flake negative as the last production operation. In comparison to all completely preserved blades, the scatter plot of the length and width shows that the laminar end-product scars on the blade platform cores belong to the lower range (Figure 41), signalling a dimensional boundary that the knappers did not intend to fall below. The minimum requirements for the length are ca. 20 mm and the width 10 mm. However, the core dimensions, especially the length-to-width ratio of the removal surfaces with a mean of 1.1 (Table 72), do not coincide with the laminar dimensions. Based

**Table 69.** Sibudu. C-A layers from the Deep Sounding: Descriptive statistics of the width of all in the width completely preserved cores.

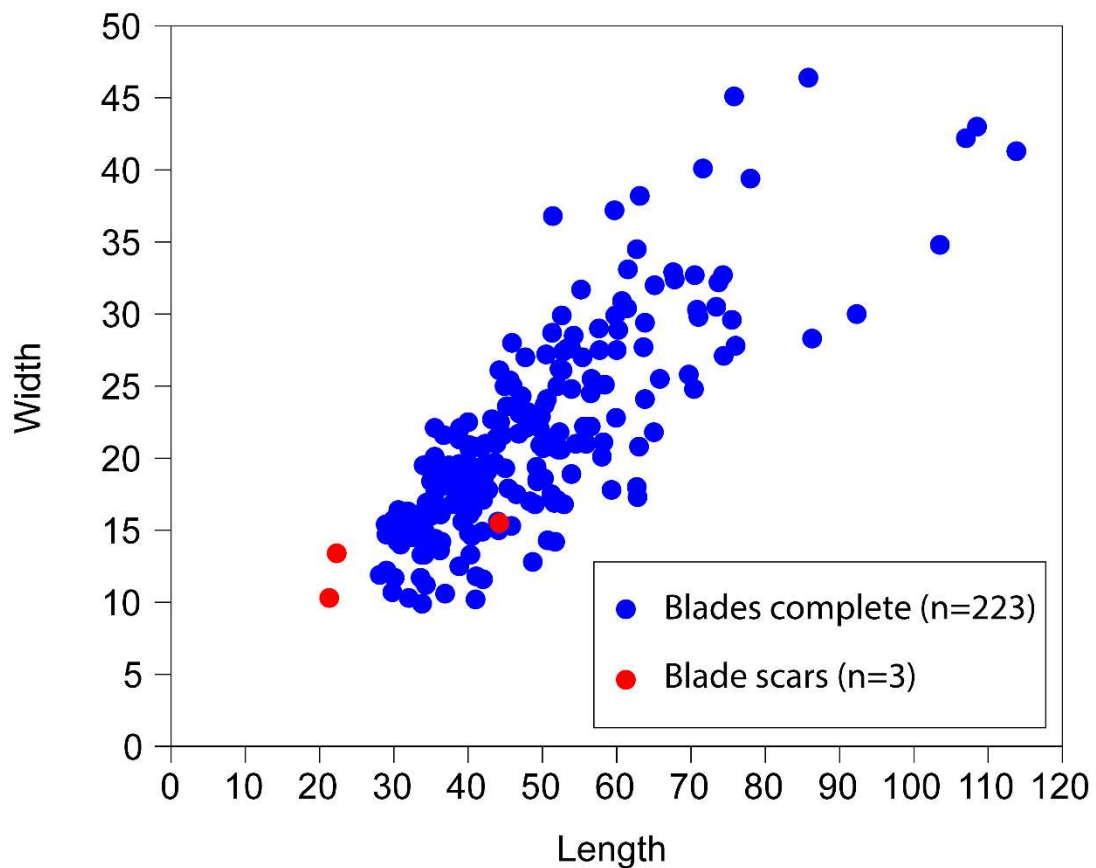
	Platform blade	platform bladelet	platform blade/bipolar	bipolar	initial Core
n	45	1	1	16	2
Min	24.2			9.3	46
Max	63.9			32	113.4
Sum	1,920.5			255	159.4
Mean	42.7	25	18.1	15.9	79.7
Std. error	1.4			1.5	33.7
Variance	88.7			35.3	2271.4
Stand. dev.	9.4			5.9	47.7
Median	41.9			15.3	79.7
25 prcntil	35.9			11.3	34.5
75 prcntil	49.7			16.2	87.8

**Table 70.** Sibudu. C-A layers from the Deep Sounding: Descriptive statistics of the thickness of all in the thickness completely preserved cores.

	Platform blade	platform bladelet	platform blade/bipolar	bipolar	initial Core
n	47	1	1	16	3
Min	12.4			6.2	16.2
Max	63.8			22.6	60.2
Sum	1,229.1			213.6	104.2
Mean	26.2	20	9.9	13.4	34.7
Std. error	1.4			1.2	13.2
Variance	87.1			22.2	520.1
Stand. dev.	9.3			4.7	22.8
Median	25.7			12.5	27.8
25 prcntil	18.9			9.6	16.2
75 prcntil	30.4			17	60.2

**Table 71.** Sibudu. C-A layers from the Deep Sounding: Frequency of last operations per core type.

Core type	production		lateral preparation		basal preparation		platform preparation		accident		indetermined		Total	
	n	%	n	%	n	%	n	%	n	%	n	%	n	%
platform blade	12	25.0%	6	12.5%	3	6.3%	4	8.3%	23	47.9%	-	0.0%	48	100%
platform bladelet	-	0.0%	-	0.0%	-	0.0%	-	0.0%	1	100.0%	-	0.0%	1	100%
platform blade/bipolar	1	100.0%	-	0.0%	-	0.0%	-	0.0%	-	0.0%	-	0.0%	1	100%
bipolar	16	100.0%	-	0.0%	-	0.0%	-	0.0%	-	0.0%	-	0.0%	16	100%
initial core	-	0.0%	1	33.3%	1	33.3%	-	0.0%	1	33.3%	-	0.0%	3	100%
indetermined	-	0.0%	-	0.0%	-	0.0%	-	0.0%	1	50.0%	1	50.0%	2	100%
<b>Total</b>	<b>29</b>	<b>40.8%</b>	<b>7</b>	<b>9.9%</b>	<b>4</b>	<b>5.6%</b>	<b>4</b>	<b>5.6%</b>	<b>26</b>	<b>36.6%</b>	<b>1</b>	<b>1.4%</b>	<b>71</b>	<b>100%</b>



**Figure 41.** Sibudu. C-A layers from the Deep Sounding: Scatter plot of length and width of completely preserved blades and of blade scars presenting last operation on laminar platform cores.

**Table 72.** Sibudu. C-A layers from the Deep Sounding: Descriptive statistics of the length-to-width ratio of all completely preserved cores.

	Platform blade	platform bladelet	platform blade/bipolar	bipolar	initial Core
n	38	1	1	14	1
Min	0.7			0.8	
Max	2.1			2.4	
Sum	42.6			20.8	
Mean	1.1	0.7	1.4	1.5	0.7
Std. error	0			0.1	
Variance	0.1			0.3	
Stand. dev.	0.3			0.5	
Median	1.1			1.4	
25 prcntil	1			1.1	
75 prcntil	1.2			1.7	

on the general description of the assemblage, the cortex coverage and dimensions of the blade platform cores, I hypothesise that a large proportion of the platform cores represents exhausted cores. Laminar cores dominate the core sample throughout all layers with the exception of layer Casper which contains a higher frequency of bipolar cores (Table 60).

One core made on quartzite exhibits bladelet scars as the last production operation (Figure 42); this might be the result of extreme core exhaustion rather than an independent reduction strategy. The knappers used a flake as the original core blank. The ventral face forms the back of the bladelet platform core. The removal surface has centrally located cortex (Table 63). This might have caused the knapping accidents, namely hinges, that represent the last operation on the core and, besides the small dimensions, may have ultimately led to its discard. Similar to the blade platform cores, this core exhibits a plain platform and unidirectional reduction, but the removal surface shape is triangular. The exploitation has reached such an advanced stage that the base of the core is non-existent due to removal scars. The core is 18.5 mm long (Table 68) and thus significantly smaller than the blade platform cores. The width is 25 mm (Table 69) and the thickness 20 mm (Table 70). This core yielded the lowest length-to-width ratio following the initial cores. The advanced stages of discard have an impact on the dimensions of the cores and most likely explain the discrepancy between the pre-determined blanks and cores. The bladelet platform core occurs only in layer Casper, which differs overall from the other layers in its core assemblage composition (Table 60).

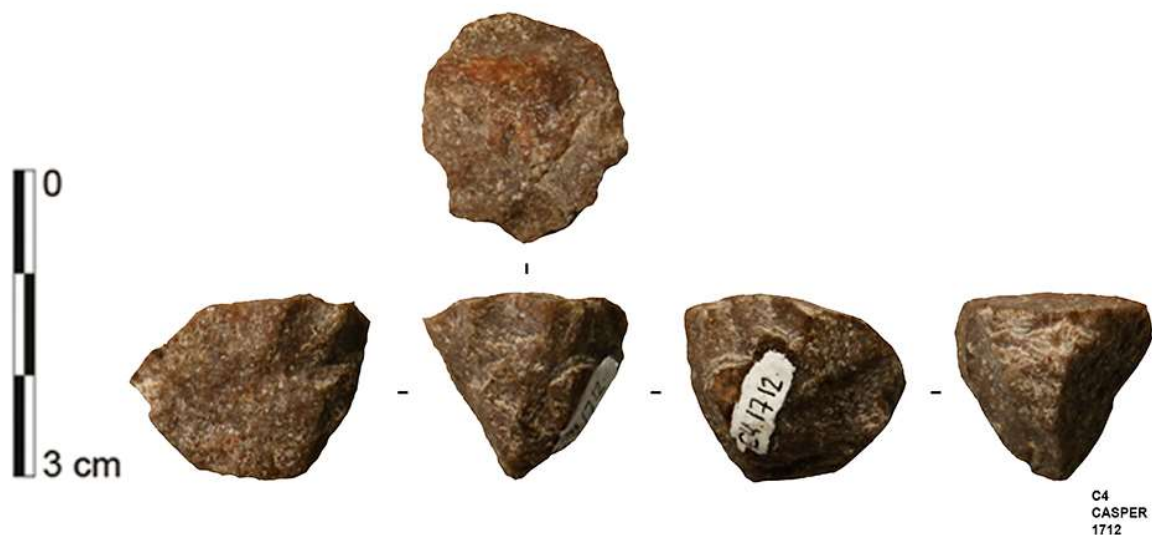
One of the quartz cores shows removals of a first exploitation as a laminar platform core and was terminated using bipolar-on-anvil percussion (Figure 39b). The core demonstrates traces of 'repercussion' (*contre-coup*) and impact scars on both the striking platform and the base. A quartz cobble served as the original core blank (Table 61). The back and one lateral surface of the core are covered with cortex (Table 63). The length of 25.1 mm falls below the minimum value of the length of the blade platform cores. The width and thickness are significantly lower than the mean values of the platform cores but fall within the range of the bipolar cores (Figure 43). The length-to-width ratio is also closer to the value of the bipolar cores (Table 72). The last

operation coincides with the extraction of elongated end-products using bipolar-on-anvil percussion (Table 71). This core type only occurs in layer Bart which, after layer Casper, has the highest proportion of bipolar cores (Table 60).

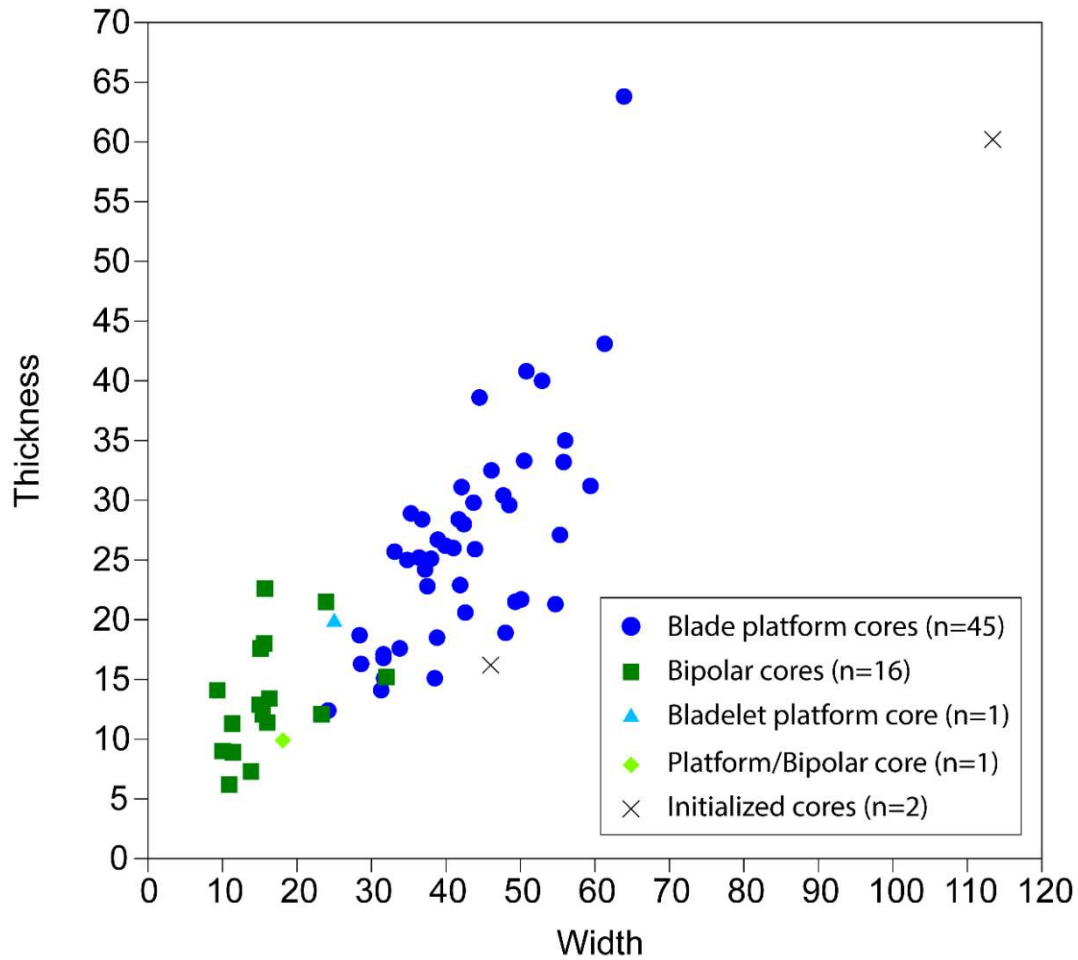
I observe bipolar cores with clear traces from bipolar-on-anvil knapping as the second most frequent core type. Quartz was mainly exploited in this manner (88.9%) (see for example Figure 39c). In most cases, the original core blank is not identifiable anymore (Table 61). A large proportion of the bipolar cores has either no cortex coverage (31.3%) or cortical remains on the back (31.3%) (Table 63). This core type clearly demonstrates smaller dimensions than the platform cores (Figure 43 & Table 68 – Table 70). The bipolar cores exhibit the highest length-to-width ratio (Table 72). Throughout the sequence, bipolar cores form the second most frequent core type, with the exception of layer Casper where they dominate (Table 60).

A few cores, including the only sandstone core (Figure 28), were classified as initial cores. Interestingly, all the initial cores are made on slabs (Table 61). They show more than 50% of cortex coverage, which is located either on the back or on the back and one lateral face (Table 62 & Table 63). Only one core is completely preserved and exhibits a cortical platform. The removal surface shape is quadrangular (Table 65). The base has either cortical remains or is prepared (Table 67). The initial cores show, with the exception of length (Table 68), greater dimensions than the platform cores (Table 69 & Table 70). The last operation involves either preparatory actions or a knapping accident (Table 71).

Finally, the two indeterminate core fragments represent the only core made on hornfels (Table 59).



**Figure 42.** Sibudu. C-A layers from the Deep Sounding: Quartzite bladelet core (Photo by Viola C. Schmid).



**FIGURE 43.** Sibudu. C-A layers from the Deep Sounding: Scatter plot of width and thickness of all in width and thickness completely preserved core types.

#### 5.4. Knapping Technique

Here, I expand on the diagnostic features allowing me to identify tendencies towards the percussion technique(s). I proceed by using blank categories to determine differences.

To begin with, I considered all completely and proximal preserved blades (n=1104). In determining whether direct or indirect application of force was used, I found that the corpus of blades exhibits a broad range of EPAs between 65° to 93° with a mean value of 82° (Figure 44) and platform depths between 0.2 mm and 22.1 mm with a mean value of 5.8 mm (Figure 45). Having said this, subgroups (1) and (2) do not demonstrate significant differences in terms of both EPA and platform depth (Table 73 & Table 74), indicating the use of the same knapping technique(s) for both subgroups. Furthermore, the laminar end-products (Figure 32 – 35) do

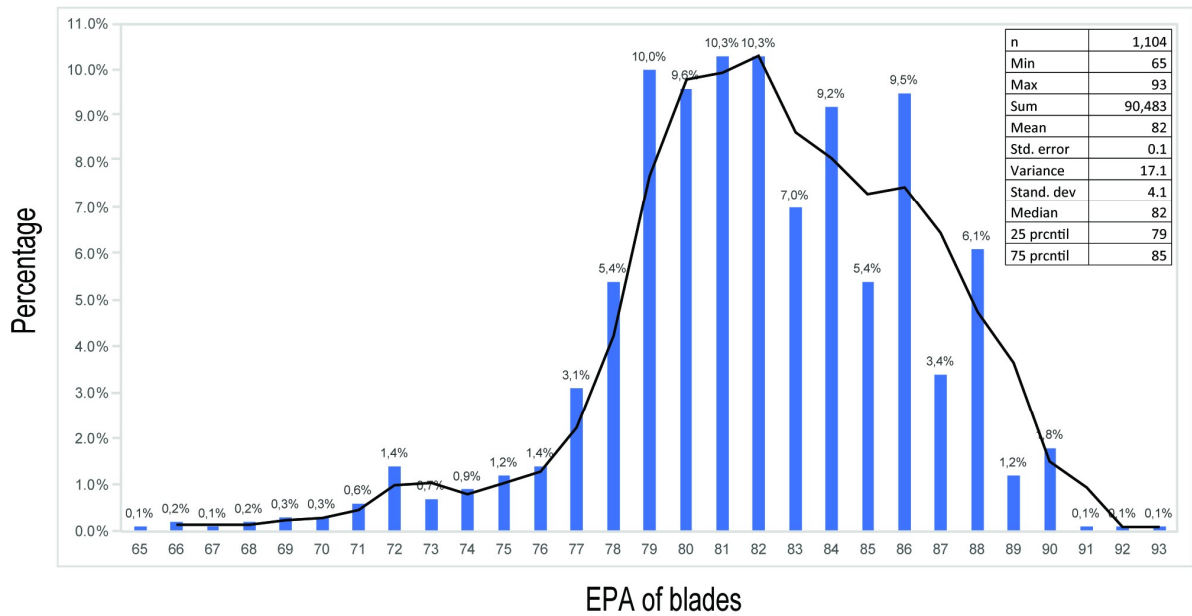


Figure 44. Sibudu. C-A layers from the Deep Sounding: Frequency distribution of EPA of blades.

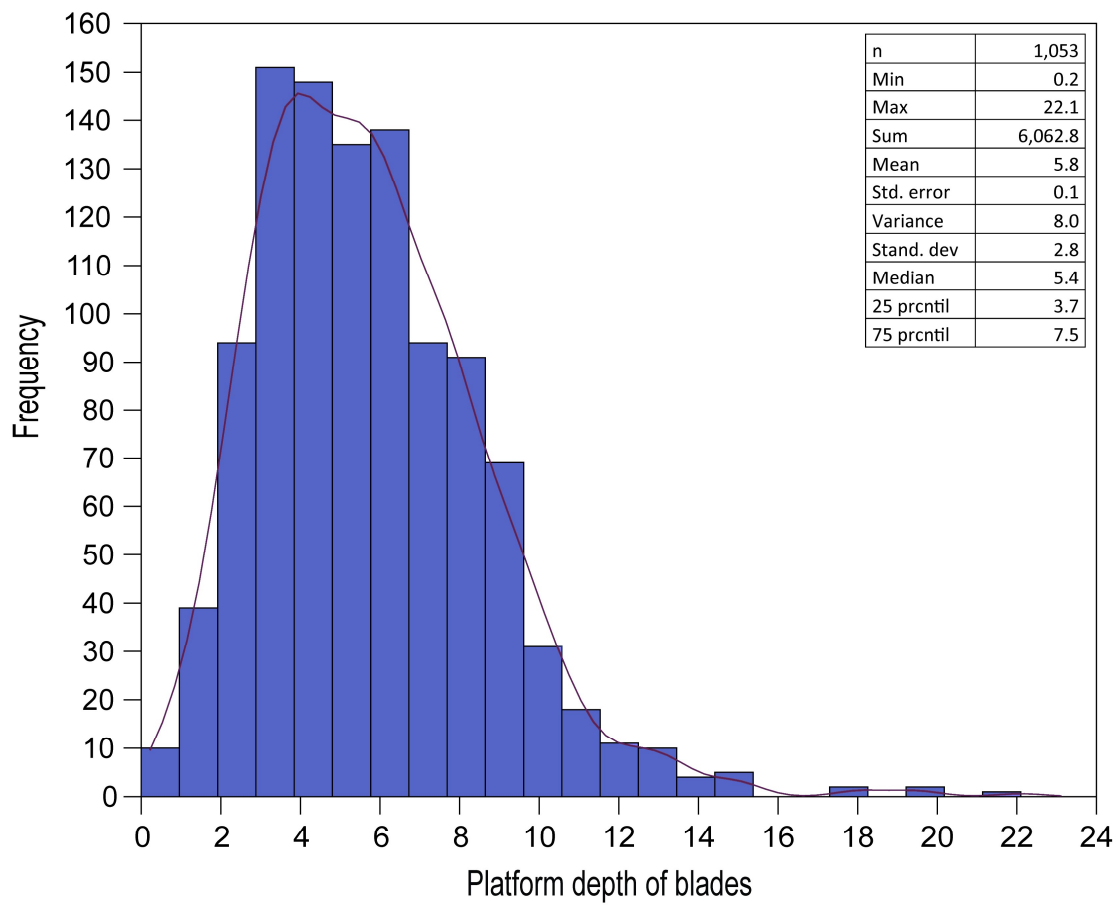






Figure 45. Sibudu. C-A layers from the Deep Sounding: Frequency distribution of platform depth of blades.

**Table 73.** Sibudu. C-A layers from the Deep Sounding: Comparison of EPA between blades with a triangular cross-section and blades with a trapezoidal cross-section (*t*-test).

		
n:	627	321
Mean:	81.938	81.891
Stand. dev.	0.332	0.423
Variance:	17.921	14.835
<b>F :</b>	<b>1.208</b>	
<b>t :</b>	<b>0.16611</b>	
<b>p :</b>	<b>0.86811</b>	

**Table 74.** Sibudu. C-A layers from the Deep Sounding: Comparison of platform depth between blades with a triangular cross-section and blades with a trapezoidal cross-section (*t*-test).

		
n:	593	314
Mean:	5.9024	5.7669
Stand. dev.	0.2467	0.2807
Variance:	9.3568	6.3884
<b>F :</b>	<b>1.4647</b>	
<b>t :</b>	<b>0.67258</b>	
<b>p :</b>	<b>0.50139</b>	

**Table 75.** Sibudu. C-A layers from the Deep Sounding: Frequency of dorsal reduction type of completely and proximal preserved blanks.

Blank Categories	abrasion		lateral notching		short hinged removals		small removals following scar ridges		none		Total	
	n	%	n	%	n	%	n	%	n	%	n	%
Blades	2	0.2%	3	0.3%	99	9.0%	6	0.5%	994	90.0%	<b>1,104</b>	<b>100%</b>
Elongated flakes	1	0.1%	-	0.0%	70	9.9%	2	0.3%	637	89.7%	<b>710</b>	<b>100%</b>
Flakes	17	0.6%	-	0.0%	215	7.6%	-	0.0%	2,586	91.8%	<b>2,818</b>	<b>100%</b>
Triangular flakes	-	0.0%	-	0.0%	10	9.6%	-	0.0%	94	90.4%	<b>104</b>	<b>100%</b>
<b>Total</b>	<b>20</b>	<b>0.4%</b>	<b>3</b>	<b>0.1%</b>	<b>394</b>	<b>8.3%</b>	<b>8</b>	<b>0.2%</b>	<b>4,311</b>	<b>91.0%</b>	<b>4,736</b>	<b>100%</b>

not show the morphological regularity and parallel sides expected from applying indirect percussion (see for example Pelegrin, 1991). Thus, the knappers most likely produced the blades by the application of direct percussion.

With respect to the motion, only a small proportion of the blades exhibits abrasion or trimming of their platforms (Table 75) and most platform depths (94.7%) exceed 2 mm. Furthermore, most of the blades show a quadrangular platform morphology, followed by oval and triangular shaped platforms (Table 76). This indicates a dominant gesture of internal percussion, i.e. striking occurred further inward from the core margin. While most of the end-products suggest

**Table 76.** Sibudu. C-A layers from the Deep Sounding: Frequency of platform morphology of completely and proximal preserved blanks.

Blank Categories	quadrangular		oval		triangular		lunate		winged		linear ridge		punctiform		irregular		crushed		indetermined		Total	
	n	%	n	%	n	%	n	%	n	%	n	%	n	%	n	%	n	%	n	%	n	%
Blades	331	30.2%	281	25.6%	184	16.8%	39	3.6%	71	6.5%	28	2.6%	1	0.1%	99	9.0%	10	0.9%	52	4.7%	<b>1,096</b>	<b>100%</b>
Elongated flakes	219	32.5%	156	23.1%	80	11.9%	31	4.6%	63	9.3%	10	1.5%		0.0%	70	10.4%	3	0.4%	42	6.2%	<b>674</b>	<b>100%</b>
Flakes	637	25.3%	539	21.4%	300	11.9%	107	4.2%	234	9.3%	44	1.7%	3	0.1%	350	13.9%	39	1.5%	268	10.6%	<b>2,521</b>	<b>100%</b>
Triangular flakes	37	36.6%	20	19.8%	10	9.9%	1	1.0%	12	11.9%	3	3.0%		0.0%	15	14.9%		0.0%	3	3.0%	<b>101</b>	<b>100%</b>
<b>Total</b>	<b>1,224</b>	<b>27.9%</b>	<b>996</b>	<b>22.7%</b>	<b>574</b>	<b>13.1%</b>	<b>178</b>	<b>4.1%</b>	<b>380</b>	<b>8.7%</b>	<b>85</b>	<b>1.9%</b>	<b>4</b>	<b>0.1%</b>	<b>534</b>	<b>12.2%</b>	<b>52</b>	<b>1.2%</b>	<b>365</b>	<b>8.3%</b>	<b>4,392</b>	<b>100%</b>

**Table 77.** Sibudu. C-A layers from the Deep Sounding: Frequency of blanks with and without lip among completely and proximal preserved blanks.

Blank Categories	with lip		without lip		Total	
	n	%	n	%	n	%
Blades	216	19.6%	888	80.4%	<b>1,104</b>	<b>100%</b>
Elongated flakes	113	15.9%	597	84.1%	<b>710</b>	<b>100%</b>
Flakes	475	16.9%	2,342	83.1%	<b>2,817</b>	<b>100%</b>
Triangular flakes	19	18.3%	85	81.7%	<b>104</b>	<b>100%</b>
<b>Total</b>	<b>823</b>	<b>17.4%</b>	<b>3,912</b>	<b>82.6%</b>	<b>4,735</b>	<b>100%</b>

**Table 78.** Sibudu. C-A layers from the Deep Sounding: Frequency of bulb type of completely and proximal preserved blanks.

Blank Categories	pronounced		weakly developed		double		absent		indetermined		Total	
	n	%	n	%	n	%	n	%	n	%	n	%
Blades	572	51.8%	420	38.0%	-	0.0%	112	10.1%	-	0.0%	<b>1,104</b>	<b>100%</b>
Elongated flakes	371	52.2%	294	41.4%	1	0.1%	41	5.8%	4	0.6%	<b>711</b>	<b>100%</b>
Flakes	1,551	55.0%	1,072	38.0%	2	0.1%	175	6.2%	22	0.8%	<b>2,822</b>	<b>100%</b>
Triangular flakes	60	57.7%	30	28.8%	-	0.0%	14	13.5%	-	0.0%	<b>104</b>	<b>100%</b>
<b>Total</b>	<b>2,554</b>	<b>53.9%</b>	<b>1,816</b>	<b>38.3%</b>	<b>3</b>	<b>0.1%</b>	<b>342</b>	<b>7.2%</b>	<b>26</b>	<b>0.5%</b>	<b>4,741</b>	<b>100%</b>

a *rentrante* motion, i.e. striking that was conducted straight in an axis of percussion perpendicular to the plane of detachment of the product, the presence of lips on 19.6% of the blades (Table 77) suggests that the motion was occasionally tangential.

To address the nature of the knapping instrument, I recorded the internal platform delineation of the blades (see for a definition Soriano, et al., 2007). A total of 21.9% of the laminar end-products demonstrate platforms where the overhang of the contact point creates an abrupt break in the delineation on the ventral face, and 2.4% of platforms have a double curve from two contact points on the ventral face. Both of these features are specific to stone hammer percussion only. This set of observations, together with a high frequency of pronounced bulbs (51.8%) (Table 78), indicates that soft and hard hammerstone percussion may have both occurred within the reduction sequence. I observe Siret fractures (7.4%), i.e. accidental



longitudinal split breaks, as a typical accident of hard hammerstone percussion, and split or shattered bulbs (33.5%) can be regarded as indicative of soft stone hammerstone percussion.

The elongated flakes comprise 712 completely or proximal preserved pieces. Like the blades, the elongated flakes also demonstrate a wide range of EPAs between 61° to 92° (Table 79) and platform depths between 1 mm and 26.1 mm (Table 80). However, the EPA of the elongated flakes averages 81.3°, differing significantly from the blades (*t*-test,  $t = -3.5692$ ;  $p = 0.00036737$ ). I also observed a significant difference in the platform depth of the elongated flakes with a mean value of 6.3 mm, higher than the blades (*t*-test,  $t = -3.6785$ ;  $p = 0.00024186$ ). Even though elongated flakes show the highest frequency of dorsal reduction (Table 75), they also encompass a greater proportion of quadrangular platform morphologies (Table 76). Additionally, 96.6% of these blanks have a platform depth exceeding 2 mm. Thus, the predominant gesture was internal percussion. Although the presence of elongated flakes with lips is low (15.9%) (Table 77), knappers also applied the *rentrante* motion for this blank category, and more occasionally the tangential motion, but this was rarer than for the blades. The range of the EPAs corresponds to suitable values for soft and hard stone hammer percussion and the high number of pieces with pronounced bulbs at 52.2% (Table 78) also makes a case for a mineral rather than an organic hammer. As would be expected for these techniques, Siret fractures (16.7%) and split or shattered bulbs (38.4%) occur among the elongated flakes.

The population of flakes includes 2823 completely or proximal preserved artefacts. The range of EPAs is the broadest, between 22° and 100°, compared to the other blank categories (Table 79) and the same is true for the platform depth which ranges from 0.7 mm to 37.6 mm (Table 80). The flakes show the lowest mean value of EPA at 80.8° and clearly differ from the blades (*t*-test,  $t = 6.7604$ ;  $p < 0.0001$ ). The platform depth averages 6.8 mm and is also significantly higher than the mean value of the blades (*t*-test,  $t = -8.0757$ ;  $p < 0.0001$ ). Flakes demonstrate the lowest number of pieces with dorsal reduction (Table 75). The platforms are mainly quadrangular in shape, followed by oval shaped (Table 76). A total of 96.8% of the platform depth of flakes exceeds 2 mm, indicating that the knappers applied internal percussion. Most of the flakes indicate a *rentrante* motion, but the flakes with lips (16.9%) (Table 77) attest that the tangential motion occurred as well. The flakes include a high proportion of pieces with pronounced bulbs (55%) (Table 78) and the range of the EPAs coincides with stone hammer use. Knapping accidents of both hard, namely Siret fractures (18.5%), and soft hammer use, namely split or shattered bulbs (37.4%), are present.

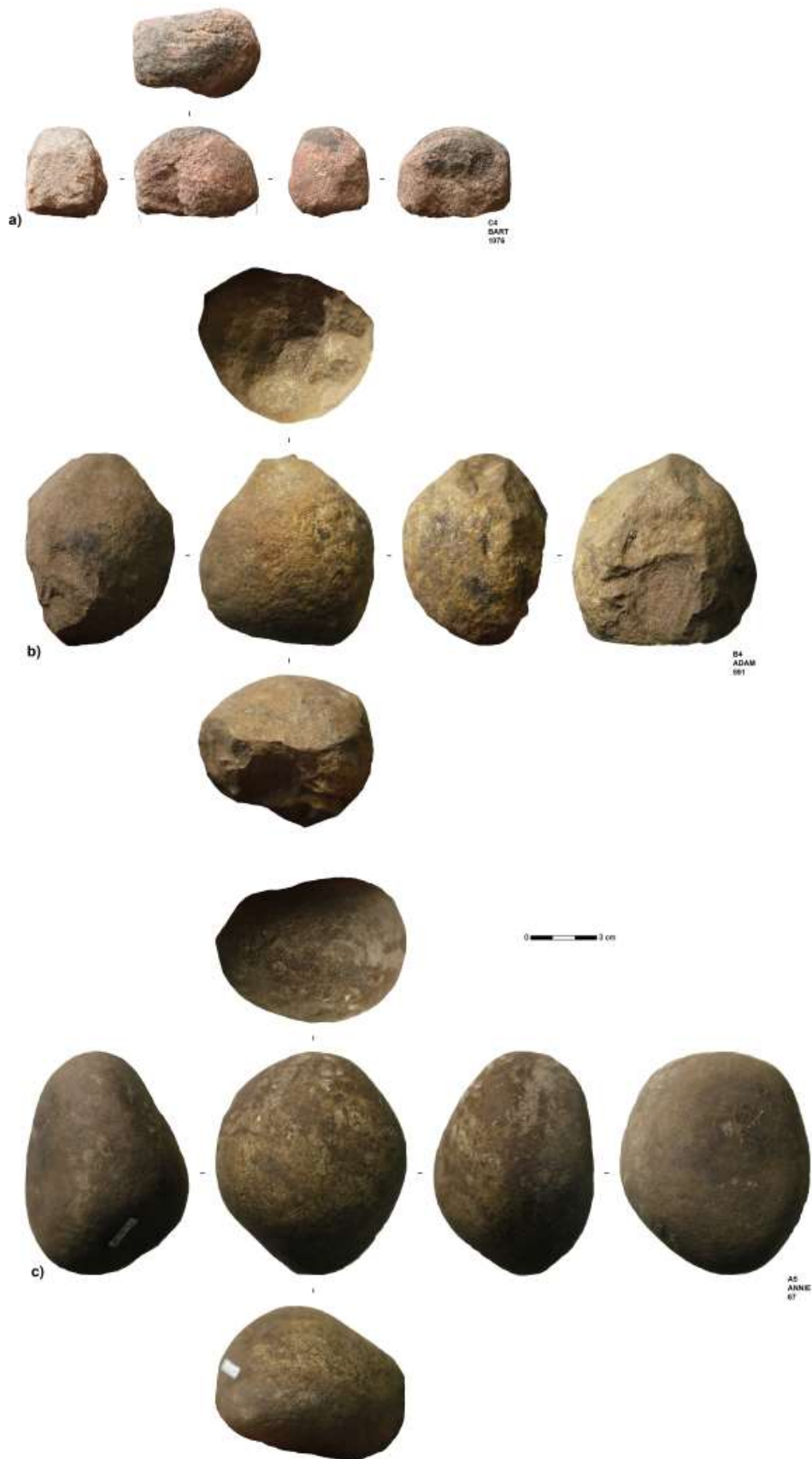
**Table 79.** Sibudu. C-A layers from the Deep Sounding: Descriptive statistics of EPA of all completely and proximal preserved blanks per blank category.

	Blades	Elongated flakes	Flakes	Triangular flakes
n	1,104	710	2,804	104
Min	65	61	22	67
Max	93	92	100	90
Sum	90,483	57,691	226,537	8,525
Mean	82	81.3	80.8	82
Std. error	0.1	0.2	0.1	0.4
Variance	17.1	16.4	26.3	18.9
Stand. dev.	4.1	4.1	5.1	4.3
Median	82	81	81	82
25 prcntil	79	79	79	80
75 prcntil	85	84	84	85

**Table 80.** Sibudu. C-A layers from the Deep Sounding: Descriptive statistics of platform depth of all completely and proximal preserved blanks per blank category.

	Blades	Elongated flakes	Flakes	Triangular flakes
n	1,053	670	2,500	103
Min	0.2	1	0.7	1.3
Max	22.1	26.1	37.6	16
Sum	6,062.8	4,219.9	16,937.2	781.8
Mean	5.8	6.3	6.8	7.6
Std. error	0.1	0.1	0.1	0.3
Variance	8	10.2	13.3	10.9
Stand. dev.	2.8	3.2	3.7	3.3
Median	5.4	5.7	6	6.9
25 prcntil	3.7	4	4.2	5
75 prcntil	7.5	7.9	8.5	10.2

Finally, 104 of the triangular flakes are completely or proximal preserved. The range of the EPAs is between 67° and 90°, averaging 82° (Table 79) which corresponds to the blades. However, the triangular flakes exhibit the highest mean value for platform depth at 7.6 mm (Table 80) and the greatest part (97.1%) exceeds 2 mm. Triangular flakes have the second largest proportion of pieces with dorsal reduction following the blades (Table 75). These blanks show the highest frequency of quadrangular platforms at 36.6% (Table 76). The detachment of triangular flakes was conducted with internal percussion combined with a *rentrante* motion, but use of a tangential motion is attested to by the presence of objects with lips (18.3%) (Table 77). This blank category has the highest frequency of artefacts with a pronounced bulb (Table 78). Both Siret fractures (6.8%) and split or shattered bulbs (31.1%) occurred.



**Figure 46.** Sibudu. C-A layers from the Deep Sounding: Hammerstones. Hammerstones made on sandstone (a, b), and hammerstone made on quartzite I (Photo (a) by Julia Becher; photos (b, c) by Viola C. Schmid).

The compilation of percussion marks for all of the blank categories leads me to the conclusion that in general, the knappers of Sibudu used hard and soft hammerstones in direct, internal percussion, while applying both *rentrante* and tangential motions. The blank categories differ mainly in the proportion of how often past people applied the tangential motion.

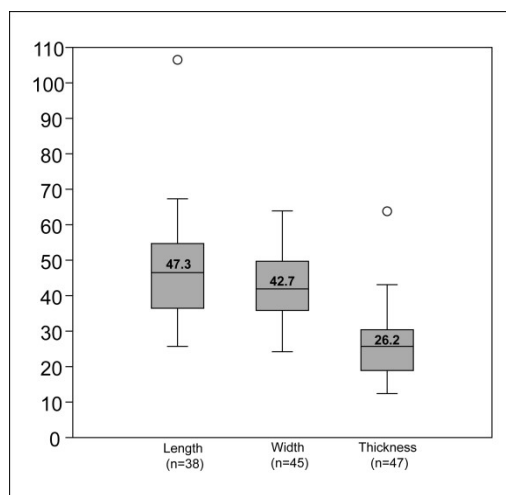
The assemblage comprises several cobbles and cobble fragments of sandstone (n=8) as well as quartzite (n=12), dolerite (n=5) and quartz (n=1) (Figure 46 & Table 11) with impact marks that can be interpreted as hammerstones, supporting the potential coexistence of both hard and soft hammerstones to detach blanks.

### 5.5. The Laminar Reduction Strategy

Based on my analysis integrating blanks and cores, I identified a specific laminar reduction strategy dominating the basal layers of Sibudu Cave that I will discuss in the following chapter. A large proportion (67.6%) of the cores (n=48; exclusively blade platform cores) corresponds to this laminar reduction system. The blanks indicate that although explicit blade cores do not exist in all raw materials, the inhabitants of the site exploited all rock types to obtain laminar end-products. These blades are characterised by unidirectional dorsal scar patterns, rectangular shapes and straight to slightly curved profiles. The recognition of this reduction system is as yet not underpinned by physical refitting, but preliminary experiments have been undertaken by C. Lepers. They will be continued and analysed in the future to test and complete the description presented here.

#### 5.5.1. Core Configuration

The cores demonstrate a systematic organisation to enable and maintain laminar production, although their dimensions vary dramatically, especially length, but this is likely due to different stages of exhaustion (Figure 47). The knappers established six different areas to achieve the geometry required to manufacture blades. Apart from striking platform, removal surface, back and base of the core, two common and essential surfaces are the lateral crest and *méplat* or lateral plane (Figure 48 – Figure 49 & Table 81):



**Figure 47.** Sibudu. C-A layers from the Deep Sounding: Box plots of dimensions of blade platform cores.

Most of the striking platforms are plain, although the knappers prepared the platforms of one core with faceting to ensure the successful extraction of the next product. In general, the outline of the platform is arched and the flaking angle is primarily in the range between 70° and 90°.

The removal surfaces show quadrangular (60.4%) followed by oval (29.2%) shapes. The cores document a rather low transversal convexity of the removal surface.

The backs of the cores are mainly formed by natural or old ventral faces (70.9%). However, 25% of the backs are overprinted by preparation removal scars belonging to either the lateral crest, base or striking platform.

Concerning the base of the core, 72.9% of the cores demonstrate complete or partial preparation to maintain the distal convexity, while only 18.8% are left with a natural surface. The toolmakers managed the longitudinal convexity with removals from the core base opposed to the knapping direction of the unidirectional reduction.

The lateral crest is made on one margin of the removal surface by detaching flakes orthogonal to the axis of exploitation with the aim of ensuring transversal convexity. The crest is prepared in different ways due to natural conditions, re-shaping and progression of reduction, and these variants can be subdivided as follows. Past people most frequently prepared the crests with bifacially alternating removals (38%) or bifacial preparation (38%). Moreover, I observe the preparation of only one face suggesting that either the preparation has been removed on one face or that the convexity was considered appropriate for reduction, thus making preparation unnecessary. One core exhibits no preparation at all as the natural configuration of the original core blank already provided a suitable transversal convexity. Finally, another core is so exhausted that the lateral crest was completely removed (Figure 50). On most cores, the angle of the crest ranges between 70° and 90° (71.1%).

The *méplat*, or lateral plane, is one of the narrow faces of the core, located opposite the lateral crest. Most of the cores (47.9%) have a natural surface that forms the lateral plane. However, 31.3% of the cores represent a stage of reduction so far advanced that the *méplat* is not recognizable due to heavy exhaustion. A few cores show orthogonal preparation removals which served to correct the angle between the removal surface and the *méplat*. The angles formed by the lateral plane and the removal surface are typically between 100° and 110°.

The lateral crest and the *méplat*, together with the typically quadrangular removal surface on the wide surface of the original core blank, form the active, or *utile*, volume (for a definition see Boëda, 2013; Boëda, et al., 2013) that provides the volume destined for exploitation. During the course of reduction, the active volume changes in shape from a triangular asymmetric cross-section to a pentagonal cross-section, resembling a house tipped over on its side. The backs of the cores represent the passive, or *inutile*, volume (see for a definition Boëda, 2013; Boëda, et al., 2013).

The last phase of production on most cores is associated with the removal of blades (41.6%) or elongated flakes (44%). One specimen shows the extraction of a triangular element. The blow to remove this triangular flake was positioned on a dihedral platform and further followed a central ridge created by two preceding converging negatives (Figure 51).

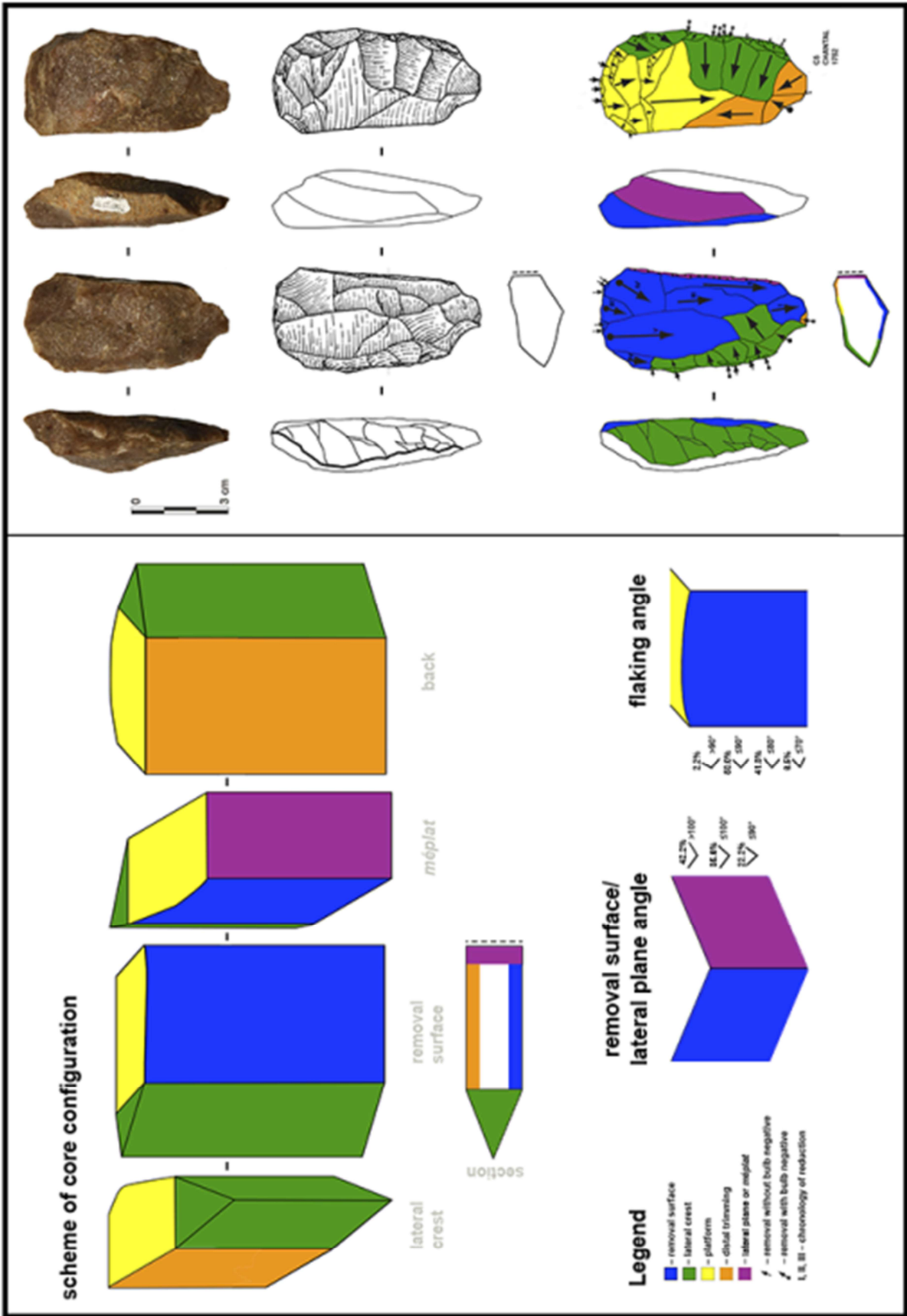
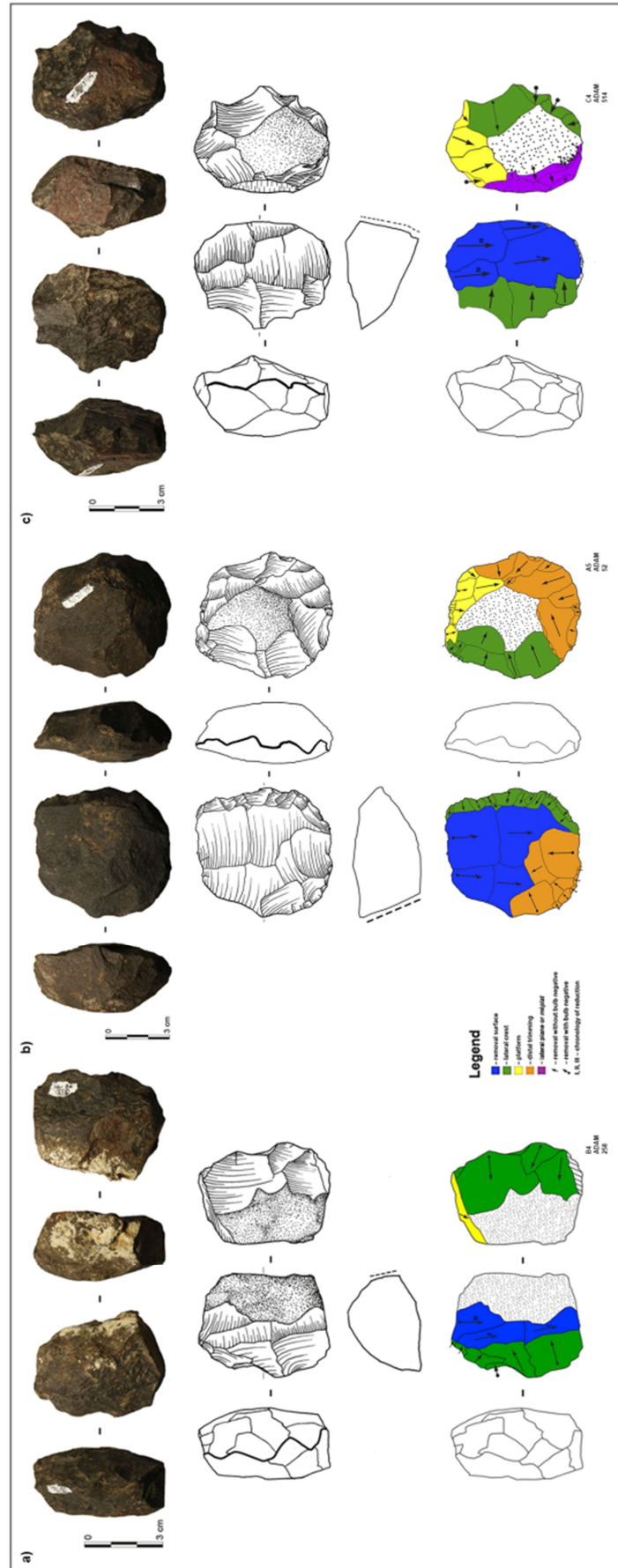


Figure 48. Sibudu. C-A layers from the Deep Sounding: Core configuration of laminar reduction strategy (Drawing after Rots, et al., 2017; photo by Viola C. Schmid).

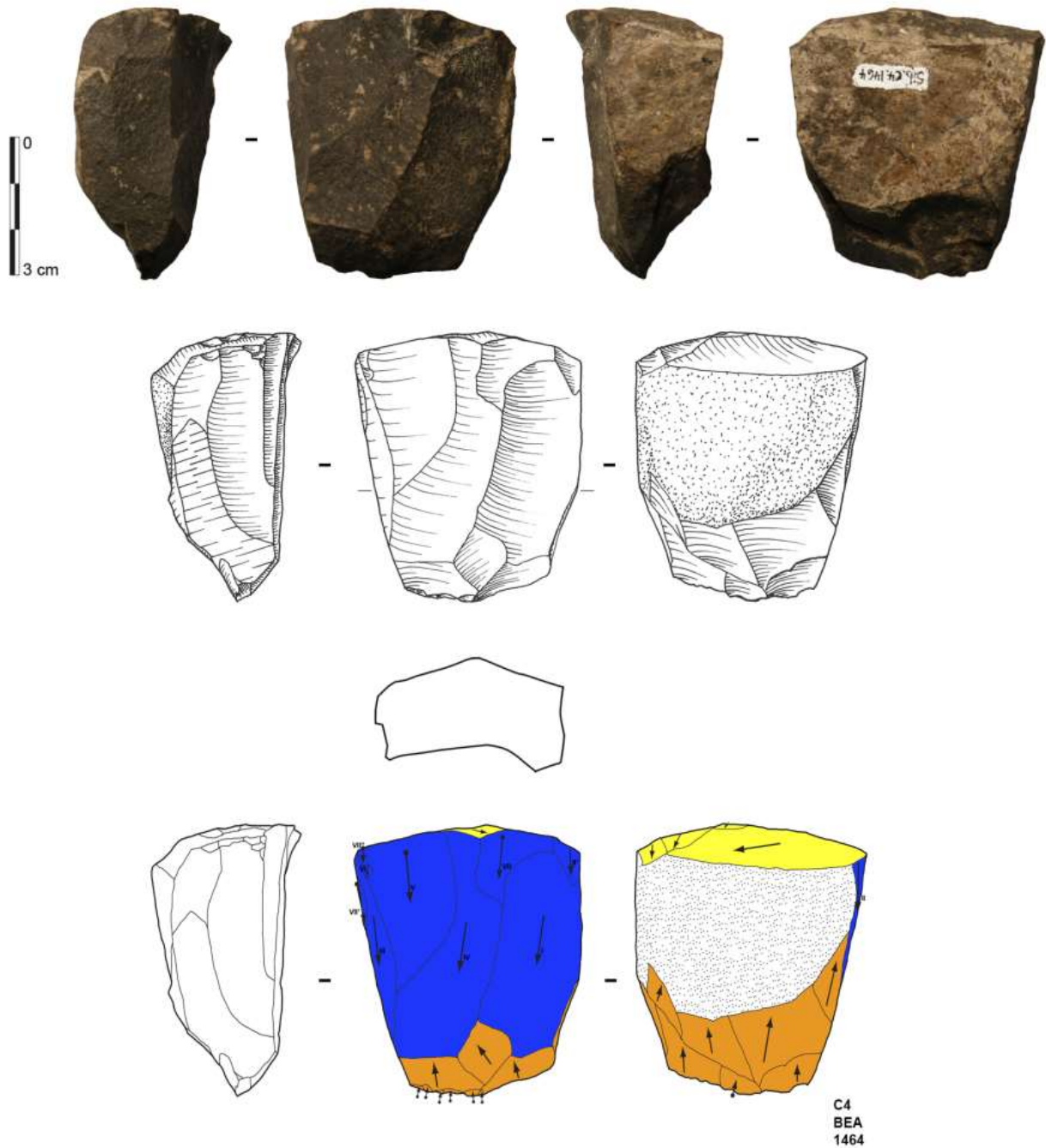


**Figure 49.** Sibudu. C-A layers from the Deep Sounding: Laminar cores (a-c) (Drawings by Heike Würschem; photos by Viola C. Schmid).

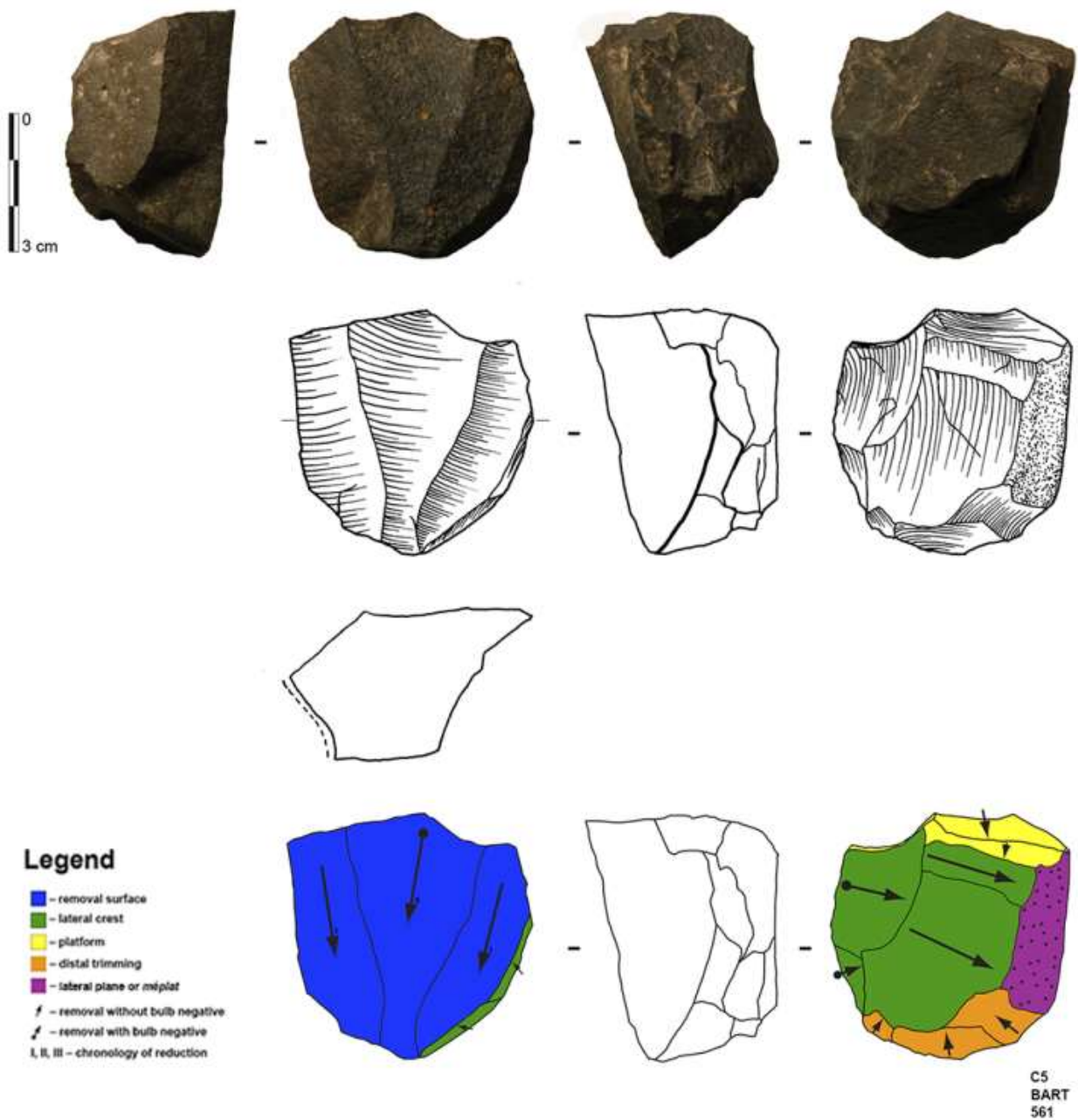
**Table 81.** Sibudu. C-A layers from the Deep Sounding: Frequencies of striking platform, base, back and last operation of laminar cores.

<b>Striking Platform</b>													
		plain		faceted		cortical		n/a					
		n	%	n	%	n	%	n	%				
		43	89.6%	1	2.1%	-	0.0%	4	8.3%				
<b>Removal Surface</b>													
		quadrangular		oval		triangular		n/a					
		n	%	n	%	n	%	n	%				
		29	60.4%	14	29.2%	3	6.3%	2	4.2%				
<b>Back</b>													
		cortex/joint surface		removals		ventral		n/a					
		n	%	n	%	n	%	n	%				
		26	54.2%	12	25.0%	8	16.7%	2	4.2%				
<b>Base</b>													
		preparation		cortex/joint surface		cortex & preparation		base removed		n/a			
		n	%	n	%	n	%	n	%	n	%		
		34	70.8%	9	18.8%	1	2.1%	1	2.1%	3	6.3%		
<b>Lateral Crest</b>													
		bifacial alternating		bifacial		unifacial		natural crest		crest removed			
		n	%	n	%	n	%	n	%	n	%		
		18	38.0%	18	38.0%	11	22.9%	-	0.0%	1	2.1%		
<b>Méplat or Lateral Plane</b>													
		cortex/joint surface		exploitation		cortex & removals		breakage surface		preparation		n/a	
		n	%	n	%	n	%	n	%	n	%	n	%
		23	47.9%	15	31.3%	5	10.4%	2	4.2%	1	2.1%	2	4.2%
<b>Last Operation</b>													
		accident		production		crest preparation		platform preparation		distal preparation			
		n	%	n	%	n	%	n	%	n	%		
		23	47.9%	12	25.0%	6	12.5%	4	8.3%	3	6.3%		





**Figure 50.** Sibudu. Layer Bea of the Deep Sounding: Exhausted laminar core, where the lateral crest was completely removed by removals from the exploitation (Drawing by Heike Würschem; photo by Viola C. Schmid).



**Figure 51.** Sibudu. Layer Bart of the Deep Sounding: Core configuration of laminar reduction strategy with extraction of triangular element in last operational phase (Drawing by Heike Würschem; photo by Viola C. Schmid).

### 5.5.2. Early Phase of reduction

The toolmakers selected many kinds of raw materials with different shapes for exploitation, although slabs were used most frequently (Table 61). Interestingly, all initialised cores are made on slabs as well. The beginning of the reduction system involves the preparation of the lateral crest and the production of a striking platform. The diagnostic flakes from the early stage of establishing the crest are trapezoidal and slightly curved to curved showing either unidirectional scars and/or cortex (n=579; 13.5% of the total flake population).

Due to the asymmetric triangular cross-section of the active volume, the effective exploitation of the volume starts on the ridge that is formed by the *méplat* and the removal surface. The knappers used either natural geometries, such as long natural edges provided by slabs, or followed a more elaborate procedure by preparing one or both *versant(s)* to facilitate the removal of the first crested blade. Uni- or bilateral primary crested blades make up 0.8% of all blades, while naturally crested cortical blades with triangular cross-sections comprise 1.8% of the assemblage. Thus, past people typically selected pieces of raw material with knapping angles and convexities that were appropriate for the extraction of blades without a great investment in core preparation.

### 5.5.3. Middle and late phase of reduction

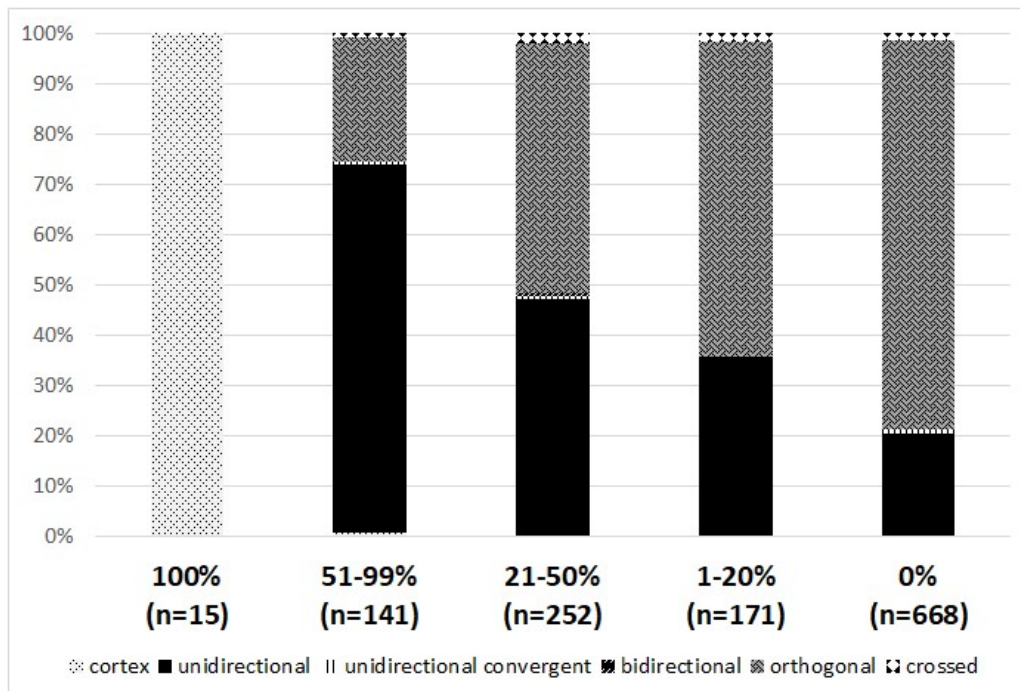
The reduction of the active volume proceeds asymmetrically on the wide surface and by reducing the *méplat*. The lateral expansion of the removal surface is reflected by the high frequency of laminar products with lateral cortex (66.7% of the blades with dorsal cortical coverage), while the presence of cortical backed blades attests to the exploitation of the *méplat* (16.8% of the blades with dorsal cortical coverage). This continuous dichotomy of the reduction sequence results in the production of two main kinds of blades (for further details see Chapter 5.2.).

As the preparation of the striking platform is minimal, most end-products have plain butts (Table 23). In general, the knappers pursued a unidirectional reduction strategy and kept the curvature of the blades low (Table 24 & Table 26). The presence of laminar elements with distal cortex (8.4% of the blades with dorsal cortical coverage) documents the lateral and distal expansions of the removal surface.

The laminar corpus includes various elements with characteristics diagnostic of this reduction system. Some of the blades (n=162; 8.5% of the total blades) and elongated flakes (n=57; 5.7% of the total elongated flakes) exhibit orthogonal or crossed dorsal negatives demonstrating their exploitation in an area of the removal surface adjacent to the lateral crest. The orthogonal dorsal scars correspond to the distal ends of removals related to the preparation of lateral crests. Apart from cortical backed blades, other core edge products (*débordants*) occur (n=11). A few of the end-products have a small shoulder next to their butt, which relates to the arched outline of the platform and the area transitional to either the lateral crest or the *méplat* (n=80). Plunging blades are present (n=41), some of which exhibit preparation to manage the distal

convexity. Laminar products with bidirectional dorsal negatives usually limited to the distal part also testify to a regulation of the distal convexity (n=68). Among the accompanying flakes, specimens also show a part of platform preparation (n=536), lateral crest preparation (n=238), and distal preparation (n=88) on their dorsal surface.

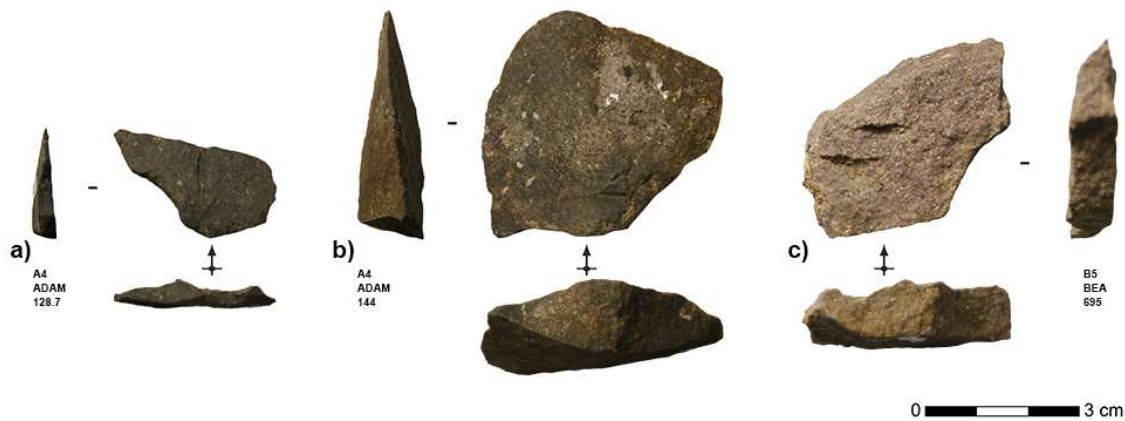
We identify two lines of evidence that indicate a discontinuous reduction sequence, suggesting that the removal surface requires partial re-shaping during knapping. First, semi-crested (n=23), non-cortical and partially cortical laminar blanks indicate that during core reduction, the toolmakers had to partially renew the ridge formed by the lateral plane and the removal surface. Second, both cores and preparation flakes show the reinstallation of the lateral crest in an advanced stage of the reduction sequence. The last operation on 12.5% of the cores involves crest preparation. The diagnostic flakes of this crest re-shaping (n=669) share features with those of the early crest preparation including the trapezoidal shape and the slightly curved to curved profile. In contrast, these blanks exhibit no cortex, but most of them show orthogonal laminar dorsal scars (Figure 52).



**Figure 52.** Sibudu. Layer Bart of the Deep Sounding: Distribution of dorsal scar patterns by cortex coverage proportions on the dorsal surface of all lateral crest preparation flakes (n=1,247).

The butts are generally plain. In some cases, these flakes (n=159) show a small shoulder, which implies their detachment close to the striking platform.

To reorganise the angle of the platform, the knappers removed partial rejuvenation core tablets (n=71). The partial rejuvenation core tablets are thick flakes with a mean value of 10.3 mm, show either trapezoidal or rectangular shapes and have backs formed by removals that came from the removal surface (Figure 53).



**Figure 53.** Sibudu. C-A layers from the Deep Sounding: Partial rejuvenation core tablets. Partial rejuvenation core tablets made on dolerite (a, b) and made on sandstone (c) (Photos by Viola C. Schmid).

We also observe a few typical flakes from distal preparation usually exhibiting bidirectional or opposed dorsal removals (n=34). They often show opposed negatives from knapping accidents (n=12), such as a hinge, attesting to the reestablishment of the distal convexities plus the correction of errors on the removal surface.

#### 5.5.4. Final phase of reduction

The cores abandoned after a long cycle of exploitation preserve information about the final stages of the reduction sequence. The moment of discard is mostly related to knapping errors. Because of core exhaustion and the imbalance in the exploitation of the active volume during the reduction as well as the preparation of crests, platforms and distal surfaces, the majority of removal surfaces is square rather than elongated. A total of 85.4% of the cores exhibit blades or elongated flakes as final end-products on their removal surfaces. In view of the final phase of production on the cores and the distribution in lengths of the blades, I posit that the minimum length of the desired blanks was about 20 mm (Figure 47).

The end of production is fixed when the removal surface reaches such flatness that further exploitation is impossible. This occurs when the toolmakers exhausted the active volume so intensely that they could not establish a transversal convexity by renewing the lateral crest. Correspondingly, the width-to-thickness ratio of cores discarded after removing the last end-product (1.9) is higher compared to the others (1.6), indicating a greater flatness.

## 5.6. Formal Tools

The formal tools from the basal layers comprise 7.7% of the total assemblage varying from 6.8% to 9.2% (Table 15). The corpus of tools (Table 82) stands out for the presence of bifacial technology (Conard, et al., 2014; Conard and Porraz, 2015), including serrated pieces (see Rots, et al., 2017).

**Table 82.** Sibudu. C-A layers from the Deep Sounding: Typological classification. (\* Including TSPs, ACTs, and Tongatis; \*\* including bifacial points, serrated pieces, and bifacially backed knives; \*\*\* including lateral scrapers, end-scrapers, and NBTs).

Layer	Unifacial pointed Forms*		Bifacial Pieces**		Scraper-like forms***		Denticulates/ Notch		Indet. Fragments		Total	
	n	%	n	%	n	%	n	%	n	%	n	%
ADAM	69	55.6%	12	9.7%	16	12.9%	8	6.5%	19	15.3%	124	100%
ANNIE	36	48.6%	12	16.2%	12	16.2%	5	6.8%	9	12.2%	74	100%
BART	36	43.4%	25	30.1%	7	8.4%	5	6.0%	10	12.0%	83	100%
BEA	64	43.5%	42	28.6%	15	10.2%	7	4.8%	19	12.9%	147	100%
CASPER	50	44.2%	31	27.4%	13	11.5%	10	8.8%	9	8.0%	113	100%
CHANTAL	48	54.5%	18	20.5%	6	6.8%	4	4.5%	12	13.6%	88	100%
<b>Total</b>	<b>303</b>	<b>48.2%</b>	<b>140</b>	<b>22.3%</b>	<b>69</b>	<b>11.0%</b>	<b>39</b>	<b>6.2%</b>	<b>78</b>	<b>12.4%</b>	<b>629</b>	<b>100%</b>

The greatest part of retouched blanks comprise different unifacially retouched pointed forms. Various scraper-like forms, as well as denticulates, are present. Within the superordinate typological classification, I tried to determine repetitive patterns in the structural positioning of working and passive edges on the artefacts and dynamic associations with reduction cycles (for further details see Chapter 3.2.9.). Subsequently based on this approach, I identified the classes of tools defined by Conard et al. (2012) and was able to define new tool classes through collaboration with use wear and residue analysts (Table 83). In this section, I will describe the superordinate typological corpus of the lowermost deposits of Sibudu and I will elaborate on the characteristics and life histories of the different tool classes.

**Table 83.** Sibudu. C-A layers from the Deep Sounding: Frequency of tool classes.

Layer	Unifacial pointed forms								Bifacial pieces				Scraper-like forms						Denticulates/ Notch		Indet. Frag.		Total			
	TSPs		ACTs		Tongatis		Unifacial Points		Bifacial Points		Bifacially Backed Knives		Serrated Pieces		Lateral Scrapers		NBTs		End-scrapers							
	n	%	n	%	n	%	n	%	n	%	n	%	n	%	n	%	n	%	n	%	n	%	n	%	n	%
ADAM	21	16.9%	30	24.2%	4	3.2%	14	11.3%	12	9.7%	-	0.0%	-	0.0%	12	9.7%	4	3.2%	-	0.0%	8	6.5%	19	15.3%	124	100%
ANNIE	12	16.2%	14	18.9%	3	4.1%	7	7.6%	11	14.9%	1	1.4%	-	0.0%	4	5.4%	8	10.8%	-	0.0%	5	6.8%	9	12.2%	74	100%
BART	12	14.5%	14	16.9%	1	1.2%	9	10.8%	20	24.1%	-	0.0%	5	6.0%	5	6.0%	2	2.4%	-	0.0%	5	6.0%	10	12.0%	83	100%
BEA	30	20.4%	22	15.0%	2	1.4%	10	7.2%	29	19.7%	3	2.0%	10	6.8%	5	3.4%	7	4.8%	3	2.0%	7	4.8%	19	12.9%	147	100%
CASPER	21	18.6%	14	12.4%	2	1.8%	13	10.8%	24	21.2%	1	0.9%	6	5.3%	8	7.1%	4	3.5%	1	0.9%	10	8.8%	9	8.0%	113	100%
CHANTAL	28	31.8%	11	12.5%	1	1.1%	8	11.1%	14	15.9%	-	0.0%	4	4.5%	4	4.5%	1	1.1%	1	1.1%	4	4.5%	12	13.6%	88	100%
<b>Total</b>	<b>124</b>	<b>19.7%</b>	<b>105</b>	<b>16.7%</b>	<b>13</b>	<b>2.1%</b>	<b>61</b>	<b>9.7%</b>	<b>110</b>	<b>17.5%</b>	<b>5</b>	<b>0.8%</b>	<b>25</b>	<b>4.0%</b>	<b>38</b>	<b>6.0%</b>	<b>26</b>	<b>4.1%</b>	<b>5</b>	<b>1.0%</b>	<b>39</b>	<b>6.2%</b>	<b>78</b>	<b>12.4%</b>	<b>629</b>	<b>100%</b>

### 5.6.1. Unifacial Pointed Forms

Unifacial pointed forms are predominant throughout the sequence accounting for 48.2% of the total tool corpus (Table 82). In layers Bart and Bea, the unifacial pointed tools decrease to 43.4% and 43.5% respectively, while they reach high percentages in the uppermost stratum Adam at 55.6% and in the lowermost stratum Chantal at 54.5%.

Most unifacial pointed forms are manufactured on dolerite (71.6%), followed by quartzite (21.8%) (Table 84). The length of the unifacial pointed forms ranges from 19.6 mm to 76.6 mm, averaging 44.7 mm (Table 85). The tools show a mean width of 26.6 mm (Table 86) and a mean thickness of 8.3 mm (Table 87). The unifacial pointed forms have an average EPA value of 82.7° (Table 88) and an average platform depth value of 7.9 mm (Table 89). Both values (*t*-test concerning EPA,  $t = 3.2732$ ;  $p = 0.0010708$ ; *t*-test concerning platform depth,  $t = 4.2843$ ;  $p = <0.001$ ) significantly exceed the mean EPA and mean platform depth of the unmodified blank population. As these two are important variables affecting the blank size (Dibble and Rezek, 2009), knappers seem to have had the desired goal to produce blanks of larger sizes to transform them into unifacial pointed forms. The blanks selected to be modified into this tool type involve primarily laminar elements (Table 90). These products come typically from the main production phase, which is also reflected by the low number of pieces with cortex remaining (Table 91). The highest proportion of this tool type with a preserved proximal part exhibits plain platforms (Table 92). However, the tools involve more elements with faceted and dihedral platforms than the unmodified blanks indicating a higher investment in the platform preparation. Knappers preferentially chose blanks with straight profiles (83.5%) to modify them into unifacial pointed forms (Table 93). Blanks with a triangular cross-section dominate at 46.5%, followed by elements with trapezoidal cross-sections at 34.7% (Table 94). Only 19.1% of these tools are completely preserved (Table 95). The majority of the specimens is present as distal fragments, comprising 44.9%.

**Table 84.** Sibudu. C-A layers from the Deep Sounding: Frequency of raw material per tool types.

Tool type	Dolerite		Hornfels		Quartz		Quartzite		Sandstone		Chert		Indetermined		Total	
	n	%	n	%	n	%	n	%	n	%	n	%	n	%	n	%
Unifacial pointed forms	217	71.6%	11	3.6%	6	2.0%	66	21.8%	-	0.0%	2	0.7%	1	0.3%	<b>303</b>	<b>100%</b>
Bifacial pieces	56	40.0%	7	5.0%	49	35.0%	24	17.1%	1	0.7%	3	2.1%	-	0.0%	<b>140</b>	<b>100%</b>
Scraper-like forms	56	81.2%	2	2.9%	1	1.4%	10	14.5%	-	0.0%	-	0.0%	-	0.0%	<b>69</b>	<b>100%</b>
Denticulates/ Notch	29	74.4%	2	5.1%	2	5.1%	5	12.8%	-	0.0%	1	2.6%	-	0.0%	<b>39</b>	<b>100%</b>
Indet. Fragments	53	67.9%	9	11.5%	4	5.1%	12	15.4%	-	0.0%	-	0.0%	-	0.0%	<b>78</b>	<b>100%</b>
<b>Total</b>	<b>411</b>	<b>65.3%</b>	<b>31</b>	<b>4.9%</b>	<b>62</b>	<b>9.9%</b>	<b>117</b>	<b>18.6%</b>	<b>1</b>	<b>0.2%</b>	<b>6</b>	<b>1.0%</b>	<b>1</b>	<b>0.2%</b>	<b>629</b>	<b>100%</b>

**Table 85.** Sibudu. C-A layers from the Deep Sounding: Descriptive statistics of length of all completely preserved tools.

	Unifacial pointed forms	Bifacial pieces	Scraper-like forms	Denticulates/Notch
n	56	22	15	4
Min	19.6	26	25.2	41.3
Max	76.6	61.7	71.4	48.2
Sum	2,502.3	892.5	629.1	176.8
Mean	44.7	40.6	41.9	44.2
Std. error	1.6	1.8	3.7	1.5
Variance	148.5	67.8	203.8	8.5
Stand. dev.	12.2	8.2	14.3	2.9
Median	42.8	40.5	38.6	43.7
25 prcntil	38	35.5	30.5	41.8
75 prcntil	49.2	44.9	54.4	47.2

**Table 86.** Sibudu. C-A layers from the Deep Sounding: Descriptive statistics of width of all in the width completely preserved tools.

	Unifacial pointed forms	Bifacial pieces	Scraper-like forms	Denticulates/Notch
n	248	102	64	32
Min	9.4	7	16.5	16.5
Max	58.3	48.4	74.2	44.5
Sum	6,606.3	2,293.2	2,065.5	873.5
Mean	26.6	22.5	32.3	27.3
Std. error	0.5	0.7	1.5	1.1
Variance	59.2	54.7	142.7	38.5
Stand. dev.	7.7	7.4	11.9	6.2
Median	26	21.2	32	26.1
25 prcntil	21.6	17.6	22.7	23.1
75 prcntil	30.5	26.9	38.8	30.1

**Table 87.** Sibudu. C-A layers from the Deep Sounding: Descriptive statistics of thickness of all in the thickness completely preserved tools.

	Unifacial pointed forms	Bifacial pieces	Scraper-like forms	Denticulates/Notch
n	294	137	67	38
Min	1.5	2.5	0.9	4.1
Max	22.1	23.6	28.7	15.9
Sum	2,450.4	1,134.8	718.4	322.7
Mean	8.3	8.3	10.7	8.5
Std. error	0.2	0.3	0.5	0.4
Variance	10.4	11.9	18.8	5.5
Stand. dev.	3.2	3.4	4.3	2.3
Median	8	7.9	9.7	8.4
25 prcntil	5.9	6.3	8.1	6.9
75 prcntil	10.2	10	12.4	9.9



**Table 88.** Sibudu. C-A layers from the Deep Sounding: Descriptive statistics of EPA of all completely and proximal preserved tools.

	Unifacial pointed forms	Bifacial pieces	Scraper-like forms	Denticulates/Notch
n	109	15	47	20
Min	62	77	67	76
Max	93	96	92	87
Sum	9,011	1,248	3,959	1,635
Mean	82.7	83.2	84.2	81.8
Std. error	0.4	1.3	0.6	0.7
Variance	21.1	26.3	17.7	10.4
Stand. dev.	4.6	5.1	4.2	3.2
Median	84	84	85	82
25 prcntil	80	79	83	78.5
75 prcntil	86	85	86	84

**Table 89.** Sibudu. C-A layers from the Deep Sounding: Descriptive statistics of platform depth of all completely and proximal preserved tools.

	Unifacial pointed forms	Bifacial pieces	Scraper-like forms	Denticulates/Notch
n	102	4	41	15
Min	1.7	7.9	1.6	4.7
Max	18.2	12.5	19.9	13.1
Sum	809.8	41.3	329.2	117.1
Mean	7.9	10.3	8.0	7.8
Std. error	0.3	1.2	0.5	0.6
Variance	10.6	5.6	10.7	5.2
Stand. dev.	3.3	2.4	3.3	2.3
Median	7.5	10.5	7.7	7.5
25 prcntil	5.3	8.1	6.2	6.1
75 prcntil	9.9	12.4	9.4	8.7

**Table 90.** Sibudu. C-A layers from the Deep Sounding: Frequency of blank type per tool types.

Tool type	blade		elongated flake		flake		triangular flake		indetermined		Total	
	n	%	n	%	n	%	n	%	n	%	n	%
Unifacial pointed forms	124	40.9%	56	18.5%	47	15.5%	12	4.0%	64	21.1%	303	100%
Bifacial pieces	35	25.0%	22	15.7%	8	5.7%	1	0.7%	74	52.9%	140	100%
Scraper-like forms	37	53.6%	15	21.7%	12	17.4%	-	0.0%	5	7.2%	69	100%
Denticulates/Notch	20	51.3%	8	20.5%	4	10.3%	1	2.6%	6	15.4%	39	100%
Indet. Fragments	27	34.6%	9	11.5%	13	16.7%	1	1.3%	28	35.9%	78	100%
<b>Total</b>	<b>243</b>	<b>38.6%</b>	<b>110</b>	<b>17.5%</b>	<b>84</b>	<b>13.4%</b>	<b>15</b>	<b>2.4%</b>	<b>177</b>	<b>28.1%</b>	<b>629</b>	<b>100%</b>

**Table 91.** Sibudu. C-A layers from the Deep Sounding: Frequency of cortex percentage per tool types.

Tool type	0%		<20%		>20%		>50%		100%		indetermined		Total	
	n	%	n	%	n	%	n	%	n	%	n	%	n	%
Unifacial pointed forms	251	82.8%	18	5.9%	17	5.6%	7	2.3%	1	0.3%	9	3.0%	303	100%
Bifacial pieces	119	85.0%	6	4.3%	12	8.6%	2	1.4%	-	0.0%	1	0.7%	140	100%
Scraper-like forms	34	49.3%	16	23.2%	12	17.4%	5	7.2%	-	0.0%	2	2.9%	69	100%
Denticulates/Notch	27	69.2%	2	5.1%	7	17.9%	3	7.7%	-	0.0%	-	0.0%	39	100%
Indet. Fragments	65	83.3%	3	3.8%	7	9.0%	1	1.3%	-	0.0%	2	2.6%	78	100%
<b>Total</b>	<b>496</b>	<b>78.9%</b>	<b>45</b>	<b>7.2%</b>	<b>55</b>	<b>8.7%</b>	<b>18</b>	<b>2.9%</b>	<b>1</b>	<b>0.2%</b>	<b>14</b>	<b>2.2%</b>	<b>629</b>	<b>100%</b>

**Table 92.** Sibudu. C-A layers from the Deep Sounding: Frequency of platform type of all completely and proximal preserved tools.

Tool type	plain		cortical		faceted		dihedral		indetermined		Total	
	n	%	n	%	n	%	n	%	n	%	n	%
Unifacial pointed forms	64	58.7%	6	5.5%	19	17.4%	19	17.4%	1	0.9%	109	100%
Bifacial pieces	16	66.7%	2	8.3%	3	12.5%	3	12.5%	-	0.0%	24	100%
Scraper-like forms	27	57.4%	2	4.3%	6	12.8%	12	25.5%	-	0.0%	47	100%
Denticulates/Notch	12	60.0%	1	5.0%	2	10.0%	5	25.0%	-	0.0%	20	100%
<b>Total</b>	<b>119</b>	<b>59.5%</b>	<b>11</b>	<b>5.5%</b>	<b>30</b>	<b>15.0%</b>	<b>39</b>	<b>19.5%</b>	<b>1</b>	<b>0.5%</b>	<b>200</b>	<b>100%</b>

**Table 93.** Sibudu. C-A layers from the Deep Sounding: Frequency of profile per tool types.

Tool type	straight		curved		twisted		indetermined		Total	
	n	%	n	%	n	%	n	%	n	%
Unifacial pointed forms	253	83.5%	30	9.9%	11	3.6%	9	3.0%	303	100%
Bifacial pieces	112	80.0%	22	15.7%	-	0.0%	6	4.3%	140	100%
Scraper-like forms	40	58.0%	19	27.5%	8	11.6%	2	2.9%	69	100%
Denticulates/Notch	30	76.9%	6	15.4%	3	7.7%	-	0.0%	39	100%
<b>Total</b>	<b>435</b>	<b>78.9%</b>	<b>77</b>	<b>14.0%</b>	<b>22</b>	<b>4.0%</b>	<b>17</b>	<b>3.1%</b>	<b>551</b>	<b>100%</b>

**Table 94.** Sibudu. C-A layers from the Deep Sounding: Frequency of cross-section per tool types.

Tool type	triangular		trapezoidal		lenticular		indetermined		Total	
	n	%	n	%	n	%	n	%	n	%
Unifacial pointed forms	141	46.5%	105	34.7%	44	14.5%	13	4.3%	303	100%
Scraper-like forms	26	37.7%	35	50.7%	4	5.8%	4	5.8%	69	100%
Denticulates/Notch	13	33.3%	17	43.6%	2	5.1%	7	17.9%	39	100%
<b>Total</b>	<b>180</b>	<b>43.8%</b>	<b>157</b>	<b>38.2%</b>	<b>50</b>	<b>12.2%</b>	<b>24</b>	<b>5.8%</b>	<b>411</b>	<b>100%</b>

**Table 95.** Sibudu. C-A layers from the Deep Sounding: Frequency of fragmentation per tool types.

Tool type	all		proximal		medial		distal		lateral		lat.-prox.		Lat.-med.		lat.-dist.		Indetermined		Total	
	n	%	n	%	n	%	n	%	n	%	n	%	n	%	n	%	n	%	n	%
Unifacial pointed forms	58	19.1%	63	20.8%	35	11.6%	136	44.9%	-	0.0%	-	0.0%	2	0.7%	-	0.0%	9	3.0%	303	100%
Bifacial pieces	22	15.7%	33	23.6%	26	18.6%	44	31.4%	2	1.4%	2	1.4%	8	5.7%	2	1.4%	1	0.7%	140	100%
Scraper-like forms	15	21.7%	32	46.4%	6	8.7%	13	18.8%	-	0.0%	-	0.0%	1	1.4%	-	0.0%	2	2.9%	69	100%
Denticulates/Notch	4	10.3%	16	41.0%	9	23.1%	3	7.7%	-	0.0%	-	0.0%	7	17.9%	-	0.0%	-	0.0%	39	100%
<b>Total</b>	<b>99</b>	<b>18.0%</b>	<b>144</b>	<b>26.1%</b>	<b>76</b>	<b>13.8%</b>	<b>196</b>	<b>35.6%</b>	<b>2</b>	<b>0.4%</b>	<b>2</b>	<b>0.4%</b>	<b>18</b>	<b>3.3%</b>	<b>2</b>	<b>0.4%</b>	<b>12</b>	<b>2.2%</b>	<b>551</b>	<b>100%</b>

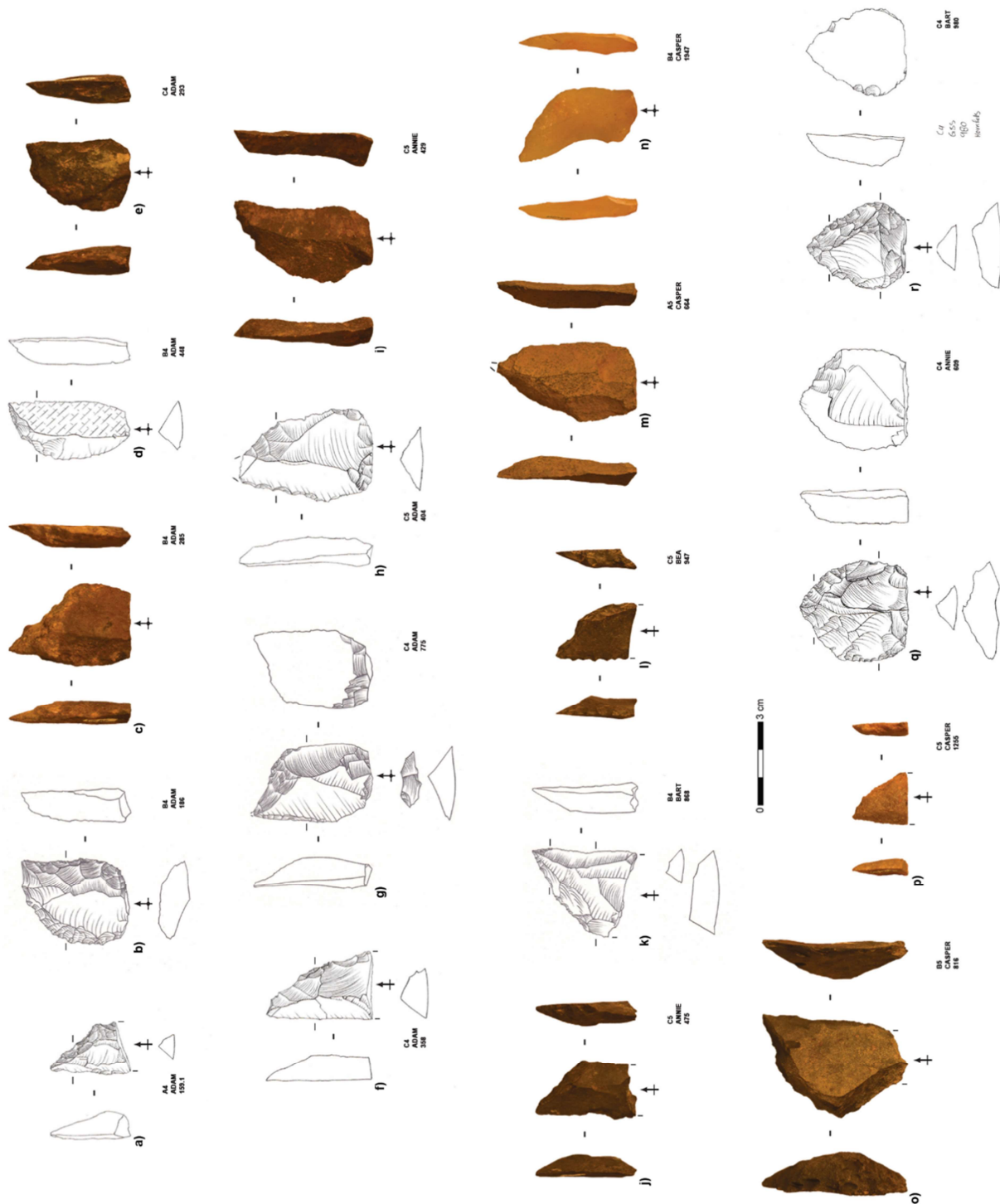
Unifacial points, in general, are defined as triangular or sub-triangular retouched blanks with the distal end pointed through retouch or by primary flaking. The retouch is almost exclusively restricted to one surface, yet a few removals on the other surface and/or thinning of the proximal end can occur. If the tip is not retouched, retouch to shape or regularise the artefact into a pointed form must be present (Volman, 1981: 26). All the specimens concur with this definition. A total of 96.9% of the tools with a preserved tip exhibit a retouched tip. Ventral thinning of the proximal end occurs in 11.6% of the completely or proximally preserved pieces.

The techno-functional study of the typological superordinate category of the unifacial pointed forms allowed me to distinguish separate tool classes that demonstrate diagnostic morphological and morphometric characteristics. First, the greatest percentage of the unifacial pointed forms features symmetrical, bilaterally retouched distal ends both in terms of plan view and angles. Additionally, their tips are trihedral with a regular triangular cross-section (Figure 54).

The medial part is usually convergent, and the base is quadrangular. I refer to this tool class as trihedral symmetric unifacial points (TSPs). Secondly, I identified that another large proportion of the unifacial points exhibits an asymmetric converging distal part, which is typically formed by a steep confected edge and an opposing unretouched edge. The confection expands in most cases to the medial part. The base has a quadrangular shape. I ranked these specimens among the ACTs (Figure 55a-p). These two tool classes will be discussed in more detail in the following section. Thirdly, a few of the unifacial pointed forms conform to the definition of Tongatis (Figure 55q-r), described as having short, bilaterally retouched distal ends in the form of



**Figure 54.** Sibudu. C-A layers from the Deep Sounding: TSPs. TSPs made on dolerite (a, c-e, g-l, k-o, q, s, t, y, z, ab), made on quartzite (b, j, p, r, u-x, aa), and made on quartz (f) (Drawings by Mojdeh Lajmiri; photos by Viola C. Schmid).



**Figure 55.** Sibudu. C-A layers from the Deep Sounding: ACTs (a-p) and Tongatis (q, r). ACTs made on hornfels (a), made on dolerite (b-f, i, j, l, m, o), made on quartzite (g, h, k, p), and made on chert (n); Tongati made on quartzite (q) and Tongati made on hornfels l (Drawings by Mojdeh Lajmiri; photos by Viola C. Schmid).

isosceles triangles. The angle of the point is typically around  $70^\circ$  and remains constant during the life cycle of the tool independent of reduction intensity. The medial part can be either convergent or parallel and exhibits often intense retouch not related to the working edge, but rather to the intermediate or prehensile part. The bases are primarily trapezoidal (Conard, et al., 2012). Finally, some of the unifacial pointed forms fulfil the general criteria of unifacial points. However, further classification was hindered by the fragmentation of many of these

pieces and the insufficiently clear manifestation of techno-functional features of some elements.

Overall, I note at this point that this techno-functional classification underpins diagnostic patterns observed within a broad typological category but is limited by a certain degree of overlap associated with blank selection, advancement of reduction cycle or state of fragmentation.

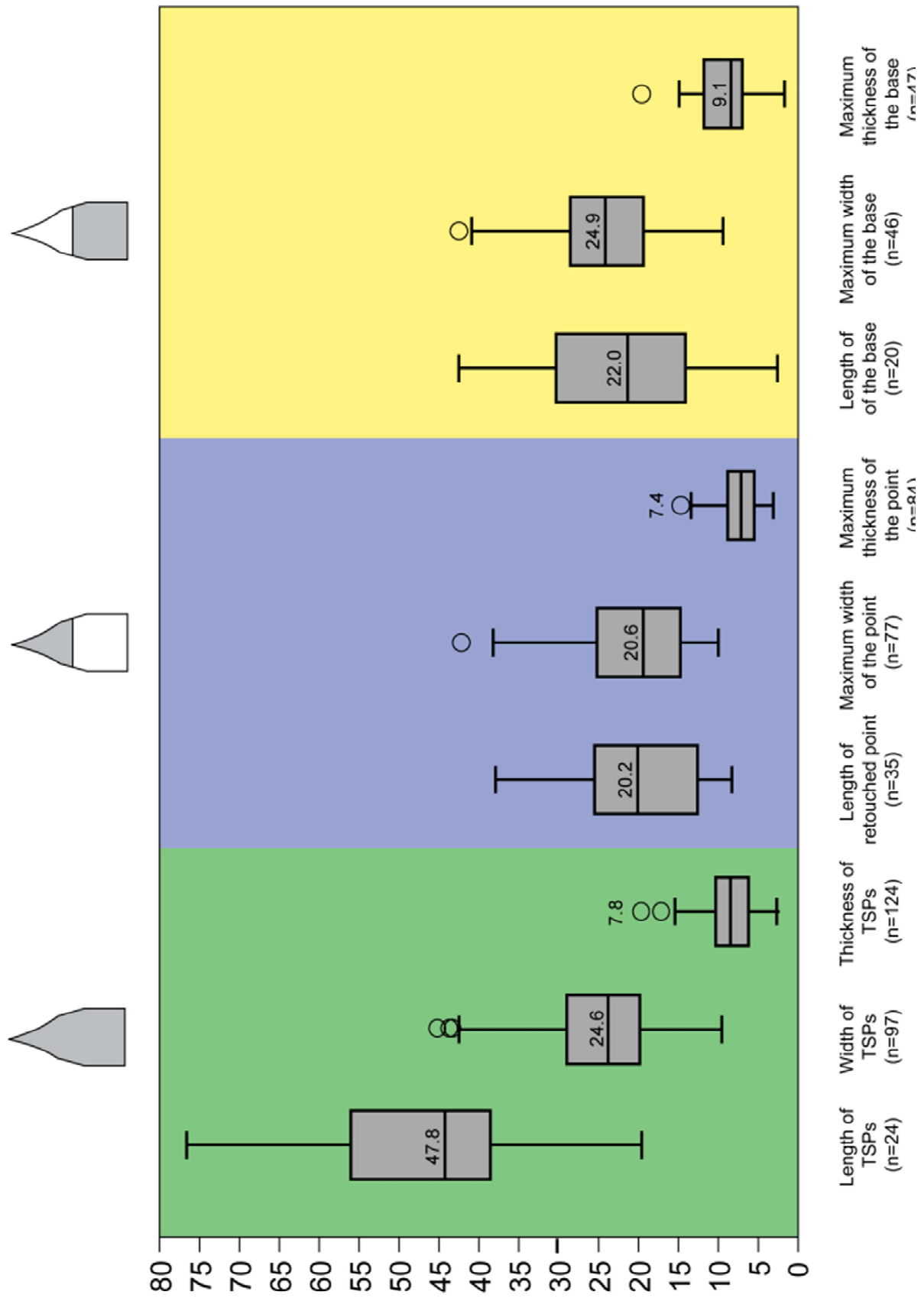
#### 5.6.1.1. TSPs

The TSPs are defined as tools with an active distal part which is thinned down by bilateral, unifacial retouch maintaining a triangular tip cross-section, as well as in terms of width and thickness, and a shape that acutely converges to a pointed end often created by two slightly curvilinear edges. The assemblage contains a total of 124 TSPs (Figure 54). TSPs occur throughout the sequence, reaching a peak at 31.8% in the layer Chantal and a low point the layer below, Bart, at 14.5% (Table 83).

Most of the TSPs (66.1%) are made on dolerite (Table 96) – mainly the medium-grained variety – followed by quartzite at 26.6%. The tools demonstrate a mean length of 47.8 mm, a mean width of 24.6 mm and a mean thickness of 7.8 mm (Figure 56). The length distribution ranges from 19.6 mm to 76.6 mm. This dimensional variability could be related to the intensity of tool reduction and/or to the blank selection for the manufacturing of TSPs. The mean debitage laminarity is 1.9 and, fittingly, the majority of selected blanks is blades and elongated flakes (Table 97). The length and thickness values of the TSPs do not significantly differ from the values of the blade population, but the TSPs are significantly wider than the unretouched blades (*t*-test, *t* = -3.1337; *p* = 0.0017528). As mentioned above for unifacial pointed forms in general,

**Table 96.** Sibudu. C-A layers from the Deep Sounding: Frequency of raw material per tool classes.

Tool class	Dolerite		Hornfels		Quartz		Quartzite		Sandstone		Chert		Indetermined		Total	
	n	%	n	%	n	%	n	%	n	%	n	%	n	%	n	%
TSPs	82	66.1%	5	4.0%	4	3.2%	33	26.6%	-	0.0%	-	0.0%	-	0.0%	124	100%
ACTs	86	81.9%	3	2.9%	-	0.0%	14	13.3%	-	0.0%	2	1.9%	-	0.0%	105	100%
Tongatis	6	46.2%	1	7.7%	1	7.7%	5	38.5%	-	0.0%	-	0.0%	-	0.0%	13	100%
Unifacial Points	43	70.5%	2	3.3%	1	1.6%	14	23.0%	-	0.0%	-	0.0%	1	1.6%	61	100%
Bifacial Points	39	35.5%	5	4.5%	41	37.3%	21	19.1%	1	0.9%	3	2.7%	-	0.0%	110	100%
Bifacially Backed Knives	2	40.0%	-	0.0%	1	20.0%	2	40.0%	-	0.0%	-	0.0%	-	0.0%	5	100%
Serrated Pieces	15	60.0%	2	8.0%	7	28.0%	1	4.0%	-	0.0%	-	0.0%	-	0.0%	25	100%
Lateral Scrapers	33	86.8%	1	2.6%	-	0.0%	4	10.5%	-	0.0%	-	0.0%	-	0.0%	38	100%
NBTs	19	73.1%	1	3.8%	1	3.8%	5	19.2%	-	0.0%	-	0.0%	-	0.0%	26	100%
End-scrapers	4	80.0%	-	0.0%	-	0.0%	1	20.0%	-	0.0%	-	0.0%	-	0.0%	5	100%
Denticulates/Notch	29	74.4%	2	5.1%	2	5.1%	5	12.8%	-	0.0%	1	2.6%	-	0.0%	39	100%
Indet. Fragments	53	67.9%	9	11.5%	4	5.1%	12	15.4%	-	0.0%	-	0.0%	-	0.0%	78	100%
<b>Total</b>	<b>411</b>	<b>65.3%</b>	<b>31</b>	<b>4.9%</b>	<b>62</b>	<b>9.9%</b>	<b>117</b>	<b>18.6%</b>	<b>1</b>	<b>0.2%</b>	<b>6</b>	<b>1.0%</b>	<b>1</b>	<b>0.2%</b>	<b>629</b>	<b>100%</b>



**Figure 56.** Sibudu. C-A layers from the Deep Sounding: Boxplot showing morphometric characteristics of the TSPs.

**Table 97.** Sibudu. C-A layers from the Deep Sounding: Frequency of blank type per tool classes.

Tool class	blade		laminar flake		flake		triangular flake		indetermined		Total	
	n	%	n	%	n	%	n	%	n	%	n	%
TSPs	61	49.2%	13	10.5%	11	8.9%	6	4.8%	33	26.6%	124	100%
ACTs	30	28.6%	30	28.6%	18	17.1%	1	1.0%	26	24.8%	105	100%
Tongatis	-	0.0%	3	23.1%	10	76.9%	-	0.0%	-	0.0%	13	100%
Unifacial Points	33	54.1%	10	16.4%	8	13.1%	5	8.2%	5	8.2%	61	100%
Bifacial Points	22	20.0%	15	13.6%	6	5.5%	-	0.0%	67	60.9%	110	100%
Bifacially Backed Knives	1	20.0%	1	20.0%	-	0.0%	-	0.0%	3	60.0%	5	100%
Serrated Pieces	12	48.0%	5	20.0%	2	8.0%	1	4.0%	5	20.0%	25	100%
Lateral Scrapers	28	73.7%	8	21.1%	2	5.3%	-	0.0%	-	0.0%	38	100%
NBTs	9	34.6%	6	23.1%	7	26.9%	-	0.0%	4	15.4%	26	100%
End-scrapers	-	0.0%	1	20.0%	3	60.0%	-	0.0%	1	20.0%	5	100%
Denticulates/Notch	20	51.3%	8	20.5%	4	10.3%	1	2.6%	6	15.4%	39	100%
Indet. Fragments	27	34.6%	9	11.5%	13	16.7%	1	1.3%	28	35.9%	78	100%
<b>Total</b>	<b>243</b>	<b>38.6%</b>	<b>109</b>	<b>17.3%</b>	<b>84</b>	<b>13.4%</b>	<b>15</b>	<b>2.4%</b>	<b>178</b>	<b>28.3%</b>	<b>629</b>	<b>100%</b>

**Table 98.** Sibudu. C-A layers from the Deep Sounding: Descriptive statistics of EPA of all completely and proximal preserved unifacial pointed forms by tool class.

	TSPs	ACTs	Tongatis	Unifacial Points
n	36	36	9	27
Min	62	75	79	74
Max	88	93	88	90
Sum	2,920	3,089	755	2,247
Mean	81.1	83.5	83.9	83.2
Std. error	0.9	0.6	1.1	0.7
Variance	32	15.2	10.1	15.2
Stand. dev.	5.7	3.9	3.2	3.9
Median	82	84	84	84
25 prcntil	79.3	80	81	80
75 prcntil	85	86	87	86

this implies that knappers chose rather wider and probably longer original laminar products to modify them into TSPs and both manufacture and re-shaping affected the width and length of these tools. The EPA averages 81° and the platform depth 8.2mm (Table 98 & Table 99). The high platform depth value points *de novo* to the selection of larger blanks, as this variable plays a major role in determining blank size (Dibble and Rezek, 2009). The selected pieces primarily involve products from the main production phase, as 90.3% of the blanks exhibit no dorsal cortex coverage and only one first blank is present. Two of the blades represent core edge blanks (*débordants*). A number of 36 of the TSPs have a platform preserved (Table 100). The majority exhibits plain platforms, but 13.9% of the platforms are faceted and further 11.1% are dihedral. Thus, the blanks of this tool class demonstrate a



higher investment in the preparation of the butt than the unretouched blanks, as already stated for the unifacial pointed forms in general. A total of 49.6% of the blanks have a triangular cross-section and 29.3% a trapezoidal cross-section. Past people preferentially selected blanks with a straight profile to manufacture TSPs, at 87.9%. Only 20.2% of the TSPs are completely preserved (Table 101). The greatest proportion of this tool class is present as tip fragments. The fractures imply that some of the points broke during production or reworking, but future use-wear studies have to confirm this.

**Table 99.** Sibudu. C-A layers from the Deep Sounding: Descriptive statistics of platform depth of all completely and proximal preserved unifacial pointed forms by tool class.

	TSPs	ACTs	Tongatis	Unifacial Points
n	33	36	9	24
Min	1.7	2.3	5	3.4
Max	14.6	11.2	18.2	17.4
Sum	270.6	264.8	95.5	178.9
Mean	8.2	7.4	10.6	7.5
Std. error	0.6	0.4	1.5	0.8
Variance	11.1	4.6	19.8	13.6
Stand. dev.	3.3	2.2	4.5	3.7
Median	8	7.4	11.3	6.3
25 prcntil	5.3	6.5	6.4	4.9
75 prcntil	10.8	9	13.9	9.2

**Table 100.** Sibudu. C-A layers from the Deep Sounding: Frequency of platform type per tool classes.

Tool class	plain		cortical		faceted		dihedral		indetermined		Total	
	n	%	n	%	n	%	n	%	n	%	n	%
TSPs	27	75.0%	-	0.0%	5	13.9%	4	11.1%	-	0.0%	36	100%
ACTs	19	51.4%	1	2.7%	8	21.6%	9	24.3%	-	0.0%	37	100%
Tongatis	4	44.4%	3	33.3%	-	0.0%	2	22.2%	-	0.0%	9	100%
Unifacial Points	14	51.9%	2	7.4%	6	22.2%	4	14.8%	1	3.7%	27	100%
Bifacial Points	9	47.4%	2	10.5%	-	0.0%	3	15.8%	5	26.3%	19	100%
Bifacially Backed Knives	2	66.6%	-	0.0%	-	0.0%	-	0.0%	1	33.3%	3	100%
Serrated Pieces	4	36.4%	-	0.0%	3	27.3%	-	0.0%	4	36.4%	11	100%
Lateral Scrapers	14	50.0%	1	3.6%	5	17.9%	8	28.6%	-	0.0%	28	100%
NBTs	10	62.5%	1	6.3%	1	6.3%	4	25.0%	-	0.0%	16	100%
End-scrapers	3	100.0%	-	0.0%	-	0.0%	-	0.0%	-	0.0%	3	100%
Denticulates/Notch	12	60.0%	1	5.0%	2	10.0%	5	25.0%	-	0.0%	20	100%
<b>Total</b>	<b>118</b>	<b>56.5%</b>	<b>11</b>	<b>5.3%</b>	<b>30</b>	<b>14.4%</b>	<b>39</b>	<b>18.7%</b>	<b>11</b>	<b>5.3%</b>	<b>209</b>	<b>100%</b>

With regard to the morphotype of TSPs, they ordinarily have a symmetrical plan view and symmetrical confected edge angles on both edges, i.e. the angles are within a range of 10° (Figure 57). The point lies generally on the percussion axis of the blank. Toolmakers installed the point of the TSPs predominantly on the distal part of the blanks. Only one TSP shows the active part on the proximal end of the blank.

The angle of the point is, for all measurable specimens (n=80), acute and predominantly ranges between 60° and 80° (Figure 58a). The point is primarily formed by bilateral retouch, at 88.7% (Figure 58b). In general, the retouch on both edges of the point is direct, but 3.9% of the TSP exhibit bifacial retouch, 2% alternate retouch, and 1% bilaterally inverse retouch. The length of the point averages 20.2 mm and is bracketed between 8.3 mm and 37.9 mm (Figure 56). The variability is probably associated with the dimensions of the original blanks and the intensity or rather extension of point reduction. The dimension distribution (Figure 58c) is continuous suggesting the existence of one single population. However, considering that both the length and the width of the TSPs determine the perforating depth and the extension of the contact zone, I suggest that this does not exclude the presence of several distinct functional populations within the sample.

The intermediate part of this tool class is prevalingly convergent (Figure 57). The greatest proportion of the TSPs was modified on both edges (61%), and a further 21% show lateral retouch on one edge. The characteristics of the retouch vary in the angle, section, length, and invasiveness. However, the majority shows rather invasive retouch, indicating that several phases of re-shaping occurred. These phases of re-shaping involved the reworking of the active part and/or the extension of the point of the TSPs. Furthermore, the intense retouch often led to the convergent shape of the lateral edges.

**Table 101.** Sibudu. C-A layers from the Deep Sounding: Frequency of fragmentation per tool classes.

Tool class	all		proximal		medial		distal		lateral		lateral-proximal		lateral-medial		lateral-distal		indetermined		Total			
	n	%	n	%	n	%	n	%	n	%	n	%	n	%	n	%	n	%	n	%		
TSPs	25	20.2%	19	15.3%	11	8.9%	68	54.8%	-	0.0%	-	0.0%	1	0.8%	-	0.0%	-	0.0%	-	0.0%	124	100%
ACTs	20	19.0%	20	19.0%	13	12.4%	52	49.5%	-	0.0%	-	0.0%	-	0.0%	-	0.0%	-	0.0%	-	0.0%	105	100%
Tongatis	9	69.2%	1	7.7%	-	0.0%	3	23.1%	-	0.0%	-	0.0%	-	0.0%	-	0.0%	-	0.0%	-	0.0%	13	100%
Unifacial Points	4	6.6%	23	37.7%	11	18.0%	13	21.3%	-	0.0%	-	0.0%	1	1.6%	-	0.0%	9	14.8%	-	0.0%	61	100%
Bifacial Points	12	10.9%	27	24.5%	21	19.1%	36	32.7%	2	1.8%	2	1.8%	7	6.4%	2	1.8%	1	0.9%	-	0.0%	110	100%
Bifacially Backed Knives	3	60.0%	1	20.0%	-	0.0%	1	20.0%	-	0.0%	-	0.0%	-	0.0%	-	0.0%	-	0.0%	-	0.0%	5	100%
Serrated Pieces	7	28.0%	5	20.0%	5	20.0%	7	28.0%	-	0.0%	-	0.0%	1	4.0%	-	0.0%	-	0.0%	-	0.0%	25	100%
Lateral Scrapers	6	15.8%	22	57.9%	4	10.5%	3	7.9%	-	0.0%	-	0.0%	1	2.6%	-	0.0%	2	5.3%	-	0.0%	38	100%
NBTs	6	23.1%	10	38.5%	2	7.7%	8	30.8%	-	0.0%	-	0.0%	-	0.0%	-	0.0%	-	0.0%	-	0.0%	26	100%
End-scrapers	3	60.0%	-	0.0%	-	0.0%	2	40.0%	-	0.0%	-	0.0%	-	0.0%	-	0.0%	-	0.0%	-	0.0%	5	100%
Denticulates/Notch	4	10.3%	16	41.0%	9	23.1%	3	7.7%	-	0.0%	-	0.0%	7	17.9%	-	0.0%	-	0.0%	-	0.0%	39	100%
<b>Total</b>	<b>99</b>	<b>18.0%</b>	<b>144</b>	<b>26.1%</b>	<b>76</b>	<b>13.8%</b>	<b>196</b>	<b>35.6%</b>	<b>2</b>	<b>0.4%</b>	<b>2</b>	<b>0.4%</b>	<b>18</b>	<b>3.3%</b>	<b>2</b>	<b>0.4%</b>	<b>12</b>	<b>2.2%</b>	<b>551</b>	<b>100%</b>		

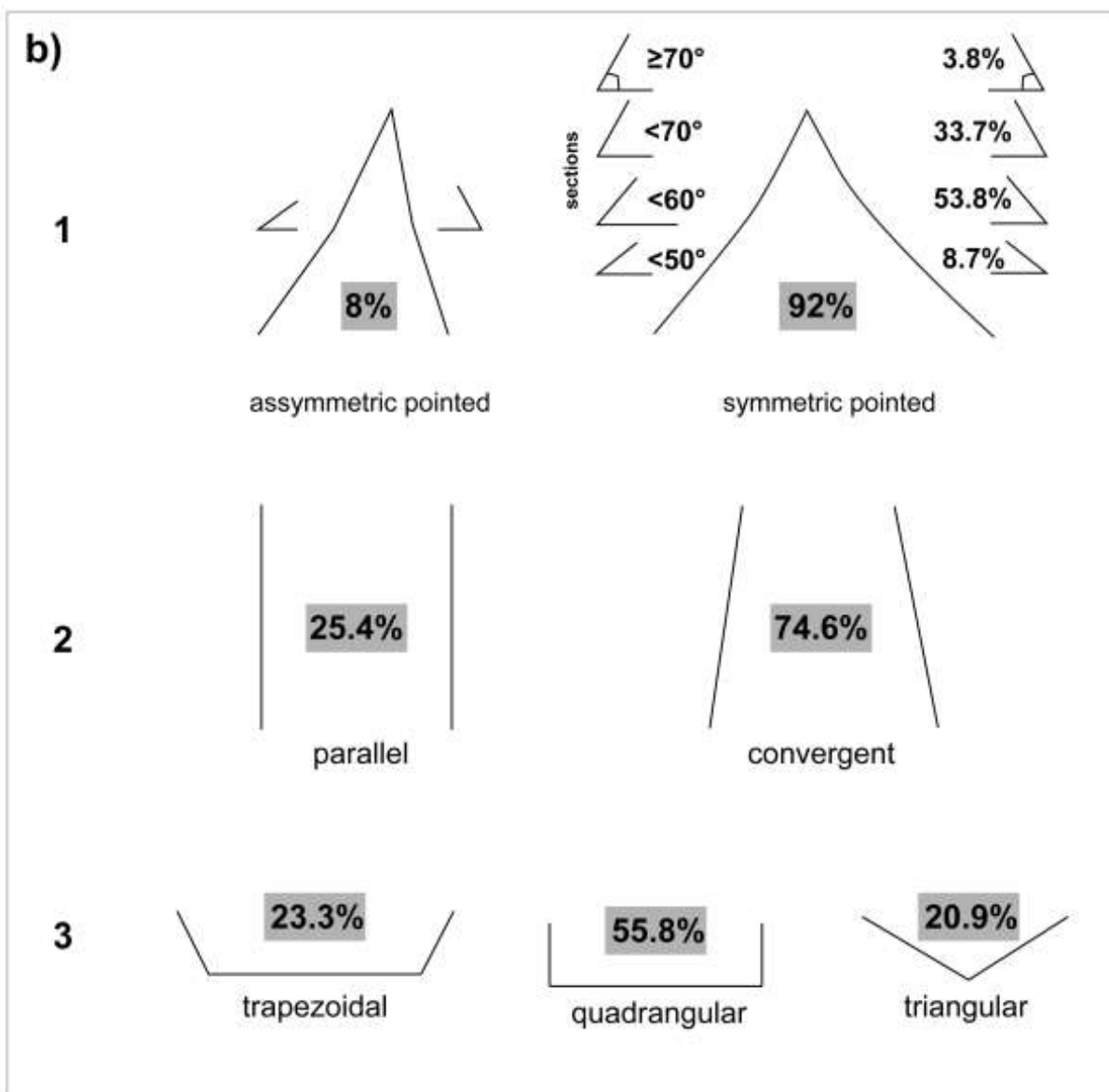
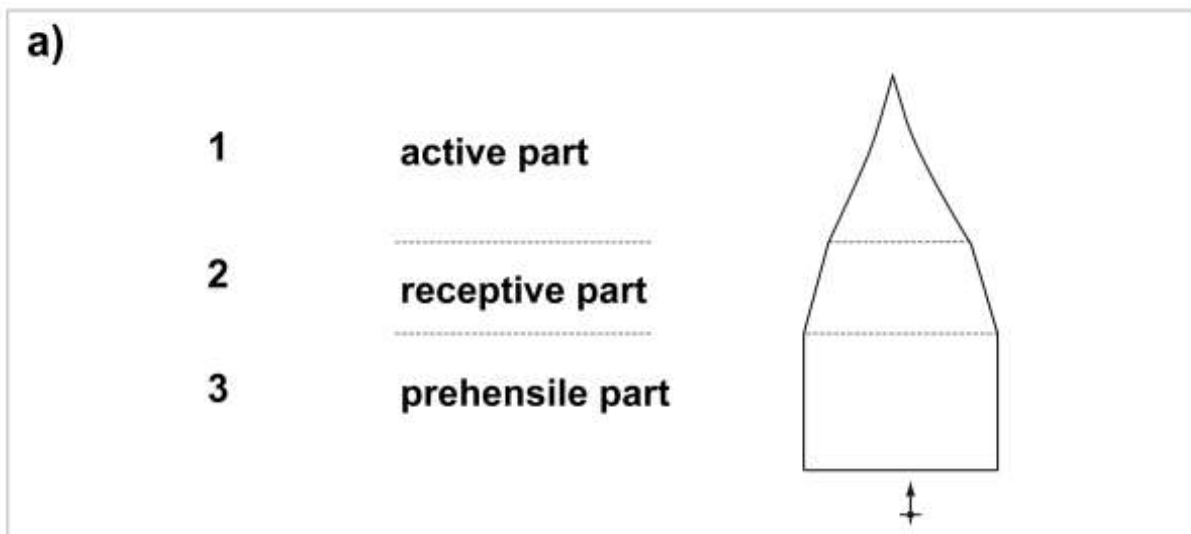
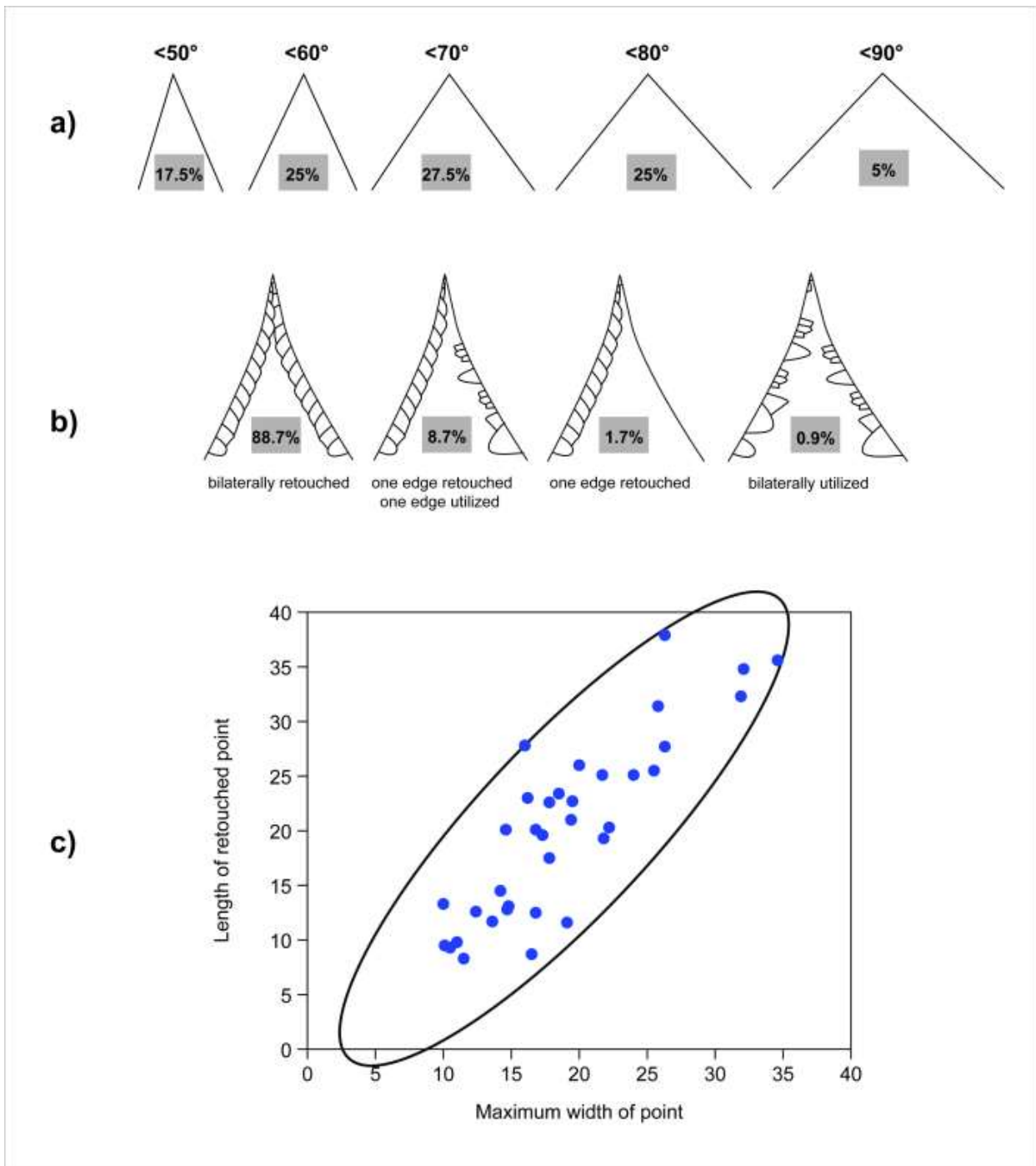
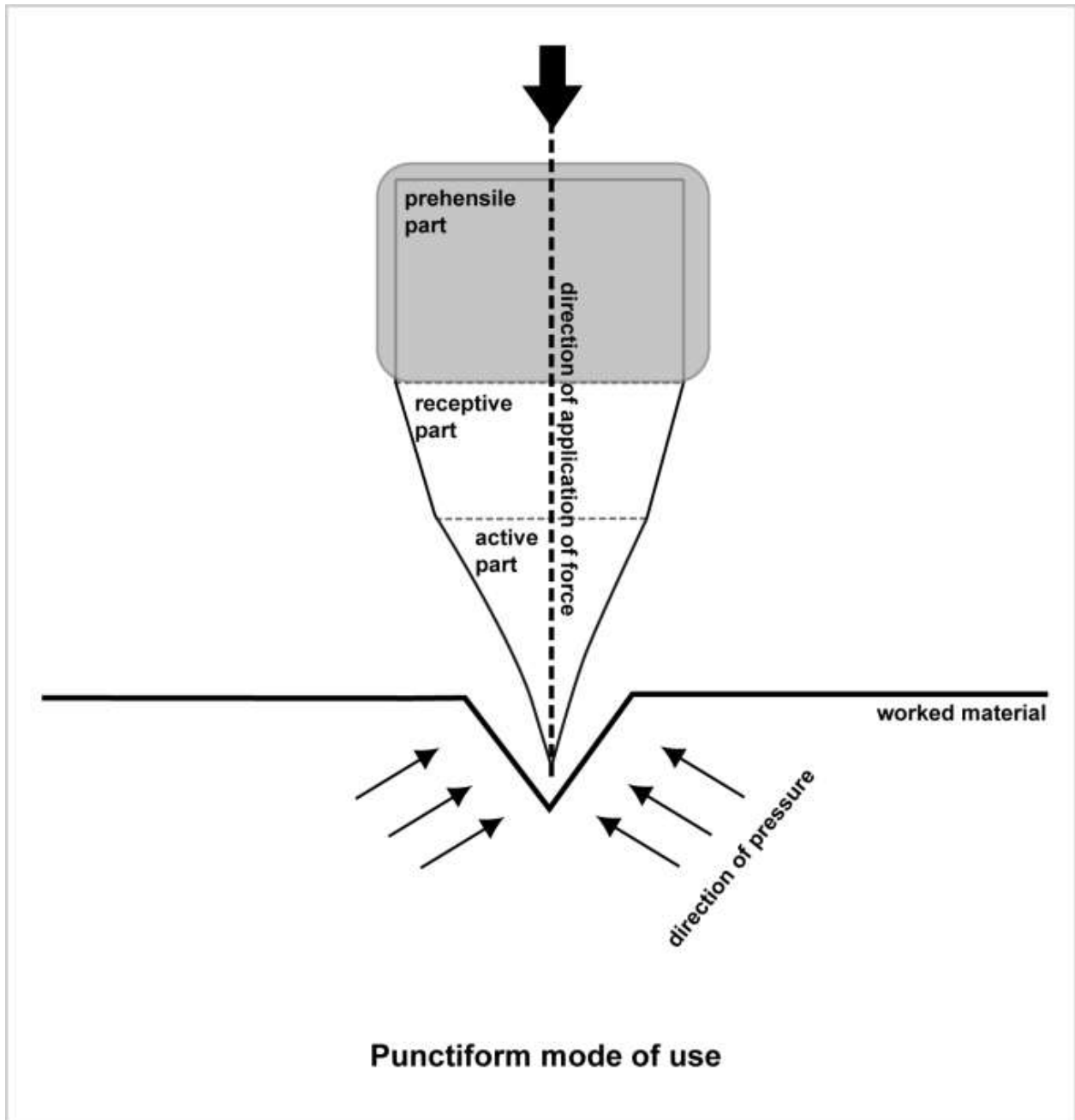


Figure 57. Sibudu. C-A layers from the Deep Sounding: TSP morphotype.

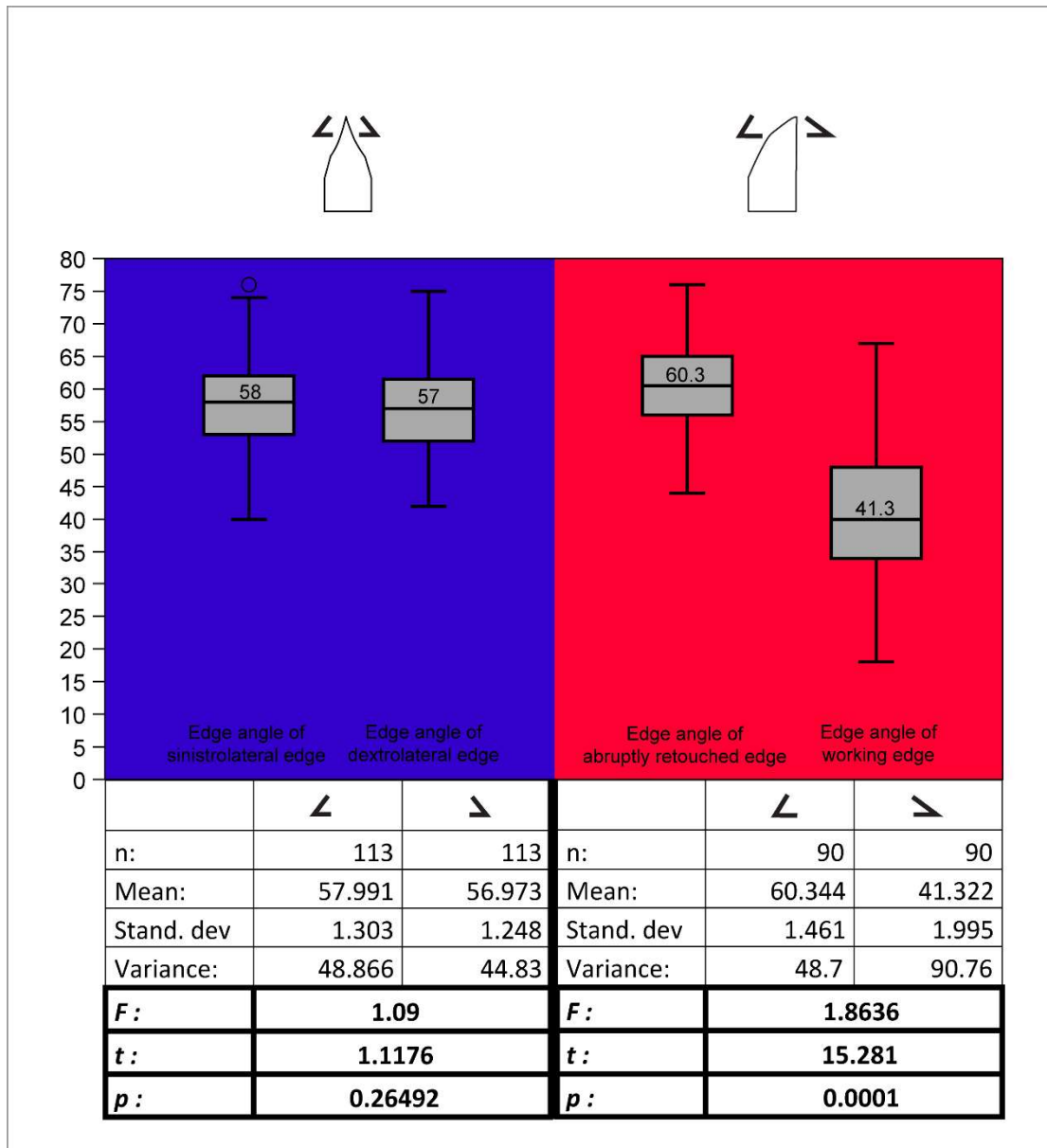


**Figure 58.** Sibudu. C-A layers from the Deep Sounding: Morphological and morphometric features of the active part of TSPs.

The bases of the TSPs with a preserved proximal end (n=43) typically have a quadrangular shape (Figure 57). A total of 20.9% of the bases demonstrate a modified basal end, mainly in the form of ventral thinning. A proportion of 34.9% of the TSPs was retouched on one basal lateral margin. The modifications involve either retouch or the detachment of one or more large removals from the ventral face. The retouch most likely concerns the correction of the delineation of the basal margins, while the large removals on the ventral face rather served to thin the proximal part of the tools.



**Figure 59.** Sibudu. C-A layers from the Deep Sounding: Techno-functional and functional characterisation of the TSPs (modified after Tringham, et al., 1974: Figure 20).

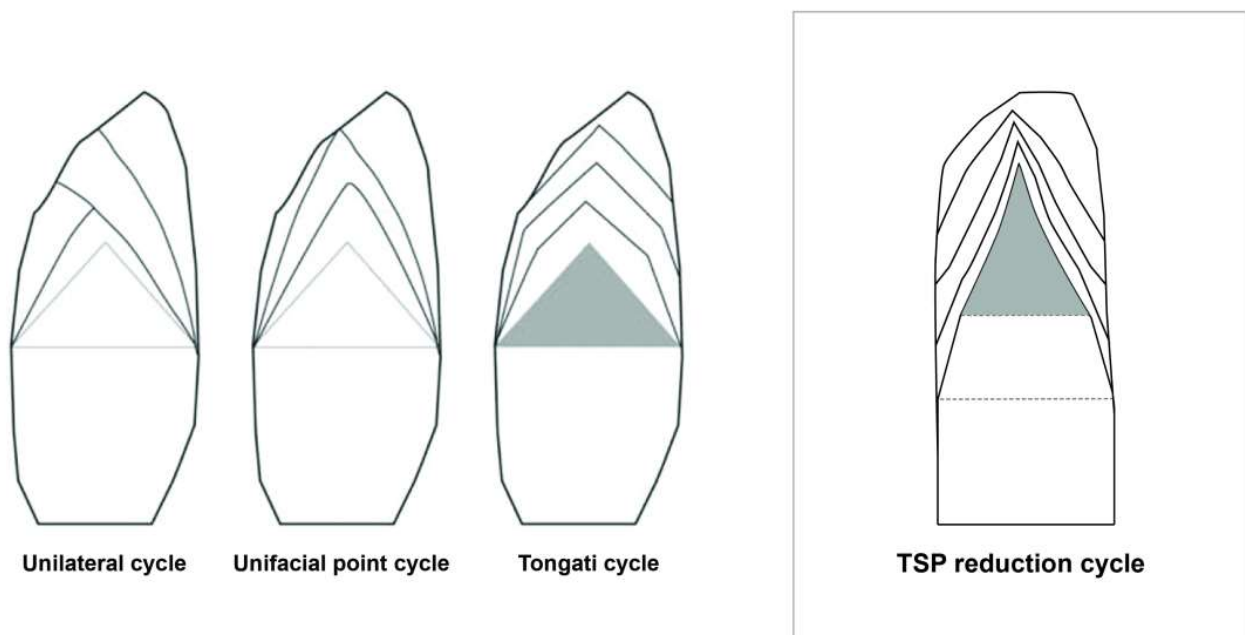


**Figure 60.** Sibudu. C-A layers from the Deep Sounding: Boxplot showing edge angles of both edges of the TSPs and ACTs.

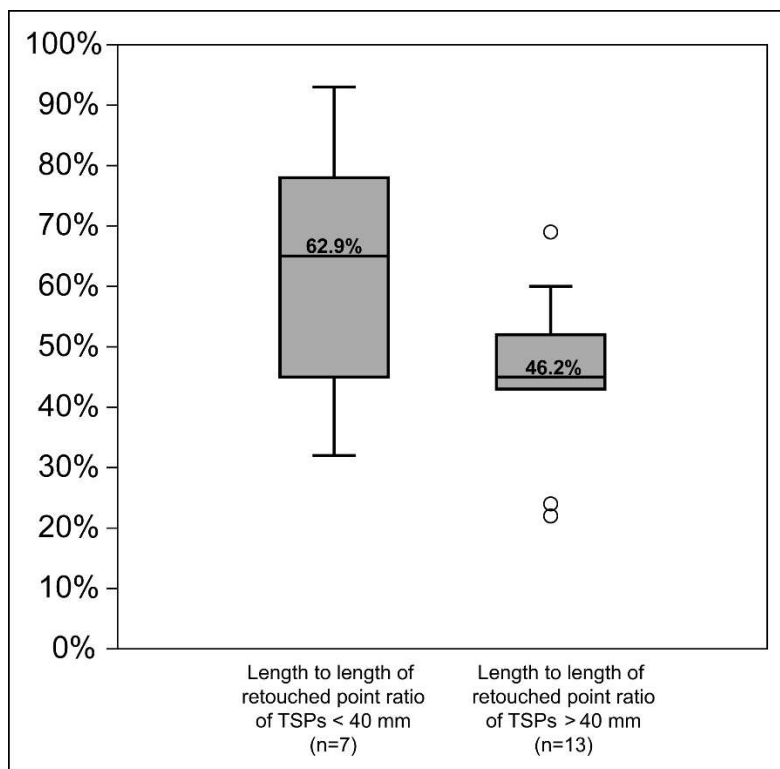
Regarding the functional features of the tool, the position and morphology of the active part and the passive zones give the first information (Soressi, 2002). The two bilaterally symmetric, converging edges form a trihedral tip and the prehensile part has a position that enables a grip perpendicular to the axis of symmetry of the point. On a macroscopic scale, I observed unintentional macro and micro removals on 33.3% of the tips, while I documented functional traces on 58.1% of the laterals of the point. The unintentional removals on the tip are located on the ventral face in 48.4% of instances, 45.2% are on the dorsal face and 6.5% are dorso-ventral. Thus, I deduced a punctiform mode of use for the TSPs (Figure 59), involving perforating, drilling, piercing or ‘burining’ (Leroi-Gourhan, 1943). These actions refer to tool use on a highly localised contact point/zone of the worked material, holding the tool at 70° to 90° to the worked material. The edge damage occurs mainly on the edges of the point rather than the tip of contact itself (Tringham, et al., 1974). However, a point can occasionally be used in a

linear mode, corresponding to scraping, slicing, or cutting. The edge angle of both laterals of the point are clearly symmetric. The edge angle of the sinistrolateral edges averages  $58^\circ$  and dextralateral edge averages  $57^\circ$  (Figure 60), meaning that the tools could be used for both directions of cutting, i.e. *coupe rentrante* and *coupe sortante*.

The examined sample of TSPs from the lowermost layers of Sibudu includes specimens reflecting different stages of the life history that this tool class undergoes. I propose here a model of the cycle of reduction for TSPs (Figure 61). In the initial stage, the tools have a small, short active part, namely the point, compared to the relatively long intermediate part. As the reduction cycle progresses, the artefacts are more heavily affected by retouch. This leads to a reduction of the receptive portion and an increase of the transformative part. Twenty TSPs have both a measurable total length and length of the retouched point. The seven pieces smaller than 40 mm show a higher total length-to-length of retouched point ratio than the pieces larger than 40 mm (Figure 62), attesting to an expansion of the active part. The length of the blank of the TSPs seems to be not so strongly reduced by the re-shaping. However, the knappers applied intense reduction of the width to configure an extension of the transformational working edge, particularly its tip cross-section involving its width and thickness. Thus, the maximum width of the point decreases and the edges of the point are slightly curved. Additionally, the originally more parallel intermediate part evolves towards a convergent morphology. Finally, the toolmakers tried to retain the axis and bilateral symmetry of the point.



**Figure 61.** Sibudu. C-A layers from the Deep Sounding: Schematic model of reduction for the TSP cycle in comparison with reduction cycles of other unifacial pointed forms (modified after Conard, et al., 2012: Figure 8).



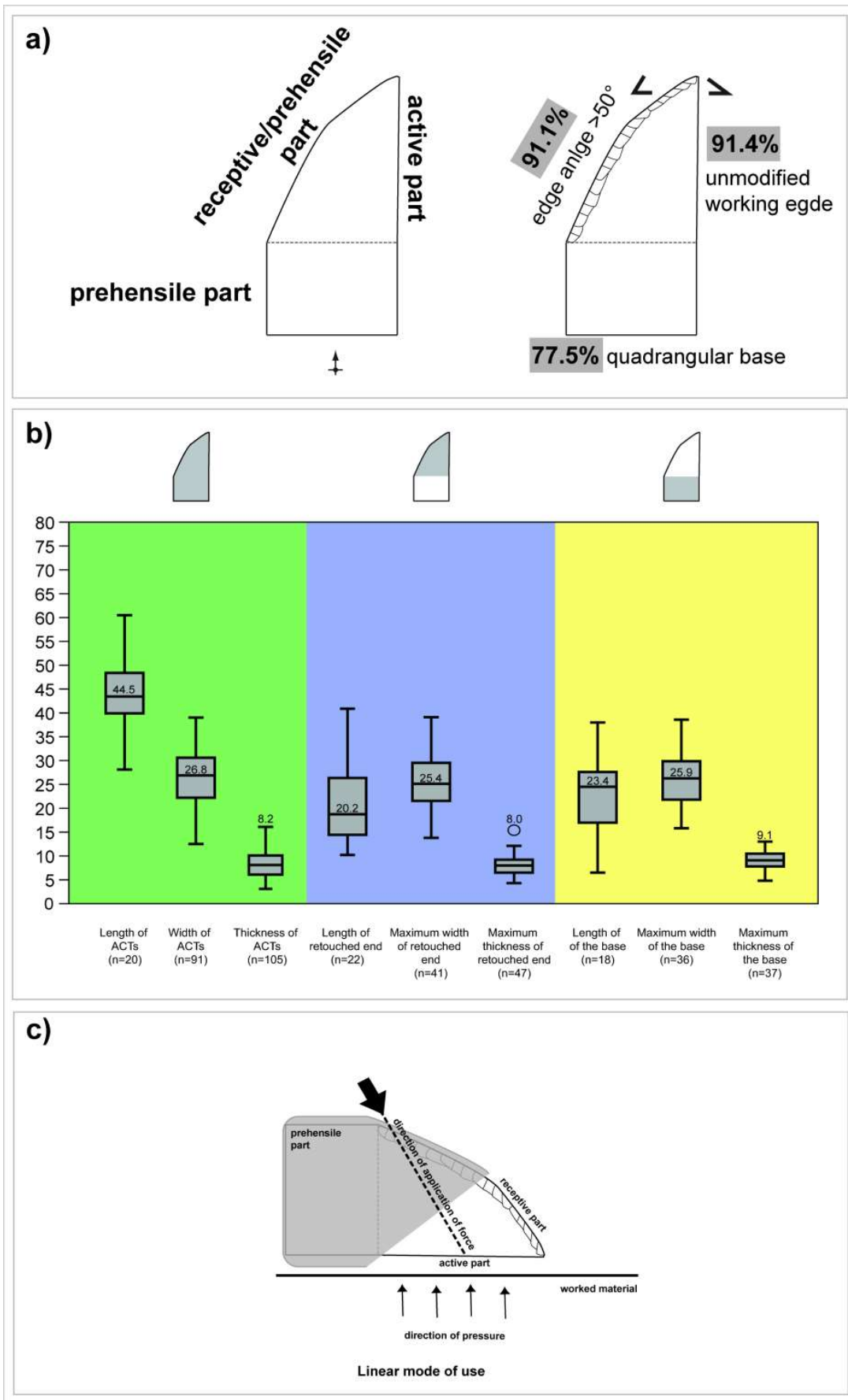
**Figure 62.** Sibudu. C-A layers from the Deep Sounding: Boxplot showing length-to-length of retouched point ratio of TSPs <40 mm and >40 mm.

### 5.6.1.2. ACTs

Asymmetric convergent tools are defined as tools with an asymmetric convergent distal part, which is formed by a convex confected edge and an opposing straight, typically unretouched working edge. The assemblage yielded 105 ACTs (Figure 55a-p & Table 83). All layers comprise ACTs, but the uppermost layer Adam yielded the highest frequency at 24.2% and layer Casper the lowest frequency at 12.4% (Table 83).

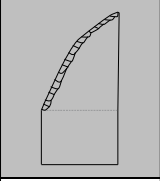
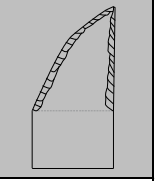
The majority of ACTs (81.9%) is made on dolerite (Table 96), mainly the medium-grained variety (75.6%). The length of these tools ranges between 28.1 mm and 60.5 mm with a mean value of 44.5 mm (Figure 63b). The width averages 26.8 mm and the thickness 8.2 mm (Figure 63b). The blank selection involved predominantly laminar products. Blades and elongated flakes both amount to 28.6% of blanks (Table 97) and the debitage laminarity is at 1.6. Blank selection most likely favoured elongated pieces, which were then reduced in length owing to the installation of the steeply retouched edges. The ACTs show similarities in width and thickness to the corpus of unretouched elongated flakes, but they are longer. The mean EPA is 83.5° (Table 98) and the mean platform depth is 7.4 mm (Table 99), both greater than the mean values of elongated flakes, indicating again the selection of larger elongated blanks. The original blanks of the ACTs come from different stages of the reduction sequence and demonstrate various morphological features. Twenty tools have remnant cortex on their dorsal face, of which a proportion of 57.9% displays more than 20% dorsal cortex coverage. A large proportion of the ACTs that retains the proximal part of the original blank preserved (n=37) exhibits a dihedral platform (24.3%) and





**Figure 63.** Sibudu. C-A layers from the Deep Sounding: a) ACT morphotype; b) boxplot showing morphometric characteristics of the ACTs; c) techno-functional and functional characterisation of the ACTs.

**Table 102.** Sibudu. C-A layers from the Deep Sounding: Descriptive statistics of edge angle of ACTs with unretouched and re-sharpened working edge.

		
n	80	10
Min	18	35
Max	60	67
Sum	3,205	514
Mean	40.1	51.4
Std. error	1	3.4
Variance	74.8	113.8
Stand. dev.	8.6	10.7
Median	39.5	53
25 prcntil	34	40
75 prcntil	46	60.3

21.6% of pieces have a faceted platform (Table 100). A total of 49.5% of the elements of this tool class show a triangular cross-section and 37.1% a trapezoidal cross-section. Past people predominantly manufactured ACTs on blanks with a straight profile at 88.6%. A low percentage of 19% of ACTs are completely preserved (Table 101).

The ACTs are typically asymmetric in plan view, hence their name (Figure 63a). Their modified distal parts are not aligned with the axis of percussion of the blank. The knappers applied modifications to the distal ends of the original blanks to manufacture ACTs, with the exception of one tool where the confection occurred on the proximal end. All specimens show direct retouch. The toolmakers seem to have had no preference for which lateral to install the abrupt convex edge, as I observed that 54.4% of the ACTs demonstrate a modification on the sinistrolateral edge and 45.6% of the ACTs on the dextralateral edge. Ten of the tools exhibit retouch on both edges, i.e. they attest to an abrupt confection and re-sharpening of the working edge. Correspondingly, the edge angles of the re-sharpened edges are more obtuse than the unretouched edges (Table 102). The length of the steeply retouched distal ends ranges from 10.2 mm to 40.9 mm with a mean value of 20.2 mm (Figure 63b). The confection of 81.1% of the tools expands from the distal end to the medial part of the blank. A total of 10% of the tools have unintentional macro and micro traces on the medial part of the blank following the retouched distal edge and a further 3.3% of the pieces exhibit a natural back as continuation of this modification. A high frequency of ACTs (83.7%) retain a medial part which is formed by one converging edge due to the modification and an opposite rectilinear edge. Furthermore, convergent edges occur on 8.7% of ACTs and parallel edges on 7.7%. Regarding the base preserved on 40 ACTs, a proportion of 77.5% has quadrangular shaped bases followed by 17.5% with a trapezoidal shape. Only two pieces attest to basal thinning. Three ACTs show a continuation of the confection from the distal end to the basal lateral margin. Seven further

pieces involve a natural back on one of the lateral basal edges. Three of the natural backs represent a continuation of the confection and two are the extension of the natural back from the medial part, while two further natural backs are located on the basal margin following the working edge. On eleven ACTs, macro or micro removals occur on the basal laterals following the abruptly retouched edge. The basal margin succeeding the working edge of 14 tools bears functional traces.

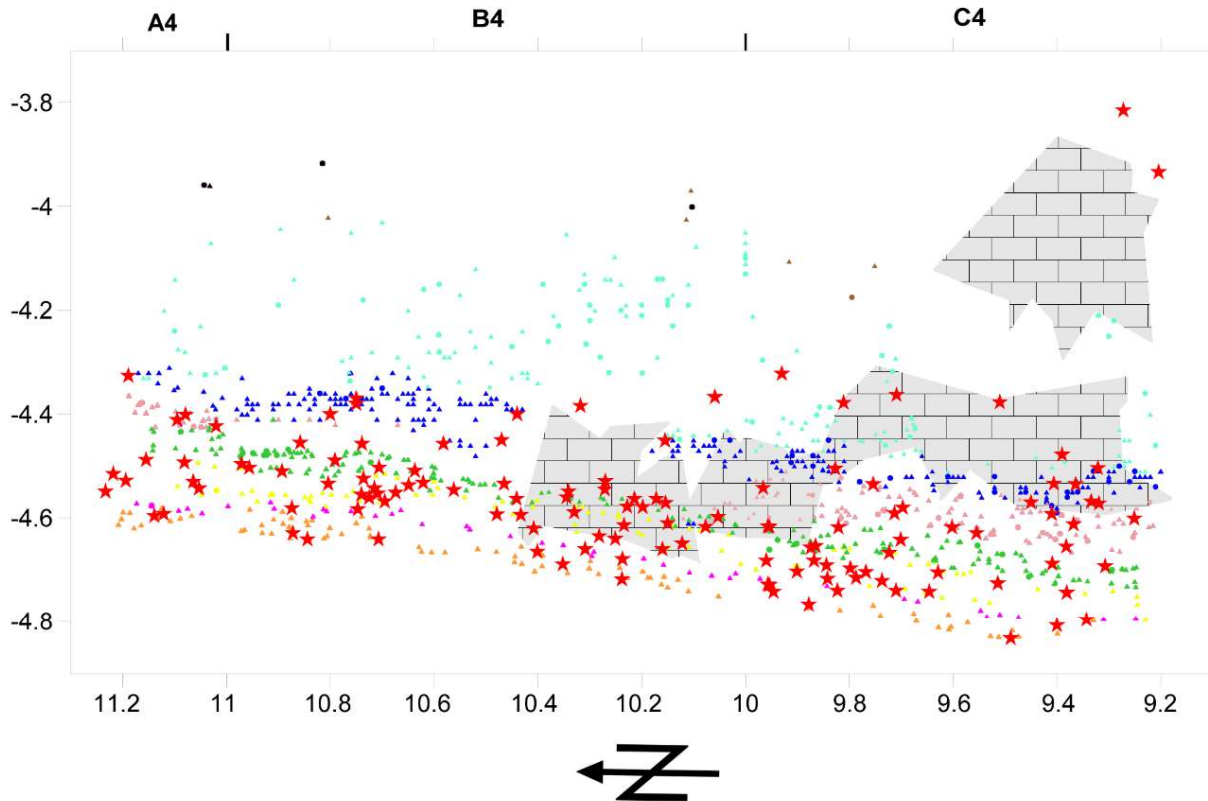
With regard to the functional characterisation of this tool class, the edge angles of the generally unretouched edge range from 18° to 67° with a mean of 41° (Figure 60), allowing both directions of cutting, i.e. *coupe rentrante* and *coupe sortante*. The edge angles differ significantly compared to those of the abruptly retouched counterparts, ranging between 44° and 76° with a mean value of 60° (Figure 60), suggesting their belonging to different functional units. Knappers most likely created blunted edges with abrupt retouch on the back of the cutting tool so that greater force could be applied to the working edges (Wilmsen, 1968). On a macroscopic scale, I observed that 60% of the tools exhibit macro and micro removals on the unmodified edge. These tools have a low angle and a feathered termination. The asymmetry of the two edges of the distal end indicates a linear mode of use (Figure 63c). The tool configuration in a linear mode, e.g. cutting, whittling and scraping, involves a prehensile edge allowing a grip perpendicular to the axis of elongation of the active part (Leroi-Gourhan, 1943; Soressi, 2002, 2004). The abruptly retouched convex edge of the distal end represents part of the passive zone enabling a prehension perpendicular to the axis of elongation of the unretouched edge with a suitable length for a linear movement. The dihedral unretouched edge functions as the active part, receiving the work-load along the intersections of its two planes during cutting actions (Tringham, et al., 1974). However, future use wear and residue analysis have to confirm or reject my hypothesis about the function of the ACTs.

Concerning the life history of the ACTs, the installation of the abruptly retouched edge seems to have been a terminal step and only the working edge experienced occasional phases of re-sharpening.

### 5.6.2. Bifacial Pieces

One striking aspect of the assemblage is the presence of bifacial technology (Figure 64) (Conard, et al., 2014; Conard and Porraz, 2015; Rots, et al., 2017). The bifacial pieces form 22.3% of the total formal tools (Table 82). The uppermost layers Adam and Annie contain the lowest numbers, while bifacial pieces reach peak numbers in layer Bart at 30.1%. In the underlying strata, the proportion of this tool type slowly but continuously decreases. Likewise, bifacial shaping flakes from the reference square C4 show the highest percentage in layer Bart (Table 103).

# EAST PROFILE



Layer	Exc. vol. liter	Density (n/m <sup>3</sup> )
■ RGS (2)	15	133
■ LBG (-)	29	-
■ BS (6)	287	21
■ ADAM (12)	128	94
■ ANNIE (12)	96	125
■ BART (25)	185	135
■ BEA (42)	229	183
■ CASPER (31)	195	159
■ CHANTAL (18)	158	114
<b>Total (148)</b>	<b><u>1320</u></b>	<b><u>112</u></b>

Legend	
★	Bifacial
▲	Lithic
●	Bone
	Rock

**Figure 64.** Sibudu. C-A layers from the Deep Sounding: Profile projection of the bifacial pieces from the Deep Sounding. The numbers in parentheses reflect the number of bifacial pieces; volume refers to the total volume of excavated sediment per layer (Status as of 2017).

**Table 103.** Sibudu. C-A layers from the Deep Sounding: Frequency of shaping and retouch flakes by raw material in square C4. (\*Shaping flakes including serrating flakes; \*\*Bias in distinguishing knapped sandstone from natural spalls.)

	Dolerite			Hornfels			Quartz			Quartzite			Sandstone			Chert			Total		
	Shap.*	Retouch	Total	Shap.*	Retouch	Total	Shap.*	Retouch	Total	Shap.*	Retouch	Total	Shap.*	Retouch	Total	Shap.*	Retouch	Total	Shap.*	Retouch	Total
ADAM	4.0%	1.4%	2856	3.6%	4.8%	166	3.4%	0.0%	89	9.3%	0.0%	108	0.0%	0.0%	43**	0.0%	0.0%	1	4.0%	1.5%	3,263
ANNIE	4.5%	1.6%	3637	7.2%	6.2%	194	9.1%	1.7%	176	11.8%	0.5%	195	0.0%	0.0%	36**	0.0%	0.0%	4	5.1%	1.8%	4,242
BART	7.0%	0.7%	2475	18.9%	4.1%	74	9.6%	0.0%	281	20.5%	1.2%	83	4.1%	0.0%	49**	0.0%	0.0%	1	7.9%	0.7%	2,963
BEA	2.2%	0.5%	2511	0.0%	5.0%	40	0.9%	0.0%	109	6.8%	0.8%	265	0.8%	0.0%	360	33.3%	0.0%	3	2.3%	0.5%	3,288
CASPER	1.2%	1.5%	1119	0.0%	0.0%	6	2.7%	2.7%	37	10.5%	1.3%	76	0.0%	0.0%	119	0.0%	0.0%	1	1.6%	1.4%	1,358
CHANTAL	0.6%	2.5%	803	0.0%	0.0%	14	0.0%	0.0%	28	0.9%	0.0%	115	0.3%	0.3%	309	0.0%	0.0%	3	0.6%	1.7%	1,272
<b>Total</b>	<b>3.9%</b>	<b>1.3%</b>	<b>13,401</b>	<b>6.9%</b>	<b>5.1%</b>	<b>494</b>	<b>6.7%</b>	<b>0.6%</b>	<b>720</b>	<b>9.1%</b>	<b>0.6%</b>	<b>842</b>	<b>0.7%</b>	<b>0.1%</b>	<b>916</b>	<b>7.7%</b>	<b>0.0%</b>	<b>13</b>	<b>4.2%</b>	<b>1.2%</b>	<b>16,386</b>

Overall, only 15.7% of bifacial pieces are completely preserved, while the majority represents either distal fragments at 31.4%, or proximal fragments at 23.6% (Table 95). The length of the completely preserved bifacial tools (n=22) lies between 26 mm and 61.7 mm, averaging 40.6 mm (Table 85). The width ranges between 7 mm and 48.4 mm, with a mean value of 22.5 mm (Table 86) and the thickness between 2.5 mm and 23.6 mm with a mean value of 8.3 mm (Table 87). The production of bifacial pieces involved mainly blades and elongated flakes where the original blank was still identifiable (Table 90). Bifacial tools comprise the highest proportion of specimens without cortex coverage (Table 91) reflecting a high degree of shaping and/or the predominant selection of products from the main production phase. A total of 17.1% of the bifacial pieces have platforms preserved from the original blanks and the majority of these platforms is plain (66.7%) (Table 92). This tool type is largely made up of pieces with straight profiles (80%) (Table 93).

Toolmakers primarily used dolerite (40%) and quartz (35%) to manufacture bifacials, followed by quartzite and hornfels (Table 84). Although dolerite is the dominant material used for bifacial pieces and shaping flakes overall, dolerite bifacial pieces are less frequent (41.4%) than dolerite shaping flakes at 75.9% in reference square C4 (Table 104). Hornfels is also more frequent as shaping flakes than bifacials, while quartz, quartzite and sandstone have a lower frequency of shaping flakes compared to bifacial pieces. Newcomer (1971) conducted experiments to manufacture handaxes from flint nodules and documented producing around

**Table 104.** Sibudu. C-A layers from the Deep Sounding: Frequency of raw material in shaping flakes and in bifacial pieces in square C4.

	Dolerite		Hornfels		Quartz		Quartzite		Sandstone		Chert		Total	
	n	%	n	%	n	%	n	%	n	%	n	%	n	%
Shaping flakes	523	75.9%	34	4.9%	77	11.2%	48	7.0%	6	0.9%	1	0.1%	689	100%
Bifacial pieces	12	41.4%	1	3.4%	6	20.7%	9	31.0%	1	3.4%	-	0.0%	29	100%

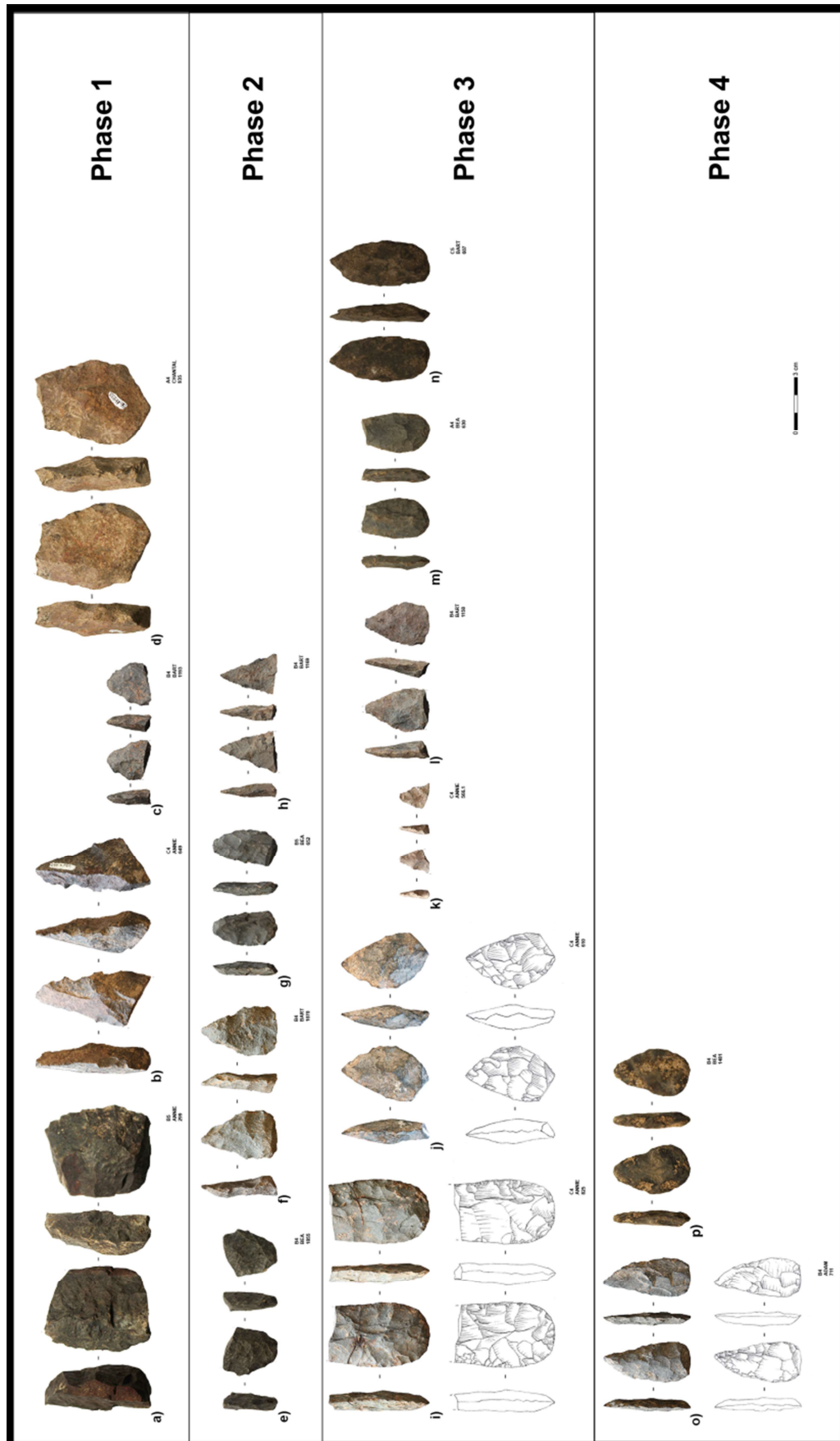
50 shaping flakes per handaxe. I acknowledge at this point certain limitations of comparability concerning the raw material and the manufacture of a different kind of bifacial tool, and I emphasize the need for experiments on comparative rocks. However, taking this as a rough benchmark, the ratio of shaping flakes to bifacial pieces made on dolerite of 43.6 indicates an agreement of numbers, while the ratio values of quartzite (5.3), sandstone (6) and quartz (12.8) are considerably lower. These discrepancies may relate to differential transport of finished and semi-finished tools and/or different intensities of sharpening, re-sharpening and maintenance for each raw material.

Bifacial retouch is defined as continuous retouch on both dorsal and ventral surfaces of a lithic along the same portion of an edge (Inizan, et al., 1999: 130). I differentiate further between bifacially retouched pieces and bifacially shaped pieces based on the degree of retouch invasiveness. Bifacially shaped pieces, as opposed to bifacially retouched pieces, have at least one surface entirely shaped by invasive flaking (Porraz, et al., 2015: 176), accounting for 61.4% of the specimens. Bifacial points, like unifacial points, are defined as triangular or sub-triangular retouched blanks with the distal end pointed, but have both surfaces intentionally modified (Volman, 1981: 26). While 96.4% of the bifacial pieces (n=135) concur with the definition of bifacial points, 3.6% of the bifacial pieces (n=5) do not exhibit all of the defining characteristics of bifacial points concerning symmetry, thinness, and a regularly pointed tip, therefore I classified these artefacts as bifacially backed knives.

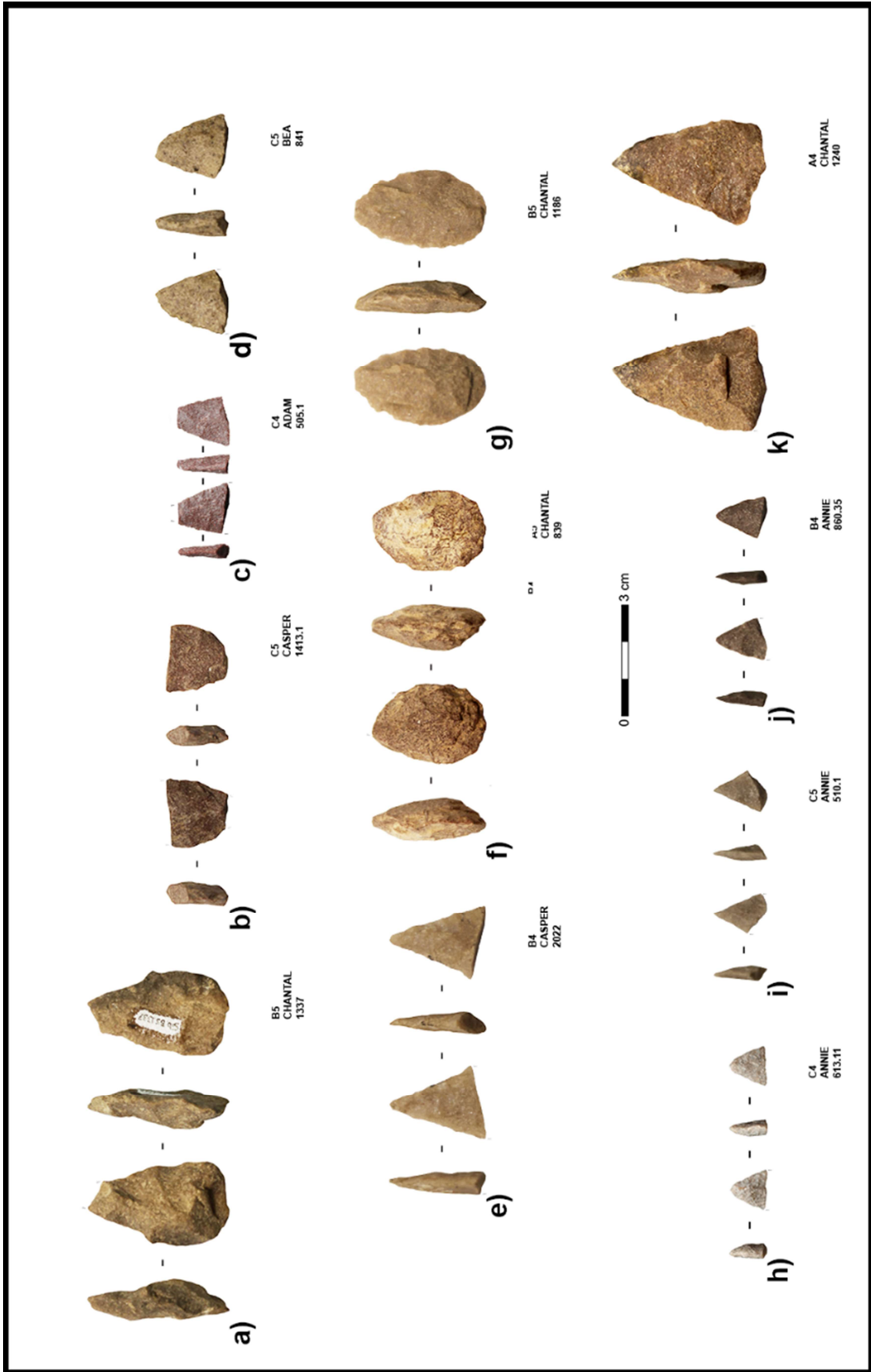
Within the bifacial point component, serrated pieces (n=25) stand out. These pieces are described as tools with margins delineated by regularly repeated small notches creating triangular teeth (Crabtree, 1972, 1973; Akerman and Bindon, 1995; Holdaway and Stern, 2004; Andrefsky, 2005; Lombard, et al., 2010). There is variability in the morphometric attributes of what have been defined as serrated pieces. For example, Akerman and Bindon (1995) establish a distinction between dentated, denticulated and serrated on the basis of the size and regularity of both the projections and the notches that separate them. In this study, I follow Rots et al. (2017: 5) using the term 'serration' as a generic term encompassing all artefacts with one or two edges that have been regularly shaped with contiguous notches forming fine triangular teeth, regardless of their dimensions and morphologies. We performed a combination of technological, wear and residue analysis to determine how toolmakers manufactured and used the serrated pieces (Rots, et al., 2017).

#### **5.6.2.1. Bifacial Points**

The assemblage contains a total of 110 bifacial points (Figures 65 – 67). This tool class is present throughout the sequence, starting with the lowest proportion, 9.7%, in layer Adam, reaching a peak of 24.1% in layer Bart and decreasing again to 15.9% towards the lowest layer Chantal (Table 83).

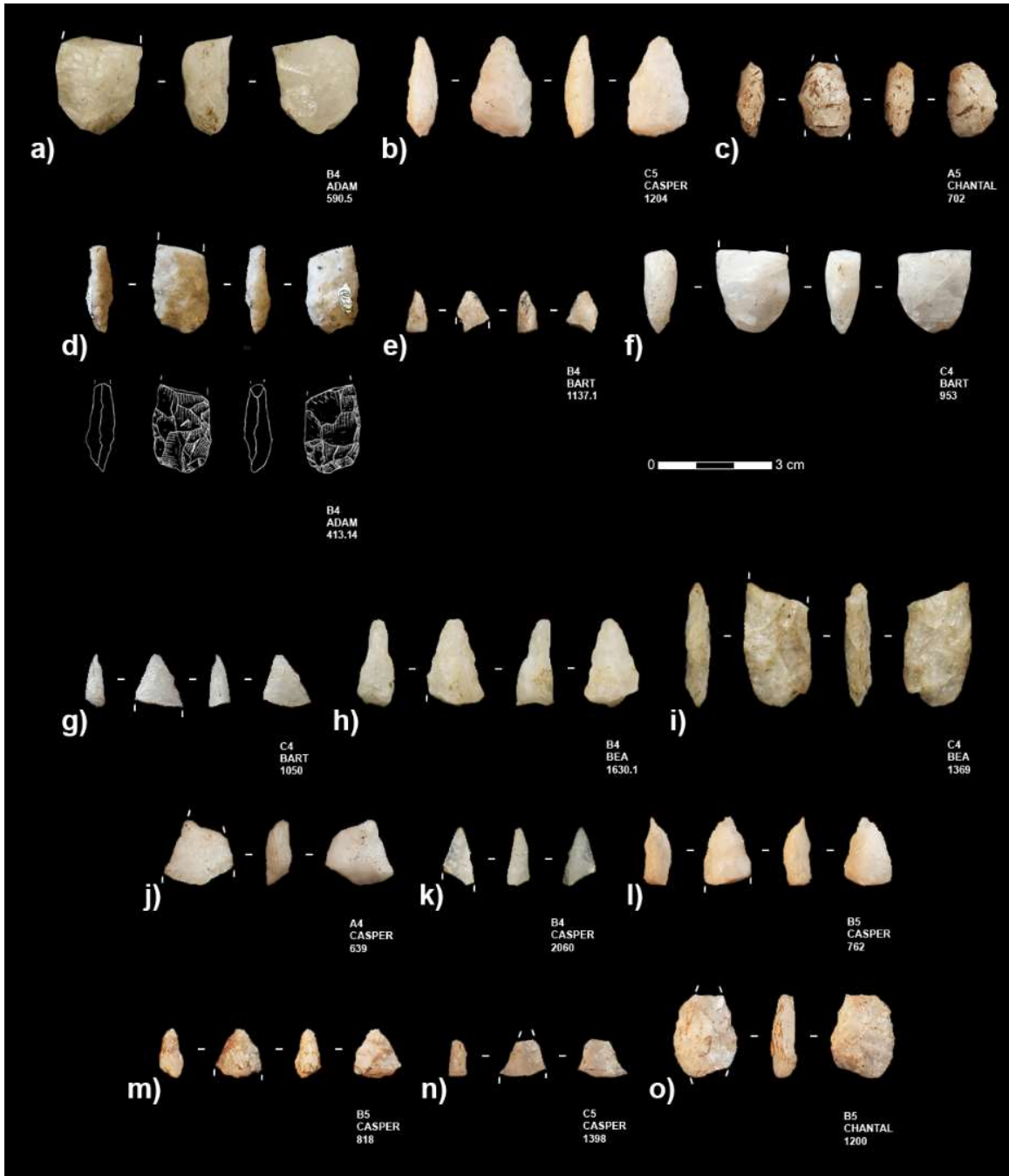


**Figure 65.** Sibudu. C-A layers from the Deep Sounding: Bifacial points made on dolerite (a-m, p) and hornfels (n, o) according to phase of manufacture (Drawings by Guillaume Porraz; photos (b, c, h, k, l) by Julia Becher; photos (i, j) by Lucía Cobo-Sánchez; photos (a, d, e, g, m, n, p) by Viola C. Schmid; (f, o) after Conard, et al., 2014: Figure 3).



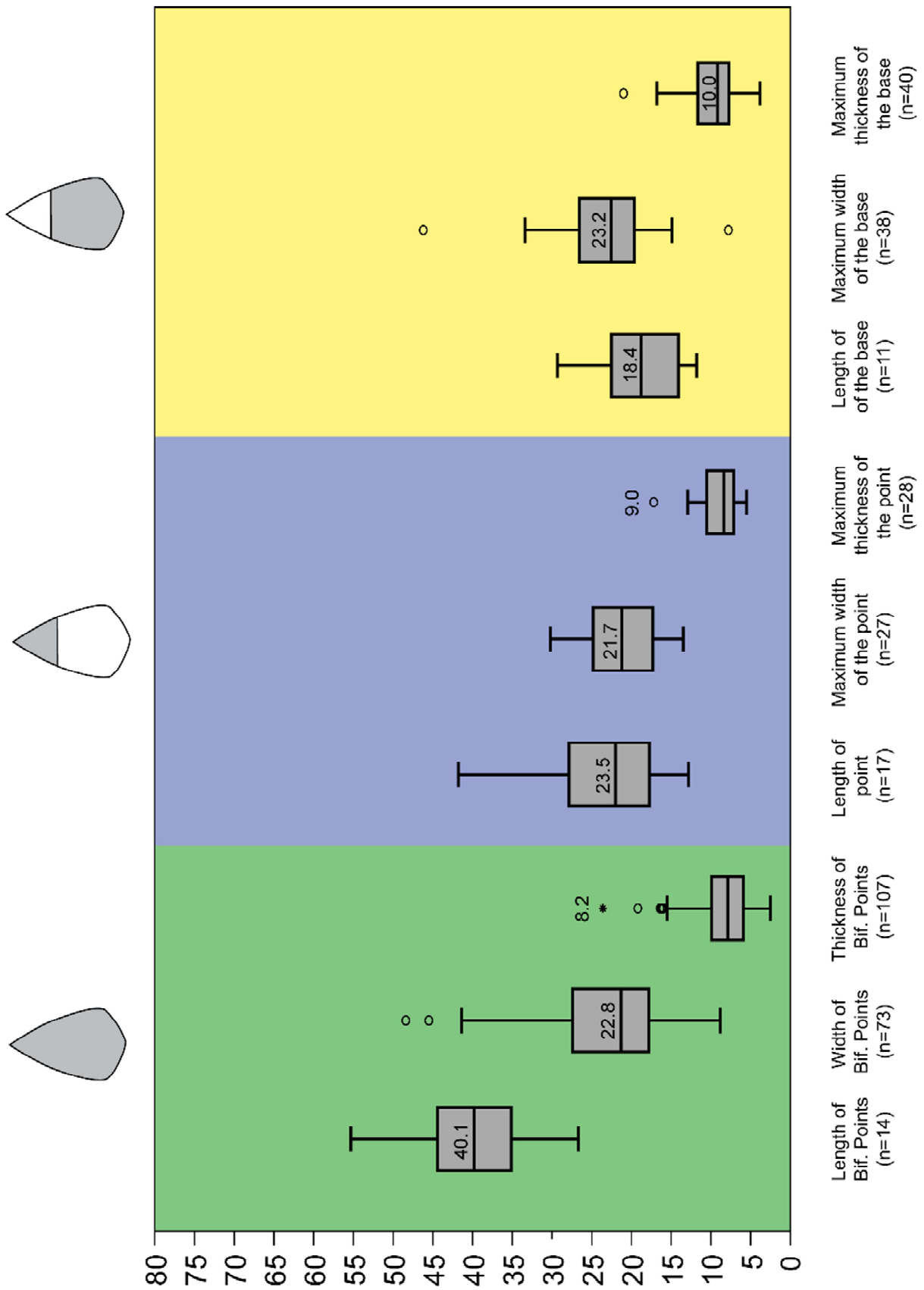
**Figure 66.** Sibudu. C-A layers from the Deep Sounding: Bifacial points made on quartzite (Photos (c, h) by Julia Becher; photos (a, b, d-g, i-k) by Viola C. Schmid).





**Figure 67.** Sibudu. C-A layers from the Deep Sounding: Bifacial points made on quartz (Drawing by Guillaume Porraz; photos (e-g) by Julia Becher; photo (d) by Lucía Cobo-Sánchez; photos (a-c, h-o) by Viola C. Schmid).

The largest proportion of bifacial points is made on quartz at 37.3%, followed by dolerite at 35.5% and quartzite at 19.1% (Table 96). Three of the pieces are made on chert, comprising half of the total formal tools made on chert ( $n=6$ ). Two of the bifacial point fragments made on chert refit and come from the adjacent squares B4 and B5 with a difference in height of 3 cm.



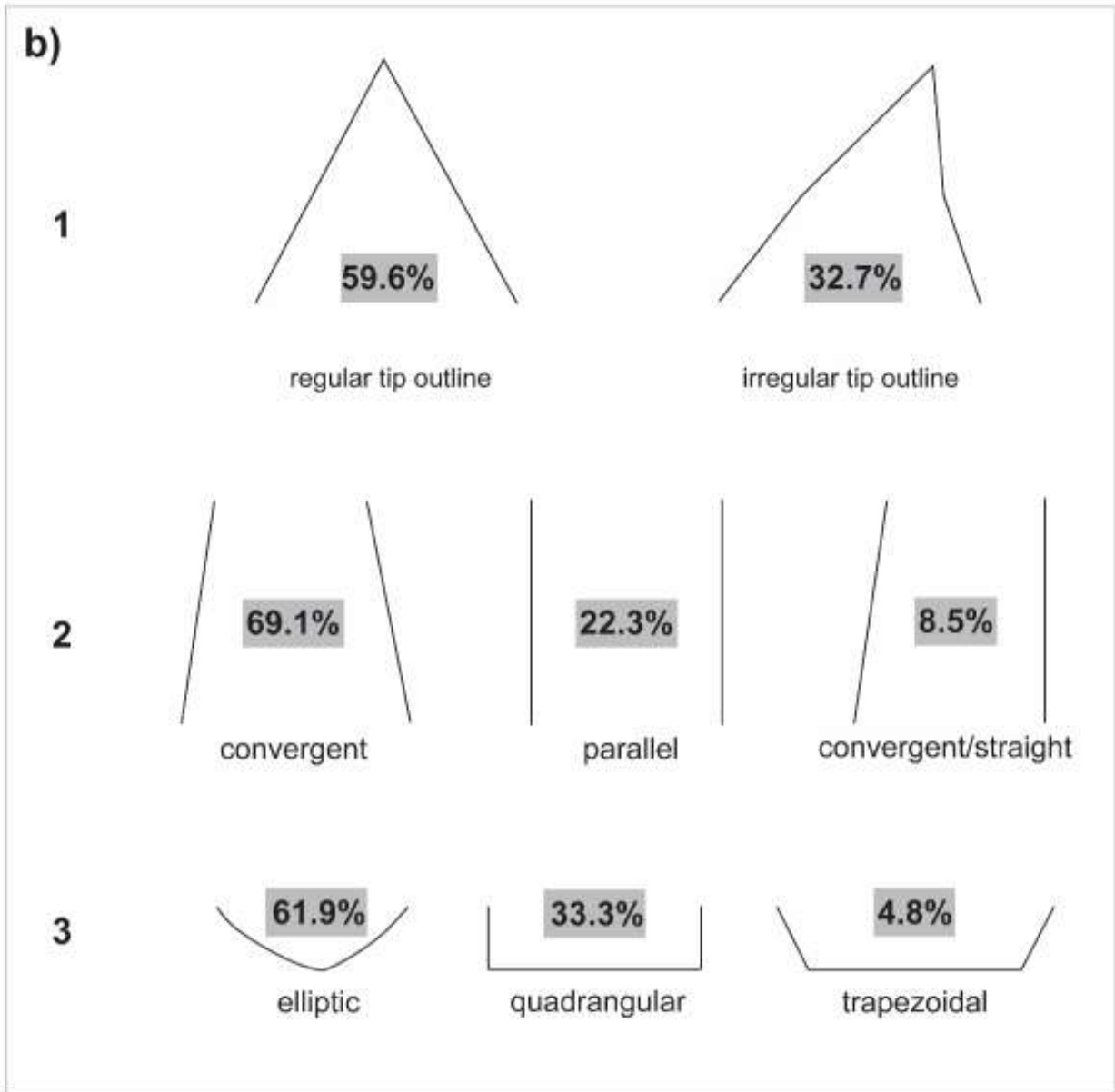
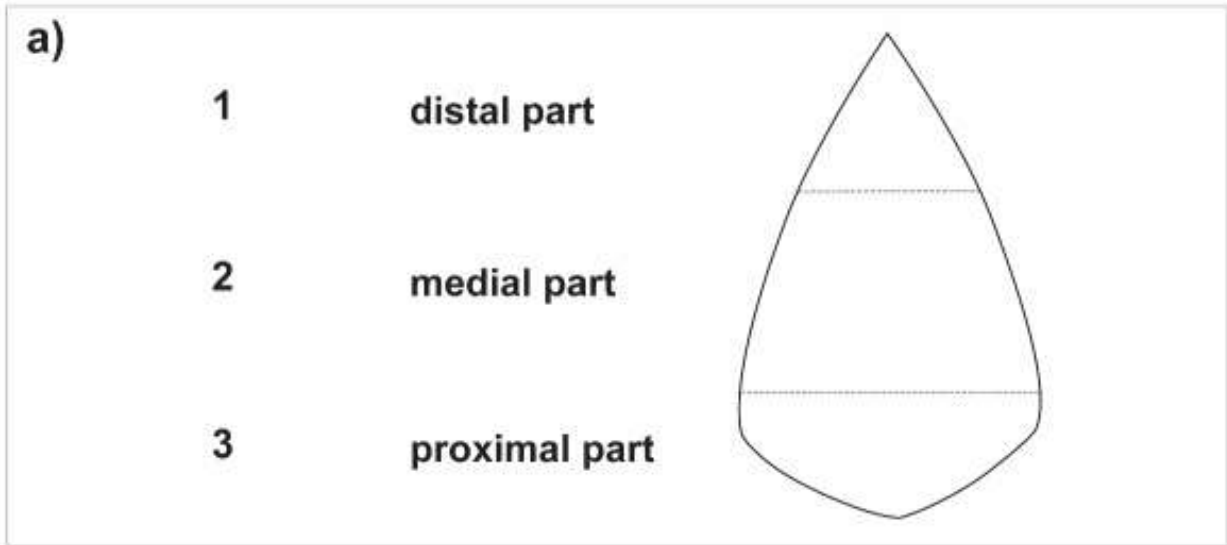
**Figure 68.** Sibudu. C-A layers from the Deep Sounding: Boxplot showing morphometric characteristics of the bifacial points.

Generally, most of the bifacial points are fragments, especially tip and distal fragments (Table 101). The length of the 14 pieces with a completely preserved length ranges between 26.7 mm and 55.3 mm, with a mean of 40.1 mm (Figure 68). The width of the bifacial points averages 22.9 mm and the thickness 8.2 mm (Figure 68). Their length-to-width ratio is  $1.6 \pm 0.2$  (n=12) and their width-thickness ratio is of  $2.5 \pm 0.4$  (n=73). While the original blank could not be determined for the majority of points due to the overall shaping, the blank selection – when identifiable (39.1%) – fell predominantly on laminar products (Table 97), with toolmakers seeming to have preferentially selected elongated products to shape them into bifacial points. A total of 86.4% of the pieces exhibit no dorsal cortex coverage. A total of 73% of the bifacial points have a straight profile. The largest proportion of the bifacial points has planoconvex cross-sections (47.3%), followed by biconvex (28.2%) and planoconvex/planoconvex (20.9%) cross-sections (Table 105).

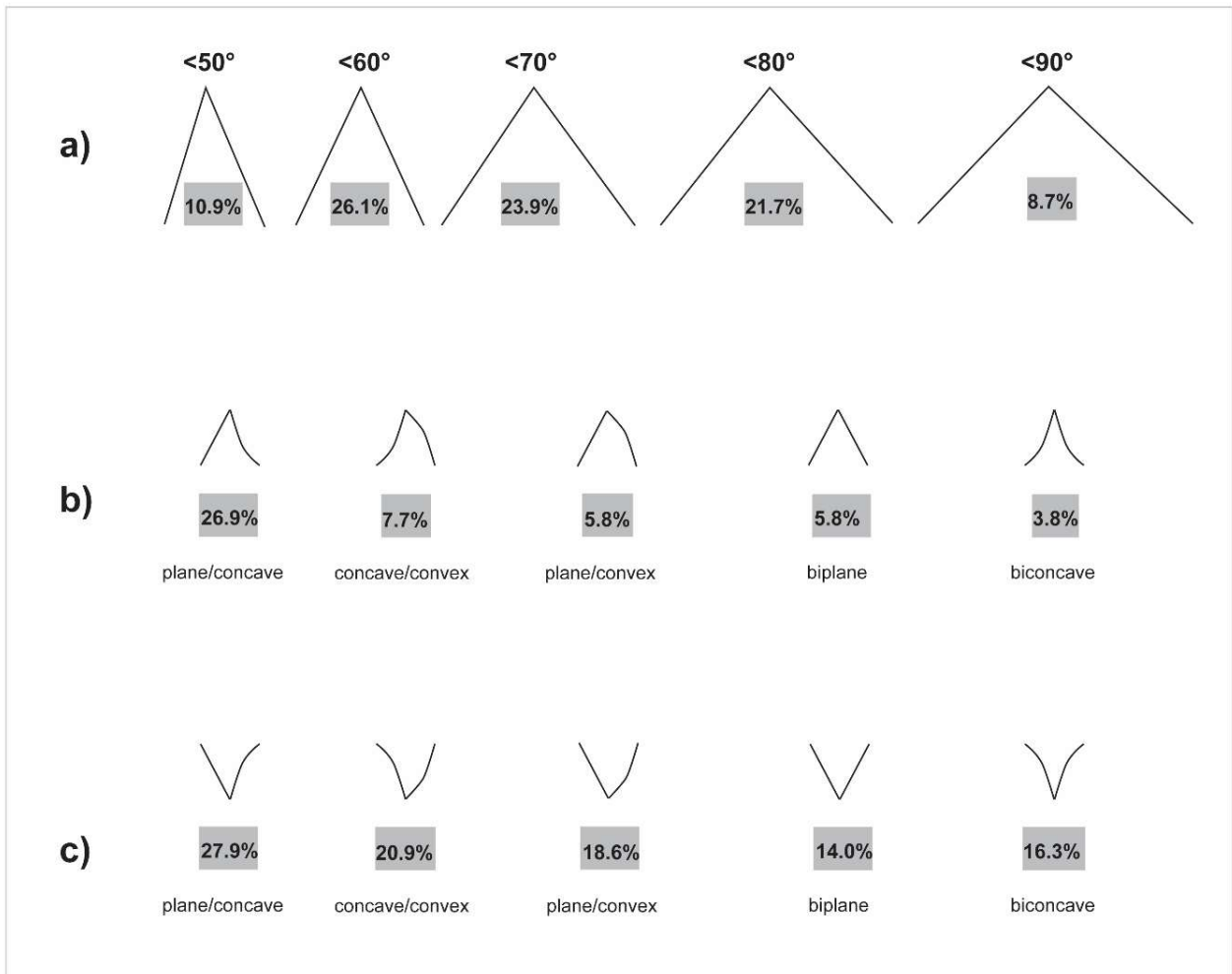
**Table 105.** Sibudu. C-A layers from the Deep Sounding: Frequency of cross-section per bifacial tool class (drawings from Boëda and Richter, 1995: 77).

Tool class	planoconvex		biconvex		planoconvex/planoconvex		indetermined		Total	
	n	%	n	%	n	%	n	%	n	%
Bifacial Points	52	47.3%	31	28.2%	23	20.9%	4	3.6%	110	100%
Bifacially Backed Knives	5	100.0%	-	0.0%	-	0.0%	-	0.0%	5	100%
Serrated Pieces	16	64.0%	6	24.0%	1	4.0%	2	8.0%	25	100%
<b>Total</b>	<b>73</b>	<b>52.1%</b>	<b>37</b>	<b>26.4%</b>	<b>24</b>	<b>17.1%</b>	<b>6</b>	<b>4.3%</b>	<b>140</b>	<b>100%</b>

Concerning the morphotype, most of the bifacial points (68.2%) show bilateral symmetry and 48.2% exhibit bifacial symmetry. I observed that the active part, when identifiable (n=38), was always installed on the distal part of the selected blank. The point is usually aligned with the percussion axis of the blank, but exceptions (6.4%) occur (see for example Figure 65j). The points have a V-shape and most bifacial points exhibit a regular pointed tip outline (Figure 69). The TPA of all measurable pieces (n=46) is acute at a mean of 65°, ranging predominantly between 55° and 75° (Figure 70a). The average length of the tip is 23.5 mm, with a range between 12.8 mm and 41.8 mm (Figure 68). The point takes between one and two thirds of the entire tool. The tip profile of the bifacial points is primarily plane/concave (Figure 70b). The body of the majority of the points (69.1%) is convergent (Figure 69). The bases of the pieces with a preserved proximal part (n=43) usually have an elliptic morphology (Figure 69) and predominantly plane/concave (27.9%) or concave/convex (20.9%) base profiles (Figure 70c).

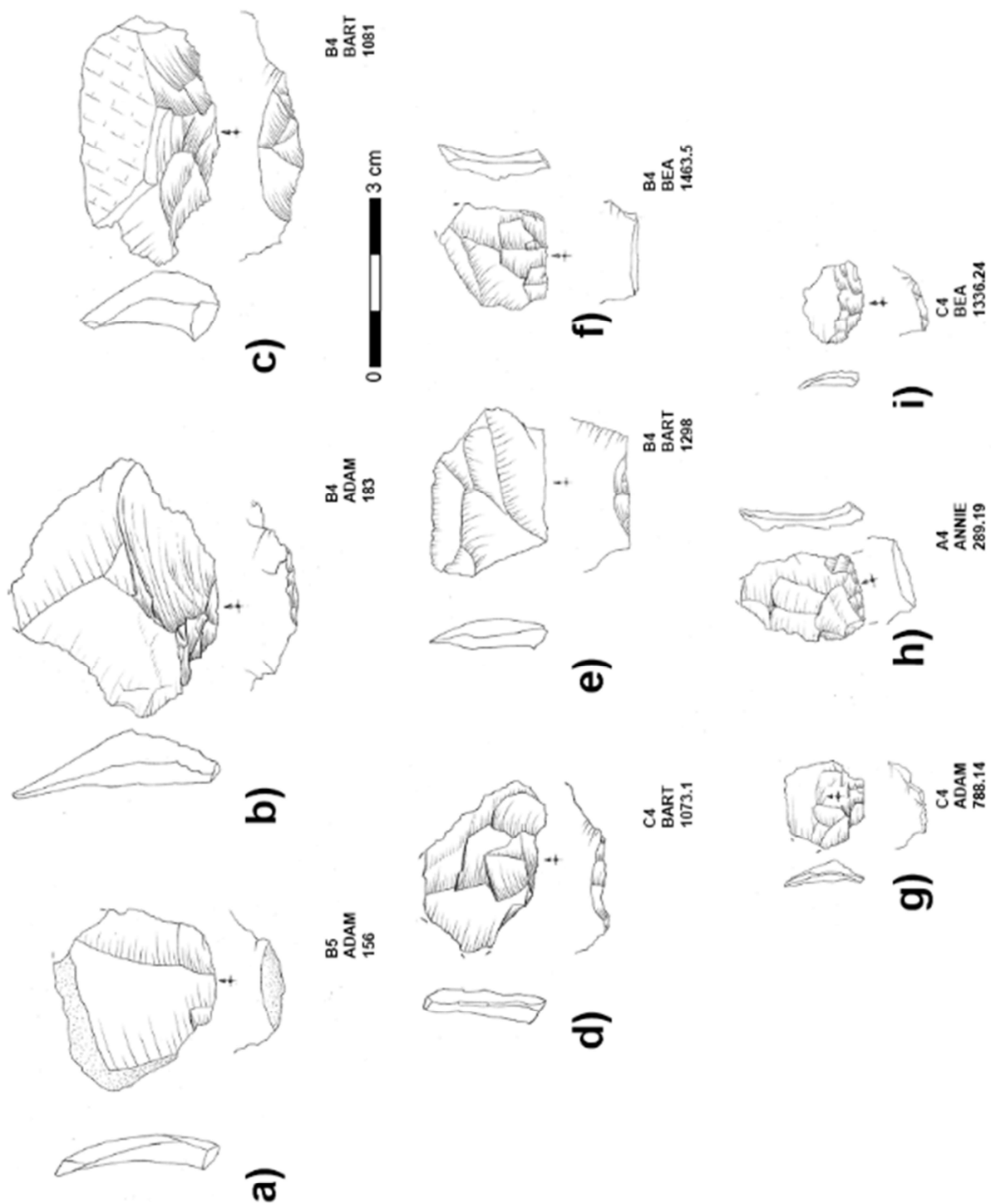


**Figure 69.** Sibudu. C-A layers from the Deep Sounding: Bifacial point morphotype.



**Figure 70.** Sibudu. C-A layers from the Deep Sounding: Morphological features, including TPA (a), tip profile (b) and base profile (c).

Toolmakers employed two knapping techniques in the bifacial reduction sequence. The initial shaping involved direct percussion with a hard hammer documented by removals on the bifacial points with concave negative bulbs and a highly localized point of percussion (i.e. Figure 65d). I also identified large shaping flakes coming from the initial shaping phase (Figure 71a-c), which exhibit wide and rather thick plain or sometimes cortical platforms (Figure 71a) with no abrasion suggesting internal hard hammer percussion (see Soriano, et al., 2015). In the advanced shaping phase, the knappers used soft hammer marginal percussion indicated by removals on the tools with shallow negative bulbs and a diffuse contact point (i.e. Figure 65i). A bone percussion tool with an encrusted quartzite flake fragment from layer Casper provides further evidence for the usage of soft organic hammers in the manufacturing of quartzite bifacial pieces at least (see Rots, et al., 2017: Figure 14). Additionally, small shaping flakes of advanced (Figure 71d-f) and final shaping (Figure 71g-i) show traces of soft hammer marginal percussion. Some blanks have abrasion of the dorsal platform edge, a curved profile and/or a lip without a bulb, while others exhibit contact points on the platform and small incipient cones (Figure 71g) suggesting the use of both organic and soft stone hammers (see Rots, et al., 2017).



**Figure 71.** Sibudu. C-A layers from the Deep Sounding: Shaping flakes made on dolerite. Shaping flakes from initial shaping phase (a-c), shaping flakes from advanced shaping phase (d-f) and shaping flakes from final shaping phase (g-i) (Drawings by Mojdeh Lajmiri).

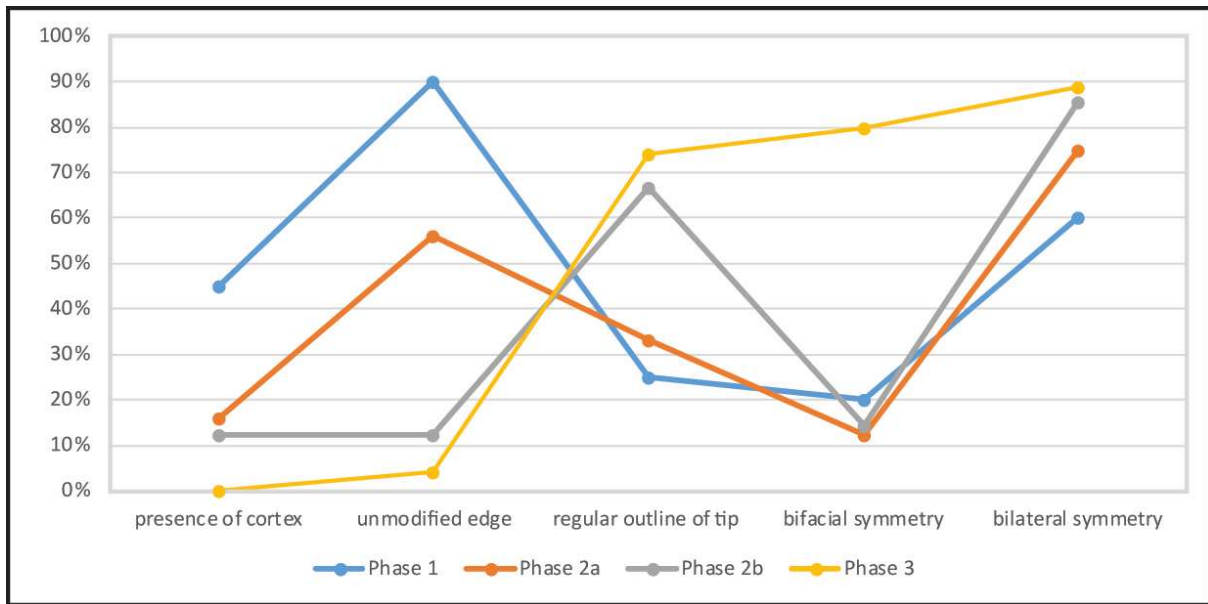
The classification of all the bifacial points according to the phases of manufacture shows that the highest frequency of pieces was discarded as finished products (Table 106). However, all phases of manufacture from initial shaping through to recycling are present which allows the reconstruction of the general manufacturing sequence.

The production of bifacial points begins with the shaping of laminar products. Knappers used often, but not exclusively, rather thick blades or elongated flakes (Table 97). Twelve out of twenty pieces from phase 1 are made on laminar elements and they are thicker (with a mean value of 13.7 mm) than the unretouched blades and elongated flakes. The inhabitants of Sibudu seem not to have highly invested in pre-determination of products since pieces from the initial and advanced phases show cortical remains or natural surfaces indicating the use of blanks from an early stage of core reduction. Once the toolmakers selected the appropriate piece, they started shaping both faces with direct hard hammer percussion. All of the pieces from the initial shaping are broken, mostly proximal or medial fragments. The breakages are likely related to knapping accidents that interrupted and ultimately terminated the shaping procedure.

**Table 106.** Sibudu. C-A layers from the Deep Sounding: Frequency of raw material per phase of manufacture of bifacial points (following Villa, et al., 2009).

	Dolerite		Hornfels		Quartz		Quartzite		Sandstone		Chert		Total	
	n	%	n	%	n	%	n	%	n	%	n	%	n	%
1. Initial shaping	12	30.8%	2	40.0%	3	7.3%	2	9.5%	1	100.0%	-	0.0%	<b>20</b>	<b>18.2%</b>
2. Advanced shaping	16	41.0%	-	0.0%	12	29.3%	6	28.6%	-	0.0%	-	0.0%	<b>34</b>	<b>30.9%</b>
3. Finished products	10	25.6%	2	40.0%	24	58.5%	11	52.4%	-	0.0%	3	100.0%	<b>50</b>	<b>45.5%</b>
4. Recycled	1	2.6%	1	20.0%	-	0.0%	2	9.5%	-	0.0%	-	0.0%	<b>4</b>	<b>3.6%</b>
Unattributed	-	0.0%	-	0.0%	2	4.9%	-	0.0%	-	0.0%	-	0.0%	<b>2</b>	<b>1.8%</b>
<b>Total</b>	<b>39</b>	<b>100%</b>	<b>5</b>	<b>100%</b>	<b>41</b>	<b>100%</b>	<b>21</b>	<b>100%</b>	<b>1</b>	<b>100%</b>	<b>3</b>	<b>100%</b>	<b>110</b>	<b>100%</b>

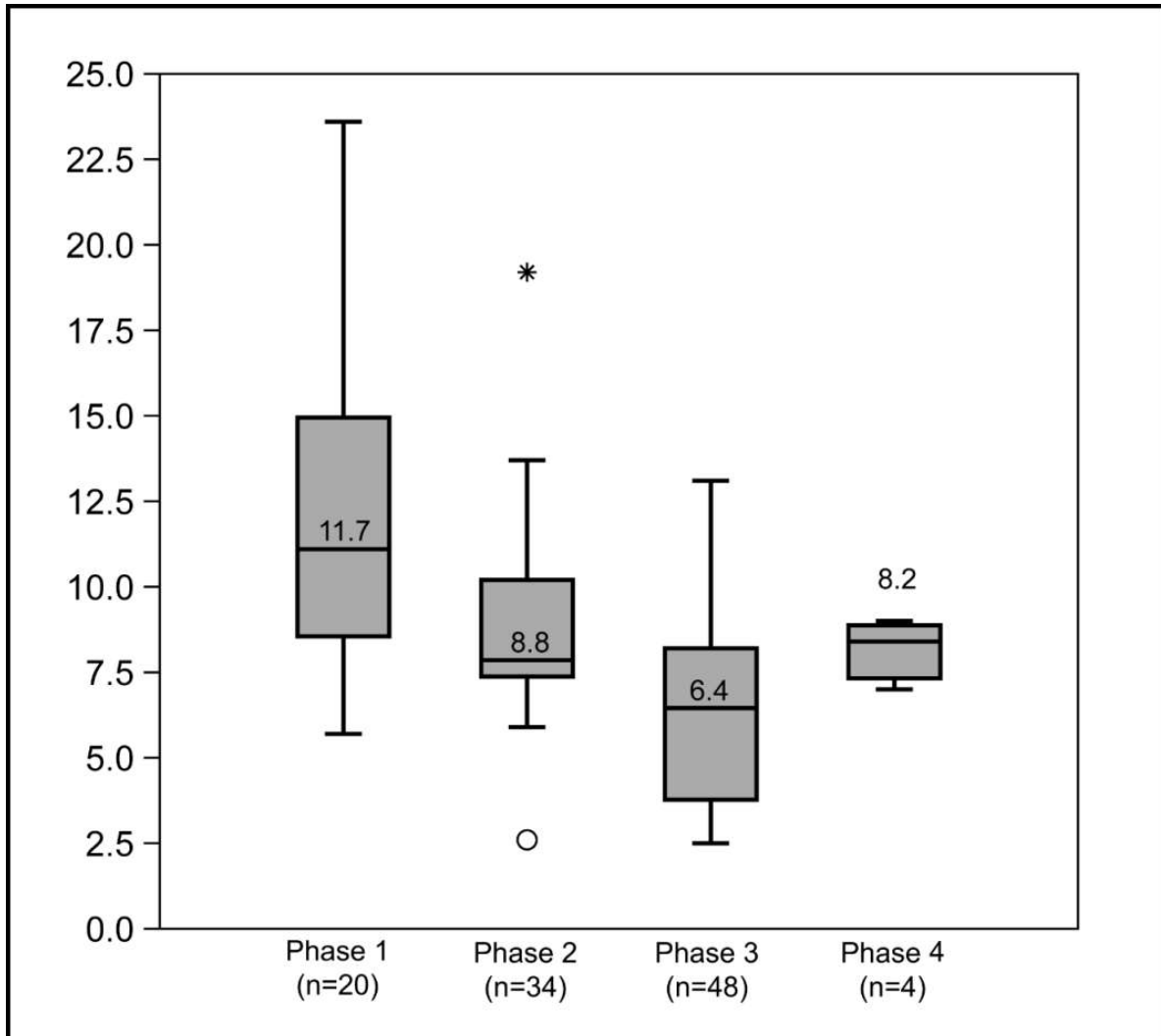
In the advanced production phases, past people started to employ soft hammers to enable more invasive shaping of the entire surface of the artefacts with the removal of long, thin flakes. Phase 2a involved the use of both hard and soft hammers, while in the subsequent phase 2b only soft hammer percussion occurred. The products have much less cortical coverage and the proportion of unmodified edges decreases progressively (Figure 72). The regularisation of the tip outline increases from only 25% in phase 1 to 66.7% in phase 2b. Moreover, bilateral symmetry is high from the beginning at 60% in accordance with preferential selection of blades and this frequency continues to increase (Figure 72). However, the occurrence of bifacial symmetry drops from 20% in phase 1 to 12.5% in phase 2a and only increases slightly in phase 2b at 14.3% (Figure 72).



**Figure 72.** Sibudu. C-A layers from the Deep Sounding: Frequency distribution of manufacturing phase attributes.

Phase 3 encompasses the finished products which only exhibit removals resulting from soft hammer percussion. The tips in particular are prepared with fine retouch and are often thinner and narrower than the rest of the piece. The toolmakers achieved the final desired bifacial point form with standardised dimensions and shapes indicated by the high frequency of regular tip outlines, bilateral and bifacial symmetry and thinness (Figure 72 & Figure 73). The shaping proceeded to such a degree that none of the finished products have any cortical coverage and only 4% of the finished points have a small proportion of unmodified blank edge (Figure 72).





**Figure 73.** Sibudu. C-A layers from the Deep Sounding: Boxplot showing thickness of the phases of manufacture of the bifacial points.

Four of the points show more concave removals of reworking, more likely related to hard hammer percussion applied after the shaping with soft hammer percussion and a change in the total outline. The reworking and resulting change of outline of the distal end of one specimen (Figure 65p) alludes to possible re-sharpening in the haft (see Villa, et al., 2009).

The high proportion of broken points (Table 95) concerns all phases of manufacture. I documented several types of breakages following the terms of Villa et al. (2009: 448f.). Most of the fractures are associated with bending fractures, forming when force is applied over a larger area but the break does not initiate at the point of applied force. Lateral snaps represent bending fractures with straight or curved profiles and 78.4% of the broken bifacial points show this fracture type. They often appear during manufacture, but can also be related to trampling or use (Villa, et al., 2009: 449). Trampling seems rather unlikely here as the whole assemblage does not show features that would suggest strong influence of trampling (see Chapter 5.7.). I cannot entirely exclude use (e.g. impact) but lateral snaps occur on pieces from phase 1 to phase 4. Additionally, a large part of the broken pieces are tip fragments. It is possible that some

breaks occurred during violent impact and were then transported back to the site inside the killed animal carcass (Villa, et al., 2009: 449). However, the shaping of the distal end requires intensive retouch and, due to the fragility related to thinness and narrowness, this part of the artefact is more prone to breakage during shaping and re-sharpening. This makes manufacture the most plausible and common explanation. Perverse fractures, which are spiral or twisting fractures initiated at the point of force along the edge of the piece, also occur on 6.2% of the pieces and also indicate manufacturing breaks.

The population of bifacial points demonstrates high variability related to the rock types used regarding size, morphology, manufacturing process, and subsequently the techno-functional interpretation. Therefore, I will present the differing trends between quartz bifacial points and the points made on the other raw materials separately from each other in the following section.

#### **5.6.2.1.1. *Bifacial Points made on Dolerite, Quartzite and Hornfels***

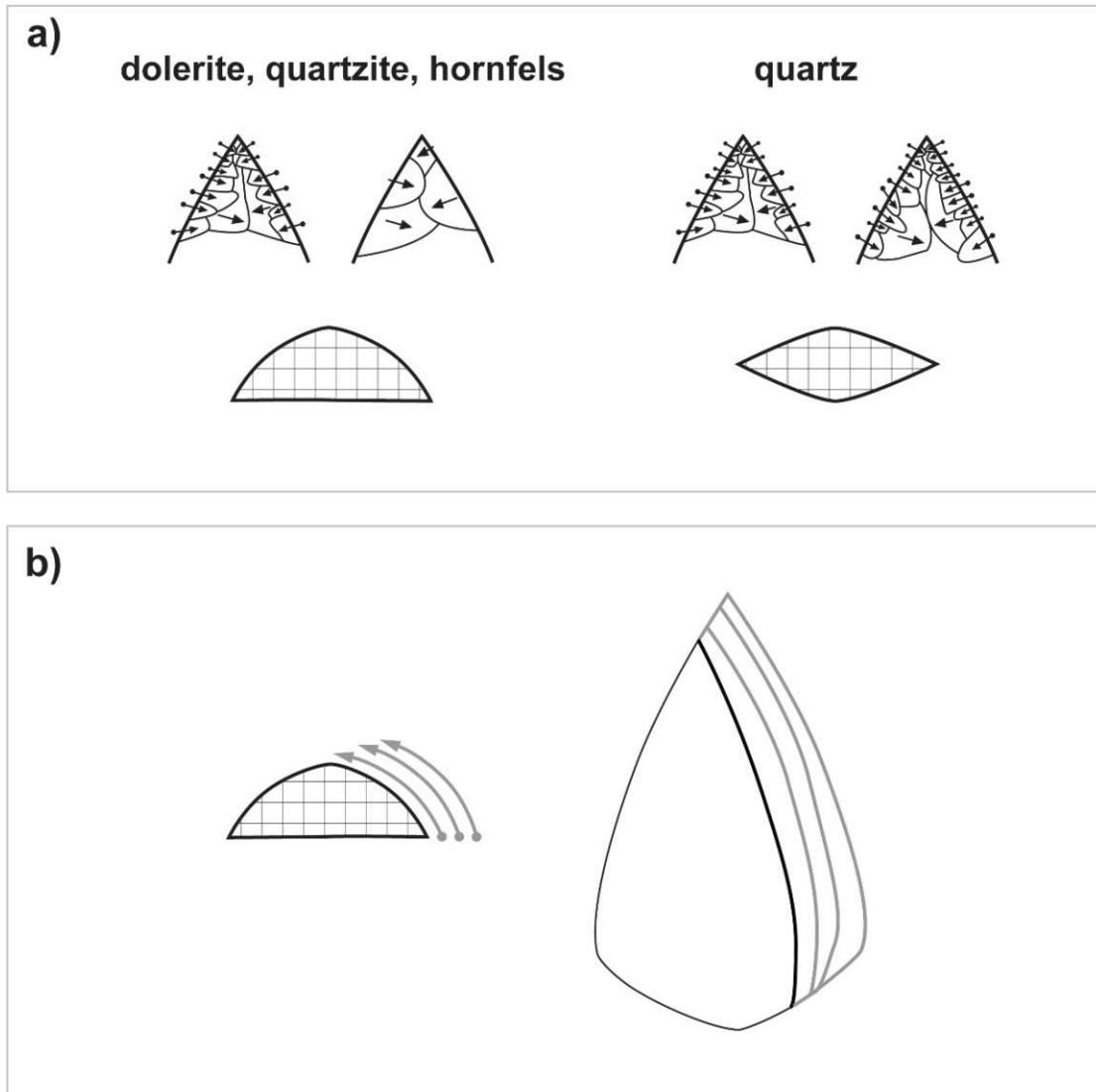
The bifacial points made on dolerite, quartzite and hornfels make up 62.7% of the total bifacial points. A total of 17.9% of the dolerite, 14.3% of the quartzite and 20% of the hornfels pieces are completely preserved. However, quartzite (23.8%) demonstrates high proportions of tip fragments compared to the lower proportion of dolerite (10.3%) and missing tip fragments of hornfels. The length of the bifacial points (n=13) made on dolerite, quartzite and hornfels averages 41.2 mm. The width of these bifacial points (n=49) lies at 25.1 mm. The mean thickness (n=64) is 9.1 mm. The width-thickness ratio of these elements amounts to  $2.6 \pm 0.4$ . A total of 81.5% of the tools exhibit straight profiles and planoconvex cross-sections (56.9%) dominate.

Concerning the morphometric characteristics, 51.4% of the points made on dolerite, quartzite and hornfels (n=35) show a regular pointed tip outline. These specimens show a high TPA with a mean value of  $67^\circ$ . The mean length of the tip is 24.1 mm. The medial parts are primarily convergent at 68.8%. Sixty percent of the tools have an elliptic base. The bases show plane/concave, concave/convex and plane/convex profiles in equal proportions of 21.9%.

Most bifacial points made on dolerite are either from the initial or advanced phase of shaping. Quartzite shows an increasing frequency from phase 1 through to phase 3. A total of 25.6% of the dolerite objects belong to the finished products, while hornfels (40%) and quartzite (52.4%) contain higher frequencies of finished points. Only one specimen made on dolerite retains a portion of unmodified blank edge. A total of 47.4% of the total dolerite points have a regular tip outline, also seen in 50% of the finished products. For quartzite, 57.1% of all points exhibit a regular tip outline, shown by 75% of the final points. Bilateral symmetry and thinness are important features of the finished points of all raw materials. The dolerite finished points include 70% of bifacially symmetric and 40% of biconvex objects; quartzite includes 81.8% of bifacially symmetric and 27.3% of biconvex elements. Quartzite, dolerite and hornfels all exhibit traces of recycling. Snap breaks are most common in all of these raw materials, reaching the highest proportion in broken pieces made on quartzite (83.3%).

The shaping of dolerite, quartzite and hornfels is generally, although probably not exclusively, organised hierarchically; i.e. the two surfaces are retouched sequentially (Figure 74). Toolmakers often started the bifacial reduction with the flat surface and continued with the convex surface leading to tools with planoconvex or planoconvex/planoconvex cross-sections. This structure and hierarchy between faces permits several re-sharpening events without any change or alteration of the entire structure, conforming to 'bifaces used as a blank for tools' (*pièces bifaciales supports*) (Boëda, 1997, 2001; Nicoud, 2013; Porraz, et al., 2013; Soriano, et al., 2015), but this affects the regularity of the pointed tip (Figure 74b).

Following a techno-functional approach, I attempted to retrace the prehensile part, working edge and function of tools from the finished and recycled products; however, upcoming use-wear and residue analysis are needed to substantiate these observations. I found some evidence for axial hafting of bifacial points. One dolerite piece with phase 4 shaping (Figure 65p) exhibits heavy reworking with large removals by hard hammer percussion on the distal part. This caused a retraction of the distal portion and slightly concave edges, the pattern and positioning of which points towards axial handling. Another phase 4 tool made on quartzite (Figure 66k) displays a step-terminating bend break on its proximal part, occurring due to pressure or counter shock in the haft or above the haft (Villa, et al., 2009: 451). The hierarchised structure and organisation of the removals on the majority of bifacial points made on dolerite, quartzite and hornfels suggest a primary use as pointed cutting tools. Their design allows multiple episodes of re-sharpening and curation ensuring long-term use (see Porraz, et al., 2013; Soriano, et al., 2015). Although these tools were probably mainly used as cutting implements, this does not preclude their use as inserts of throwing or thrusting spears. Additionally, the TCSA values of the dolerite and quartzite pieces comply with the values of hand-delivered spears (Table 107).



**Figure 74.** Sibudu. C-A layers from the Deep Sounding: a) Removal organisation during manufacture of bifacial points; b) Schematic model showing re-sharpening of bifacial points with two hierarchised surfaces and change of tip outline.

**Table 107.** Sibudu. C-A layers from the Deep Sounding: Descriptive statistics of TCSA in mm<sup>2</sup>. (\*Data sets from (Villa, et al., 2009: Table 5).)

	n	Min	Max	Mean	Stand. dev.
Arrowheads*	118	8	146	33	10
Dart tips*	40	20	94	58	18
Spear tips*	28	50	392	168	89
Quartz bifacial points, phase 3, C-A layers Sibudu	12	18	95	59	21
Dolerite bifacial points, phase 3, C-A layers Sibudu	7	35	193	111	59
Quartzite bifacial points, phase 3, C-A layers Sibudu	5	30	128	74	37
Quartz finished serrated points, C-A layers Sibudu	3	14	46	27	17
Dolerite finished serrated points, C-A layers Sibudu	4	72	176	100	51
Hornfels finished serrated points, C-A layers Sibudu	2	104	126	115	16

#### **5.6.2.1.2. Bifacial Points Made on Quartz**

The quartz bifacial points alone form more than a third of the bifacial points. Only 2.4% of these points are not fragmented. A total of 24.4% of the specimens represent tip fragments. With regard to the metrical data, the only completely preserved quartz bifacial point (Figure 67b) yielded a minimum length value of 26.7 mm. The width of the bifacial points with a completely preserved width (n=22) averages 17.3 mm. The mean thickness of pieces with a completely preserved thickness (n=39) is 6.6 mm. The width-thickness ratio of the tools is  $2.3 \pm 0.3$ . A total of 70.7% of the pieces have a straight profile. The highest frequency of quartz tools (41.5%) shows biconvex cross-sections.

In terms of morphometric characteristics, 76.5% of the quartz points with a preserved tip (n=17) have a regular pointed tip outline. The TPA of the pieces averages  $61^\circ$ . The length of the tip of the only completely preserved quartz point is 14.2 mm. A total of 56% of the elements have a convergent medial part. The highest proportion of the bases is elliptic (63.6%) and 45.5% demonstrate plane/concave profiles.

In terms of the phases of manufacture, the bifacial points occur in increasing frequency from the initial phase to the finishing phase. Most of the points (58.5%) are finished products (Table 106). None of the quartz finished elements show unmodified edges. The tools show a high frequency of regular pointed tip outlines, both overall (76.5%) and specifically the finished artefacts (91.7%). The large proportion of bifacial symmetric (90.5%) and biconvex (61.9%) pieces distinguishes the quartz finished points from other raw materials. None of the quartz specimens exhibit traces of recycling. Snap breaks are the most common breakage type.

The manufacture of bifacial points from quartz seems to be managed by alternating removals resulting in biconvex finished products with pointed regular tip outlines. This hypothesis is also supported by observations regarding the chronology of the removals. The quartz bifacial points correspond to 'bifaces as tools' (*pièces bifaciales outils*) consisting of two non-hierarchical surfaces (Figure 74a) (Boëda, et al., 1990; Boëda, 1997; Nicoud, 2013). The installation of these two surfaces is simultaneous to create an active edge that can be retouched to shape the entire volume of the desired tool.

With regard to the functional role of quartz bifacial points, they might have served as axially hafted armatures in a hunting weapon. The mean TCSA value falls in the range of both dart tips thrown with an atlatl and arrowheads delivered with a bow (Table 107). Furthermore, I identified two possible impact fractures, both on finished quartz bifacial points.

#### **5.6.2.2. Serrated Pieces**

The toolkit comprises a total of 25 serrated pieces (Figure 75). This tool class is represented only in the lower layers from Bart to Chantal reaching the highest frequency in layer Bea at 6.8% (Table 83). However, serrating flakes also appear in the uppermost layers, Adam and Annie (see below).

The toolmakers made the greatest proportion of serrated pieces on dolerite (60%) followed by quartz (28%) (Table 96). Other raw materials play a minor role; two serrated pieces are hornfels and one is quartzite. Most tools are either complete or distally fragmented (Table 101). The artefacts have a mean length of 42.1 mm, a mean width of 21.1 mm and a mean thickness of 7.8 mm (Table 108).

**Table 108.** Sibudu. C-A layers from the Deep Sounding: Descriptive statistics of length, width and thickness of the serrated pieces.

	Length	Width	Thickness
n	7	23	25
Min	26	7	3.3
Max	61.7	39	12.5
Sum	294.7	484.7	195.1
Mean	42.1	21.1	7.8
Std. error	4	1.7	0.4
Variance	110.5	64	4.2
Stand. dev.	10.5	8	2.1
Median	41	20	8
25 prcntil	40	16	6.4
75 prcntil	45	26	9

Their length-to-width ratio is  $1.6 \pm 0.3$  (n=6) and their width-thickness ratio is of  $2.8 \pm 0.9$  (n=23). The knappers predominantly chose blades and elongated flakes as blanks to shape into serrated elements (Table 97). Cortex remains are present on 12% of the pieces, but never covering more than 50% of the dorsal surface. The tools exhibit almost exclusively straight profiles (96%). The pieces have primarily planoconvex (64%) or biconvex (28%) cross-sections (Table 105).

Most of the serrated pieces (n=16) exhibit bilateral symmetry. The active part is associated with the distal ends of the tools. The point is usually aligned with the percussion axis of the blank. The delineation of the edges is variable, more regular in the distal end and often sinuous in the proximal end. The regularity of the distal part partly relates to the installation of the notches. When they are bifacial, either the notches are bifacially symmetric (e.g. the alternating bifacial notches originate from the same contact point) or asymmetric (e.g. the alternating bifacial notches originate from adjacent contact points) (Rots, et al., 2017: 7).

The tips are V-shaped and demonstrate generally a regular pointed outline (71.4%). The TPA of all measurable pieces (n=10) is acute, at a mean of  $52^\circ$  measured with a goniometer and at a mean of  $46^\circ$  calculated with a formula (Table 109). A total of 56% of the serrated pieces



**Figure 75.** Sibudu. C-A layers from the Deep Sounding: Serrated Pieces. Serrated pieces made on dolerite (f, h, i, k, m, p-x), made on quartz (a-e, n, o), made on hornfels (g, l), and made on quartzite (j) (modified after Rots, et al., 2017).

**Table 109.** Sibudu. C-A layers from the Deep Sounding: Descriptive statistics of TPA of all measurable serrated pieces measured with the goniometer and calculated with the formula:  $\arctan(\text{width}/10 \text{ mm (known distance from tip)})/\text{Pi} \times 180$ .

	TPA (goniometer)	TPA (formula)
n	10	10
Min	22	32.2
Max	71	58
Sum	522	455.1
Mean	52.2	45.5
Std. error	5.2	3.1
Variance	275.1	96.6
Stand. dev.	16.6	9.8
Median	57	48.8
25 prcntil	38	33.9
75 prcntil	66.8	52.8

have a convergent medial part, while 40% exhibit a parallel medial part. The serration of 87.5% of the pieces (n=21) continues from the point area towards the medial part. Eleven of these tools demonstrate bilateral continuation, while five each show sinistrolateral or dextralateral continuation of the serration. Twelve artefacts have their base preserved, of which four show basal thinning. Two thirds of these bases are quadrangular and one third is elliptic.

In spite of the limited sample size, technological variability within the serrated pieces can be observed, specifically in terms of their reduction sequences (Rots, et al., 2017: 9ff.). The population can be subdivided into two subgroups: bifacially shaped blanks that were bilaterally (n=11) serrated, and bifacially (or unifacially) retouched blanks that were bilaterally (or laterally) serrated (n=14). No firm traces of reworking were recognised on the serrated pieces, suggesting that the serration was not only the last stage of the manufacturing process but also its final stage (Rots, et al., 2017: 10).

Concerning the first subgroup, the toolmakers started with the selection of a usually elongated blank, proceeding first with bifacial shaping and subsequently serrating. They shaped it by direct percussion until they achieved the desired dimension and suitable bilateral and bifacial symmetries. The set-up and, in particular, the preparation of the final bifacial forms is thus strongly associated with the different parameters of the percussive technique; i.e. the applied force, the motion of the percussion, and the location of the impact point. Only after this bifacial shaping procedure, was a series of notches set up, intended to serrate the edges. Seven of the pieces are made on quartz, three on dolerite and one on quartzite. Together with use-wear and residue analysis, we could show that three of the tools were not used and two definitely either broke or were discarded during manufacture (Figure 75n, o, t) (see Rots, et al., 2017: Table 11). Four of the bifacially shaped serrated pieces show only one serrated edge, but two of them represent unfinished products discarded in production and two others are basal fragments.



The reduction sequence of the second subgroup involves bifacially retouched blanks that were bilaterally (or laterally) serrated (n=9) and unifacially retouched blanks that were laterally serrated (n=5). As for the first subgroup, the knappers preferentially selected laminar products, then applied bifacial or unifacial retouch to prepare the edges in terms of angle and platform for the serration. Twelve of the tools are made on dolerite and two on hornfels. All of the unifacially retouched blanks that were laterally serrated seem to have been discarded during production and were therefore not considered for functional analysis (Rots, et al., 2017: 11). The bifacially retouched population encompasses three elements that most likely were not completed and again were excluded from functional analysis (Figure 75r, s, v). The serrated piece B4-1552 (Figure 75r) clearly demonstrates that the toolmaker(s) encountered problems in shaping the dextralateral edge and abandoned the piece. Two of the three unfinished tools are only laterally serrated, while all finished bifacially retouched blanks were bilaterally serrated.



**Figure 76.** Sibudu. C-A layers from the Deep Sounding: Pressure flaking experiments. a) Christian Lepers conducting the pressure flaking; b) pressure flaking of crystal quartz (Exp. 84/12 piece fractured in the production sequence); c) pressure flaking of dolerite (Exp. 82/22 piece finished used as projectile (see Rots, et al., 2017: Figure 7)).

Rots et al. (2017) combined multiple lines of evidence, including my technological study, as well as functional analysis and experiments (Figure 76). They examined different types of data, including the negative traces on the serrated pieces themselves, positive traces from the shaping flakes, and wear and residue evidence representing the remnant traces of the manufacturing process, to verify that the final series of notches creating the serrations was applied by pressure technique.

The width and depth of the notches and their spacing are important parameters to deduce the use of pressure (Akerman and Bindon, 1995; Akerman, et al., 2002; Lombard, et al., 2010). The regularity of notches on a single piece indicates a clear control of the locations of the contact points as well as of the applied force. The serrated pieces demonstrate variation in their notches. The serration is not equally explicit on all pieces. Some tools – generally the finished products – are regularly serrated all along their edges (see Rots, et al., 2017: Figure 9), while others show more discontinuous serrations. Some tools have deep notches while notches on others are very shallow. The serration never occurs at the base of the pieces, whereas notches are always visible on the medial part and, to a lesser extent, on the distal part. Taking into account all the finished and completely preserved pieces (n=5), these tools average 16 notches per finished piece (i.e. eight notches per edge). The notches have a mean width of  $3.1 \pm 1.7$  mm and a mean depth of  $0.5 \pm 0.3$  mm. When considering the finished tools (n=13), eleven pieces have a notch width with a standard deviation less than 1.7 mm and the values of only two pieces exceed the standard deviation for the notch depth of 0.3 mm. The serration seems to have been more regular on each piece than between pieces, indicating strong internal homogeneity and control of the notches on individual pieces. Furthermore, in contrast to percussion where the edges need to be convex or rectilinear to ensure a good contact with the hammer, pressure technique allows detachment of removals in areas that cannot be reached by percussion. The serration of a few pieces is symmetric; i.e. the last notch was initiated within the concavity of the previous one (Rots, et al., 2017: 23). Additionally, the negatives of the serrating removals exhibit small hackles, negative bulbs, parallel edges and feathered terminations which are diagnostic of a narrow contact point (Mourre, et al., 2010; Högberg and Lombard, 2016; Rots, et al., 2017). Minor abrasion occurring on some of the finished and unfinished pieces is typically applied before the use of pressure technique to create an artificial placement of the compressor tip interior of the edge (Rots, et al., 2017: 23).

Concerning the serration flakes, a study of all flakes (<30-5 mm) made on quartz was undertaken, with flakes from square C4 and layer Bart serving as reference to illustrate proportions of retouch, shaping and serration flakes (Rots, et al., 2017: 26ff.). Quartz was selected because it represents one of the primary raw materials for the serrated pieces and the visibility of technical damages is clearer compared to dolerite or quartzite. The distinction of shaping and serrating flakes is based on the thickness of the platform and the overall morphology. A number of 281 of the flakes < 30 mm made on quartz (out of a total of 2963) involve a strict minimum of 27 (9.6%) shaping flakes, including three serrating flakes. The serrating flakes have a mean platform width value of  $3.9 \pm 1.9$  mm and a mean platform thickness value of  $1.5 \pm 0.6$  mm in accordance with the measurements on the serrated pieces directly. The shape of the platforms' surfaces is either straight (n = 12), convex (n = 4) or concave

(n = 2). The convex and concave examples are characteristic of the presence of the contact point within a concavity suggesting a phase of symmetric bifacial serration. However, one serrating flake has a contact point directly on the convexity of a ridge indicating a phase of asymmetric bifacial serration. The serration blanks are short and have predominantly parallel edges. Nine flakes exhibit a clear bulb, while neither contact points nor lips occur. Abrasion of the dorsal overhang of the butt is rare and therefore does not represent an absolute precondition for notching. Shattered bulbs and bulbar scars are rare, but eight serrating flakes show parasite shatters initiating obliquely to the axis of the flake. While this might relate to the nature of the raw material, the parasite shatters could also point to the presence of an opposite force while the flake was detached, such as the force of a pressure tool slightly opposed to the force applied by the hand holding the piece.

Microscopic study revealed bone residues in association with negatives of the serrations (Rots, et al., 2017: 23). Correspondingly among the corpus of bone tools, one bone fragment from layer Casper is identified as a bone compressor since it exhibits macro- and microscopic wear traces consisting of crushing, small fracture negatives and striations that are similar to the experimentally-used bone compressor (Rots, et al., 2017: Figure 12 & Figure 13). Moreover, several small bone flakes from the sieved buckets match the experimental bone flakes that occasionally unintentionally come off the tip of a bone compressor during its use. Their features are a rectangular to trapezoidal shape, a crushed platform, a small bulb, a straight profile and unidirectional dorsal removals. In conclusion, the width of the extremity of the purported bone compressor (2.5 mm) concurs with the width of the notches on the serrated pieces, ranging between 2 mm and 4 mm.

The evidence outlined above strongly points to the application of pressure technique in tool serration. While pressure flaking usually aims at regularising an edge and thinning the sections of the tool, here the serrated edges more likely result from pressure notching. In the case of pressure notching, the compressor has to be placed slightly interior of the edge and the force has to be applied at an angle roughly perpendicular to the plane of the blank (Crabtree, 1973; Callahan, 1985 (revised 1989); Whittaker, 1994; Lepers, 2010). This angle influences the depth of the notch and determines the thickness and breadth of the platform and the overall morphology of the serration flakes.

Largely as a result of the use-wear and residue analyses and their associated experiments, a wide range of functional data was able to shed light on the use and handling of the serrated pieces (Rots, et al., 2017: 30ff.). The impact-related damage and the protein residues associated with usage on animal material (see for an example Rots, et al., 2017: Figure 20) in the distal area of thirteen serrated pieces from this assemblage attest to their use as mounted tips on shafts of hunting weapons. One quartz distal fragment had abundant starch granules strongly adhered to the tip, which might point to the attaching of plant-based poison (Rots, et al., 2017: Figure 23).

The proximal parts of several pieces show wear traces (see for an example Rots, et al., 2017: Figures 15 – 17) and residues which can be recognised as evidence for hafting. Toolmakers at least occasionally utilised bindings of sinew, skin and plant tissue combined with

resin to attach the points. Different residues of *Podocarpus falcatus* wood strongly suggest that this species played an important role as an adhesive (Rots, et al., 2017: Figure 27). Moreover, the appearance of resinous residues in conjunction with, among other things, red ochre/haematite of a small particle size, strongly suggest the manufacture and use of compound adhesives made from finely ground red ochre mixed with plant gum (see for an example Rots, et al., 2017: Figures 24a-c). One small cobble with ochre staining comes from layer Chantal and has likely been employed as a grinder/polisher to prepare the red ochre for use as a loading agent (Rots, et al., 2017: Figure 28). Finally, residue analysis identified remains of either *Urena lobata* L. or *Pavonia spp.* belonging to the family Malvaceae. Both genera have a strong bast fibre commonly used for cordage, but additionally the wood of both is light and strong with straight stems, suitable for shafts. The basal width averages 17.4 mm in total (n=14); 19.8 mm for dolerite, 11.3 mm for quartz, and 20 mm for hornfels (Rots, et al., 2017: Table 6). The basal width together with the thickness represent important size parameters for the shaft width; for example, the shaft cannot be wider than the projectile as it would impede its intrusion into the target. Therefore, the shafts must have a maximum of approximately 12 mm in diameter which corresponds well to the stem size of the Malvaceae shrubs.

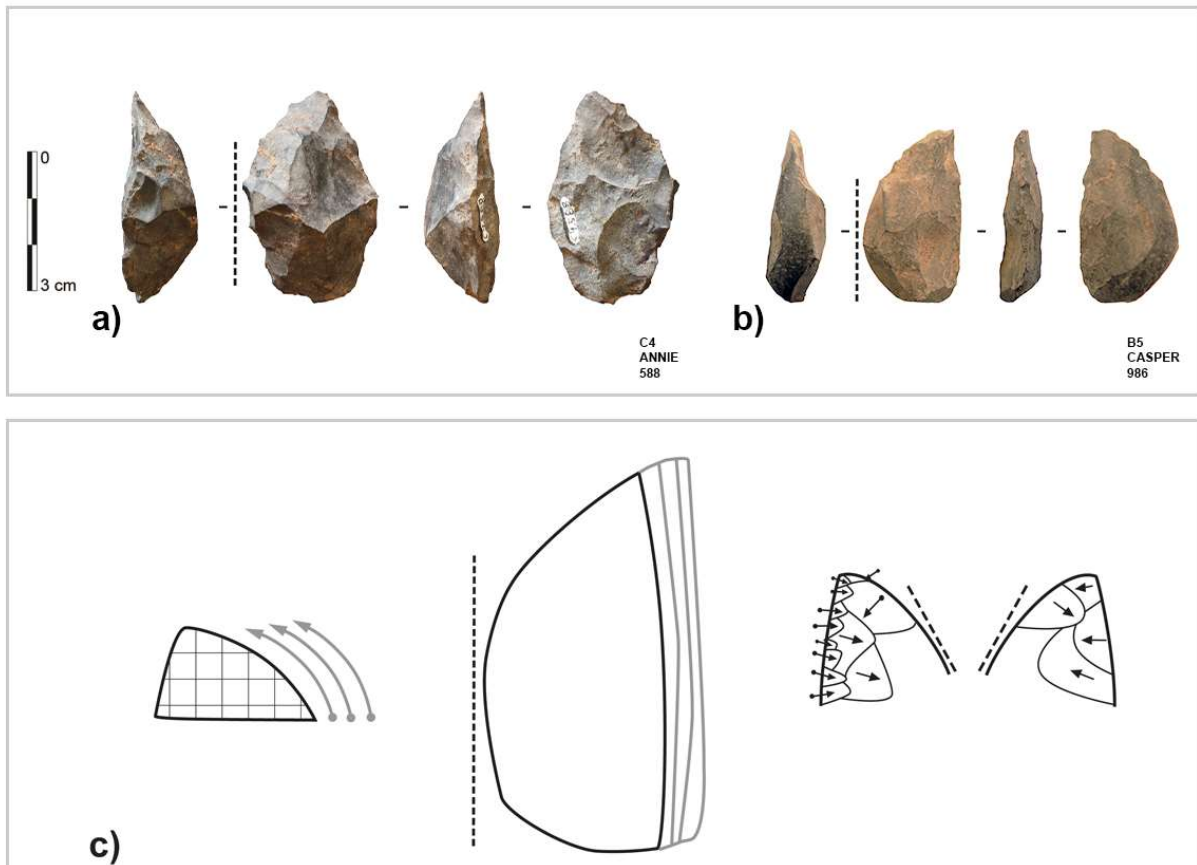
### 5.6.2.3. Bifacially Backed Knives

The assemblage contains a total of five bifacially backed knives (Figure 77). Their structure, in terms of the techno-functional characterisation, complies with what has been called asymmetrically bifacially backed knives (*Keilmesser*) in the literature (see Jöris, 2006; Frick, et al., 2018). One bifacial tool originates from layer Annie and another one from layer Casper, with the remaining three from layer Bea (Table 83).

Two each of the bifacially backed knives are made on dolerite and quartzite, and one on quartz (Table 96). Three of the tools are complete, while the other two represent a proximal and a distal fragment (Table 101). The length ranges between 35.3 mm and 44.9 mm. The mean width is 23.1 mm and the mean thickness 11.8 mm. The complete pieces have a mean length-to-width ratio of 1.6. The total width-thickness ratio is  $2 \pm 0.2$ . The original blank of two tools could be determined; one is an elongated flake and the other one a blade (Table TOOL 97). Three of these bifacial tools show dorsal cortex coverage. Four tools have straight profiles and only one demonstrates a curved profile. The tool class is characterised by exclusively planoconvex cross-sections (Table 105).

Concerning the morphotype, the bifacial tools are shaped bifacially asymmetrically. The toolmakers designed these tools to create a robust working edge opposite to either a natural back or one prepared with steep, large removals. Towards the distal end on the lateral with the back, the retouch changes to a less abrupt angle forming a sharp edge which converges with the opposing working edge. The distal part exhibits a tip lacking a regular pointed outline. The medial part is composed of the rectilinear working edge and the towards the distal part converging edge with the back. The base most commonly has a quadrangular morphology.

With regard to the manufacture process, all of the bifacial tools seem to be finished products, with one exception. Piece C4-588 (Figure 77a) exhibits large removals on the dextralateral working edge truncating the more carefully spaced and less deep previous removals, suggesting that this tool is in a phase of reworking. The organisation of the shaping generally proceeded hierarchically. The knappers started with shaping of the flat surface and then modified the working edge. Due to this procedure, the bifacial tools have an asymmetric section allowing for frequent re-sharpening episodes, especially on the convex face.



**Figure 77.** Sibudu. C-A layers from the Deep Sounding: Bifacial tools. a & b) made on dolerite (Photos by Viola C. Schmid); c) Schematic model showing re-sharpening of bifacial tools and removal organisation.

### 5.6.3. Scrapper-like Forms

Scrapper-like forms, including lateral scrapers, NBTs and a few end-scrapers, occur throughout the sequence reaching the highest proportion at 16.2% in layer Annie and the lowest proportion at 6.8% in layer Chantal (Table 82). This tool type includes lateral scrapers (n=38), NBTs (n=26), and end-scrapers (n=5).

### 5.6.3.1. Lateral Scrapers

The lateral scrapers are most common in the uppermost layer Adam at 9.7% and show the lowest frequency in layer Bea at 3.4% (Table 83).

Large dolerite blades or elongated flakes often served as original blanks for the manufacturing of lateral scrapers (Figure 74a-e). A total of 86.8% of the lateral scrapers are made on dolerite (Table 96). The remaining tools are made on quartzite (10.5%) and hornfels (2.6%). Blades form 73.7% of the original blanks of this tool class and elongated flakes 21.1% (Table 97). The majority of the pieces is fragmented, mostly comprising proximal fragments (57.9%) (Table 101). Only six pieces are completely preserved showing a mean length value of 47.3 mm (Table 110). The pieces have a robustness demonstrating a mean width value of 33.6 mm and a mean thickness value of 10.7 mm (Table 110). The EPA averages 85.8° and the platform depth 8.3 mm. The mean EPA value significantly exceeds that of the unifacial pointed forms ( $t = 3.4631$ ;  $F = 3.5852$   $p = <0.001$ ) and the denticulates ( $t = 4.9518$ ;  $F = 1.7706$   $p = <0.001$ ). Both values are significantly greater than the mean values of the unmodified blank population ( $t$ -test concerning EPA,  $t = 5.2061$ ;  $p = <0.001$ ;  $t$ -test concerning platform depth,  $t = 5.2061$ ;  $p = 0.0066$ ). These variables strongly related to the blank size indicate that the knappers preferably selected blanks of large size – even larger than the blanks for the other tool classes – to use them as lateral scrapers. The width-to-thickness ratio is  $3.8 \pm 3.7$ . A total of 55.3% of the tools show no cortical remains. The cortex of the specimens with cortical coverage is primarily laterally and, to a lesser extent, distally located, sometimes covering more than 50% of the dorsal surface. Therefore, past people partially transformed pieces of the earliest stage of reduction when the lateral and distal expansion of the removal surface was conducted. Fifty percent of the elements have a plain

**Table 110.** Sibudu. C-A layers from the Deep Sounding: Descriptive statistics of length, width and thickness of the lateral scrapers.

	Length	Width	Thickness
n	6	33	36
Min	35	17.6	0.9
Max	71.4	68	20.5
Sum	283.6	1110.1	384.7
Mean	47.3	33.6	10.7
Std. error	5.6	1.8	0.7
Variance	189.5	106.5	15.6
Stand. dev.	13.8	10.3	3.9
Median	42.5	33.9	9.9
25 prcntil	37.2	24.4	8.4
75 prcntil	58.7	38.9	12

platform, while 28.6% of platforms are dihedral and 17.9% are faceted (Table 100). The profiles of lateral scrapers are prevalingly straight at 52.6%, but curved and twisted original blanks are also frequent indicating that straightness was not a prerequisite for this tool type. In contrast, 81.6% of the objects show parallel edges which seems to have been a selection criterion. The artefacts show either a triangular (45.9%) or trapezoidal (43.2%) cross-section.

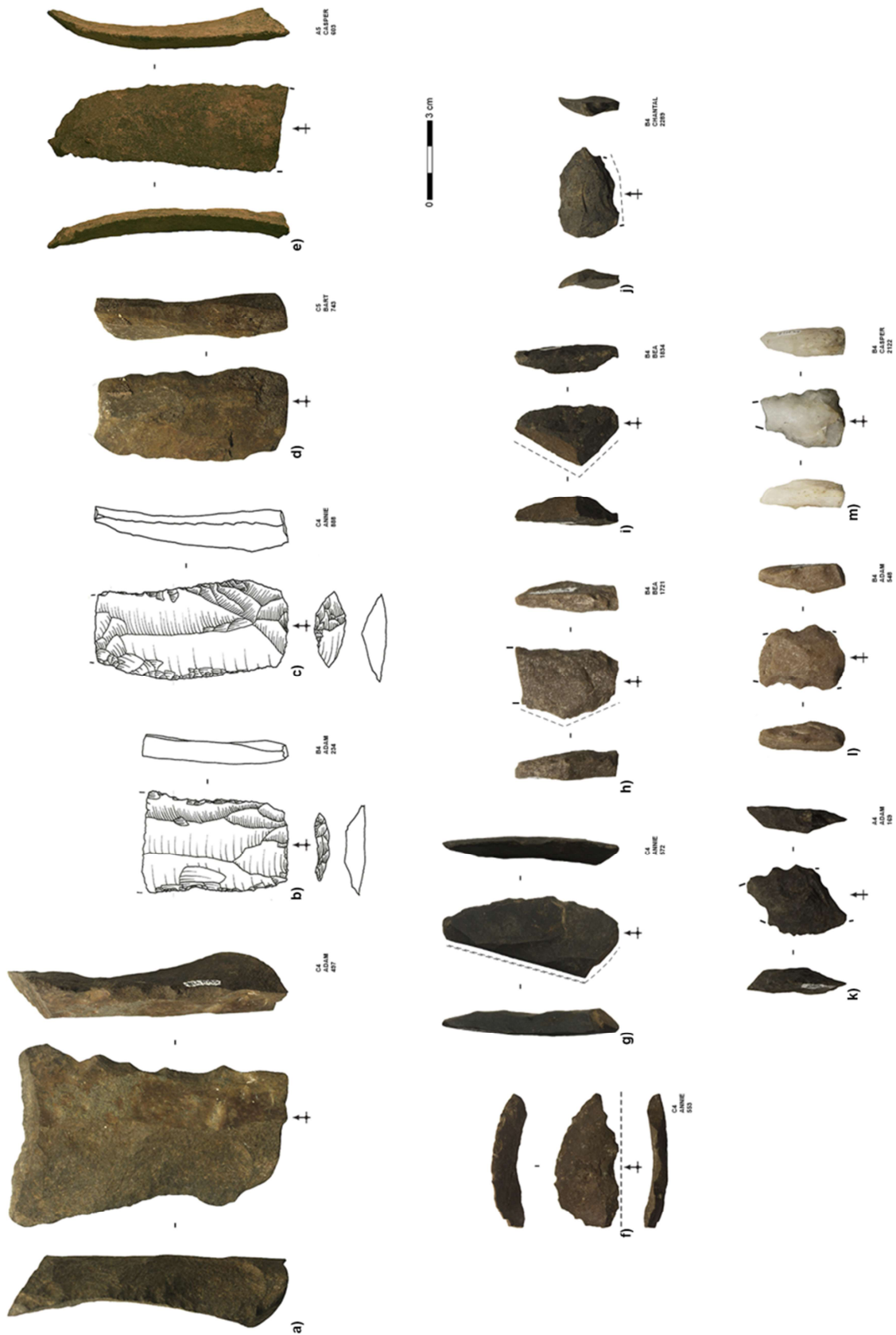
47.4% of the lateral scrapers show retouch on both edges, while 13.2% exhibit retouch only on their sinistrolateral edge and 31.6% on their dextralateral edge. The retouch is variable, ranging from fine retouch scars to large removals.

### **5.6.3.2. NBTs**

The NBTs (Figure 78f-j) are most frequent in layer Annie at 10.8% and least frequent in layer Chantal at 1.1% (Table 83).

The highest percentage (73.1%) is made on dolerite, followed by 19.2% made on quartzite (Table 96). One hornfels and one quartz tool are present as well. The toolmakers used a variety of original blanks to transform them into NBTs. A total of 34.6% of blades and 23.1% of elongated flakes were used (Table 97). Additionally, 26.9% of the NBTs were made on flakes, including crest and platform preparation flakes and a shaping flake (Figure 78f). The blank of the remaining pieces (15.4%) was not identifiable. A proportion of 23.1% is completely preserved, while the majority (38.5%) is proximal fragments (Table 101). The length of the NBTs ranges from 25.2 mm to 63.9 mm with a mean value of 40.3 mm (Table 111). The width averages 29.8 mm and the thickness 10.9 mm (Table 111). The width-to-thickness ratio amounts to  $3.1 \pm 1.7$ . A total of 69.2% of the artefacts exhibit cortex coverage primarily in the form of a back or laterally. The largest proportion has plain platforms at 62.5% followed by dihedral platforms at 25% (Table 100). Straight profiles (65.4%) dominate the NBT population. Fifty percent have parallel edges, while 34.6% show one rectilinear and one converging edge. A total of 57.5% of the tools exhibit trapezoidal cross-sections, followed by 34.6% of triangular cross-sections.

The transformative part is dextralateral at 57.7% and sinistrolateral at 34.6%. Most of the time the retouch is direct, but in a few cases knappers installed the retouch ventrally (11.5%). The backing is located opposite to the working edge. Although the back is sometimes created by removals (23.1%), the back is usually natural concurring with the defining characteristic. The backs are predominantly formed by cortex (34.6%), but can be a Siret fracture (26.9%), the platform of a blank (7.7%) or from a core-edge product (7.7%).



**Figure 78.** Sibudu. C-A layers from the Deep Sounding: Lateral scrapers (a-e), NBTs (f-j) and denticulates (k-m). All lateral scrapers made on dolerite; NBTs made on dolerite (f, i, j), made on hornfels (g), and made on quartzite (h); denticulate made on dolerite (k), denticulate made on quartzite (l), and denticulate made on quartz (m) (Drawings by Heike Würschem and Mojdeh Lajmiri; photos by Viola C. Schmid).



**Table 111.** Sibudu. C-A layers from the Deep Sounding: Descriptive statistics of length, width and thickness of the NBTs.

	Length	Width	Thickness
n	6	26	26
Min	25.2	16.5	4.4
Max	63.9	74.2	28.7
Sum	241.9	774.6	282.4
Mean	40.3	29.8	10.9
Std. error	7.1	2.8	1
Variance	302.8	202.2	26.6
Stand. dev.	17.4	14.2	5.2
Median	33.1	25.2	9.7
25 prcntil	26.6	21.1	7.2
75 prcntil	60.8	34.4	12.9

#### 5.6.4. Denticulates/Notch

Denticulates (Figure 78k-m) or notched pieces are consistently present in all strata. Six tools have a single notch and are therefore classified as notched pieces, rather than the succession of adjacent notches that defines denticulates (n=33) (see Inizan, et al., 1999: 138). The highest proportion (8.8%) comes from layer Casper and the lowest proportion (4.5%) from the lowermost layer Chantal.

The greatest number of denticulates are made on dolerite (74.4%), followed by quartzite (12.8%) (Table 84). Two pieces each of hornfels and quartz, and one chert artefact are also present. The knappers preferentially modified blades at 51.3% and elongated flakes at 20.5% into denticulates and notched pieces (Table 90). Only 10.3% of the tools are completely preserved, while the greatest proportion represents either proximal or medial fragments. The length of the four complete artefacts averages 44.2 mm (Table 85). The denticulates and notched pieces show a mean width of 27.3 mm (Table 86) and a mean thickness of 8.5 mm (Table 87). The width-to-thickness ratio has a value of  $3.3 \pm 0.8$ . Cortex coverage was documented on only 30.8% of the pieces (Table 91). The platforms of the original blanks are mostly plain (60%), but 25% of the platforms are dihedral and further 10% are faceted (Table 92). Most of the tools have a straight profile at 76.9% (Table 93). The edges are primarily parallel at 56.4%. Trapezoidal cross-sections dominate at 43.6%, ahead of triangular cross-sections at 33.3% (Table 94).

The single concave indents of the six notched pieces have a mean width of  $12.7 \pm 6.6$  mm and mean depth of  $2.7 \pm 1.6$  mm. The denticulation of the remaining denticulates (n=33) occurs either sinistrolaterally (48.5%), dextrilaterally (36.4%) or bilaterally (15.2%). In total, 129 notches have been identified across all tools. The highest number counted on one denticulate is eight notches. The tools demonstrate a denticulation with rather wide notches, of which some are deep, but some are very shallow. The notches generally have a mean width of  $7 \pm 2.9$

mm and a mean depth of  $1.1 \pm 0.5$  mm. The denticulation shows more regularity on each piece than between pieces. The value of the width of the notches on only one piece exceeds the standard deviation of 3 mm and three pieces demonstrate a greater standard deviation for the notch depth of 0.5 mm. However, great variability stands out between the denticulates as their mean notch width ranges between 3.2 mm and 12.7 mm and their mean notch depth between 0.2 mm and 2.2 mm.

### *5.7. Taphonomy*

Here, I present the data relating to edge damage, thermal alteration, and heavy encrustations observed on the lithics to emphasize their primary anthropogenic character, but also to document the effect of diagenetic processes.

I identified edge damage, which involves damage caused either by utilisation or by post-depositional influences, including solifluction or trampling, on the blanks of all raw materials (Table 112). Chert and hornfels show the highest proportion of objects with edge damage. This is largely related to the rock properties as these rocks are more prone to breakage than other raw materials, such as dolerite.

Furthermore, thermal alteration in the form of irregular breakage surface and shelled spalling occurs predominantly on hornfels, followed by chert (Table 113).

Finally, during the recording process, I noticed that even after washing, some of the artefacts had heavy sintering of sediment still attached to their surfaces and showed traces of weathering. A trend becomes apparent whereby the encrustation on the artefacts of virtually all raw materials increases towards the lowermost layer Chantal (Table 114). A total of 77.4% of the pieces with extreme attachment of encrustation originate from the eastern part of the excavation area, namely squares A4, B4, and C4. Interestingly, from layer Bea onwards an absence of bone is also documented in the area of the south-eastern corner further expanding in the layers below (Figure 22), indicating diagenetic alteration.

**Table 112.** Sibudu. C-A layers from the Deep Sounding: Frequency of edge damage on all blanks by raw material.

Layer	Dolerite			Hornfels			Quartz			Quartzite			Sandstone			Chert			Total		
	edge damage	no edge damage	Total	edge damage	no edge damage	Total	edge damage	no edge damage	Total	edge damage	no edge damage	Total	edge damage	no edge damage	Total	edge damage	no edge damage	Total	edge damage	no edge damage	Total
ADAM	49.4%	50.6%	1459	76.2%	23.8%	21	30.0%	70.0%	20	52.9%	47.1%	68	51.7%	48.3%	58	75.0%	25.0%	4	49.8%	50.2%	1630
ANNIE	50.8%	49.2%	789	27.3%	72.7%	11	40.0%	60.0%	5	56.7%	43.3%	60	55.8%	44.2%	86	100.0%	0.0%	2	51.4%	48.6%	953
BART	58.8%	41.2%	896	81.8%	18.2%	11	38.5%	61.5%	13	56.9%	43.1%	51	49.5%	50.5%	91	40.0%	60.0%	5	57.8%	42.2%	1067
BEA	50.7%	49.3%	1194	50.0%	50.0%	12	20.0%	80.0%	15	61.2%	38.8%	49	62.5%	37.5%	152	80.0%	20.0%	5	52.1%	47.9%	1427
CASPER	55.7%	44.3%	990	90.9%	9.1%	11	50.0%	50.0%	22	69.8%	30.2%	43	72.1%	27.9%	179	66.7%	33.3%	3	58.7%	41.3%	1248
CHANTAL	53.2%	46.8%	806	71.4%	28.6%	7	64.3%	35.7%	14	46.7%	53.3%	60	54.9%	45.1%	122	100.0%	0.0%	1	53.4%	46.6%	1010
<b>Total</b>	<b>52.7%</b>	<b>47.3%</b>	<b>6134</b>	<b>67.1%</b>	<b>32.9%</b>	<b>73</b>	<b>40.4%</b>	<b>59.6%</b>	<b>89</b>	<b>56.5%</b>	<b>43.5%</b>	<b>331</b>	<b>60.2%</b>	<b>39.8%</b>	<b>688</b>	<b>70.0%</b>	<b>30.0%</b>	<b>20</b>	<b>53.6%</b>	<b>46.4%</b>	<b>7335</b>

**Table 113.** Sibudu. C-A layers from the Deep Sounding: Frequency of thermal alteration by raw material.

Layer	Dolerite		Hornfels		Quartz		Quartzite		Sandstone		Chert		Indetermined		Total		
	thermally altered	not thermally altered	thermally altered	not thermally altered	thermally altered	not thermally altered	thermally altered	not thermally altered	thermally altered	not thermally altered	thermally altered	not thermally altered	thermally altered	not thermally altered	thermally altered	not thermally altered	Total
ADAM	5.1%	94.9%	18.8%	81.3%	0.0%	100.0%	3.1%	96.9%	1.6%	98.4%	14.3%	85.7%	0.0%	0.0%	5.1%	94.9%	1814
ANNIE	5.6%	94.4%	23.8%	76.2%	10.0%	90.0%	2.6%	97.4%	1.1%	98.9%	50.0%	50.0%	0.0%	0.0%	5.5%	94.5%	1057
BART	3.7%	96.3%	18.8%	81.3%	0.0%	100.0%	4.5%	95.5%	1.1%	98.9%	0.0%	100.0%	0.0%	100.0%	3.6%	96.4%	1183
BEA	3.0%	97.0%	22.2%	77.8%	0.0%	100.0%	0.0%	100.0%	0.0%	100.0%	0.0%	100.0%	0.0%	0.0%	2.7%	97.3%	1595
CASPER	3.1%	96.9%	26.1%	73.9%	0.0%	100.0%	0.0%	100.0%	1.1%	98.9%	0.0%	100.0%	0.0%	100.0%	2.9%	97.1%	1393
CHANTAL	4.9%	95.1%	11.1%	88.9%	0.0%	100.0%	0.0%	100.0%	1.6%	98.4%	100.0%	0.0%	0.0%	0.0%	4.3%	95.7%	1122
<b>Total</b>	<b>4.2%</b>	<b>95.8%</b>	<b>21.0%</b>	<b>79.0%</b>	<b>0.6%</b>	<b>99.4%</b>	<b>1.7%</b>	<b>98.3%</b>	<b>1.0%</b>	<b>99.0%</b>	<b>12.9%</b>	<b>87.1%</b>	<b>0.0%</b>	<b>100.0%</b>	<b>4.0%</b>	<b>96.0%</b>	<b>8164</b>

**Table 114.** Sibudu. C-A layers from the Deep Sounding: Frequency of heavy sintering by raw material.

Layer	Dolerite			Hornfels			Quartz			Quartzite			Sandstone			Chert			Indetermined			Total		
	heavy sintering	no heavy sintering	Total	heavy sintering	no heavy sintering	Total	heavy sintering	no heavy sintering	Total	heavy sintering	no heavy sintering	Total	heavy sintering	no heavy sintering	Total	heavy sintering	no heavy sintering	Total	heavy sintering	no heavy sintering	Total	heavy sintering	no heavy sintering	Total
ADAM	0.6%	99.4%	1584	0.0%	100.0%	32	0.0%	100.0%	33	0.0%	100.0%	97	0.0%	100.0%	61	0.0%	100.0%	7	0.0%	0.0%	0	0.5%	99.5%	1814
ANNIE	0.3%	99.7%	859	0.0%	100.0%	21	0.0%	100.0%	10	0.0%	100.0%	78	0.0%	100.0%	87	0.0%	100.0%	2	0.0%	0.0%	0	0.3%	99.7%	1057
BART	0.4%	99.6%	962	0.0%	100.0%	16	0.0%	100.0%	38	0.0%	100.0%	66	1.1%	98.9%	94	0.0%	100.0%	5	0.0%	100.0%	2	0.4%	99.6%	1183
BEA	3.0%	97.0%	1304	0.0%	100.0%	18	0.0%	100.0%	32	0.0%	100.0%	75	1.9%	98.1%	157	0.0%	100.0%	9	0.0%	0.0%	0	2.6%	97.4%	1595
CASPER	5.8%	94.2%	1068	0.0%	100.0%	23	0.0%	100.0%	44	2.9%	97.1%	69	3.9%	96.1%	181	0.0%	100.0%	6	0.0%	100.0%	2	5.1%	94.9%	1393
CHANTAL	9.2%	90.8%	879	0.0%	100.0%	9	5.6%	94.4%	18	3.4%	96.6%	88	5.6%	94.4%	126	0.0%	100.0%	2	0.0%	0.0%	0	8.2%	91.8%	1122
<b>Total</b>	<b>3.0%</b>	<b>97.0%</b>	<b>6656</b>	<b>0.0%</b>	<b>100.0%</b>	<b>119</b>	<b>0.6%</b>	<b>99.4%</b>	<b>175</b>	<b>1.1%</b>	<b>98.9%</b>	<b>473</b>	<b>2.5%</b>	<b>97.5%</b>	<b>706</b>	<b>0.0%</b>	<b>100.0%</b>	<b>31</b>	<b>0.0%</b>	<b>100.0%</b>	<b>4</b>	<b>2.7%</b>	<b>97.3%</b>	<b>8164</b>

## 6. Discussion

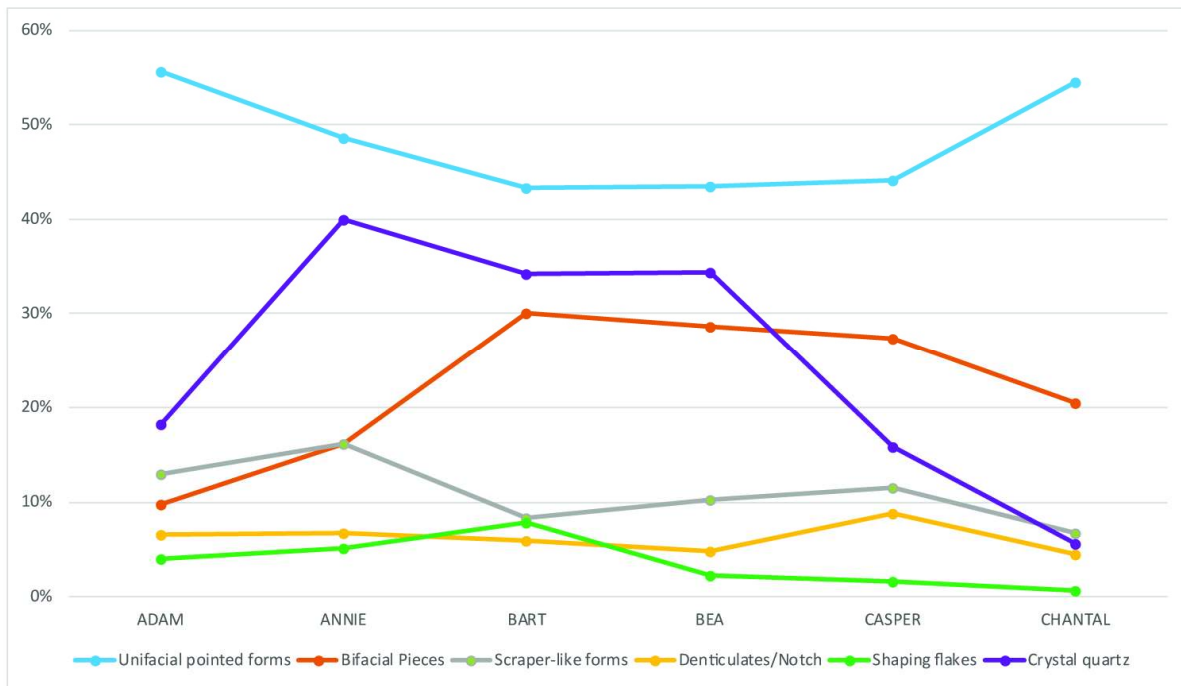
### 6.1. Insights into the way of life

In this sub-chapter, I will summarise the data presented in the results section and then overview the technological and techno-economic features of the C-A layers. This will formulate statements about the core reduction strategy, tool design and variability, raw material economy, subsistence patterns and mobility strategies, allowing me to provide an interpretation of how past people organised their daily life and settlement system at Sibudu in response to their resource needs and the environmental conditions.

To begin with, I underline the overall similarities documented in terms of raw material selection, blank production and tool manufacture that unite the lithic assemblages of the C-A layers. **The homogeneity of the assemblages leads to the conclusion that they can be considered as one technological tradition.** All strata are characterised by a predominance of dolerite (Table 6), a blank population involving >20% of blades, >10% of elongated flakes and >50% of flakes (Table 16), a low occurrence of triangular flakes, the presence of mainly platform blade cores and bipolar cores (Table 60), and a tool corpus including primarily unifacial pointed forms, followed by bifacial tools, scraper-like forms and denticulates (Table 82). The specific laminar reduction strategy which results in two subgroups of laminar end-products, together with diagnostic preparation flakes and typical exhausted cores, stretches as a main feature through the sequence. Moreover, the tool types and the tool classes of importance occur in all deposits (Table 83).

In spite of this overall homogeneity, I identified five trends within the sequence concerning the emergence and frequency of particular formal tools in different layers:

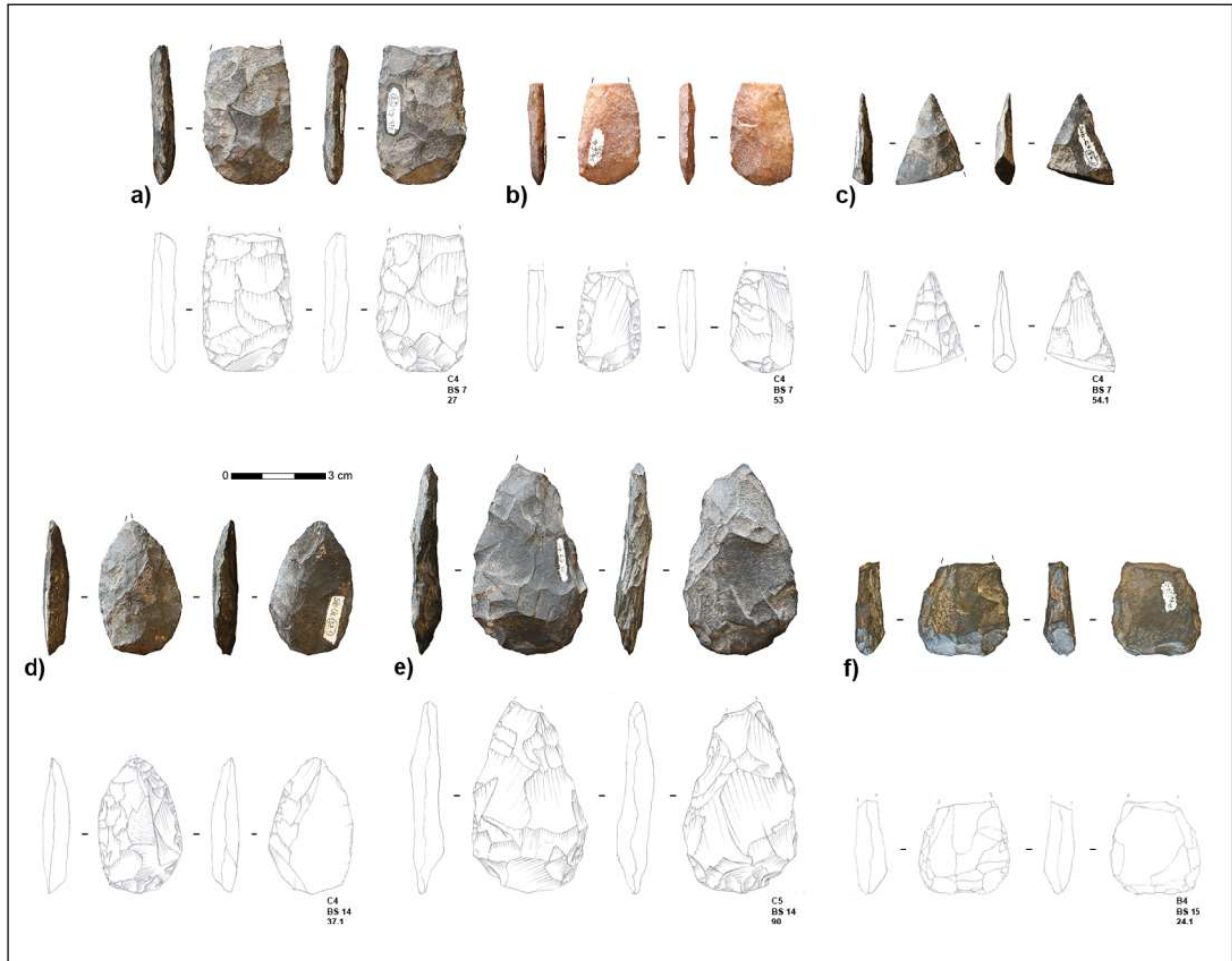
- (1) The unifacial pointed forms are most frequent in the uppermost layer Adam. They decrease in layer Annie and have their lowest proportion in layer Bart, then increasing again towards the lowermost layer Chantal.
  - (2) The tool class of TSPs has its lowest occurrence in Bart and increases in the strata below showing a peak in layer Chantal.
  - (3) ACTs are most frequent in Adam and decrease subsequently.
  - (4) The bifacial pieces show the opposite trend to the unifacial pointed forms with their lowest number in the uppermost deposit Adam, but increasing towards layer Bart. In fact, Bart contains the peak number of bifacial elements and shaping flakes in the whole sequence, after which bifacial tool frequencies decrease again.
  - (5) The serrated pieces appear only from layer Bart onwards and have the highest proportions in layers Bea and Bart. However, the occurrence of serrating flakes in the strata above indicates that toolmakers also produced these tools during the occupation period of deposits Adam and Annie but the pieces were probably discarded elsewhere. Regardless, serrated pieces might in fact be less present in the uppermost deposits considering that bifacial shaping or retouching precedes the serrating of a tool and bifacial pieces are less common in these layers generally.
- (5) Scraper-like forms are most frequent in the two uppermost layers. Adam contains the most lateral scrapers, while Annie has the most NBTs.



**Figure 79.** Sibudu. C-A layers from the Deep Sounding: Frequency distribution of tool types and shaping flakes.

**The distribution curve (Figure 79) of tool types highlights the peak of bifacial technology, together with shaping flakes, in layer Bart which also marks the low point of almost all other tool types.** A trend becomes apparent that bifacial piece numbers increase from Adam to Bart, after which they slowly decrease, while the unifacial pointed forms present the reverse pattern. Additionally, quartz and crystal quartz in particular, plays an important role in the manufacturing of bifacial tools, since 82.8% of the tools made on crystal quartz are bifacial pieces. Interestingly, the proportion of crystal quartz is highest in layers Annie, Bart, and Bea, with both a sharp increase before and decrease after these layers (Figure 79).

In order to hypothesise about a possible start and end of the technological phase encompassed by layers C-A, I have to consider the SUs above and below my sample for context. The BS member is located directly on top of the uppermost layer Adam. Wadley (2012a, 2013) provides a preliminary description of the BS strata, stating that the lower part (BS 11 to BS 16) features large blades and flakes made on different raw materials, including dolerite, hornfels, quartz, and quartzite, and typologically is characterised by bifacial points. The younger deposits (BS to BS 10) include flakes and blades, but besides unifacial points and denticulates made on dolerite, other tools are rare. The University of Tübingen also excavated a total volume of 287 litres in the BS member (Figure 64). A first examination of the tool corpus resulted in the identification of six bifacial pieces coming from BS 7, BS 14, and BS 15 (Figure 80). I additionally undertook a preliminary study of the eleven cores from the BS member. Eight cores came from layers BS 12 to BS 15, including five platform blade cores exhibiting a configuration that corresponds to the laminar reduction strategy identified in the C-A layers, two bipolar cores and one indeterminate broken core. Three cores were from layers BS and BS 6 comprising one unidirectional recurrent Levallois core, one initial core and one core fragment. These first very

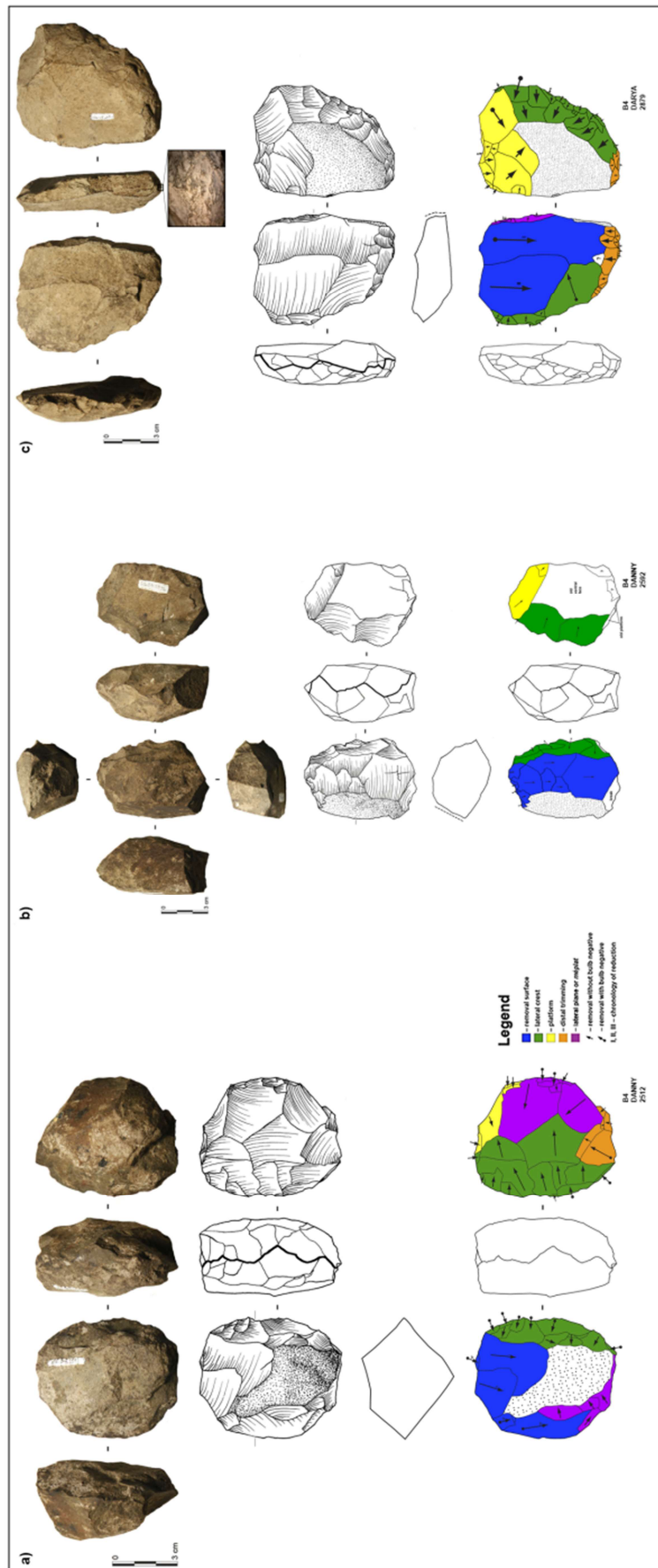


**Figure 80.** Sibudu. Deep Sounding: Bifacial tools from BS member. Bifacial tools made on hornfels (a, c, d, e), made on quartzite (b), and made on dolerite (f) (Drawings by Guillaume Porraz; photos by Lucía Cobo-Sánchez).

limited observations suggest that the lower part of BS might also belong to the ‘C-A’ technological phase.

In terms of the excavated layers stratigraphically below my sample – Danny and Darya – I had the opportunity to analyse the typological composition (Rots, et al., 2017: Table 5), cores and core fragments in order to reveal possible similarities or differences. Danny contains a total of 108 tools, while Darya comprises 73 formal tools. Bifacial technology continues in these deposits (Conard, 2016: Figure 7), but decreases to 17.6% and 17.8% respectively in comparison to layer Chantal above where it represents 20.5% of tools. One complete serrated piece made on dolerite occurs in layer Darya (Rots, et al., 2017: Figure 4, A5-1021). Unifacial





**Figure 81.** Sibudu. Deep Sounding: Laminar cores from layers Danny and Darya (a-c) (Drawings by Heike Würschem; photos by Viola C. Schmid).

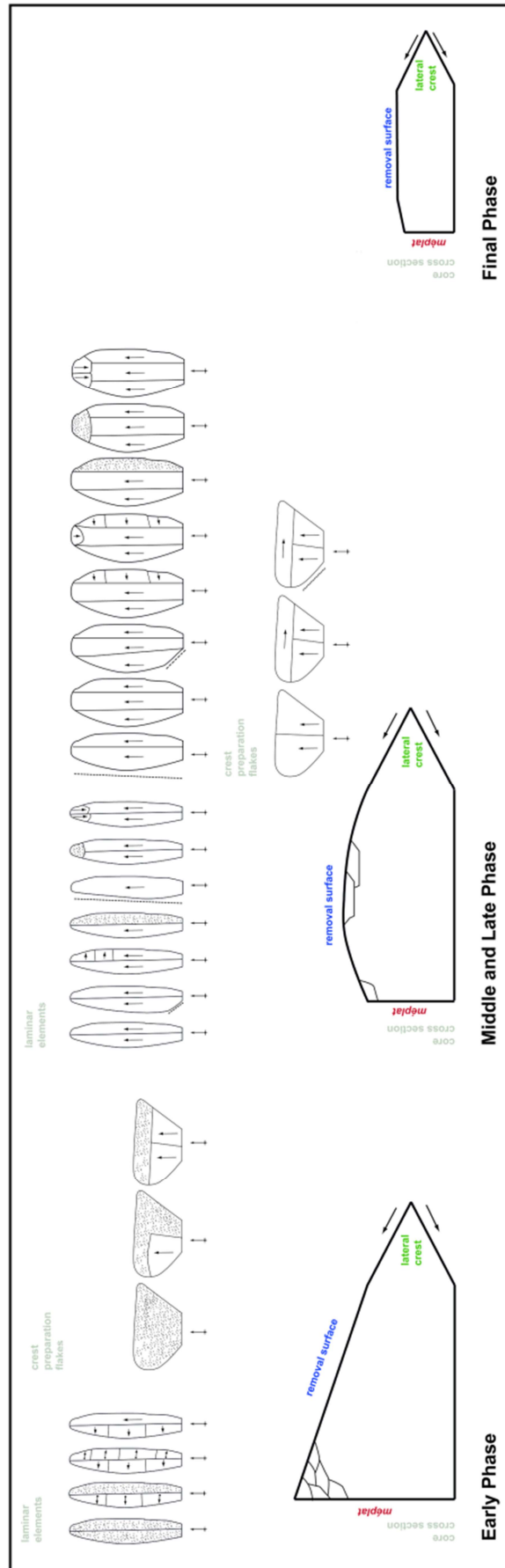
pointed forms (Conard, 2016: Figure 8) are still the most frequent tool type at 42.6% and 34.2% though this number diminishes. In contrast, scraper-like forms increase to 28.7% and 27.4%. Among the 18 cores from strata Danny and Darya, twelve objects follow the laminar reduction strategy of the C-A layers (Figure 81). The remaining pieces include two bipolar cores, two core fragments, one bladelet core, and one initial core. Therefore, I conclude that both the tool repertoire and the structure of the cores point to a continuation of the technological tradition into layers Danny and Darya.

The selection of my sample seems not to reflect the complete stratigraphic extent of the technological expression. Nevertheless, the noticeable peak in bifacial technology, including serrated pieces, in layer Bart, together with its rise and subsequent decline strongly indicate that the assemblage of **the C-A layers captures the central era of the technological tradition**. The layers featuring the laminar reduction strategy and formal tools, including primarily unifacially pointed forms with the tool classes TSPs and ACTs and bifacial tools with the diagnostic tool class of serrated pieces, encompasses a total thickness of about 50 cm. They share characteristics with the lower BS layers above and the D deposits below pointing to a longer duration overall. **This technological tradition seems therefore to constitute a considerable part of the sequence indicating a persistence rather than a short episode or a transitional period.**

#### 6.1.1. Technical system of the C-A layers

In general the assemblage shows little taphonomic disturbance. The only noticeable post-depositional impact is the strong encrustation of sediment on the artefacts made on all raw materials which increases towards the lowermost layer Chantal (Table 114).

The inhabitants of the C-A layers at Sibudu predominantly used the raw material dolerite. **The lithic assemblage demonstrates one main reduction sequence oriented towards the production of laminar elements.** Bipolar cores also play a minor role but are associated with one specific rock type, namely quartz. I recognised a laminar reduction strategy with a particular structural procedure from its early to final phases (Figure 82). In this strategy, past people preferentially chose dolerite slabs and used either the natural ridges of the core's original blanks or installed artificial crests to initiate the exploitation by extracting naturally or primary crested blades. The cores and blanks indicate a unidirectional reduction sequence involving direct internal percussion with a hammerstone, possibly with both soft and hard stones, while applying both *rentrante* and tangential motions. The organisation of the cores to allow laminar production involves setting up a striking platform, removal surface, core back and base, and the establishment of two additional essential areas, a lateral crest and a lateral plane/*méplat*. The lateral crest adjacent to the removal surface serves to create a transversal convexity. If necessary, it is re-shaped during core exploitation indicating a discontinuous reduction sequence. The lateral plane of the core situated opposite to the lateral crest is, in most cases, a natural surface. The *méplat*, the removal surface and crest, which together form the active volume, therefore provide the necessary volume for exploitation. During the reduction, the





**Figure 82.** Sibudu. C-A layers from the Deep Sounding: Box Scheme of laminae reduction system showing early, middle/late and final phase of reduction sequence with diagnostic products.

active volume is increasingly exploited and lateral expansion of the removal surface occurs. Different exploitation patterns generated two sub-groups of blades: on the one hand, reduction towards the *méplat* produced tall, laterally centralized blades with a triangular cross-section, and on the other hand, more central reduction of the removal surface produced flat, laterally diffuse blades with a trapezoidal cross-section. Typical preparation flakes originate from this reduction system, especially concerning the establishment and maintenance of the lateral crest. The crest preparation flakes from the early phase of reduction are trapezoidal and slightly curved to curved with unidirectional scars and/or dorsal cortex coverage, whereas preparation flakes from the later phases that show a similar shape and profile exhibit no cortex and orthogonal laminar dorsal scars. Core reduction ceased as soon as the removal surface reached a flatness that restricted further exploitation. The discarded cores exhibit a pentagonal cross-section resembling a house tipped over on its side, rather than the asymmetric triangular cross-section seen at the beginning and during the main (middle and late) phase of reduction.

I have also identified diagnostic features within the typological corpus. The toolmakers primarily (although not exclusively) selected elongated products for transformation into tools. **Consequently, the laminar reduction strategy and the tool manufacture seem to be strongly interlinked.**

**Different unifacial pointed forms account for the major part of the retouched elements. Two tool classes, TSP and ACT, stand out within the unifacial pointed forms,** although a few Tongatis appear as well. Both demonstrate clearly distinguishable technological and techno-functional characteristics justifying the subdivision as separate tool classes (Figure 83). The TSPs are defined as unifacial points having symmetrical, bilaterally retouched trihedral tips with a regular triangular cross-section, convergent medial parts, and quadrangular bases. ACTs are characterised by asymmetric converging distal ends usually consisting of a steep retouched edge and an opposing unretouched edge, medial parts with a converging and a rectilinear edge, and quadrangular proximal ends. Pieces from both classes are primarily made on dolerite, but for TSPs in particular quartzite plays a role. Regarding the dimensions, the TSPs are longer, thinner and significantly narrower than the ACTs ( $t$ -test,  $t = -2.2665$ ;  $p = 0.024572$ ). Additionally, the TSPs show a higher variability in size than the ACTs. Blank selection predominantly involved laminar products larger than the accompanying blank population, also supported by EPA and platform depth. In contrast, for ACTs, elongated flakes and even flakes are important blank types, with correspondingly lower debitage laminarity of 1.6. The blanks modified into TSPs are mostly from the main production phase and only few elements exhibit dorsal cortex coverage, while the original blanks of the ACTs come from different reduction stages and comprise more pieces with cortical remains. Plain platforms dominate, but ACTs especially show a great proportion of elements with dihedral and faceted platforms. Toolmakers preferentially chose blanks with a straight profile and a triangular or trapezoidal cross-section to transform them into both TSPs and ACTs. The clearly different techno-functional features of both point forms are reflected in their names. The TSPs are bilaterally symmetric and have similar tip edge angles,

	TSP	ACT
		
Main Raw Materials	Dolerite, Quartzite	
Length	47.8 mm	44.5 mm
Width	24.6 mm	26.8 mm
Thickness	7.8 mm	8.2 mm
Blank selection	Blade, elongated flake	Blade, elongated flake, flake
EPA	81°	83.5°
platform depth	8.2 mm	7.4 mm
platform type	plain, faceted, dihedral	plain, dihedral, faceted
cross-section	triangular, trapezoidal	
profile	straight	
Bilateral Point Symmetry	Yes	No
Angles of Tip forming edges	symmetric	assymmetric
Tip forming edges	both retouched	1 retouched, 1 unmodified
Medial part	bilaterally retouched, convergent	1 retouched converging, 1 straight
Base	quadrangular	
Mode of use	punctiform	linear
Life history	different stages of reduction	occasional phases of re-sharpening

**Figure 83.** Sibudu. C-A layers from the Deep Sounding: Summarized comparison of TSPs and ACTs.

while the ACTs are asymmetric and demonstrate significantly differing edge angles. Furthermore, both edges of the points of the TSPs are typically retouched, whereas the ACTs usually have one steeply retouched and one unretouched edge. For the techno-functional units (UTFs), both edges of the points of the TSPs belong to the active part. Conversely, the retouched part of the ACTs represents a receptive or prehensile part and only the unmodified edge is the transformative part. Most TSPs have a bilaterally retouched convergent medial part as an extension of the retouched distal end. The retouching of the distal end of the ACTs continues in most cases towards the medial part of the blank, creating a converging edge opposite to a straight unretouched edge. The bases of both tool classes are usually quadrangular. Several TSPs exhibit basal thinning but very few ACTs are basally thinned. In term of a functional interpretation of TSPs, the trihedral tip and the position of the prehensile part that enables a grip perpendicular to the axis of symmetry of the point strongly indicate a punctiform mode of use. The ACTs with asymmetry of the two edges of the distal end and a prehensile edge allowing a grip perpendicular to the axis of elongation of the active part seem to have most likely had a linear mode of use. While TSPs proceed through different stages of reduction in their life cycle, from a shorter working edge at the initial stage to an expansion of the active part and a consequent reduction of the receptive part at an advanced stage, the ACTs are equipped with an abruptly retouched passive edge therefore only rarely show re-sharpening of the unmodified working edge.

**As recognised from initial studies of the assemblage, bifacial technology plays an important role in the assemblage as well (Conard, et al., 2014; Conard and Porraz, 2015). The majority of the pieces concurs with the definition of bifacial points,** being triangular retouched blanks with pointed distal ends and both surfaces intentionally modified. Toolmakers mainly used quartz for bifacial point production, followed by dolerite and quartzite. They preferentially chose elongated products to modify them into bifacial points. Only a few pieces exhibit cortex coverage due to the high degree of shaping and also likely related to the selection of blanks from the main production phase. The bifacial reduction sequence involves two knapping techniques: direct internal percussion with a hard hammer in the initial phase, and direct marginal percussion with a soft hammer in the advanced phases. Large shaping flakes with thick platforms and no abrasion confirm the use of internal hard hammer percussion at the beginning of the shaping process, and small shaping flakes with abrasion, curved profiles, and lips indicate the application of marginal soft hammer percussion in the advanced and final shaping. All manufacture phases (1-4) occur, but finished products are most frequent. High numbers of all points are fragmented, mostly occurring as tip fragments demonstrating lateral snaps, which represent bending fractures with straight or curved profiles. These fractures are associated with breakage during manufacture indicating a high rate of knapping accidents. The finished bifacial points exhibit finely retouched tips and a regular tip outline. The bilaterally symmetric tools have either planoconvex, biconvex or planoconvex/planoconvex cross-sections. Their V-shaped tips are usually installed on the percussion axis of the blank constituting one or even up to two thirds of the tool. The medial part is convergent and the bases have an elliptic morphology.

**Within the bifacial population, serrated pieces – that is, tools with edges delineated by regularly repeated small notches creating triangular teeth converging into a point – stand out as a tool class on their own (Rots, et al., 2017).** The pieces are predominantly made on dolerite and quartz. Knappers selected mainly blades and elongated flakes to modify into serrated elements. This selection did not necessarily involve products from the main reduction phase, as I documented dorsal cortical coverage up to 50%. Despite the small sample, the population of serrated pieces encompasses two subgroups with differing manufacturing processes: bifacially shaped blanks that were bilaterally serrated, and bifacially retouched blanks that were bilaterally serrated. The former are initially shaped bifacially by direct percussion into the desired bifacial preforms and subsequently, after a new preparatory set up, their edges are serrated. Thus, the reduction sequence of this subgroup is strongly interconnected with the manufacture of bifacial points. The latter pertain to blanks that were first bifacially retouched to prepare the angles and platforms for the ensuing serration on both edges. Some of the serrated pieces exhibit no traces of use, lack bilateral symmetry, and additionally, the serration occurs only on one edge, suggesting discard during manufacture. The phase of serrating most likely was not only the last in the manufacturing process, but also its final phase due to the absence of evidence of re-sharpening. The finished tools have straight profiles, bilateral symmetry, and either planoconvex or biconvex cross-sections. The tip, as the active part, is usually installed on the distal ends in alignment with the percussion axis of the blank and has a V-shape and a regular pointed outline. The regularity of the point partly relates to the installation of the notches. The convergent or parallel medial parts typically show a

bilateral continuation of the serration, while the quadrangular or elliptic bases never have serrations. Before discussing the functional role of this tool class, I will address the percussive technique which produced the serrations. The toolmakers seem to have achieved the series of regular small notches forming the serrated edges by pressure notching with bone compressors. To do this, they applied the force of the compressor on the interior of the artefact edge at an angle approximately perpendicular to the plane of the blank. The regularity of the notches on the pieces themselves in terms of width, depth and spacing imply clear control of the location of the contact point and of the applied force, indicating pressure technique. Typical serrating flakes diverge from shaping flakes with regard to the thickness of the platform, the presence of lips, and the overall morphology, demonstrating a platform width of  $3.9 \pm 1.9$  mm and thickness of  $1.5 \pm 0.6$  mm that is in accordance with the measurements of the width ( $3.1 \pm 1.7$  mm) and depth ( $0.5 \pm 0.3$  mm) of the notches on the serrated pieces. Use wear and residue analysis provided solid evidence for the function and handling of these tools. Past people used the serrated pieces as projectiles mounted on shafts to hunt animals. They fabricated compound adhesives, mixing plant material of *Podocarpus falcatus* with finely ground red ochre for the hafting of the points. Bindings of sinew, skin and plant tissue combined with resin were likely also involved. For the shafts, the toolmakers seem to have used wood of the plant family Malvaceae. The dimensions of the serrated pieces point to assisted projection with three possible options: spear/arrow shafts that were delivered with a flexible spear-thrower, thin spear shafts delivered with a hard spear-thrower, or arrows delivered with a bow. Delivery with a flexible spear-thrower or as arrows with a bow seems most likely (Rots, et al., 2017: 51).

A small number of the bifacial tools lack the typical characteristics in terms of symmetry, morphology and thinness, and were therefore classified as asymmetrically bifacially backed knives. These objects are made on dolerite, quartzite and quartz. The average length and width of these tools overlaps with the values of the bifacial points, while the mean thickness of 11.8 mm contrasts with that of the bifacial points, at 8.2 mm. This difference is also reflected in the width-thickness ratio of  $2 \pm 0.2$  for the bifacially backed knives and  $2.5 \pm 0.4$  for the bifacial points. Cortex coverage is not unusual on the tool blanks. The tool class has exclusively planoconvex cross-sections caused by their bifacial asymmetry. The bifacially asymmetrical shape results from the hierarchical manufacture process, starting with shaping of the flat surface and then working the convex face. The pieces are distinguished by their robust lateral transformative part, allowing for a series of re-sharpening events on the edge opposite either a natural back or one prepared with large steep removals, functioning as reprehensive part. The distal ends lack a regular pointed outline. The medial part is formed by the rectilinear working edge and the converging back, in contrast to the convergent medial parts of the bifacial points. The bases are quadrangular.

**To a lesser extent, scraper-like forms are present in the assemblage. The highest proportion of this tool type is lateral scrapers, followed by NBTs.** A very small number of pieces comply with the definition of end-scrapers exhibiting a front as the active part.

Dolerite blades and elongated flakes served as blanks for the manufacture of lateral scrapers. The toolmakers primarily selected either products with more than 50% of cortex

originating from the earliest stage of reduction, or specimens with lateral or distal cortical coverage from the phase of reduction when the lateral and distal expansion occurred. These tools stand out due to their large size and robusticity in comparison with the other tools. Straightness was not essential in determining blank form, as curved and twisted lateral scrapers also are numerous. However, parallel edges seem to have been prerequisites, and the majority shows retouch on both edges. The modifications are variable, ranging from fine to large retouch removals indicating use for different tasks or different degrees of reworking.

The NBTs are commonly made on dolerite. In contrast to the other tools, knappers used a broad range of blanks to transform them into this tool class. Blades and elongated flakes were selected, but also variable flake types, including crest and platform preparation flakes, and shaping flakes. The pieces demonstrate the highest mean thickness of all tool classes, at 10.9 mm. The tool is distinguished by a natural back as the prehensile part, opposite to the lateral active part, usually formed by direct retouch although ventral retouch does occur. Most pieces have a cortical back, but some backs are associated with Siret fractures, platforms of a blank or core edges on a product.

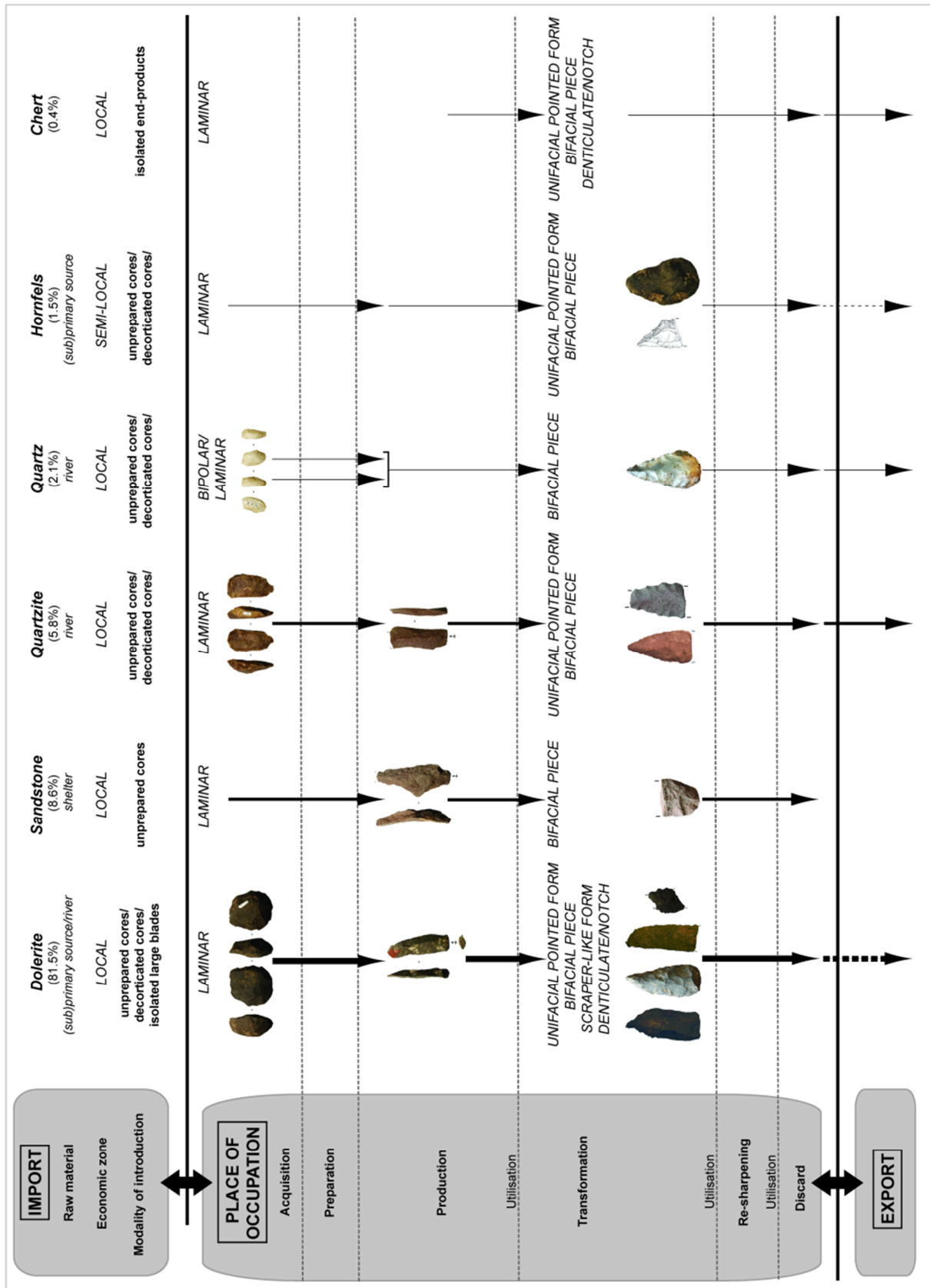
**Finally, the tool corpus includes denticulates and notched pieces.** The few notched pieces, as opposed to the denticulates, have only one single pronouncedly concave notch rather than a series of adjacent notches. Generally, the tools were made on dolerite laminar elements. The mean width at 27.3 mm and the width-to-thickness ratio  $3.3 \pm 0.8$  is only exceeded by the lateral scrapers. The tools have parallel edges and straight profiles.

The denticulates display a set of technological features that clearly distinguishes them from the serrated pieces. Denticulates commonly have only one edge retouched, with the working edges located laterally and not towards the distal working edge like the serrated pieces. The highest number of notches on a complete tool is eight, compared to an average of sixteen notches on a complete serrated piece, although their mean length values do not differ considerably. The mean width of the notches on the denticulates averages  $7 \pm 2.9$  mm and the depth  $1.1 \pm 0.5$  mm. The notches of the denticulates are significantly greater than those of the serrated pieces (*t*-test concerning width of notches,  $t = 15.364$ ;  $p = <0.001$ ; *t*-test concerning depth of notches,  $t = 14.304$ ;  $p = <0.001$ ) indicating different manufacturing procedures, including the organisation of preparation, percussive techniques connected to the modifications, and probably differing functions. However, as for the serrated pieces, the denticulates demonstrate a certain regularity on each piece but high variability between specimens.

#### 6.1.2. Techno-economic System of the C-A layers (Figure 84)

**The inhabitants of the C-A layers at Sibudu predominantly procured locally available raw materials, including primarily dolerite, followed by sandstone, quartzite, quartz, hornfels, and chert.** While dolerite and hornfels seem to have been mostly quarried from (sub)primary sources, past people collected quartzite and, to a lesser extent, quartz as cobbles from the nearby river. The rock shelter is formed of sandstone and so this rock was directly available at





**Figure 84.** Sibudu. C-A layers from the Deep Sounding: Dynamic model of the techno-economic procedures concerning the different raw materials in the assemblage (modified after Porráz, 2005: Figure 60).

the site. Only a few pieces of chert are present in the assemblage, thus its procurement is not easily determined.

The dominant raw material dolerite appears in different qualities, but the toolmakers mostly used the medium-grained variety. The presence of all phases of the reduction sequence supports the argument that the knappers partially exploited the raw material on site without preparation of the original core blanks. However, the low frequency of completely cortical artefacts and the presence of isolated large blades indicate the occasional import of end-products manufactured off-site. **The high blank-to-core ratio and the great proportion of intensively exhausted cores attests to long reduction sequences.** The blanks and cores highlight the manufacturing of elongated products. **Although the laminar reduction strategy occurs on all raw materials, I observe a pattern of raw material selection favouring dolerite, particularly in the form of slabs.** The natural geometry of slabs provides an optimal set-up for starting the reduction sequence without having to install a primary crest and investing a lot in preparation beforehand. **While tools made on dolerite are most frequent numerically, the low tool-to-blank ratio for this raw material suggests that tool production, namely retouching and shaping, was not the central focus of knapping.** With the exception of the bifacial pieces (on which I will elaborate below), all other tool types encompass more than 60% of artefacts made on dolerite. Firstly, the scraper-like forms, especially the lateral scrapers, make up the highest proportion of tools made on this rock type. The knappers selected large dolerite blades and elongated flakes from the initial and early expanding phases of the reduction because of their long parallel working edges. The pieces sometimes produced off-site and brought to Sibudu are suitable for long-lasting use. Furthermore, the extreme width of the tools compared to the other retouched elements allows for several re-sharpening episodes. The variability of the retouch on the lateral scrapers may be associated with different intensity of edge reworking before discard. Additionally, the tool class of denticulates has a lot in common with the lateral scrapers, that is a high number of dolerite specimens, a great mean width and width-to-thickness ratio, a predominance of laminar products selected as blanks and a high percentage of pieces with dorsal cortex coverage. The shared characteristic of denticulates is the series of notches, but otherwise these encompass a diversity of morphological features and I suggest that some of denticulates represent strongly reworked lateral scrapers (Picin, et al., 2011). Unifacially pointed forms, particularly the ACTs, also involve a high frequency of dolerite tools. **Overall, the toolmakers of Sibudu most probably preferentially chose the raw material dolerite to produce tools with a long life-span.** One explanation could be the rock properties, namely toughness and rigidity, ensuring durable edges on unmodified blanks that allow a long use without needing to be retouched as often as other rock types, such as hornfels (Wadley and Kempson, 2011).

Quartzite and hornfels also show that the whole reduction sequence took place to a limited extent on-site, and that the transport of already prepared cores and debitage products to Sibudu was common. With regard to quartzite, the knappers prevalently used a light to dark purple fine-grained variety, especially for the tool production. **Both quartzite and hornfels exhibit a high tool-to-blank ratio, indicating an increased investment in modifying blanks and manufacturing tools.** This fact is partly related to the rock properties of hornfels, which is highly

suitable for knapping, producing thin sharp edges, but is prone to breakage and needs frequent re-sharpening (Wadley and Kempson, 2011).

The quartz assemblage demonstrates that, to a certain degree, the knappers conducted the whole reduction sequence on-site. Quartz shows the highest ratio of small debitage products to single lithics implying intense on-site knapping events, but also small-sized natural raw material occurrences. Translucent and milky quartz occur in the assemblage. The structure of crystal quartz has uniquely glass-like qualities compared to the other southern African rock types producing notably smoother and sharper cutting edges (Mourre, 1996; Delagnes, et al., 2006; Pargeter and Hampson, 2019). The translucent quartz was mainly used for the manufacture of tools. **Numerous bipolar cores of both quartz categories and blanks of primarily milky quartz bear testimony to the main exploitation of quartz by bipolar-on-anvil percussion.** A low proportion of debitage products and cores made on quartz demonstrates that the laminar reduction system played a minor role in working this raw material. A few cores made on quartz also point towards a change of knapping technique during the reduction sequence. The toolmakers first exploited quartz as laminar cores and, at a later or the final stage of reduction, applied bipolar-on-anvil technique. **Quartz is of great importance for tool production, especially the manufacture of bifacial and bifacially serrated pieces (see below).**

**The inhabitants of Sibudu occasionally fell back on sandstone which is directly available at the site.** The high frequency of first flakes made on sandstone combined with the low proportion of end-products and tools suggests that the short reduction sequences occurred entirely on-site.

Only a few pieces of chert are present in the assemblage indicating a fragmented reduction sequence. **Past people seem to have introduced isolated end-products to the site, where they used, curated and finally discarded them.**

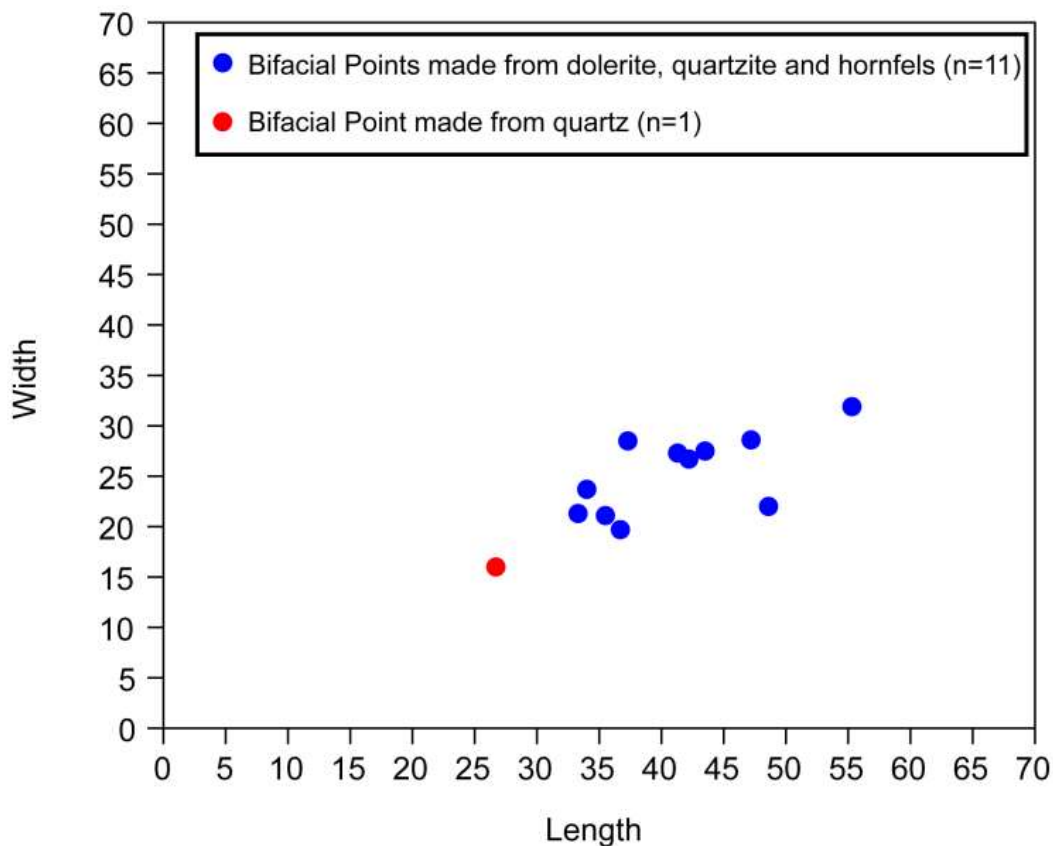
I discuss bifacial technology here separately to highlight striking techno-economic differences between the raw materials.

**First of all, some rock types seem to demonstrate an *in situ* bifacial production.** Dolerite is predominant within the bifacial pieces and shaping flakes, but less frequent in bifacial pieces than in shaping flakes. The resulting ratio of shaping flakes to bifacial pieces indicates that the artisans executed the whole bifacial manufacturing cycle on-site. Hornfels exhibits also a relative high ratio of shaping flakes to bifacials. With the exception of sandstone comprising only one bifacial specimen from initial shaping, hornfels and dolerite encompass the highest proportion of pieces from phase 1, indicating additionally the complete manufacturing cycle occurred at the site. On the contrary, quartz and especially quartzite have low ratio values and a low number of elements from the initial shaping attesting primarily utilisation, re-sharpening and maintenance at the site, while less often production. Chert is only present as finished products, which together with a very low frequency of shaping flakes suggest that the knappers transported, used and finally discarded the finished tools at Sibudu. Additionally, the greatest percentage of bifacial tools represents tip or distal fragments and the percentage is even higher considering only the finished products (41.2%). The fractures mostly relate to accidents during re-sharpening. The complementary larger fragments were either moved to an unexcavated area of the site or exported from the site (Soriano, et al., 2015). Interestingly, quartz (50%) and

quartzite (50%) include a higher number of distally broken finished products compared to dolerite (35.2%) indicating on the one hand that these raw materials are more prone to break, but on the other hand that they possibly were transported away more often.

**Moreover, the quartz bifacial points vary greatly from the bifacial points made on the other rocks in terms of morphometric features, life history, and techno-functional classification indicating a differential techno-economic behaviour.**

Concerning the tool size, the bifacial points made on quartz are noticeably smaller than the other raw materials in all dimensions (Figure 85). The only completely preserved quartz bifacial point (Figure 67b) yielded the minimum length value of 26.7 mm in the assemblage. The width of the quartz tools with a completely preserved width averages 17.3 mm, while the width of the other raw materials lies at 25.3 mm. The mean thickness of the quartz points with a completely preserved thickness is 6.6 mm and the one of the other raw materials is 9.2 mm. Thus, the quartz pieces are significantly narrower and thinner than the ones made on other raw materials (*t*-test concerning the width,  $t = 4.7405$ ;  $p = <0.001$ ; *t*-test concerning the thickness,  $t = 3.6349$ ;  $p = 0.003$ ). The width-thickness ratio of the bifacial points made on quartz is  $2.3 \pm 0.3$  and the one of the elements made on the other raw materials is  $2.6 \pm 0.4$  showing a clear difference (*t*-test,  $t = 2.6075$ ;  $p = 0.0116$ ). The highest frequency of pieces made on quartz (41.5%) shows biconvex cross-sections, while planoconvex cross-sections (56.5%) dominate among the tools made on the other raw materials.



**Figure 85.** Sibudu. C-A layers from the Deep Sounding: Scatter plot of width and length of all complete bifacial points.

The morphotype of the bifacial points made on quartz differs from the one made on other raw materials mainly with regard to the distal end. A total of 76.5% of the quartz points with a preserved tip show a regular pointed tip outline and only 51.4% of the other points. The TPA of the quartz pieces averages 61°, while the other bifacial points show a higher mean value of 67°. The length of the tip of the only completely preserved quartz point is 14.2 mm, whereas the mean value for the other points is 24.1 mm.

I observe a discrepancy also in terms of manufacturing processes and life histories. The highest frequency of finished points is made on quartz. Most bifacial points made on dolerite are either from the initial or advanced shaping. Only 20% of the total finished products belong to dolerite, while 48% are made on quartz. The bifacial tool population encompasses significantly more finished quartz bifacial points than such made on dolerite (Table 115). None of the quartz finished products show unmodified edge, while one specimen made on dolerite demonstrates a proportion of unmodified blank edge. The quartz finished tools show a higher percentage of regular pointed tip outlines (91.7%) than the finished products of dolerite (50%) and quartzite (75%). The large number of bifacial symmetric (90.5%) and biconvex (61.9%) pieces also distinguishes the quartz finished points from the dolerite with 70% of bifacial symmetric and 40% of biconvex objects and quartzite with 81.8% of bifacial symmetric and 27.3% of biconvex elements. The trend is even more noticeable, when only the distal parts of the finished products are considered. The quartz finished products involve 66.7% of tip and distal fragments with biconvex cross-sections, while dolerite has 33.3% and quartzite 25% of biconvex cross-sections. In contrast to quartzite, dolerite and hornfels, no specimen made on quartz exhibits traces of recycling. This may find an explanation in the fact that quartz pieces are the smallest making a reworking with hard hammer percussion seem like a less rewarding operation.

These differences between quartz and the other raw materials most possibly relate to a differential organisation of the bifacial point manufacture. The shaping of the quartz seems to be managed by alternating removals resulting in biconvex finished products with regular

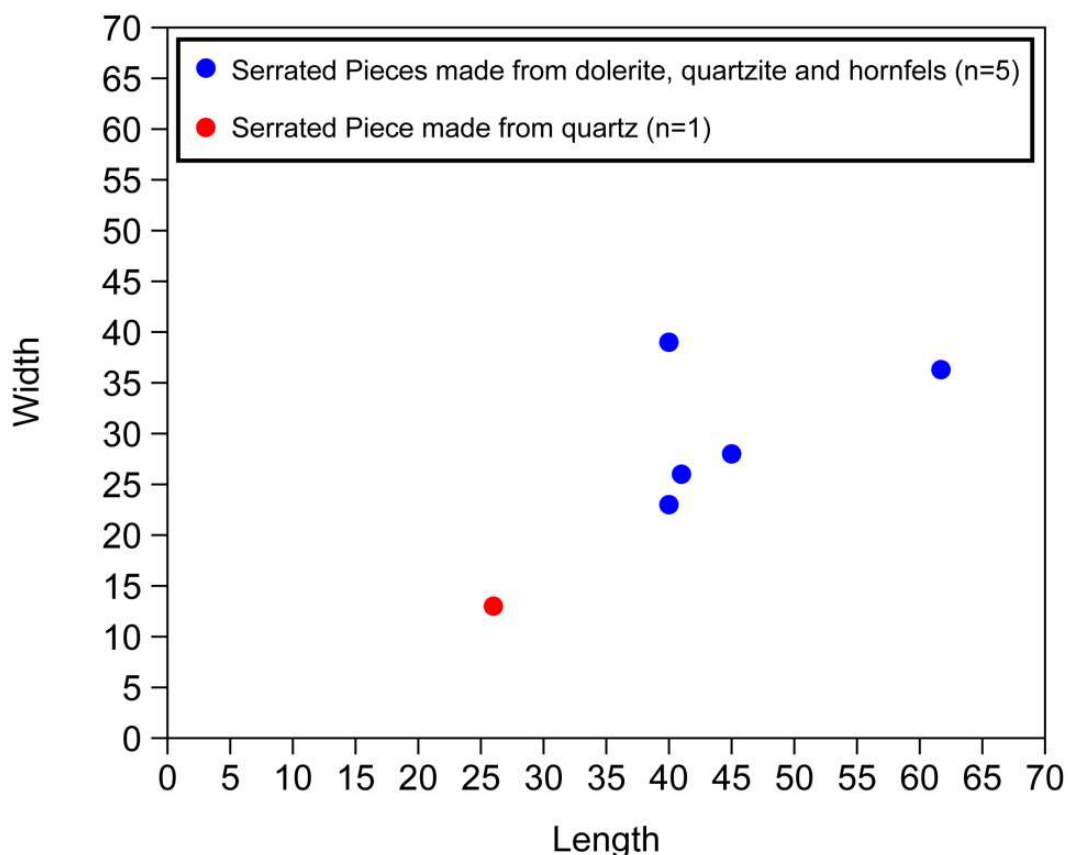
**Table 115.** Sibudu. C-A layers from the Deep Sounding: Comparison of finished bifacial points & points from other phases of manufacture between quartz and dolerite (chi-squared test).

Raw Material	Finished product	Initial & Advanced Shaping, Recycling	Total
Quartz	24	17	41
Dolerite	10	29	39
<i><b>chi-squared test</b></i>			
<b>F=</b>		<b>1</b>	
<b>χ<sup>2</sup>=</b>		<b>8,8507</b>	
<b>p=</b>		<b>0,0029298</b>	
<b>Fisher exact p=</b>		<b>0,0035651</b>	

pointed tip outlines. The two symmetric surfaces are installed simultaneously without hierarchisation corresponding to ‘bifaces as tools’ (Boëda, et al., 1990; Boëda, 1997; Nicoud, 2013). However, the shaping of the other raw materials, although not exclusively, is organised hierarchically. The bifacial reduction started with the confection of the flat surface and continued with the shaping of the convex surface leading to a planoconvex or planoconvex/planoconvex cross-sections of the finished tools and allowing for multiple re-sharpening events without structural changes. This bifacial reduction sequence complies with ‘bifaces used as a blank for tools’ (Boëda, 1997, 2001; Nicoud, 2013; Porraz, et al., 2013; Soriano, et al., 2015).

The application of the active part and the use of the bifacial points likely diverges between quartz and the other raw materials. The symmetric structure, organisation of removals and sizes of the quartz bifacial points indicates a use as projectiles in hunting weapons. On the contrary, the hierarchised structure and organisation of the removals of the points made on other rock types demonstrate an employment as tools in a different context. These bifacial points suggest that they functioned mainly as pointed cutting tools and might have been used as armatures in throwing or thrusting spears occasionally.

**Finally, the serrated pieces represent ultimate tools in terms of morphometric characteristics, i.e. a reworking is excluded as distinguished from the bifacial points, which could be re-sharpened or reworked at different moments throughout their life cycles. Thus, the variability of quartz and the other raw materials concerning dimensions, shapes, and manufacturing is not associated with differences in stages of discard (Rots, et al., 2017: 10).**



**Figure 86.** Sibudu. C-A layers from the Deep Sounding: Scatter plot of lengths and widths of all complete serrated pieces.

Serrated pieces made on quartz stand out due to their dimensions (Figure 86). The only completely preserved quartz tool has a length of 26 mm, while dolerite (45.7 mm) and hornfels (43 mm) show greater mean length values. The pieces made on quartz are narrower and thinner than the pieces made on other raw materials (Table 116 & Table 117). The width-thickness ratio is lesser concerning the quartz artefacts at  $2.1 \pm 0.6$  compared to the ratio of the other raw materials at  $3.1 \pm 0.9$ . The serrated pieces made on quartz show primarily biconvex (71.4%) cross-sections, whereas the pieces made on other raw materials are mostly planoconvex (82.4%).

Concerning the morphotype, the quartz tools exclusively demonstrate regular pointed tip outlines, while only 60% of the other raw materials have a regular pointed tip. The majority of the quartz objects exhibits elliptic bases at 75%, while quadrangular bases dominate among the other rocks at 88%.

**Table 116.** Sibudu. C-A layers from the Deep Sounding: Descriptive statistics of width of all in the width completely preserved serrated pieces made on quartz compared to the other raw materials.

	Serrated pieces made on quartz	Serrated pieces made on dolerite, hornfels & quartzite
n	7	16
Min	7	14.2
Max	20	39
Sum	99	385.7
Mean	14.1	24.1
Std. error	2.0	1.8
Variance	28.8	50.1
Stand. dev	5.4	7.1
Median	16	23.1
25 prcntil	7	18
75 prcntil	19	28.1

**Table 117.** Sibudu. C-A layers from the Deep Sounding: Descriptive statistics of thickness of all in the thickness completely preserved serrated pieces made on quartz compared to the other raw materials.

	Serrated pieces made on quartz	Serrated pieces made on dolerite, hornfels & quartzite
n	7	18
Min	4	3.3
Max	8	12.5
Sum	47	148.1
Mean	6.7	8.2
Std. error	0.6	0.5
Variance	2.2	4.5
Stand. dev	1.5	2.1
Median	7	8
25 prcntil	6	6.9
75 prcntil	8	9.3

The first of the two serrated reduction sequences, namely bifacially shaped blanks that were bilaterally serrated, concerns all of the serrated pieces made on quartz. Consequently, it has to be acknowledged that the first subgroup is strongly interlinked with the tool class of bifacial points. The comparison of the finished bifacial points made on quartz and the finished respectively used serrated pieces made on quartz reveals great similarities concerning the high frequency of biconvex cross-sections and the thickness (Table 118). On the contrary, only 22.2% of the serrated pieces made on other raw materials count to the first subgroup. The remaining pieces belong to bifacially (or unifacially) retouched blanks that were bilaterally (or laterally) serrated, whereby the bifacially retouched blanks with lateral serration and the unifacially retouched blanks with laterally serration seem to have been discarded during production and do not represent finished tools. Fewer accidents have occurred on quartz during the serrating, as all pieces are finished bearing traces of use apart from one specimen (Rots, et al., 2017).

**Table 118.** Sibudu. C-A layers from the Deep Sounding: Descriptive statistics of thickness of all in the thickness completely preserved bifacial points of phase 3 and finished serrated pieces made on quartz.

	Quartz bifacial points. phase 3	Quartz serrated pieces finished
n	23	5
Min	2.6	4
Max	11.5	8
Sum	142.9	31
Mean	6.2	6.2
Std. error	0.5	0.7
Variance	5.8	2.2
Stand. dev	2.4	1.5
Median	6.6	6
25 prcntil	3.4	5
75 prcntil	7.9	7.5

Concerning the serrations, the only completely preserved finished quartz serrated piece includes 18 notches and shows a mean notch width of  $2.1 \pm 1$  mm and a mean notch depth of  $0.2 \pm 0.1$  mm. The completely preserved finished products made on dolerite and hornfels, conversely, demonstrate an average of 16 notches per piece with a mean notch width of  $3.4 \pm 1.8$  mm and a mean notch depth of  $0.5 \pm 0.3$  mm. Taking into account the serrations of all finished tools made on quartz, the mean notch width is  $2.1 \pm 1.1$  mm and the mean notch depth is  $0.2 \pm 0.1$  mm concurring with the completely preserved finished piece. The notch width of all finished serrated pieces made on other rock types averages  $3.4 \pm 1.7$  mm and a mean depth of  $0.5 \pm 0.3$  mm coinciding with the completely preserved finished products as well. Both values significantly distinguish the quartz tools from the others (*t*-test concerning the width of the notches,  $t = 5.2378$ ;  $p = <0.001$ ; *t*-test concerning the depth of the notches,  $t = 5.6894$ ;  $p = <0.001$ ). **Hence, the quartz serrated pieces have narrower and shallower notches and generally a greater regularity of the serration.**

The differences in size and shape concerning the raw materials point to the possibility of variation in function respectively weapon types between quartz and the other raw materials,



but further evidence must be provided to substantiate this argument. As stated before, the functional analysis determined two projection modes, namely as spear/arrows delivered with a flexible spear-thrower or as arrows delivered with a bow. Considering the small sample size and the need of more and systematic experimentation, Rots et al. (2017: 51) suggest that particularly the quartz serrated points could have been used in bow and arrow. I additionally found that the TCSA of the quartz serrated pieces matches with the value of arrowheads (Table 107). Dolerite and hornfels pieces correspond more with spear tips (Table 107). The TPA of the quartz pieces is at a mean of 39° measured with the goniometer as well as calculated with the formula, while the TPA measured for serrated pieces made on dolerite is 60.8° and calculated 49.5°. **The quartz points have aerodynamic properties, such as relative lightness (the only completely preserved finished quartz weighs 1.9 g), thinness, symmetry, narrow penetrating angle and biconvex cross-section (Villa and Lenoir, 2009: 79), which are supposedly in accordance with arrows. The serrated pieces made on other raw materials seem to rather comply with spear tips insinuating the presence of two projection modes.**

The plenitude of data from the whole bifacial population allows for a substantial interpretation. Quartz is mainly, though not exclusively, interlinked with bifacial technology and shows particularities concerning the reduction sequence, morphometric characteristics as well as function compared to the other raw materials. The evidence strongly suggests that the artisans selected quartz with rock properties leading to extremely sharp cutting edges to produce bifacial and bifacially serrated arrowheads for hunting animals. The serration of the bifacial points could have been an advantage to increase the contact surface of the point with the target upon insertion causing poorer plausibility of wound closure, greater haemorrhage and infection risk of the animal potentially overcoming the decrease cutting capacity of the edges by bifacial retouch (Rots, et al., 2017). Conversely, the focus of the other raw materials is not primarily centred on bifacial technology and the products resulting from bifacial shaping, including the serrated pieces, rather concur with spear tips which often seemed to be used as knives. The design of these bifacial tools points to multifunctionality and economic efficiency (Kelly, 1988; Whittaker, 1994, Soressi and Hays, 2003; Soressi, 2004; McCall and Thomas, 2012). The knappers could use the cutting edges in combination with the pointed distal ends of the bifacials in a broad range of tasks (Soressi, 2004; McCall and Thomas, 2012). Ethnographically, the tool use of projectiles for other purposes has been documented, e.g. among Australian aboriginal groups (Hayden, 1979; Binford, 1986; McCall and Thomas, 2012). The so-called *leiliras* well comparable to bifacial points were hafted either as knives or spear tips and frequently exchanged from one purpose to the other (Hayden, 1979). The high level of efficiency is achieved by the re-sharpening potential of the hierarchised surfaces of the points, as the loss of width and functional surface is minimized and a long use-live is ensured (Jeske, 1989; Soressi and Hays, 2003; Soressi, 2004; McCall and Thomas, 2012; Porraz, et al., 2013, Soriano, et al., 2015). **Consequently, a complex composition of the technological organisation based on different raw material economies marks the C-A layers of Sibudu (sensu Perlès, 1992). Past people seem to have chosen preferably quartz as cynegetic equipment, while the other raw materials served mostly as domestic tools.**

At last, the accumulated information provides the opportunity to draw conclusions about the provisioning strategy or mix of provisioning strategies, meaning the calculation of past people to keep themselves supplied with tools or raw material when and where needed. Mobility and land use heavily impact the choice of provisioning strategies (Binford, 1980; Bamforth, 1986; Shott, 1986; Geneste, 1991; Kuhn, 1995, 2004). **The exploitation of mostly local raw materials and the presence of the entire reduction sequence for all rock types except chert strongly plead for a main provisioning of place strategy.** This provisioning strategy requires that raw materials are transported from the sources to the site and amassed there as ready supply for foreseeable activities (for definition see Kuhn, 2004). The import of isolated large end-products made on dolerite, the export of multifunctional as well as long-lasting bifacial tools predominantly made on quartzite, and the techno-economic handling of chert suggest, admittedly, the provisioning of individuals aiming at the constant supply of mobile people with artefacts or raw materials they most probably are going to use (for definition see Kuhn, 2004). Finally, the exploitation of sandstone could possibly indicate a provisioning of activities corresponding to the ad hoc manufacturing of blanks for immediate needs (for definition see Kuhn, 2004). **General interpretative models of the lithic assemblages (Binford, 1980; Kuhn, 1995, 2004; Kelly, 2013) propose that Sibudu was not occupied for short-term activities but represents a base camp.** This hypothesis is supported by the enormous wealth of all classes of material at the site throughout the sequence (see Wadley and Whitelaw, 2006), and the C-A layers also document a phase of intense occupation of the site.

## *6.2. The chrono-cultural classification of the C-A layers*

After providing a detailed synthesis of the technological and techno-economic features, I will present here comparisons first to bifacial-bearing MSA assemblages in MIS 5 and furthermore expand to all well-dated MSA sites of MIS 5 to elucidate technological affiliations and furthermore probable cultural relationships. The correlation with MIS 5 does not imply environmental determinism causing technological change during this stage, but merely specifies the broad timeframe (following Lombard, et al., 2012: 125). Finally, I will provide my evaluation of the position of the C-A layers within the chrono-cultural framework of the MSA considering taxonomic and scale-related obstacles.

### 6.2.1. The MSA bifacial phenomenon

**The SB technocomplex represents the main manifestation presently defined for MSA bifacial technologies** (Figure 2 & Figure 3) (Goodwin and van Riet Lowe, 1929; Clark, 1959; Wadley, 2007; Henshilwood, 2012). The presence of bifacial points served for a long time as diagnostic criterion to assign an assemblage to the SB (Henshilwood, 2012: 218). In recent years, voices of more and more researcher grew louder to be cautious in the acceptance of the SB as a short-lived, technologically uniform cultural marker due to great differences concerning the manufacturing process, morphometric characteristics, status within the assemblage,

appearance of other reduction strategies as well as formal tools and apart from that the uncertainty related to its absolute chronology (see Chapter 1.2.1).

Hence, the occurrence and spectrum of **bifacial tools in the C-A deposits of Sibudu underlying pre-SB layers without bifacial technology and SB layers characterised precisely by bifacial elements further fuel the debate on the SB in particular and the temporal and spatial distribution of the bifacial phenomenon in the southern African MSA** in general. I confront here, following up on Rots et al. (2017: 52f.), the C-A toolkit with the assemblages first of the SB from Sibudu, furthermore affiliated to the SB in general and finally, of bifacial-bearing MSA technocomplexes in MIS 5 by extending from the bifacial corpus to the whole technical subsystem. With this comparison, I elaborate even more profoundly on the question of how and if the C-A strata relate to the SB (Lombard, et al., 2012; Porraz, et al., 2013; Soriano, et al., 2015; Archer, et al., 2016). **The SB technocomplex is defined on the predominance of bifacial technology and the presence of bifacial points with a specific morphotype, i.e. foliate or lanceolate points “[...] with semi-circular, or wide-angled pointed butt.”**(Goodwin and van Riet Lowe, 1929: 119). The typical sites assigned to the SB include Sibudu Cave, UMH, BBC, DRP, PC, DRS and HRS.

#### **6.2.1.1. The C-A layers within the MIS 5 occupations at Sibudu**

As mentioned above, **Sibudu** itself represents one of the sites, which yielded a SB occupation dated to  $69.5 \pm 2.1$  ka BP, namely layers **RGS and RGS 2**(Wadley, 2007; Soriano, et al., 2009, 2015). The SB assemblage is dominated by bifacial reduction sequences with bifacial shaping flakes forming 91.8% of the assemblage (Soriano, et al., 2015). Flakes, elongated flakes and blades not associated with bifacial shaping amount to only 1.9% of the artefacts. The blades detached from platform cores with internal hard hammer percussion are usually short as well as highly variable in shape (Soriano, et al., 2015: 7). The knappers used the available raw materials, including dolerite, hornfels, quartzite, quartz, and sandstone, with a strong preference toward dolerite. The tool corpus also illustrates the overall focus on bifacial points accounting for 53.1% in the SB layers. The toolmakers hardly shaped quartz into a bifacial tool, meaning that this rock received no special consideration during manufacture or in the functional system. The foliate bifacial pieces have primarily V-shaped tips, usually broad or wide arched bases and planoconvex cross-sections (Soriano, et al., 2015). They are variable in size with a maximum width of 27.2 mm and maximum thickness of 8.5 mm (Wadley, 2007: Table 2). The extent of retouch appearing identical on both edges and functional data suggest an axial hafting of the points. The structure and organization of the removals points to a main design as cutting devices that knappers could often re-sharpen and use for a long time. However, the bifacial pieces also show traces of the use as tips of throwing or thrusting spears (Lombard, 2006b; Soriano, et al., 2015). Among the remaining formal tools, *pieces esquillées* (splintered pieces), scrapers, and unifacial points occur (Wadley, 2007).

**The C-A layers of Sibudu differ in many aspects from the SB layers of the same site,** though the toolmakers used the same range of rock types and preferably dolerite. The

main differences concern firstly to their reduction sequences, as the SB is almost exclusively dominated by bifacial reduction sequences, while the C-A layers show that the knappers aimed prevalingly to produce laminar elements. Secondly, the bifacial pieces account for the greatest proportion of the SB tool corpus, while most of the tools from the C-A layers are unifacial pointed forms. Thirdly, although the bifacial points made from other raw materials than quartz share similarities regarding morphometric, techno-functional, and functional features, the number of quartz points from the SB layers is negligibly small. In contrast, quartz stands apart from the other rocks in the C-A layers concerning manufacturing and function. Finally, serrated pieces do not occur in the SB assemblage.

The informally called 'pre-SB' strata below, namely **LBG** dated to  $70.9 \pm 2.1$  ka BP respectively  $70.8 \pm 2.1$  ka BP and the **younger BS layers**  $72.4 \pm 1.9$  ka BP (Jacobs and Roberts, 2017), have a thickness of approximately 40 cm. They contain flakes as well as blades and exhibit a typological corpus comprising denticulates made on dolerite and only rarely unifacial points, but completely lacking bifacial technology and (Wadley, 2012a, 2013b).

Though more in-depth technological analyses concerning the reduction strategies of the flakes and blades are still to be undertaken, the absence of bifacial technology and the low significance of pointed forms generally distinguish the LBG and younger BS deposits from the C-A layers.

I have already elaborated on the **older BS strata** directly above the C-A layers and their strong resemblance to the C-A layers in Chapter 5.1.

In conclusion, the sequence of Sibudu comprises layers complying with the SB technocomplex and being clearly differentiated from the C-A strata. The LBG and younger BS deposits separate these two bifacial-bearing phases stratigraphically constituting a hiatus in bifacial technology. Therefore, on the scale of the site itself the C-A layers and the SB deposits cannot be grouped together.

### 6.2.1.2. The C-A layers and the Still Bay

After having addressed the C-A layers and the SB on the site level of Sibudu, I discuss here the SB in general in relation to the C-A layers:

**UMH**, in KwaZulu-Natal ca 90 km from Sibudu, comprises serrated pieces associated with bifacial points in the lowermost **levels 25 to 28** (Kaplan, 1990; Lombard, et al., 2010; Mohapi, 2013; Högberg and Lombard, 2016a, 2016b). Level 25 yielded an age of  $70.5 \pm 4.7$  ka BP (Lombard, et al., 2010). **UMH has been interpreted as a localised variation of the SB considering the co-occurrence** (Lombard, et al., 2010, 2012). However, due to the systematic discovery of serrated pieces in layers below the SB at Sibudu, and uncertainties concerning the

stratigraphic context of UMH, Rots et al. (2017) recently questioned the unambiguous evidence for serrated bifacial pieces during the conventional phase of the SB.

The knappers used quartz as well as hornfels and to a lesser degree quartzite as well as chert. Quartz seems to be the preferred raw material, but hornfels and quartzite play also an important role concerning the tool manufacturing. The assemblage includes irregular, single platform and bipolar cores (Kaplan, 1990). Flakes account for the greatest proportion of the blank population, though blades are present (Kaplan, 1990; Högberg and Lombard, 2016b). Bifacial and serrated points are made on quartzite, hornfels, and quartz. They result from different point production strategies (Högberg and Lombard, 2016b). Most frequently, especially concerning quartz, the toolmakers manufactured the points according to the bifacial nodule point-production strategy version 1, i.e. the shaping starts from a nodule and leads to a finished bifacial or serrated point with a biconvex cross-section. At the beginning of this bifacial reduction sequence, the knappers applied internal percussion with hard hammer, while they used later marginal percussion with soft hammer and sometimes at the final stage created serrations with pressure technique (Högberg and Lombard, 2016a). Moreover, quartzite and hornfels bifacial or serrated points were also produced according to bifacial blade point production strategy and to a lesser extent flake point production strategy. Blades and flakes instead of nodules are selected and the shaping starts usually on the dorsal face continuing afterwards on the ventral face. During the manufacture process, the roughout is flipped several times from one face to the other. The finished products have diamond-shaped cross-sections. In contrast to the bifacial nodule point-production strategy, the outline of the original blank changes less. Finally, the unifacial point-production strategy concerns almost exclusively hornfels. This reduction strategy is similar to the bifacial blade or flake point production strategy, but the ventral face of the original face stays unworked leading to a planoconvex cross-section of the points (Högberg and Lombard, 2016b). In general, most of the bifacial points seem to be finished products and exhibit biconvex cross-sections and elliptical bases (Lombard, et al., 2010). Their width-thickness-ratio averages  $2.4 \pm 0.4$ . The serrated points are primarily made on quartz (milky and crystal) and bifacially shaped. They show a mean width-thickness-ratio of  $2.1 \pm 0.3$ . The serration is located on both laterals on most specimens. The width of the notches ranges from circa 1 mm to 5 mm (Lombard, et al., 2010). The presence of shaping flakes made on quartz, hornfels, and quartzite often with abrasion confirms on site manufacturing. The discrepancy of the quartzite bifacial points to the shaping flakes indicates that finished tools made on quartzite were transported to the site. Supposed pressure flakes suggests the production of serrated pieces at UMH (Högberg and Lombard, 2016b). Other formal tools, such as scrapers and backed pieces, occur (Kaplan, 1990).

**A lot of similarities between UMH and the C-A layers are evident**, though further technological studies on the blanks, cores and other formal tools than bifacial and serrated points are needed to clarify the nature of the technical sub-system. Both assemblages are characterised by bifacial technology, including serrated pieces. Similar raw materials were preferred. The inhabitants of Sibudu and UMH show a corresponding techno-economic behaviour, in which they brought along quartzite bifacial points with them to only use, maintain and abandoned at the site. The bifacial reduction strategies

seem to overlap in many aspects, the use of blades as original blanks, the occurrence of unifacial serrated pieces, and the peculiar status of quartz associated with one main manufacturing process. Though the serrated points of Sibudu Cave seem to be less elongated and the serrations overall less indented than those of UMH (see Rots, et al., 2017), some morphological compliance is documented notably regarding the shape of the base. Finally, the dimensions of the serrated pieces themselves and the width of their notches are similar between UMH and the C-A layers supporting the hypothesis that pressure technique with a bone tool compressor was applied (see Rots, et al., 2017). This two assemblages share strong technological similarities and seemingly differ mainly in terms of chronology. The time lag between UMH and the C-A layers needs to be addressed again to resolve potential inconsistencies.

The SB assemblage of the **M1 and M2 upper phases from BBC**, Western Cape Province, dates between 77 and 70 ka (Villa, et al., 2009; Soriano, et al., 2015). The toolkit attests to a reduction strategy independent from bifacial technology. The short reduction sequence is oriented towards the production of flakes and laminar flakes (Soressi, 2005; Soriano, et al., 2015). Bifacial tools dominate the formal tools. Silcrete from two sources in an exotic economic sector is the preferential raw material, followed by quartzite, quartz, and chert. Flakes mainly served as original blanks. All stages of production from preform to finished and recycled objects appear. Most of the pieces conform to the phase of advanced shaping and in general, the largest proportion was discarded unfinished (Villa, et al., 2009; Soriano, et al., 2015). Initial shaping with hard hammer percussion is documented by removals with concave bulbs and highly localized points of percussion, while advanced and finalising shaping executed by soft hammer marginal percussion by negatives with shallow bulbs and diffuse contact points (Villa, et al., 2009: 446). Pressure flaking on silcrete points attested by deep bulb negatives and hackles on the bulb negatives  $\leq 10\text{mm}$  was applied in the final phase of the manufacturing process only after heat-treatment to regularise and finish the point (Mourre, et al., 2010: 660f.). Finished points exhibit bilateral as well as bifacial symmetry, regular tip outline and regular tip profile. They have V-shaped points with straight or curved sides. The base of the finished points is pointed or narrow elliptic often with a truncated end. Point length of finished bifacial points ranges between 34 mm and 74.5 mm. The majority of the bifacial points are fragmented. Bending fractures most probably related to production failures are most common. A few points exhibit impact scars. Several lines of evidence indicate that the points were handled axially and used as spear tips (Villa, et al., 2009; Soriano, et al., 2015). High proportions of shaping and silcrete pressure flakes occur in the assemblage (Villa, et al., 2009; Mourre, et al., 2010). The bifacial shaping flakes have occasionally been transformed into tools (Soressi, 2005). Different scraper forms, including characteristic circular scrapers, are frequent besides the bifacial points (Soriano, et al., 2015).

Though further analyses are needed to provide a detailed technological description, **the knappers of BBC aimed at the production of flakes rather than blades**. In contrast to the C-A layers, the toolmakers of BBC selected mainly exotic raw materials for the manufacturing of bifacial points. While the manufacture process shows many

similarities, heat-treatment and pressure flaking to rectify the tip is not observed in Sibudu. Furthermore, the two assemblages differ concerning the proportion of finished tools. At both sites, at least partial *in situ* shaping was identified. Morphologically, the tips and bases of both bifacial point populations are similar, but the specimens from the C-A layers have no bases with truncated ends. Dimensional differences concerning the length are apparent. The bifacial points of BBC exhibit a high frequency of bifacial symmetry in contrast to the points made from other raw materials than quartz at Sibudu suggesting also different main functions. **No serrated pieces occur in the assemblage of BBC. Circular scrapers are diagnostic of the BBC typological corpus, but are absent in the C-A layers.**

At **DRS** (Porraz, et al., 2013, 2014), Western Cape Province, the **SB type 'Larry'** encompassing 5 SUs has an age of  $109 \pm 10$  ka (following Tribolo, et al., 2013) and of  $76.5 \pm 3.3$  ka (following Jacobs and Roberts, 2015). The assemblage is dominated by flakes, but also exhibits a high frequency of blanks related to bifacial shaping. Some of the large bifacial shaping flakes were transformed into formal tools. Blades amount up to only 8.4% of the assemblage. The knappers preferentially used local quartzite. A reduction strategy aiming at the production of laminar blanks and flakes occurs, but the end-products are morphologically variable. Bifacial pieces form the largest proportion of the tool corpus. Most bifacial points, like most elements of the whole toolkit, are made on the local coarse-grained quartzite, followed by quartz and semi-local yellowish-brown silcrete. Exotic silcrete and fine-grained quartzite pieces are also present. All manufacturing phases were discerned in the assemblage: initial shaping by direct, internal percussion with a hard hammer, advanced shaping by marginal percussion with a soft hammer, and final regularisation of the bifacial piece and recycling. The exclusive use of direct percussion was documented. The bifacial reduction sequence was started with slabs, angular blocks or flakes. The points have a lanceolate morphology and the base is elliptic or pointed. The bifacial pieces are typically thin and the point thickness is standardised. Finished points show a mean thickness of 8.5 mm. The objects are bilaterally symmetric, but bifacially asymmetric. They have planoconvex cross-sections and the organisation of the removals points to an independently, hierarchised bifacial reduction sequence. The toolmakers aimed for a standardised morphology of the bifacial points, but provided flexibility to re-sharpen and modify the piece in the required way, if necessary, in the last phase (Porraz, et al., 2013, 2014). Hence, the bifacial tools conform to 'bifaces used as a blank for tools' (Boëda, 1997, 2001; Nicoud, 2013; Porraz, et al., 2013; Soriano, et al., 2015). Nearly all bifacial points are unintentionally broken probably resulting from the extensively reduced nature of the products. A rarity of impact-like fractures was observed, but a high frequency of curation and retooling of the edges suggesting primarily a use as cutting device (Porraz, et al., 2013). Bifacial pieces of different raw materials indicate different implementation of the manufacture process at the site. Bifacial tool production of local quartzite was conducted on site, as products of all stages of reduction are present. All stages of the reduction sequence, except of the initial blank selection, were observed also for the yellowish-brown silcrete and fine-grained quartzite. Exotic silcrete and quartz were mainly introduced to the site as finished products, as only finished

specimens are present and the small shaping flakes <20 mm clearly dominate among the shaping flakes. No bifacial tools made on hornfels exist, but shaping flakes, suggesting a similar scenario as for silcrete and quartz. A techno-economic pattern can be recognised that bifacial elements made on exotic fine-grained rock types, in contrast to the local and semi-local raw materials, were extensively transported within the territory confirmed additionally by the high ratio of unfinished bifacial pieces made on local rocks and the high ratio of fragmented finished pieces made on non-local rocks represent. The assemblage yielded additionally other tools, such as different forms of scrapers, denticulates, *pieces esquillées*, and a few wide and circular end-scrapers (Porraz, et al., 2013).

**Blade production at DRS plays a minor part and the products are not standardised compared to the C-A layers of Sibudu.** Bifacial technology holds a more important place in the assemblage of DRS than Sibudu. The bifacial populations of both sites yet bear common features concerning the manufacturing process, including soft and hard hammer, morpho-metric characteristics, and the techno-functional characterisation. Furthermore, the techno-economic behaviour of past people to transport the bifacial pieces made on higher quality raw materials as ready tools suitable for long-term use with them is observed in both assemblages. However, **DRS contains neither a particular manufacturing and functional treatment of quartz nor serrated pieces.**

The SB of **HRS**, Western Cape Province, with an OSL age between 80 and 72 ka (Evans, 1994; Högberg and Larsson, 2011; Högberg, 2014, 2016; Högberg and Lombard, 2016b), involves an independent laminar and flake reduction strategy besides the manifestation of bifacial technology. The main raw material is local quartzite. Furthermore hornfels, silcrete, and quartz occur in assemblage, which are all locally available or in short distance to the site (Högberg and Lombard, 2016b). The blade population has a mean length of 59 mm. One-half of the blades have triangular cross-sections and the other half trapezoidal. The platforms of laminar end-products are relatively thick and often faceted. Abrasion is also present on 13% of the blades. Crested blades occur in a low proportion. The knappers pursued a unidirectional reduction from single-platform cores. The set-up of the removal surfaces was by all appearances semi-circumferential (see Högberg, 2016: Figure 16) and thus, the transversal convexity is managed by means of the knapping cycle. A few blade cores resemble HP-cores. An independent flake reduction strategy corresponding to centripetal Levallois method exists (Högberg, 2016).

The bifacial points of HRS were predominantly made on quartzite and silcrete followed by quartz. Hornfels was not used for the production of bifacial points (Evans, 1994; Högberg and Larsson, 2011; Högberg and Lombard, 2016b). The knappers employed different bifacial reduction strategies to produce bifacial points (Högberg and Larsson, 2011; Högberg and Lombard, 2016b). Most frequently in general and exclusively concerning quartz, the toolmakers followed the bifacial nodule point-production strategy version 1, i.e. the manufacturing process starts from a nodule resulting in a finished bifacial with a biconvex cross-sections. This bifacial reduction sequence involves internal percussion with a hard hammer at the beginning and later the use of marginal percussion with soft hammer. Furthermore, a few bifacial specimens made



on silcrete and quartzite were manufactured according to bifacial nodule point-production strategy version 2. The difference to version 1 relate to the set-up of the reduction, including a hierarchical organisation. The two faces are alternately retouched sequentially, leading to planoconvex/planoconvex cross-sections. The manufacture of the silcrete points mainly concerned flake point production strategy. Flakes instead of nodules are selected. The finished products demonstrate diamond-shaped cross-sections and the outline of the original blank changed less during the reduction sequence. Finally, the knappers used the unifacial point-production strategy on silcrete blanks to obtain points leaving the ventral face unworked. (Högberg and Larsson, 2011; Högberg and Lombard, 2016b). The use of pressure technique to shape the edges with fine retouch in the finishing phase of the reduction on different raw materials has been hypothesised (Högberg and Larsson, 2011; Högberg and Lombard, 2016b), but is not confirmed (see Porraz, et al., 2013: 3394). With regard to silcrete, heat treatment in an early stage of reduction has been occasionally documented, but the silcrete bifacial points experienced no special treatment than the other end-products (Schmidt and Högberg, 2018). The finished bifacial points have typically either a biconvex or planoconvex cross-section, a sharp point, and a wide-angled pointed butt. The length of the completely preserved, finished points ranges between 37 mm and 76 mm (Högberg and Larsson, 2011), whereas the quartz pieces are in general smaller than the other raw materials. A high proportion of the bifacial points is fragmented. Bending fractures most probably associated with production failures are most frequent. Some bifacial elements with impact scars occur. A large number of shaping flakes, mostly made on quartzite, is present in the assemblage. The difference in ratio of shaping flakes to bifacial pieces between quartzite and silcrete suggests that quartzite points were manufactured on site, while silcrete points were imported (Högberg and Larsson, 2011; Högberg and Lombard, 2016b). Along with the bifacial points different forms of scrapers and denticulates were observed (Evans, 1994; Högberg and Larsson, 2011).

In comparison with the C-A layers, the blades of HRS are larger. The differences concerning the attributes of the platform between Sibudu and HRS are likely associated with a different use and combination of percussion techniques. Furthermore, **the reduction sequence in terms of convexity maintenance is managed differently at HRS.** Though the bifacial points of HRS seem to be larger than those from Sibudu, the manufacture process and the morphology show similarities. Both bifacial populations indicate a peculiar position of quartz compared to the other raw materials due to production strategy as well as the resulting morphological features. Additionally, the techno-economic pattern of carrying bifacial tools as part of a mobile toolkit is evident in both assemblages. **Although the knappers at HRS supposedly used pressure technique to achieve to final regularisation of the points, pressure notching, like in the C-A layers, is absent.** The stratigraphic context of HRS seems to be a palimpsest of occupations and thus the exact associations between the technological events, i.e. bifacial technology and laminar production, need to be clarified and interpreted in the light of local and well stratified sequences.

The site of **DRP**, Western Cape Province, was excavated by amateurs in 1936 and Schirmer (1975) produced the only description of the assemblage as well as the excavations and

a reconstruction of the stratigraphy. Silcrete dominates the assemblage, followed by quartzite and quartz. The knappers produced primarily flakes, while blade types seem to be absent. A total of 76.7% of the formal tools are either unifacial or bifacial points, whereby the bifacial specimens are more common. Most of the bifacial pieces are made on quartzite (65.8%) and to a lesser extent on silcrete (33%). Only a few quartz bifacial points occur in the toolkit (Schirmer, 1975). All phases of manufacture are documented. The points in total show great standardisation concerning size and morphology (Minichillo, 2005). The complete points studied by Minichillo (2005: Table 5.2) show a mean length of 63.6 mm for silcrete and of 56.5 mm for quartzite. A high proportion of the bifacial elements is broken. Other tool types concern pieces with miscellaneous retouch, backed tools, and a few scrapers (Schirmer, 1975). The difficult accessibility of the site led Minichillo (2005: 118) to hypothesise that DRP was not functioning as a base camp or a hunting station, but rather as a bifacial point workshop. Shaping flakes occur in the assemblage confirming at least certain production or maintenance activities at the site (Minichillo, 2005).

Although comparability is limited due to the problematic research history, **the knappers of DRP seem to not have aimed at the production of blades like in the C-A layers of Sibudu. Quartz plays only a minor concerning the bifacial technology.** The bifacial points of DRP are larger than those of Sibudu. The backed tools are absent from the tool corpus of the C-A layers.

**PC**, Western Cape Province, has a turbulent research history and was the research aim of numerous excavations (Goodwin, 1949; Minichillo, 2005; Andreasson, 2010). The largest-scale excavations were conducted by Victor and Bertie Peers from 1926-1929. A summary of their field notes was published by Goodwin (1949). He provided a basic stratigraphic description from top to bottom: LSA, MSA ('Coarse Stillbay'), Howiesons Poort, Still Bay ('Finer Stillbay'), MSA ('Proto-Stillbay'), and ESA. This stratigraphy led to confusion due to the use of variants of the SB and the positioning of the HP in-between. A subsequent excavation by Jolly in the 1940s (Jolly, 1948) yielded a similarly vague stratigraphic sequence with some contradictions to the Peers observations. Later excavations by (Anthony, 1972) have recovered only materials of the lower deposits containing early MSA (Volman, 1981; Schmid, et al., 2016). Several attempts since the Peers excavations have been undertaken to resolve the relationship of the HP and SB at Peers Cave. Though this may never be clarified as almost all of the upper deposits have been removed, it is likely that the HP overlies the SB and is not interposed (Minichillo, 2005). The assemblage includes numerous irregular, radial, and change of orientation cores and blanks in the quartzite. The bifacial points seem to have been made on non-local silcrete primarily, whereas the toolkit encompasses no cores and debitage products of non-local raw materials indicating that knappers executed the earlier stages of the reduction sequence somewhere else (Andreasson, 2010). The presence of preforms as well as finished points attest different phases of the manufacturing process took place at PC. Toolmakers used large thick flakes and cobbles to shape bifacial pieces. The removals of the finished products point to the use of direct soft hammer percussion. Evidence of re-sharpening is present and some points demonstrate recycling by notching of the edges. The base of the finished objects is either thin elongated

double pointed or more elliptic. The typical laurel-leaf shape is common, but also examples with a wider teardrop shape exist. The length of the completely preserved points ranges between 35 mm and 100 mm. They are between 20 mm and 50 mm wide and between 5 mm and 20 mm thick. Some of the specimens are fragmented and the breaks mostly represent snap or bending fractures of the distal end. Denticulates, scrapers, and an unifacial point appear as other tools in the assemblage (Andreasson, 2010).

Though the statement possibilities are limited due to insecurities concerning the stratigraphy of the site and the conditions of the lithic collections, **some differences are apparent concerning the blank production and tool corpus**. The cores suggest a different organisation and aim of the reduction sequence at PC than at Sibudu. The techno-economic organisation involving a discrepancy between the exploitation of exotic raw materials exclusively for bifacial point production and local rocks predominantly for reduction strategies is not the case in the C-A layers. The sizes of the bifacial points differ and serrated pieces respectively pressure technique are absent at PC.

The putative SB occupation of **VR3**, Western Cape Province, yielded a young age of between <59.9 and 45.7 ka (Steele, et al., 2016). Bifacial pieces together with backed pieces and unifacial points originate mostly from Unit 04 of the main area. The unifacial and bifacial points are spatially not distinct from one another, while the backed artefacts occur largely slightly higher. The layer is dominated by quartz, followed by silcrete, hornfels and quartzite. Most of the cores are atypical or fragmented. However, among the remaining cores, Discoid and Levallois cores are most frequent. Flakes are the most common blank category. Only a few blades are present, but from fine-grained raw materials. The bifacial points are predominantly made on quartz. Two large, elongated hornfels points with ventral thinning and bifacial retouch on the tip appear in the assemblage. Knappers executed tool manufacture and maintenance at the site indicated by the presence of unfinished bifacial points and shaping flakes. The tool corpus involves furthermore notched pieces, scrapers, *pieces esquillées*, and denticulates (Steele, et al., 2016).

A comparison between VR3 and the C-A layers is currently not appropriate, as the stratigraphic separation of the lithic assemblage of layer 04, including bifacial elements suggesting an affinity to the SB and backed pieces potentially indicative of the HP, needs further clarification. Moreover, the layers of VR3 date younger than MIS 5

**MRS**, Western Cape Province, is a further rock shelter that yielded SB layers (Will, et al., 2015), but data concerning the lithic technology have not been published yet.

Bifacial-bearing surface collections assigned to the SB technocomplex are known from near the modern town of Still Bay, Western Cape Province, including **Blombos Sands**, **Blombos Schoolhouse**, and **Kleinjongensfontein**. The dune field site of Kleinjongensfontein yielded one of the assemblages that led to the naming of the SB and involves primarily bifacial points made on silcrete (Minichillo, 2005).

Another open-air site **Cape Hangklip**, Western Cape Province, located at the first cape east of the Cape of Good Hope produced a collection of 27 bifacials mainly made on silcrete (Minichillo, 2005).

Several systematic surveys conducted in the northern Cederberg mountains, Western Cape Province, lead to the discovery of open-air sites comprising bifacial points indicative of the SB (Mackay, et al., 2018). In the Clanwilliam area, the locality **Clanwilliam Dam East** yielded 50 bifacial points prevailingly made on silcrete. The assemblages demonstrates pieces from unfinished tools with cortical remains from the earliest phase of production, finished products, and recycled points (Hallinan, 2013; Mackay, et al., 2018). During Doring River survey, a large MSA scatter called **Kleinhoek 1** was discovered containing more than 140 bifacial points (Mackay, et al., 2018: Figure 2.6). Most of the pieces are made on local fine-grained quartzite and the whole bifacial manufacturing process from early to later phases is documented (Mackay, et al., 2018). The open-air site **Soutfontein-001** is located on the banks of the Varsche River close to an outcrop of quartz and encompasses an assemblage of 142 points. Three of the points are unifacial points, while the rest concerns bifacial specimens. The majority of the tools are made on quartz (Mackay, et al., 2010, 2018). The metrical data of 60 points showed a mean width of 27 mm, a mean thickness of 11 mm and a TCSA value of 152 with a minimum of 63 and a maximum of 418 (Mackay, et al., 2010).

The comparability to the C-A layers of Sibudu is very limited, as for the most part the technological data are not published or restricted to only some criteria, like raw material, of the bifacial component.

To sum up, **the assemblages of the SB comply with the definition with regard to the prevalence of bifacial technology and the occurrence of the typical bifacial points. The foliate or lanceolate morphology represents indeed a uniting feature of all points.** Generally, the tools exhibit V-shaped tips and elliptic bases. However, the bifacial pieces differ with regard to cross-section as well as bifacial symmetry. The bifacial points of BBC have biconvex cross-sections and bifacial symmetry, while the SB layers of Sibudu and DRS are planoconvex cross-sectional and bifacially asymmetric. UMH and HRS involve bifacially symmetric quartz bifacial points with biconvex cross-sections and bifacially asymmetric points made on other raw materials with planoconvex cross-sections. The bifacial tools vary in length and width, but are in general thin at mean thickness values of less than 10 mm with the exception of PC.

All assemblages attest the application of at the beginning direct internal percussion with a hard hammer and in later phases the introduction of direct marginal percussion with a soft hammer. However at BBC, the last phase of the bifacial reduction of silcrete involved pressure flaking after heat treatment to regularise the tip. As a side note here, heat treatment has thus a special status in the manufacturing process of bifacial points at BBC. At HRS, knappers also heat treated their silcrete yet in an early stage of the reduction sequence and did not apply heat treatment particularly to the point production. The points of HRS might have undergone pressure technique as a last trimming as well. Though, the manufacture of serrated bifacial pieces appears only in UMH.

Multiple lines of evidence confirm the assumption that the bifacial tools were handled axially. Dissension persists concerning the techno-functional and functional characterisation. The BBC bifacial specimens seem to represent mainly spear tips, while the points of the SB deposits of Sibudu and DRS were primarily used as cutting implements and only occasionally as spearheads.

The toolmakers of BBC and PC selected non-local fine-grained rock types for the shaping of bifacial pieces, while the SB layers of Sibudu, UMH, DRS, and HRS demonstrate the use of local available raw materials. However, past people seem to have curated bifacial specimens made on fine-grained varieties for a long-term use in different places of their territory. UMH and HRS indicate a differential treatment of quartz concerning the manufacturing process and the functional focus, whereas quartz is of minor importance in the SB strata of Sibudu, BBC, DRS, and DRP.

The SB is largely dominated by bifacial technology. The accompanying reduction strategies concern flake production in BBC and DRP. Blade technology appears in the SB context of HRS and Sibudu. However the stratigraphic sequence of a maximum depth of 0.3 m is complicated at HRS, as no divisions were observed within the sediments (Evans 1994; Högberg and Larsson, 2011). Additionally, most of the SB points occur in the upper part of the stratigraphy, while the blades appear throughout the sequence, but are more numerous in the lower part (Högberg, 2014, 2016). At PC, the aim of the reduction sequence is not clear.

Except UMH, the bifacial pieces dominate the typological spectrum of the SB assemblages. Other tool types concern scrapers, denticulates, and *pieces esquillées*. Among the scrapers, the variant of convergent scrapers or respectively unifacial points occurs rarely at the SB layers of Sibudu, BBC, and DRS. Large circular scrapers are characteristic at BBC and are present in low proportion at DRS. The tool corpus of UMH and DRP comprises additionally backed tools. Interestingly, knappers chose shaping flakes for the transformation into tools at DRS and BBC.

The comparison between the SB sites and the C-A layers of Sibudu revealed that **bifacial technology turns out to be an outstanding component in all the assemblages. But I observed several differences in terms of raw material provisioning patterns, organisation of the manufacturing process, morphometric, techno-functional characteristics, accompanying reduction sequences and the remaining formal tools.** Morphologically, the C-A strata of Sibudu together with UMH and HRS demonstrate on the one hand bifacially symmetric quartz bifacial points with biconvex cross-sections and on the other hand bifacially asymmetric points made on other raw materials with planoconvex cross-sections. The C-A layers, UMH and HRS evince a techno-economic management of quartz concerning manufacture and function. Relating to the functional aspect, the bifacial corpus of the C-A strata shows a dichotomy of bifacial points made on quartz used as armatures, likely as arrowheads, and those made on other raw materials used prevalingly as knives and at times as spears tips. The manufacture of serrated bifacial pieces with pressure notching in a final and ultimate phase emerges only in UMH and the C-A layers. The C-A deposits as well as the SB layers of Sibudu, UMH, DRS, and HRS involve the use of local available rocks. In contrast to the SB

assemblages, the C-A layers are of a predominantly laminar character. Additionally, unifacial pointed forms and not bifacial pieces as in the SB dominate the typological spectrum of the assemblages from the C-A strata. Shaping flakes for the modification into tools attested at DRS, BBC, also occur in the C-A layers.

### 6.2.1.3. The C-A layers within the MIS 5 bifacial expressions

It is of eye-opening importance to point out that **bifacial technology is not exclusively associated with the SB**. Bifacial reduction strategies indeed emerge in MSA sub-stages later than the SB: The Early HP of DRS involves a small number of bifacial pieces and shaping flakes (Porraz, et al., 2013). The HP at Sibudu yet comprises the manufacture of small quartz bifacials as one typical component in its technological repertoire (de la Peña, et al., 2013). In the Sibudan of Sibudu, the production of bifacial tools primarily made on quartz was identified (Will and Conard, 2018). Additionally, the final MSA of Sibudu, UMH, and Umbeli belli, KwaZulu-Natal, yielded morphologically distinct bifacial points with hollow bases (Kaplan, 1989, 1990; Wadley, 2005; Mohapi, 2012, 2013; Bader, 2018).

Interestingly in this context is the **evidence confirming earlier expressions of bifacial technology than the SB in the southern African MSA**.

The MSA sequence of **DRS** contains the so-termed **Pre-SB type 'Lynn'** (Porraz, et al., 2013, 2014) represented by one SU of 10 cm thickness, which is of interest in this discussion. Tribolo et al. (2013) published an age of  $100 \pm 10$  ka for the layer, while dissonantly, (Jacobs and Roberts, 2015) dated the SB to  $76.5 \pm 3.3$  ka and SU Marc below to  $88.4 \pm 4$  ka providing a age range from 73.2 to 92.4 for Pre-SB type 'Lynn'. Knappers used predominantly local raw materials, especially quartzite. The assemblage is dominated by irregular flakes and laminar blanks resulting from two reduction strategies. The first reduction sequence concerns the exploitation of the cores with centripetal removals, while the second reduction proceeds in a unidirectional manner. The characteristics of the blanks indicate the use of direct internal percussion with a hard hammer. The tool corpus comprises a high proportion of lateral scrapers and convergent scrapers corresponding to unifacial pointed forms. The toolmakers selected variable blank types for the transformation imparting these formal tools different morphological features. Two unifacial points show a basal thinning. Furthermore, notched pieces, denticulates and *pieces esquillées* occur as well among the retouched elements. Past people followed a particular techno-economic behaviour correlating the transport distance of the raw materials with certain tool types and intensities of re-sharpening. The local available quartzite encompasses mainly denticulates and notched pieces, while tools on exotic fine-grained rocks are more frequent and more intensely re-sharpened. Finally, the toolkit encompasses a few bifacial pieces, yet more numerous than *pieces esquillées*, and shaping flakes. Although the stratigraphic context of the bifacial elements needs further clarification, as a possible intrusion from the overlying SB layers cannot be excluded at present, Pre-SB 'Lynn' could constitute the onset of bifacial technology preceding the SB at DRS (Porraz, et al., 2013, 2014). The assemblage seemingly shares similarities with the end of MSA 2b corresponding

MSA II or Mossel Bay sub-stage (see Table 1), which has been said to include unifacial and bifacial points (Volman, 1981, 1984). NBC tentatively assigned to MSA II or Mossel Bay sub-stage contains convergent scrapers with ventral basal thinning (Volman, 1981, 1984). At KRM, the presence of a few unifacial and bifacial pieces and a subtle change in raw material provisioning marks the top of the MSA II (Singer and Wymer, 1982; Wurz, 2000, 2002). Layer T of AP11 (Vogelsang, 1998) could also coincide with this phase.

**In contrast to the C-A layers of Sibudu, the assemblage of the Pre-SB ‘Lynn’ demonstrates not one main reduction sequence, but two of which one concerns the exploitation of cores centripetally.** In the C-A layers, both internal hard and soft hammer percussion occurs, while only hard hammer percussion technique was documented at DRS. The prevailing use of local raw materials characterises both toolkits. The techno-economic pattern of intensified maintaining and re-sharpening of tools made on fine-grained raw materials of higher quality and the high frequency of unifacial pointed forms seem to be similarities as well. **However, *pieces esquillées* are absent in the C-A layers and moreover, bifacial technology is a centrepiece within the tool corpus.**

The **lower occupational unit T of AP11** (Vogelsang, 1998; Vogelsang, et al., 2010) yielded a lithic assemblage of 5521 artefacts, including four bifacial points (0.1%). The presence of bifacial pieces lead to the dismissing of the original classification as MSA 2 (Vogelsang, 1998) and the affiliation to the SB (Vogelsang, et al., 2010; Lombard and Högberg, 2018). However as mentioned in Chapter 1.2.2., Vogelsang et al. (2010) made this claim with reservations, as the SB is defined on the basis of a central status of bifacial technology and a high frequency of bifacial points rather than the appearance of a small fraction of bifacial tools. Thus, AP11 belongs to the MSA bifacial phenomenon of MIS 5, but a designation to the SB is highly questionable. The knappers used predominantly local quartzite to produce regular blades and triangular flakes with a high proportion of faceted butts from single-platform cores, cores with two opposed platforms and Levallois cores. Crested blades are also present. The tool corpus comprises, other than bifacial pieces, unifacial points, edge-retouched points and basal end-scrapers on pointed blades (Vogelsang, 1998; Vogelsang, et al., 2010).

Faceted platforms occur frequently at AP11, while rarely in the C-A layers at Sibudu.

**The reduction at Sibudu is predominantly unidirectional and differs from the Levallois method. The production of triangular elements is of importance at AP11 in contrast to Sibudu.** The typological corpus of AP11 and Sibudu differ in terms of the frequency of bifacial pieces and the presence of basal end-scrapers on pointed blades.

The **Pietersburg** involves the manufacture of bifacial pieces and is thus of interest in this discussion. The reinvestigation of several sites of the Pietersburg, as mentioned in Chapter 1.2.2., widespread in the interior of South Africa (see Figure 4) add new data to contribute to the technological description and a refined definition of this technocomplex.

**CH** comprising a long sequence of Pietersburg occupations was described in detail by Mason (1957), Mason et al (1988), and McNabb and Sinclair (2009). Local available raw

materials, including quartzite, quartz, andesite, chert, felsite and hornfels, were preferably used. Knappers followed a variety of reduction strategies to produce laminar elements. They exploited unidirectional prismatic and pyramidal cores starting with the installation of a crest. Moreover, prepared core technologies occur to manufacture blades and parallel-sided elongated flakes. Large flakes are also used as cores and shaped by centripetal flaking. Further exploitation continues either as uni- or bidirectional recurrent Levallois core. The end-products often exhibit faceted platforms. The reduction sequences are discontinuous, as indicated by non-cortical core maintaining products. Blades and elongated flakes as well as triangular flakes and flakes were selected for tool production. The tool corpus encompasses a large number of unifacial points, followed by side scrapers. A low proportion of bifacial points is present as well (McNabb and Sinclair, 2009). Based on his analysis of tools and blanks, (Mason, 1962, Mason, 1971, Mason, 1957) subdivided the Pietersburg sequence of CH into an Early, Middle and Later Pietersburg. McNabb and Sinclair (2009) conformingly documented a noticeable variability through time. The production of unifacial points increases in upper strata.

The Pietersburg of **BC** first described by Beaumont (1978) and Beaumont et al. (1978) involves flakes and blades made on rhyolite and quartzite, which decrease in dimensions from the oldest to the younger layers. The typical products exhibit plain platforms and large dimensions with length values ranging between 80 mm to 90 mm as well as width values of 40 mm to 50 mm. Toolmakers used the Levallois concept to produce their blanks. The formal tools contain a variety of bifacial as well as unifacial points and scrapers (Beaumont, 1978; Beaumont, et al., 1978). Preliminary lithic analysis of the new excavations at BC (Backwell, et al., 2018b) show that rhyolite, hornfels and basalt are the dominating raw materials. Flakes are most frequent among the blanks, but blades are also common. Levallois points occur abundantly. Knappers employed the Levallois concept to obtain their desired blanks. An independent bladelet production stands out. Retouched elements are yet quite rare.

Porraz et al. (2015, 2018) confirmed a strong technological and typological affinity of the **upper MSA occupations of BRS** to the Pietersburg industry. The upper phase 21 is dated by luminescence dating to  $73 \pm 6$  on quartz or to  $91 \pm 10$  ka on feldspar and the lower phase 28 to  $75 \pm 6$  ka respectively  $97 \pm 10$  ka (Porraz, et al., 2018). Most of the artefacts are made on hornfels and quartz from the surroundings of the site. Both raw materials have been exploited in similar ways, but retouching of hornfels is more frequent probable due to the properties of the rock type. The assemblages exhibit the production of laminar elements of different morphologies involving unidirectional Levallois as well as prismatic cores and a high frequency of end-products with faceted platforms. The blades of phase 28 exhibit a mean length of 38.7 mm, a mean width of 16 mm, and a mean thickness of 4 mm. Discoid and centripetal Levallois cores to obtain flakes of variable shapes are present as well. The percussion traces of some blanks point to an occasional application of marginal soft hammer percussion additionally to internal hard hammer percussion (Porraz, et al., 2015, 2018). The tool corpus of phase 21 is characterised by the presence of unifacial as well as bifacial points. However, the bifacial reduction sequence is of minor importance and no particular blank selection for the transformation into bifacial elements has been observed. 'Kostienki' pieces represent another noteworthy component of phase 21 (Porraz, et al., 2015). Phase 28 encompasses a typological



spectrum of side scrapers, notched pieces/denticulates, and as a diagnostic feature end-scrapers largely made on hornfels. Characteristic retouch flakes occur in the assemblage indicating *in situ* tool manufacture (Porraz, et al., 2018).

A new research project concerns the site of **MC** (de la Peña, et al., 2018b), Limpopo, which was first excavated in 1947 by Tobias and attributed to the Pietersburg industry (Tobias, 1949). A first technological description (de la Peña, et al., 2018b) shows that the lithic assemblages of layers I to V encompasses artefacts made on quartzite, quartz, and chert. The dominating rock type quartzite comes from the surroundings of the site. Flakes form the majority of the blanks, but the percentage of blades accounts for around 10% in all the layers. The blade production seemingly is integrated in the flake reduction sequence. Most of the products exhibit centripetal scars and most likely belong to the Levallois concept. The proportion of formal tools is low, including mainly side scrapers, unifacial points, notched pieces and denticulates, whereas the collection of Tobias' comprised bifacial pieces. The strata show differences concerning raw materials, the presence of triangular flakes, and the occurrence of unifacial points.

Though the Pietersburg technocomplex and its subdivision needs further clarification in the next years, some trends stand out allowing a comparison to the C-A layers of Sibudu. **Different laminar reduction strategies were used at CH and BRS, in contrast to Sibudu, where one reduction strategy clearly dominates.** The reduction of prismatic and pyramidal cores begins with the formation crested blades, which is also the case in the initial reduction phase at Sibudu. However, the convexities during the reduction are not managed with a lateral crest. Phases of core preparation interrupt phases of production in both systems of reduction. The remaining laminar cores show characteristics of the laminar Levallois method (Boëda, 1994, 2013; Boëda, et al., 2013). **The laminar reduction system of Sibudu differs from the laminar Levallois method, supposedly present in all Pietersburg assemblages, in so far as most of the cores exhibit no faceting and the flaking angles are below 90°.** Moreover, unlike the laminar cores from Sibudu, the intersection of the removal surface and the surface of the platform of Levallois cores is a plane allowing a parallel detachment of pre-determined products. Even though the Pietersburg sequences of CH and BC demonstrate a tendency towards the decrease in length of laminar elements, the end-products are still larger than those from Sibudu. No independent bladelet production was observed in the C-A layers. BRS demonstrates the application of both hard hammer percussion and soft hammers percussion, similar to Sibudu. The knappers of the C-A layers as well as those of the Pietersburg used mainly local available raw materials. The typological composition of the C-A strata involves unifacial and bifacial points as well as scraper-like forms complying with the Pietersburg. **The typical end-scrapers of phase 28 in BRS are absent at Sibudu. The toolkits of the Pietersburg lack serrated pieces associated with the use of pressure technique.**

This overview with a focus on the SB first and then an extension to the other bifacial-bearing industries in MIS 5 illustrates the **diversity of the bifacial phenomenon in MIS 5 apart from the common presence of bifacial reduction sequences** (see also Rots, et al., 2017). Accordingly, the

conception of bifacial technology in the MSA of southern Africa bursting as one single and consistent technological expression is untenable. Consequently, the proposition of 'Synthetic Model' (so named by Conard, et al., 2014) that SB represents a well-defined chrono-cultural marker horizon of short duration characterised by bifacial points (Jacobs, et al., 2008a; Henshilwood, 2012) needs to be reconsidered. **The MSA bifacial technologies seem rather to be a broader technological phenomenon comprising more spatial variability and potential temporal differences** highlighted by others as well (e.g. de la Peña, et al., 2013; Porraz, et al., 2013; Conard, et al., 2014; Conard and Porraz, 2015; Soriano, et al., 2015; Archer, et al., 2016; Rots, et al., 2017; Will and Conard, 2018). However, the typical assemblages assigned to the SB, including the SB layers of Sibudu Cave, BBC, DRP, DRS and HRS, conform with the defined features, in fact the prominence of bifacial technology within the toolkit and the morphology of the bifacial products, justifying to be aggregated under the term SB, despite to technological heterogeneities and chronological uncertainties already pointed out by other authors (Porraz, et al., 2013; Soriano, et al., 2015; Archer, et al., 2016).

**Besides, more and more data seem to confirm that bifacial technology arises and vanishes in various regions at different times.** The variability is visible on a sub-continental scale. In fact, Sibudu itself attests, on the level of an individual site, the occurrence of bifacial shaping in different phases, including the C-A layers, SB, HP, Sibudan and final MSA. Yet, the assemblages reveal great variabilities concerning the implementation and importance of bifacial manufacturing, the morphometric, techno-functional and functional features of the bifacial elements, the raw material economy, the concomitant reduction strategies, and the remaining formal tools (Wadley, 2005, 2007, Soriano, et al., 2009, 2015; Mohapi, 2012; de la Peña, et al., 2013; Conard, et al., 2014; de la Peña, 2015; Rots, et al., 2017; Will and Conard, 2018). **Consequently, the craftspeople of the southern African MSA seem to have autonomously invented bifacial technology due to varied cultural and techno-social reasons during different times indicating convergence in lithic technology** (see also Will and Conard, 2018). Convergence, i.e. repeated evolution/innovation of analogous traits in multiple species/cultures, represents a common evolutionary process in biological (e.g. Moore and Willmer, 1997; McGhee, et al., 2011) and cultural (e.g. O'Brien, et al., 2018) systems. Convergent technologies cannot be used straightforwardly to make claims about relationships between assemblages, cultures or populations in archaeological studies. However, hypotheses should be built on an approach focusing on numerous aspects, qualitatively and quantitatively, of the whole lithic assemblage rather than one singled out element (Tostevin, 2012; Will, et al., 2015; Will and Conard, 2018). **Accordingly, this study followed such a more holistic technological approach and due to a scarcely significant number of common features of the C-A layers with the SB especially, I argue that they should not be consolidated under the same label.**

Based on the current state of knowledge and re-affirmed by the comparison above, UMH interpreted as a localised variant of the SB shares a great number of similarities with the C-A layers at Sibudu. Until now, serrated artefacts have only been documented this early from the assemblages of these two sites (Rots, et al., 2017). A few serrated specimens seem to be present

in Zimbabwean sites, such as Bambata Cave and Zombepata Cave, assigned to the so-called Bambata Complex (Jones 1926, 1949; Armstrong, 1931a, 1931b; Cooke, 1971; Sampson, 1974), but future studies have to verify this. Despite stratigraphic insecurities, **UMH could belong to the same technological tradition as the C-A layers at Sibudu.**

#### 6.2.2. Cultural developments in the MSA context of MIS 5

In this section, I am now extending the focus and elaborate on the relation of the C-A deposits of Sibudu to assemblages of MIS 5 within the southern African context. My aim here is to tackle questions concerning the cultural-technological dynamics in this time period and furthermore to enhance the understanding of past hunter-gatherer populations in terms of, for example, resource management or technological innovations. Hence, I explore the differences and similarities to relevant industries from the known literature.

**KRM**, as stated in Chapter 1.2.2., yielded the reference assemblage for the **'MSA I' or 'Klasies River'**. Other sites comprising layers with technological similarities that might be assigned to this sub-stage of the MSA are HRS (Evans, 1994) and HBC (Volman, 1981, 1984; Hendey and Volman, 1986; Lombard, et al., 2012). The Klasies River technocomplex features the exploitation of local raw materials, which are, in the case of KRM, quartzite cobbles. Several traits related to knapping technique indicate that aside from internal direct hard hammer percussion, past people used marginal direct soft hammer percussion. The blades are produced by reduction of pyramidal or flat cores. The exploitation starts with the extraction of initial blades with thick cross sections. The lower faces or backs of the core exhibit low investment in the preparation. The platforms are, however, highly prepared. The cores and end-products attest a recurrent unidirectional reduction sequence. Some flat cores demonstrate a triangular flake scar as the last removal resembling Levallois point cores. This suggests either the coexistence of a laminar reduction with a triangular flake reduction or a last stage in the laminar reduction system. These blades, often with curved profiles, have a thin symmetrical shape. Furthermore, they are on average 81 mm long. The tool spectrum is small, including denticulates, notched pieces, retouched blades and triangular flakes (Wurz, 2000, 2002, 2012).

**The heavy use of cobbles as raw materials for cores and the use of pyramidal as well as flat cores distinguishes the laminar reduction of the Klasies River sub-stage from that of the C-A layers at Sibudu.** Both assemblages exhibit the use of soft and hard hammer, whereas marginal percussion and frequent preparation of the striking platforms common at KRM are absent at Sibudu. The reduction sequence at KRM does not start with crested blades. Though both reduction systems proceed unidirectionally, the end-products differ with regard to their curvature and dimensions. **A triangular flake reduction strategy lacking at Sibudu co-occurs with the laminar reduction at KRM. The C-A layers show a higher frequency of tools and a different spectrum of tool types as well as classes.**

The **'MSA II' or 'Mossel Bay'** defined on the according assemblage from **KRM** is associated with the **MSA-Mike from DRS** (Porraz, et al., 2013), the **M3 phase of BBC** (Douze, et

al., 2015), and **PP13B dating to MIS 5** (Thompson, et al., 2010). Furthermore, the undated sites CSB (Thompson and Marean, 2008), NBC (Volman, 1981, 1984), and KFR (Volman, 1981; Mackay, et al., 2014) might belong to the Mossel Bay industry as well. Future technological analyses have to show, if MLK belongs to this technocomplex. The lower occupational unit T of AP11 (Vogelsang, 1998; Vogelsang, et al., 2010) shows characteristics justifying a designation to the Mossel Bay despite the appearance of a few bifacial pieces (Vogelsang, 1998; Vogelsang, et al., 2010). The main raw materials in the Mossel Bay are from local sources; quartzite in KRM. Platform characteristics imply the exclusive use of hard-hammer percussion. The reduction systems reflect prevalingly unidirectional convergent and parallel Levallois methods on split cobbles. The blades are shorter with a mean length of 75.9 mm in the MSA II lower respectively 68.8 mm in the MSA II upper, thicker with a mean thickness of 11 mm in the MSA II lower respectively 10.3 mm in the MSA II upper and more irregular than those from the preceding MSA I sub-stage. Levallois points constitute the actual end-products with well-prepared platforms, regular dorsal scar patterns and a central ridge. Among the few formal tools, notched as well as denticulated blades and triangular flakes occur (Wurz, 2000, 2002, 2012; Wurz, et al., 2018).

The Mossel Bay and the C-A layers from Sibudu share similarities concerning the use of hard hammer percussion and the unidirectional reduction strategies aiming towards the production of blades. **However, the high investment in the platform preparation of the end-products, the occurrence of the Levallois concept, the importance of triangular flake production and the low frequency of tools are clear differences** in comparison with the technology documented in the C-A layers at Sibudu.

The sites **YFT** (Halkett, et al., 2003; Avery, et al., 2008; Wurz, 2012), **HDP1** (Will, 2011; Will, et al., 2013), and **SH** (Volman, 1978, 1981; Grine and Klein, 1993) comprise highly similar toolkits and seem to belong to a distinct variant of MIS 5 (Wurz, 2012, 2013). The procurement of local raw materials is observed, but also end-products and especially tools made on rocks of semi-local or non-local origin occur implying a particular techno-economic organisation of transport and curation. The reduction sequences are primarily oriented towards the production of flakes. The cores exhibit minimal preparation. Most of the blanks have plain platforms. Core-edge flakes are common. The toolmakers applied direct hard hammer percussion and, for the knapping of quartz, bipolar-on-anvil technique. The assemblages are characterised by a relatively high frequency of tools, including denticulates, notched pieces and scrapers.

**The comparison of the C-A layers of Sibudu to the three sites on the West Coast highlights great differences regarding the aim of the reduction strategies, the presence of bifacial technology and the composition of the tool corpus.**

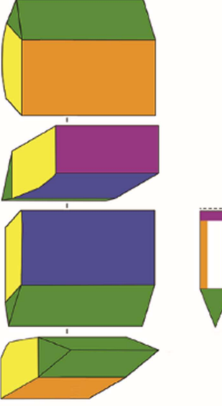
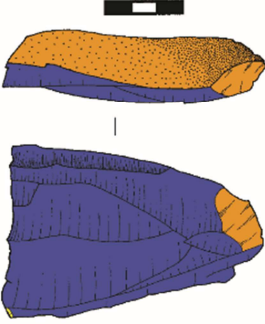
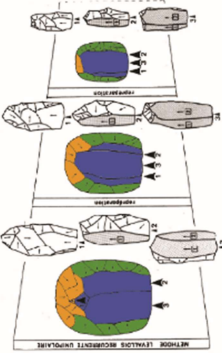
**This comprehensive overview of the MSA context in MIS 5** points out that with the exception of the sites YFT, HDP1 and SH, which seem to portray a specific functional adaptation to the coastal environment of the Western Cape and/or an earlier phase (Wurz, 2012; Will, et al., 2013; Douze, et al., 2015), **one technological expression, namely blade technology, emerges in the southern African technocomplexes during this time period** (see also Schmid, et al.,

2019). It must be mentioned that laminar production appears temporally and spatially scattered as early as the first half of the Middle Pleistocene in Africa. The earliest emergence of laminar reduction strategies comes from the Kapthurin Formation, East Africa, dating to at least 500 ka BP (Johnson and McBrearty, 2010). The oldest evidence blade producing industry in southern Africa is associated with Stratum 4a of KP1, belonging to the Fauresmith techno-complex with an age of  $464 \pm 47$  ka BP (Wilkins and Chazan, 2012). However, the manufacture of laminar blanks becomes established as a widespread phenomenon not before MIS 5. Interestingly, while the blade production is widely used from MIS 5 onwards, I observe not only the existence of different reduction strategies (Table 119) and differing roles of the laminar blanks within the functional system, but also great differences concerning the tool manufacturing and typological spectrum suggesting considerable spatial variability. Therefore, **MIS 5 in South Africa seemingly constitutes a period associated with a diversification in innovative blade technologies related to the expression of regional cultural traditions** (see Clark, 1988). The significance of these findings is further that during MIS 5, blade technology prevails in southern Africa, but the realisation of the technological goal differs regionally indicating that past populations organised themselves over distances with complex systems of connectedness and selective technology transfer. Based on the set of original traits of the C-A layers of Sibudu I described, the laminar reduction sequence together with the tool corpus comprising particular tool classes of unifacial pointed forms and bifacial technology, including serrated pieces, have not been presented before and thus, should be regarded as distinctive technological features of this assemblage. **The strata correspond to the rise of blade technology as an innovation within MIS 5, but also reflect the diversity in laminar reduction strategies and the emergence of other novelties, such as serrated pieces manufactured by pressure notching with a bone compressor and used as projectiles.**

### 6.2.3. The C-A layers of Sibudu matter – So what label?

After presenting the results and interpretations of my technological analysis of the C-A layers of Sibudu and drawing comparisons with assemblages relevant in this context, I return here to one of my central research questions engaging with a better understanding of the cultural dynamics and developments during MIS 5 in KwaZulu-Natal in a sparsely studied ecological zone. Furthermore, I provide a contribution to a purposeful terminological resolution for the chrono-cultural classificatory system of the southern African MSA. Historically, informal terminology, such as post-HP and pre-SB, implicating that material cultural remains can be characterised by what they lack rather than by what they contain, served for a preliminary description of an assemblage. In contrast, **I followed, as described in detail above, an approach explicitly requiring the underlining of positive key elements of the assemblages.** Only after this essential step has been undertaken, I am in an appropriate position to determine eventual similarities with other assemblages allowing for a cultural designation (see Conard, et al., 2012). My study showed that **the lithic technology of the C-A layers manifests a composition of positive characteristics.** The specific laminar reduction strategy with the installation of a lateral

**Table 119.** Comparison of the laminar reduction strategy of the C-A layers to other laminar reduction systems in southern Africa (+ = <10%; ++ = >10% and <50%; +++ = >50%) (scheme of pyramidal or flat core modified after Wurz, 2002; scheme of unidirectional recurrent Levallois core modified after Boëda, 1994) (modified after Schmid, et al., 2019).

<p><b>Scheme</b></p> <ul style="list-style-type: none"> <li>— removal surface</li> <li>— lateral crest</li> <li>— platform</li> <li>— distal trimming/back</li> <li>— <i>méplat</i></li> </ul>			
<b>Laminar Core configuration</b>	core with <i>méplat</i> , removal surface, lateral crest) + base, striking platform, back (C-A layers)	pyramidal or flat cores (Klasies River/MSA I)	unidirectional recurrent Levallois cores
<b>Reduction Organisation</b>	unidirectional (+++)	unidirectional (+++)	unidirectional (+++)
<b>Platform faceting</b>	+	+++	+++
<b>Technique</b>	internal direct hard/possible soft stone hammer percussion	internal direct hard stone hammer percussion/marginal direct soft stone hammer percussion	internal direct hard stone hammer percussion

crest and a lateral plane, the prevailing use of the laminar end-products for the modification into tools, the manufacturing of a variety of unifacial pointed forms, including primarily TSPs and ACTs, the occurrence of bifacial technology together with a particular status of quartz concerning the tool production illustrate diagnostic technological and techno-economic features branding the C-A deposits of Sibudu. Moreover, the appearance of serrated pieces transformed by pressure technique present on top of that a clear techno-functional signature (see Rots, et al., 2017). After establishing the wealthy set of key elements, I took the next step by comparing the techno-cultural ensemble of the C-A strata to available data from relevant assemblages from MIS 5 in the southern African context to evaluate technological affiliations and cultural relations. I determined that apart from bifacial technology, **the C-A layers have only a few commonalities with bifacial-bearing industries, above all the SB technocomplex.** The comparison to further demonstrate that blade technology seemingly arose during this period presenting a shared cognitive project, but was transposed in variable conceptual schemes and implemented through different operational schemes. **Besides the differing laminar reduction sequences, the techno-typological expressions show great differences to MSA I, MSA II and the coastal sites YFT, SH and HDP1.**

The assemblage of the C-A deposits comes from the site of Sibudu that meets basic prerequisites, such as the large number of lithic artefacts ( $n=8,164 >30$  mm; total for C-A layers), the good chronological control of the strata and the high quality of the spatial and technological data (see Conard, et al., 2012). In addition, the thickness of approximately 50 cm of the C-A strata, which exhibit great homogeneity with regard to the technical sub-system justifying their shared identity, implies a robust lasting archaeological signal within the stratigraphic sequence rather than an impulsive short moment in time or transitional horizon. **Based on these outstanding conditions together with the identification of clear peculiarities and the outcome of the comparative study, I propose that the C-A layers, descriptively referred to as 'serrates layers' by Rots et al. (2017), deserve a new techno-cultural term 'iLembian'.** The iLembian is named after the district municipality iLembe, where Sibudu is located. I follow the argumentation made by (Brew, 1946) viewing cultural taxonomy as meaningful analytical tool or heuristic device only in the context of answering specific research questions about past human lifeways and the organisation of our concepts and ideas about the past (Will, et al., 2014; Conard and Will, 2015; Will and Conard, 2018). I consider the **use of the term 'iLembian' as helpful to characterise and individualise the assemblage on the level of the site and on a broader scale, to construct a chrono-cultural framework for a better communication and understanding of behavioural changes and more generally cultural evolution in a time period and region, where little research has been done so far.** The usefulness and extent of the taxonomic unit can only be tested and underpinned by future studies, preferably technological analyses, and systematic comparisons with the growing body of the archaeological record, as there is no way to predict *a priori*, if term is useful for the area around Sibudu, the geographic zone of KwaZulu-Natal or the whole of southern Africa. Therefore, only additional research will be able to pinpoint the positioning of the iLembian within the taxonomic hierarchy of assemblages, phases, industries and technocomplexes respectively industrial complexes (Bishop and Clark, 1966; Clark, et al., 1966; Lombard, et al., 2012).

This clarification of the C-A layers within the chrono-cultural framework of the MSA has further implications concerning historical processes. Socio-economic, demographic and/or ecological mechanisms seemingly sparked the emergence of the cultural identity representing the iLembian. The recognition of the technological advancements of the groups belonging to the iLembian, such as bone tools (Rots, et al., 2017), blade technology, the application of pressure technique and the manufacture of serrated pieces for the use as projectiles, testifies the thriving of innovations in MIS 5, which by all appearances portrays a critical period concerning cultural evolution.



## 7. Summary

Over the last decades of research, the Middle Stone Age (MSA) has emerged as a key period for the biological and cultural evolution of modern humans. The MSA is generally considered to have started around 300 ka ago and lasted until circa 40 to 20 ka. In their pioneer monograph '*The Stone Age cultures of South Africa*' from 1929, A. J. H. Goodwin and C. van Riet Lowe defined the term MSA and introduced the tripartite division of the African Stone Age into Earlier Stone Age (ESA) ESA, MSA and Later Stone Age (LSA). Currently, the African fossil record has yielded the oldest specimens of anatomically modern humans (AMH) from Jebel Irhoud and associated with one of the oldest MSA assemblages (Hublin, et al., 2017). Since the 1980s, several independent genetic studies have demonstrated that *Homo sapiens* originated in Africa, but only increased availability of genomic data in the future and the constant progress of analytical methodologies will allow us to fully examine the complex scenario of modern human origins. The material culture of the MSA demonstrates a suite of technological and behavioural innovations of spatial and temporal diversity. The disappearance of large cutting tools (LCTs), such as handaxes and cleavers, the development of prepared core technologies for the production of flakes, blades and triangular flakes (points), and the manufacture of new tool-types suitable for hafting mark the major technological changes in the MSA. The onset of the MSA seems to represent a period of diversification in lithic technology associated with cultural regionalisation of past populations, resulting in different trajectories of change. Additionally, a variety of non-lithic cultural items appears as novelties in the MSA, signalling the emergence of more complex social behaviours. Organic technologies include a range of bone tools (such as knives, points, harpoons, awls, pins and engraved bones); personal ornamentation (marine shell beads); objects related to symbolically mediated behaviour (engraved ochre pieces and ostrich eggshell). These technologies, alongside the manufacture of compound paint and production of adhesives for hafting tools and advances in the lithic technical sub-system, can be seen as behavioural proxies for cognitive complexity. Complex cognition includes abstract thought, analogical reasoning, cognitive fluidity, flexibility in problem-solving, multitasking and long-term planning, comparable with the cognitive abilities of living people and falling within the variability of modern populations. Yet the nature, timing and tempo of factors that triggered all these early behavioural innovations still require further clarification.

Historically, researchers focused primarily on investigating two distinct Late Pleistocene technocomplexes: the Still Bay (SB) and the Howiesons Poort (HP), which were considered

particularly innovative. These two sub-stages were claimed to display clear cultural markers despite their relatively short timescales (Jacobs, et al., 2008a). The toolkit of the HP is characterised by blade production with high-quality raw materials of good knapping suitability, that were transformed into backed tools (Henshilwood, 2012; Wadley, 2015), whilst the toolkit of the SB features bifacial technology, partially produced by pressure-flaking and silcrete heat-treatment that was adopted to improve the knapping properties (Mourre, et al., 2010; Henshilwood, 2012; Schmidt, et al., 2013; Schmidt and Högberg, 2018). The categorisation of the HP as a cultural unit with a wide geographic range has been validated, but with a relatively long-lasting temporal duration from Marine Isotope Stage (MIS) 5 to 3, encompassing diachronic technological change and regional variability (Villa, et al., 2010; Porraz, et al., 2013; de la Peña, 2015; Soriano, et al., 2015; Douze, et al., 2018). In contrast, the SB period dating to MIS 5 and 4 is less well-defined and has a more problematic research history. This technocomplex was defined by Goodwin and van Riet Lowe (1929) based on the presence of bifacial points within several unstratified, undated, MSA open-air sites in the Western Cape Province. After the initial description, confusion arose about the SB, as the taxonomic label SB was applied to both assemblages lacking the *fossile directeur* and to assemblages from insecure stratigraphic contexts. Eventually, the SB industry was not listed in Volman's (1981, 1984) revised classification scheme of the MSA phases nor in of Singer and Wymer's (1982) formal subdivision. The term SB was not reintroduced until the excavations at Hollow Rock Shelter (HRS) (Evans, 1993, 1994) and at Blombos Cave (BBC) (Henshilwood, et al., 2001b) yielded stratified assemblages which seemingly corresponded to the original definition. Furthermore, the latest revision of the southern African MSA sequence reaffirmed the SB as a technocomplex (Lombard, et al., 2012). Jacobs et al.'s (2008a) synthesized chronological model argued that the SB is short-lived, lasting only from ca. 75 ka to 71 ka BP. However, Tribolo et al. (2013) demonstrated instead that the SB layers of Diepkloof Rock Shelter (DRS) are significantly older, extending up to  $109 \pm 10$  ka BP. The relatively short nature of the SB has been further challenged (see Guérin, et al., 2013; Feathers, 2015; Galbraith, 2015; Jacobs and Roberts, 2017). Sites containing assemblages assigned to the SB include Varsche Rivier 003 (VR3) (Steele, et al., 2016), Mertenhof Rock Shelter (MRS) (Will, et al., 2015), HRS (Evans, 1994; Högberg and Larsson, 2011; Högberg and Lombard, 2016a), DRS (Porraz, et al., 2013), Peers Cave (PC) (Minichillo, 2005), Dale Rose Parlour (DRP) (Schirmer, 1975), BBC (Villa, et al., 2009; Soriano, et al., 2015), Umhlatuzana Rock Shelter (UMH) (Kaplan, 1990; Lombard, et al., 2010; Högberg and Lombard, 2016b) and Sibudu Cave (Wadley, 2007; Soriano, et al., 2015). The SB assemblages

share strikingly similar bifacial technology; but growing evidence seems to point towards technological heterogeneity and temporal expansiveness of the SB (Porráz, et al., 2013; Conard and Porráz, 2015; Soriano, et al., 2015; Archer, et al., 2016; Rots, et al., 2017).

In recent years, technological studies on MIS 5 assemblages are growing in the literature, all of which point towards a more complex picture of cultural evolution than the uniform and stagnant scenario that was previously assumed. A number of sites assigned to the Pietersburg technocomplex are known from the north-eastern interior part of South Africa (Sampson, 1974; Wadley, 2015). Some of the Pietersburg sites are currently being re-investigated, such as Bushman Rock Shelter (BRS) (Porráz, et al., 2015, 2018), Border Cave (BC) (Backwell, et al., 2018b), Mwulu's Cave (MC) (de la Peña, et al., 2018), and Olieboomspoot (Val, personal communication). Furthermore, the 'MSA I' or 'Klasies River' and the 'MSA II' or 'Mossel Bay' technocomplexes were originally defined by Singer and Wymer (1982) based on assemblages at KRM and confirmed by Wurz (2000, 2002). MSA-Mike from DRS (Porráz, et al., 2013), M3 phase of BBC (Douze, et al., 2015), and Pinnacle Point (PP13B) dating to MIS 5 (Thompson, et al., 2010) resemble the KRM Mossel Bay. Three sites from the West Coast, Ysterfontein 1 (YFT) (Wurz, 2012), Hoedjiespunt 1 (Will, et al., 2013), and Sea Harvest (Volman, 1978), share distinct similarities, suggesting that they belong to a particular regional and/or chronological variant of the MSA (Wurz, 2013). Additionally, the Pre-SB type 'Lynn' (Porráz, et al., 2013, 2014) is also associated to the MSA of MIS 5, and presents a transitional unit with the emergence of bifacial technology preceding the SB. Thus, the archaeological record seems to indicate that cultural change and inventiveness are not restricted to the HP and SB technocomplexes. It suggests a complex scenario of distinct co-existing techno-typological traditions structured regionally in southern Africa during MIS 5 influencing the territorial and social organisation and the occurrence and diffusion of innovations. However, to increase our understanding of behavioural shifts, such as new technological achievements and symbolic practices, and beyond that, to contribute to the refinement of the chrono-cultural framework, the exploration of long regional sequences and the extension of the research focus from purportedly precocious phases, such as the SB and the HP, to the whole of the MSA is of great importance.

The site of Sibudu Cave, KwaZulu-Natal, South Africa, comprises a long and well-dated MSA sequence. Current excavations conducted by the University of Tübingen in the Deep Sounding of Sibudu have yielded MIS 5 lithic assemblages. These findings contribute to the discussion on

the driving mechanisms, appearance of technological novelties, and the cultural variability in the MSA during this period.

In the introduction, I start with the quote '*Giving substance to shadows*' from the song '*Crucify your mind*' by Sixto Rodriguez. These words summarise the five main research aims of this work: 1) Provide a first and detailed description of layers preceding the as particularly innovative considered SB by highlighting the diagnostic positive features concerning the lithic technology and raw material economy; 2) Identify technological novelties during MIS 5 in a under-studied region 3) Determine the potential mechanisms that drive behavioural changes and technological variability in MIS 5; 4) Exploring relationships and/or differences with other relevant assemblages of MIS 5, in particular the SB technocomplex; 5) Contribute to a refinement of the chrono-cultural framework of the southern African MSA during MIS 5.

The site of Sibudu Cave is located 40 km north of Durban in the local municipality KwaDukuza, which belongs to the district municipality iLembe. The site is perched on a steep cliff above the uThongathi River and the rock shelter is cut into the Natal Group sandstone. The excavation area is located at an altitude of approximately 100 m above mean sea-level in the north-eastern part of the shelter. With regards to the research history, A. Mazel excavated the first trial trench in 1983, and then further excavations were conducted by L. Wadley from 1998 until 2011. A team from the University of Tübingen led by N. J. Conard has continued the fieldwork since 2011.

The high-resolution stratigraphic sequence mainly consists of MSA layers ranging from more than 74 to 33 ka BP, followed by Iron Age occupations. The stratigraphy is predominantly composed of anthropogenic deposits and the organic preservation is generally in a good condition. Several OSL and radiocarbon dates have been obtained from the MSA deposits (e.g. Wadley and Jacobs, 2006; Jacobs, et al., 2008a; Jacobs and Roberts, 2017) and new luminescence dates are currently being finalised by C. Tribolo. The part of the chrono-cultural sequence that provided the lithic material for my thesis encompassed the six layers: BMo, RBS, GSS, GBP, LBC and PSS, which were identified at the start of the new excavations in 2011. In addition to these descriptive field designations, every new layer was assigned first a male and then a female name in alphabetical order, starting with the letter A: Adam, Annie, Bart, Bea, Casper and Chantal. The preliminary results of luminescence dating suggest that these strata date to between 92 and 72 ka BP (Tribolo, personal communication). The deposits BS and LBG, informally named 'pre-SB', are located above in the stratigraphy. Within the BS sequence, a

change in the typological corpus stands out as bifacial points occur in the deeper layer BS 11 to BS 16 (Wadley, 2013b). The deposits above, belonging to the SB, with an age of  $69.5 \pm 2.1$  ka BP, exhibit as the main diagnostic characteristic bifacial lithic technology, including bifacial points (Wadley, 2007; Soriano, et al., 2015). Strata assigned to the HP overlie the SB dating to between  $60.5 \pm 1.8$  and  $58 \pm 1.7$  ka BP feature different lithic reduction strategies that were used to make blades that were then frequently transformed into a variety of backed tools (Delagnes, et al., 2006; de la Peña, 2015; Soriano, et al., 2015). Furthermore, the manufacture of small quartz bifacial points is part of the HP toolkit as well (de la Peña, et al., 2013). The following part of the sequence has an age of roughly 58 ka BP corresponding to the post-HP. In response to concerns surrounding the informal name of 'post-HP', it has been suggested that Sibudu be considered as type-site for this phase (Conard, et al., 2012; Lombard, et al., 2012). Lombard et al. (2012) proposed the term 'Sibudu technocomplex', characterised by point production using the Levallois concept and typical unifacial points with faceted platforms and elongated shapes. Conard et al. (2012) argue instead for the term 'Sibudan', as it presents distinctive techno-functional signatures, such as Tongatis, Ndwedwes, *biseaux* and naturally backed tools. Moreover, this high-resolution sequence dating to around 58 ka BP revealed short-term changes and strong diachronic signals (Will and Conard, 2018). The overlying strata, referred to as late MSA dated to ca. 48 ka BP, are characterised by a high frequency of unifacial points (Villa et al. 2005). The layers at the top of the MSA sequence are described as final MSA, with an age of around 38 ka BP, and their most characteristic feature are hollow-based points (Wadley, 2005).

Today Sibudu is situated in the KwaZulu-Natal Coastal Belt of the Indian Ocean Coastal Belt Biome, falling within the Summer Rainfall Zone. This vegetation zone is dominated by forest only interrupted by patches of grassland, and characterised by hot and moist tropical climatic conditions in the summer and mild, dry subtropical conditions in winter (Mucina, et al., 2006). The indigenous vegetation directly around the site comprises evergreen species, deciduous savannah woodland and grassland (Wadley, 2013b).

With regards to palaeoenvironmental reconstructions, Sibudu provides a wide range of high-resolution environmental data (e.g. Allott, 2006; Herries, 2006; Pickering, 2006; Renaut and Bamford, 2006; Schiegl and Conard, 2006; Clark, 2013; Sievers, 2013; Hall, et al., 2014; Val, 2016; Murungi, 2017; Robinson and Wadley, 2018). This evidence, spanning several fields, depicts a mosaic of habitats that persisted during all of the occupation layers of Sibudu, perhaps due to the location of the site and its proximity to the uThongathi River (Robinson and Wadley,

2018). A large part of the taxa surrounding Sibudu today was most likely also present during the MSA, suggesting similar conditions as today existed at the site. However, some plant species have been identified in the archaeological record that are seemingly absent today, implying that, perhaps due to the more northerly vegetation elements, the dry woodland component of the vegetation may have been more extensive (Wadley and Jacobs, 2006). With regard to the layers Chantal to Adam relevant for this thesis, a preliminary faunal identification of layer Casper revealed the presence of blue duiker and bush pig, which are commonly found in forest habitats.

Following the *chaîne opératoire* approach (e.g. Leroi-Gourhan, 1943; Tixier, 1980; Pelegrin, et al., 1988; Boëda, et al., 1990; Geneste, 1991; Inizan, et al., 1999; Soressi and Geneste, 2011), I carried out a technological analysis of the artefacts from layers C-A at Sibudu. With regards to my theoretical background, I proposed that the lithic production first emerged as a cognitive project, which was then converted, on an intellectual level, into a conceptual scheme that finally underwent concretisation through a series of events representing the operational scheme. Each of these steps is dependent upon and influenced by several, partly interacting, natural and human parameters (Pigeot, 1991; Inizan, et al., 1999; Soressi and Geneste, 2011; Porraz, et al., 2016). Thus, the documentation of patterns in a lithic assemblage provide the basis for interpretation as intentional (Soressi and Geneste, 2011). Knappers' ultimate goal is to produce tools designed in a way that they can serve a distinct function (Porraz, et al., 2016). As the tool is considered the integral part of a deliberate, non-random system of fabrication, maintenance and abandonment, I would expect a strong relationship between raw material selection, core reduction strategies, outcome of blanks and the transformation and use and discard of tools (Conard, et al., 2012). In addition to adopting a traditional typological approach, I follow the Pradnik Cycle (Krukowski, 1939) concept, which assumes that the regulated phases of tool production, usage and discard leave recurrent patterns on the lithic assemblage, as tools from different stages occur allowing for the determination of the life-cycle of the tool. Furthermore, I adopt a techno-functional approach to provide functional characterisations of the tools based on technical features (e.g. Lepot, 1993; Bourguignon, 1997; Soriano, 2000; Bonilauri, 2010; Nicoud, 2011; Chevrier, 2012; Boëda, 2013). The aim of this approach is to identify the three essential techno-functional units of a tool: the transformative part, the prehensile part and the intermediate part. The technological and techno-functional methods, combined with use-wear and residue analyses (Rots, et al., 2017), and further supplemented with experimental data,

provide multiple lines of evidence to underpin specific hypotheses about the dynamics of production, use and discard of tools. This comprehensive framework of methodological procedures enables me to gain maximum information from limited archaeological data, to describe technical events and to make inferences about human behaviours in the C-A layers from Sibudu. Finally, detailed technological analyses allow comparisons with other assemblages to identify similarities and differences in technical choices to achieve a better understanding of temporal and spatial variability of lithic technology in a broader cultural context (see Lechtman, 1977; Wiessner, 1983).

The archaeological sample that formed the basis of my doctoral work consisted of all of the lithic objects  $\geq 30$  mm, plus all cores, core fragments, tools and tool fragments regardless of their size from layers Chantal to Adam. The pieces originated from an excavation area of circa 4 m<sup>2</sup> excavated between 2012-2016. The six deposits comprise a total of 8,164 artefacts.

Returning to the results of this study, during this phase of occupation, the knappers exploited a range of different raw materials mostly available locally (less than 5 km), including primarily dolerite followed by sandstone, quartzite, quartz, hornfels and chert, which are of variable prominence with regards to blank production and tool manufacture. Past people procured the rock types from different sources, e.g. as cobbles from the river or from (sub)primary outcrops, and thus the raw materials show variable shapes as well as physical characteristics. The proportion of cortex coverage as well as the presence of products from the earliest stages of reduction imply that the toolmakers at least to some extent carried out the whole reduction sequence with regard to all raw materials, except chert, at the site. Dolerite comprises the highest frequency of blanks, cores and tools and, seems to have been intensely exploited by knapping activities on site. A few large dolerite blades occur in the assemblage, indicating that some elements were imported as end-products to the site. Although dolerite is the dominant raw material, the tool-to-blank ratio suggests that blanks were (relatively) rarely made into tools. Sandstone, originating from the shelter itself, is second most common raw material in the assemblage and displays the lowest degree of modification. Quartzite and hornfels seem to have been more often transported to the site as finished blanks. The tools made out of these rock types show a high degree of investment into their curation. The assemblage also comprises crystal and milky quartz. This rock type makes up the second largest number of cores, which are the smallest in size compared to the cores made with other raw materials. Quartz, especially

crystal quartz, is of great importance for the production of tools, in particular bifacial and serrated pieces.

The toolkit demonstrates a strong emphasis on the production of blades and elongated flakes in relation to different raw materials. Some of the blades have very large dimensions with a maximum length of up to 114 mm, whilst the majority have an average length between 39 mm and 55 mm. However, the blade assemblage contains a high proportion of fragmented elements. In contrast to the length, which comprises a wide range, the width and thickness of the blades show a higher degree of standardisation. Most blades show no cortex coverage on the dorsal face. The platforms of the majority of these laminar end-products are plain and the morphology is almost exclusively rectangular. The pieces predominantly exhibit unidirectional dorsal scar patterns, whereas some end-products have orthogonal or bidirectional negatives attesting to respectively lateral distal preparation. The knappers aimed for blades with straight to slightly curved profiles. Within the blade category, I identify two distinctive concerning the cross-section as well as the width-thickness ratio subgroups: (1) tall, laterally centralised blades with a triangular cross-section, and (2) flat, laterally diffuse blades with a trapezoidal cross-section. Subgroup (1) dominates the assemblage and shows clear lower vertical convexities. Interestingly, none of the blades in subgroup (2) had complete dorsal cortex coverage and only a few blanks had more than 50% of cortical remains, suggesting that subgroup (2) is not involved in the earliest stages of reduction. The blades exhibit similar metric dimensions and shapes throughout the sequence.

The elongated flakes generally display similar tendencies to blades. In contrast to the blades, however, more elongated flakes show cortical remains on their dorsal face. Elongated flakes are shorter, wider and thicker than blades. Most of these blanks are not fragmented and a clearly higher percentage of pieces than blades are completely preserved. The trend of the dichotomy of laterally centralised specimens with a triangular cross-section and flat, laterally diffuse ones with a trapezoidal cross-section stands out among the elongated flakes as well. I also observe similar tendencies in all layers in terms of elongated flake size and shape.

Flakes make up the largest part of the blank population and exhibit a set of diagnostic features. Quartz and sandstone include a lower frequency of laminar elements, but a higher percentage of flakes than the other raw materials. The flake category demonstrates a mean length of 31.9 mm with a corresponding mean width of 33 mm and a mean thickness of 8.9 mm. These blanks consist of a higher proportion of completely preserved elements than their laminar



counterparts. The flakes, more often than the blades and elongated flakes, display cortex coverage on their dorsal faces. Most of the flakes have plain platforms, but involving the highest number of pieces with cortical platforms. The prevailing dorsal scar pattern is unidirectional, yet a large number demonstrates orthogonal negatives – often an orthogonal laminar scar. Interestingly, the flake population with orthogonal scars exhibit more non-cortical elements, and additionally, involve fewer pieces with over 50% cortical remains plus no completely cortical artefacts. Hence, the orthogonal flakes presumably come from more advanced stages of the reduction sequence. The greatest part shows a trapezoidal morphology and straight to slightly curved profiles. The cross-sections are either triangular or trapezoidal. I documented diachronic similarities concerning metric dimensions and shape.

Triangular flakes are present in low proportion throughout the sequence, but play a marginal role within the assemblage.

I classified the cores following Conard et al.'s 2004 unified taxonomy. Accordingly, most of the cores conform with platform types and, more precisely, almost exclusively to blade platform cores. The blade platform cores are primarily made on dolerite and quartzite. The knappers seemed to select predominately slabs to configure them into these core type. The low percentage of cortex coverage is most often located on the backs and/or on one lateral surface of the cores. The majority of the specimens is equipped with one striking platform, which is usually plain. The main removal surfaces prevailingly have a quadrangular shape. The blade platform cores are almost solely exploited by unidirectional removals. Most often, the bases of this core type exhibit a distal trimming preparation. The variability within the blade platform cores seems to be associated with different stages of discard. The last operations on the cores correspond primarily to knapping accidents or preparational activities. The last production operations clearly highlight the focus on laminar elements. The laminar end-product scars on the blade platform cores indicate minimum requirements for the length of circa 20 mm and the width of 10 mm. However, the core dimensions, especially the length-width ratio of the removal surfaces, do not coincide with the laminar dimensions. Based on the general description of the assemblage, the cortex coverage and dimensions of the blade platform cores, I argue that a high frequency of the platform cores represents exhausted cores. Platform cores dominate throughout all layers, except in the Casper layer, in which bipolar cores are more common.

One core made on quartzite exhibits bladelet scars as the last production operation. The similarities between the configuration and morphology of the blade platform cores suggest that

this core might be the result of extreme core exhaustion rather than an independent reduction strategy.

One of the quartz cores shows removals of a first exploitation as a laminar platform core and traces of a termination by bipolar-on-anvil percussion.

The second most frequent core types are bipolar cores, mainly made on quartz. These cores have smaller dimensions than the platform cores.

A few cores belong to the category of initial cores. All of them are made on slabs and exhibit more than 50% of cortex coverage, located either on the back or on the back and one lateral face. The removal surfaces have quadrangular shapes and the bases are either cortical or prepared. The initial cores show greater dimensions than the platform cores. The last operation is related to either preparatory actions or a knapping accident.

The tendencies of the identified percussion marks for all of the blanks suggest that the Sibudu knappers used both hard and soft hammerstones in direct, internal percussion, while applying both *rentrante* and tangential motions. The assemblage comprises several cobbles and cobble fragments of sandstone, quartzite, dolerite and quartz with impact traces that can be interpreted as hammerstones, supporting the potential coexistence within the toolkit of hard and soft hammerstones to detach blanks.

Aggregating all the data from the blanks and cores, I found that the inhabitants of Sibudu in the MSA focused mainly on the production of laminar elements and developed a specific unidirectional reduction strategy to create blades and elongated flakes on all raw materials. The typical blades are characterised by unidirectional dorsal scar patterns, rectangular shapes and straight to slightly curved profiles. The systematic core configuration enables and maintains laminar production. The knappers established six different areas to achieve the geometry required to manufacture their end-products: striking platform, removal surface, back as well as base of the core, plus the two further essential surfaces: the lateral crest and *méplat* or lateral plane. The platforms are usually plain and have an arched outline. Primarily, the removal surfaces show quadrangular shapes and are of a rather low transversal convexity. The backs of the cores are mainly formed by natural or old ventral faces. However, some backs are overprinted by preparational removals belonging to either the lateral crest, base or striking platform. Most of the bases demonstrate complete or partial preparation with negatives opposed to the knapping direction of the unidirectional reduction to maintain the distal convexity. The lateral crest is made on one lateral of the removal surface by detaching flakes

orthogonal to the axis of exploitation with the goal to sustain transversal convexity. Past people most likely frequently prepared the crests with either bifacially alternating removals or bifacial preparation. The *méplat*, or lateral plane, is located opposite the lateral crest on one of the narrow faces of the core. The lateral plane commonly is formed by a natural surface. However, a few cores display a rather advanced stage of reduction so that the *méplat* is not recognizable anymore due to heavy exhaustion. A few cores show orthogonal preparation removals to correct the angle between the removal surface and the *méplat*. The lateral crest and the lateral plane, together with the removal surface form the volume destined for exploitation. During the progress of the reduction, this active volume changes morphologically from a triangular asymmetric cross-section to a pentagonal cross-section, resembling a house tipped over on its side. The backs of the cores represent the passive volume.

In the early phase of laminar reduction system, the toolmakers preferentially selected slabs to begin with the preparation of the lateral crest and the installation of a striking platform. The diagnostic flakes from the early stage are trapezoidal and slightly curved to curved showing either unidirectional scars and/or cortex. The asymmetric triangular cross-section of the active volume enables the start of the effective exploitation from the ridge formed by the *méplat* and the removal surface. The knappers used either natural geometries to detach first naturally crested cortical blades or prepared one or both *versant(s)* to facilitate the removal of first crested blades.

In the middle and late phases of the reduction, the exploitation of the active volume proceeds asymmetrically on the wide surface and by reducing the lateral plane. The high frequency of laminar products with lateral cortex attests to the lateral expansion of the removal surface, while the presence of cortical backed blades testify to the exploitation of the *méplat*. This continuous dichotomy of the reduction sequence results in the production of two subgroups of blades. The reduction sequence is discontinuous, as on the one hand semi-crested laminar blanks indicate that the toolmakers had to partially renew the ridge formed by the lateral plane and the removal surface. On the other hand, cores and preparation flakes show the reinstallation of the lateral crest in an advanced stage of the reduction sequence. The diagnostic flakes of the crest re-shaping share characteristics with those of the early crest preparation including the trapezoidal shape and the slightly curved to curved profile, but they show no cortical remains and orthogonal laminar dorsal scars. To reorganise the angle of the platform, past people most likely removed partial rejuvenation core tablets. Distal trimming to manage the longitudinal convexity occurs as well.

The final phase of reduction involves the abandonment of the cores after a long cycle of exploitation, mostly due to knapping errors. The extreme core exhaustion, the imbalance in the exploitation of the active volume as well as the preparation of crests, platforms and distal surfaces cause a squarer rather than elongated shape of most removal surfaces. The end of production is inevitable, when the active volume is so intensely exhausted that the establishment of a transversal convexity by renewing the lateral crest and thus a further exploitation is impossible.

The assemblage stands out because of the presence of bifacial technology, including serrated pieces, but the greatest part of the formal tools in all layers concerns a variety of unifacially retouched pointed forms. Various scraper-like forms, as well as denticulates, are present as well. Within the superordinate typological classification, I defined tool classes based on the identification of patterns in the structural positioning of working and passive edges on the tools and dynamic associations with reduction cycles.

All of the unifacial pointed forms conform to the definition of triangular or sub-triangular blanks retouched almost exclusively on one surface with the distal end pointed through retouch or by primary flaking. Most of these tools are manufactured on dolerite, followed by quartzite. The blanks selected to be modified into this tool type involve primarily straight laminar elements of larger sizes from the main production phase. Among the unifacial pointed forms, I distinguished the tool classes: trihedral symmetric unifacial points (TSPs), asymmetric convergent tools (ACTs), Tongatis (for definition see Conard, et al., 2012) and unifacial points, which fulfil the general criteria, but were not classified further.

The TSPs make up the greatest percentage of the unifacial pointed forms. They feature symmetrical, bilaterally retouched distal ends formed by slightly curvilinear edges. Their tips are trihedral and of a regular triangular cross-sections. The intermediate parts are convergent and often invasively retouched on both edges suggesting several re-shaping phases, which cause the extension of the active part. The bases have usually a quadrangular shape and sometimes demonstrate ventral thinning. These tools demonstrate a mean length of 47.8 mm, a mean width of 24.6 mm and a mean thickness of 7.8 mm. The wide range of the length as well as the length of the retouched point could be related to the intensity of tool reduction and/or to the blank selection for the manufacturing of TSPs. The laminar products selected for the modification into TSPs are originally wider and probably longer than the unretouched blades and are then affected in length and width by manufacture and re-shaping. Most of the TSPs are

present as tip fragments probably broken during tool production or reworking. Concerning the techno-functional characteristics, these tools were probably primarily used in a punctiform mode related to perforating, drilling or piercing. The cycle of reduction comprises TSPs with small, short active parts compared to a relatively long intermediate part in an initial stage, while the advanced reduction of the tools, including several events of reworking, leads to a decline of the intermediate part and an expansion of the transformational working edge. Consequently, the maximum width of the point decreases and the delineation of the edges of the point are slightly concave rather than rectilinear. Additionally, the originally more parallel intermediate part changes into a convergent morphology.

ACTs represent the second largest proportion within the unifacial pointed forms exhibiting asymmetric convergent distal parts not aligned with the axis of percussion of the original blank and typically formed by a steep convex retouched edge together with an opposing straight unretouched edge. The confection expands from the distal end to the medial part commonly constituted by one converging edge and an opposite rectilinear edge. The base is usually quadrangular in shape. The length averages 44.5 mm, the width 26.8 mm and the thickness 8.2 mm. The blank selection involved predominantly straight laminar products from different stages of the reduction sequence. A low percentage of the ACTs are completely preserved. With regard to the functional characterisation, the toolmakers seemingly installed the blunted edges with abrupt retouch as backs of cutting tools to apply greater force to the working edges. The unmodified edges often exhibiting macroscopically visible macro and micro removals have low angles and feathered terminations. The asymmetry of the two edges indicates a linear mode of use, e.g. cutting, whittling and scraping. Concerning the life history of the ACTs, the installation of the steeply retouched edge seems to have been a terminal step and only the working edge was occasionally re-sharpened.

The bifacial pieces form the second most common tool type within the typological corpus. All specimens comply with tools exhibiting retouch on both surfaces along the same proportion of edge. This tool type comprises bifacial points and bifacially backed knives as tool classes. Furthermore, the tool class of serrated pieces defined as tools with margins delineated by regularly repeated small notches creating triangular teeth (Crabtree, 1972; Akerman and Bindon, 1995; Andrefsky, 2005) stands out.

Toolmakers primarily used quartz to manufacture bifacial points, followed by dolerite and quartzite. A large proportion of the bifacial points are fragments, especially tip and distal

fragments. The length shows a mean of 40.1 mm, while the width averages 22.9 mm and the thickness 8.2 mm. Most often the specimens are so overprinted by the bifacial shaping that the original blanks could not be determined anymore, but, when identifiable, knappers selected preferentially thick laminar products. The majority of the bifacial points have a straight profile. Concerning the morphotype, most of the bifacial points demonstrate bilateral symmetry. The points have a V-shape as well as a regular pointed tip outline and take between one and two thirds of the entire tool. The mediate part is usually convergent and the bases of the pieces have an elliptic morphology. The bifacial reduction sequence involves two knapping techniques: direct percussion with a hard hammer in the initial shaping process and soft hammer marginal percussion in the advanced phase of shaping. All phases of manufacture from preforms to finished products and recycled elements occur. The bifacial points demonstrate a high variability related to the rock types regarding size, morphology, organisation of the manufacturing process and subsequently the techno-functional interpretation.

The points made on dolerite, quartzite and hornfels are on average 41.2 mm long, 25.1 mm wide and 9.1 mm thick. These tools exhibit planoconvex cross-sections. The shaping of dolerite, quartzite and hornfels bifacial points is generally, although not exclusively, organised hierarchically. Toolmakers often started the bifacial reduction on the flat surface and continued with the convex surface resulting in tools with planoconvex cross-sections. This configuration and hierarchy between faces permits a series of re-sharpening events without alteration of the entire structure, conforming to 'bifaces used as a blank for tools' (*pièces bifaciales supports*) (see Boëda, 1997; Porraz, et al., 2013; Soriano, et al., 2015). This design of the bifacial points made on dolerite, quartzite and hornfels suggests a long-term use primarily as pointed cutting implements.

The quartz bifacial points yielded a minimum length value of 26.7 mm. The width averages 17.3 mm and the thickness 6.6 mm. The highest frequency of quartz tools shows biconvex cross-sections. The manufacture of bifacial points made on quartz seems to be managed non-hierarchically by alternating removals resulting in biconvex finished products with pointed regular tip outlines. These bifacial points correspond to 'bifaces as tools' (*pièces bifaciales outils*) (see Boëda, et al., 1990; Nicoud, 2013). The bifacials most likely have functioned as axially hafted armatures in hunting weapons.

The tool corpus contains 25 serrated pieces mainly made on dolerite followed by quartz. The artefacts have a mean length of 42.1 mm, a mean width of 21.1 mm and a mean thickness of 7.8 mm. Blades and elongated flakes served predominantly as original blanks. The serrated

pieces have straight profiles and bilateral symmetry. Their morphotype consists of V-shaped and regular pointed tips, convergent or parallel medial parts exhibiting a continuation of from the point area and quadrangular basal parts. Technological variability concerning the reduction sequence results in two subgroups within the serrated pieces: bifacially shaped blanks that were bilaterally serrated and bifacially (or unilaterally) retouched blanks that were bilaterally (or laterally) serrated. The serrating of the artefacts constitutes the last and final phase of the manufacturing process. Multiple lines of evidence from technological and functional analyses as well as experiments indicate that the knappers applied pressure technique with a bone compressor to create the serrations. The series of notches on the pieces demonstrate great regularity indicating a clear control of the location of the contact points and applied force. Furthermore, the serrating removals exhibit characteristics, such as small hackles, negative bulbs, parallel edges and feathered terminations typical for a narrow contact point (see Mourre, et al., 2010). Moreover, the occurrence of quartz serrating flakes could be verified, as they differ from the shaping flakes with regard to platform thickness and overall morphology. The application of bone compressors is attested by microscopically identified bone residues in relation with the serration, the appearance of a bone tool with diagnostic use traces of a compressor and the presence of small bone flakes resembling the experimental bone flakes coming off the tip of a compressor unintentionally during use. The toolmakers at Sibudu rather than employing pressure flaking to regularise an edge and thinning the sections of the tools used pressure notching to create the notches of the serrated pieces by placing the compressor slightly interior of the edge and applying the force at an angle perpendicular to the plane of the blank (see Crabtree, 1973; Whittaker, 1994). The results of the use-wear and residue analyses in combination with experimental data provide insights on the function and handling of the serrated pieces (Rots, et al., 2017). These tools represent mounted tips on shafts of hunting weapons. Past people manufactured and utilised compound adhesives of ground red ochre mixed with plant gum for the hafting of the pieces.

Among the bifacial tools occur also five specimens that concur with the definition of asymmetrically bifacially backed knives (*Keilmesser*) (see Jöris, 2006; Frick, et al., 2018). They have robust working edges opposite to natural or with steep, large removals prepared backs. Towards the distal end on the lateral related to the back, the retouch changes to a less abrupt angle forming a sharp edge which converges with the opposing working edge. The distal end exhibits a tip lacking a regular pointed outline. The medial part is composed of the rectilinear working edge and the towards the distal part converging edge with the back. The base has a

quadrangular morphology. The organisation of the manufacturing proceeded hierarchically and resulted in an asymmetric section allowing for frequent re-sharpening episodes.

Furthermore, the scraper-like forms include lateral scrapers, naturally backed tools (NBTs) and a few end-scrapers.

The lateral scrapers make up the greatest part of the scraper-like forms. The highest frequency of the lateral scrapers shows modifications on both edges. I observe a variability concerning the retouching ranging from fine retouch to large removals. Large dolerite blades or elongated flakes partially from early stages of the reduction commonly served as original blanks for the manufacturing of lateral scrapers. The pieces have a mean length value of 47.3 mm. They are robust demonstrated by a mean width of 33.6 mm and a mean thickness of 10.7 mm.

The NBTs refer to objects with a natural backing located opposite to a retouched working edge. The back is in a few cases created by removals, but usually formed naturally by cortex, Siret fractures, platforms of the blank or from a core-edge product. The highest proportion is made on dolerite, followed by quartzite. The knappers selected a variety of original blanks, including blades, elongated flakes, flakes, preparational flakes and shaping flakes, to transform them into NBTs. The length of the elements averages 40.3 mm, the width 29.8 mm and the thickness 10.9 mm.

Finally, denticulates and notched pieces are consistently present in the typological composition of all strata. The notched pieces have a single deeply concave notch in contrast to the denticulates, which show a succession of adjacent notches (see Inizan, et al., 1999). The preferentially chosen original blanks are either blades or elongated flakes. The specimens demonstrate a mean length of 44.2 mm, a mean width of 27.3 mm and a mean thickness of 8.5 mm. The denticulations of the tools primarily occurring only on one lateral have rather wide notches; some of which are deep, while some are shallow. The mean notch width and mean notch depth show broad ranges attesting a great variability.

In general, the lithics of the C-A layers show little influence of taphonomic disturbances. The only noticeable post-depositional impact is the strong encrustation of sediment on the artefacts made on all raw materials which increases towards the lowermost layer Chantal.

The results of my study highlight great similarities of the C-A layers in relation to raw material selection, blank production, tool manufacture and spectrum. Due to this homogeneity, I consider the lithic assemblages as belonging to one technological tradition. Despite the overall



concordance, some trends are apparent within the sequence concerning the appearance and frequency of particular tools. Unifacial points reach a low point in layer Bart, while bifacial pieces and associated shaping flakes peak in this deposit. Serrated pieces, in contrast to serrating flakes, which occur in all the strata, emerge only from Bart onwards and have their highest frequency in layers Bea and Bart. Additionally, the proportion of crystal quartz strongly related to the manufacturing of bifacials is highest in strata Annie, Bart, and Bea with a sharp increase before and decrease after. Consequently, layer Bart marks the high point of bifacial technology.

In order to hypothesise about a possible start and end of the technological phase represented by layers C-A, I consider the SUs above and below within the stratigraphic sequence of Sibudu. The lower BS member located directly on top of the layer Adam, though only preliminary described, comprise large blades as well as flakes made on different raw materials, platform blade cores and bifacial points. The younger deposits include flakes and blades, but besides unifacial points and denticulates made on dolerite, other tools are rare. Thus, the limited available data suggest that the lower part of BS might belong to the 'C-A' technological phase. I had the possibility to analyse the tools and cores from the layers Danny and Darya stratigraphically directly below my sample. Base on their tool repertoire comprising bifacial pieces, a large proportion of unifacial pointed forms as well as scraper-like forms and the core populations demonstrating a high frequency of blade platform cores with a configuration resembling the laminar reduction strategy from the C-A layers, I argue that Danny and Darya represent a continuation of the technological tradition. Nevertheless, the C-A layers showing a striking peak in bifacial technology, including the serrated pieces, capture the central part of this technological tradition. These strata with a considerable thickness of circa 50 cm seem to constitute a phase of longer duration rather than a short episode.

The C-A layers are characterised by clear technological and techno-economic features:

The assemblage demonstrates one main unidirectional reduction strategy with a particular organisation oriented towards the production of blades and elongated flakes. The structure of the cores involves additionally to the striking platform, removal surface, core back and base, a lateral crest for the management of the transversal convexity and a lateral plane/*méplat* for providing the exploitable volume. Two subgroups of laminar end-products result from the exploitation of either the narrower lateral plane or the wider removal surface. Furthermore, typical preparation flakes originate from this reduction system, especially

concerning the establishment and maintenance of the lateral crest. Blades and elongated flakes often served as original blanks for different tool types indicating a strong interrelation. The tool corpus contains different unifacial pointed forms, whereas TSPs and ACTs stand out with particular morphometric and techno-functional characteristics. The striking typological elements however are the bifacial tools, including bifacial points, serrated pieces and a few asymmetrically bifacially backed knives. The manufacturing of the serrated pieces involved the application of pressure notching with a bone compressor. Past people used these objects as hafted projectiles to hunt animals. Scraper-like forms, such as lateral scrapers and NBTs, are also present within the toolkit. Finally, denticulates and notched pieces occur and are clearly different from the serrated pieces due to the number, location, width and depth of the notches.

The raw material procurement of the knappers from Sibudu involved preferentially locally available raw materials; first and foremost dolerite. Although the toolmakers exploited all raw materials with their particular laminar reduction strategy, they favoured dolerite slabs and exhausted them intensively as cores with long reduction cycles. Though the highest number of tools is made on dolerite, retouching and shaping of the blanks seemingly constitutes not the main focus of the knapping indicated by the low tool-to-blank ratio. This rock type was primarily selected to produce tools with a long life-span probably due to its toughness and rigidity ensuring durable edges. On the contrary, the inhabitants of Sibudu often modified blanks and invested in the curation of tools made on quartzite and hornfels. Quartz was mainly exploited by bipolar-on-anvil percussion played a central role for tool production, especially bifacial technology. Sandstone shows a high frequency of cortical blanks and a low percentage of tools as well as end-products suggesting the occasional exploitation by short reduction sequences on site. The assemblage exhibits the import of isolated end-products made on chert.

Concerning the bifacial technology, the raw materials demonstrate outstanding techno-economic differences. First, the whole bifacial manufacturing process of dolerite and hornfels seems to have been executed *in situ*, while bifacials made on quartz and especially quartzite got to the site primarily as finished products, where they were used, re-sharpened and discarded. Furthermore, the quartz bifacial points differ greatly from the other rocks in terms of morphometric features, organisation of the manufacturing process, life history, and ultimately the techno-functional and functional classification indicating a differential techno-economic behaviour. The size, the symmetric structure and the organisation of removals of the quartz points suggest a use as projectiles, whereas the other raw materials served rather as cutting implements. Finally, the serrated pieces also display a variability between quartz and

the other raw materials concerning dimensions, shapes, and manufacturing. The quartz points show properties, such as thinness, symmetry, narrow penetrating angle and biconvex cross-section, which putatively correspond to arrows, while the specimens made on other raw materials seem to rather comply with spear tips.

The exploitation of mostly local raw materials and the presence of entire reduction sequences for all rock types, except chert, indicates a main provisioning of place strategy, yet the provisioning of individuals and the provisioning of activities came into play to a limited extent as well.

Concerning the chrono-cultural classification, I compare the C-A layers to bifacial-bearing MSA assemblages in MIS 5 and subsequently to well-dated MSA sites of MIS 5 known from the literature.

Before discussing the MSA bifacial phenomenon in MIS 5 in general, I consider the C-A layers within the stratigraphic sequence of Sibudu itself. I observe great differences to the SB layers of the site concerning the reduction sequences, the dominance of bifacial technology and raw material economy. The layers interposed LBG and younger BS strata, though the technological data are preliminary, lack bifacial technology and exhibit an overall low importance of pointed forms. On the site level, the C-A layers and the SB deposits thus cannot be grouped together.

The comparison with the SB, as the main manifestation of MSA bifacial technologies, first and further bifacial expressions of MIS 5, including the Pre-SB type 'Lynn' of DRS, the lower occupational unit T of Apollo 11 (AP11) and the Pietersburg technocomplex, demonstrates the distinctiveness of the C-A layers and illustrates the diversity of the bifacial phenomenon. The bifacial technologies seem to be spatially variable and temporally different rather than related to one short-lived technocomplex (e.g. Porraz, et al., 2013; Conard, et al., 2014; Conard and Porraz, 2015; Soriano, et al., 2015; Rots, et al., 2017). The increasing body of archaeological evidence shows that bifacial technology emerges and vanishes in various regions at different times. The toolmakers of the MSA seem to have invented bifacial technology independently in a variety of contexts implying convergence, i.e. repeated innovation of analogous traits in multiple cultures, in lithic technology (see Will and Conard, 2018). As the C-A layers and the assemblages of the SB have, apart from the presence of bifacial technology, few characteristics in common, I argue that they should not be merged under the same label.

UMH interpreted as a localised variant of the SB shares numerous similarities, such as the early emergence of serrated pieces, with the C-A layers at Sibudu and thus, the two assemblages seem to belong to the same technological tradition.

The comprehensive comparative overview of the further MSA context in MIS 5 illustrates striking differences regarding the tool manufacturing, the spectrum of tool types, and the organisation of the reduction strategies, but reveals that a general trend towards the production of blades becomes more widely spread during this period. Past populations living synchronously in different regions of southern Africa and sharing cognitive competences seemingly aimed at similar technological goals. They shared the laminar reduction sequences as a joint cognitive project, which was translated into varied conceptual schemes that were realised through different operational schemes (see Inizan et al, 1999; Soressi and Geneste, 2011). Consequently, the MSA of MIS 5 apparently represents a period associated with a diversification in innovative blade technologies related to the expression of regional cultural traditions (see Clark 1988). The C-A layers conform to the appearance of blade technology as an innovation within MIS 5, but also reflect the diversity and the emergence of other novelties, such as serrated pieces involving pressure notching.

The assemblage of the C-A layers shows clear positive central elements and is noticeably different from the bifacial-bearing industries, above all the SB, and other technocomplexes of MIS 5, such as MSA I and MSA II. The data converge in such a way that I propose a new techno-cultural term 'iLembian' for the C-A layers. The name refers to the district municipality iLembe, where Sibudu is located. In my opinion, the use of the term 'iLembian' serves to contribute to the establishment of a chrono-cultural framework for a better communication and understanding of behavioural changes and cultural evolution in a time period and region, where little research has been done so far. More generally, I emphasise the observation that blade technology, the application of pressure technique and the manufacture of serrated pieces for the use as projectiles belong to the key set of innovations that help to characterise cultural dynamics in southern Africa during MIS 5.

## 8. Résumé

Au cours des dernières décennies de recherche, le *Middle Stone Age* (MSA) apparaît comme une période clé de l'évolution biologique et culturelle de l'homme moderne. On considère généralement que le MSA a débuté il y a environ 300 ka et a duré jusqu'à environ 40 à 20 ka. Dans leur monographie pionnière '*The Stone Age cultures of South Africa*' de 1929, A. J. H. Goodwin et C. van Riet Lowe ont, pour la première fois, défini le terme MSA et introduit la division tripartite de l'Âge de la pierre africain en *Earlier Stone Age* (ESA), MSA et *Later Stone Age* (LSA). Depuis les années 1980, plusieurs études génétiques indépendantes ont montré que l'Afrique est la patrie d'origine de l'*Homo sapiens*, mais que seule la disponibilité accrue de données génomiques dans le futur et le progrès constant des méthodologies analytiques permettront de retracer le scénario complexe des origines de l'homme moderne. La culture matérielle du MSA témoigne d'un ensemble d'innovations technologiques et comportementales d'une grande diversité spatiale et temporelle. La disparition des *large cutting tools* (LCT), tels que les bifaces et les hachereaux, le développement de technologies pour la production prédéterminée d'éclats, de lames et d'éclats triangulaires (pointes) et la fabrication de nouveaux types d'outils adaptés à un manche marquent les principaux changements technologiques dans le MSA. Le début du MSA semble représenter une période de diversification de la technologie lithique, associée à la régionalisation culturelle des populations précédentes qui se traduit par différentes trajectoires de changement. En outre, une variété d'éléments culturels non-lithiques apparaissent comme des nouveautés dans le MSA, signalant l'émergence de comportements sociaux plus complexes. Les technologies sur matières dures animales produisant une large palette d'outils sur os, tels que les couteaux, les pointes, les harpons, les poinçons et les os gravés, les parures sous forme de perles en coquillages marins, les objets liés à des comportements symboliques, comme les pièces gravées en ocre et les coquilles d'œufs d'autruche gravées, la fabrication de peinture composite et production d'adhésifs pour l'emmanchement d'outils en lien avec les progrès du sous-système technique lithique constituent des indicateurs de comportement montrant une complexité cognitive. La cognition complexe comprend la pensée abstraite, le raisonnement analogique, la fluidité cognitive, la souplesse dans la résolution de problèmes, l'adaptabilité à des tâches multiples" et la planification à long terme, comparable aux compétences mentales des êtres vivants et s'inscrivant dans la variabilité des populations modernes. Pourtant, la nature, la

temporalité et le rythme des facteurs qui déclenchent toutes ces innovations comportementales précoces nécessitent encore beaucoup plus de précisions.

Longtemps, les chercheurs n'ont concentré leur attention que sur l'étude des deux complexes technologiques distincts du Pléistocène tardif, le Still Bay (SB) et l'Howiesons Poort (HP), considérés comme particulièrement innovants. Ces deux sous-étapes du MSA étaient décrites comme étant de courte durée et possédant des marqueurs culturels clairs (Jacobs, et al., 2008a). Les industries lithique de l'HP se caractérisent par la production de lames sur des matières premières de haute qualité et de bonne aptitude à la taille, ensuite transformées en outils à dos (Henshilwood, 2012; Wadley, 2015), tandis que celles du SB présentent une technologie bifaciale, partiellement produite par façonnage par pression et traitement thermique du silicrète qui a servi à en améliorer les propriétés de coupe (Mourre et al., 2010; Henshilwood, 2012; Schmidt, et al., 2013; Schmidt et Högberg, 2018). La définition du HP comme une unité culturelle ayant une large couverture géographique s'est maintenue, mais avec une durée relativement longue allant du stade isotopique 5 au stade 3 (MIS), englobant des changements technologiques diachroniques et une variabilité régionale (Villa, et al., 2010; Porraz, et al., 2013; de la Peña, 2015; Soriano, et al., 2015; Douze, et al., 2018). En revanche, la période SB datant des MIS 5 et 4 est moins bien définie et a un historique de recherche plus problématique. Ce complexe technologique a été défini par Goodwin et van Riet Lowe (1929) sur la base de la présence de pointes bifaciales dans plusieurs sites non stratifiés et non datés du MSA en plein air dans la province du Cap occidental. Après la description initiale, la confusion s'est installée au sujet du SB, puisque l'étiquette taxonomique SB a été appliquée d'une part aux assemblages dépourvus du fossile directeur et d'autre part aux assemblages provenant de contextes stratigraphiques peu sûrs. Finalement, l'industrie SB n'a pas été inscrite dans le système de classification révisé des phases MSA de Volman (1981, 1984) et de la subdivision formelle de Singer et Wymer (1982). Le terme SB n'a pas été réhabilité avant que les fouilles à Hollow Rock Shelter (HRS) (Evans, 1993, 1994) et à Blombos Cave (BBC) (Henshilwood, et al., 2001b) ne produisent des ensembles stratifiés correspondant à la définition originale. La dernière révision de la séquence MSA de l'Afrique australe a réaffirmé le SB comme un complexe technologique (Lombard, et al., 2012). Le modèle chronologique synthétisé de Jacobs et al. (2008a) prétend que le SB est de courte durée et ne dure que de 75 ka à 71 ka BP environ. Cependant, Tribolo et al. (2013) ont montré que les couches SB de Diepkloof Rock Shelter (DRS) sont significativement plus anciennes, s'étendant jusqu'à  $109 \pm 10$  ka BP. Le caractère éphémère du SB a été remis en question depuis (Guérin, et al., 2013; Feathers, 2015 ; Galbraith,

2015 ; Jacobs et Roberts, 2017). Les sites contenant des assemblages attribués au SB comprennent Varsche Rivier 003 (VR3) (Steele et al., 2016), Mertenhof Rock Shelter (MRS) (Will et al., 2015), HRS (Evans, 1994; Högberg et Larsson, 2011; Högberg et Lombard, 2016a), DRS (Porraz, et al, 2013), Peers Cave (PC) (Minichillo, 2005), Dale Rose Parlour (DRP) (Schirmer, 1975), BBC (Villa et al., 2009; Soriano et al., 2015), Umhlatuzana Rock Shelter (UMH) (Kaplan, 1990; Lombard, et al., 2010; Högberg et Lombard, 2016b) et Sibudu Cave (Wadley, 2007; Soriano et al., 2015) Les assemblages du SB ont en commun une similitude frappante de technologie bifaciale, mais de plus en plus de preuves démontrent également son hétérogénéité technologique et sa durée (Porraz, et al., 2013; Conard et Porraz, 2015; Soriano, et al., 2015; Archer, et al., 2016; Rots, et al., 2017).

Ces dernières années, les études technologiques sur les assemblages MIS 5 sont de plus en plus publiées et donnent une image plus complexe de l'évolution culturelle que le scénario uniforme et stagnant supposé précédemment. Un certain nombre de sites attribués au complexe technologique de Pietersburg sont connus dans la partie nord-est de l'Afrique du Sud (Sampson, 1974 ; Wadley, 2015). Certains des sites de Pietersburg font actuellement l'objet d'une nouvelle étude, comme le Bushman Rock Shelter (BRS) (Porraz, et al., 2015, 2018), Border Cave (BC) (Backwell, et al., 2018b), Mwulu's Cave (MC) (de la Peña, et al., 2018) et Olieboomspoort (Val, communication personnelle). En outre, les complexes technologiques 'MSA I' ou 'Klasies River' et 'MSA II' ou 'Mossel Bay' ont été initialement définis par Singer et Wymer (1982) à partir des assemblages de KRM et confirmés par Wurz (2000, 2002). MSA-Mike de DRS (Porraz, et al., 2013), la phase M3 de BBC (Douze, et al., 2015), et Pinnacle Point (PP13B) datant du MIS 5 (Thompson, et al., 2010) ressemblent au KRM Mossel Bay. Trois sites de la côte ouest, Ysterfontein 1 (YFT) (Wurz, 2012), Hoedjiespunt 1 (Will et al., 2013) et Sea Harvest (Volman, 1978), présentent de grandes similitudes suggérant une expression du MSA distincte (Wurz, 2013). Enfin, le pré-SB de type 'Lynn' (Porraz, et al., 2013, 2014) appartient également au MSA du MIS 5 et présente une unité de transition avec l'émergence de la technologie bifaciale précédant le SB. Ainsi, les données archéologiques semblent indiquer que le changement culturel et les innovations ne se limitent pas aux complexes technologiques HP et SB et suggèrent un scénario complexe de coexistence de traditions techno-typologiques distinctes, structurées au niveau régional en Afrique australe au cours du MIS 5 et ayant un impact sur l'organisation territoriale et sociale et sur la présence et la diffusion des innovations. Cependant, il reste très important d'accroître nos connaissances sur les changements de comportements, tels que les nouvelles réalisations technologiques et les pratiques

symboliques, et au-delà, de contribuer à affiner le cadre chrono-culturel, d'explorer de longues séquences régionales et d'étendre l'objectif de la recherche des phases prétendument précoces, telles que le SB et le HP, pour l'ensemble du MSA.

Le site de la grotte de Sibudu, KwaZulu-Natal, Afrique du Sud, comprend une séquence MSA longue et bien datée. Les fouilles menées actuellement par l'Université de Tübingen dans le *Deep Sounding* (sondage profond) de Sibudu ont permis d'obtenir des assemblages lithiques MIS 5 qui contribuent à la discussion sur les mécanismes des changements, l'apparition de nouveautés technologiques et la variabilité culturelle dans le MSA pendant cette période.

Dans l'introduction, je commence par la citation '*Giving substance to shadows*' de la chanson '*Crucify your mind*' de Sixto Rodriguez. Ces quatre mots résument avec une merveilleuse concision les principales questions de recherche qui sous-tendent ce travail : 1) Fournir une première description détaillée des couches qui précèdent et pour ainsi dire restent longtemps dans l'ombre du SB considéré comme particulièrement innovant en mettant en évidence les caractéristiques diagnostiques positives concernant la technologie lithique et l'économie des matières premières ; 2) Identifier les nouveautés technologiques au cours du MIS 5 dans une région peu étudiée à la fois zone écologique et géologique ; 4) Explorer les liens et/ou les différences avec d'autres ensembles pertinents du MIS 5, en particulier le complexe technologique SB ; 5) Contribuer à l'affinement du cadre chrono-culturel du MSA de l'Afrique australe pendant le MIS 5.

Le site de la grotte de Sibudu est situé à 40 km au nord de Durban dans la municipalité locale KwaDukuza appartenant à la municipalité de district iLembe. Le site est perché sur une falaise abrupte au-dessus de la rivière uThongathi. L'abri sous roche est taillé dans le grès du *Natal Group*. La zone d'excavation est située à une altitude d'environ 100 m au-dessus du niveau moyen de la mer dans la partie nord-est de l'abri. Concernant l'historique de la recherche, une première tranchée de test a été creusée en 1983 par A. Mazel. D'autres fouilles ont été menées par L. Wadley de 1998 à 2011. Depuis 2011, une équipe de l'Université de Tübingen dirigée par N. J. Conard poursuit le travail de terrain.

La séquence stratigraphique à haute résolution se compose principalement de couches du MSA allant de plus de 74 à 33 ka BP, suivies par les occupations de l'Âge du fer. La stratigraphie est principalement composée de couches anthropiques. La conservation organique est généralement bonne. Plusieurs dates OSL et radiocarbone ont été obtenues à partir des



couches du MSA (par exemple, Wadley et Jacobs, 2006; Jacobs, et al, 2008a; Jacobs et Roberts, 2017) et de nouvelles dates de luminescence sont actuellement en cours par C. Tribolo. La partie de la séquence chrono-culturelle qui fournit le matériel lithique pour ma thèse comprend les six couches BMo, RBS, GSS, GBP, LBC et PSS identifiées depuis le début des nouvelles fouilles en 2011. En plus de ces dénominations descriptives de terrain, un nom masculin et ensuite un nom féminin ont été attribués à chaque nouvelle couche par ordre alphabétique, en commençant par la lettre A : Adam, Annie, Bart, Bea, Casper et Chantal. Les résultats préliminaires de la datation par luminescence suggèrent que ces strates datent entre 92 et 72 ka BP (Tribolo, communication personnelle). Les couches BS et LBG, officiellement appelés 'pré-SB', sont stratigraphiquement situées au-dessus. Un changement dans le corpus typologique se note au sein de la séquence BS car des pointes bifaciales apparaissent dans les couches plus profondes, de BS 11 à BS 16 (Wadley, 2013b). Les strates au-dessus appartiennent au SB, avec un âge de  $69,5 \pm 2,1$  ka BP et présentent comme principale caractéristique diagnostique une technologie lithique bifaciale, incluant des pointes bifaciales (Wadley, 2007; Soriano, et al., 2015). Les niveaux attribués au HP recouvrent le SB datant entre  $60,5 \pm 1,8$  et  $58 \pm 1,7$  ka BP et présentent différentes chaînes opératoires pour produire des lames fréquemment transformées en une variété d'outils à dos (Delagnes, et al., 2006; de la Peña, 2015; Soriano, et al., 2015). De plus, la fabrication de petites pointes bifaciales en quartz fait également partie de corpus d'outils du HP (de la Peña, et al., 2013). La partie suivante de la séquence a un âge d'environ 58 ka BP correspondant au post-HP. En réponse aux problèmes entourant le nom informel de 'post-HP', il a été suggéré que Sibudu soit considéré comme un site-type pour cette phase (Conard, et al., 2012; Lombard, et al., 2012). Lombard et al. (2012) ont proposé le terme 'Sibudu technocomplex', caractérisé par une production de pointes utilisant le concept Levallois et de pointes unifaciales typiques avec des talons facettés et de forme allongée. Conard et al. (2012) plaident pour le terme 'Sibudan' qui présente des signatures techno-fonctionnelles distinctes, telles que Tongatis, Ndwedwes, des biseaux et des outils à dos naturel. De plus, cette séquence à haute résolution datant d'environ 58 ka BP a révélé des changements sur le court terme et de forts signaux diachroniques (Will et Conard, 2018). Les strates sus-jacentes sont appelées MSA tardives, datées d'environ 48 ka BP, et se caractérisent par une fréquence élevée de pointes unifaciales (Villa et al. 2005). Les couches au sommet de la séquence du MSA sont décrites comme MSA final, avec un âge d'environ 38 ka BP, et impliquent comme caractéristiques les plus diagnostiques des pointes à base concave (Wadley, 2005).

Sibudu est aujourd'hui situé dans le *KwaZulu-Natal Coastal Belt* du biome du *Indian Ocean Coastal Belt*, dans la zone *Summer Rainfall*. Cette zone de végétation est dominée par une forêt interrompue par des prairies et caractérisée par des conditions climatiques tropicales chaudes et humides en été, ainsi que par des conditions subtropicales douces et plus sèches en hiver (Mucina, et al., 2006). La végétation primaire directement autour du site comprend des espèces à feuilles persistantes, des savanes à feuilles caduques et des prairies (Wadley, 2013b).

En ce qui concerne la reconstitution paléoenvironnementale, Sibudu fournit un large éventail de données environnementales de substitution à haute résolution (par exemple Allott, 2006; Herries, 2006; Pickering, 2006; Renaut and Bamford, 2006; Schiegl and Conard, 2006; Clark, 2013; Sievers, 2013; Hall, et al., 2014; Val, 2016; Murungi, 2017; Robinson and Wadley, 2018). Ces données multidisciplinaires indiquent qu'une mosaïque d'habitats a persisté durant tous les niveaux d'occupation de Sibudu en raison de l'aspect du site et de la proximité de la rivière uThongathi (Robinson et Wadley, 2018). Beaucoup des taxons qui poussent autour de Sibudu aujourd'hui étaient également présents pendant le MSA, ce qui indique des conditions similaires à celles actuelles. Cependant, certaines espèces végétales sont absentes aujourd'hui, du fait de nombreux éléments de végétation plus septentrionale, la composante boisée sèche de la végétation pouvait être plus étendue (Wadley et Jacobs, 2006). En ce qui concerne plus particulièrement les couches Chantal à Adam, une identification faunique préliminaire de la couche Casper a révélé la présence de céphalopodes bleus et de porcs de brousse, que l'on trouve généralement dans les habitats forestiers.

Suivant l'approche de la chaîne opératoire (Leroi-Gourhan, 1943; Tixier, 1980; Pelegrin, et al, 1988; Boëda, et al, 1990; Geneste, 1991; Inizan, et al, 1999; Soressi et Geneste, 2011), j'ai effectué une analyse technologique des artéfacts des couches C-A à Sibudu. Mon fondement théorique repose sur la considération que la production lithique ait d'abord émergé comme un projet cognitif qui a ensuite été converti, sur le plan intellectuel, en un schéma conceptuel qui s'est finalement concrétisé par une série d'opérations représentant le schéma opérationnel. Chacune de ces étapes dépend de plusieurs paramètres naturels et humains qui interagissent en partie (Pigeot, 1991; Inizan, et al., 1999; Soressi et Geneste, 2011; Porraz, et al., 2016). Ainsi, la récurrence de modèles dans un assemblage lithique permet de l'interpréter comme intentionnelle (Soressi et Geneste, 2011). L'objectif ultime des tailleurs est de produire un outil conçu de manière à servir pour une fonction spécifique (Porraz, et al., 2016). Comme l'outil est

considéré comme faisant partie intégrante d'un système intentionnel et non aléatoire de fabrication, d'entretien et d'abandon, on s'attend à des liens solides entre la sélection des matières premières, les stratégies d'exploitation des nucléus, les résultats des produits du débitage et la transformation, l'utilisation et l'abandon des outils (Conard, et al., 2012). En plus d'adopter une approche typologique traditionnelle, je suis le concept du cycle de Pradnik (Krukowski, 1939) qui suppose que les phases régulées de production, d'utilisation et d'abandon de l'outil ont laissé des modèles récurrents sur l'assemblage lithique, les outils provenant de différentes étapes permettant une détermination du cycle de vie de l'outil. De plus, j'adopte une approche techno-fonctionnelle pour fournir des caractérisations fonctionnelles des outils basés sur des caractéristiques techniques (par exemple Lepot, 1993; Bourguignon, 1997; Soriano, 2000; Bonilauri, 2010; Nicoud, 2011; Chevrier, 2012 ; Boëda, 2013). Cette approche vise à identifier les trois unités techno-fonctionnelles (UTF) essentielles d'un outil : la partie transformatrice, la partie préhensile et la partie réceptive. Les méthodes technologiques et techno-fonctionnelles, combinées à des analyses d'utilisation et de résidus (Rots, et al., 2017), et complétées par des données expérimentales, fournissent de multiples sources de données pour étayer certaines hypothèses sur la dynamique de la production, de l'utilisation et du rejet des outils. Ce cadre complet de différentes approches méthodologiques me permet d'obtenir un maximum d'informations à partir de données archéologiques limitées pour décrire des événements techniques et faire des inférences sur les comportements humains dans les couches C-A de Sibudu. Enfin, des analyses technologiques détaillées permettent de faire des comparaisons avec d'autres assemblages pour identifier les similitudes et les différences dans les choix techniques afin de mieux comprendre la variabilité temporelle et spatiale de la technologie lithique dans un contexte culturel élargi (voir Lechtman, 1977; Wiessner, 1983).

L'échantillon archéologique à la base de mon travail de doctorat concerne tous les objets lithiques  $\geq 30$  mm, ainsi que tous les nucléus, fragments de nucléus, outils et fragments d'outils, quelle que soit leur taille, des couches Chantal à Adam. Les pièces proviennent d'une zone d'excavation d'environ 4 m<sup>2</sup> et fouillée de 2012 à 2016. Les six couches comprennent un total de 8 164 artefacts.

Résumant les résultats de cette étude, les tailleurs, au cours de cette phase d'occupation, ont exploité une gamme de différentes matières premières principalement disponibles localement (moins de 5 km), dont notamment de la dolérite suivie de grès, quartzite, quartz, hornfels et

chert, qui ont une importance variable dans la production des enlèvements et la fabrication des outils. Les populations préhistoriques se procuraient les types de roches dans différentes sources, par exemple sous forme de galets provenant de la rivière ou d'affleurements (sub)primaires. Les matières premières présentent donc des formes ainsi que des propriétés physiques variables. La proportion de couverture du cortex ainsi que la présence de produits dès les premières étapes de la chaîne opératoire impliquent que les tailleurs ont réalisé au moins partiellement l'ensemble de la chaîne opératoire pour toutes les matières premières, sauf le chert, sur le site. La dolérite est la plus fréquente, parmi les produits du débitage, les nucléus et les outils, et semble avoir été intensément exploitée par les activités de taille sur place. Quelques grosses lames de dolérite sont présentes dans l'assemblage, ce qui indique que certains éléments ont été importés comme produits finis sur le site. Bien que la dolérite soit la matière première dominante, le ratio outil/enlèvements suggère que les enlèvements étaient relativement rarement transformés en outils. Le grès provenant de l'abri lui-même est la seconde matière la plus commune dans l'assemblage et présente le plus faible degré de modification. Le quartzite et le hornfels semblent avoir été plus souvent transportés sur le site sous forme de produits finis. Les outils de ces types de roches montrent un haut degré d'investissement dans leur entretien. L'assemblage comporte aussi du quartz hyalin et laiteux. Ce type de roche présente le deuxième plus grand nombre de nucléus, qui sont toutefois plus petits que les nucléus réalisés sur d'autres matières premières. Le quartz, spécialement le quartz hyalin, est d'une grande importance pour la production d'outils, en particulier les pièces bifaciales et crénelées.

L'assemblage montre une importante production de lames et d'éclats allongés également liés à différentes matières premières. Certaines des lames sont de très grandes dimensions avec une longueur maximale de 114 mm, tandis que la plupart ont une longueur moyenne entre 39 mm et 55 mm. Cependant, la population de lames contient une forte proportion d'éléments fragmentés. Contrairement à la longueur, qui couvre une large gamme, la largeur et l'épaisseur présentent un degré de standardisation plus élevé. La plus grande proportion des lames ne présente aucun cortex sur la face dorsale. Les talons de la majorité de ces produits finis laminaires sont lisses et la morphologie est presque exclusivement rectangulaire. Les pièces montrent principalement des négatifs dorsaux unidirectionnels, tandis que certains produits finis présentent des négatifs orthogonaux ou bidirectionnels attestant d'une préparation latérale ou distale. Les tailleurs cherchaient à obtenir des lames aux profils droits à légèrement

courbés. Au sein de la catégorie des lames, j'identifie deux sous-groupes significativement distincts en ce qui concerne la section transversale ainsi que le rapport largeur-épaisseur : (1) des lames épaisses et étroites, de section triangulaire, et (2) des lames plus fines et larges, de section trapézoïdale. Le sous-groupe (1) domine dans l'assemblage et montre clairement une convexité en partie distale. Il est intéressant de noter qu'aucune lame du sous-groupe (2) ne présente une face dorsale complètement corticale et que seuls quelques éléments ont plus de 50% de surface corticale, ce qui implique que le sous-groupe (2) n'est pas concerné dans les premiers stades de l'exploitation. Les lames présentent des dimensions et des morphologies similaires tout au long de la séquence.

Les éclats allongés présentent généralement des tendances similaires à celles des lames. Contrairement aux lames, davantage d'éclats allongés présentent des restes corticaux sur leur face dorsale. Les éclats allongés sont plus courts et significativement plus larges et plus épais que les lames. La plupart de ces éclats ne sont pas fragmentés et un pourcentage significativement plus élevé de pièces que les lames est complètement préservé. La tendance à la dichotomie de supports étroits avec une section triangulaire et de supports fins et larges avec une section trapézoïdale, se remarque également parmi les éclats allongés. J'observe également des tendances similaires dans toutes les couches en termes de taille et de forme des éclats allongés.

Les éclats constituent la plus grande partie de la population des produits de débitage et présentent un ensemble de caractéristiques diagnostiques. Le quartz et le grès apportent une plus faible fréquence d'éléments laminaires, mais un pourcentage plus élevé d'éclats que les autres matières premières. La catégorie des éclats présente une longueur moyenne de 31,9 mm avec une largeur moyenne de 33 mm et une épaisseur moyenne de 8,9 mm. Ces supports comprennent une plus grande proportion d'éléments complètement préservés que leurs homologues laminaires. Les éclats plus souvent que les lames et les éclats allongés ont une face dorsale corticale. La plupart des éclats ont des talons lisses, mais avec le plus grand nombre de pièces avec des talons corticaux. Les négatifs dorsaux dominants sont unidirectionnels, mais un grand nombre présente des négatifs orthogonaux - souvent un négatif laminaire orthogonal. Il est intéressant de noter que la population des éclats présentant des négatifs orthogonaux présente davantage d'éléments non corticaux et comporte en outre moins de pièces avec plus de 50 % de restes corticaux et aucun artefact entièrement cortical. Par conséquent, les éclats orthogonaux proviennent vraisemblablement de stades plus avancés de la chaîne opératoire.

La plus grande partie présente une morphologie trapézoïdale et des profils droits à légèrement courbés. Les sections transversales sont triangulaires ou trapézoïdales. J'ai documenté les similitudes diachroniques concernant les dimensions et les morphologies.

Les éclats triangulaires sont en faible proportion présents tout au long de la séquence, mais jouent un rôle marginal dans l'assemblage.

J'ai classé les nucléus selon la taxonomie unifiée de Conard et al. (2004) et, par conséquent, la plupart des nucléus sont conformes aux types de *platform* et plus précisément presque exclusivement aux *blade platform cores*. Les *blade platform cores* sont principalement constitués de dolérite et de quartzite. Les tailleurs ont surtout choisi des blocs pour les configurer dans ces types de nucléus. Le faible pourcentage de cortex est le plus souvent situé sur le dos et/ou sur une surface latérale des nucléus. La majorité des spécimens comporte un plan de frappe, qui est généralement lisse. Les principales surfaces d'enlèvement sont majoritairement de forme quadrangulaire. Les *blade platform cores* sont presque exclusivement exploités par des enlèvements unidirectionnels. Les bases de ce type de nucléus présentent le plus souvent une préparation des convexités distales. La variabilité à l'intérieur des *blade platform cores* semble être associée à différents stades de rejet. Les dernières opérations sur les nucléus correspondent principalement à des accidents de taille ou à des activités de préparation. Les dernières opérations de production ont clairement mis l'accent sur les éléments laminaires. Les négatifs laminaires du produit fini sur les *blade platform cores* indiquent les exigences minimales pour la longueur d'environ 20 mm et 10 mm de largeur. Cependant, les dimensions du nucléus, en particulier le ratio longueur-largeur des surfaces d'enlèvement, ne coïncident pas avec les dimensions laminaires. D'après la description générale de l'assemblage, la présence de cortex et les dimensions des *blade platform cores*, je déduis qu'un nombre élevé de spécimens représente des nucléus épuisés. Les *blade platform cores* dominant dans toutes les couches, à l'exception de la couche Casper, où les nucléus bipolaires sont plus courants.

Un nucléus en quartzite présente des enlèvements lamellaires comme dernière opération de production. Les similitudes concernant la configuration et la morphologie par rapport aux *blade platform cores* suggèrent que ce nucléus pourrait être le résultat d'un épuisement extrême du nucléus plutôt que d'une chaîne opératoire indépendante.

L'un des nucléus de quartz montre l'enlèvement d'une première exploitation comme *blade platform core* et des traces finales d'une percussion bipolaire sur enclume.

Les nucléus bipolaires fabriqués principalement sur quartz représentent le deuxième type de nucléus le plus fréquent. Ces nucléus montrent clairement des dimensions plus petites que les nucléus de *platform*.

Quelques nucléus appartiennent à la catégorie des nucléus initiaux. Tous sont réalisés sur blocs et présentent une surface corticale de plus de 50% située soit sur le dos ou sur le dos et une face latérale. Les surfaces d'enlèvement ont des formes quadrangulaires et les bases sont soit corticales, soit préparées. Les nucléus initiaux ont des dimensions plus grandes que les nucléus de *platform*. La dernière opération est liée soit à des actions préparatoires, soit à un accident de taille.

Les tendances des marques de percussion identifiées pour tous les enlèvements indiquent que les tailleurs de Sibudu utilisaient des percuteurs durs et tendre en percussion interne directe, en appliquant à la fois des mouvements rentrants et tangentiels. L'assemblage comprend plusieurs galets et fragments de galets de grès, quartzite, dolérite et quartz avec des traces d'impacts qui peuvent être interprétés comme des percuteurs en pierre, favorisant la coexistence potentielle de percuteurs durs et tendre pour détacher les enlèvements.

En rassemblant toutes les données des produits du débitage et des nucléus, j'ai constaté que les habitants de Sibudu à cette époque se concentraient sur la production d'éléments laminaires et développaient une chaîne opératoire unidirectionnelle spécifique pour obtenir des lames et des éclats allongés sur toutes les matières premières. Les lames typiques se caractérisent par des négatifs dorsaux unidirectionnels, une morphologie rectangulaire et des profils droits à légèrement courbés. La configuration systématique du nucléus permet et maintient la production laminaire. Pour obtenir la configuration du nucléus nécessaire à la fabrication de leurs produits finis, les tailleurs ont établi six zones différentes : le plan de frappe, la surface de débitage, le dos ainsi que la base du nucléus, plus les deux autres surfaces essentielles, la crête latérale et le méplat. Les plans de frappe sont généralement lisses et ont un contour arqué/semi-circulaire. Les surfaces de débitage présentent principalement des formes quadrangulaires et sont d'une convexité transversale assez faible. Les dos des nucléus sont principalement formés par des faces naturelles ou ventrales anciennes. Cependant, certains dos montrent des enlèvements préparatoires appartenant soit à la crête latérale, soit à la base, soit au plan de frappe. La plupart des bases présentent une préparation complète ou partielle avec des négatifs opposés au sens du débitage unidirectionnel, afin de maintenir la convexité distale. La crête latérale est réalisée sur un côté de la surface de débitage en détachant des éclats

orthogonaux à l'axe d'exploitation dans l'objectif de maintenir la convexité transversale. Le plus souvent, les populations préhistoriques préparaient les crêtes en alternant les enlèvements bifaciaux ou par une préparation bifaciale. Le méplat est situé en face de la crête latérale sur l'une des faces étroites du nucléus. Il est généralement formé par une surface naturelle. Cependant, quelques nucléus reflètent un stade d'exploitation assez avancé de sorte que le méplat n'est plus reconnaissable en raison d'un épuisement important. Quelques nucléus présentent des enlèvements orthogonaux de préparation réalisés afin de corriger l'angle entre la surface de débitage et le méplat. La crête latérale et le méplat, ainsi que la surface de débitage du volume sont configurés pour l'exploitation. Au cours de la production, ce volume utile passe morphologiquement d'une section triangulaire asymétrique à une section pentagonale, ressemblant à une maison basculée sur le côté. Les dos des nucléus représentent le volume inutile.

Dans la phase initiale du système de débitage laminaire, les tailleurs ont choisi de préférence des blocs pour commencer par la préparation de la crête latérale et l'installation du plan de frappe. Les éclats diagnostiques du stade initial sont trapézoïdaux et légèrement courbés à courbés, montrant soit des négatifs unidirectionnels, soit du cortex. La section triangulaire asymétrique du volume utile permet de commencer l'exploitation effective à partir de la crête formée par le méplat et la surface d'enlèvement. Les tailleurs utilisaient soit des convexités naturelles pour détacher les premières lames corticales à crête naturelle, soit préparaient l'un ou les deux versants pour faciliter l'enlèvement des premières lames à crête.

À la phase intermédiaire et à la fin du débitage, l'exploitation du volume utile se fait de manière asymétrique sur la grande surface et en réduisant le méplat. La grande fréquence des produits laminaires à partie corticale latérale témoigne de l'expansion latérale de la surface de débitage, tandis que la présence de lames à dos cortical témoigne de l'exploitation du méplat. Cette dichotomie continue de la séquence du débitage entraîne la production de deux sous-groupes de lames. La chaîne opératoire est discontinue, car d'une part des enlèvements laminaires à semi-crête indiquent que les tailleurs ont dû renouveler partiellement la crête formée par le méplat et la surface d'enlèvement. En revanche, les nucléus et les éclats de préparation montrent la réinstallation de la crête latérale à un stade avancé du débitage. Les éclats diagnostiques de reconfiguration de la crête présentent les mêmes caractéristiques que ceux de la préparation initiale de la crête, y compris la forme trapézoïdale et le profil légèrement courbés à courbés, mais ils ne présentent aucun cortex ni négatifs dorsaux laminaires orthogonaux. Pour réorganiser l'angle du plan de frappe, les artisans ont retiré des tablettes de



ravivage partiel. La préparation distale pour gérer la convexité longitudinale se produit également.

La dernière phase du débitage implique l'abandon des nucléus après un long cycle d'exploitation, principalement dû à des erreurs de taille. L'épuisement extrême du nucléus, le déséquilibre dans l'exploitation du volume utile ainsi que la préparation des crêtes, des plans de frappe et des surfaces distales provoquent une forme plutôt carrée qu'allongée de la plupart des négatifs d'enlèvement. La fin de la production est inévitable, lorsque le volume utile est si intensément épuisé que la mise en place d'une convexité transversale en renouvelant la crête latérale et donc une exploitation ultérieure n'est plus possible.

L'assemblage se distingue par la présence de la technologie bifaciale, incluant des pièces crénelées, mais la majeure partie des outils formels dans toutes les couches est constitué par une variété de formes pointues unifaciales. Divers types de racloir, ainsi que des denticulés, sont également présents. Dans la classification typologique, j'ai défini des classes d'outils basées sur l'identification de modèles à partir des structures et localisation des parties transformatives et des parties préhensives sur les outils et leur intégration dynamique dans les cycles de chaîne opératoire.

Toutes les formes pointues unifaciales correspondent à la définition des supports triangulaires ou sous-triangulaires retouchés presque exclusivement sur une surface, l'extrémité distale étant pointue par retouche ou par débitage. La plupart de ces outils sont fabriqués sur de la dolérite, suivie de quartzite. Les supports sélectionnés pour être modifiés dans ce type d'outil sont principalement des éléments laminaires droits de plus grandes dimensions issus de la phase de production principale. Parmi les formes pointues unifaciales, j'ai distingué les classes d'outils : pointes unifaciales symétriques trièdres (TSPs), outils convergents asymétriques (ACTs), Tongatis (pour la définition voir Conard, et al., 2012) et pointes unifaciales, qui répondent aux critères généraux mais ne sont plus classés.

Les TSPs constituent le plus grand pourcentage des formes pointues unifaciales. Elles ont une extrémité distale symétrique, retouchée bilatéralement et formée par des bords légèrement curvilignes. Leurs pointes sont triédriques et d'une section triangulaire régulière. Les parties réceptives sont convergentes et souvent retouchées de manière invasive sur les deux bords, ce qui suggère plusieurs phases de réaffûtage qui provoquent l'extension de la partie transformative. Les bases ont généralement une forme quadrangulaire et présentent parfois

un amincissement ventral. Ces outils ont une longueur moyenne de 47,8 mm, une largeur moyenne de 24,6 mm et une épaisseur moyenne de 7,8 mm. La grande gamme de longueur ainsi que la longueur de la pointe retouchée peuvent être liées à l'intensité de la confection de l'outil et/ou à la sélection des supports pour la fabrication des TSPs. Les produits laminaires sélectionnés pour la modification en TSP sont à l'origine plus larges et probablement plus longs que les lames non retouchées et sont ensuite affectés dans leur longueur et leur largeur par la production et le réaffûtage. La plupart des TSPs sont présentes sous forme de fragments de pointes probablement cassés lors de la fabrication ou de la reprise de l'outil. En ce qui concerne les caractéristiques techno-fonctionnelles, ces outils ont probablement été utilisés principalement dans un mode punctiforme lié à la perforation, au perçage ou au forage. Le cycle de confection comprend des TSPs avec de petites parties transformatives courtes par rapport à une partie réceptive relativement longue dans une phase initiale, tandis que la confection avancée des outils, y compris après plusieurs opérations de reprise, entraîne une perte de la partie intermédiaire et une expansion de partie transformative. Par conséquent, la largeur maximale de la pointe diminue et la délimitation des bords de la pointe devient légèrement concave plutôt que rectiligne. De plus, la partie intermédiaire à l'origine parallèle acquiert une morphologie convergente.

Les ACTs représentent la deuxième plus grande proportion des formes pointues unifaciales présentant des parties distales convergentes asymétriques non alignées avec l'axe de percussion du support d'origine et généralement formées par un bord abrupt retouché convexe et un bord droit opposé non retouché. La confection s'étend de l'extrémité distale à la partie réceptive communément constituée d'un bord convergent et d'un bord rectiligne opposé. La base est généralement de forme quadrangulaire. La longueur moyenne est de 44,5 mm, la largeur de 26,8 mm et l'épaisseur de 8,2 mm. La sélection des supports a porté principalement sur des produits laminaires droits provenant de différentes étapes de la chaîne opératoire. Un faible pourcentage des ACTs est totalement préservé. En ce qui concerne la caractérisation techno-fonctionnelle, les tailleurs ont apparemment installé des bords émoussés par une retouche abrupte pour former un dos aux outils de coupe pour appliquer une plus grande force sur les parties transformatives. Les bords non modifiés qui présentent souvent des enlèvements macroscopiques visibles à l'échelle macroscopique ont des angles aigus et sont tranchants. L'asymétrie des deux bords indique un mode d'utilisation linéaire, par exemple la coupe, l'ébavurage et le raclage. En ce qui concerne le cycle de vie des ACTs, l'installation du bord

fortement retouché semble avoir été une étape finale et seul le bord opposé était parfois réaffûté.

Les pièces bifaciales constituent le deuxième type d'outil le plus courant dans le corpus typologique. Tous les exemplaires sont conformes aux outils présentant des retouches sur les deux faces dans la même proportion du bord. Ce type d'outil comprend des pointes bifaciales et des couteaux bifaciaux à dos. De plus, la classe d'outils des pièces crénelées, définies comme des outils à bords délimités par de petites encoches régulièrement répétées créant des dents triangulaires (Crabtree, 1972; Akerman et Bindon, 1995; Andrefsky, 2005) se distingue.

Les tailleurs utilisaient principalement le quartz pour fabriquer des pointes bifaciales, suivi de la dolérite et du quartzite. Une grande partie des pointes bifaciales sont des fragments, en particulier les fragments de la pointe. La longueur moyenne est de 40,1 mm, la largeur moyenne est de 22,9 mm et l'épaisseur de 8,2 mm. Le plus souvent, les pièces sont tellement modifiées par le façonnage bifacial que les supports d'origine ne peuvent plus être déterminés, mais, lorsqu'ils sont identifiables, les tailleurs choisissent de préférence des produits laminaires épais. La majorité des pointes bifaciales ont un profil droit. En ce qui concerne le morphotype, la plupart des pointes bifaciales présentent une symétrie bilatérale. Les pointes ont une forme en V ainsi qu'un contour régulier de pointe bien appointée et couvrent entre un et deux tiers de l'outil entier. La partie réceptive est généralement convergente et les bases des pièces ont une morphologie elliptique. La séquence de confection bifaciale implique deux techniques de taille : la percussion directe avec un percuteur dur dans le processus de façonnage initial et la percussion marginale à percuteur tendre dans la phase avancée du façonnage. Toutes les phases de fabrication, des préformes aux produits finis, ainsi que les éléments recyclés, sont présentes. Les pointes bifaciales montrent une grande variabilité liée aux types de roches en ce qui concerne la taille, la morphologie, l'organisation du processus de fabrication et par conséquent l'interprétation techno-fonctionnelle.

Les pointes en dolérite, quartzite et cornéenne mesurent en moyenne 41,2 mm de long, 25,1 mm de large et 9,1 mm d'épaisseur. Ces outils présentent des sections transversales plan-convexes. Le façonnage des pointes bifaciales de dolérite, quartzite et hornfels est généralement, mais pas exclusivement, organisé de manière hiérarchique. Les tailleurs commençaient souvent la confection bifaciale sur la surface plane et continuaient avec la surface convexe, ce qui donnait des outils avec des sections transversales plan-convexes. Cette configuration et hiérarchie entre les faces permet une série d'événements de réaffûtage sans

altération de l'ensemble de la structure, conformément aux pièces bifaciales supports (Boëda, 1997 ; Porraz, et al, 2013 ; Soriano, et al, 2015). Cette conception des pointes bifaciales réalisées sur la dolérite, le quartzite et la hornfels suggère une utilisation à long terme principalement comme outils de coupe pointus.

Les pointes bifaciales de quartz ont donné une longueur minimale de 26,7 mm. La largeur moyenne est de 17,3 mm et l'épaisseur de 6,6 mm. La majeure partie des outils à quartz présente des sections biconvexes. La fabrication de pointes bifaciales sur quartz semble être gérée de façon non hiérarchique en alternant les enlèvements qui aboutissent à des produits finis biconvexes avec des contours de pointes régulières et pointues. Ces pointes bifaciales correspondent à des pièces bifaciales outils (voir Boëda, et al., 1990 ; Nicoud, 2013). Les pièces bifaciales ont très probablement fonctionné comme des armatures insérées axialement dans un manche comme armes de chasse.

Le corpus de l'outil contient 25 pièces crénelées principalement faites de dolérite suivie de quartz. Les artefacts ont une longueur moyenne de 42,1 mm, une largeur moyenne de 21,1 mm et une épaisseur moyenne de 7,8 mm. Les lames et les éclats allongés servaient principalement de support d'origine. Les pièces crénelées ont des profils droits et une symétrie bilatérale. Leur morphotype se compose de pointes en forme de V et de pointes régulières, de parties mésiales convergentes ou parallèles prolongeant la zone de la pointe et de parties basales quadrangulaires. La variabilité technologique concernant la séquence de production entraîne la formation de deux sous-groupes à l'intérieur des pièces crénelées : les supports de forme bifaciale qui étaient crénelés bilatéralement et les supports retouchés de manière bifaciale (ou unifaciale) qui étaient crénelés de manière bilatérale (ou latérale). La retouche crénelée des artefacts constitue la dernière et ultime phase du processus de fabrication. De multiples sources de données issues d'analyses technologiques et fonctionnelles ainsi que d'expérimentations indiquent que les tailleurs ont appliqué une technique par pression avec un compresseur en os pour créer les dents crénelées. La série d'encoches sur les pièces montre une grande régularité indiquant un contrôle clair de l'emplacement des points de contact et de la force appliquée. De plus, les enlèvements de crénelage présentent des caractéristiques telles que de petites lancettes, des bulbes négatifs, des bords parallèles et des bords tranchants typiques d'un point de contact étroit (voir Mourre, et al., 2010). Par ailleurs, la présence d'éclats de quartz de crénelage a pu être vérifiée, car elles diffèrent des éclats de façonnage en ce qui concerne l'épaisseur et la morphologie globale du talon. L'application de compresseurs en os est attestée par des résidus osseux identifiés au microscope en relation avec les crans,

l'apparition d'un outil osseux avec des traces d'utilisation diagnostique d'un compresseur et la présence de petits enlèvements osseux ressemblant aux enlèvements osseux expérimentaux qui se détachent accidentellement de la pointe du compresseur pendant son utilisation. Les tailleurs de Sibudu, plutôt que de tailler par pression pour régulariser un bord et d'amincir les sections des outils, ont utilisé l'encoche par pression pour créer les encoches des pièces crénelées en plaçant légèrement le compresseur à l'intérieur du bord et en appliquant la force selon un angle perpendiculaire au point de vue du enlèvements (voir Crabtree, 1973; Whittaker, 1994). Les résultats des analyses tracéologique et de résidus, combinés à des données expérimentales, donnent un aperçu de la fonction et de l'emmanchement des pièces crénelées (Rots, et al., 2017). Ces outils représentent des pointes montées sur des manches d'armes de chasse. Dans le passé, les populations fabriquaient et utilisaient des adhésifs composés d'ocre rouge broyé mélangé à de la gomme végétale pour l'emmanchement des pièces.

Parmi les outils bifaciaux, on trouve également cinq pièces qui correspondent à la définition des couteaux bifaciaux à dos asymétrique (Keilmesser) (voir Jöris, 2006; Frick, et al., 2018). Ils ont des parties transformatives robustes opposées à des bords naturels ou préparées avec des enlèvements importants et abrupts. Vers l'extrémité distale sur le côté latéral par rapport au dos, la retouche passe à un angle moins abrupt formant un bord tranchant qui converge avec le bord opposé. L'extrémité distale présente une pointe sans contour pointu régulier. La partie mésiale est composée du bord rectiligne et du bord convergeant vers la partie distale avec le dos. La base a une morphologie quadrangulaire. L'organisation de la fabrication s'est déroulée de manière hiérarchique et s'est traduite par une section asymétrique permettant des réaffûtages fréquents.

De plus, les types racloir comprennent des racloirs latéraux, des outils à dos naturel (NBT) et quelques grattoirs.

Les racloirs latéraux constituent la plus grande partie des types de racloir. Un nombre élevé de racloirs latéraux présente des confections sur les deux bords. J'observe une variabilité au niveau de la retouche allant de la retouche fine à des enlèvements plus grands. De grosses lames de dolérite ou des éclats allongés, provenant en partie des premiers stades de la chaîne opératoire, servaient généralement de supports d'origine pour la fabrication des racloirs latéraux. Les pièces ont une longueur moyenne de 47,3 mm. Leur robustesse est démontrée par une largeur moyenne de 33,6 mm et une épaisseur moyenne de 10,7 mm.

Les NBTs se réfèrent à des objets avec un dos naturel situé à l'opposé d'un bord retouché. Le dos est dans quelques cas créé par des enlèvements, mais généralement formé naturellement par du cortex, des fractures de Siret, le talon de l'éclat-support ou un produit débordant. La proportion la plus élevée se trouve dans la dolérite, suivie du quartzite. Les tailleurs ont sélectionné une variété de supports, y compris des lames, des éclats allongés, des éclats, des éclats de préparation et des éclats de façonnage, pour les transformer en NBTs. La longueur moyenne des pièces est de 40,3 mm, la largeur de 29,8 mm et l'épaisseur de 10,9 mm.

Enfin, les denticulés et les pièces à coche sont toujours présents dans la composition typologique de toutes les couches. Les pièces à coche présentent une seule encoche profondément concave contrairement aux denticulés qui présentent une succession d'encoches adjacentes (voir Inizan, et al., 1999). Les supports d'origine choisis de préférence sont soit des lames, soit des éclats allongés. Les échantillons présentent une longueur moyenne de 44,2 mm, une largeur moyenne de 27,3 mm et une épaisseur moyenne de 8,5 mm. La denticulation des outils, principalement située sur un seul côté, a des encoches assez larges ; certaines sont profondes, d'autres sont peu profondes. La largeur moyenne de l'encoche et la profondeur moyenne de l'encoche montrent de larges gammes attestant d'une grande variabilité.

En général, le matériel lithique des couches C-A a été peu affecté par des perturbations taphonomiques. Le seul impact post-dépositionnel notable est la forte incrustation de sédiments sur les artefacts de toutes les matières premières qui augmente vers la couche inférieure Chantal.

Les résultats de mon étude mettent en évidence de grandes similitudes entre les couches C-A en ce qui concerne la sélection des matières premières, la production des supports, la fabrication et le spectre des outils. En raison de cette homogénéité, je considère les assemblages lithiques comme appartenant à une seule tradition technologique. Malgré la concordance générale, certaines tendances se dégagent dans la séquence en ce qui concerne l'apparence et la fréquence de certains outils. Les pointes unifaciales atteignent la fréquence la plus basse dans la couche Bart, tandis que les pièces bifaciales et les éclats de façonnage associés atteignent leur maximum dans cette couche. Les pièces crénelées, contrairement aux éclats de production des crans, qui se produisent dans toutes les strates, n'émergent qu'à partir de Bart et ont leur fréquence la plus élevée dans les couches Bea et Bart. De plus, la

proportion de quartz hyalin fortement liée à la fabrication des outils bifaciaux est la plus élevée dans les strates Annie, Bart et Bea avec une forte augmentation avant et une diminution après. Par conséquent, la couche Bart marque le point culminant de la technologie bifaciale.

Afin d'émettre l'hypothèse d'un début et d'une fin possible de la phase technologique représentée par les couches C-A, je considère les unités stratigraphiques au-dessus et au-dessous de la séquence de Sibudu. La partie inférieure de BS située directement au-dessus de la couche Adam, bien que décrit de manière préliminaire, comprend de grandes lames ainsi que des éclats fabriqués sur différentes matières premières, des *blade platform cores* et des pointes bifaciales. Les niveaux les plus récents de BS comprennent des éclats et des lames, mais également des pointes unifaciales et des denticulées faits sur dolérite, d'autres outils sont rares. Par conséquent, les données limitées dont on dispose donnent à penser que la partie inférieure de BS pourrait appartenir à la phase technologique "C-A". J'ai eu la possibilité d'analyser les outils et les nucléus des couches Danny et Darya stratigraphiquement située sous les niveaux d'analyse. En me basant sur leur gamme d'outils qui comprend des pièces bifaciales, une grande proportion de formes pointues unifaciales ainsi que des types de racloirs et les populations de nucléus démontrant une fréquence élevée de *blade platform cores* avec une configuration ressemblant à la chaîne opératoire laminaire des couches C-A, je soutiens que Danny et Darya représentent une continuation de la tradition technologique. Néanmoins, les couches C-A qui présentent le point culminant de la technologie bifaciale, incluant crénelées, capturent l'essence de cette tradition technologique. Ces strates d'une épaisseur considérable, d'environ 50 cm, semblent constituer une phase de plus longue durée plutôt qu'un épisode court.

Les couches C-A se définissent par des caractéristiques technologiques et techno-économiques claires :

L'assemblage démontre une chaîne opératoire principale unidirectionnelle, avec une organisation particulière, orientée vers la production de lames et d'éclats allongés. La structure des nucléus comprend en plus du plan de frappe, la surface de débitage, le dos et la base du nucléus, une crête latérale pour la gestion de la convexité transversale et un méplat pour fournir le volume exploitable. Les deux sous-groupes de produits finis laminaires résultent de l'exploitation soit du méplat plus étroit, soit de la surface d'enlèvement plus large. De plus, des éclats de préparation typiques proviennent de cette chaîne opératoire, notamment en ce qui concerne la mise en place et l'entretien de la crête latérale. Les lames et les éclats allongés servaient souvent de supports pour différents types d'outils, ce qui indique une forte

interrelation. Le corpus des outils contient différentes formes pointues unifaciales, tandis que les TSPs et les ACTs se distinguent par des caractéristiques morphométriques et technofonctionnelles particulières. Les éléments typologiques frappants sont cependant les outils bifaciaux, y compris les pointes bifaciales, les pièces crénelées et quelques couteaux bifaciaux à dos asymétrique. La fabrication des pièces crénelées impliquait l'application d'un encochage par pression à l'aide d'un compresseur en os. Dans le passé, les populations utilisaient ces objets comme des projectiles emmanchés pour chasser les animaux. Les objets de type racloir, tels que des racloirs latéraux et des NBTs, sont également présents dans l'assemblage. Enfin, des denticulés et des pièces à coche sont également produits et sont clairement différents des pièces crénelées en raison du nombre, de l'emplacement, de la largeur et de la profondeur des encoches.

L'approvisionnement en matières premières des tailleurs de Sibudu s'est fait de préférence à partir de matières premières disponibles localement, en premier lieu de la dolérite. Bien que les artisans aient exploité toutes les matières premières avec leur chaîne opératoire laminaire particulière, ils ont favorisé les blocs de dolérite et les ont épuisées en tant que nucléus de manière intensive, avec de longs cycles de production. Bien que la majorité des outils soient fabriqués en dolérite, la retouche et le façonnage des enlèvements ne constituent apparemment pas l'objectif principal de la taille, comme l'indique le faible ratio outil/support. Ce type de roche a été principalement sélectionné pour produire des outils à longue durée de vie, probablement en raison de sa ténacité et de sa dureté qui garantissent des bords durables. Au contraire, les habitants de Sibudu ont souvent modifié des supports investis dans la conservation d'outils en quartzite et en hornfels. Le quartz exploité principalement par percussion bipolaire sur enclume a joué un rôle central dans la production d'outils, en particulier la technologie bifaciale. Le grès présente une grande fréquence de produits corticaux et un faible pourcentage d'outils et de produits finis, ce qui suggère une exploitation occasionnelle par de courtes chaînes opératoires sur site. L'assemblage montre l'importation de produits finis isolés fabriqués sur chert.

En ce qui concerne la technologie bifaciale, les matières premières présentent des différences techno-économiques remarquables. Tout d'abord, l'ensemble du processus de fabrication bifacial de la dolérite et de l'hornfels semble avoir été réalisé *in situ*, tandis que les pièces bifaciales fabriquées à partir de quartz et surtout de quartzite sont arrivées sur le site principalement en tant que produits finis, où ils ont été utilisés, réaffûtés et abandonnés. De



plus, les pointes bifaciales du quartz diffèrent grandement des autres roches en termes de caractéristiques morphométriques, d'organisation du processus de fabrication, de cycle de vie, et finalement de leur classification techno-fonctionnelle et fonctionnelle suggérant un comportement techno-économique différentiel. La taille, la structure symétrique et l'organisation des enlèvements des pointes de quartz suggère une utilisation comme projectiles, alors que les autres matières premières servaient plutôt d'outils de coupe. Enfin, les pièces crénelées présentent également une variabilité du quartz et des autres matières premières en ce qui concerne les dimensions, les formes et la fabrication. Les pointes de quartz présentent des propriétés telles que la finesse, la symétrie, l'angle de pénétration étroit et la section transversale biconvexe, qui correspondent supposément à des flèches, tandis que les spécimens réalisés sur d'autres matières premières semblent plutôt se correspondre à des pointes de lance.

L'exploitation de matières premières principalement locales et la présence de chaînes opératoires entières pour tous les types de roches, à l'exception du chert, indiquent un approvisionnement principal de la stratégie de place (*provisioning of place*), mais l'approvisionnement des individus (*provisioning of individuals*) et l'approvisionnement des activités (*provisioning of activities*) ont également joué dans une certaine mesure.

En ce qui concerne la classification chrono-culturelle, je compare les couches C-A aux assemblages bifaciaux du MSA du MIS 5 et ensuite aux sites du MSA bien datés du MIS 5.

Avant de discuter du phénomène bifacial du MSA du MIS 5, en général, je considère les couches C-A dans la séquence stratigraphique de Sibudu elle-même. J'observe de grandes différences par rapport aux couches de SB du site en ce qui concerne les chaînes opératoires, la prédominance de la technologie bifaciale et l'économie des matières premières. Bien que les données technologiques soient préliminaires, les couches situées entre LBG et la partie la plus récente de BS manquent de technologie bifaciale et présentent une importance globalement faible pour les formes pointues. Au niveau du site, les couches C-A et les couches SB ne peuvent donc pas être regroupées.

La comparaison avec le SB, en tant que principale manifestation des technologies bifaciales MSA, premièrement et d'après avec les expressions bifaciales di MIS 5, y compris Pré-SB type 'Lynn' de DRS, l'unité stratigraphique T d'Apollo 11 (AP11) et le complexe technologique de Pietersburg, démontre le caractère distinct des couches C-A et illustre la diversité du phénomène bifacial. Les technologies bifaciales semblent être variables dans l'espace et

différentes dans le temps plutôt que liées à un seul complexe technologique à courte durée de vie (p. ex. Porraz, et al. 2013; Conard, et al. 2014; Conard et Porraz, 2015; Soriano, et al. 2015; Rots, et al. 2017). Les données archéologiques de plus en plus nombreuses montrent que la technologie bifaciale émerge et disparaît dans diverses régions à des moments différents. Les tailleurs du MSA semblent avoir inventé indépendamment la technologie bifaciale dans une variété de contextes impliquant une convergence, c'est-à-dire une innovation répétée de traits analogues dans plusieurs cultures, en technologie lithique (voir Will et Conard, 2018). Étant donné que les couches C-A et les assemblages du SB ont, hormis la présence de la technologie bifaciale, peu de caractéristiques en commun, je soutiens qu'ils ne devraient pas être fusionnés sous la même étiquette.

L'UMH interprétée comme une variante localisée du SB présente de nombreuses similitudes, comme l'émergence précoce de pièces crénelées, avec les couches C-A à Sibudu et donc, les deux assemblages semblent appartenir à la même tradition technologique.

L'aperçu comparatif exhaustif du contexte MSA du MIS 5 illustre les différences frappantes en ce qui concerne la fabrication d'outils, le spectre des types d'outils et l'organisation des chaînes opératoires, mais révèle qu'une tendance générale vers la production de lames se répand de plus en plus pendant cette période. Les populations passées contemporaines dans différentes régions d'Afrique australe et partageant des compétences cognitives semblent viser des objectifs technologiques similaires. Ils ont partagé la production laminaire comme un projet cognitif commun, qui s'est traduit par des schémas conceptuels variés qui ont été réalisés par différents schémas opérationnels (voir Inizan et al, 1999; Soressi et Geneste, 2011). Par conséquent, le MSA du MIS 5 représente apparemment une période associée à une diversification des technologies de lames innovantes liées à l'expression des traditions culturelles régionales (voir Clark 1988). Les couches C-A sont conformes à l'apparence de la technologie des lames en tant qu'innovation du MIS 5, mais reflètent également la diversité et l'émergence d'autres nouveautés, telles que les pièces crénelées avec encochage par pression.

L'assemblage des couches C-A présente des éléments centraux clairement positifs et se distingue nettement des industries bifaciales, surtout du SB, et d'autres technocomplexes du MIS 5, tels que le MSA I et le MSA II. Les données convergent de telle manière que je propose un nouveau terme techno-culturel 'iLembian' pour les couches C-A. Le nom fait référence à la municipalité de district iLembe, où se trouve Sibudu. A mon avis, l'utilisation du terme 'iLembian' contribue à l'établissement d'un cadre chrono-culturel pour une meilleure

communication et compréhension des changements de comportement et de l'évolution culturelle dans une période et une région où peu de recherches ont été faites jusqu'ici. Plus généralement, j'insiste sur l'observation que la technologie des lames, l'application de la technique de pression et la fabrication de pièces crénelées utilisées comme projectiles font partie des innovations clés qui aident à caractériser la dynamique culturelle en Afrique australe lors du MIS 5.

## 9. Zusammenfassung

In den letzten Jahrzehnten der Forschung hat sich das *Middle Stone Age* (MSA) als Schlüsselperiode für die biologische und kulturelle Evolution des modernen Menschen herausgestellt. Es herrscht allgemeiner Konsens, dass das MSA vor circa 300.000 Jahren begann und bis ungefähr 40.000 bzw. 20.000 Jahre andauerte. A. J. H. Goodwin und C. van Riet Lowe definierten in ihrer bahnbrechenden Monographie 'The Stone Age cultures of South Africa' von 1929 den Begriff des MSA und führten die Dreiteilung der afrikanischen Steinzeit in *Early Stone Age* (ESA), MSA und *Later Stone Age* (LSA) ein. Aktuell liefert der afrikanische Fossilbestand das bisher älteste bekannte Individuum mit Zugehörigkeit zum anatomisch modernen Menschen und in Vergesellschaftung mit einem der ältesten MSA-Inventare aus der Fundstelle Jebel Irhoud (Hublin, et al., 2017). Seit den 1980er Jahren belegen mehrere unabhängige genetische Studien, dass *Homo sapiens* ursprünglich aus Afrika stammte, aber nur eine zukünftige, erhöhte Zugänglichkeit zu genomischen Daten und der stätige Fortschritt bezüglich der analytischen Methoden werden es uns ermöglichen, das komplexe Szenario der Entstehungsgeschichte moderner Menschen in vollem Ausmaß zu erforschen. Die materielle Kultur des MSA weist eine Reihe von technologischen und verhaltensbezogenen Innovationen von räumlicher und zeitlicher Vielfalt auf. Das Verschwinden von *Large Cutting Tools* (LCTs), wie Faustkeilen und Cleavern, die Entwicklung von Abbaustrategien an präparierten Kernen für die Produktion von Abschlügen, Klingen und triangulären Abschlügen (Spitzen) und die Herstellung neuer Werkzeugtypen, die sich zum Schäften eignen, kennzeichnen die großen technologischen Umwälzungen im MSA. Der Beginn des MSA scheint eine Periode der Vervielfältigung in der Steintechnologie gekoppelt mit kultureller Regionalisierung vergangener menschlicher Populationen darzustellen, was zu unterschiedlichen Verlaufsrichtung des Wandels führte. Darüber hinaus kommen eine Vielzahl von nicht-lithischen Kulturgegenständen als Neuerungen im MSA vor, die das Entstehen komplexerer sozialer Verhaltensweisen signalisieren. Zu den organischen Technologien gehören eine Reihe von Knochenwerkzeugen (wie z.B. Messer, Spitzen, Harpunen, Ahlen, Pfrieme und gravierte Knochen), persönliche Schmuckgegenstände (wie z.B. durchlochte Schneckengehäuse als Perlen), Objekte, die mit symbolischem Verhalten in Verbindung stehen (wie z.B. gravierte Ockerstücke sowie Straußeneischalen). Diese Technologien können zusammen mit der Herstellung von Farben aus zusammengesetzten Komponenten und der Zubereitung von Klebstoffen für das Befestigen von Werkzeugen und den Fortschritten in der Steinbearbeitung als verhaltensbezogene Anzeiger für die kognitive

Komplexität angesehen werden. Komplexe Kognition umfasst abstraktes Denken, Analogieschlussfolgerung, kognitive Fluidität, Flexibilität in der Problemlösung, Multitasking und langfristige Planung, vergleichbar mit den kognitiven Fähigkeiten lebender Menschen und in der Variabilität moderner menschlicher Populationen. Art, Zeitpunkt und Tempo der Faktoren, die all diese frühen verhaltensmäßigen Innovationen auslösten, bedürfen jedoch noch weiterer Klärung.

Historisch gesehen setzten Forscher vor allem einen Schwerpunkt auf die Erforschung zweier ausgeprägter spätpleistozäner Technokomplexe: des Still Bay (SB) und des Howiesons Poort (HP), die als besonders innovativ galten. Von diesen beiden Unterstufen des MSA wurde trotz ihrer relativ kurzen zeitlichen Ausdehnung behauptet, dass sie eindeutige kulturelle Merkmale aufweisen (Jacobs, et al., 2008a). Die Steintechnologie des HP zeichnet sich durch ihre Klingenproduktion an hochwertigen Rohmaterialien mit guten Schlageigenschaften aus und der Weiterverarbeitung der Klingen zu rückengestumpften Elementen (Henshilwood, 2012; Wadley, 2015), während der Werkzeugbestand des SB durch bifaziale Technologie gekennzeichnet ist, die teilweise durch Druckretusche und durch Tempern von Silcrete, um die Schlageigenschaften zu verbessern, angebracht wurde (Mourre, et al., 2010; Henshilwood, 2012; Schmidt, et al., 2013; Schmidt und Högberg, 2018). Die Einstufung des HP als kulturelle Einheit mit einem breiten geographischen Spektrum wurde validiert, jedoch mit einer relativ langen zeitlichen Spanne vom Marinen Isotopenstadium (MIS) 5 bis 3 und diachrone technologische Veränderung sowie regionale Variabilität umfassend (Villa, et al., 2010; Porraz, et al., 2013; de la Peña, 2015; Douze, et al., 2018; Soriano, et al., 2015). Im Gegensatz dazu ist die ins MIS 5 und 4 datierte Periode des SB weniger gut definiert und hat eine wesentlich problematischere Forschungsgeschichte. Dieser Technokomplex wurde von Goodwin und van Riet Lowe (1929) definiert basierend auf dem Vorkommen von bifaziellen Spitzen aus mehreren unstratifizierten und undatierten MSA-Freilandfundstellen in der Provinz Westkap. Nach der ersten Beschreibung kam es zu Ungereimtheiten bezüglich des SB, da eine taxonomische Zuweisung zum SB sowohl von Inventaren mit fehlenden Leitfossilien als auch von Inventaren aus unsicheren stratigraphischen Kontexten erfolgte. Schließlich wurde das SB weder in Volmans (1981, 1984) überarbeitetem Klassifizierungsschema der MSA-Phasen noch in der formalen Untergliederung von Singer und Wymer (1982) aufgeführt. Der Begriff SB erhielt erst durch die Ausgrabungen an den Fundstellen Hollow Rock Shelter (HRS) (Evans, 1993, 1994) und Blombos Cave (BBC) (Henshilwood, et al., 2001b) Rehabilitation, da diese stratifizierten

Inventare lieferten, die der ursprünglichen Definition zu entsprechen schienen. Darüber hinaus bestätigte die aktuellste Revision der südafrikanischen MSA-Abfolge das SB als Technokomplex (Lombard, et al., 2012). Dem synthetisierten chronologischen Modell von Jacobs et al. (2008a) zufolge ist das SB kurzlebig und reicht von nur ca. 75.000 bis 71.000 Jahre BP. Tribolo et al. (2013) zeigten hingegen, dass die SB-Schichten von Diepkloof Rock Shelter (DRS) deutlich älter sind und sich zeitlich bis zu  $109.000 \pm 10$  BP erstrecken. Die relativ kurze Dauer des SB wurde weiter noch in Frage gestellt (siehe Guérin, et al., 2013; Feathers, 2015; Galbraith, 2015; Jacobs und Roberts, 2017). Zu den Fundstellen, die dem SB zugeordnete Inventare enthalten, zählen Varsche Rivier 003 (VR3) (Steele, et al., 2016), Mertenhof Rock Shelter (MRS) (Will, et al., 2015), HRS (Evans, 1994; Högberg und Larsson, 2011; Högberg und Lombard, 2016a), DRS (Porráz, et al., 2013), Peers Cave (PC) (Minichillo, 2005), Dale Rose Parlour (DRP) (Schirmer, 1975), BBC (Villa, et al., 2009; Soriano, et al., 2015), Umhlatuzana Rock Shelter (UMH) (Kaplan, 1990; Lombard, et al., 2010; Högberg und Lombard, 2016b) und Sibudu Cave (Wadley, 2007; Soriano, et al., 2015). Die SB-Inventare haben als auffallend ähnliches Merkmal die bifaziale Technologie gemein; doch scheint die zunehmende Beweislage auf technologische Heterogenität und zeitliche Ausdehnung des SB hinzudeuten (Porráz, et al., 2013; Conard und Porráz, 2015; Soriano, et al., 2015; Archer, et al., 2016; Rots, et al., 2017). In den letzten Jahren tauchen in der Literatur mehr und mehr technologische Studien zu MIS 5-Inventaren auf, die alle ein komplexeres Bild der kulturellen Evolution als das bisher angenommene einheitliche und stagnierende Szenario andeuten. Eine Reihe von Fundstellen, die dem Technokomplex Pietersburg angehören, sind aus dem nordöstlichen Landesinneren Südafrikas bekannt (Sampson, 1974; Wadley, 2015). Einige der Pietersburg-Fundstellen werden derzeit neu untersucht, wie z.B. Bushman Rock Shelter (BRS) (Porráz, et al., 2015, 2018), Border Cave (BC) (Backwell, et al., 2018b), Mwulu's Cave (MC) (de la Peña, et al., 2018) und Olieboomspoort (Val, persönliche Mitteilung). Darüber hinaus wurden die Technokomplexe ‚MSA I‘ oder ‚Klasies River‘ und ‚MSA II‘ oder ‚Mossel Bay‘ ursprünglich basierend auf den Inventaren von KRM von Singer und Wymer (1982) definiert und von Wurz (2000, 2002) bestätigt. MSA-Mike aus DRS (Porráz, et al., 2013), M3-Phase aus BBC (Douze, et al., 2015) und Pinnacle Point (PP13B) aus MIS 5 (Thompson, et al., 2010) ähneln dem Mossel Bay von KRM. Drei Fundstellen von der südafrikanischen Westküste, Ysterfontein 1 (YFT) (Wurz, 2012), Hoedjiespunt 1 (Will, et al., 2013) und Sea Harvest (Volman, 1978), weisen herausragende Ähnlichkeiten auf, was darauf hindeutet, dass diese zu einer bestimmten regionalen und/oder chronologischen Variante des MSA gehören könnten (Wurz, 2013). Zusätzlich ist Pre-SB type ‚Lynn‘ (Porráz, et al., 2013, 2014)

mit dem MSA des MIS 5 verbunden und stellt eine Übergangsindustrie mit aufkommender bifazieller Technologie vor dem SB dar. Somit scheint der archäologische Bestand darauf hinzudeuten, dass kultureller Wandel und Erfindungsreichtum nicht auf die Technokomplexe, HP und SB, beschränkt sind. Die Datenlage schlägt eher ein komplexes Szenario mit unterschiedlichen koexistierenden techno-typologischen Traditionen vor, die während des MIS 5 im südlichen Afrika regional strukturiert waren, was sich auf die territoriale und soziale Organisation sowie das Auftreten und die Verbreitung von Innovationen auswirkte. Es ist jedoch von großer Bedeutung, um unser Verständnis von Verhaltensänderungen, wie neuen technologischen Errungenschaften und symbolischen Praktiken, zu erweitern und darüber hinaus zur Verfeinerung des chrono-kulturellen Gerüsts beizutragen, lange regionale Abfolgen zu erforschen und den Forschungsschwerpunkt von angeblich besonders innovativen Phasen wie dem SB und dem HP auf das gesamte MSA auszuweiten.

Die Fundstelle Sibudu Cave, KwaZulu-Natal, Südafrika, umfasst eine lange und gut datierte MSA-Sequenz. Aktuelle Ausgrabungen der Universität Tübingen im Deep Sounding (Tiefsondage) von Sibudu haben zur Freilegung von lithischen Inventaren aus MIS 5 geführt. Diese Funde tragen zur Diskussion in Bezug auf die Antriebsmechanismen sowie das Auftreten technologischer Neuerungen und die kulturelle Variabilität des MSA in diesem Zeitabschnitt bei.

In der Einleitung beginne ich mit dem Zitat *'Giving substance to shadows'* aus dem Lied *'Crucify your mind'* von Sixto Rodriguez. Diese Worte fassen die fünf Hauptforschungsziele dieser Arbeit zusammen: 1) Präsentation einer ersten und detaillierten Beschreibung der Schichten, die dem als besonders innovativ betrachteten SB vorausgehen, durch Hervorhebung der diagnostischen positiven Merkmale in Bezug auf die Steintechnologie und die Rohmaterialökonomie; 2) Identifizierung technologischer Neuerungen während des MIS 5 in einer bislang unzureichend untersuchten Region; 3) Bestimmung der potenziellen Mechanismen, die Verhaltensänderungen und technologische Variabilität im MIS 5 bewirken; 4) Erforschung von Verbindungen und/oder Unterschieden mit anderen relevanten Inventaren des MIS 5, insbesondere dem SB-Technokomplex; 5) Beitrag zur Verfeinerung des chrono-kulturellen Klassifizierungssystems des südafrikanischen MSA während des MIS 5.

Die Fundstelle Sibudu-Höhle befindet sich 40 km nördlich von Durban in der Gemeinde KwaDukuza, die zum Distrikt iLembe gehört. Der Fundplatz liegt auf einer steilen Klippe über dem uThongathi-Fluss und das Abri ist in den Sandstein der Natal Group geschnitten. Das

Ausgrabungsgelände befindet sich auf einer Höhe von ca. 100 m über dem Meeresspiegel im nordöstlichen Teil der Fundstelle. In Bezug auf die Forschungsgeschichte führte A. Mazel 1983 die erste Testgrabung durch, während dann weitere Ausgrabungen in den Jahren 1998 bis 2011 von L. Wadley stattfanden. Eine Grabungsmannschaft der Universität Tübingen unter der Leitung von N. J. Conard setzt seit die Feldarbeit 2011 fort.

Die hochauflösende stratigraphische Abfolge besteht hauptsächlich aus MSA-Schichten datiert auf älter als 74.000 bis 33.000 BP, gefolgt von eisenzeitlichen Besiedlungen. Die Stratigraphie besteht überwiegend aus anthropogenen Ablagerungen und die organische Erhaltung ist in der Regel gut. Die MSA-Schichten lieferten zahlreiche OSL- und Radiokohlenstoffdaten (z.B. Wadley und Jacobs, 2006; Jacobs, et al., 2008a; Jacobs und Roberts, 2017), und neue Lumineszenzdatierungen werden von C. Tribolo derzeit ermittelt. Der Teil der chronokulturellen Sequenz, dem das lithische Material meiner Arbeit zugrunde liegt, umfasst die folgenden sechs Schichten: BMo, RBS, GSS, GBP, LBC und PSS, die seit dem Beginn der neuen Ausgrabungen im Jahr 2011 identifiziert wurden. Zusätzlich zu diesen deskriptiven Feldbezeichnungen wurde jeder neuen Schicht in alphabetischer Reihenfolge zuerst ein männlicher und dann ein weiblicher Name zugewiesen, beginnend mit dem Buchstaben A: Adam, Annie, Bart, Bea, Casper und Chantal. Die vorläufigen Ergebnisse der Lumineszenzdatierungen zeigen an, dass diese Schichten ein Alter zwischen 92.000 und 72.000 BP aufweisen (Tribolo, persönliche Mitteilung). Die Schichten BS und LBG, informell als ‚pre-SB‘ bezeichnet, befinden sich in der Stratigraphie darüber. Innerhalb der BS-Abfolge wird eine Änderung der typologischen Zusammensetzung deutlich, da in den tieferen archäologischen Horizonten BS 11 bis BS 16 bifaziale Spitzen auftreten (Wadley, 2013). Die oben genannten Ablagerungen mit einem Alter von  $69.500 \pm 2.100$  BP, die dem SB zugeordnet werden, weisen als diagnostische Hauptmerkmal die bifaziale Steintechnologie auf, einschließlich bifazieller Spitzen (Wadley, 2007; Soriano, et al., 2015). Die Schichten zum HP gehörig liegen über dem SB mit Datierung zwischen  $60.500 \pm 1.800$  und  $58.000 \pm 1.700$  BP und zeichnen sich durch verschiedene Abbaustrategien, welche zur Herstellung von Klingen führten, die dann häufig in eine Vielfalt von rückengestumpften Werkzeugen modifiziert wurden (Delagnes, et al., 2006; de la Peña, 2015; Soriano, et al., 2015). Darüber hinaus ist auch die Herstellung von kleinen bifaziellen Quarzspitzen Teil des Werkzeugbestands im HP (de la Peña, et al., 2013). Der folgende Abschnitt der Sequenz hat ein Alter von circa 58.000 BP und entspricht dem post-HP. Als Reaktion auf die Unklarheiten bezüglich des informellen Namens ‚post-HP‘ wurde vorgeschlagen, Sibudu als Referenzfundstelle für diese Phase heranzuziehen (Conard, et al.,



2012; Lombard, et al., 2012). Lombard et al. (2012) schlugen den Begriff ‚Sibudu Technokomplex‘ vor, der sich durch Spitzenproduktion nach dem Levallois-Konzept und typische unifaziale Spitzen mit facettierten Schlagflächenresten und länglichen Formen auszeichnet. Conard et al. (2012) plädierten stattdessen für den Begriff ‚Sibudan‘, da dieser markante techno-funktionale Signaturen wie Tongatis, Ndwedwes, *biseaux* und Werkzeuge mit natürlichem Rücken präsentiert. Darüber hinaus offenbart diese hochauflösende Sequenz, die auf circa 58.000 BP datiert, kurzfristige Veränderungen und starke diachrone Signale (Will und Conard, 2018). Die darüber liegenden Schichten, die als *late MSA* bezeichnet werden und auf ca. 48.000 BP datiert sind, zeichnen sich durch das häufige Vorkommen von unifaziellen Spitzen aus (Villa et al. 2005). Die obersten Schichten der MSA-Abfolge werden als *final MSA* mit einem Alter von etwa 38.000 BP bezeichnet, und haben als ihr charakteristischstes Merkmal bifaziale Spitzen mit konkaver Basis (Wadley, 2005).

Heute liegt Sibudu im *KwaZulu-Natal Coastal Belt* des *Indian Ocean Coastal Belt Biome*, das in die *Summer Rainfall Zone* fällt. Diese Vegetationszone wird von Wäldern dominiert, die nur von Graslandflächen unterbrochen werden, und ist durch heiße, feuchte tropische Klimabedingungen im Sommer sowie milde, trockene subtropische Bedingungen im Winter gekennzeichnet (Mucina, et al., 2006). Die einheimische Vegetation direkt um die Fundstelle herum umfasst immergrüne Arten, Savannenlaubwälder und Grasland (Wadley, 2013).

Im Hinblick auf paläo-ökologische Rekonstruktionen bietet Sibudu eine weite Bandbreite von hochauflösenden Umweltdaten (z.B. Allott, 2006; Herries, 2006; Pickering, 2006; Renaut und Bamford, 2006; Schiegl und Conard, 2006; Clark, 2013; Sievers, 2013; Hall, et al., 2014; Val, 2016; Murungi, 2017; Robinson und Wadley, 2018). Diese multidisziplinären Belege deuten auf ein Mosaik an Lebensräumen, das durch alle Besiedlungsschichten Sibudus hindurch erhalten blieb, vielleicht aufgrund der Lage der Fundstelle und seiner Nähe zum uThongathi-Fluss (Robinson und Wadley, 2018). Ein großer Teil der Taxa, die Sibudu heute umgeben, war höchstwahrscheinlich auch während des MSA vorhanden, was auf ähnliche Bedingungen, wie sie heute an diesem Ort herrschen, schließen lässt. Allerdings wurden im archäologischen Material einige Pflanzenarten identifiziert, die heute scheinbar nicht mehr vorhanden sind, was bedeutet, dass die Trockenwaldkomponente der Vegetation vielleicht aufgrund der nördlicheren Vegetationselemente umfangreicher gewesen sein könnte (Wadley und Jacobs, 2006). Im Hinblick auf die Schichten Chantal bis Adam, die relevant für diese Arbeit sind, ergab eine vorläufige archäozoologische Identifizierung in der Schicht Casper das Vorhandensein von Blauducker und Buschschwein, die häufig in Waldgebieten vorkommen.

Dem *chaîne opératoire*-Ansatz (vgl. Leroi-Gourhan, 1943; Tixier, 1980; Pelegrin, et al., 1988; Boëda, et al., 1990; Geneste, 1991; Inizan, et al., 1999; Soressi und Geneste, 2011) folgend führte ich eine technologische Analyse der Steinartefakte der Schichten C-A von Sibudu durch. Meinem theoretischen Hintergrund zufolge gehe ich davon aus, dass die Steinartefaktproduktion zunächst als kognitives Projekt entstand, das dann auf intellektueller Ebene in ein konzeptionelles Schema umgewandelt wurde, welches schließlich durch eine Reihe von Ereignissen, die das operative Schema repräsentieren, konkretisiert wurde. Jeder dieser Schritte ist abhängig und wird beeinflusst von mehreren, teilweise interagierenden, natürlichen und menschlichen Parametern (Pigeot, 1991; Inizan, et al., 1999; Soressi und Geneste, 2011; Porraz, et al., 2016). So bildet die Dokumentation von wiederkehrenden Mustern in einem lithischen Inventar die Grundlage für die Interpretation als intentional (Soressi und Geneste, 2011). Das oberste Ziel für einen Steinschläger ist die Herstellung von Werkzeugen, die so konzipiert sind, dass sie einer bestimmten Funktion dienen können (Porraz, et al., 2016). Da das Werkzeug als integraler Bestandteil eines intentionellen, nicht zufälligen Systems von Zurichtung, Instandhaltung und Verwerfung betrachtet wird, gehe ich von einer starken Beziehung zwischen der Rohmaterialelektion, den Kernabbaustrategien, der Ausbeute an Grundformen und der Retuschierung, dem Einsatz sowie der Verwerfung von Werkzeugen aus (Conard, et al., 2012). Neben einem traditionellen typologischen Ansatz verfolge ich das Konzept des Pradnik-Zyklus (Krukowski, 1939), welches darauf beruht, dass die regulierten Phasen der Werkzeugherstellung, -nutzung und -entsorgung wiederkehrende Muster im lithischen Inventar hinterlassen, da Werkzeuge aus verschiedenen Phasen auftreten, die eine Bestimmung des Lebenszyklus der Werkzeuge ermöglichen. Darüber hinaus verfolge ich einen techno-funktionalen Ansatz, um funktionale Charakterisierungen der Werkzeuge auf der Grundlage technischer Merkmale bereitstellen zu können (z.B. Lepot, 1993; Bourguignon, 1997; Soriano, 2000; Bonilauri, 2010; Nicoud, 2011; Chevrier, 2012; Boëda, 2013). Ziel dieses Ansatzes ist es, die drei wesentlichen techno-funktionalen Einheiten eines Werkzeugs zu identifizieren: die Arbeitskante, den Griff und das Zwischenstück. Die technologischen und techno-funktionalen Methoden, kombiniert mit Gebrauchsspuren- und Residuenanalysen (Rots, et al., 2017), die durch experimentelle Daten noch ergänzt werden, liefern mehrere Beweislinien, um spezifische Hypothesen über die Dynamik der Produktion, des Gebrauchs und der Entsorgung von Werkzeugen zu untermauern. Dieser umfassende methodische Verfahrensrahmen ermöglicht es mir, aus begrenzten archäologischen Daten maximale Informationen zu gewinnen, technische Ereignisse zu beschreiben und Rückschlüsse auf menschliches Verhalten

in den C-A-Schichten von Sibudu zu ziehen. Schließlich ermöglichen detaillierte technologische Analysen Vergleiche mit anderen Inventaren, um Ähnlichkeiten und Unterschiede bei den technischen Entscheidungen hervorzuheben und ein besseres Verständnis der zeitlichen und räumlichen Variabilität der Steintechnologie in einem breiteren kulturellen Kontext zu erreichen (siehe Lechtman, 1977; Wiessner, 1983).

Das archäologische Material, das die Grundlage meiner Doktorarbeit bildet, beinhaltet alle lithischen Objekte  $\geq 30$  mm, sowie alle Kerne, Kernfragmente, Werkzeuge und Werkzeugfragmente unabhängig von ihrer Größe aus den Schichten Chantal bis Adam. Die Stücke stammen aus einer Ausgrabungsfläche von ca. 4 m<sup>2</sup>, die zwischen 2012-2016 gegraben wurde. Die sechs Schichten lieferten insgesamt 8.164 Artefakte.

Zu den Ergebnissen dieser Studie, die Steinschläger nutzten in dieser Phase der Besiedlung eine Reihe verschiedener, meist lokal verfügbarer (weniger als 5 km) Rohmaterialien, darunter vor allem Dolerit, gefolgt von Sandstein, Quarzit, Quarz, Hornfels und Chert, die in Bezug auf die Grundformenproduktion und den Werkzeugbestand von unterschiedlicher Bedeutung waren. Die Menschen beschafften die Gesteinsarten aus verschiedenen Lagerstätten, z.B. als Knollen aus dem Fluss oder aus (sub)primären Aufschlüssen, und daher weisen die Rohmaterialien sowohl unterschiedliche Formen als auch physikalische Eigenschaften auf. Der Anteil der Kortextbedeckung sowie das Vorhandensein von Produkten aus den frühesten Phasen des Abbaus weist daraufhin, dass die Werkzeughersteller zumindest teilweise die gesamte Abbausequenz in Bezug auf alle Rohmaterialien, mit Ausnahme von Chert, am Fundplatz durchführten. Dolerit umfasst die höchste Anzahl an Grundformen, Kernen und Werkzeugen und wurde offenbar intensiv vor Ort durch verschiedene Schlagaktivitäten ausgenutzt. Einige große Klingen aus Dolerit treten im Inventar auf, was darauf hindeutet, dass einige Elemente als fertige Zielprodukte in die Fundstelle importiert wurden. Obwohl Dolerit das dominierende Gestein ist, deutet das Verhältnis von Werkzeug zu Grundform daraufhin, dass die Grundformen (relativ) selten zu Werkzeugen weiterverarbeitet wurden. Sandstein, der aus dem Abri selbst stammt, stellt das zweithäufigste Rohmaterial im Inventar dar und weist den geringsten Retuschierungsgrad auf. Quarzit und Hornfels scheinen häufiger als fertige Zielprodukte zur Fundstelle transportiert worden zu sein. Die aus diesen Gesteinsarten hergestellten Werkzeuge belegen ein hohes Maß an Investition in ihre Instandhaltung. Das Inventar enthält zusätzlich sowohl Bergkristall als auch Milchquarz. Dieses Gestein stellt die zweitgrößte Anzahl an Kernen, die aber im Vergleich zu den Kernen aus anderen Rohmaterialien

die kleinste Größe aufweisen. Quarz, insbesondere Bergkristall, ist von großer Bedeutung für die Werkzeugherstellung, insbesondere von bifaziellen Stücken und sogenannten *serrated pieces*.

Das Steinartefaktinventar zeigt einen starken Fokus auf die Herstellung von Klingen und Klingenabschlägen in Bezug auf die verschiedenen Rohmaterialien. Einige der Klingen sind von sehr großem Ausmaß mit einer maximalen Länge von bis zu 114 mm, während die meisten eine durchschnittliche Länge zwischen 39 mm und 55 mm haben. Die Klingenkategorie enthält jedoch einen hohen Anteil an fragmentierten Stücken. Im Gegensatz zur Länge, die ein weites Spektrum umfasst, weisen die Breite und Dicke der Klingen einen höheren Standardisierungsgrad auf. Die meisten Klingen haben keine Kortextbedeckung auf der Dorsalfläche. Die Schlagflächenreste der meisten dieser laminaren Zielprodukte sind glatt und die Morphologie ist fast ausschließlich rechteckig. Die Elemente zeigen überwiegend unidirektionale dorsale Negative, wobei einige Zielprodukte orthogonale oder bidirektionale Negative aufweisen, die eine laterale bzw. distale Präparation belegen. Die Steinschläger zielten auf Klingen mit geraden bis leicht gekrümmten Profilen ab. Innerhalb der Klingenkategorie identifizierte ich zwei Untergruppen, die sich sowohl durch den Querschnitt als auch durch das Breiten-Dicken-Verhältnis unterscheiden: (1) hohe, seitlich zentrierte Klingen mit dreieckigem Querschnitt und (2) flache, seitlich diffuse Klingen mit trapezförmigem Querschnitt. Die Untergruppe (1) dominiert das Inventar und zeigt eine deutlich niedrigere vertikale Konvexität. Interessanterweise ist keine der Klingen der Untergruppe (2) vollständig mit Kortext bedeckt und nur wenige dieser Grundformen haben mehr als 50% kortikale dorsale Überreste, was darauf hindeutet, dass die Untergruppe (2) nicht in den frühesten Phasen des Abbaus auftritt. Die Klingen weisen ähnliche morphometrische Charakteristika durch die Schichtenabfolge hindurch auf.

Die Klingenabschläge zeigen im Allgemeinen ähnliche Tendenzen zu den Klingen. Im Gegensatz zu den Klingen haben sie jedoch häufiger kortikale Reste auf ihrer Dorsalfläche. Klingenabschläge sind kürzer, breiter und dicker als Klingen. Die meisten dieser Grundformen sind nicht fragmentiert und ein deutlich höherer Anteil als bei den Klingen ist vollständig erhalten. Der Trend der Dichotomie von seitlich zentralisierten Stücken mit dreieckigem Querschnitt und flachen, seitlich diffusen mit trapezförmigem Querschnitt zeichnet sich auch unter den Klingenabschlägen ab. Ich beobachte ebenso ähnliche Tendenzen in Bezug auf Größe und Form der Klingenabschläge in allen Schichten.

Die Abschlage machen den grosten Teil des Inventars aus und weisen eine Reihe von diagnostischen Merkmalen auf. Quarz und Sandstein beinhalten eine geringere Anzahl an laminaren Elementen, aber einen hoheren Anteil an Abschlagen im Vergleich zu den anderen Rohmaterialien. Die Abschlagklasse weist eine durchschnittliche Lange von 31,9 mm mit einer entsprechenden durchschnittlichen Breite von 33 mm und einer mittleren Dicke von 8,9 mm auf. Diese Grundformen umfassen einen hoheren Anteil an vollstandig erhaltenen Elementen als ihre laminaren Gegenstucke. Die Abschlage zeigen haufiger als die Klingen und Klingenabschlage Kortexbedeckung auf ihren dorsalen Flachen. Die meisten der Abschlage haben glatte Schlagflachenreste, aber die groste Stuckzahl an kortikalen Schlagflachenresten tritt ebenso auf. Das vorherrschende dorsale Negativmuster ist unidirektional, dennoch besitzen eine groe Anzahl von Abschlagen orthogonale Negative – oft ein orthogonales laminares Negativ. Interessanterweise weist die Abschlagpopulation mit orthogonalen Negativen mehr Elemente ohne Kortex auf, und zusatzlich sind weniger Stucke mit ber 50% kortikalen Resten sowie keine vollstandig kortikalen Artefakte vorhanden. Daher stammen die orthogonalen Abschlage vermutlich aus fortgeschrittenen Phasen der Abbausequenz. Der grote Teil zeigt eine trapezformige Morphologie und gerade bis leicht gekrumnte Profile. Die Querschnitte sind entweder dreieckig oder trapezformig. Ich dokumentierte diachrone ahnlichkeiten in Bezug auf metrische Dimensionen und Form unter den Abschlagen.

Triangulare Abschlage sind in geringer Anzahl in der gesamten Sequenz vorhanden, spielen aber eine marginale Rolle.

Die Kerne wurden nach der einheitlichen Taxonomie fur Kerne von Conard et al. (2004) klassifiziert. Dementsprechend fallen die meisten Kerne unter die sogenannten *platform cores* (Plattformkerne) und, praziser gesagt, fast ausschlielich unter die *blade platform cores* (Klingenplattformkerne). Diese Kerne werden hauptsachlich aus Dolerit und Quarzit hergestellt. Die Steinschlager schienen uberwiegend Platten auszuwahlen, um sie zu diesem Kerntyp zuzurichten. Der geringe Prozentsatz von Kortexbedeckung befindet sich zumeist auf dem Rucken und/oder auf einer Lateralflache der Kerne. Die Mehrheit der Kerne ist mit einer Schlagflache ausgestattet, die in der Regel glatt ist. Die Hauptabbauf্লachen haben uberwiegend viereckige Formen. Die *blade platform cores* wurden fast ausschlielich durch unidirektionalen Abbau genutzt. Meistens weisen die Kernfue dieser Kerne eine distale Preparation auf. Die Variabilitat innerhalb der *blade platform cores* scheint mit verschiedenen Verwerfungsstadien zusammenzuhangen. Die letzten Operationen an den Kernen entsprechen in erster Linie

Schlagunfällen oder Präparationen. Die letzten Produktionsschritte unterstreichen deutlich den Fokus auf laminierte Elemente. Die Negative der laminaren Zielprodukte auf den *blade platform cores* verweisen auf Mindestanforderungen für die Länge von ca. 20 mm und der Breite von 10 mm. Die Maße der Kerne, insbesondere das Längen-Breiten-Verhältnis der Abbauflächen, stimmen jedoch nicht mit den laminaren Dimensionen überein. Basierend auf der allgemeinen Beschreibung des Inventars, der Kortextbedeckung und den Dimensionen der *blade platform cores* argumentiere ich, dass viele dieser Kerne stark abgebaute Restkerne darstellen. *Blade platform cores* dominieren in allen Schichten, außer in der Schicht Casper, in der bipolare Kerne häufiger vorkommen.

Ein aus Quarzit hergestellter Kern weist als letzten Produktionsschritt Lamellennegative auf. Die Ähnlichkeit zur Struktur und Morphologie der *blade platform cores* deuten darauf hin, dass dieser Kern eher das Ergebnis einer extremen Kernerschöpfung darstellt als von einer unabhängigen Abbaustrategie stammen könnte.

Einer der Quarzkerne scheint zuerst als *blade platform cores* abgebaut worden zu sein und weist Negative und Aufsplitterungen durch bipolaren Abbau als letztes Abbaustadium auf.

Die zweithäufigste Kernart sind bipolare Kerne, die hauptsächlich mit Quarz zusammenhängen. Diese Kerne haben kleinere Maße als die *blade platform cores*.

Einige wenige Kerne gehören zu Kernen im Anfangsstadium. Alle wurden an Platten hergestellt und weisen mehr als 50% kortikale Überreste auf, die sich entweder auf dem Rücken oder auf dem Rücken und einer Lateralfäche befinden. Die Abbauflächen haben viereckige Formen und die Kernfüße sind entweder kortikal oder präpariert. Diese Kerne weisen größere Dimensionen auf als die *blade platform cores*. Die letzte Operation an diesen Kernen bezieht sich entweder auf Präparationen oder auf einen Schlagunfall.

Die durch die Schlagmerkmale der Grundformen identifizierten Trends deuten darauf hin, dass die Werkzeughersteller aus Sibudu sowohl harte als auch weiche Schlagsteine für den direkten, internen Schlag verwendeten, wobei sowohl *rentrante* als auch tangentielle Bewegungen ausgeführt wurden. Das Inventar enthält mehrere Knollen und Knollenfragmente aus Sandstein, Quarzit, Dolerit und Quarz mit Schlagspuren, die als Schlagsteine interpretiert werden können und die eine mögliche Koexistenz von harten und weichen Schlagsteinen in der Steintechnologie zum Lösen der Grundformen untermauern.

Alle Daten von Grundformen und Kernen zusammennehmend stellte ich fest, dass sich die Bewohner von Sibudu im MSA hauptsächlich auf die Herstellung laminarer Elemente

fokussierten und eine spezifische unidirektionale Abbaustrategie entwickelten, um Klingen und Klingenabschläge von allen Rohmaterialien zu gewinnen. Die typischen Klingen zeichnen sich durch unidirektionale dorsale Negative, rechteckige Formen und gerade bis leicht gekrümmte Profile aus. Die systematische Kernkonfiguration ermöglicht die laminare Produktion und hält sie gleichzeitig instand. Um die für die Gewinnung ihrer Zielprodukte erforderliche Geometrie zu erreichen, richteten die Steinschläger sechs verschiedene Bereiche ein: Schlagfläche, Abbaufäche, Rücken und Kernfuß sowie zwei weitere wesentliche Flächen: die laterale Kernkante und den *méplat* bzw. die laterale Fläche. Die Schlagflächen sind in der Regel glatt und haben einen gewölbten Umriss. Die Abbaufächen zeichnen sich in erster Linie durch quadratische Formen aus und sind von eher geringen transversalen Konvexität. Die Rücken der Kerne werden hauptsächlich durch natürliche Flächen oder alte Ventralflächen gebildet. Einige Rücken sind jedoch durch Präparationsnegative, die entweder zur lateralen Kernkante, zum Kernfuß oder zur Schlagfläche gehören, überprägt. Die meisten Kernfüße zeigen eine vollständige oder teilweise Präparation mit Negativen, die der unidirektionalen Abbaurichtung entgegengesetzt sind, um die distale Konvexität zu erhalten. Die laterale Kernkante wird auf einer Seite der Abbaufäche durch das Ablösen von Negativen orthogonal zur Abbaurichtung mit dem Ziel der Erhaltung der transversalen Konvexität hergestellt. Die Steinzeitmenschen präparierten die laterale Kernkante höchstwahrscheinlich häufig mit entweder bifaziell alternierenden oder bifaziellen Negativen. Der *méplat*, befindet sich gegenüber der lateralen Kernkante auf einer der schmalen Seiten des Kerns. Diese Fläche wird üblicherweise durch eine natürliche Oberfläche gebildet. Einige wenige Kerne weisen jedoch ein so fortgeschrittenes Abbaustadium auf, dass der *méplat* aufgrund starker Erschöpfung nicht mehr erkennbar ist. Weitere Kerne zeigen orthogonale Präparationsnegative, die den Winkel zwischen der Abbaufäche und dem *méplat* korrigieren sollten. Die laterale Kernkante und der *méplat* zusammen mit der Abbaufäche formen das Volumen, das für den Abbau bestimmt ist. Im Laufe des fortschreitenden Kernabbaus verändert sich dieses aktiv nutzbare Volumen morphologisch von einem dreieckigen asymmetrischen Querschnitt zu einem fünfeckigen Querschnitt, der an ein umgefallenes Haus erinnert. Die Rücken der Kerne stellen das passive (*inutile*) Volumen dar. In der Frühphase des laminaren Abbausystems wählten die Werkzeugmacher vorzugsweise Platten, um mit der Anlage der lateralen Kernkante und der Installation einer Schlagfläche beginnen zu können. Die diagnostischen Abschläge aus dem Frühstadium sind trapezförmig sowie leicht gekrümmt bis gekrümmt und zeigen auf der Dorsalfäche entweder unidirektionale Negative und/oder Kortex. Der asymmetrische dreieckige Querschnitt des aktiven Volumens

ermöglicht es mit der effektiven Nutzung des Grates, der durch den *méplat* und die Abbaufäche gebildet wird, zu starten. Die Steinschläger nutzten entweder die natürliche Geometrie aus, um die ersten Klingen mit einer natürlichen, kortikalen Kernkante zu lösen, oder sie präparierten den Grat, sodass der Abbau durch eine einseitige oder zweiseitige primäre Kernkantenklinge erleichtert wurde.

In der mittleren und späten Phase erfolgt die Nutzung des aktiven (*utile*) Volumens asymmetrisch auf der breiten Abbaufäche und durch den Abbau des *méplat*. Der hohe Anteil an laminaren Produkten mit lateralen Kortexresten belegt die laterale Erweiterung der Abbaufäche, während das Vorhandensein von Klingen mit kortikalem Rücken von der Nutzung des *méplat* zeugt. Diese kontinuierliche Dichotomie der Abbaufolge führt zur Herstellung von zwei Untergruppen der Klingen. Der Abbau verläuft nicht kontinuierlich, da einerseits partielle Kernkantenklingen darauf hindeuten, dass die Werkzeugmacher den durch die laterale Fläche und die Abbaufäche gebildeten Grat teilweise erneuern mussten und andererseits bezeugen die Kerne und Präparationsabschläge die Neuinstallation der lateralen Kernkante in einem fortgeschrittenen Stadium der Abbaufolge. Die diagnostischen Abschläge der lateralen Kernkantenerneuerung haben ähnliche Eigenschaften wie jene der frühen lateralen Kernkantenpräparation, einschließlich der trapezförmigen Form und des leicht gekrümmten bis gekrümmten Profils, besitzen hingegen keine kortikalen Reste und orthogonale, laminare dorsale Negative. Die prähistorischen Bewohner von Sibudu lösten höchstwahrscheinlich partielle Kernscheiben, um einen für den Abbau optimal geeigneten Winkel der Schlagfläche wiederherzustellen. Eine distale Präparation zur Regulation der longitudinalen Konvexität erfolgte auch.

Die letzte Phase des Abbaus betrifft die Verwerfung der Kerne nach einem langen Nutzungszyklus meist aufgrund von Schlagunfällen. Die extreme Kernerschöpfung, das Ungleichgewicht in der Ausnutzung des aktiven Volumens sowie die Präparation der lateralen Kernkanten, Schlagflächen und der Kernfüße führen zu einer eher quadratischen statt länglichen Form der meisten Abbaufächen. Das Ende der Produktion ist unvermeidlich, wenn das aktive Volumen so stark erschöpft ist, dass die Anbringung einer transversalen Konvexität durch Erneuerung der lateralen Kernkante und damit eine weitere Nutzung unmöglich ist.

Das Inventar zeichnet sich durch das Vorhandensein der bifaziellen Technologie, inklusive *serrated pieces*, aus, aber beim größten Teil der Werkzeuge in allen Schichten handelt es sich um eine Vielzahl von unifaziell retuschierten Spitzenformen. Es kommen außerdem



verschiedene schaberartige Formen und gezähnte Stücke vor. Innerhalb der übergeordneten typologischen Klassifikation definierte ich Werkzeugklassen, die auf der Identifizierung von Mustern in Bezug auf die strukturelle Positionierung der Arbeitskanten und den passiven Bereichen an den Werkzeugen und dynamischen Verbindungen mit den Werkzeugherstellungs- und Nachbearbeitungszyklen basieren.

Alle unifaziell retuschierten Spitzenformen entsprechen der Definition von dreieckigen oder ansatzweise dreieckigen Grundformen, die fast ausschließlich auf einer Oberfläche retuschiert wurden, wobei das distale Ende durch Retusche zugespitzt wurde oder durch die Zurichtung beim Abbau eine spitze Form erhielt. Die meisten dieser Werkzeuge wurden aus Dolerit gefertigt; gefolgt von Quarzit. Bei den Grundformen, die zu diesem Werkzeugtyp modifiziert wurden, handelt es sich in erster Linie um gerade laminare Elemente von größeren Ausmaßen aus der Hauptproduktionsphase. Unter den unifaziell retuschierten Spitzenformen unterschied ich die Werkzeugklassen: dreiflächige, symmetrische unifaziale Spitzen (TSPs), asymmetrische konvergente Werkzeuge (ACTs), Tongatis (bezüglich Definition siehe Conard, et al., 2012) und unifaziale Spitzen, die den allgemeinen Kriterien entsprechen, aber nicht weiter klassifiziert wurden.

Die TSPs kommen am häufigsten von den unifaziell retuschierten Spitzenformen vor. Sie verfügen über symmetrische, bilateral retuschierte Distalenden, die von leicht kurvenförmigen Kanten geformt werden. Ihre Spitzen sind dreiflächig und sie weisen regelmäßige dreieckige Querschnitte auf. Die medialen Abschnitte sind konvergent und oft flächendeckend an beiden Kanten retuschiert, was auf mehrere Nachschärfungsphasen hindeutet, die die Verlängerung des Kraft überleitenden Teils des Werkzeugs bewirken. Die basalen Enden haben in der Regel eine viereckige Form und wurden manchmal ventral verjüngt. Diese Werkzeuge weisen einen Längenmittelwert von 47,8 mm, einen Breitenmittelwert von 24,6 mm und einen Dickenmittelwert von 7,8 mm auf. Die große Bandbreite der Länge sowie der Länge der retuschierten Spitze könnte mit der Intensität der Werkzeugnachschärfung und/oder mit der Grundformenauswahl für die Herstellung von TSPs zusammenhängen. Die für die Modifikation zu TSPs ausgewählten laminaren Produkte sind ursprünglich breiter und wahrscheinlich auch länger als die unretuschierten Klingen und werden erst durch die Zurichtung und Nachbearbeitung in Länge und Breite verändert. Die meisten TSPs liegen als Spitzenfragmente vor, die wahrscheinlich bei der Werkzeugherstellung oder Nachschärfung gebrochen sind. Was die funktionellen Eigenschaften betrifft, so wurden diese Werkzeuge wahrscheinlich

vorwiegend in einem punktuellen Modus zum Perforieren, Bohren oder Lochen eingesetzt. Der Werkzeugherstellungs- und Nachbearbeitungszyklus umfasst TSPs mit kleinen, kurzen Kraft überleitenden Teilen verglichen mit relativ langen mittleren Abschnitten in der Anfangsphase, während das Fortschreiten der Werkzeugbearbeitung, einschließlich mehrerer Nachschärfungsereignisse, zu einem Rückgang des Zwischenteils und einer Ausweitung der Arbeitskante führt. Folglich nimmt die maximale Breite der Spitze ab und der Verlauf der Kanten der Spitze ist leicht konkav und nicht geradlinig. Zusätzlich ändert sich die Morphologie des medialen Teils von ursprünglich mehr parallel zu konvergent.

Die ACTs stellen den zweitgrößten Anteil innerhalb der unifaziell retuschierten Spitzenformen dar und weisen asymmetrische, konvergente Distalenden auf, die nicht mit der Schlagachse der ursprünglichen Grundform übereinstimmen und typischerweise durch eine steile, konvex retuschierte Kante zusammen mit einer gegenüberliegenden, geraden, unretuschierten Kante gebildet werden. Die Modifikation erstreckt sich vom distalen Ende bis zum medialen Teil, der üblicherweise von einer konvergierenden Kante und einer gegenüberliegenden geradlinigen Kante geformt wird. Das basale Ende ist in der Regel viereckig. Die Länge beträgt durchschnittlich 44,5 mm, die Breite 26,8 mm und die Dicke 8,2 mm. Die Grundformenselektion umfasst überwiegend gerade laminare Produkte aus verschiedenen Phasen der Abbaufolge. Ein geringer Anteil der ACTs ist vollständig erhalten. In Bezug auf die funktionale Charakterisierung installierten die Werkzeugmacher die abgestumpfte Kante mit Steilretusche scheinbar als Rücken von Schneidwerkzeugen, um mehr Kraft auf die Arbeitskanten ausüben zu können. Die unmodifizierten Kanten, die oft makroskopisch sichtbare Makro- und Mikronegative aufweisen, weisen spitze Winkel und Federbrüche auf. Die Asymmetrie der beiden Kanten deutet auf eine lineare Gebrauchsweise, wie z.B. Schneiden, Schnitzen und Schaben, hin

Die Historie der ACTs betreffend scheint die Anlage der steilretuschierten Kante ein terminaler Schritt gewesen zu sein und nur die Arbeitskante wurde gelegentlich nachbearbeitet.

Die bifaziellen Stücke bilden den zweithäufigsten Werkzeugtyp innerhalb der typologischen Zusammensetzung des Inventars. Alle Stücke entsprechen Werkzeugen, die auf beiden Flächen im gleichen Kantenbereich retuschiert wurden. Dieser Werkzeugtyp umfasst bifaziale Spitzen und Keilmesser als Werkzeugklassen. Darüber hinaus sticht die Werkzeugklasse der *serrated pieces* hervor. Diese Werkzeuge zeichnen sich durch Ränder mit regelmäßig mehrfachen kleinen

Kerben, die dreieckige Zähne erzeugen, aus (Crabtree, 1972; Akerman und Bindon, 1995; Andrefsky, 2005).

Die Werkzeugmacher verwendeten hauptsächlich Quarz zur Herstellung von bifaziellen Spitzen; gefolgt von Dolerit und Quarzit. Bei einem großen Teil der bifaziellen Spitzen handelt es sich um Fragmente, insbesondere Distalfragmente. Die Länge zeigt einen Mittelwert von 40,1 mm, während die Breite durchschnittlich 22,9 mm und die Dicke 8,2 mm beträgt. Meistens sind die Stücke durch die bifazielle Formgebung so überprägt, dass die originale Grundform nicht mehr bestimmt werden konnten, aber, wenn identifizierbar, wurden vorzugsweise dicke laminare Produkte ausgewählt. Die Mehrheit der bifaziellen Spitzen hat ein gerades Profil. Was den Morphotyp angeht, so weisen die meisten bifaziellen Spitzen bilaterale Symmetrie auf. Deren Spitze haben eine V-Form sowie eine regelmäßig spitzzulaufende Kontur und machen zwischen einem und zwei Dritteln des gesamten Werkzeugs aus. Der mittlere Teil ist in der Regel konvergent und die Basen der Stücke haben eine elliptische Morphologie. Die bifazielle Abbausequenz involviert zwei Schlagtechniken: den direkten Schlag mit einem harten Schlagstein in der Anfangsphase des Formgebungsprozesses und den weichen marginalen Schlag in der fortgeschrittenen Phase der Formgebung. Alle Phasen der Zurichtung von Vorformen über die fertigen Produkte bis hin zu recycelten Elementen treten auf. Die bifaziellen Spitzen zeigen eine hohe Variabilität zusammenhängend mit den verwendeten Rohmaterialien Größe, Morphologie, Organisation des Herstellungsprozesses und anschließend daran die technofunktionale Interpretation der Gesteine betreffend.

Die Spitzen aus Dolerit, Quarzit und Hornfels sind im Durchschnitt 41,2 mm lang, 25,1 mm breit und 9,1 mm dick. Diese Werkzeuge weisen einen plankonvexen Querschnitt auf. Die Formgebung dieser bifazieller Spitzen ist im Allgemeinen, wenn auch nicht ausschließlich, hierarchisch organisiert. Werkzeugmacher begannen oft mit der bifaziellen Bearbeitung auf der flachen Oberfläche und setzten diese mit der konvexen Oberfläche fort, was zu Werkzeugen mit plankonvexen Querschnitten führte. Diese Konfiguration und Hierarchie zwischen den Flächen erlaubt eine Serie von Nachschärfungen ohne die gesamte Struktur zu verändern, entsprechend den bifaziellen Grundformen (*pièces bifaciales supports*) (vgl. Boëda, 1997; Porraz, et al., 2013; Soriano, et al., 2015). Diese Gestaltung der bifaziellen Spitzen aus Dolerit, Quarzit und Hornfels deutet auf eine langfristige Nutzung vor allem als spitzzulaufendes Schneidwerkzeug hin.

Die bifaziellen Spitzen aus Quarz zeigen einen Mindestlängenwert von 26,7 mm. Die Breite beträgt durchschnittlich 17,3 mm und die Dicke durchschnittlich 6,6 mm. Der Hauptanteil dieser

Quarzwerkzeuge weist bikonvexe Querschnitte auf. Die Herstellung von bifaziellen Spitzen aus Quarz scheint nicht-hierarchisch, sondern durch alternierende Negative gesteuert worden zu sein, was zu bikonvexen Fertigprodukten mit regelmäßigen spitzzulaufenden Konturen führt. Diese bifaziellen Spitzen entsprechen den 'bifaziellen Stücken als Werkzeug' (*pièces bifaciales outils*) (vgl. Boëda, et al., 1990; Nicoud, 2013). Diese bifaziellen Werkzeuge haben höchstwahrscheinlich als axial geschäftete Einsätze in Jagdwaffen fungiert.

Der Werkzeugbestand enthält 25 *serrated pieces*, die hauptsächlich aus Dolerit hergestellt wurden; gefolgt von Quarz. Die Artefakte haben eine mittlere Länge von 42,1 mm, eine mittlere Breite von 21,1 mm und eine mittlere Dicke von 7,8 mm. Klingen und Klingensplitter dienten überwiegend als Originalgrundformen. Die *serrated pieces* besitzen gerade Profile und bilaterale Symmetrie. Ihr Morphotyp besteht aus V-förmigen und regelmäßigen Spitzen, konvergenten oder parallelen medialen Teilen, die eine Fortsetzung des Spitzenbereichs darstellen, und viereckige Basalenden. Die technologische Variabilität in Bezug auf die Formgebungsfolge führt zu zwei Untergruppen innerhalb dieser Werkzeugklasse: bifaziell geformte Werkzeuge, die bilateral mit feinen Zähnen versehen wurden, und bifaziell (oder unifaziell) retuschierte Werkzeuge, die bilateral (oder lateral) mit feinen Zähnen ausgestattet wurden. Die Zähnung der Artefakte stellt die letzte und ultimative Phase des Herstellungsprozesses dar. Mehreren Beweislinien von technologischen und funktionellen Analysen sowie Experimenten zufolge setzten die Steinschläger die Drucktechnik mit Knochenkompressoren ein, um die feinen Zähne anzubringen. Die Abfolge der Kerben auf den Stücken zeugt von einer großen Regelmäßigkeit, die auf eine klare Kontrolle der Lage der Kontaktpunkte und der angebrachten Kraft hinweist. Darüber hinaus weisen die Zähnungsabschläge Merkmale wie kleine Lanzettsprünge, Negativbulben, parallele Kanten und Federbrüche auf, die für einen engen Kontaktpunkt typisch sind (vgl. Mourre, et al., 2010). Außerdem konnte das Auftreten von Quarzzähnungsabschlägen nachgewiesen werden, da sie sich hinsichtlich der Schlagflächenrestdicke und Gesamtmorphologie von den Formgebungsabschlägen unterscheiden. Die Anwendung von Knochenkompressoren wird durch mikroskopisch identifizierte Knochenreste assoziiert mit der Zähnung, das Auftreten eines Knochenwerkzeugs mit diagnostischen Gebrauchsspuren und das Vorhandensein von kleinen Knochenabschlägen, die den experimentellen Knochenabschlägen ähneln, die unbeabsichtigt während des Gebrauchs von der Spitze des Kompressors abgehen, bestätigt. Die Werkzeugmacher in Sibudu wendeten nicht Druckretusche an, um die Kante zu regulieren und die Verjüngung des Querschnitts der Werkzeuge bewirken, sondern Druckkerbung, um die

Kerben der *serrated pieces* zu erzeugen, indem sie den Kompressor leicht innerhalb der Kante platzierten und die Kraft in einem Winkel senkrecht zur Ebene der Grundform anbrachten (vgl. Crabtree, 1973; Whittaker, 1994). Die Ergebnisse der Gebrauchsspuren- und Residuenanalyse in Kombination mit experimentellen Daten geben Einblicke zur Funktion und Handhabung der *serrated pieces* (Rots, et al., 2017). Diese Werkzeuge stellen in Schäftungen eingesetzte Spitzen von Jagdwaffen dar. Die prähistorischen Menschen fertigten und verwendeten eine Klebstoffmischung aus gemahlenem rotem Ocker und Pflanzenklebstoff zum Befestigen der Stücke.

Unter den bifaziellen Werkzeugen befinden sich auch fünf Exemplare, die der Definition von Keilmessern entsprechen (vgl. Jöris, 2006; Frick, et al., 2018). Sie haben robuste Arbeitskanten gegenüber von natürlichen oder mit steilen, großen Negativen präparierten Rücken. In Richtung des distalen Endes auf der Lateralen, auf der sich der Rücken befindet, ändert sich der Winkel der Retusche zu weniger abrupt und bildet somit eine scharfe Kante, die mit der gegenüberliegenden Arbeitskante distal zusammenläuft. Das Distalende weist eine Spitze ohne regelmäßig spitzzulaufende Kontur auf. Der mediale Teil besteht aus der geradlinigen Arbeitskante und der zum distalen Abschnitt konvergierenden Kante mit dem Rücken. Die Basis hat eine viereckige Morphologie. Die Organisation der Fertigung verlief hierarchisch und führte zu einem asymmetrischen Querschnitt, der häufige Nachschärfungsepisoden ermöglicht.

Des Weiteren beinhalten die schaberartigen Formen Schaber, Werkzeuge mit natürlichem Rücken (NBTs) und einige Kratzer.

Die Schaber machen den größten Teil der schaberartigen Formen aus. Der höchste Anteil dieser Werkzeugklasse zeigt Modifikationen an beiden Kanten. Ich beobachtete eine Variabilität die Retusche betreffend, die von Perlretusche bis hin zu stark retuschiert reicht. Große Doleritklingen oder -klingenabschläge, die teilweise aus frühen Phasen des Abbaus stammen, dienen üblicherweise als Originalgrundformen für die Zurichtung der Schaber. Die Stücke haben einen Längenmittelwert von 47,3 mm. Sie zeichnen sich durch eine mittlere Breite von 33,6 mm und eine mittlere Dicke von 10,7 mm aus.

Die NBTs beziehen sich auf Objekte mit einem natürlichen Rücken, der gegenüber einer retuschierten Arbeitskante angeordnet ist. Der Rücken wird in einigen wenigen Fällen durch Negative präpariert, aber in der Regel auf natürliche Weise durch Kortex, Siretbrüche, Schlagflächenreste der Grundformen oder Kernkanten von Kernkantenprodukten gebildet. Der

größte Anteil entfällt auf Dolerit; gefolgt von Quarzit. Die Steinschläger wählten eine Vielfalt an Originalgrundformen, darunter Klingen, Klingenabschläge, Abschläge, Präparationsabschläge und Formgebungsabschläge, um sie in NBTs zu retuschieren. Die Länge der Elemente beträgt durchschnittlich 40,3 mm, die Breite 29,8 mm und die Dicke 10,9 mm.

Schließlich sind in der typologischen Zusammensetzung aller Schichten immer wieder gezähnte und gekerbte Stücke zu finden. Die gekerbten Stücke besitzen eine einzige tief konkave Kerbe im Gegensatz zu den gezähnten Stücken, die eine Abfolge von nebeneinander gereihten Kerben aufweisen (cf. Inizan, et al., 1999). Bei den bevorzugt gewählten Originalgrundformen handelt es sich entweder um Klingen oder Klingenabschläge. Die Stücke weisen eine mittlere Länge von 44,2 mm, eine mittlere Breite von 27,3 mm und eine mittlere Dicke von 8,5 mm auf. Die vornehmlich an einer Seite auftretenden Zählungen der Werkzeuge haben relativ breite Kerben, von denen einige tief, aber andere seicht sind. Die durchschnittliche Kerbbreite und -tiefe haben eine weite Spanne, die eine große Variabilität belegen.

Im Allgemeinen weisen die Steinartefakte der C-A-Schichten wenig Beeinträchtigung durch taphonomische Prozesse auf. Die einzig auffällige post-depositionelle Beeinflussung ist die starke Verkrustung von Sedimenten auf Stücken aller Rohmaterialien, die bis zur untersten Schicht Chantal ansteigt.

Die Ergebnisse meiner Arbeit heben die großen Ähnlichkeiten der C-A-Schichten in Bezug auf Rohmaterialelektion, Grundformenproduktion, Werkzeugherstellung und Werkzeugtypenspektrum hervor. Aufgrund dieser Homogenität betrachte ich die lithischen Inventare als zu einer technologischen Tradition gehörend. Trotz der allgemeinen Übereinstimmung sind einige Trends innerhalb der Abfolge bezüglich des Auftretens und der Häufigkeit einzelner Werkzeugklassen erkennbar. Unifazielle Spitzen erleben einen Tiefpunkt in der Schicht Bart, während bifazielle Stücke und die damit zusammenhängenden Formgebungsabschläge in diesem archäologischen Horizont ihren Peak erreichen. Die *serrated pieces* treten im Gegensatz zu den Zählungsabschlägen, die in allen Schichten vorkommen, erst ab Bart auf und sind am häufigsten in den Schichten Bea und Bart. Darüber hinaus ist der Anteil an Bergkristall, der stark mit der Herstellung von bifaziellen Werkzeugen verbunden ist, in den Schichten Annie, Bart und Bea am höchsten, wobei ein starker Anstieg davor und ein Rückgang zu bemerken ist. Die Schicht Bart markiert somit den Höhepunkt der bifaziellen Technologie.

Um über einen möglichen Beginn und ein mögliches Ende der technologischen Phase, die durch die Schichten C-A repräsentiert wird, zu hypothetisieren, betrachte ich die archäologischen Einheiten darüber und darunter innerhalb der stratigraphischen Sequenz von Sibudu. Der untere Abschnitt von BS, welcher sich direkt oberhalb der Schicht Adam befindet, obwohl nur vorläufig beschrieben, umfasst sowohl große Klingen als auch Abschlüge aus verschiedenen Rohmaterialien, *blade platform cores* und bifazielle Spitzen. In den jüngeren Ablagerungen finden sich Abschlüge und Klingen, aber neben einigen wenigen unifaziellen Spitzen und gezähnten Stücken aus Dolerit treten Werkzeuge eher selten auf. Die begrenzt verfügbaren Daten deuten also darauf hin, dass der untere Teil von BS zur technologischen Phase ‚C-A‘ gehören könnte. Ich hatte die Möglichkeit, die Werkzeuge und Kerne aus den Schichten Danny und Darya stratigraphisch direkt unter den von mir bearbeiteten Schichten zu analysieren. Basierend auf ihrem Werkzeugrepertoire, das bifazielle Stücke, einen hohen Anteil an unifaziellen Spitzenformen sowie schaberartigen Formen umfasst, und den Kernen, bei welchen es sich häufig um *blade platform cores* mit einer Konfiguration, die der laminaren Abbaustrategie aus den C-A-Schichten ähnelt, handelt, argumentiere ich, dass Danny und Darya eine Fortsetzung der technologischen Tradition darstellen. Dennoch bilden die C-A-Schichten, die einen markanten Höhepunkt in der bifaziellen Technologie, einschließlich der *serrated pieces*, repräsentieren, den zentralen Abschnitt dieser technologischen Tradition. Diese Schichten mit einer beträchtlichen Dicke von ca. 50 cm scheinen eher eine Phase von längerer Dauer als eine kurze Episode gewesen zu sein.

Die C-A-Schichten zeichnen sich durch klare technologische und technoökonomische Merkmale aus:

Das Inventar ist gekennzeichnet durch eine unidirektionale Hauptabbaustrategie mit einer speziellen Organisation, die auf die Herstellung von Klingen und Klingenabschlägen ausgerichtet ist. Die Struktur der Kerne besteht neben der Schlagfläche, der Abbaufäche, dem Rücken und dem Kernfuß, aus einer lateralen Kernkante für die Regelung der transversalen Konvexität und einer lateralen Fläche bzw. *méplat* für die Bereitstellung des nutzbaren Volumens. Die beiden Untergruppen der laminaren Zielprodukte ergeben sich aus dem Abbau entweder der schmalen lateralen Fläche oder der breiteren Abbaufäche. Darüber hinaus fallen bei diesem Abbausystem typische Präparationsabschlüge, insbesondere bei der Einrichtung und Erhaltung der lateralen Kernkante, an. Klingen und Klingenabschlüge dienten oft als Originalgrundformen für verschiedene Werkzeugtypen, wodurch eine starke

Wechselbeziehung belegt sein dürfte. Der Werkzeugbestand enthält verschiedene unifaziell retuschierte Spitzenformen, wobei TSPs und ACTs durch besondere morphometrische und technofunktionale Eigenschaften hervorstechen. Die auffallendsten typologischen Elemente sind jedoch die bifaziellen Werkzeuge, darunter bifazielle Spitzen, *serrated pieces* und einige Keilmesser. Die Herstellung der *serrated pieces* erfolgte unter Anwendung der Druckkerbung mit einem Knochenkompressor. Die Menschen der damaligen Zeit nutzten diese Objekte als geschäftete Projektile, um Tiere zu jagen. Schaberartige Formen, wie Schaber und NBTs, sind ebenfalls im Werkzeugrepertoire vorhanden. Schlussendlich kommen auch gezähnte und gekerbte Stücke vor und unterscheiden sich deutlich von den *serrated pieces* durch die Anzahl, Lage, Breite und Tiefe der Kerben.

Die Rohmaterialbeschaffung der Steinschläger in Sibudu bezog sich vorzugsweise auf lokal verfügbare Gesteine, allen voran Dolerit. Obwohl die Werkzeugmacher alle Rohmaterialien mit ihrer speziellen laminaren Abbaustrategie nutzten, favorisierten sie Doleritplatten und erschöpften diese als Kerne intensiv mit langen Abbauzyklen. Obwohl der Großteil der Werkzeuge aus Dolerit hergestellt wird, bildete die Retusche und Formgebung der Grundformen scheinbar nicht den Schwerpunkt der Schlagaktivitäten, worauf das niedrige Werkzeug-Grundformen-Verhältnis hinweist. Diese Gesteinsart wurde in erster Linie für die Zurichtung von Werkzeugen mit langer Lebensdauer ausgewählt, was wahrscheinlich auf ihre Zähigkeit und Festigkeit zurückzuführen ist, die dauerhafte, langverwendbare Kanten gewährleisten. Im Gegensatz dazu modifizierten die Bewohner von Sibudu oft Grundformen und investierten in die Instandhaltung von Werkzeugen aus Quarzit und Hornfeldern. Quarz, der hauptsächlich bipolar abgebaut wurde, spielte eine zentrale Rolle bei der Werkzeugherstellung, insbesondere in der bifaziellen Technologie. Sandstein umfasst zahlreiche kortikale Grundformen und einen geringen Anteil an Werkzeugen sowie Zielprodukten, was auf eine gelegentliche Nutzung durch kurze Abbaufolgen vor Ort hindeutet. Das Inventar zeigt den Import von isolierten Produkten aus Chert.

Die bifazielle Technologie betreffend manifestieren sich herausragende technoökonomische Unterschiede bei den Rohmaterialien. Erstens scheint der gesamte bifazielle Formgebungsprozess von Dolerit und Hornfels *in situ* vorgenommen worden zu sein, während bifazielle Stücke, die aus Quarz und insbesondere Quarzit gefertigt wurden, in erster Linie als fertige Produkte in die Fundstelle eingebracht wurden, wo sie verwendet, nachgeschärft und verworfen wurden. Außerdem unterscheiden sich die bifaziellen Spitzen aus Quarz stark von den anderen Gesteinen in Bezug auf morphometrische Merkmale, Organisation des



Herstellungsprozesses, Historie und schließlich die technofunktionale sowie funktionale Klassifizierung, was auf ein differenziertes technoökonomisches Verhalten hinweist. Die Größe, die symmetrische Struktur und die Organisation der Negative der Quarzspitzen deuten auf einen Einsatz als Projektile hin, während die anderen Rohmaterialien eher als Schneidewerkzeuge dienten. Schließlich zeigen die *serrated pieces* auch eine Variabilität von Quarz zu den anderen Gesteinsarten hinsichtlich der Maße, Formen und Zurichtung. Die Quarzspitzen zeichnen sich durch Eigenschaften wie Dünnhheit, Symmetrie, enger Penetrationswinkel und bikonvexer Querschnitt aus, die vermeintlich Pfeilen entsprechen, während die Objekte aus anderen Rohmaterialien eher mit Speerspitzen übereinstimmen. Die Ausnutzung überwiegend lokaler Rohstoffe und das Vorhandensein ganzer Abbaufolgen für alle Gesteinsarten mit Ausnahme von Chert deuten auf eine Hauptbeschaffungsstrategie den Standort (*provisioning of place*) betreffend hin, aber auch die Ausstattung des Individuums (*provisioning of individuals*) und die ad-hoc Versorgung bei Aktivitäten (*provisioning of activities*) kamen bis zu einem gewissen Grad ins Spiel.

Was die chrono-kulturelle Gliederung betrifft, vergleiche ich die C-A-Schichten mit MSA-Inventaren mit einer bifaziellen Komponente in MIS 5 und anschließend mit gut datierten, aus der Literatur bekannten MSA-Fundstellen aus MIS 5.

Bevor ich das bifazielle Phänomen im MSA von MIS 5 im Allgemeinen diskutiere, betrachte ich die C-A-Schichten innerhalb der stratigraphischen Sequenz von Sibudu selbst. Ich beobachte große Unterschiede zu den SB-Schichten der Fundstelle hinsichtlich der Abbaufolgen, der Dominanz der bifaziellen Technologie und der Rohmaterialienökonomie. Die Schichten dazwischengelegten LBG und der jüngere Abschnitt von BS, obwohl die technologischen Daten vorläufig sind, haben keine bifazielle Komponente und weisen eine insgesamt geringe Bedeutung von Spitzenformen auf. Auf der Ebene der Fundstelle können daher die C-A-Schichten und die SB-Ablagerungen nicht zusammengefasst werden.

Der Vergleich erstens mit dem SB als Hauptmanifestation der bifaziellen Technologien im MSA und dann weiteren bifaziellen Expressionen aus MIS 5, einschließlich des Pre-SB type ‚Lynn‘ aus DRS, der unteren Besiedlungsschicht T von Apollo 11 (AP11) und des Pietersburg-Technokomplexes, hebt die Besonderheit der C-A-Schichten hervor und veranschaulicht die Vielfalt des bifaziellen Phänomens. Die bifaziellen Technologien scheinen räumlich variabel und zeitlich unterschiedlich aufzutreten und nicht mit einem einzigen kurzlebigen Technokomplex assoziiert zu sein (siehe Porraz, et al., 2013; Conard, et al., 2014, Conard und Porraz, 2015;

Soriano, et al., 2015; Rots, et al., 2017). Die zunehmende Datenlage an archäologischen Beweisen zeigt, dass die bifazielle Komponente in verschiedenen Regionen zu unterschiedlichen Zeiten auftaucht und wieder verschwindet. Die Werkzeugmacher des MSA scheinen die Herstellung von bifaziellen Stücken in einer Vielzahl von Kontexten, die Konvergenz implizieren, d.h. wiederholte Innovation analoger Merkmale in mehreren Kulturen, in der Steintechnologie unabhängig voneinander, erfunden zu haben (siehe Will und Conard, 2018). Da die C-A-Schichten und die SB-Inventare, abgesehen vom Vorhandensein der bifaziellen Komponente, nur wenige gemeinsame Eigenschaften aufweisen, plädiere ich dafür, dass sie nicht unter demselben Etikett zusammengeführt werden sollten.

UMH, das als eine lokalisierte Variante des SB interpretiert wird, hat zahlreiche Charakteristika, wie z.B. das frühe Auftauchen von *serrated pieces*, mit den C-A-Schichten von Sibudu gemein und daher scheinen die beiden Inventare zur gleichen technologischen Tradition zu gehören.

Der umfassende vergleichende Überblick über die weiteren MSA-Kontexte in MIS 5 verdeutlicht markante Unterschiede in Bezug auf die Werkzeugzurichtung, das Spektrum der Werkzeugtypen und die Organisation der Abbaustrategien, zeigt jedoch auf, dass sich in diesem Zeitraum ein allgemeiner Trend zur Herstellung von Klingen immer weiter ausbreitet. Die Bevölkerungsgruppen von damals, die synchron in verschiedenen Regionen des südlichen Afrikas lebten und dieselben kognitiven Kompetenzen besaßen, zielten scheinbar auf ähnliche technologische Ziele ab. Sie teilten die laminaren Abbausequenzen als gemeinsames kognitives Projekt, das in verschiedene konzeptionelle Schemata übersetzt wurde, die durch verschiedene operative Schemata realisiert wurden (siehe Inizan et al, 1999; Soressi und Geneste, 2011). Folglich stellt das MSA aus MIS 5 offenbar einen Zeitraum dar, der mit einer Diversifizierung der innovativen Klingentechnologien zusammenfällt, die mit der Ausprägung regionaler kultureller Traditionen zusammenhängt (siehe Clark 1988). Die C-A-Schichten unterstreichen ebenso dieses Auftreten von Klingentechnologien als Innovation innerhalb des MIS 5, spiegeln aber auch die Vielfalt und das Aufkommen anderer Neuerungen wider, wie z.B. *serrated pieces* durch Druckkerbung.

Das Inventar der C-A-Schichten zeigt deutlich positive Schlüsselemente und unterscheidet sich deutlich von Industrien mit bifazieller Komponente, vor allem dem SB, und anderen Technokomplexen des MIS 5, wie MSA I und MSA II. Die Daten lassen sich so auslegen, dass ich einen neuen technokulturellen Begriff ‚iLembian‘ für die C-A-Schichten vorschlage. Der Name bezieht sich auf den Distrikt iLembe, in welchem sich Sibudu befindet. Meiner Meinung nach

trägt die Verwendung des Begriffs ‚iLembian‘ dazu bei, einen chrono-kulturellen Rahmen zur besseren Kommunikation und zum besseren Verständnis von Verhaltensänderungen und kultureller Evolution in einem Zeitraum und einer Region, in der bisher wenig Forschung betrieben wurde, zu schaffen. Generell betone ich die Feststellung, dass die Klingentechnologie, die Anwendung der Drucktechnik und die Herstellung von *serrated pieces*, die als Geschosse eingesetzt wurden, zu zentralen Innovationen gehören, die dazu beitragen, die kulturelle Dynamik im südlichen Afrika während des MIS 5 zu charakterisieren.

## 10. Bibliography

- Adler, D.S., 2002. Late Middle Palaeolithic Patterns of Lithic Reduction, Mobility, and Land Use in the Southern Caucasus, Unpublished PhD thesis, Harvard University, Cambridge.
- Akerman, K., Bindon, P., 1995. Dentate and related stone biface points from Northern Australia, *The Beagle Records of the Museums and Art Galleries of the Northern Territory* 12, 89-99.
- Akerman, K., Fullagar, R., van Gijn, A., 2002. Weapons and wunan: production, function and exchange of Kimberley points, *Australian Aboriginal Studies* 2002, 13-42.
- Allott, L.F., 2006. Archaeological charcoal as a window on palaeovegetation and wood-use during the Middle Stone Age at Sibudu Cave, *Southern African Humanities* 18, 173-201.
- Andreasson, H., 2010. The Forgotten Cave and the Still Bay - A Technological Lithic Analysis of the Middle Stone Age Layers from Peers Cave, South Africa, Unpublished Master's thesis, University of Oslo, Oslo.
- Andrefsky, W.J., 1994. Raw-material availability and the organization of technology, *American Antiquity* 59, 21-34.
- Andrefsky, W.J., 2005. *Lithics: Macroscopic Approaches to Analysis*, Cambridge University Press, Cambridge.
- Andrefsky, W.J., 2006. Experimental and archaeological verification of an index of retouch for hafted bifaces, *American Antiquity* 71, 743-757.
- Anthony, B.W., 1972. The Stillbay Question, in: Hugot, H.J. (Ed.), *Actes du VIe Congrès panafricain de préhistoire*, Dakar, 1967, Les Imprimeries Réunies de Chambéry, Chambéry, pp. 80-82.
- Archer, W., Gunz, P., van Niekerk, K.L., Henshilwood, C.S., McPherron, S.P., 2015. Diachronic Change within the Still Bay at Blombos Cave, South Africa, *PLoS ONE* 10, e0132428.
- Archer, W., Pop, C.M., Gunz, P., McPherron, S.P., 2016. What is Still Bay? Human biogeography and bifacial point variability, *Journal of Human Evolution* 97, 58-72.
- Armstrong, A.L., 1931a. The Antiquity of Man in Rhodesia as Demonstrated by Stone Implements of the Ancient Zambezi Gravels, South of Victoria Falls, *The Journal of the Royal Anthropological Institute of Great Britain and Ireland* 66, 331-348.
- Armstrong, A.L., 1931b. Rhodesian Archæological Expedition (1929): Excavations in Bambata Cave and Researches on Prehistoric Sites in Southern Rhodesia, *The Journal of the Royal Anthropological Institute of Great Britain and Ireland* 61, 239-276.
- Assefa, Z., Lam, Y.M., Mienis, H.K., 2008. Symbolic Use of Terrestrial Gastropod Opercula during the Middle Stone Age at Porc-Epic Cave, Ethiopia, *Current Anthropology* 49, 746-756.
- Aubert, M., Pike, A.W.G., Stringer, C.B., Bartsiokas, A., Kinsley, L., Eggins, S., Day, M.H., Grün, R., 2012. Confirmation of a late Middle Pleistocene age for the Omo Kibish 1 cranium by direct uranium-series dating, *Journal of Human Evolution* 63, 704-710.
- Auffermann, B., Burkert, W., Hahn, J., Pasda, C., Simon, U., 1990. Ein Merkmalsystem zur Auswertung von Steinartefaktinventaren, *Archäologisches Korrespondenzblatt* 20, 259-270.
- Avery, G., Halkett, D.J., Orton, J., Steele, T., Tusenius, M., Klein, R.G., 2008. The Ysterfontein 1 Middle Stone Age Rock Shelter and the evolution of coastal foraging, *South African Archaeological Society Goodwin Series* 10, 66-89.

- Backwell, L., Bradfield, J., Carlson, K.J., Jashashvili, T., Wadley, L., d'Errico, F., 2018a. The antiquity of bow-and-arrow technology: evidence from Middle Stone Age layers at Sibudu Cave, *Antiquity*, 289-303.
- Backwell, L., d'Errico, F., 2016. Chapter 2. Osseous projectile weaponry from Early to Late Middle Stone Age Africa, in: Langley, M.C. (Ed.), *Osseous Projectile Weaponry*, Springer, Dordrecht, pp. 15-29.
- Backwell, L., d'Errico, F., Wadley, L., 2008. Middle Stone Age bone tools from the Howieson's Poort layers, Sibudu Cave, South Africa, *Journal of Archaeological Science* 35, 1566-1580.
- Bader, G.D., 2018. A return to Umbeli Belli: New insights of recent excavations and implications for the final MSA of eastern South Africa, *Journal of Archaeological Science: Reports* 21, 733-757.
- Bader, G.D., Will, M., 2017. Recent Research on the MSA in KwaZulu-Natal, South Africa, *Mitteilungen der Gesellschaft für Urgeschichte* 26, 53-82.
- Bader, G.D., Will, M., Conard, N.J., 2015. The lithic technology of Holley Shelter, KwaZulu-Natal, and its place within the MSA of southern Africa, *South African Archaeological Bulletin* 70, 149-165.
- Bamforth, D.B., 1986. Technological efficiency and tool curation, *American Antiquity* 51, 38-50.
- Barham, L.S., 2000. *The Middle Stone Age of Zambia, South Central Africa*, Western Academic and Specialist Press, Bristol.
- Barham, L.S., 2002. Backed tools in the Middle Pleistocene Central Africa and their evolutionary significance, *Journal of Human Evolution* 43, 585-603.
- Barham, L.S., 2012. Clarifying some fundamental errors in Herries' (2011) "A chronological perspective on the Acheulian and its transition to the Middle Stone Age in southern Africa: The question of the Fauresmith", *International Journal of Evolutionary Biology* 2012, 1-5.
- Barham, L.S., Mitchell, P.J., 2008. *The First Africans: African Archaeology from the Earliest Tool Makers to Most Recent Foragers*, Cambridge University Press, Cambridge.
- Barham, L.S., Tooth, S., Duller, G.A.T., Plater, A.J., Turner, S., 2015. Excavations at site C North, Kalambo Falls, Zambia: New insights into the Mode 2/3 transition in south-central Africa, *Journal of African Archaeology* 13, 187-214.
- Bar-Yosef, O., 1998. On the nature of transitions: the Middle to Upper Paleolithic and Neolithic Revolution, *Cambridge Archaeological Journal* 8, 141-163.
- Beaumont, P., 1990a. Pniel 1, McGregor Museum, Kimberley.
- Beaumont, P., 1990b. Pniel 6, McGregor Museum, Kimberley.
- Beaumont, P., 1990c. Roidam 1 & 2 and Biesiesput, McGregor Museum, Kimberley.
- Beaumont, P., 1990d. Nooitgedacht 2 and Roseberry Plain 1, McGregor Museum, Kimberley.
- Beaumont, P., McNabb, J., 2000. Canteen Koppie - the recent excavations, *The Digging Stick* 17, 3-7.
- Beaumont, P.B., 1978. *Border Cave*, Unpublished Master's thesis, University of Cape Town, Cape Town.
- Beaumont, P.B., de Villiers, H., Vogel, J.C., 1978. Modern man in sub-Saharan Africa prior to 49 000 years B.P.: a review and evaluation with particular reference to Border Cave, South

- African Journal of Science 74, 409-419.
- Becher, J., 2016. Die organischen Artefakte von Sibudu, Südafrika, Unpublished Bachelor's thesis, Eberhard Karls Universität Tübingen, Tübingen.
- Bertouille, H., 1989. Theories Physiques et Mathématiques de la Taille des Outils Préhistoriques, Cahiers du Quaternaire 15, 1-100.
- Bews, J.W., 1920. The plant ecology of the coast belt of Natal, Annales Natal Museum 4, 367-467.
- Biberson, P., 1956. Le gisement de l' « Atlanthrope » de Sidi Abderrahmane (Casablanca), Bulletin d'Archéologie Marocaine 1, 39-92.
- Binford, L.R., 1980. Willow smoke and dogs' tails: hunter-gatherer settlement systems and archaeological site formation, American Antiquity 45, 4-20.
- Binford, L.R., 1986. An Alyawara day: Making men's knives and beyond, American Antiquity 51, 547-562.
- Bintanja, R., van de Wal, R.S.W., Oerlemans, J., 2005. Modelled atmospheric temperatures and global sea levels over the past million years, Nature 437, 125-128.
- Bishop, W.W., Clark, J.D., 1966. Systematic investigation of the African later Tertiary and Quaternary, Current Anthropology 7, 253-256.
- Bishop, W.W., Clark, J.D., 1967. Background to Evolution in Africa, Chicago University Press, Chicago.
- Blegen, N., 2017. The earliest long-distance obsidian transport: Evidence from the ~200 ka Middle Stone Age Sibilo School Road Site, Baringo, Kenya, Journal of Human Evolution 103, 1-19.
- Boëda, É., 1991. Approche de la variabilité des systèmes de production lithique des industries du Paléolithique inférieur et moyen: chronique d'une variabilité attendue, Culture et technique 17-18, 37-79.
- Boëda, É., 1994. Le concept Levallois: variabilité des méthodes, Édition du CNRS, Paris.
- Boëda, É., 1997. Technogenèse de systèmes de production lithique au Paléolithique inférieur et moyen en Europe occidentale et au Proche-Orient, Habilitation, Université Paris Ouest Nanterre La Défense, Nanterre.
- Boëda, É., 2001. Détermination des unités techno-fonctionnelles de pièces bifaciales provenant de la couche acheuléenne C'3 base du site de Barbis I., in: Cliquet, D., Otte, M. (Eds.), Les industries à outils bifaciaux du Paléolithique moyen d'Europe occidentale, ERAUL, Liège, pp. 51-75.
- Boëda, É., 2013. Techno-logique & technologie: une paléo-histoire des objets lithiques tranchants, @rchéo-éditions, Paris.
- Boëda, É., Geneste, J.-M., Meignen, L., 1990. Identification de chaînes opératoires lithiques du Paléolithique ancien et moyen, Paléo 2, 43-80.
- Boëda, É., Hou, Y.M., Forestier, H., Sarel, J., Wang, H.M., 2013. Levallois and non-Levallois blade production at Shuidonggou in Ningxia, North China, Quaternary International 295, 191-203.
- Boëda, É., Richter, J., 1995. Steinartefakt-Produktionssequenzen im Micoquien der Kulna-Höhle, Quartär 45, 75-98.

- Bonilauri, S., 2010. Les outils du Paléolithique moyen: une mémoire technique oubliée? Approche techno-fonctionnelle appliquée à un assemblage lithique de conception Levallois provenant du site d'Umm el Tlel (Syrie centrale), Unpublished PhD thesis, Université Paris Ouest Nanterre La Défense, Nanterre.
- Botha, G.A., 1996. The geology and palaeopedology of Late Quaternary colluvial sediments in northern KwaZulu-Natal/Natal, Council for Geoscience Memoires 83, 1-165.
- Botha, G.A., Partridge, T.C., 2000. Colluvial deposits, in: Partridge, T.C., Maud, R.R. (Eds.), *The Cenozoic of Southern Africa*, Oxford University Press, New York, pp. 88-99.
- Botha, G.A., Scott, L., Vogel, J.C., von Brunn, V., 1992. Palaeosols and palaeoenvironments during the Late Pleistocene Hypothermal in northern Natal, *South African Journal of Science* 88, 508-512.
- Botha, G.A., Temme, A.J.A.M., Singh, R.G., 2016. Colluvial deposits and slope instability, in: Knight, J., Grab, S.W. (Eds.), *Quaternary Environmental Change in Southern Africa: Physical and Human Dimensions*, Cambridge University Press, Cambridge.
- Bourguignon, L., 1997. Le Moustérien de type Quina: nouvelle définition d'une entité technique, Unpublished PhD thesis, Université Paris Ouest Nanterre La Défense, Nanterre.
- Bouzouggar, A., Barton, N., Vanhaeren, M., d'Errico, F., Collcutt, S., Higham, T., Hodge, E., Parfitt, S., Rhodes, E., Schwenninger, J.-L., Stringer, C., Turner, E., Ward, S., Moutmir, A., Stambouli, A., 2007. 82,000-year-old shell beads from North Africa and implications for the origins of modern human behavior, *Proceedings of the National Academy of Sciences* 104, 9964-9969.
- Bouzouggar, A., Humphrey, L.T., Barton, N., Parfitt, S.A., Balzan, L.C., Schwenninger, J.-L., El Hajraoui, M.A., Nespoulet, R., Bello, S.M., 2018. 90,000 year-old specialised bone technology in the Aterian Middle Stone Age of North Africa, *PLoS ONE* 13, e0202021.
- Bräuer, G., 1984. The 'Afro-European Sapiens Hypothesis' and Hominid Evolution in East Asia during the Late Middle and Upper Pleistocene, *Cour. Forsch.-Inst. Senckenberg* 69, 145-156.
- Bräuer, G., 1992. Africa's Place in the Evolution of *Homo sapiens*, in: Bräuer, G., Smith, F.H. (Eds.), *Continuity or Replacement - Controversies in Homo Sapiens Evolution*, A. A. Balkem, Rotterdam, pp. 83-98.
- Breuil, H., 1944. Le Paléolithique au Congo Belge d'après les recherches de Docteur Cabu, *Transactions of the Royal Society of South Africa* 30, 143-174.
- Brew, J.O., 1946. The use and abuse of taxonomy, *The archaeology of Alkali Ridge Utah. Papers of the Peabody Museum of Archaeology and Ethnology* 21, 44-66.
- Brooks, A.S., Helgren, D.M., Cramer, J.S., Franklin, A., Hornyak, W., Keating, J.M., Klein, R.G., Rink, W.J., Schwarcz, H., Leith Smith, J.N., Stewart, K., Todd, N.E., Verniers, J., Yellen, J.E., 1995. Dating and context of three Middle Stone Age sites with bone points in the Upper Semliki Valley, Zaire, *Science* 268, 548-553.
- Brooks, A.S., Yellen, J.E., Potts, R., Behrensmeier, A.K., Deino, A.L., Leslie, D.E., Ambrose, S.H., Ferguson, J.R., d'Errico, F., Zipkin, A.M., Whittaker, S., Post, J., Veatch, E.G., Foecke, K., Clark, J.B., 2018. Long-distance stone transport and pigment use in the earliest Middle Stone Age, *Science* 360, 90-94.
- Brown, F.H., McDougall, I., Fleagle, J.G., 2012. Correlation of the KHS Tuff of the Kibish Formation to volcanic ash layers at other sites, and the age of early *Homo sapiens* (Omo I

- and Omo II), *Journal of Human Evolution* 63, 577-585.
- Brown, K.S., Marean, C.W., Herries, A.I.R., Jacobs, Z., Tribolo, C., Braun, D.R., Roberts, D.L., Meyer, M.C., Bernatchez, J., 2009. Fire as an engineering tool of early modern humans, *Science* 325, 859-862.
- Bruch, A.A., Sievers, C., Wadley, L., 2012. Quantification of climate and vegetation from southern African Middle Stone Age sites e an application using Late Pleistocene plant material from Sibudu, South Africa, *Quaternary Science Reviews* 45, 7-17.
- Cain, C.R., 2004. Notched, flaked and ground bone artefacts from Middle Stone Age and Iron Age layers of Sibudu Cave, KwaZulu-Natal, South Africa, *South African Journal of Science* 100, 195-197.
- Cain, C.R., 2006. Human activity suggested by the taphonomy of 60ka and 50ka faunal remains from Sibudu Cave, *Southern African Humanities* 18, 241-260.
- Cairncross, B., 2004. Field guide to rocks & minerals of Southern Africa, Struik, Cape Town.
- Callahan, E., 1979. The Basics of Biface Knapping: A Manual for Flint Knappers and Lithic Analysis, *Archaeology of Eastern North America* 7, 1-179.
- Callahan, E., 1985 (revised 1989). *Flintknapping Flashcards: Pressure Flaking off Flakes*, Piltown Productions, Lynchburg VA.
- Campmas, E., Amani, F., Morala, A., Debenath, A., El Hajraoui, M.A., Nespoulet, R., 2016. Initial insights into Aterian hunter-gatherer settlements on coastal landscapes: The example of Unit 8 of El Mnasra Cave (Témara, Morocco), *Quaternary International* 413, 5-20.
- Cann, R.L., Stoneking, M., Wilson, A.C., 1987. Mitochondrial DNA and human evolution, *Nature* 325, 31-36.
- Carr, A.S., Bateman, M.D., Roberts, D.L., Murray-Wallace, C.V., Jacobs, Z., Holmes, P.J., 2010. The Last interglacial sea-level high stand on the southern Cape coastline of South Africa, *Quaternary Research* 73, 351-363.
- Chase, B.M., 2010. South African palaeoenvironments during marine oxygen isotope stage 4: a context for the Howiesons Poort and Still Bay industries, *Journal of Archaeological Science* 37, 1359-1366.
- Chase, B.M., Meadows, M.E., 2007. Late Quaternary dynamics of southern Africa's winter rainfall zone, *Earth-Science Reviews* 84, 103-138.
- Chazan, M., 2015. The Fauresmith and archaeological systematics, in: Runge, J. (Ed.), *Changing Climates, Ecosystems and Environments within Arid Southern Africa and Adjoining Regions*, *Palaeoecology of Africa* 33, CRC Press/Balkema, Leiden, pp. 59-70.
- Chazan, M., Horwitz, L.K., 2009. Milestones in the development of symbolic behaviour: a case study from Wonderwerk Cave, South Africa, *World Archaeology* 41, 521-539.
- Chazan, M., Horwitz, L.K., 2015. An Overview of Recent Research at Wonderwerk Cave, South Africa, *Proceedings of the 2010 joint meeting of the Panafrican Archaeological Congress and the Society of Africanist Archaeologists*, Dakar, pp. 2-4.
- Chazan, M., Wilkins, J., Morris, D., Berna, F., 2012. Bestwood 1: a newly discovered Earlier Stone Age living surface near Kathu, Northern Cape Province, South Africa, *Antiquity* 86, 1-8.
- Chevrier, B., 2012. Les assemblages à pièces bifaciales au Pléistocène inférieur et moyen ancien en Afrique de l'Est et au Proche-Orient: : nouvelle approche du phénomène bifacial



- appliquée aux problématiques de migrations, de diffusion et d'évolution locale, Unpublished PhD thesis, Université Paris Ouest Nanterre La Défense, Nanterre.
- Chevrier, B., Huysecom, É., Soriano, S., Rasse, M., Lespez, L., Lebrun, B., Tribolo, C., 2018. Between continuity and discontinuity: An overview of the West African Paleolithic over the last 200,000 years, *Quaternary International* 466, 3-22.
- Chimusa, E.R., Defo, J., Thami, P.K., Awany, D., Mulisa, D.D., Allali, I., Ghaza, H., Moussa, A., Mazandu, G.K., 2018. Dating admixture events is unsolved problem in multi-way admixed populations, *Briefings in Bioinformatics* 00, 1-12.
- Clark, J.D., 1959. *The Prehistory of Southern Africa*, Penguin Books, Harmondsworth.
- Clark, J.D., 1970. *The Prehistory of Africa*, Praeger, New York.
- Clark, J.D., 1982. *The Cambridge History of Africa*, Cambridge University Press, Cambridge.
- Clark, J.D., 1988. The Middle Stone Age of East Africa and the beginnings of regional identity, *Journal of World Prehistory* 2, 235-305.
- Clark, J.D., 2001. Kalambo Falls prehistoric site. Volume III, the earlier cultures: Middle and Earlier Stone Age, Cambridge University Press, Cambridge.
- Clark, J.D., Beyene, Y., Wolde, G., Hart, W.K., Renne, P., Gilbert, H., Defleur, A., Suwa, G., Katoh, S., Ludwig, K.R., Boisserie, J.R., Asfaw, B., White, T.D., 2003. Stratigraphic, chronological and behavioural contexts of Pleistocene Homo sapiens from Middle Awash, Ethiopia, *Nature* 423, 747-752.
- Clark, J.D., Brown, K.S., 2001. The Twin Rivers Kopje, Zambia: Stratigraphy, fauna, and artefact assemblages from the 1954 and 1956 excavations, *Journal of Archaeological Science* 28, 305-330.
- Clark, J.D., Cole, G.H., Isaac, G.L., Kleindienst, M.R., 1966. Precision and definition in African archaeology, *South African Archaeological Bulletin* 21, 114-121.
- Clark, J.L., 2009. Testing models on the emergence and nature of modern human behaviour: Middle Stone Age fauna from Sibudu Cave (South Africa), Unpublished PhD thesis, Ann Arbor University of Michigan, Ann Arbor.
- Clark, J.L., 2011. The evolution of human culture during the later Pleistocene: Using fauna to test models on the emergence and nature of "modern" human behavior, *Journal of Anthropological Archaeology* 30, 273-291.
- Clark, J.L., 2013. Exploring the relationship between climate change and the decline of the Howieson's Poort at Sibudu Cave (South Africa), in: Clark, J.L., Speth, J.D. (Eds.), *Zooarchaeology and Modern Human Origins: Human Hunting Behavior during the Later Pleistocene*, Springer, Dordrecht, pp. 9-18.
- Clark, J.L., 2017. The Howieson's Poort fauna from Sibudu Cave: Documenting continuity and change within Middle Stone Age industries, *Journal of Human Evolution* 107, 49-70.
- Clark, J.L., Plug, I., 2008. Animal exploitation strategies during the South African Middle Stone Age: Howieson's Poort and post Howieson's Poort fauna from Sibudu Cave, *Journal of Human Evolution* 54, 886-898.
- Clarke, B.M., Schoeman, P., Kota, M.W., 2007. *The geology of the Verulam area*, Council for Geoscience, Pretoria.
- Clarke, M.L., Vogel, J.C., Botha, G.A., Wintle, A.G., 2003. Late Quaternary hillslope evolution

- recorded in eastern South African colluvial badlands, *Palaeogeography, Palaeoclimatology, Palaeoecology* 197, 199-212.
- Clarkson, C., 2002a. An index of invasiveness for the measurement of unifacial and bifacial retouch: a theoretical, experimental and archaeological verification, *Journal of Archaeological Science* 29, 65-75.
- Clarkson, C., 2002b. Holocene scraper reduction, technological organization and landuse at Ingaladdi Rockshelter, Northern Australia, *Archaeology in Oceania* 37, 79-86.
- Cochrane, G.W.G., 2006. An analysis of lithic artefacts from the ~60 ka layers of Sibudu Cave, *Southern African Humanities* 18, 69-88.
- Cochrane, G.W.G., 2008. The transition from Howieson's Poort to post-Howieson's Poort industries in southern Africa, *South African Archaeological Society Goodwin Series* 10, 157-167.
- Collins, M.B., 1975. Lithic Technology as a Mean of Processual Inference, in: Swanson, E. (Ed.), *Lithic Technology, Making and Using Stone Tools*, Mouton publishers, Chicago, pp. 15-34.
- Compton, J.S., 2011. Pleistocene sea-level fluctuations and human evolution on the southern coastal plain of South Africa, *Quaternary Science Reviews* 30, 506-527.
- Compton, J.S., Wiltshire, J.G., 2009. Terrigenous sediment export from the western margin of South Africa on glacial/interglacial cycles, *Marine Geology* 266, 212-222.
- Conard, N.J., 2004. Die Entstehung der kulturellen Modernität, in: Conard, N.J. (Ed.), *Woher kommt der Mensch?*, Attempto Verlag, Tübingen, pp. 188-218.
- Conard, N.J., 2005. An overview of the patterns of behavioural change in Africa and Eurasia, in: d'Errico, F., Blackwell, L. (Eds.), *From Tools to Symbols: from Early Hominids to Modern Humans*, Witwatersrand University Press, Johannesburg, pp. 294-332.
- Conard, N.J., 2007. Cultural Evolution in Africa and Eurasia During the Middle and Late Pleistocene, in: Henke, W., Tattersall, I. (Eds.), *Handbook of paleoanthropology*, Springer, Berlin, Heidelberg, New York, pp. 2001-2037.
- Conard, N.J., 2008. A critical view of the evidence for a southern African origin of behavioral modernity, *South African Archaeological Society Goodwin Series* 10, 175-179.
- Conard, N.J., 2010. Cultural modernity: Consensus or conundrum?, *Proceedings of the National Academy of Sciences* 107, 7621-7622.
- Conard, N.J., 2012. World Heritage and the Middle Stone Age: examples from East Africa and South Africa, *World Heritage papers* 33, 18-29.
- Conard, N.J., 2013. The 2013 Excavation of the University of Tübingen in MSA deposits at Sibudu Rockshelter, KwaZulu-Natal, Excavation Report on file at the KwaZulu-Natal Museum, Pietermaritzburg.
- Conard, N.J., 2014. The 2014 Excavation of the University of Tübingen in MSA deposits at Sibudu Rockshelter, KwaZulu-Natal, Excavation Report on file at the KwaZulu-Natal Museum, Pietermaritzburg.
- Conard, N.J., 2015. The 2015 Excavation of the University of Tübingen in MSA deposits at Sibudu Rockshelter, KwaZulu-Natal, Excavation Report on file at the KwaZulu-Natal Museum, Pietermaritzburg.
- Conard, N.J., 2016. The 2016 Excavation of the University of Tübingen in MSA deposits at Sibudu

- Rockshelter and the LSA and MSA layers of Umbeli Belli Rockshelter, KwaZulu-Natal, Excavation Report on file at the KwaZulu-Natal Museum, Pietermaritzburg.
- Conard, N.J., Adler, D.S., 1997. Lithic Reduction and Hominid Behavior in the Middle Paleolithic of the Rhineland, *Journal of Anthropological Research* 53, 147-175.
- Conard, N.J., Bader, G.D., Schmid, V.C., Will, M., 2014. Bringing the Middle Stone Age into Clearer Focus, *Mitteilungen der Gesellschaft für Urgeschichte* 23, 121-128.
- Conard, N.J., Porraz, G., 2015. Revising models for the cultural stratigraphic sequence of the Middle Stone Age, *South African Archaeological Bulletin* 70, 124-130.
- Conard, N.J., Porraz, G., Wadley, L., 2012. What is in a name? Characterizing the 'post-Howieson's Poort' at Sibudu, *South African Archaeological Bulletin* 67, 180-199.
- Conard, N.J., Soressi, M., Parkington, J.E., Wurz, S., Yates, R., 2004. A unified lithic taxonomy based on patterns of core reduction, *South African Archaeological Bulletin* 59, 13-17.
- Conard, N.J., Will, M., 2015. Examining the Causes and Consequences of Short-Term Behavioral Change during the Middle Stone Age at Sibudu, South Africa, *PLoS ONE* 10, e0130001.
- Cooke, C.K., 1971. Excavation in Zombepata Cave, Sipolilo District, Mashonaland, Rhodesia, *South African Archaeological Bulletin* 26, 104-127.
- Cotterell, B., Kamminga, J., 1979. The Mechanics of Flaking, in: Hayden, B. (Ed.), *Lithic Use-Wear Analysis*, Academic Press, New York, pp. 97-112.
- Cotterell, B., Kamminga, J., 1987. The Formation of Flakes, *American Antiquity* 52, 675-708.
- Cotterell, B., Kamminga, J., 1990. *Mechanics of Pre-Industrial Technology*, Cambridge University Press, Cambridge.
- Cotterell, B., Kamminga, J., Dickson, F.P., 1985. The essential mechanics of conchoidal flaking, *International Journal of Fracture* 29, 205-221.
- Crabtree, D.E., 1972. An Introduction to Flintworking, *Occasional Papers of the Idaho State Museum*, Pocatello.
- Crabtree, D.E., 1973. Experiments in replicating Hohokam points, *TEBIWA - The Journal of the Idaho State University Museum* 16, 10-45.
- Cresswell, R., 1983. Transferts de techniques et chaînes opératoires, *Techniques et Culture* 2, 143-163.
- Dauvois, M., 1976. *Précis de dessin dynamique et structural des industries lithiques préhistoriques*, Édition du CNRS, Fanlac.
- Day, M.H., 1969. Omo human skeletal remains, *Nature* 222, 1135-1138.
- Day, M.H., Leakey, M.D., Magori, C., 1980. New hominid fossil skull (Lh-18) from the Ngaloba Beds, Laetoli, northern Tanzania, *Nature* 284, 55-56.
- Dayet, L., Texier, P.-J., Daniel, F., Porraz, G., 2013. Ochre resources from the Middle Stone Age sequence of Diepkloof Rock Shelter, Western Cape, South Africa, *Journal of Archaeological Science* 40, 3492-3505.
- de la Peña, P., 2015. Refining Our Understanding of Howiesons Poort Lithic Technology: The Evidence from Grey Rocky Layer in Sibudu Cave (KwaZulu-Natal, South Africa), *PLoS ONE* 10, e0143451.
- de la Peña, P., Taipale, N., Wadley, L., Rots, V., 2018. A techno-functional perspective on quartz

- micro-notches in Sibudu's Howiesons Poort indicates the use of barbs in hunting technology, *Journal of Archaeological Science* 93, 166-195.
- de la Peña, P., Val, A., Stratford, D.J., Colino, F., Esteban, I., Fitchett, J.M., Hodgskiss, T., Matembo, J., Moll, R., 2018. Revisiting Mwulu's Cave: new insights into the Middle Stone Age in the southern African savanna biome, *Archaeological and Anthropological Sciences* 11, 3239-3266.
- de la Peña, P., Wadley, L., 2014a. Quartz Knapping Strategies in the Howiesons Poort at Sibudu (KwaZulu-Natal, South Africa), *PLoS ONE* 9, e101534.
- de la Peña, P., Wadley, L., 2014b. New knapping methods in the Howiesons Poort at Sibudu (KwaZulu- Natal, South Africa), *Quaternary International* 350, 26-42.
- de la Peña, P., Wadley, L., 2017. Technological variability at Sibudu Cave: The end of Howiesons Poort and reduced mobility strategies after 62,000 years ago, *PLoS ONE* 12, e0185845.
- de la Peña, P., Wadley, L., Lombard, M., 2013. Quartz Bifacial Points in the Howiesons Poort of Sibudu, *South African Archaeological Bulletin* 68, 119-136.
- De Loecker, D., Schlanger, N., 2004. Analysing Middle Palaeolithic flint assemblages: the system used for studying the flint artefacts at Maastricht-Belvédère (The Netherlands), in: De Loecker, D. (Ed.), *Beyond the site - The Saalian archaeological record at Maastricht-Belvedere (The Netherlands)*, *Analecta Praehistorica Leidensia*, Leiden, pp. 303-345.
- de Ruiter, D.J., Brophy, J.K., Lewis, P.J., Churchill, S.E., Berger, L.R., 2008. Faunal assemblage composition and paleoenvironment of Plovers Lake, a Middle Stone Age locality in Gauteng Province, South Africa, *Journal of Human Evolution* 55, 1102-1117.
- Deacon, H.J., 2008. The context of the 1967–8 sample of human remains from Cave 1 Klasies River Main Site, *South African Archaeological Society Goodwin Series* 10, 143-149.
- Deacon, H.J., Deacon, J., 1999. *Human Beginnings in South Africa: Uncovering the Secrets of the Stone Age*, David Philip Publishers, Cape Town.
- Deacon, J., 1990. Weaving the fabric of Stone Age research in southern Africa, in: Robertshaw, P. (Ed.), *A history of African archaeology*, James Currey Ltd, Oxford, pp. 39-58.
- Debenath, A., Raynal, J.-P., Texier, J.-P., 1984. Fouilles du Cap Chatelier in *Activités de la mission préhistorique et paléontologique française au Maroc. Années 1981-1982*, *Bulletin d'Archéologie Marocaine* 15, 18-20.
- Deino, A.L., Behrensmeyer, A.K., Brooks, A.S., Yellen, J.E., Sharp, W.D., Potts, R., 2018. Chronology of the Acheulean to Middle Stone Age transition in eastern Africa, *Science* 360, 95-98.
- Delagnes, A., Wadley, L., Villa, P., Lombard, M., 2006. Crystal quartz backed tools from the Howiesons Poort at Sibudu Cave, *Southern African Humanities* 18, 43-56.
- d'Errico, F., 2003. The invisible frontier. A multiple species model for the origin of behavioral modernity, *Evolutionary Anthropology: Issues, News, and Reviews* 12, 188-202.
- d'Errico, F., Backwell, L., 2016. Earliest evidence of personal ornaments associated with burial: The *Conus* shells from Border Cave, *Journal of Human Evolution* 93, 91-108.
- d'Errico, F., Backwell, L., Villa, P., Degano, I., Lucejko, J.J., Bamford, M.K., Higham, T.F.G., Colombini, M.P., Beaumont, P.B., 2012a. Early evidence of San material culture represented by organic artifacts from Border Cave, South Africa, *Proceedings of the National Academy of*

- Sciences of the United States of America 109, 13214–13219.
- d'Errico, F., Backwell, L., Wadley, L., 2012b. Identifying regional traditions in Middle Stone Age bone technology. The case of Sibudu Cave, *Journal of Archaeological Science* 39, 2479-2495.
- d'Errico, F., Henshilwood, C.S., 2007. Additional evidence for bone technology in the southern African Middle Stone Age, *Journal of Human Evolution* 52, 142-163.
- d'Errico, F., Henshilwood, C.S., Lawson, G., Vanhaeren, M., Tillier, A.-M., Soressi, M., Bresson, F., Maureille, B., Nowell, A., Lakarra, J., Backwell, L., Julien, M., 2003. Archaeological evidence for the emergence of language symbolism and music—an alternative multidisciplinary perspective, *Journal of World Prehistory* 17, 1-70.
- d'Errico, F., Henshilwood, C.S., Vanhaeren, M., van Niekerk, K.L., 2005. *Nassarius kraussianus* shell beads from Blombos Cave: evidence for symbolic behaviour in the Middle Stone Age, *Journal of Human Evolution* 48, 3-24.
- d'Errico, F., Henshilwood, C.S., Vanhaeren, M., van Niekerk, K., 2005. *Nassarius kraussianus* shell beads from Blombos cave: evidence for symbolic behaviour in the Middle Stone Age, *Journal of Human Evolution* 48, 3-34.
- d'Errico, F., Moreno-García, R., Rifkin, R.F., 2012b. Technological, elemental and colorimetric analysis of an engraved ochre fragment from the Middle Stone Age levels of Klasies River Cave 1, South Africa, *Journal of Archaeological Science* 39, 942-952.
- d'Errico, F., Vanhaeren, M., Barton, N., Bouzouggar, A., Mienis, H., Richter, D., Hublin, J.-J., McPherron, S.P., Lozouet, P., 2009. Additional evidence on the use of personal ornaments in the Middle Paleolithic of North Africa, *Proceedings of the National Academy of Sciences* 106, 16051-16056.
- d'Errico, F., Vanhaeren, M., Wadley, L., 2008. Possible shell beads from the Middle Stone Age layers of Sibudu Cave, South Africa, *Journal of Archaeological Science* 35, 2675-2685.
- Dibble, H.L., 1987. The Interpretation of Middle Paleolithic Scraper Morphology, *American Antiquity* 52, 109-117.
- Dibble, H.L., 1991. Local raw material exploitation and its effects on assemblage variability, in: Montet-White, A., Holen, S. (Eds.), *Raw Material Economies Among Prehistoric Hunter-Gatherers*, University of Kansas Publications in Anthropology, Lawrence, pp. 33-47.
- Dibble, H.L., Aldeias, V., Jacobs, Z., D.I., O., Rezek, Z., Lin, S.C., Alvarez-Fernández, E., Barshay-Szmidt, C.C., Hallett-Desguez, E., Reed, D., Reed, K., Richter, D., Steele, T.E., Skinner, A., Blackwell, B., Doronicheva, E., El-Hajraoui, M., 2013. On the industrial attributions of the Aterian and Mousterian of the Maghreb, *Journal of Human Evolution* 64, 194-210.
- Dibble, H.L., Bernard, M.C., 1980. A Comparative Study of Basic Edge Angle Measurement Techniques, *American Antiquity* 45, 857-865.
- Dibble, H.L., McPherron, S.P., 1996. A multimedia companion to the Middle Paleolithic site of Combe-Capelle Bas (France), University of Pennsylvania Museum, Philadelphia.
- Dibble, H.L., McPherron, S.P., 2006. The Missing Mousterian, *Current Anthropology* 47, 777-803.
- Dibble, H.L., Pelcin, A.W., 1995. The Effect of Hammer Mass and Velocity on Flake Mass, *Journal of Archaeological Science* 22, 429-439.
- Dibble, H.L., Rezek, Z., 2009. Introducing a new experimental design for controlled studies of

- flake formation: results for exterior platform angle, platform depth, angle of blow, velocity, and force, *Journal of Archaeological Science* 36, 1945-1954.
- Dibble, H.L., Schurmans, U.A., Iovita, R.P., McLaughlin, M.V., 2005. The measurement and interpretation of cortex in lithic assemblages, *American Antiquity* 70, 545-560.
- Dibble, H.L., Whittaker, J.C., 1981. New experimental evidence on the relation between percussion flaking and flake variation, *Journal of Archaeological Science* 8, 283-296.
- Dies, K., 1975. Physikalische Betrachtungen an einem Pseudo-Geröllartefakt, *Quartär* 26, 147-157.
- Douze, K., 2012. Le Early Middle Stone Age d'Éthiopie et les changements techno-économiques à la période de l'émergence des premiers *Homo sapiens*, Unpublished PhD thesis, Université de Bordeaux I, Bordeaux.
- Douze, K., Delagnes, A., 2016. The pattern of emergence of a Middle Stone Age tradition at Gademotta and Kulkuletti (Ethiopia) through convergent tool and point technologies, *Journal of Human Evolution* 91, 93-121.
- Douze, K., Delagnes, A., Wurz, S., 2018. The Howiesons Poort lithic sequence of Klipdrift Shelter, southern Cape, South Africa, *PLoS ONE* 13, e0206238.
- Douze, K., Wurz, S., Henshilwood, C.S., 2015. Techno-cultural characterization of the MIS 5 (c. 105–90 Ka) lithic industries at Blombos Cave, Southern Cape, South Africa, *PLoS ONE* 10, e0142151.
- Dreyer, T.F., 1935. A human skull from Florisbad, Orange Free State, with a note on the endocranial cast, by C. U. Ariens Kappers, *Proceedings of the Academy of Science of Amsterdam* 38, 3-12.
- Duller, G.A.T., Tooth, S., Barham, L.S., Tsukamoto, S., 2015. New investigations at Kalambo Falls, Zambia: Luminescence chronology, site formation, and archaeological significance, *Journal of Human Evolution* 85, 111-125.
- Dusseldorp, G.L., Lombard, M., Wurz, S., 2013. Pleistocene Homo and the updated Stone Age sequence of South Africa, *South African Journal of Science* 109, 46-52.
- Ecker, M., Morris, D., 2017. Excavating the fossil-bearing strata of the lower Vaal River, South Africa: First results from Pniel 6, ESHE, PESHE, Leiden, p. 61.
- El Hajraoui, M.A., 1994. L'industrie osseuse atérienne de la grotte d'El Mnasra (région de Témara, Maroc), *Préhistoire Anthropologie Méditerranéennes* 3, 91-94.
- El Hajraoui, M.A., Debenath, A., 2012. Partie 3-Grotte d'El Mnasra: Chapitre XXIV. L'industrie osseuse, in: El Hajraoui, M.A., Nespoulet, R., Debenath, A., Dibble, H.L. (Eds.), *La Préhistoire de la Région de Rabat-Témara, Villes et Sites d'Archéologie Marocaine*, Royaume du Maroc, Ministère de la Culture, Institut National des Sciences de l'Archéologie et du Patrimoine, Rabat, pp. 179-188.
- Evans, U., 1993. Hollow Rock Shelter (or Sevilla 48): Lithic Analysis a small but significant contribution to future MSA studies, Unpublished Master's thesis, University of Cape Town, Cape Town.
- Evans, U., 1994. Hollow Rock Shelter, a Middle Stone Age site in the Cederberg, *Southern African Field Archaeology* 3, 63-73.
- Feathers, J.K., 2002. Luminescence dating in less than ideal conditions: case studies from Klasies

- River main site and Duinefontein, South Africa, *Journal of Archaeological Science* 29, 177-194.
- Feathers, J.K., 2015. Luminescence dating at Diepkloof Rock Shelter e new dates from single-grain quartz, *Journal of Archaeological Science* 63, 164-174.
- Finch, J.M., Hill, T.R., 2008. A late Quaternary pollen sequence from Mfabeni Peatland, South Africa: Reconstructing forest history in Maputaland, *Quaternary Research* 70, 442-450.
- Frick, J.A., Herkert, K., Hoyer, C.T., Floss, H., 2018. Keilmesser with tranchet blow from Grotte de la Verpillière I (Germolles, Saône-et-Loire, France), in: Valde-Nowak, P., Sobczyk, K., Nowak, M., Żrałka, J. (Eds.), *Multas per gentes et multa per saecula*, Jagiellonian University, Kraków, pp. 25-36.
- Frison, G.C., 1968. A functional analysis of certain chipped stone tools, *American Antiquity* 33, 149-155.
- Galbraith, R.F., 2015. On the mis-use of mathematics: A comment on “How confident are we about the chronology of the transition between Howieson's Poort and Still Bay?” by Guérin et al. (2013), *Journal of Human Evolution* 80, 184-186.
- Geneste, J.-M., 1985. Analyse lithique d’industries moustériennes du Périgord: approche technologique du comportement des groupes humains au Paléolithique moyen, Unpublished PhD thesis, Université de Bordeaux I, Bordeaux.
- Geneste, J.-M., 1988. Systèmes d’approvisionnement en matières premières au Paléolithique moyen et supérieur en Aquitaine, in: Otte, M. (Ed.), *L’Homme de Néandertal 8 : La mutation*, ERAUL, Liège, pp. 61-70.
- Geneste, J.-M., 1991. Systèmes techniques de production lithique: variations techno-économiques dans les processus de réalisation des outillages paléolithiques, *Techniques et Culture* 17-18, 1-35.
- Geneste, J.-M., 1992. L’approvisionnement en matières premières dans les systèmes de production lithique: la dimension spatiale de la technologie, in: Mora, R., Terradas, X., Parpal, A., Plana, C. (Eds.), *Tecnologia y cadenas operativas líticas*, Treballs d’Arqueologia, Universitat Autònoma de Barcelona, Barcelona, pp. 1-36.
- Gibson, N.E., Wadley, L., Williamson, B.S., 2004. Residue analysis of backed tools from the 60,000- to 68,000-year-old Howieson’s Poort layers of Rose Cottage Cave, South Africa, *Southern African Humanities* 16, 1-11.
- Glenny, W., 2006. Report on the micromammal assemblage analysis from Sibudu Cave, *Southern African Humanities* 18, 270-288.
- Goldberg, P., Miller, C.E., Schiegl, S., Ligouis, B., Berna, E., Conard, N.J., Wadley, L., 2009. Bedding, hearths, and site maintenance in the Middle Stone Age of Sibudu Cave, KwaZulu-Natal, South Africa, *Archaeological und Anthropological Sciences* 1, 95-122.
- Goodman, M.E., 1944. The physical properties of stone tool materials, *American Antiquity* 9, 415-433.
- Goodwin, A.J.H., 1928. Sir Langham Dale's collection of stone implements, *South African Journal of Science* 25, 410-418.
- Goodwin, A.J.H., 1949. What to see at the cave, in: Jager, H.S. (Ed.), *Guide to the Peer’s Cave Tunnel Cave and Rock Shelters at Skildergat*, Fish Hoek.

- Goodwin, A.J.H., 1958. Formative years of our prehistoric terminology, *South African Archaeological Bulletin* 13, 25-33.
- Goodwin, A.J.H., van Riet Lowe, C., 1929. *The Stone Age cultures of South Africa*, AMS Press, Edinburgh.
- Gould, R.A., Koster, D.A., Sontz, A.H., 1971. The lithic assemblage of the western desert Aborigines of Australia, *American Antiquity* 36, 149-169.
- Grine, F.E., 2012. Observations on Middle Stone Age human teeth from Klasies River Main Site, South Africa, *Journal of Human Evolution* 63, 750-758.
- Grine, F.E., Klein, R.G., 1993. Late Pleistocene human remains from the Sea Harvest site, Saldanha Bay, South Africa, *South African Journal of Science* 89, 145-152.
- Grine, F.E., Pearson, O.M., Klein, R.G., Rightmire, G.P., 1998. Additional human fossils from Klasies River Mouth, South Africa, *Journal of Human Evolution* 35, 95-107.
- Grine, F.E., Wurz, S., Marean, C.W., 2017. The Middle Stone Age human fossil record from Klasies River Main Site, *Journal of Human Evolution* 103, 53-78.
- Grove, M., Lamb, H., Roberts, H., Davies, S., Marshall, M., Bates, R., Huws, D., 2015. Climatic variability, plasticity, and dispersal: a case study from Lake Tana, Ethiopia, *Journal of Human Evolution* 87, 32-47.
- Grün, R., Beaumont, P., Tobias, P.V., Eggins, S., 2003. On the Age of Border Cave 5 Human Mandible, *Journal of Human Evolution* 45, 155-167.
- Grün, R., Beaumont, P.B., 2001. Border Cave revisited: a revised ESR chronology, *Journal of Human Evolution* 40, 467-482.
- Grün, R., Brink, J.S., Spooner, N.A., Taylor, L., Stringer, C.B., Franciscus, R.G., Murray, A.S., 1996. Direct dating of Florisbad hominid, *Nature* 382, 500-501.
- Guérin, G., Murray, A.S., Jain, M., Thomsen, K.J., Mercier, N., 2013. How confident are we in the chronology of the transition between Howieson's Poort and Still Bay?, *Journal of Human Evolution* 64, 314-317.
- Gunz, P., Bookstein, F.L., Mitteroecker, P., Stadlmayr, A., Seidler, H., Weber, G.W., 2009. Early modern human diversity suggests subdivided population structure and a complex out-of-Africa scenario, *Proceedings of the National Academy of Sciences* 106, 6094-6098.
- Hahn, J., 1977. *Aurignacien: Das ältere Jungpaläolithikum in Mittel- und Osteuropa*, Böhlau, Köln, Wien.
- Hahn, J., 1982. *Der Speckberg bei Meilenhofen, Teil II: Archäologie des Jungpaläolithikums, Kataloge der Prähistorischen Staatssammlung, Lasselben, Kallmünz.*
- Hahn, J., 1988. *Die Geißenklösterle-Höhle im Achtal bei Blaubeuren I. Fundhorizontbildung und Besiedlung im Mittelpaläolithikum und im Aurignacien, Forschungen und Berichte zur Vor- und Frühgeschichte in Baden-Württemberg* 26, Stuttgart.
- Hahn, J., 1991. *Erkennen und Bestimmen von Stein- und Knochenartefakten: Einführung in die Artefaktmorphologie*, Verlag Archaeologica Venatoria, Tübingen.
- Halkett, D.J., Hart, T., Yates, R.J., Volman, T.P., Parkington, J.E., Orton, J., Klein, R.G., Cruz-Uribe, K., Avery, G., 2003. First excavation of intact Middle Stone Age layers at Ysterfontein, Western Cape Province, South Africa: implications for Middle Stone Age ecology, *Journal of Archaeological Science* 30, 955-971.



- Hall, G., Wadley, L., Woodborne, S., 2014. Past environmental proxies from the Middle Stone Age at Sibudu, KwaZulu-Natal, South Africa, *Journal of African Archaeology* 12, 7-24.
- Hall, G., Woodborne, S., Scholes, M., 2008. Stable carbon isotope ratios from archaeological charcoal as palaeoenvironmental indicators, *Chemical Geology* 247, 384-400.
- Hallinan, E., 2013. Stone Age landscape use in the Olifants River Valley, Western Cape, Unpublished Master's Thesis, University of Cape Town, Cape Town.
- Hammer, Ø., Harper, D.A.T., Ryan, P.D., 2001. PAST: Paleontological statistics software package for education and data analysis, *Palaeontologia Electronica* 4, 9.
- Harper, P.T.N., 1997. The Middle Stone Age sequence at Rose Cottage Cave: a search for continuity and discontinuity, *South African Journal of Science* 93, 470-475.
- Haudricourt, G., 1964. La technologie, science humaine, *La Pensée* 115, 28-35.
- Hayden, B., 1979. Palaeolithic reflections. Lithic technology and ethnographic excavation among the Australian Aborigines, Australian Institute of Aboriginal and Torres Strait Island, New Jersey.
- Hendey, Q.B., Volman, T.P., 1986. Last Interglacial Sea Levels and Coastal Caves in the Cape Province, South Africa, *Quaternary Research* 25, 189-198.
- Henshilwood, C.S., 2012. Late Pleistocene Techno-traditions in Southern Africa: A Review of the Still Bay and Howiesons Poort, c. 75–59 ka, *Journal of World Prehistory* 25, 205-237.
- Henshilwood, C.S., d'Errico, F., Yates, R.J., Jacobs, Z., Tribolo, C., Duller, G.A., Mercier, N., Sealy, J.C., Valladas, H., Watts, I., Wintle, A.G., 2002. Emergence of modern human behavior: Middle Stone Age engravings from South Africa, *Science* 295, 1278-1280.
- Henshilwood, C.S., d'Errico, F., Marean, C.W., Milo, R.G., Yates, R., 2001b. An early bone tool industry from the Middle Stone Age at Blombos Cave, South Africa: implications for the origins of modern human behaviour, symbolism and language, *Journal of Human Evolution* 41, 631-678.
- Henshilwood, C.S., d'Errico, F., van Niekerk, K.L., Coquinot, Y., Jacobs, Z., Lauritzen, S.-E., Menu, M., Moreno-García, R., 2011. A 100,000-Year-Old Ochre-Processing Workshop at Blombos Cave, South Africa, *Science* 334, 219-222.
- Henshilwood, C.S., d'Errico, F., van Niekerk, K.L., Dayet, L., Queffelec, A., Pollarolo, L., 2018. An abstract drawing from the 73,000-year-old levels at Blombos Cave, South Africa, *Nature* 562, 115.
- Henshilwood, C.S., d'Errico, F., Vanhaeren, M., van Niekerk, K.L., Jacobs, Z., 2004. Middle Stone Age Shell Beads from South Africa, *Science* 304, 404.
- Henshilwood, C.S., d'Errico, F., Watts, I., 2009. Engraved ochres from the Middle Stone Age levels at Blombos Cave, South Africa, *Journal of Human Evolution* 57, 27-47.
- Henshilwood, C.S., Lombard, M., 2014. Becoming human: Archaeology of the sub-Saharan Middle Stone Age, in: Renfrew, C., Bahn, P.G. (Eds.), *The Cambridge World Prehistory*, Cambridge University Press, Cambridge, pp. 106-113.
- Henshilwood, C.S., Marean, C.W., 2003. The origin of modern human behavior: Critique of the models and their test implications, *Current Anthropology* 44, 627-651.
- Henshilwood, C.S., Sealy, J.C., Yates, R.J., Cruz-Uribe, K., Goldberg, P., Grine, F.E., Klein, R.G., Poggenpoel, C., van Niekerk, K., Watts, I., 2001a. Blombos Cave, Southern Cape, South Africa:

- Preliminary report on the 1992–1999 excavations of the Middle Stone Age levels, *Journal of Archaeological Science* 28, 421-448.
- Henshilwood, C.S., van Niekerk, K.L., Wurz, S., Delagnes, A., Armitage, S.L., Rifkin, R.F., Douze, K., Keene, P., Haaland, M.M., Reynard, J., Discamps, E., Mienies, S.S., 2014. Klipdrift Shelter, southern Cape, South Africa: preliminary report on the Howiesons Poort layers, *Journal of Archaeological Science* 45, 284-303.
- Herries, A.I.R., 2006. Archaeomagnetic evidence for climate change at Sibudu Cave, Southern African Humanities 18, 131-147.
- Herries, A.I.R., 2011. A Chronological Perspective on the Acheulian and Its Transition to the Middle Stone Age in Southern Africa: The Question of the Fauresmith, *International Journal of Evolutionary Biology* 2011, 1-25.
- Hiscock, P., Tabrett, A., 2010. Generalization, inference and the quantification of lithic reduction, *World Archaeology* 42, 545-561.
- Hodgskiss, T.P., 2013. Ochre use in the Middle Stone Age at Sibudu, South Africa: grinding, rubbing, scoring and engraving, *Journal of African Archaeology* 11, 75-95.
- Hoffmann, D.L., Standish, C.D., García-Diez, M., Pettitt, P.B., Milton, J.A., Zilhão, J., Alcolea-González, J.J., Cantalejo-Duarte, P., Collado, H., de Balbín, R., Lorblanchet, M., Ramos-Muñoz, J., Weniger, G.-C., Pike, A.W.G., 2018. U-Th dating of carbonate crusts reveals Neandertal origin of Iberian cave art, *Science* 359, 912-915.
- Högberg, A., 2014. Chronology, stratigraphy and spatial distribution of artefacts at Hollow Rock Shelter, cape province, South Africa, *South African Archaeological Bulletin* 69, 142-151.
- Högberg, A., 2016. A Lithic Attribute Analysis on Blades from the Middle Stone Age Site, Hollow Rock Shelter, Western Cape Province, South Africa, *Lithic Technology* 41, 93-113.
- Högberg, A., Larsson, L., 2011. Lithic technology and behavioural modernity: new results from the Still Bay site, Hollow Rock Shelter, Western Cape Province, South Africa, *Journal of Human Evolution* 61, 133-155.
- Högberg, A., Lombard, M., 2016a. Still Bay Point-Production Strategies at Hollow Rock Shelter and Umhlatuzana Rock Shelter and Knowledge-Transfer Systems in Southern Africa at about 80-70 Thousand Years Ago, *PLoS ONE* 11, e0168012.
- Högberg, A., Lombard, M., 2016b. Indications of pressure flaking more than 70 thousand years ago at Umhlatuzana Rock Shelter, *South African Archaeological Bulletin* 71, 53-59.
- Holdaway, S., Douglass, M., 2015. Use beyond manufacture: non-flint stone artifacts from Fowlers Gap, Australia. *Lithic Technology*, *Lithic Technology* 40, 94-111.
- Holdaway, S., Stern, N., 2004. *A Record in Stone: the Study of Australia's Flaked Stone Artefacts*, Aboriginal Studies Press, Melbourne.
- Hublin, J.-J., Ben-Ncer, A., Bailey, S.E., Freidline, S.E., Neubauer, S., Skinner, M.M., Bergmann, I., Le Cabec, A., Benazzi, S., Harvati, K., Gunz, P., 2017. New fossils from Jebel Irhoud, Morocco and the pan-African origin of *Homo sapiens*, *Nature* 546, 289-292.
- Hughes, S.S., 1998. Getting to the point: evolutionary change in prehistoric weaponry, *Journal of Archaeological Method and Theory* 5, 345-408.
- Ingman, M., Kaessmann, H., Pääbo, S., Gyllensten, U., 2000. Mitochondrial genome variation and the origin of modern humans, *Nature* 408, 708.

- Inizan, M.-L., Reduron-Ballinger, M., Roche, H., Tixier, J., 1999. Technology of Knapped Stone, CREP, Nanterre.
- Jacobs, Z., Hayes, E.H., Roberts, R.G., Galbraith, R.F., Henshilwood, C.S., 2013. An improved OSL chronology for the Still Bay layers at Blombos Cave, South Africa: further tests of single-grain dating procedures and a re-evaluation of the timing of the Still Bay industry across southern Africa, *Journal of Archaeological Science* 40, 579-594.
- Jacobs, Z., Roberts, R.G., 2008. Testing times: old and new chronologies for the Howieson's Poort and Still Bay industries in environmental context, *South African Archaeological Society Goodwin Series* 10, 9-34.
- Jacobs, Z., Roberts, R.G., 2015. An improved single grain OSL chronology for the sedimentary deposits from Diepkloof Rockshelter, Western Cape, South Africa, *Journal of Archaeological Science* 63, 175-192.
- Jacobs, Z., Roberts, R.G., 2017. Single-grain OSL chronologies for the Still Bay and Howieson's Poort industries and the transition between them: Further analyses and statistical modelling, *Journal of Human Evolution* 107, 1-13.
- Jacobs, Z., Roberts, R.G., Galbraith, R.E., Deacon, H.J., Grün, R., Mackay, A., Mitchell, P., Vogelsang, R., Wadley, L., 2008a. Ages for the Middle Stone Age of southern Africa: implications for human behaviour and dispersal, *Science* 322, 733-735.
- Jacobs, Z., Roberts, R.G., Nespoulet, R., El Hajraoui, M.A., Debenath, A., 2012. Single-grain OSL chronologies for Middle Palaeolithic deposits at El Mnasra and El Harhoura 2, Morocco: Implications for Late Pleistocene human-environment interactions along the Atlantic coast of northwest Africa, *Journal of Human Evolution* 62, 377-394.
- Jacobs, Z., Wintle, A.G., Duller, G.A.T., Roberts, R.G., Wadley, L., 2008b. New ages for the post-Howieson's Poort, late and final Middle Stone Age at Sibudu Cave, South Africa, *Journal of Archaeological Science* 35, 1790-1807.
- Jacobs, Z., Wintle, A.G., Roberts, R.G., Duller, G.A.T., 2008c. Equivalent dose distributions from single grains of quartz at Sibudu, South Africa: context, causes and consequences for optical dating of archaeological deposits, *Journal of Archaeological Science* 35, 1808-1820.
- Jelinek, A.J., 1976. Form, function, and style in lithic analysis, *Cultural change and continuity: essays in honor of James Bennett Griffin*, Academic Press, New York, San Francisco, London, pp. 19-33.
- Jeske, R.J., 1989. Economies in raw material use by prehistoric hunter-gatherers, in: Torrence, R. (Ed.), *Time, energy, and stone tools*, Cambridge University Press, Cambridge, pp. 34-45.
- Johnson, C.R., McBrearty, S., 2010. 500,000 year old blades from the Kapthurin Formation, Kenya, *Journal of Human Evolution* 58, 193-200.
- Johnson, J.K., 1979. Archaic biface manufacture : production failures, a chronicle of the misbegotten, *Lithic Technology* 7, 25-35.
- Jolly, K., 1948. The development of the Cape Middle Stone Age in the Skildergat Cave, Fish Hoek, *South African Archaeological Bulletin* 3, 106-107.
- Jones, N., 1926. *The Stone Age in Rhodesia*, Oxford University Press, London.
- Jones, N., 1949. *The Prehistory of Southern Rhodesia*, Cambridge University Press, Cambridge.
- Jöris, O., 2006. Bifacially backed knives (Keilmesser) in the Central European Middle

- Palaeolithic, in: Goren-Inbar, N., Sharon, G. (Eds.), *Axe age: Acheulian tool-making from quarry to discard*, Equinox Publishing, London, pp. 287-310.
- Kaplan, J., 1989. 45000 Years of Hunter-Gatherer History in Natal as Seen from Umhlatuzana Rock Shelter, *South African Archaeological Society Goodwin Series* 6, 7-16.
- Kaplan, J., 1990. The Umhlatuzana rock shelter sequence: 100 000 years of Stone Age history, *Natal Museum Journal of Humanities* 2, 1-94.
- Karlin, C., Bodu, P., Pelegrin, J., 1991. Processus techniques et chaînes opératoires. Comment les préhistoriens s'approprient un concept élaboré par les ethnologues, in: Balfet, H. (Ed.), *Observer l'action technique, les chaînes opératoires, pour quoi faire?*, Édition du CNRS, Paris, pp. 101-117.
- Kelly, R.L., 1988. The three sides of a biface, *American Antiquity* 53, 717–734.
- Kerkhof, F., Müller-Beck, H., 1969. Zur bruchmechanischen Deutung der Schlagmarken an Steingeräten, *Glastechnische Berichte* 42, 439-448.
- Kieselbach, P., 1993. Die Artefakte der mesolithischen Freilandstation Rottenburg - Siebenlinden II, Unpublished Master's thesis, Universität Tübingen, Tübingen.
- Klein, R.G., 2009. *The Human Career: Human Biological and Cultural Origins*, University of Chicago Press, Chicago.
- Klein, R.G., Edgar, B., 2002. *The dawn of human culture*, Wiley, New York.
- Kot, M., 2013. The Earliest Middle Palaeolithic Bifacial Leafpoints in Central and Southern Europe. Technological Approach, Unpublished PhD thesis, Warsaw University, Warsaw.
- Krukowski, S., 1939. Paleolit. *Prehistoria Ziemi Polskiej*, in: Krukowski, S., Kostrzewski, J., Jakimowicz, R. (Eds.), *Prehistoria Ziemi Polskiej*, Polska Akademia Umiejętności, Krakow.
- Kuhn, S.L., 1990. A geometric index of reduction for unifacial stone tools, *Journal of Archaeological Science* 17, 583-593.
- Kuhn, S.L., 1991. 'Unpacking' Reduction: Lithic Raw Material Economy in the Mousterian of West-Central Italy, *Journal of Anthropological Archaeology* 10, 76-106.
- Kuhn, S.L., 1992. On Planning and Curated Technologies in the Middle Paleolithic, *Journal of Anthropological Research* 48, 185-214.
- Kuhn, S.L., 1995. *Mousterian Lithic Technology: an Ecological Perspective*, Princeton University Press, Princeton.
- Kuhn, S.L., 2004. Upper Paleolithic raw material economies at Ücagızlı cave, Turkey, *Journal of Anthropological Archaeology* 23, 431-448.
- Kuman, K.A., 1989. Florisbad and #Gi: The contribution of open-air sites to study of the Middle Stone Age in southern Africa, Unpublished PhD thesis, University of Pennsylvania, Philadelphia.
- Kuman, K.A., Gibbon, R., Kempson, H., Langejans, G.H.J., Le Baron, J.L., Pollarolo, L., Sutton, M., 2005. Stone Age signatures in northernmost South Africa: early archaeology in the Mapungubwe National Park and vicinity, in: d'Errico, F., Backwell, L. (Eds.), *From Tools to Symbols: From Early Hominids to Modern Humans*, Witwatersrand University Press, Johannesburg, pp. 163-182.
- Kuman, K.A., Inbar, M., Clarke, R.J., 1999. Palaeoenvironments and Cultural Sequence of the

- Florisbad Middle Stone Age Hominid Site, South Africa, *Journal of Archaeological Science* 26, 1409-1425.
- Kyriacou, K., Parkington, J.E., Marais, A.D., Braun, D.R., 2014. Nutrition, modernity and the archaeological record: Coastal resources and nutrition among Middle Stone Age hunter-gatherers on the western Cape coast of South Africa, *Journal of Human Evolution* 77, 64-73.
- Lachance, J., Vernot, B., Elbers, C.C., Ferwerda, B., Froment, A., Bodo, J.-M., Lema, G., Fu, W., Nyambo, T.B., Rebbeck, T.R., Zhang, K., Akey, J.M., Tishkoff, S.A., 2012. Evolutionary history and adaptation from high-coverage whole-genome sequences of diverse African hunter-gatherers, *Cell* 150, 457-469.
- Lahr, M.M., Foley, R.A., 1998. Towards a theory of modern human origins: geography, demography, and diversity in recent human evolution, *American Journal of Physical Anthropology* 107, 137-176.
- Lechtman, H., 1977. *Style in Technology - Some Early Thoughts*, in: Lechtman, H., Merrill, R.S. (Eds.), *Material Culture: Styles, Organization, and Dynamics of Technology*, West Publishers, New York.
- Lemonnier, P., 1976. La description des chaînes opératoires: contribution à l'analyse des systèmes techniques, *Techniques et Culture* 1, 101-150.
- Lepers, C., 2010. Tailler et retoucher par pression, *Bulletin des Chercheurs de la Wallonie* 2, 37-50.
- Lepot, M., 1993. Approche techno-fonctionnelle de l'outillage lithique moustérien: essai de classification des parties actives en terme d'efficacité technique, Unpublished Master's thesis, Université Paris Ouest Nanterre La Défense, Nanterre.
- Leroi-Gourhan, A., 1943. *Evolution et technique I - L'Homme et la Matière*, Albin Michel, Paris.
- Leroi-Gourhan, A., 1964. *Le geste et la parole I - Technique et langage*, Albin Michel, Paris.
- Li, H., Kuman, K., Lotter, M.G., Leader, G.M., Gibbon, R.J., 2017. The Victoria West: earliest prepared core technology in the Acheulean at Canteen Kopje and implications for the cognitive evolution of early hominids, *Royal Society Open Science* 4, 170288.
- Lisiecki, L.E., Raymo, M.E., 2005. A Pliocene-Pleistocene stack of 57 globally distributed benthic  $\delta^{18}O$  records, *Paleoceanography* 20, PA1003.
- Lombard, M., 2006a. Direct evidence for the use of ochre in the hafting technology of Middle Stone Age tools from Sibudu Cave, *Southern African Humanities* 18, 57-67.
- Lombard, M., 2006b. First impressions of the functions and hafting technology of Still Bay pointed artefacts from Sibudu Cave, *Southern African Humanities* 18, 27-41.
- Lombard, M., 2007. The gripping nature of ochre: the association of ochre with Howieson's Poort adhesives and Later Stone Age mastics from South Africa, *Journal of Human Evolution* 53, 406-419.
- Lombard, M., 2008. Finding resolution for the Howiesons Poort through the microscope: micro-residue analysis of segments from Sibudu Cave, South Africa, *Journal of Archaeological Science* 35, 26-41.
- Lombard, M., Högberg, A., 2018. The Still Bay points of Apollo 11 Rock Shelter, Namibia: an inter-regional perspective, *Azania: Archaeological Research in Africa* 53, 312-340.
- Lombard, M., Phillipson, L., 2010. Indications of bow and stone-tipped arrow use 64,000 years

- ago in KwaZulu-Natal, South Africa, *Antiquity* 84, 635-648.
- Lombard, M., Schlebusch, C., Soodyall, H., 2013. Bridging disciplines to better elucidate the evolution of early *Homo sapiens* in southern Africa, *South African Journal of Science* 109, 1-8.
- Lombard, M., Wadley, L., Deacon, J., Wurz, S., Parsons, I., Mohapi, M., Swart, J., Mitchell, P., 2012. South African and Lesotho Stone Age Sequence Updated (I), *South African Archaeological Bulletin* 67, 120-144.
- Lombard, M., Wadley, L., Jacobs, Z., Mohapi, M., Roberts, R.G., 2010. Still Bay and serrated points from Umhlatuzana Rock Shelter, KwaZulu-Natal, South Africa, *Journal Archaeological Science* 37, 1773-1784.
- Lourdeau, A., 2010. Le technocomplexe Itaparica: Définition technofonctionnelle des industries à pièces façonnées unifacielmant à une face plan dans le centre et le nord-est du Brésil pendant la transition Pleistocène-Holocène et L'Holocène ancien, Unpublished PhD thesis, Université Paris Ouest Nanterre La Défense, Nanterre.
- Lubsen, K.D., Corruccini, R.S., 2011. Morphometric analysis of the Herto Cranium (BOU-VP-16/1): where does it fit?, *Journal of Contemporary Anthropology* 2, 1.
- MacCalman, H.R., Viereck, A., 1967. Peperkorrel, a factory site of Lupemban affinities from central south west Africa, *South African Archaeological Bulletin* 22, 41-50.
- Mackay, A., 2008. A method for estimating edge length from flake dimensions: use and implications for technological change in the southern African MSA, *Journal of Archaeological Science* 35, 614-622.
- Mackay, A., 2010. The Late Pleistocene archaeology of Klein Kliphuis Rock Shelter, Western Cape, South Africa: 2006 excavations, *South African Archaeological Bulletin* 65, 132-147.
- Mackay, A., Hallinan, E., Steele, T.E., 2018. Provisioning responses to environmental change in South Africa's winter rainfall zone: MIS 5-2, in: Robinson, E., Sellet, F. (Eds.), *Lithic Technological Organization and Paleoenvironmental Change*, Springer, Cham, pp. 13-36.
- Mackay, A., Jacobs, Z., Steele, T.E., 2015. Pleistocene archaeology and chronology of Putslaagte 8 (PL8) Rockshelter, Western Cape, South Africa, *Journal of African Archaeology* 13, 71-98.
- Mackay, A., Orton, J., Schwartz, S., Steele, T.E., 2010. Soutfontein (SFT)-001: Preliminary report on an open-air bifacial point-rich site in southern Namaqualand, South Africa. *South African Archaeological Bulletin* 65, 84-95.
- Mackay, A., Stewart, B.A., Chase, B.M., 2014. Coalescence and fragmentation in the late Pleistocene archaeology of southernmost Africa, *Journal of Human Evolution* 72, 1-26.
- Mackay, A., Welz, A., 2008. Engraved ochre from a Middle Stone Age context at Klein Kliphuis in the Western Cape of South Africa, *Journal of Archaeological Science* 35, 1521-1532.
- Magnani, M., Rezek, Z., Lin, S.C., Chan, A., Dibble, H.L., 2014. Flake variation in relation to the application of force, *Journal of Archaeological Science* 46, 37-49.
- Magori, C.C., Day, M.H., 1983. Laetoli Hominid 18: an early *Homo sapiens* skull, *Journal of Human Evolution* 12, 747-753.
- Malan, B.D., 1955. The Archaeology of the Tunnel Cave and Skildergat Kop, Fish Hoek, Cape of Good Hope, *South African Archaeological Bulletin* 10, 3-9.
- Malan, B.D., 1962. Biographical sketch, in: Malan, B.D., Cooke, H.B.S. (Eds.), *The contribution of*

- C. van Riet Lowe to prehistory in southern Africa, South African Archaeological Society, Cape Town, pp. 38-42.
- Mallick, S., Li, H., Lipson, M., Mathieson, I., Gymrek, M., Racimo, F., Zhao, M., Chennagiri, N., Nordenfelt, S., Tandon, A., Skoglund, P., Lazaridis, I., Sankararaman, S., Fu, Q., Rohland, N., Renaud, G., Erlich, Y., Willems, T., Gallo, C., Spence, J.P., Song, Y.S., Poletti, G., Balloux, F., van Driem, G., de Knijff, P., Gallego Romero, I., Jha, A.R., Behar, D.M., Bravi, C.M., Capelli, C., Hervig, T., Moreno-Estrada, A., Posukh, O.L., Balanovska, E., Balanosky, O., Karachanak-Yankova, S., Sahakyan, H., Toncheva, D., Yepiskoposyan, L., Tyler-Smith, C., Xue, Y., Abdullah, M.S., Ruiz-Linares, A., Beall, C.M., Di Rienzo, A., Jeong, C., Starikovskaya, E.B., Metspalu, E., Parik, J., VILLEMS, R., Henn, B.M., Hodoglugil, U., Mahley, R., Sajantila, A., Stamatoyannopoulos, G., Wee, J.T.S., Khusainova, R., Khusnutdinova, E., Litvinov, S., Ayodo, G., Comas, D., Hammer, M.F., Kivisild, T., Klitz, W., Winkler, C., Labuda, D., Bamshad, M., Jorde, L.B., Tishkoff, S.A., Watkins, W.S., Metspalu, M., Dryomov, S., Sukernik, R., Singh, L., Thangaraj, K., Pääbo, S., Kelso, J., Patterson, N., Reich, D., 2016. The Simons Genome Diversity Project: 300 genomes from 142 diverse populations, *Nature* 538, 201-206.
- Marwick, B., 2008. What attributes are important for the measurement of assemblage reduction intensity? results from an experimental stone artefact assemblage with relevance to the Hoabinhian of mainland Southeast Asia, *Journal of Archaeological Science* 35, 1189-1200.
- Mason, R.J., 1957. The Transvaal Middle Stone Age and statistical analysis, *South African Archaeological Bulletin* 12, 119-137.
- Mason, R.J., 1962. *Prehistory of the Transvaal*, Witwatersrand University Press, Johannesburg.
- Mason, R.J., 1971. *Multivariate analysis of Cave of Hearths Middle Stone Age artefact assemblages*, University of the Witwatersrand, Johannesburg.
- Mason, R.J., Brain, C.K., Brown, A.J.V., Cooke, H.B.S., Deacon, H.J., Ewer, R.F., De Graaff, B., Hofmeyr, I., Malan, B.D., Tobias, P.V., du Toit, A.P., Turton, K., Wells, L.H., 1988. *Cave of Hearths, Makapansgat, Transvaal*, University of the Witwatersrand, Johannesburg.
- Maud, R.R., Botha, G.A., 2000. Deposits of the south eastern and southern coasts, in: Partridge, T.C., Maud, R.R. (Eds.), *The Cenozoic of Southern Africa*, Oxford University Press, New York, pp. 19-32.
- McBrearty, S., 1988. The Sangoan-Lupemban and Middle Stone Age Sequence at the Muguruk Site, Western Kenya, *World Archaeology* 19, 388-420.
- McBrearty, S., 2005. The Kapthurin Formation: What We Know Now That We Didn't Know Then, in: Lieberman, D.E., Smith, R.J., Kelly, J. (Eds.), *Interpreting the Past: Essays on Human, Primate, and Mammal Evolution in Honor of David Pilbeam*, Brill, Boston, pp. 263-274.
- McBrearty, S., Brooks, A.S., 2000. The revolution that wasn't: a new interpretation of the origin of modern human behavior, *Journal of Human Evolution* 39, 453-563.
- McBrearty, S., Tryon, C.A., 2006. From Acheulean to Middle Stone Age in the Kapthurin Formation, Kenya, in: Hovers, E., Kuhn, S.L. (Eds.), *Transitions Before the Transition: Evolution and Stability in the Middle Palaeolithic and Middle Stone Age*, Springer, New York, pp. 257-277.
- McCall, G.S., Thomas, J.T., 2012. Still Bay and Howiesons Poort Foraging Strategies: Recent Research and Models of Culture Change, *African Archaeological Review* 29, 7-50.

- McCarthy, R.C., Lucas, L., 2014. A morphometric reassessment of BOU-VP-16/1 from Herto, Ethiopia, *Journal of Human Evolution* 74, 114-117.
- McDougall, I., Brown, F.H., Fleagle, J.G., 2005. Stratigraphic placement and age of modern humans from Kibish, Ethiopia, *Nature* 433, 733-736.
- McGhee, G.R., Müller, G.B., Schäfer, K., 2011. *Convergent evolution: limited forms most beautiful*, MIT Press Cambridge, Cambridge.
- McNabb, J., Beaumont, P., 2011. A Report on the Archaeological Assemblages from Excavations by Peter Beaumont at Canteen Koppie, Northern Cape, South Africa, Archaeopress, Southampton.
- McNabb, J., Beaumont, P., 2012. Excavations in the Acheulean levels at the Earlier Stone Age site of Canteen Koppie, Northern Province, South Africa, *Proceedings of the Prehistoric Society* 78, 51-71.
- McNabb, J., Sinclair, A., 2009. *The Cave of Hearths: Makapan Middle Pleistocene Research Project: Field Research by Anthony Sinclair and Patrick Quinney, 1996–2001*, Archaeopress, Oxford.
- McPherron, S.P., Braun, D.R., Dogandžić, T., Archer, W., Desta, D., Lin, S.C., 2014. An experimental assessment of the influences on edge damage to lithic artifacts: a consideration of edge angle, substrate grain size, raw material properties, and exposed face, *Journal of Archaeological Science* 49, 70-82.
- Meadows, M.E., Quick, L.J., 2016. Terrestrial ecosystem changes in the late Quaternary, in: Knight, J., Grab, S.W. (Eds.), *Quaternary Environmental Change in Southern Africa: Physical and Human Dimensions*, Cambridge University Press, Cambridge, pp. 269-283.
- Mellars, P., 1989. Major Issues in the Emergence of Modern Humans, *Current Anthropology* 30, 349-385.
- Mellars, P., Stringer, C.B., 1989. *The human revolution: Behavioural and biological perspectives on the origins of modern humans*, Edinburgh University Press, Edinburgh.
- Miller, C.E., 2014. High-resolution geoarchaeology and settlement dynamics at the Middle Stone Age sites of Diepkloof and Sibudu, South Africa, in: Conard, N.J., Delagnes, A. (Eds.), *Settlement dynamics of the Middle Paleolithic and Middle Stone Age*, Kerns Verlag, Tübingen, pp. 27-46.
- Minichillo, T., 2005. *Middle Stone Age Lithic Study, South Africa: an Examination of Modern Human Origins*, Unpublished PhD thesis, University of Washington, Washington.
- Mitchell, P.J., 2008. Developing the Archaeology of Marine Isotope Stage 3, *South African Archaeological Society Goodwin Series* 10, 52-65.
- Mithen, S.J., 1996. *The prehistory of the mind: a search for the origins of art, religion, and science*, Thames & Hudson, London.
- Mohapi, M., 2008. *A new angle on Middle Stone Age hunting technology in South Africa*, Unpublished PhD thesis, University of the Witwatersrand, Johannesburg.
- Mohapi, M., 2012. Point morphology and the Middle Stone Age cultural sequence of Sibudu Cave, KwaZulu-Natal, South Africa, *South African Archaeological Bulletin* 67, 5-15.
- Mohapi, M., 2013. The Middle Stone Age point assemblage from Umhlatuzana Rock Shelter: a morphometric study, *Southern African Humanities* 25, 25-51.



- Moll, E.J., White, F., 1978. The Indian Ocean Coastal Belt, in: Werger, M.J.A., Van Bruggen, A.C. (Eds.), *Biogeography and ecology of southern Africa*, Springer, Dordrecht, pp. 561-598.
- Moore, J., Willmer, P., 1997. Convergent evolution in invertebrates, *Biological Reviews* 72, 1-60.
- Moreau, L., 2009. *Geißenklösterle – Das Gravettien der Schwäbischen Alb im europäischen Kontext*, Kerns Verlag, Tübingen.
- Morgan, L.E., Renne, P.R., 2008. Diachronous dawn of Africa's Middle Stone Age: New 40Ar/39Ar ages from the Ethiopian Rift, *Geology* 36, 967-970.
- Mourre, V., 1996. Les industries en quartz au Paléolithique. Terminologie, méthodologie et technologie, *Paléo* 8, 205-223.
- Mourre, V., Villa, P., Henshilwood, C.S., 2010. Early Use of Pressure Flaking on Lithic Artifacts at Blombos Cave, South Africa, *Science* 330, 659-662.
- Mucina, L., Scott-Shaw, C.R., Rutherford, M.C., Camp, K.G.T., Matthews, W.S., Powrie, L.W., Hoare, D.B., 2006. Indian Ocean Coastal Belt, in: Mucina, L., Rutherford, M.C. (Eds.), *The Vegetation of South Africa, Lesotho and Swaziland*, South African National Biodiversity Institute, Pretoria, pp. 570-583.
- Murungi, M.L., 2017. *Phytoliths at Sibudu (South Africa): Implications for vegetation, climate and human occupation during the MSA*, Unpublished PhD thesis, University of the Witwatersrand, Johannesburg.
- Nicoud, E., 2011. *Le phénomène acheuléen en Europe occidentale: approche chronologique, technologie lithique et implications culturelles*, Unpublished PhD thesis, Università degli studi di Roma La Sapienza/Aix-Marseille Université I, Rome, Aix en Provence.
- Nicoud, E., 2013. What Does the Acheulean Consist of? The Example of Western Europe (MIS 16-9), *Mitteilungen der Gesellschaft für Urgeschichte* 22, 41-60.
- Nigst, P.R., 2012. *The Early Upper Palaeolithic of the Middle Danube Region*, Leiden University Press, Leiden.
- O'Brien, M.J., Buchanan, B., Eren, M.I., 2018. *Convergent Evolution in Stone-Tool Technology*, MIT Press Cambridge, Cambridge.
- Odell, G.H., 1996. Economizing Behavior and the Concept of "Curation.", in: Odell, G.H. (Ed.), *Stone Tools: Theoretical Insights into Human Prehistory*, Plenum Press, New York, pp. 51-80.
- Opperman, H., 1996. Strathalan Cave B, North-Eastern Cape Province, South Africa: Evidence for human behavior 29,000–26,000 years ago, *Quaternary International* 33, 45-53.
- Ossendorf, G., 2013. *Spätpleistozäne Jäger-Sammler des südwestlichen Namibias*, Unpublished PhD thesis, University of Cologne, Cologne.
- Ott, I., 1996. Die Artefakte der jungpaläolithischen Fundstelle von Rosenberg am Kamp, Niederösterreich, *Archaeologia Austriaca* 80, 43-114.
- Pargeter, J., Hampson, J., 2019. Quartz crystal materiality in Terminal Pleistocene Lesotho, *Antiquity* 93, 11-27.
- Parkington, J.E., 2001. Milestones: the impact of systematic exploitation of marine foods on human evolution, in: Tobias, P., Raath, M.A., Moggi-Cechi, J., Doyle, G.A. (Eds.), *Humanity from African Naissance to Coming Millennia*, Florence University Press, Florence, pp. 327-336.

- Parkington, J.E., 2010. Coastal diet, encephalization, and innovative behaviors in the late Middle Stone Age of southern Africa, in: Cunnane, S.C., Stewart, K.M. (Eds.), *Human brain evolution - the influence of freshwater and marine food resources*, John Wiley & Sons, Hoboken, pp. 189-202.
- Pelcin, A.W., 1996. Controlled experiments in the production of flake attributes, Unpublished PhD thesis, University of Pennsylvania, Philadelphia.
- Pelcin, A.W., 1998. The Formation of Flakes: The Role of Platform Thickness and Exterior Platform Angle in the Production of Flake Initiations and Terminations, *Journal of Archaeological Science* 24, 1107-1113.
- Pelegrin, J., 1986. Technologie lithique: une méthode appliquée à l'étude de deux séries du Périgordien ancien (Roc de Combe, couche 8 - La Cote, niveau III), Unpublished PhD thesis, Université Paris Ouest Nanterre La Défense, Paris.
- Pelegrin, J., 1991. Sur une recherche technique expérimentale des techniques de débitage laminaire, in: *Archéologie expérimentale – Tome 2 - L'os et la pierre, la maison et les champs, Actes du Colloque International "Expérimentation en archéologie: Bilan et Perspectives"*, Éditions Errance, Paris, pp. 118-128.
- Pelegrin, J., 1995. Technologie lithique: Le Châtelperronien de Roc-de-Combe (Lot) et de la Cote (Dordogne), *Cahiers du Quaternaire*, Édition du CNRS, Paris.
- Pelegrin, J., 2000. Les techniques de débitage laminaire au Tardiglaciaire : critères de diagnose et quelques réflexions, in: Valentin, B., Bodu, P., Christensen, M. (Eds.), *L'Europe centrale et septentrionale au Tardiglaciaire*, Mémoires du Musée de Préhistoire d'Île de France 7, Édition APRAIF, Nemours, pp. 73-86.
- Pelegrin, J., 2005. Remarks About Archaeological Techniques and Methods of Knapping: Elements of a Cognitive Approach to Stone Knapping, in: Roux, V., Bril, B. (Eds.), *Stone Knapping, the Necessary Conditions for a Uniquely Hominin Behavior*, McDonald Institute for Archaeological Research, Cambridge, pp. 23-34.
- Pelegrin, J., 2006. Long blade technology in the Old World: an experimental approach and some archaeological results, in: Apel, J., Knutsson, K. (Eds.), *Skilled Production and Social Reproduction - Aspects of Traditional Stone-Tool Technologies*, Societas Archaeologica Upsaliensis & The Department of Archaeology and Ancient History, Uppsala University, Uppsala, pp. 37-68.
- Pelegrin, J., Karlin, C., Bodu, P., 1988. «Chaînes opératoires»: un outil pour le préhistorien. *Technologie préhistorique*, Édition du CNRS, Paris.
- Perlès, C., 1992. Economie des matières premières et économie du débitage: deux conceptions opposées?, in: *Actes des rencontres 19-20 octobre 1990 (Ed.)*, Bilan et perspectives, Éditions APDCA, pp. 35-45.
- Peterkin, G.L., 1993. Lithic and organic hunting technology, in: Peterkin, G.L., Bricker, H., P.A., M. (Eds.), *Hunting and Animal Exploitation in the Later Paleolithic and Mesolithic of Eurasia*, American Anthropological Association, Washington, DC, pp. 49-68.
- Picin, A., Peresani, M., Vaquero, M., 2011. Application of a new typological approach to classifying denticulate and notched tools: the study of two Mousterian lithic assemblages, *Journal of Archaeological Science* 38, 711-722.
- Pickering, R., 2002. A sedimentological analysis of six archaeological soil samples from Sibudu

- Cave, KwaZulu-Natal, South Africa, Research report on file at the University of the Witwatersrand, Johannesburg.
- Pickering, R., 2006. Regional geology, setting and sedimentology of Sibudu Cave, Southern African Humanities 18, 123-129.
- Pienaar, M., Woodborne, S., Wadley, L., 2008. Optically stimulated luminescence dating at Rose Cottage Cave, South African Journal of Science 104, 65-69.
- Pigeot, N., 1991. Réflexions sur l'histoire technique de l'homme: de l'évolution cognitive à l'évolution culturelle, Paléo 3, 167-200.
- Plug, I., 2004. Resource exploitation: animal use during the Middle Stone Age at Sibudu Cave, KwaZulu-Natal, South African Journal of Science 100, 151-158.
- Plug, I., 2006. Aquatic animals and their associates from the Middle Stone Age levels at Sibudu, Southern African Humanities 18, 289-299.
- Plug, I., Clark, J., 2008. In the air: preliminary report on the birds from Sibudu Cave, KwaZulu-Natal, South Africa, South African Archaeological Society Goodwin Series 10, 133-142.
- Porat, N., Chazan, M., Grün, R., Aubert, M., Eisenmann, V., Horwitz, L.K., 2010. New radiometric ages for the Fauresmith industry from Kathu Pan, southern Africa: Implications for the Earlier to Middle Stone Age transition, Journal of Archaeological Science 37, 269-283.
- Porraz, G., 2005. En marge du milieu alpin – Dynamiques de formation des ensembles lithiques et modes d'occupation des territoires au Paléolithique moyen, Unpublished PhD thesis, Aix-Marseille Université I, Aix en Provence.
- Porraz, G., Igreja, M., Schmidt, P., Parkington, J.E., 2016. A shape to the microlithic Robberg from Elands Bay Cave (South Africa), Southern African Humanities 29, 203-247.
- Porraz, G., Texier, P.-J., Archer, W., Piboule, M., Rigaud, J.-P., Tribolo, C., 2013. Technological successions in the Middle Stone Age sequence of Diepkloof Rock Shelter, Western Cape, South Africa, Journal of Archaeological Science 40, 3376-4300.
- Porraz, G., Texier, P.-J., Miller, C.E., 2014. Le complexe bifacial Still Bay et ses modalités d'émergence à l'abri Diepkloof (Middle Stone Age, Afrique du Sud), in: Brenet, M., Bourguignon, L., Jarry, M.E., Mémoires de la Société Préhistorique Française, in press. (Eds.), Emergence et diversité des techno-complexes au Paléolithique moyen ancien. Relations entre productions de débitage et de façonnage, Session C Du XXVIIe Congrès Préhistorique de France, Mémoires de la Société Préhistorique Française, Paris, pp. 155-175.
- Porraz, G., Texier, P.-J., Rigaud, J.-P., Parkington, J.E., Poggenpoel, C., Roberts, D.L., 2008. Preliminary characterization of an MSA lithic assemblage preceding the "classic" Howiesons Poort complex at Diepkloof Rock Shelter, Western Cape Province, South Africa, South African Archaeological Society Goodwin Series 10, 105-121.
- Porraz, G., Val, A., Dayet, L., de La Peña, P., Douze, K., Miller, C.E., Murungi, M., Tribolo, C., Schmid, V.C., Sievers, C., 2015. Bushman Rock Shelter (Limpopo, South Africa): A Perspective From The Edge Of The Highveld, South African Archaeological Bulletin 70, 166–179.
- Porraz, G., Val, A., Tribolo, C., Mercier, N., de la Peña, P., Haaland, M.M., Igreja, M., Miller, C.E., Schmid, V.C., 2018. The MIS5 Pietersburg at '28' Bushman Rock Shelter, Limpopo Province, South Africa, PLoS ONE 13, e0202853.
- Ramos, J., Bernal, D., Domínguez-Bella, S., Calado, D., Ruiz, B., Gil, M.J., Clemente, I., Durán, J.J., Vijande, E., Chamorro, S., 2008. The Benzú rockshelter: a Middle Palaeolithic site on the

- North African coast, *Quaternary Science Reviews* 27, 2210-2218.
- Ramsay, P.J., Cooper, J.A.G., 2002. Late Quaternary sea-level change in South Africa, *Quaternary Research* 57, 82-90.
- Rasse, M., Soriano, S., Tribolo, C., Stokes, S., Huysecom, É., 2004. La séquence pléistocène supérieur d'Ounjougou (Pays Dogon, Mali, Afrique de l'Ouest): évolution géomorphologique, enregistrements sédimentaires et changements culturels, *Quaternaria* 15, 329-341.
- Raynal, J.-P., Sbihi Alaoui, F.-Z., Geraads, D., Magoga, L., Mohib, A., 2001. The earliest occupation of North-Africa: the Moroccan perspective, *Quaternary International* 75, 65-75.
- Raynal, J.-P., Sbihi Alaoui, F.-Z., Mohib, A., Geraads, D., 2009. Préhistoire ancienne au Maroc atlantique : bilan et perspectives régionales, *Bulletin d'Archéologie Marocaine* 21, 9-53.
- Reher, C.A., 1991. Large scale lithic quarries and regional transport systems on the High Plains of Eastern Wyoming: Spanish Diggings revisited, in: Montet-White, A., Holen, S. (Eds.), *Raw Material Economies Among Prehistoric Hunter-Gatherers*, University of Kansas Publications in Anthropology, Lawrence, pp. 251-284.
- Reindl, E., Apperly, I.A., Beck, S.R., Tennie, C., 2017. Young children copy cumulative technological design in the absence of action information, *Scientific Reports* 7, 1788.
- Renaut, R., Bamford, M.K., 2006. Results of a preliminary palynological analysis at Sibudu Cave, *Southern African Humanities* 18, 235-240.
- Reynolds, S., 2006. Temporal changes in vegetation and mammalian communities during Oxygen Isotope Stage 3 at Sibudu Cave, KwaZulu-Natal, *Southern African Humanities* 18, 301-314.
- Rezek, Z., Lin, S.C., Iovita, R.P., Dibble, H.L., 2011. The relative effects of core surface morphology on flake shape and other attributes, *Journal of Archaeological Science* 38, 1346-1359.
- Richter, D., Grün, R., Joannes-Boyau, R., Steele, T.E., Amani, F., Rué, M., Fernandes, P., Raynal, J.-P., Geraads, D., Ben-Ncer, A., Hublin, J.-J., McPherron, S.P., 2017. The age of the hominin fossils from Jebel Irhoud, Morocco, and the origins of the Middle Stone Age, *Nature* 546, 293-296.
- Riga, A., Oxilia, G., Panetta, D., P.A., S., Benazzi, S., Wadley, L., Moggi-Cecchi, J., 2018. Human deciduous teeth from the Middle Stone Age layers of Sibudu Cave (South Africa), *Journal of Anthropological Sciences* 96, 1-14.
- Rigaud, J.-P., Texier, P.-J., Poggenpoel, C., Parkington, J.E., 2006. Le mobilier Stillbay et Howieson's Poort de l'abri Diepkloof. La chronologie du Middle Stone Age sud-africain et ses implications, *Comptes Rendus Palevol* 5, 839-849.
- Rightmire, G.P., Deacon, H.J., 1991. Comparative studies of Late Pleistocene human remains from Klasies River Mouth, South Africa, *Journal of Human Evolution* 20, 131-156.
- Robinson, J.R., Wadley, L., 2018. Stable isotope evidence for (mostly) stable local environments during the South African Middle Stone Age from Sibudu, KwaZulu-Natal, *Journal of Archaeological Science* 100, 32-44.
- Roche, H., Tixier, J., 1982. Les accidents de taille, *Studia Praehistorica Belgica* 2, 65-76.
- Rohling, E.J., Grant, K., Bolshaw, M., Roberts, A.P., Siddall, M., Hemleben, C., Kucera, M., 2009. Antarctic temperature and global sea level closely coupled over the past five glacial cycles,

- Nature Geoscience 2, 500-504.
- Rolland, N., Dibble, H.L., 1990. A new synthesis of Middle Paleolithic variability, *American Antiquity* 55, 480-499.
- Roth, B.J., Dibble, H.L., 1998. Production and transport of blanks and tools at the French Middle Paleolithic site of Combe-Capelle Bas, *American Antiquity* 63, 47-62.
- Rots, V., Lentfer, C., Schmid, V.C., Porraz, G., Conard, N.J., 2017. Pressure flaking to serrate bifacial points for the hunt during the MIS5 at Sibudu Cave (South Africa), *PLoS ONE* 12, e0175151.
- Rots, V., Van Peer, P., 2006. Early evidence of complexity in lithic economy: core-axe production, hafting and use at Late Middle Pleistocene site 8-B-11, Sai Island (Sudan), *Journal of Archaeological Science* 33, 360-371.
- Sackett, J.R., 1982. Approaches to style in lithic archaeology, *Journal of Anthropological Archaeology* 1, 59-112.
- Sahle, Y., Morgan, L.E., Braun, D.R., Atnafu, B., Hutchings, W.K., 2014. Chronological and behavioral contexts of the earliest Middle Stone Age in the Gademotta Formation, Main Ethiopian Rift, *Quaternary International* 331, 6-19.
- Sampson, C.G., 1974. *The Stone Age Archaeology of Southern Africa*, Academic Press, London.
- Scally, A., Durbin, R., 2012. Revising the human mutation rate: implications for understanding human evolution, *Nature Reviews Genetics* 13, 745-753.
- Scerri, E.M.L., 2017. The North African Middle Stone Age and its place in recent human evolution, *Evolutionary Anthropology: Issues, News, and Reviews* 26, 119-135.
- Scerri, E.M.L., Thomas, M.G., Manica, A., Gunz, P., Stock, J.T., Stringer, C.B., Grove, M., Groucutt, H.S., Timmermann, A., Rightmire, G.P., d'Errico, F., Tryon, C.A., Drake, N.A., Brooks, A.S., Dennell, R.W., Durbin, R., Henn, B.M., Lee-Thorp, J., deMenocal, P., Petraglia, M.D., Thompson, J.C., Scally, A., Chikhi, L., 2018. Did Our Species Evolve in Subdivided Populations across Africa, and Why Does It Matter?, *Trends in Ecology & Evolution* 33, 582-594.
- Schiegl, S., Conard, N.J., 2006. The Middle Stone Age sediments at Sibudu: results from FTIR spectroscopy and microscopic analyses, *Southern African Humanities* 18, 149-172.
- Schiegl, S., Stockhammer, P., Scott, C., Wadley, L., 2004. A mineralogical and phytoliths study of the Middle Stone Age hearths in Sibudu Cave, KwaZulu-Natal, South Africa, *South African Journal of Science* 100, 185-194.
- Schirmer, G.R., 1975. An analysis of lithic material from Dale Rose Parlour, Trappies Kop, Kalk Bay, Cape Peninsula, Unpublished Archaeology Additional report, University of Cape Town, Cape Town.
- Schlanger, N., 2003. The Burkitt affair revisited. Colonial implications and identity politics in early South African prehistoric research, *Archaeological Dialogues* 10, 5-26.
- Schlebusch, C.M., Lombard, M., Soodyall, H., 2013. MtDNA control region variation in populations from southern Africa, *BMC Evolutionary Biology* 13, 56.
- Schlebusch, C.M., Malmström, H., Günther, T., Sjödin, P., Coutinho, A., Edlund, H., Munters, A.R., Vicente, M., Steyn, M., Soodyall, H., Lombard, M., Jakobsson, M., 2017. Southern African ancient genomes estimate modern human divergence to 350,000 to 260,000 years ago, *Science* 358, 652-655.

- Schlebusch, C.M., Skoglund, P., Sjödin, P., Gattepaille, L.M., Hernandez, D., Jay, F., Li, S., De Jongh, M., Singleton, A., Blum, M.G.B., Soodyall, H., Jakobsson, M., 2012. Genomic variation in seven Khoe-San groups reveals adaptation and complex African history, *Science* 338, 374-379.
- Schmid, V.C., Conard, N.J., Parkington, J.E., Texier, P.-J., Porraz, G., 2016. The 'MSA 1' of Elands Bay Cave (South Africa) in the context of the southern African Early MSA technologies, *Southern African Humanities* 29, 153-201.
- Schmid, V.C., Porraz, G., Zeidi, M., Conard, N.J., 2019. Blade technology characterizing the MIS 5 D-A layers of Sibudu Cave, South Africa, *Lithic Technology* 44, 1-38.
- Schmidt, P., Högberg, A., 2018. Heat treatment in the Still Bay - A case study on Hollow Rock Shelter, South Africa, *Journal of Archaeological Science: Reports* 21, 712-720.
- Schmidt, P., Porraz, G., Slodczyk, A., Bellot-Gurlet, L., Archer, W., Miller, C.E., 2013. Heat treatment in the South African Middle Stone Age: temperature induced transformations of silcrete and their technological implications, *Journal of Archaeological Science* 40, 3519-3531.
- Shadrach, K., 2018. Investigating the Fauresmith stone tool industry from Pit 4 West at Canteen Kopje, Northern Cape Province, South Africa, Unpublished Master's thesis, University of Witwatersrand, Johannesburg.
- Shea, J.J., 2003. The Middle Palaeolithic of the East Mediterranean Levant, *Journal of World Prehistory* 17, 313-394.
- Shea, J.J., 2006. The origins of lithic projectile point technology: evidence from Africa, the Levant, and Europe, *Journal of Archaeological Science* 33, 823-846.
- Shea, J.J., 2009. The Impact of Projectile Weaponry on Late Pleistocene Hominin Evolution, in: Hublin, J.-J., Richards, M.P. (Eds.), *The Evolution of Hominin Diets: Integrating Approaches to the Study of Palaeolithic Subsistence*, Springer, Dordrecht, pp. 189-199.
- Shott, M.J., 1986. Technological organization and settlement mobility: an ethnographic examination, *Journal of Anthropological Research* 42, 15-52.
- Siegel, P., 1985. Edge angle as a functional indicator: a test, *Lithic Technology* 14, 90-94.
- Sievers, C., 2006. Seeds from the Middle Stone Age layers at Sibudu Cave, *Southern African Humanities* 18, 203-222.
- Sievers, C., 2013. Sedges as bedding in Middle Stone Age Sibudu, Unpublished PhD thesis, University of the Witwatersrand, Johannesburg.
- Sinclair, I., Hockey, P., Tarboton, W., Ryan, P., 2011. *Sasol Birds of Southern Africa IV*, Struik Nature, Cape Town.
- Singer, R., Wymer, J.J., 1982. *The Middle Stone Age at Klasies River Mouth in South Africa*, University of Chicago Press, Chicago.
- Skinner, J.D., Chimimba, C.T., 2005. *The Mammals of the Southern African Subregion*, Cambridge University Press, Cape Town.
- Skoglund, P., Thompson, J.C., Prendergast, M.E., Mittnik, A., Sirak, K., Hajdinjak, M., Salie, T., Rohland, N., Mallick, S., Peltzer, A., Heinze, A., Olalde, I., Ferry, M., Harney, E., Michel, M., Stewardson, K., Cerezo-Román, J.I., Chiumia, C., Crowther, A., Gomani-Chindebvu, E., Gidna, A.O., Grillo, K.M., Helenius, I.T., Hellenthal, G., Helm, R., Horton, M., López, S., Mabulla,

- A.Z.P., Parkington, J.E., Shipton, C., Thomas, M.G., Tibesasa, R., Welling, M., Hayes, V.M., Kennett, D.J., Ramesar, R., Meyer, M., Pääbo, S., Patterson, N., Morris, A.G., Boivin, N., Pinhasi, R., Krause, J., Reich, D., 2017. Reconstructing Prehistoric African Population Structure, *Cell* 171, 59-71.
- Sonneville-Bordes, D., 1960. Le Paléolithique supérieur en Périgord, Delmas, Bordeaux.
- Soressi, M., 2002. Le Moustérien de tradition acheuléenne du sud-ouest de la France, Unpublished PhD thesis, Université de Bordeaux I, Bordeaux.
- Soressi, M., 2004. From the Mousterian of Acheulian Tradition type A to type B: A change in technical tradition, raw material, task, or settlement dynamics?, in: Conard, N.J. (Ed.), *Settlement Dynamics of the Middle Paleolithic and Middle Stone Age*, Kerns Verlag, Tübingen, pp. 343-366.
- Soressi, M., 2005. Aux origines de la 'modernité' comportementale en Afrique du sud il ya 75 000 ans, *Annales de la Fondation Fyssen* 20, 125-131.
- Soressi, M., Geneste, J.-M., 2011. Special Issue: Reduction Sequence, Chaîne Opératoire, and Other Methods: The Epistemologies of Different Approaches to Lithic Analysis The History and Efficacy of the Chaîne Opératoire Approach to Lithic Analysis: Studying Techniques to Reveal Past Societies in an Evolutionary Perspective, *PaleoAnthropology* 2011, 334-350.
- Soressi, M., Hays, M., 2003. Manufacture, transport and use of Mousterian bifaces - A case study from the Perigord (France), in: Soressi, M., Dibble, H.L. (Eds.), *Multiple Approaches to the Study of Bifacial Technologies*, University of Pennsylvania, Philadelphia, pp. 125-147.
- Soriano, S., 2000. Outillage bifacial et outillage sur éclat au Paléolithique ancien et moyen : coexistence et interaction, Unpublished PhD thesis, Université Paris Ouest Nanterre La Défense, Nanterre.
- Soriano, S., 2001. Statut fonctionnel de l'outillage bifacial dans les industries du Paléolithique moyen: propositions méthodologiques, in: Cluquet, D., Otte, M. (Eds.), *Les industries à outils bifaciaux du Paléolithique moyen d'Europe occidentale*, ERAUL, Liège, pp. 77-83.
- Soriano, S., Rasse, M., Tribolo, C., Huysecom, E., 2010. Ounjougou: a long Middle Stone Age sequence in the Dogon country (Mali), in: Allsworth-Jones, P. (Ed.), *West African Archaeology. New Developments, New Perspectives*, British Archaeological Reports International Series, Oxford, pp. 1-14.
- Soriano, S., Villa, P., Delagnes, A., Degano, I., Pollarolo, L., Lucejko, J.J., Henshilwood, C.S., Wadley, L., 2015. The Still Bay and Howiesons Poort at Sibudu and Blombos: Understanding Middle Stone Age Technologies, *PLoS ONE* 10, e0131127.
- Soriano, S., Villa, P., Wadley, L., 2007. Blade technology and tool forms in the Middle Stone Age of South Africa: the Howiesons Poort and post-Howiesons Poort at Rose Cottage Cave, *Journal of Archaeological Science* 35, 681-703.
- Soriano, S., Villa, P., Wadley, L., 2009. Ochre for the toolmaker: Shaping the Still Bay points at Sibudu (Kwa-Zulu-Natal, South Africa), *Journal of African Archaeology* 7, 41-54.
- Speth, J., 1972. Mechanical Basis of Percussion Flaking, *American Antiquity* 37, 34-60.
- Steele, T., Mackay, A., Orton, J., Schwartz, S., 2012. Varsche Rivier 003, a new Middle Stone Age site in southern Namaqualand, South Africa, *South African Archaeological Bulletin* 67, 108-119.
- Steele, T.E., Mackay, A., Fitzsimmons, K.E., Igreja, M., Marwick, B., Orton, J., Schwartz, S.,

- Stahlschmidt, M., 2016. Varsche Rivier 003: A Middle and Later Stone Age Site with Still Bay and Howiesons Poort Assemblages in Southern Namaqualand, South Africa, *PaleoAnthropology* 2016, 100-163.
- Stewart, B.A., Dewar, G.I., Morley, M.W., Inglis, R.H., Wheeler, M., Jacobs, Z., Roberts, R.G., 2012. Afromontane foragers of the Late Pleistocene: site formation, chronology and occupational pulsing at Melikane Rockshelter, Lesotho, *Quaternary International* 270, 40-60.
- Stringer, C.B., 1992. Reconstructing recent human evolution, *Philosophical Transactions Royal Society London B Biological Sciences* 337, 217-224.
- Stringer, C.B., 1996. Current issues in modern human origins, in: Meikle, W.E., Howell, F.C., Jablonski, N.G. (Eds.), *Contemporary issues in human evolution*, California Academy of Sciences, San Francisco, pp. 115-134.
- Stringer, C.B., 2016. The origin and evolution of *Homo sapiens*, *Philosophical Transactions Royal Society B* 371, 20150237.
- Stringer, C.B., Andrews, P., 1988. Genetic and fossil evidence for the origin of modern humans, *Science* 239, 1263-1268.
- Surovell, T.A., 2012. *Toward a behavioral ecology of lithic technology: cases from Paleoindian archaeology*, University of Arizona Press, Tucson.
- Sutton, M.B., 2013. *The Archaeology of Swartkrans Cave, Gauteng, South Africa: new excavations of Members 1 and 4*, Unpublished PhD thesis, University of the Witwatersrand, Johannesburg.
- Sutton, M.B., Pickering, T.R., Pickering, R., Brain, C.K., R.J., C., Heaton, J.L., Kuman, K., 2009. Newly discovered fossil- and artifact-bearing deposits, uranium-series ages, and Plio-Pleistocene hominids at Swartkrans Cave, South Africa, *Journal of Human Evolution* 57, 688-696.
- Taylor, N., 2016. Across rainforests and woodlands: a systematic reappraisal of the Lupemban Middle Stone Age in Central Africa, in: Jones, S.C., Stewart, B.A. (Eds.), *Africa from MIS 6-2: Population Dynamics and Paleoenvironments*, Springer, Dordrecht, pp. 273-299.
- Templeton, A.R., Hedges, S.B., Kumar, S., Tamura, K., Stoneking, M., 1992. Human origins and analysis of mitochondrial DNA sequences, *Science* 255, 737-739.
- Texier, P.-J., Porraz, G., Parkington, J.E., Rigaud, J.-P., Poggenpoel, C., Miller, C.E., Tribolo, C., Cartwright, C.R., Coudenneau, A., Klein, R.G., Steele, T., Verna, C., 2010. A Howiesons Poort tradition of engraving ostrich eggshell containers dated to 60,000 years ago at Diepkloof Rock Shelter, South Africa, *Proceedings of the National Academy of Sciences of the United States of America* 107, 6180-6185.
- Thompson, E., Marean, C.W., 2008. The Mossel Bay lithic variant: 120 years of Middle Stone Age research from Cape St Blaize Cave to Pinnacle Point, *South African Archaeological Society Goodwin Series* 10, 90-104.
- Thompson, E., Williams, H.M., Minichillo, T., 2010. Middle and late Pleistocene Middle Stone Age lithic technology from Pinnacle Point 13B (Mossel Bay, Western Cape Province, South Africa), *Journal of Human Evolution* 59, 358-377.
- Tishkoff, S.A., Reed, F.A., Friedlaender, F.R., Ehret, C., Ranciaro, A., Froment, A., Hirbo, J.B., Awomoyi, A.A., Bodo, J.-M., Doumbo, O., Ibrahim, M., Juma, A.T., Kotze, M.J., Lema, G., Moore, J.H., Mortensen, H., Nyambo, T.B., Omar, S.A., Powell, K., Pretorius, G.S., Smith,



- M.W., Thera, M.A., Wambebe, C., Weber, J.L., Williams, S.M., 2009. The genetic structure and history of Africans and African Americans, *Science* 324, 1035-1044.
- Tixier, J., 1967. Procédés d'analyse et questions de terminologie dans l'étude des ensembles industriels du Paléolithique récent et de l'Épipaléolithique en Afrique du Nord-Ouest, in: Bishop, W.W., Clark, J.D. (Eds.), *Background to Evolution in Africa*, The University of Chicago Press, Chicago, London, pp. 771-820.
- Tixier, J., 1980. *Préhistoire et technologie lithique*, Édition du CNRS, Meudon.
- Tixier, J., 2012. A method for the study of stone tools = méthode pour l'étude des outillages lithiques : guidelines based on the work of J. Tixier = notice sur les travaux scientifiques de J. Tixier, Musée national d'histoire et d'art/Centre national de recherche archéologique du Luxembourg.
- Tobias, P.V., 1949. The excavation of Mwułu's cave, Potgietersrust district, South African Archaeological Bulletin 4, 2-13.
- Tobias, P.V., 1971. Human skeletal remains from the Cave of Hearths, Makapansgat, northern Transvaal, *American Journal of Physical Anthropology* 34, 335–367.
- Tomasello, M., 1999. The human adaptation for culture, *Annual review of anthropology* 28, 509-529.
- Tostevin, G., 2000. Behavioral Change and Regional Variation across the Middle to Upper Paleolithic Transition in Central Europe, Eastern Europe, and the Levant, Unpublished PhD thesis, Harvard University, Cambridge.
- Tostevin, G., 2003. Attribute analysis of the lithic technologies of Stránská skála II–III in their regional and inter-regional context, in: Svoboda, J.A., Bar-Yosef, O. (Eds.), *Stránská skála: Origins of the Upper Paleolithic in the Brno Basin*, Peabody Museum, Harvard University, Cambridge, pp. 77-118.
- Tostevin, G., 2012. Seeing Lithics: A Middle-Range Theory for Testing for Cultural Transmission in the Pleistocene, Peabody Museum, Harvard University & Oxbow Books, Oxford, Oakville.
- Tribolo, C., Mercier, N., Douville, E., Joron, J.-L., Reyss, J.-L., Rufer, D., Cantin, N., Lefrais, Y., Miller, C.E., Parkington, J.E., Porraz, G., Rigaud, J.-P., Texier, P.-J., 2013. OSL and TL dating of the Middle Stone Age sequence of Diepkloof Rock Shelter (Western Cape, South Africa): a clarification, *Journal of Archaeological Science* 40, 3401-3411.
- Tribolo, C., Rasse, M., Soriano, S., Huysecom, É., 2015. Defining a chronological framework for the Middle Stone Age in West Africa: Comparison of methods and models for OSL ages at Ounjougou (Mali), *Quaternary Geochronology* 29, 80-96.
- Tringham, R., Cooper, G., Odell, G., Voytek, B., Whitman, A., 1974. Experimentation in the Formation of Edge Damage: A New Approach to Lithic Analysis, *Journal of Field Archaeology* 1, 171-196.
- Tryon, C.A., 2006. 'Early' Middle Stone Age lithic technology of the Kapthurin Formation (Kenya), *Current Anthropology* 47, 367-375.
- Tryon, C.A., Faith, J.T., 2013. Variability in the Middle Stone Age of Eastern Africa, *Current Anthropology* 54, S234-S254.
- Tryon, C.A., McBrearty, S., Texier, P.-J., 2005. Levallois Lithic Technology from the Kapthurin Formation, Kenya: Acheulian Origin and Middle Stone Age Diversity, *African Archaeological Review* 22, 199-229.

- Tsirk, A., 1974. Mechanical basis of percussion flaking: some comments, *American Antiquity* 39, 128-130.
- Tyson, P.D., 1986. *Climatic Change and Variability in Southern Africa*, Oxford University Press, Oxford.
- Underhill, D., 2011a. A history of Stone Age archaeological study in South Africa, *South African Archaeological Bulletin* 66, 3-14.
- Underhill, D., 2011b. The study of the Fauresmith: a review, *South African Archaeological Bulletin* 66, 15-26.
- Val, A., 2016. New data on the avifauna from the Middle Stone Age layers of Sibudu Cave, South Africa: Taphonomic and palaeoenvironmental implications, *Quaternary International* 421, 173-189.
- Valentin, B., 2000. L'usage des percuteurs en pierre tendre pour le débitage des lames. Circonstances de quelques innovations au cours du Tardiglaciaire dans le Bassin parisien, in: Pion, G. (Ed.), *Le Paléolithique supérieur récent: nouvelles données sur le peuplement et l'environnement*, Actes de la 5e table ronde de Chambéry, 12 mars 1999, *Mémoires de la Société Préhistorique Française* 28, pp. 253-260.
- van Campo, E., Duplessy, J.C., Prell, W.L., Barratt, N., Sabatier, R., 1990. Comparison of terrestrial and marine temperature estimates for the past 135 kyr off southeast Africa: a test for GCM simulations of palaeoclimate, *Nature* 348, 209-212.
- Van Peer, P., Fullagar, R., Stokes, S., Bailey, R.M., Moeyersons, J., Steenhoudt, F., Geerts, A., Vanderbeken, T., De Dapper, M., Geus, F., 2003. The Early to Middle Stone Age transition and the emergence of modern human behaviour at site 8-B-11, Sai Island, Sudan, *Journal of Human Evolution* 45, 187-193.
- Van Peer, P., Rots, V., Vroomans, J.-M., 2004. A story of colourful diggers and grinders: The Sangoan and Lupemban at site 8-B-11, Sai Island, Northern Sudan, *Before Farming* 2004, 1-28.
- Vanhaeren, M., d'Errico, F., Stringer, C., James, S.L., Todd, J.A., Mienis, H.K., 2006. Middle Paleolithic Shell Beads in Israel and Algeria, *Science* 312, 1785-1788.
- Vaquero, M., Vallverdu, J., Rosell, J., Pasto, I., Allue, E., 2001. Neandertal behavior at the Middle Palaeolithic site of Abric Romani, Capellades, Spain, *Journal of Field Archaeology* 28, 93-114.
- Veeramah, K.R., Wegmann, D., Woerner, A., Mendez, F.L., Watkins, J.C., Destro-Bisol, G., Soodyall, H., Louie, L., Hammer, M.F., 2011. An early divergence of KhoeSan ancestors from those of other modern humans is supported by an ABC-based analysis of autosomal resequencing Data, *Molecular Biology and Evolution* 29, 617-630.
- Vigilant, L., Stoneking, M., Harpending, H., Hawkes, K., Wilson, A.C., 1991. African populations and the evolution of human mitochondrial DNA, *Science* 253, 1503-1507.
- Villa, P., Delagnes, A., Wadley, L., 2005. A late Middle Stone Age artifact assemblage from Sibudu (KwaZulu-Natal): comparisons with the European Middle Paleolithic, *Journal of Archaeological Science* 32, 399-422.
- Villa, P., Lenoir, M., 2006. Hunting weapons of the Middle Stone Age and the Middle Palaeolithic: spear points from Sibudu, Rose Cottage and Bouheben, *Southern African Humanities* 18, 89-122.
- Villa, P., Lenoir, M., 2009. Hunting and Hunting Weapons of the Lower and Middle Paleolithic

- of Europe, in: Hublin, J.-J., Richards, M.P. (Eds.), *The Evolution of Hominin Diets: Integrating Approaches to the Study of Palaeolithic Subsistence*, Springer, Dordrecht, pp. 59-85.
- Villa, P., Soressi, M., Henshilwood, C.S., Mourre, V., 2009. The Still Bay points of Blombos Cave (South Africa), *Journal of Archaeological Science* 36, 441-460.
- Villa, P., Soriano, S., 2010. Hunting weapons of Neanderthals and early Modern Humans in South Africa: Similarities and differences, *Journal of Anthropological Research* 66, 5-38.
- Villa, P., Soriano, S., Teyssandier, N., Wurz, S., 2010. The Howieson's Poort and MSA III at Klasies River main site, Cave 1A, *Journal of Archaeological Science* 37, 630-655.
- Villa, P., Soriano, S., Tsanova, T., Degano, I., Higham, T.F.G., d'Errico, F., Backwell, L., Lucejko, J.J., Colombini, M.P., Beaumont, P.B., 2012. Border Cave and the beginning of the Later Stone Age in South Africa, *Proceedings of the National Academy of Sciences of the United States of America* 109, 13208–13213.
- Vogelsang, R., 1998. *Middle Stone Age Fundstellen in Südwest-Namibia*, Heinrich Barth Institut, Köln.
- Vogelsang, R., Richter, J., Jacobs, Z., Eichhorn, B., Linseele, V., Roberts, R.G., 2010. New excavations of Middle Stone Age deposits at Apollo 11 Rock Shelter, Namibia: stratigraphy, archaeology, chronology and past environments, *Journal of African Archaeology* 8, 185-218.
- Volman, T.P., 1978. Early archaeological evidence for shellfish collecting, *Science* 201, 911-913.
- Volman, T.P., 1981. *The Middle Stone Age in the Southern Cape*, Unpublished PhD thesis, University of Chicago, Chicago.
- Volman, T.P., 1984. Early prehistory of southern Africa, in: Klein, R.G. (Ed.), *Southern African Prehistory and Palaeoenvironments*, Balkema, Rotterdam, pp. 169-220.
- Wadley, L., 2001a. Preliminary report on excavations at Sibudu Cave, KwaZulu-Natal, *Southern African Humanities* 13, 1-17.
- Wadley, L., 2001b. What is cultural modernity? A general view and a South African perspective from Rose Cottage Cave, *Cambridge Archaeological Journal* 11, 201-221.
- Wadley, L., 2004. Vegetation changes between 61 500 and 26 000 years ago: the evidence from seeds in Sibudu Cave, KwaZulu-Natal, *South African Journal of Science* 100, 167-173.
- Wadley, L., 2005. A typological study of the final Middle Stone Age stone tools from Sibudu Cave, KwaZulu-Natal, *South African Archaeological Bulletin* 60, 51-63.
- Wadley, L., 2006. Partners in grime: results of multi-disciplinary archaeology at Sibudu Cave, *Southern African Humanities* 18, 315-341.
- Wadley, L., 2007. Announcing a Still Bay Industry at Sibudu Cave, *Journal of Human Evolution* 52, 681-689.
- Wadley, L., 2008. The Howieson's Poort industry of Sibudu Cave, *South African Archaeological Society Goodwin Series* 10, 122-132.
- Wadley, L., 2010a. Compound-Adhesive Manufacture as a Behavioral Proxy for Complex Cognition in the Middle Stone Age, *Current Anthropology* 51, S111-S119.
- Wadley, L., 2010b. Cemented ash as a receptacle or work surface for ochre powder production at Sibudu, South Africa, 58,000 years ago, *Journal of Archaeological Science* 37, 2397-2406.
- Wadley, L., 2012a. Two 'moments in time' during Middle Stone Age occupations of Sibudu,

- South Africa, *Southern African Humanities* 24, 79-97.
- Wadley, L., 2012b. Some combustion features at Sibudu, South Africa, between 65,000 and 58,000 years ago, *Quaternary International* 247, 341-349.
- Wadley, L., 2013a. Recognizing Complex Cognition through Innovative Technology in Stone Age and Palaeolithic Sites, *Cambridge Archaeological Journal* 23, 163-183.
- Wadley, L., 2013b. MIS 4 and MIS 3 Occupations in Sibudu, KwaZulu-Natal, South Africa, *South African Archaeological Bulletin* 68, 41-51.
- Wadley, L., 2015. Those marvellous millennia: The Middle Stone Age of Southern Africa, *Azania: Archaeological Research in Africa* 50, 155-226.
- Wadley, L., Hodgskiss, T., Grant, M., 2009. Implications for complex cognition from the hafting of tools with compound adhesives in the Middle Stone Age, South Africa, *Proceedings of the National Academy of Sciences* 106, 9590-9594.
- Wadley, L., Jacobs, Z., 2004. Sibudu Cave, KwaZulu-Natal: Background to the excavations of Middle Stone Age and Iron Age occupations, *South African Journal of Science* 100, 145-151.
- Wadley, L., Jacobs, Z., 2006. Sibudu Cave: background to the excavations, stratigraphy and dating, *Southern African Humanities* 18, 1-26.
- Wadley, L., Kempson, H., 2011. A review of rock studies for archaeologists, and an analysis of dolerite and hornfels from the Sibudu area, KwaZulu-Natal, *Southern African Humanities* 23, 87-107.
- Wadley, L., Mohapi, M., 2008. A segment is not a monolith: evidence from the Howiesons Poort of Sibudu, South Africa, *Journal of Archaeological Science* 35, 2594-2605.
- Wadley, L., Plug, I., Clark, J.L., 2008. The contribution of Sibudu fauna to an understanding of KwaZulu Natal environments at ~58ka, ~48ka and ~35ka, in: Badenhorst, S., Mitchell, P.J., Driver, J.C. (Eds.), *Animals and People: Archaeozoological Papers in Honour of Ina Plug*, *British Archaeological Reports International Series*, Oxford, pp. 34-45.
- Wadley, L., Sievers, C., Bamford, M., Goldberg, P., Berna, F., Miller, C.E., 2011. Middle Stone Age Bedding Construction and Settlement Patterns at Sibudu, South Africa, *Science* 334, 1388-1391.
- Wadley, L., Whitelaw, G. (Eds.), 2006. *Sibudu Cave: background to the excavations, stratigraphy and dating*, *Southern African Humanities* 18, Council of the Natal Museum, Pietermaritzburg.
- Waelbroeck, C., Labeyrie, L., Michel, E., Duplessy, J.C., McManus, J.F., Lambeck, K., Balbon, E., Labracherie, M., 2002. Sea-level and deep water temperature changes derived from benthic foraminifera isotopic records, *Quaternary Science Reviews* 21, 295-305.
- Watts, I., 2010. The pigments from Pinnacle Point Cave 13B, Western Cape, South Africa, *Journal of Human Evolution* 59, 392-411.
- Wayland, E.G., Smith, R., 1923. Some Primitive Stone Tools from Uganda, *Geological Survey of Uganda Occasional Paper* 1, Entebbe.
- Weißmüller, W., 1991. Die graphische Simulation des Kanteneffekts zum besseren Verständnis der Kernpräparation, *Archäologisches Korrespondenzblatt* 21, 173-186.
- Weißmüller, W., 1995. Die Silexartefakte der Unteren Schichten der Sesselfelsgrötte. Ein Beitrag zum Problem des Moustérien, *Quartär-Bibliothek* 6, Saarbrücken.

- Wells, C.R., 2006. A sample integrity analysis of faunal remains from the RSp layer at Sibudu Cave, Southern African Humanities 18, 261-277.
- Wendorf, F., Close, A.E., Schild, R., 1994. Africa in the period of *Homo sapiens neanderthalensis* and contemporaries, in: De Laet, S.J., Dani, A.H., Lorenzo, J.L., Nunoo, R.B. (Eds.), History of Humanity, Prehistory and the Beginnings of Civilization, Routledge/UNESCO, New York, pp. 117-131.
- Wendorf, F., Schild, R., 1974. A Middle Stone Age Sequence from the Central Rift Valley, Ethiopia, Polska Akademia Nauk, Wroclaw.
- White, T.D., Asfaw, B., Degusta, D., Gilbert, H., Richards, G.D., Suwa, G., Clark Howell, F., 2003. Pleistocene *Homo sapiens* from Middle Awash, Ethiopia, Nature 426, 742-747.
- Whiten, A., Horner, V., Marshall-Pescini, S., 2003. Cultural panthropology, Evolutionary Anthropology: Issues, News, and Reviews 12, 92–105.
- Whittaker, J.C., 1994. Flint Knapping. Making and Understanding Stone Tools, University of Texas Press, Austin.
- Wiessner, P., 1983. Style and Social Information in Kalahari San Projectile Points, American Antiquity 48, 253-276.
- Wilkins, J., 2013. Technological Change in the Early Middle Pleistocene: The Onset of the Middle Stone Age at Kathu Pan 1, Northern Cape, South Africa, Unpublished PhD thesis, University of Toronto, Toronto.
- Wilkins, J., Chazan, M., 2012. Blade production ~500 thousand years ago at Kathu Pan 1, South Africa: support for a multiple origins hypothesis for early Middle Pleistocene blade technologies, Journal of Archaeological Science 39, 1883-1900.
- Wilkins, J., Pollarolo, L., Kuman, K., 2010. Prepared core reduction at the site of Kudu Koppie in northern South Africa: temporal patterns across the Earlier and Middle Stone Age boundary, Journal of Archaeological Science 37, 1279-1292.
- Will, M., 2011. Das MSA-Steinartefaktinventar von Hoedjiespunt 1, Westkap, Südafrika – Implikationen für frühe aquatische Adaptationen von *Homo sapiens*, Unpublished Bachelor's thesis, Eberhard Karls Universität Tübingen, Tübingen.
- Will, M., Bader, G.D., Conard, N.J., 2014. Characterizing the Late Pleistocene MSA Lithic Technology of Sibudu, KwaZulu-Natal, South Africa, PLoS ONE 9, e98359.
- Will, M., Conard, N.J., 2018. Assemblage variability and bifacial points in the lowermost Sibudan layers at Sibudu, South Africa, Archaeological and Anthropological Sciences 10, 389-414.
- Will, M., El-Zaatari, S., Harvarti, K., Conard, N.J., 2019. Human teeth from securely stratified Middle Stone Age contexts at Sibudu, South Africa, Archaeological and Anthropological Sciences 11, 3491-3501.
- Will, M., Mackay, A., Phillips, N., 2015. Implications of Nubian-like core reduction systems in southern Africa for the identification of early modern human dispersals, PLoS ONE 10, e0131824.
- Will, M., Parkington, J.E., Kandel, A.W., Conard, N.J., 2013. Coastal adaptations and the Middle Stone Age lithic assemblages from Hoedjiespunt 1 in the Western Cape, South Africa, Journal of Human Evolution 64, 518-537.
- Wilmsen, P., 1968. Functional analysis of flaked stone artifacts, American Antiquity 33, 156-161.

- Wintle, A.G., Botha, G.A., Li, S.-H., Vogel, J.C., 1995. A chronological framework for colluviation during the last 110 kyr in KwaZulu-Natal, South African Journal of Science 91, 134-139.
- Wirminghaus, J.O., Downs, C.T., Symes, C.T., Perrin, M.R., 2012. Diet of the Cape Parrot, *Poicephalus robustus*, in Afromontane forests in KwaZulu-Natal, South Africa, Ostrich: Journal of African Ornithology 73, 20-25.
- Wurz, S., 2000. The Middle Stone Age at Klasies River, South Africa, Unpublished PhD thesis, University of Stellenbosch, Stellenbosch.
- Wurz, S., 2002. Variability in the Middle Stone Age lithic sequence, 115,000 – 60,000 years ago at Klasies River, South Africa, Journal of Archaeological Science 29, 1001-1015.
- Wurz, S., 2012. The significance of MIS 5 shell middens on the Cape coast: lithic perspective from Klasies River and Ysterfontein 1, Quaternary International 270, 61-69.
- Wurz, S., 2013. Technological trends in the Middle Stone Age of South Africa between MIS 7 and MIS 3, Current Anthropology 54 (Supplement 8), S305-S319.
- Wurz, S., 2014. Southern and East African Middle Stone Age: Geography and Culture, Encyclopedia of Global Archaeology, Springer, Dordrecht, pp. 6890-6912.
- Wurz, S., 2016. Development of the archaeological record during the middle stone age of South Africa, in: Knight, J., Grab, S. (Eds.), Quaternary Environmental Change in Southern Africa: Physical and Human Dimensions, Cambridge University Press, Cambridge, pp. 371-384.
- Wurz, S., Bentsen, S.E., Reynard, J., Van Pletzen-Vos, L., Brenner, M., Mentzer, S., Pickering, R., Green, H., 2018. Connections, culture and environments around 100 000 years ago at Klasies River main site, Quaternary International 495, 102-115.
- Yellen, J.E., 1998. Barbed bone points: tradition and continuity in Saharan and sub-Saharan Africa, African Archaeological Review 15, 173-198.
- Yellen, J.E., Brooks, A.S., Cornelissen, E., Mehlman, M.H., Stewart, K.A., 1995. Middle Stone Age worked bone industry from Katanda, Upper Semliki Valley, Zaire, Science 268, 553-556.
- Zilhão, J., 2001. Anatomically Archaic, Behaviorally Modern: The Last Neanderthals and Their Destiny, Stichting Nederlands Museum voor Anthropologie en Praehistorie, Amsterdam.
- Zilhão, J., 2011. The emergence of language, art and symbolic thinking, in: Henshilwood, C.S., d'Errico, F. (Eds.), Homo symbolicus: the dawn of language, imagination and spirituality, John Benjamins B.V., Amsterdam, Philadelphia, pp. 111-131.

## 11. Supplementary Information

[E4]

Filename=SibuduCave\_DS  
Com=COM2:1200,E,7,1,OP0  
Instrument=MitutoyoAbsoluteDigimatic  
Sound=Yes  
Delaytime=1  
Table=recordingNEW  
BackColor=15724527

[unit]

Type=Menu  
Prompt=Enter the square:  
Menu=B5 C5 A5 B4 C4 A4  
Length=20

[ID]

Type=Text  
Prompt=Enter the artifact ID please:  
Length=20

[Suffix]

Type=Text  
Prompt=Enter the artifact ID Suffix please:  
Length=20

[layer]

Type=Menu  
Prompt=Select the layer:  
Menu=PSS LBC GBP GSS RBS BMO  
Length=50

[refitting]

Type=Menu  
Prompt=Is this artifact part of a refit group?  
Menu=No,Yes  
Length=20

[refitGroup]

Type=Text  
Prompt=Enter the refit group ID please:  
Length=20  
Condition1=refitting Yes

[refitType]

Type=Menu  
Prompt=Select the refit type:  
Menu=sequence,breakage,retouch,temperature  
Length=80  
Condition1=refitting Yes

[RM]  
Type=Menu  
Prompt=Select the raw material:  
Menu=dolerite,sandstone,quartzite,quartz,hornfels,chert/ccs  
Length=20

[RMU]  
Type=Menu  
Prompt=Select the raw material unit:  
Menu=RMU1qu RMU2qu RMU3qu RMU1ho RMU2ho RMU3ho RMULowdol RMUMeddol RMUHighdol  
milky crystal RMU4qu RMU5qu RMU6qu RMU7qu RMU8qu RMU9qu RMU10qu RMU11qu RMU12qu  
RMU13qu RMU14qu RMU15qu RMU16qu RMU1ccs RMU2ccs RMU3ccs RMU4ccs RMU17qu  
Length=20  
Condition1=RM quartzite hornfels dolerite quartz

[thermalAlteration1]  
Type=Menu  
Prompt=Thermal alteration?  
Menu=No,Yes  
Length=30

[thermalAlteration2]  
Type=Menu  
Prompt=Select the type of thermal alteration:  
Menu=colourChange,craquelation,shelledSpallings,irregularBreakageSurface,colourChange+craquelati  
on,colourChange+irregularBreakageSurface,colourChange+craquelation+irregularBreakageSurface,col  
ourChange+shelledSpallings,colourChange+irregularBreakageSurface+shelledSpall,shelledSpallings+irr  
egularBreakageSurface  
Length=50  
Condition1=thermalAlteration1 Yes

[cortexPercentage]  
Type=Menu  
Prompt=Select the percentage of cortex:  
Menu=100%,>50%,>20%,<20%,0%  
Length=20

[cortexType]  
Type=Menu  
Prompt=Select the type of cortex:  
Menu=alluvial,diaclastic,weathered,thermal,indetermined  
Length=20  
Condition1=cortexPercentage 100% >50% >20% <20%

[cortexPosition]  
Type=Menu  
Prompt=Select the position of cortex:  
Menu=distal proximal sinistrolateral dextralateral lateral distal+lateral proximal+lateral middle/centre  
100%cortex backed entame indetermined backed+lateral backed+middle/centre distal+proximal  
Length=50  
Condition1=cortexPercentage 100% >50% >20% <20%



[edgeDamage/Taphonomy1]

Type=Menu

Prompt=Are there postdepositional changes or edge damages?

Menu=No,Yes

Length=20

[edgeDamage/Taphonomy2]

Type=Menu

Prompt=Select the edge damage type:

Menu=damage,use,rounding,burnt,modern,weathered,indetermined

Length=20

Condition1=edgeDamage/Taphonomy1 Yes

[fragmentation]

Type=Menu

Prompt=Which part of the blank is preserved:

Menu=all,proximal,medial,distal,lateral,lateral-proximal,lateral-medial,lateral-distal,proximal/medial,medial/distal,indetermined

Length=20

[technologicalAccident1]

Type=Menu

Prompt=Is there a technological accident:

Menu=Yes,No

Length=20

[technologicalAccident2]

Type=Menu

Prompt=Select technological accident:

Menu=hinge, plunging, Siretbreak, hinge+Siretbreak, plunging+hinge, Siretbreak+plunging, step, Siretbeak+step

Length=29

Condition1=technologicalAccident1 Yes

[length]

Type=Instrument

Prompt=Enter a value for length

Length=12

Condition1=fragmentation all lateral

[width]

Type=Instrument

Prompt=Enter a value for width

Length=12

Condition1=fragmentation all proximal medial distal proximal/medial medial/distal

[thickness]

Type=Instrument

Prompt=Enter a value for thickness

Length=12

[weight]  
Type=Instrument  
Prompt=Enter a value for weight  
Length=12

[maximalDimension]  
Type=Instrument  
Prompt=Enter a value for maximal dimension  
Length=12  
Condition1=fragmentation all lateral

[product1]  
Type=Menu  
Prompt=Select the product:  
Menu=flake,blade,bladelet,debris,triangularFlake  
Length=26

[product2]  
Type=Menu  
Prompt=Specify the product:  
Menu=indifferent, dosLimité, débordant, preferential, BladeWithPartofPlatformPreparation, BladeWithDistalPreparation, BladeWithLateralPreparation, BladeletWithLateralPreparation, FlakeDistalPreparation, FlakeLateralPreparation, FlakeLateralPreparationWithPartofPlatform, FlakeWithDistalPreparation, FlakeWithLateralPreparation, FlakeWithPartofPlatformPreparation, FlakePlatformPreparation, Kombewa, bipolarFlake, laminarFlake, blade, bladelet, triangularFlake, shapingFlake, slabFlake, LevalloisPreparationFlake, plungingBlade, primaryCrestedBlade, SecondaryOneSidedCrestedBlade, SecondaryTwoSidedCrestedBlade, SemicrestedPrimaryBlade, SemicrestedSecondaryOneSidedBlade, SemicrestedSecondaryTwoSidedBlade, burinSpall, slab+bipolarFlake, BladeWithDistalPrep, BladeWithLateralPreparation+PartofPlatform, BladeWithLateralPreparation, débordant+WithLateralPreparation, FlakeWithLateral+DistalPreparation, FlakeWithLateralPreparation+PartofPlatform, laminarFlakeWithDistalPreparation, plungingFlake, primaryCrestedBladelet, primaryOneSidedCrestedBlade, SecondaryOneSidedCrestedBladelet, SecondaryOneSidedCrestedFlake, SemicrestedPrimaryFlake, SemicrestedSecondaryOneSidedFlake, triangularFlakeWithPartofPlatform, FlakeDébordant+DistalPreparation, FlakeDébordantWithDistalPreparation, BladeWithLateral+DistalPreparation, laminarFlake+dosLimité, laminarFlake+débordant  
Length=44  
Condition1=product1 flake blade bladelet triangularFlake

[morphology]  
Type=Menu  
Prompt=Select the morphology:  
Menu=triangular,circular,rectangular,trapezoidal,irregular,indetermined  
Length=26  
Condition1=product1 flake blade bladelet triangularFlake

[dorsalScarsNumber]  
Type=Numeric  
Prompt=Enter the number of dorsal scars:  
Length=20  
Condition1=product1 flake blade bladelet triangularFlake

[dorsalScarsOrient]

Type=Menu

Prompt=orientation of dorsal scars:

Menu=cortex,unidirectional,bidirectional,unidirectionalConvergent,opposed,centripedal,orthogonal,Kombewa,crossed,indetermined

Length=50

Condition1=product1 flake blade bladelet triangularFlake

[platformType]

Type=Menu

Prompt=Select type of platform remnant:

Menu=cortical,plain,faceted,crushed,dihedral,punctiform,linearRidge,indeterminable

Length=30

Condition1=product1 flake blade bladelet triangularFlake AND

Condition2=fragmentation all proximal lateral-proximal proximal/medial lateral indetermined

[platformForm]

Type=Menu

Prompt=Select type of platform remnant:

Menu=oval,ventrallySplittedOut,crushed,lunate,chapeaudeGendarme,quadrangular,punctiform,triangular,irregular,linearRidge,indeterminable

Length=30

Condition1=product1 flake blade bladelet triangularFlake AND

Condition2=fragmentation all proximal lateral-proximal proximal/medial lateral indetermined

[platformWidth]

Type=Instrument

Prompt=Enter a value for platformWidth

Length=12

Condition1=product1 flake blade bladelet triangularFlake AND

Condition2=fragmentation all proximal lateral-proximal proximal/medial lateral indetermined

[platformThickness]

Type=Instrument

Prompt=Enter a value for platformThickness

Length=12

Condition1=product1 flake blade bladelet triangularFlake AND

Condition2=fragmentation all proximal lateral-proximal proximal/medial lateral indetermined

[dorsalReduction]

Type=Menu

Prompt=Is there a dorsal reduction?

Menu=none,shortHingedRemovals,abrasion,abrasion+shortHingedRemovals,smallRemovalsFollowingScarRidges,lateralNotching

Length=32

Condition1=product1 flake blade bladelet triangularFlake AND

Condition2=fragmentation all proximal lateral-proximal proximal/medial lateral indetermined

[delinationVentral]

Type=Menu

Prompt=What is the delination of the platform on the ventral face?

Menu=regularCurve,curvedOverhangingImpactPointWithoutBreak,curvedOverhangingImpactPointWithBreak,doublecurved,rectilinear,irregular,indeterminate

Length=40  
Condition1=product1 flake blade bladelet triangularFlake AND  
Condition2=fragmentation all proximal lateral-proximal proximal/medial lateral indetermined

[lip]  
Type=Menu  
Prompt=Is there a lip?  
Menu=No,Yes  
Length=20  
Condition1=product1 flake blade bladelet triangularFlake AND  
Condition2=fragmentation all proximal lateral-proximal proximal/medial lateral indetermined

[cone]  
Type=Menu  
Prompt=Is there a cone?  
Menu=No,Yes  
Length=20  
Condition1=product1 flake blade bladelet triangularFlake AND  
Condition2=fragmentation all proximal lateral-proximal proximal/medial lateral indetermined

[Bulb]  
Type=Menu  
Prompt=Is there a bulb?  
Menu=No,absentLip,pronounced,poorlyDeveloped,double,indeterminate  
Length=20  
Condition1=product1 flake blade bladelet triangularFlake AND  
Condition2=fragmentation all proximal lateral-proximal proximal/medial lateral indetermined

[BulbShattered]  
Type=Menu  
Prompt=Is the bulb shattered?  
Menu=No,Yes  
Length=20  
Condition1=product1 flake blade bladelet triangularFlake AND  
Condition2=fragmentation all proximal lateral-proximal proximal/medial lateral indetermined

[BulbarScar]  
Type=Menu  
Prompt=Is there a bulbar scar?  
Menu=No,Yes  
Length=20  
Condition1=product1 flake blade bladelet triangularFlake AND  
Condition2=fragmentation all proximal lateral-proximal proximal/medial lateral indetermined

[exteriorPlatformAngle]  
Type=Numeric  
Prompt=Enter a value for exteriorPlatformAngle  
Length=12  
Condition1=product1 flake blade bladelet triangularFlake AND  
Condition2=fragmentation all proximal lateral-proximal proximal/medial lateral indetermined

[distalTermination]

Type=Menu

Prompt=Select type of distal termination:

Menu=pointed,straight,convex,concave,plunging,hinged,step,indetermined

Length=30

Condition1=product1 flake blade bladelet triangularFlake AND

Condition2=fragmentation all distal lateral-distal medial/distal lateral indetermined

[crossSection]

Type=Menu

Prompt=Select type of cross section:

Menu=lenticular,triangular,trapezoidal,irregular,indeterminable

Length=30

Condition1=product1 flake blade bladelet triangularFlake indetermined

[profile]

Type=Menu

Prompt=Select type of profile:

Menu=rectilinear,slightlyCurved,curved,highlyCurved,irregular,indeterminate

Length=30

Condition1=product1 flake blade bladelet triangularFlake indetermined

[SedimentAttached]

Type=Menu

Prompt=Is sediment attached to this artefact?

Menu=No,Yes

Length=20

[photo]

Type=Menu

Prompt=Is this artefact photographed?

Menu=No,Yes

Length=20

[notes]

Type=Text

Prompt=Insert any additional notes here:

Length=255

[date]

Type=Menu

Prompt=Enter the date:

Menu=04/07/2017

Length=20